The role of histone kinases in controlling transcription in B cell lymphoma and leukaemia

Sarah Kreuz

Submitted in accordance with the requirements for the degree of
Doctor of Philosophy

The University of Leeds

School of Medicine and Health

January 2015

The candidate confirms that the work submitted is her own and that appropriate credit has been given where reference has been made to the work of others.

Acknowledgements

I would like to thank everybody, who made this work possible and who helped me throughout the process. First, I would like to acknowledge Yorkshire Cancer Research for funding my PhD. Many thanks to Pascal Lefevre and Reuben Tooze for giving me the opportunity to conduct this work under their supervision. Thanks to Pascal, for everything he taught me in the last three years and to Reuben, who was open for discussion of my results and often helped me see the data from a different perspective. I would also like to acknowledge Gina Doody, who gave me a lot of helpful advice on my project and provided many good ideas for the next experiments. A big thank you also to Peter Hillmen, who proposed the work on CLL and who was an invaluable source of advice in this field.

Special thanks go to all the people in the lab, who were always happy to help with ideas, protocols and materials. Thanks to Darren Newton, with whom I had a lot of lively and fruitful discussion about CLL. Further, I would like to specially acknowledge Talha Munir, who introduced me to CLL and made sure that I had a constant supply of CLL samples, Mario Cocco, who helped me with the ChIP-seq experiment and Matt Care, who analysed the raw sequencing data. I would like to thank Sophie Stephenson, who was always happy to help me with protocols, chemicals and advice, and John Sinfield, who motivated me throughout my PhD. Thanks to James Thorne and Lylia Ouboussad, who helped me in the first months of the PIM1 project. Very special thanks go to Rachael Barlow, without whom the lab just would not function, and to Richard Ingram and Deborah Clarke, who made sure that we always had enough consumables.

The people, who helped me the most during my PhD, were my friends, who saw me through a lot of difficult times and made me feel at home in Leeds. My greatest thanks go to Justin Gillespie, who is a very good and understanding friend and also helped me with the scientific side of the project. Many thanks to Annemarie, Layal, Katie and Orla for all the lovely days and evenings we spent together and to Muna, Geetha, Basmah and Sara.

A huge thank you to my family, especially my parents, who supported me throughout my studies in Germany and through the whole PhD. Without their help, I would not have been able to achieve any of this.

Abstract

Protein kinases are central mediators of signal transduction pathways and transcriptional regulation. Lymphoid malignancies are characterised by aberrant activation of key signal transduction pathways and specific gene expression programmes. Consequently, targeting kinases involved in these signal transduction pathways is a promising therapeutic strategy. Because gene expression is regulated at the level of chromatin, the aim of this study was to assess the effects of chromatin-modifying kinases on histone phosphorylation and transcriptional regulation in B cell lymphoma and the consequences of kinase inhibition for tumour cell viability and the chromatin structure of target genes.

The kinase PIM1, whose mRNA is highly expressed in the aggressive activated B cell-like diffuse large B cell lymphoma (ABC-DLBCL), but not germinal centre B cell-like DLBCL (GCB-DLBCL), has been shown to associate with the transcription factor MYC and to regulate the expression of MYC target genes by phosphorylating histone H3S10. Therefore, effects of PIM1 on viability and gene expression were evaluated in ABC-DLBCL and in the MYC-dependent Burkitt lymphoma (BL). However, pan-PIM kinase inhibition or knockdown of PIM1 did not effectively reduce viability of ABC-DLBCL or Burkitt lymphoma cell lines. Further, the expression of the MYC- and PIM1-bound *GNL3* gene was largely unaffected by alterations in PIM kinase levels or activity. In conclusion, PIM kinases do not seem to be bona fide therapeutical targets in DLBCL and BL.

The second part of this project aimed to understand the effects of Ibrutinib on chromatin structure in chronic lymphocytic leukaemia (CLL) cells. Ibrutinib inhibits Bruton's tyrosine kinase, and thus B cell receptor (BCR) signalling, and is currently being tested in clinical trials for the treatment of CLL. *In vitro*, Ibrutinib inhibited BCR-induced gene expression and histone H3T6 and T11 phosphorylation. A possible kinase targeting H3T6 and H3T11 downstream of the BCR might be zipper-interacting protein kinase (ZIPK), a ZIPK inhibitor blocked H3T6p and H3T11p and gene expression. Short-term Ibrutinib treatment appeared to inhibit histone turnover but did not reduce H3K4me3, H3K9ac, H2A.Z or POL II recruitment at target genes, indicating that it inhibits only some aspects of transcription. In contrast, long-term Ibrutinib treatment decreased H3K4me3 and H3K9ac in promoter regions, possibly by an indirect, gene silencing-dependent mechanism. In summary, the results suggest that Ibrutinib blocks progression of CLL by inhibiting only some branches of BCR signalling and interestingly, many transcription-associated changes to the chromatin remain unaltered, while transcription is effectively inhibited.

Table of Contents

List of Tables

List of Figures

Abbreviations

14-3-3 protein	Adapter protein
4EBP1	Eukaryotic initiation factor 4E binding protein 1
A	(Desoxy-)adenosine
AATF	Apoptosis antagonising transcription factor
ABC	ATP-binding cassette
ABC-DLBCL	Activated B cell-like diffuse large B cell lymphoma
ABL	Abelson murine leukaemia viral oncogene
Ac	Acetyl-
ADP	Adenosine diphosphate
AID	Activation-induced cytidine deaminase
AML	Acute myeloid leukaemia
AP1	Activator protein 1
APS	Ammonium persulfate
AR	Androgen receptor
ARE	3'-AU-rich element
ARF	alternate reading frame, protein product of the *CDKN2A* locus
ARID3A	AT-rich interactive domain 3A
ASHM	Aberrant somatic hypermutation
ASK1	Apoptosis signalling kinase 1
ATCC	American Type Culture Collection
ATF4	Activating transcription factor 4
ATP	Adenosine triphosphate
AUF1	AU-rich element-binding factor 1
BAD	BCL2-associated agonist of cell death
BAH domain	Bromo-adjacent homology domain
BAX	BCL2-associated X protein
BCAP	B cell adaptor for PI3K
BCL	B cell lymphoma
BCL2	B CLL/B cell lymphoma 2
BCL2L1	BCL2-like 1
BCL6	B cell lymphoma 6
BCR	B cell receptor
BCR-ABL	breakpoint cluster region-Abelson murine leukaemia viral oncogene fusion protein
BET	Bromodomain and extra terminal domain
bHLHZ	Basic helix-loop-helix leucine zipper
BIM	BCL2-interacting mediator of cell death
BL	Burkitt lymphoma
BLK	B lymphoid kinase
BLNK	B cell linker
BMX	Bone marrow tyrosine kinase
bp	Base pair(s)
BRD4	Bromodomain-containing protein 4
BRE1	Ring finger protein 20, E3 ubiquitin protein ligase
BRK	Breast tumour kinase
BSA	Bovine serum albumin
BTK	Bruton's tyrosine kinase
C	(Desoxy-)cytidine
Ca^{2+}	Calcium
$CaCl_2$	Calcium chloride
CaMKII	Calcium/Calmodulin-dependent kinase
cAMP	Cyclic adenosine monophosphate
CARD	Caspase recruitment domain
CARMA1	CARD-containing and MAGUK protein

CBP	CREB-binding protein
CCL	chemokine (C-C motif) ligand
CCND1/2/3	Cyclin D1/2/3
CCR	chemokine (C-C motif) receptor
CD	Cluster of differentiation
CD40L	CD40 ligand
CDC25C	Cell division cycle 25C
CDK	Cyclin-dependent kinase
cDNA	Complementary DNA
CDS	Coding DNA sequence
CE	Capping enzymes
ChIP	Chromatin immunoprecipitation
ChIP-seq	ChIP sequencing
CLL	Chronic lymphocytic leukaemia
CML	Chronic myeloid leukaemia
CMV	Cytomegalovirus
CO_2	Carbondioxide
COMPASS	Complex proteins associated with Set1
COT	Cancer Osaka thyroid oncogene
COX2	Cyclooxygenase 2
CREB	cAMP-response element binding
CSK	C-terminal Src kinase
CSR	Class switch recombination
CTCF	CCCTC-binding factor
CTD	C-terminal domain
CXCL	chemokine (C-X-C motif) ligand
CXCR	chemokine (C-X-C motif) receptor
D	Aspartate
DAG	Diacylglycerol
DAPK	Death-associated protein kinase
dATP	Desoxyadenosine triphosphate
dCDP	Desoxycytidine diphosphate
dCTP	Desoxycytidine triphosphate
ddH_2O	Twice desalted water
dGTP	Desoxyguanosine triphosphate
dH_2O	Desalted water
DLK	DAP-like kinase
DMEM	Dulbecco's modified Eagle medium
DMSO	Dimethylsulfoxide
DNA	Desoxyribonucleic acid
DNase	Desoxyribonuclease
DNMT	DNA methyltransferase
dNTP	Desoxynucleotide triphosphate
DOK	Docking protein
DRAK1/2	Death-associated protein kinase-related protein 1/2
DRB	5,6-Dichloro-1-β-D-ribofuranosylbenzimidazole
DSIF	DRB sensitivity-inducing factor
DTT	Dithiotreitol
dTTP	Desoxythymidine triphosphate
DUSP2/4	Dual specificity phosphatase
DYRK1/2/3	Dual-specificity tyrosine phosphorylation-regulated kinase 1A
E box	Enhancer box
E_μ	IGH enhancer
E2F	Adenovirus *E2* gene promoter region binding factor
eBL	Endemic Burkitt lymphoma
EBNA2	Epstein–Barr virus nuclear antigen 2
EBV	Epstein-Barr virus

ECL	Enhanced chemiluminescence
EDTA	Ethylenediaminetetraacetic acid
EGF	Epidermal growth factor
EGFP	Enhanced green fluorescent protein
EGFR	Epidermal growth factor receptor
EGR1	Early growth response 1
EGTA	Ethyleneglycol tetraacetic acid
eIF	Eukaryotic translation initiation factor
ER	Endoplasmic reticulum/ oestrogen receptor
ERBB2	erythroblastic leukaemia viral oncogene homolog 2
ERK	Extracellular signal-regulated kinase
ETS	E-twenty-six oncogene homolog
EZH1/2	Enhancer of zeste homolog 1/2
F	Phenylalanine
Fab	Fragment, antigen-binding (Ig fragment of heavy and light chain)
FACS	Fluorescence-assisted cell sorter
FACT	Facilitates transcription
FADD	FAS-associated via death domain
FAS	Fas cell surface death receptor
FASL	FAS ligand
FBW7	F box and WD repeat domain-containing 7
Fc	Fragment, crystallisable (Ig fragment of two heavy chains)
FCRL	FcR-like
FCS	Foetal calf serum
FcγR	Fcγ receptor
FGR	Gardner-Rasheed feline sarcoma viral (Fgr) oncogene homolog, SRC family kinase
FLICE	FADD-like interleukin-1 beta-converting enzyme
FLIP	FLICE-like inhibitory protein
FLT3	Fms-related tyrosine kinase 3
FOS	Finkel–Biskis–Jinkins murine osteosarcoma oncogene
FOSL1	FOS-like 1
FOXO	Forkhead box O
FRK	FYN-related SRC family tyrosine kinase
FYN	FGR/YES related novel protein
G	(Desoxy-)guanosine/ Glycine
G9A	Histone H3K9 methyltransferase 3
GADD45	Growth arrest and DNA damage 45
GAP	GTPase-activating protein
GAPDH	Glyceraldehyde 3-phosphate dehydrogenase
GC	Germinal centre
GCB-DLBCL	Germinal centre B cell-like diffuse large B cell lymphoma
GCN5	general control of amino-acid synthesis, yeast, homolog
gDNA	Genomic DNA
GDP	Guanosine diphosphate
GEF	Guanine nucleotide exchange factor
GLP	G9A-like protein
GLT8D1	Glycosyltransferase 8 domain containing 1
GNAT family	GCN5-related N-acetyltransferase family
GNL3	Guanine nucleotide binding protein-like 3, nucleolar; nucleostemin
GRB2	Growth factor receptor-bound protein 2
GSK3β	Glycogen synthase kinase 3 beta
GTP	Guanosine triphosphate
Gy	Gray
HAT	Histone acetyltransferase

HBO1	Histone acetyltransferase bound to ORC
HCDR	Human complementarity determining region
HCK	Haematopoietic cell kinase
HCl	Hydrogen chloride
HCLB	Hypotonic cell lysis buffer
HDAC	Histone deacetylase
HEPES	4-(2-hydroxyethyl)-1-piperazineethanesulfonic acid
hnRNA	Heterogeneous nuclear RNA
HP1	Heterochromatin protein 1
HPRT	Hypoxanthine phosphoribosyltransferase 1
HRP	Horseradish peroxidase
HSP90	Heat shock protein, 90kDa
hTERT	human telomerase reverse transcriptase
IAP	Inhibitor of apoptosis
ID2	Inhibitor of DNA binding 2
Ig	Immunoglobulin
IGH	Immunoglobulin heavy chain
IGK/Igκ	Immunoglobulin kappa chain
IGL	immunoglobulin light chain
IGL/Igλ	Immunoglobulin lambda chain
IKK	Inhibitor of NF kappa B kinase
IL	Interleukin
IMDM	Iscove's modified Dulbecco's medium
Inh	Inhibitor
INI1	Integrase interactor 1 protein
iNOS	Inducible nitric oxide synthase
IP	Immunoprecipitation
IP_3	Inositoltrisphosphate
IPTG	Isopropyl β-D-1-thiogalactopyranoside
IRF1	Interferon regulatory factor 1
ITAM	Immunoreceptor tyrosine-based activation motif
ITIM	Immunoreceptor tyrosine-based inhibition motif
ITK	IL2-inducible T cell kinase
JAK3	Janus kinase 3
JHDM	Jumonji domain-containing histone demethylase
JMJD	Jomonji domain-containing protein
JNK	JUN N-terminal kinase
JUN	jun proto-oncogene
K	Lysine
KAc	Potassium acetate
KCl	Potassium chloride
kDa	Kilo Dalton
KDM	Lysine-specific demethylase
Ki67	antigen identified by monoclonal antibody Ki 67
L	Leucine
LacO	Lactose operator
LAIR1	Leukocyte-associated Ig-like receptor 1
LB	Lysogeny broth
LCK	Lymphocyte protein tyrosine kinase, SRC family kinase
LiCl	Lithium chloride
LIF	Leukaemia inhibitory factor
LILRB	Leukocyte immunoglobulin-like receptor, subfamily B
LSD	Lysine-specific demethylase
LYN	Member of the Src family kinases
M	Methionine
MAGUK	Membrane-associated guanylate cyclase
MALT	Mucosa-associated lymphoid tissue

MALT1	Mucosa-associated lymphoma translocation gene 1
MAPK	Mitogen-activated protein kinase
MARK3	MAP/microtubule affinity-regulating kinase 3
MAX	MYC-associated factor X
MB	MYC box
Mb	Megabases
MBP1	MYC-binding protein 1
MCL	Mantle cell lymphoma
MCL1	Myeloid cell leukaemia 1
M-CLL	Mutated CLL
MDM2	Mouse double minute 2 homolog
Me	Methyl-
Me3	Trimethyl-
MeCP2	Methyl-CpG binding protein 2
MEK	Mitogen/extracellular signal-regulated kinase
$MgAc_2$	Magnesium diacetate
$MgCl_2$	Magnesium chloride
MHC	Major histocompatibility complex
MIB2	Mind bomb 2
miR/miRNA	Micro RNA
MIZ1	MYC-interacting Zinc-finger protein 1
MKP1	MAP kinase phosphatase 1
MLL	Mixed lineage leukaemia
MM1	Myc modulator 1
MMLV	Moloney murine leukaemia virus
MMS2	Ubiquitin-conjugating enzyme E2 variant 2
$MnCl_2$	Manganese chloride
MNK	Mitogen-activated kinase-interacting kinase
MnSOD	Manganese superoxide dismutase
MNT	MAX network transcriptional repressor
MOF	Ortholog of *Drosophila* Males absent on the first
MOPS	3-(N-morpholino)propansulfonic acid
MORF	MOZ-related factor
MOZ	Monocytic leukaemia zinc finger protein
MRG15	MORF-related gene on chromosome 15
mRNA	Messenger RNA
MSK	Mitogen- and stress-activated protein kinase
MSRB1/SEPX1	Methionine sulfoxide reductase B1 gene
mTORC	Mammalian target of rapamycin complex
MTT	3-(4,5-Dimethylthiazol-2-yl)-2,5-diphenyltetrazolium bromide
MXD	MAX dimerization protein
MYC	v-myc avian myelocytomatosis viral oncogene homolog
MYCL	v-myc avian myelocytomatosis viral oncogene lung carcinoma-derived homolog
MYCN	v-myc avian myelocytomatosis viral oncogene neuroblastoma-derived homolog
MYND domain	myeloid, Nervy, and DEAF-1 homology domain
MyoD	myogenic differentiation
MYST family	MOZ, Ybf2, Sas2, Tip60 acetyltransferase family
NaCl	Sodium chloride
NaF	Sodium fluoride
$NaHCO_3$	Sodium hydrogen carbonate
$NaVO_3$	Sodium vanadate
NCK	Non-catalytic region of tyrosine kinase adaptor protein
NCL	Nucleolin
ncRNA	Non-coding RNA
NELF	Negative elongation factor

NEMO	NF kappa B essential modulator
NFAT	Nuclear factor of activated T cells
NFR	Nucleosome-free region
NF-YA	Nuclear factor YA
NFκB	Nuclear factor kappa B
NHL	Non-Hodgkin lymphoma
NK cells	Natural killer cells
NLC	Nurse-like cell
NLS	Nuclear localisation sequence
NPM1	Nucleophosmin
NSD3	Nuclear receptor binding SET domain-containing protein 3
nt	Nucleotide(s)
ORC	Origin recognition complex
P	Proline
p	Phosphate
PAF1	POL II-associated factor, homolog (*S. cerevisiae*)
PAGE	Polyacrylamide gelelectrophoresis
PALS	Periarterial lymphoid sheath
PAP1	PIM-associated protein 1
Par4	Prostate apoptosis response
PARP	Poly-(ADP-ribose)-polymerase
Pat	Patient
PBMCs	Peripheral blood mononuclear cells
PBRM1	Polybromo 1
PBS	Phosphate buffered saline
PCAF	p300/CBP-associated factor
PCR	Polymerase chain reaction
PD1	Programmed cell death 1
PDK1	PIP_3-dependent kinase 1
PECAM	Platelet/endothelial cell adhesion molecule
Pen/Strep	Penicillin/Streptomycin
PEST	Proline, glutamate, serine, threonine-rich sequence
PF1	PHD finger protein 12
PFs	Polyadenylation factors
PH	Pleckstrin homology
PHD finger	Plant homeodomain finger
PI	Propidium iodide
PI3K	Phosphatidylinositol-3-kinase
PI-4,5-P_2	Phosphatidylinositol-4,5-bisphosphate
PIC	Proteinase inhibitor cocktail
PIM1/2/3	Proviral insertion site for Moloney murine leukaemia virus
PIN1	Peptidyl-prolyl *cis-trans* isomerase NIMA-interacting 1
PIP_3	Phosphatidylinositol-3,4,5-trisphosphate
PKA	Protein kinase A
PKB/AKT	Protein kinase B
PKC	Protein kinase C
PKM2	Pyruvate kinase M2
PLCγ	Phospholipase C gamma
PMA	Phorbol 12-myristate 13-acetate
PMSF	Phenylmethylsulfonyl fluoride
POL	RNA polymerase
PP1	Protein phosphatase 1
PP2A	Protein phosphatase 2A
PPP6C	Protein phosphatase 6, catalytic subunit
PRAS40	Proline-rich AKT substrate of 40 kDa
PRC1/2	Polycomb repressive complex 1/2
PRDM2	PR domain-containing 2

PRDX1	Peroxiredoxin 1
P-TEFb	Positive transcription elongation factor b
PTEN	Phosphatase and tensin homolog
PTM	Posttranslational modification
PU.1/SPI1	Spleen focus forming virus (SFFV) proviral integration oncogene
PVDF	Polyvinylidene fluoride
R	Arginine
RAC1	RAS-related C3 botulinum toxin substrate 1
RAD6	Ubiquitin-conjugating enzyme E2A
RAF	Rapidly accelerated fibrosarcoma
RAG1/2	Recombination-activating gene 1/2
RAS	Rat sarcoma
RASGAP	RAS GTPase activating protein
RASGRP	RAS guanine nucleotide-releasing protein
R-CHOP	Rituximab, cyclophosphamide, doxorubicin, vincristine, prednisone
rDNA	Ribosomal DNA
RefSeq	Reference sequence
RET	Receptor tyrosine-protein kinase, proto-oncogene
RHEB	RAS homolog enriched in brain
RHO	Ras homolog
RING1	Really interesting new gene 1
RIPA	Radioimmunoprecipitation assay buffer
RIPK2	Receptor-interacting serine-threonine kinase 2
RNA	Ribonucleic acid
RNase	Ribonuclease
ROCK	Rho kinase
Rpd3S	Rpd3 histone deacetylase complex, small
rRNA	Ribosomal RNA
RSK	Ribosomal S6 kinase, 90 kDa
RT-qPCR	Reverse transcription quantitative PCR
RUNX	Runt-related transcription factor
S	Serine
S6K	Ribosomal S6 kinase, 70 kDa
Sas2	Something about silencing 2
sBL	Sporadic Burkitt lymphoma
sd	Standard deviation
SDS	Sodium dodecyl sulfate
SET domain	Su(var)3-9, enhancer of zeste and trithorax homology domain
SET1A/B	SET domain-containing 1A/B
SETD2	SET domain-containing 2
SETDB1	SET domain-containing B1
SFK	Src family kinase
SH2/3	Src homology 2/3 domain
SHIP	SH2 domain-containing inositol polyphosphate-5-phosphatase
SHM	Somatic hypermutation
SHP	SH2 domain-containing phosphotyrosine phosphatase
shRNA	Short hairpin RNA
SIGLEC10	Sialic acid-binding Ig-like lectin
SIN3A/B	SIN3 transcription regulator family members A and B
SKP2	S phase kinase-associated protein 2
SLL	Small lymphocytic lymphoma
SMAD	Mothers against decapentaplegic homolog
SMARCA	SWI/SNF related, matrix associated, actin-dependent regulator of chromatin, subfamily A
SMYD3	SET and MYND domain-containing 3

SNORD69	Box C/D snoRNA 69
snoRNA	Small nucleolar RNA
SOS	Son of sevenless
SP1	Specificity protein 1
SPIB, SPIC	Spi-1/PU.1-related transcription factors
SPT3	Suppressor of Ty 3 homolog (*S. cerevisiae*)
SPT5	Suppressor of Ty 5 homolog (*S. cerevisiae*)
SRC	Rous sarcoma oncogene
SSB	SDS sample buffer
STAGA	SPT3-TAF9-GCN5 acetyltransferase
STAT	Signal transducer and activator of transcription
SUMO	Small ubiquitin-like modifier
SUV39H1/2	Suppressor of variegation 3-9 homolog 1/2
SWI/SNF	Switch/sucrose non-fermentable
SYK	Spleen tyrosine kinase
T	Threonine/ Deoxythymidine
TAB2/3	TAK1 binding protein 2/3
TAD	Topologically associating domain
TAE	Tris-acetate-EDTA
TAF	TBP-associated factor
TAK1	TGF-beta-activated kinase 1
Taq	*Thermophilus aquaticus* RNA-dependent DNA polymerase
TBP	TATA-binding protein
TBST	Tris-buffered saline with 0.1% Tween-20
TCF	Ternary complex factor
TE	Tris-EDTA
TEC	Transient erythroblastopenia of childhood, proto-oncogene
TEM	Trans-endothelial migration
TEMED	Tetramethylethylenediamine
TF	Transcription factor
TFIID/H	General transcription factors for POL II
TFIIIB	General transcription factor for POL III
TFTC	TBP-free TAFII-containing complex
TGFβ	Transforming growth factor beta
TIAR	Translational repression by RNA binding
TIF1β	Transcription intermediary factor 1 beta
TIP60	60 kDa Trans-Activator of Transcription (Tat)-interacting protein
TLR10	Toll-like receptor 10
TNF	Tumour necrosis factor
Tpl2	Tumour progression locus 2
TRAF6	TNF receptor-associated factor 6
tRNA	Transfer RNA
TRRAP	Transformation/transcription domain-associated protein
TSC	Tuberous sclerosis complex
TSS	Transcription start site
TTP	Tristetraprolin
TTS	Transcription termination site
U	Uridine
ub	Ubiquitin-
UBC13	Ubiquitin-conjugating enzyme 13
UK	United Kingdom
UM-CLL	Unmutated CLL
UTR	Untranslated region
VAV	VAV guanine nucleotide exchange factor
VDR	Vitamin D receptor
W	Tryptophan

WDR5	WD repeat domain 5
WHO	World Health Organisation
WNT	Wingless/integration family
X	Any amino acid
Y	Tyrosine
Ybf2	Yeast binding factor 2
YES	Yamaguchi sarcoma viral oncogene homolog
ZAP70	Zeta-chain-associated protein kinase 70
ZIC	Zinc finger protein of the Cerebellum
ZIPK	Zipper-associated protein kinase

1 Introduction

1.1 Overview

B cell malignancies can arise from different stages of normal B cell development through B cells acquiring mutations that result in the reduction of apoptosis and enhance proliferation. Often, B cell intrinsic properties, e.g. the expression of the DNA mutating machinery used for immunoglobulin hypermutation (Lenz et al., 2007; Pasqualucci et al., 2001) or the chronic activation of B cell receptor signalling (Burger & Chiorazzi, 2013; Davis et al., 2010), facilitate malignant transformation. Further, other cells of the immune system or the lymphoid organs play a role in driving proliferation of the malignant cells (Bhattacharya et al., 2011; Burger et al., 2000; Ito et al., 2012; Lagneaux et al., 1998; Os et al., 2013; Patten et al., 2008).

Malignant cells often show aberrant gene expression profiles and, consistently, important drivers of malignant transformation are key transcription factors, like MYC in Burkitt lymphoma, NFκB in activated B cell-like diffuse large B cell lymphoma (ABC-DLBCL) and BCL6 in germinal centre B cell-like DLBCL (GCB-DLBCL), and/or the activation of key signal transduction pathways, like the B cell receptor pathway, through aberrant signalling in DLBCL, through chronic signalling in CLL or through tonic signalling in Burkitt lymphoma (Alizadeh et al., 2000; Hatzi & Melnick, 2014; Z. Li et al., 2003; Niemann & Wiestner, 2013). Because kinases are currently the preferred therapeutic targets, targeting kinases involved in these transformation-driving pathways can provide a good means of treating B cell malignancies. However, treating patients with drugs targeting only a single enzyme often leads to rapid induction of resistance (le Coutre et al., 2000; Woyach et al., 2014). Thus, identifying novel targetable kinases is important to improve the treatment of B cell malignancies. Interesting targets in DLBCL and Burkitt lymphoma might be the kinases PIM1 and PIM2. mRNAs for both kinases are highly expressed in the more aggressive ABC-DLBCL as compared to GCB-DLBCL (Alizadeh et al., 2000; Care et al., 2013; Wright et al., 2003). Further, PIM1 has been associated with transcriptional regulation at MYC target genes (Zippo et al., 2007) and might therefore contribute to the transcriptional deregulation and thus tumour formation or progression in ABC-DLBCL and the MYC-dependent Burkitt lymphoma. Of note, PIM kinase knockout mice only show a very mild phenotype: they are viable and fertile, although they have a reduced body size and their peripheral T cells show a reduced proliferative response towards T cell receptor and IL-2 stimulation

(Mikkers et al., 2004). This indicates that therapeutic inhibition of PIM kinases might have a desirable side-effect profile.

On the other hand, it is important to understand how drugs work, which are already used for treating B cell malignancies, for example the Bruton's tyrosine kinase inhibitor Ibrutinib, which is currently evaluated in clinical trials for the treatment of CLL. It leads to remission and thus knowledge about its mechanism of action will help us to better understand the disease, which ultimately provides a means of developing novel drugs targeting the essential survival pathways. These drugs can be used in conjunction with the original drug to prevent resistances or in patients, who have already become resistant to Ibrutinib.

This study mainly focussed on effects of kinases and kinase inhibitors on the chromatin, because the ultimate driving force for B cell malignancies is aberrant gene expression and the chromatin is the platform, at which gene expression is regulated (Taylor et al., 2013). Through histone tail modifications or the use of histone variants, transcription can be activated or repressed (Berger, 2007; Li, Carey, et al., 2007). Understanding which changes to the chromatin structure are mediated by certain signal transduction pathways and kinases and which of these are important for tumour maintenance, will eventually allow for the identification of drugable targets. Moreover, histone modifications are indicative of the activation status of a gene and thus the phenotype of a cell. They can therefore also be used as a diagnostic tool and to predict drug sensitivity and drug response (Taylor et al., 2013).

1.2 B cells and B cell receptor signalling

1.2.1 B and T lymphocytes in lymphoid tissues

B and T lymphocytes are cells of the adaptive immune system. B cells develop in the bone marrow, T cells in the thymus (Janeway et al., 2001). T cell responses are cell-mediated, which means that direct contact between the T cell and target cell is usually required. Cytotoxic T cells kill infected or abnormal cells, while T helper cells stimulate other cells of the immune system and help them to carry out their specific function. In contrast, B lymphocytes mediate the humoral immune response by producing immunoglobulins in response to an antigenic challenge, which serve to either neutralise or opsonise the antigen (Alberts, 2008).

Mature B and T cells circulate in the blood or home to the secondary lymphoid tissues (lymph node, spleen, mucosa-associated lymphoid tissues (MALT)) (Janeway et al., 2001). These have a specific architecture: B and T cells migrate to different areas

which are associated with specific stromal cells and other leukocytes (Koning & Mebius, 2012; Mebius & Kraal, 2005). In the lymph nodes, B cells form follicles, which are surrounded by more diffusely distributed T cells (Figure 1.1) (Janeway et al., 2001; Koning & Mebius, 2012). The spleen consists of the red pulp, where the blood is cleared of old cells and foreign particles, and the white pulp, which is formed by lymphoid cells (Mebius & Kraal, 2005). The central arteries are surrounded by the periarterial lymphoid sheath (PALS), which mainly consists of T cells. B cells form follicles adjacent to the PALS (Koning & Mebius, 2012). The perifollicular zone also contains some scattered B and T cells (Steiniger et al., 1997). Specialised marginal zone B cells can be found in the marginal zone between the follicles and the perifollicular zone. In contrast to rodents, human marginal zone-like B cells can also be found in the circulation and beneath the subcapsular sinus in lymph nodes (Figure 1.1) (Weill et al., 2009).

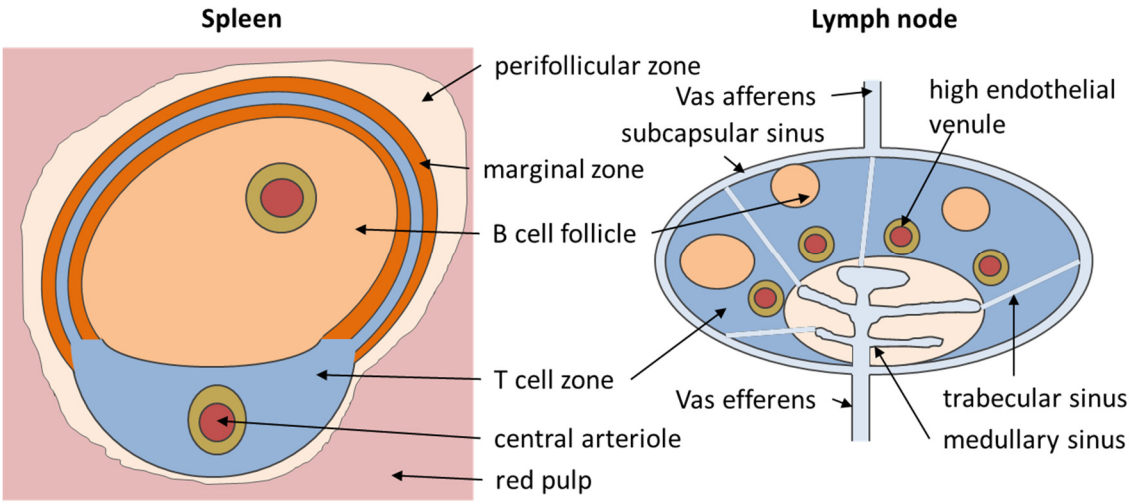

Figure 1.1 Schematic composition of the spleen and lymph nodes (adapted from Koning and Mebius, 2012 and Mebius and Kraal 2005).
One section of the spleen depicting one central arteriole with the PALS is shown, while a section of the whole lymphnode is depicted.

1.2.2 The B cell receptor

Immunoglobulins and the signalling molecules CD79a and b form the B cell receptor (BCR) on the surface of the cell, allowing for specific responses to antigens (Figure 1.2) (Jung et al., 2006).

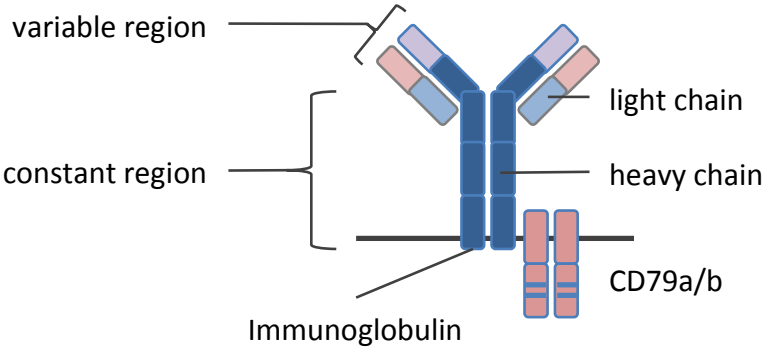

Figure 1.2 The B cell receptor.
The core B cell receptor consisting of the immunoglobulin and the accessory CD79a and b chains.

The immunoglobulins consist of two heavy (IgH) and two light chains (Igλ or Igκ), each of which has a variable, antigen-recognising and a constant dimerization and effector region. The large diversity of immunoglobulins, which allows for the recognition of almost unlimited numbers of antigens, is generated by genomic rearrangement of the IGH and IGK or IGL loci (Jung et al., 2006; Watson & Breden, 2012). In the germ line, the genomic loci for the light chains consist of multiple V (variable) and J (joining) segments and the constant region(s), while the heavy chain locus has additional D (diversity) segments in between the V and J regions (Figure 1.3) (Cook & Tomlinson, 1995; Early et al., 1980).

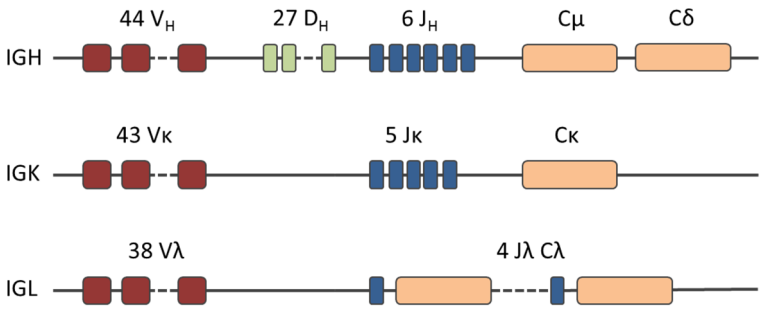

Figure 1.3 The immunoglobulin loci.
Schematic representation of the IGH, IGK and IGL genomic loci with variable (V), diversity (D), joining (J) and constant (C) regions. The IGH gene has different C segments encoding for different immunoglobulin isotypes (μ, δ, γ, ε, α).

Through homologous recombination events during B cell development, different V(D)J segments are joined, leading to the expression of distinct BCRs (Figure 1.4). The lymphocyte-specific enzymes recombination-activating gene 1 (RAG1) and RAG2, as well as the general DNA-double strand break repair pathway play an essential role in this process (Gellert, 2002; Mombaerts et al., 1992; Shinkai et al., 1992). In humans, 44 functional V_H, grouped into 7 different families, 27 functional D_H and 6 functional J_H segments have been identified (Cook & Tomlinson, 1995; van Dongen et al., 2003). For IGK and IGL 43 and 38 functional V and 5 and 4 functional J regions are known (van Dongen et al., 2003). In addition to this combinatorial diversity, further diversification is achieved during the recombination process through insertions or deletions in the joining regions, which increases the heterogeneity of the BCR (Gellert, 2002; Tonegawa, 1983). And last, activated B cells undergo somatic hypermutation of the V region, which leads to almost unlimited diversity of the receptor (Pascual et al., 1994). Importantly, malignant B cells often use stereotyped B cell receptors with a restricted repertoire of V, D and J regions and distinct mutation patterns, implicating the stimulation by common antigens in disease pathogenesis (Darzentas & Stamatopoulos, 2013; Sutton et al., 2013).

T cell receptors are generated by a similar mechanism but do not undergo somatic hypermutation (Gellert, 2002). Further, while B cell receptors can recognise both soluble and surface-bound antigens and even non-protein substrates, T cells can recognise only peptides that are bound to major histocompatibility complex (MHC) molecules on the surfaces of other cells (Janeway et al., 2001).

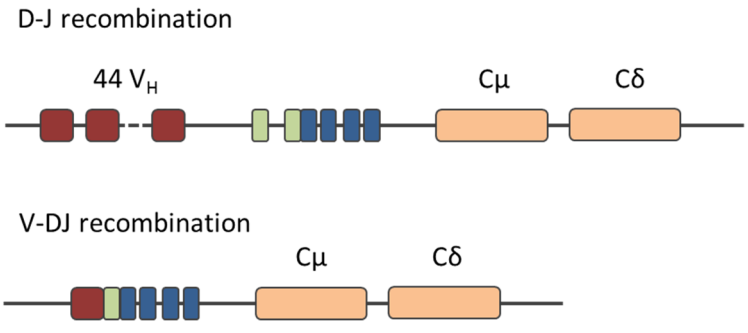

Figure 1.4 VDJ recombination.
VDJ recombination generates a functional IGH chain by altering the genomic composition of the IGH locus.

1.2.3 B cell development and maturation

Because the development of B cell malignancies is intricately linked to B cell development and activation, these will be reviewed in the following sections. With the support of bone marrow stromal cells, B cells develop from haematopoietic stem cells into pro- and then pre-B cells (Janeway et al., 2001). During this development, B cells rearrange their B cell receptor genes. The heavy chain rearrangement occurs in pro-B cells and when a functional μ heavy chain is generated, which means that in-frame recombination occurred, the cell becomes a pre-B cell (Boekel et al., 1998; Pieper et al., 2013). As there are two IGH alleles, the cell has two chances to generate such a functional μ heavy chain or it undergoes apoptosis. The newly generated heavy chain and the surrogate light chain then form the pre-B cell receptor, which triggers cell division and reorganisation of the IGK light chain genes (Pieper et al., 2013). In contrast to the heavy chain locus, each allele can undergo several attempts of recombination to generate a functional gene, before recombination of the other allele occurs (Langerak & Dongen, 2012). If IGK gene rearrangement is unsuccessful, IGL rearrangement is initiated, so that most cells proceed to the next developmental stage (Burg et al., 2001). Immature B cells express a functional IgM receptor, consisting of IgH and Igκ or Igλ chains (Figure 1.5) (Pieper et al., 2013).

Immature B cells first home to the spleen, where they develop into marginal zone or follicular B cells (Figure 1.5) (Pieper et al., 2013). Marginal zone B cells express hypermutated IgM and form the first line of defence against blood-borne pathogens (Weill et al., 2009; Weller et al., 2004). In a T cell-independent response, they develop into IgM-secreting plasma cells (Oliver et al., 1999; Spencer et al., 1998; Timens et al., 1989). But most of the B cells in the periphery are follicular B cells that can be found in the follicles in spleen and lymph nodes and are involved in the germinal centre reaction (Srivastava et al., 2005). In humans, both marginal zone and follicular B cells circulate between the lymphoid tissues and the blood until they encounter their antigen and become activated (Steiniger et al., 2005; Weller et al., 2004). B cell malignancies can develop from pre-B cells (B cell acute lymphocytic leukaemia), from marginal zone or follicular B cells and their activated progeny (Rickert, 2013).

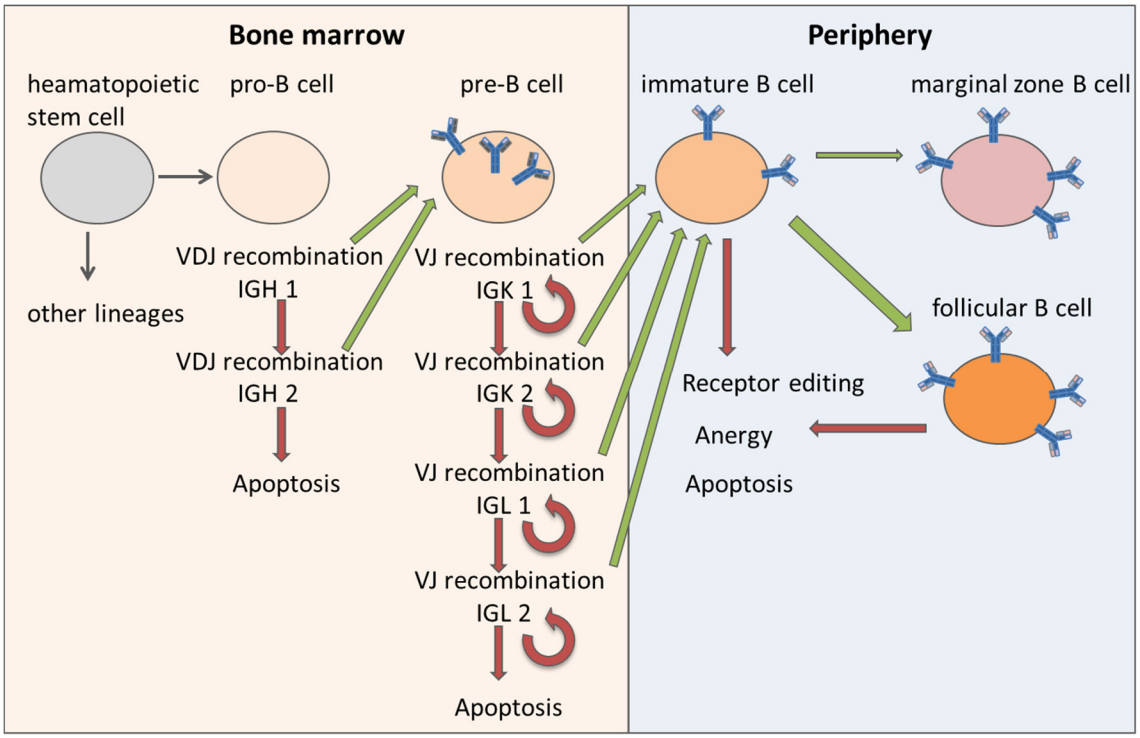

Figure 1.5 B cell development.
A haematopoietic stem cell gives rise to a pro-B cell, which activates IGH recombination. Upon successful recombination, the pre-B cell receptor is expressed and the cell undergoes light chain rearrangement. The immature B cell leaves the bone marrow and homes to the spleen, where it develops into either a marginal zone or a follicular B cell. If the cell recognises an autoantigen, it can undergo receptor editing, become anergic or undergo apoptosis.

1.2.4 The humoral immune response

When the mature B cell encounters its cognate antigen, the BCR is cross-linked and signal transduction is triggered. However, to become fully activated, a follicular B cell normally requires T cell help. T cells can only provide this, if they have previously been primed by an encounter with their antigen on dendritic cells (Mempel et al., 2004; Stoll et al., 2002). B cells internalise the Ig-bound antigen, process and present it via their MHC class II receptors (Abbas et al., 1985; Zotos & Tarlinton, 2012). They migrate into the T cell zone to make contact with primed T cells (Reif et al., 2002) and if a T cell recognises the antigen, it stimulates the B cell via cell surface receptors like CD40 ligand (CD40L) and CD28, as well as cytokines like interleukin-4 (IL-4) and IL-21 (Figure 1.6) (Damle et al., 1991; Ettinger et al., 2005; Lane et al., 1992; Lederman et al., 1992; Zotos & Tarlinton, 2012).

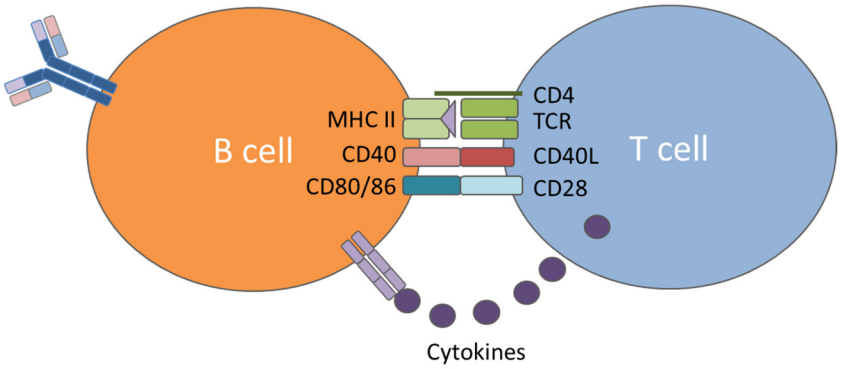

Figure 1.6 B cell activation.
Primed T cells activate antigen-specific B cells through interactions of cell surface receptors and cytokines.

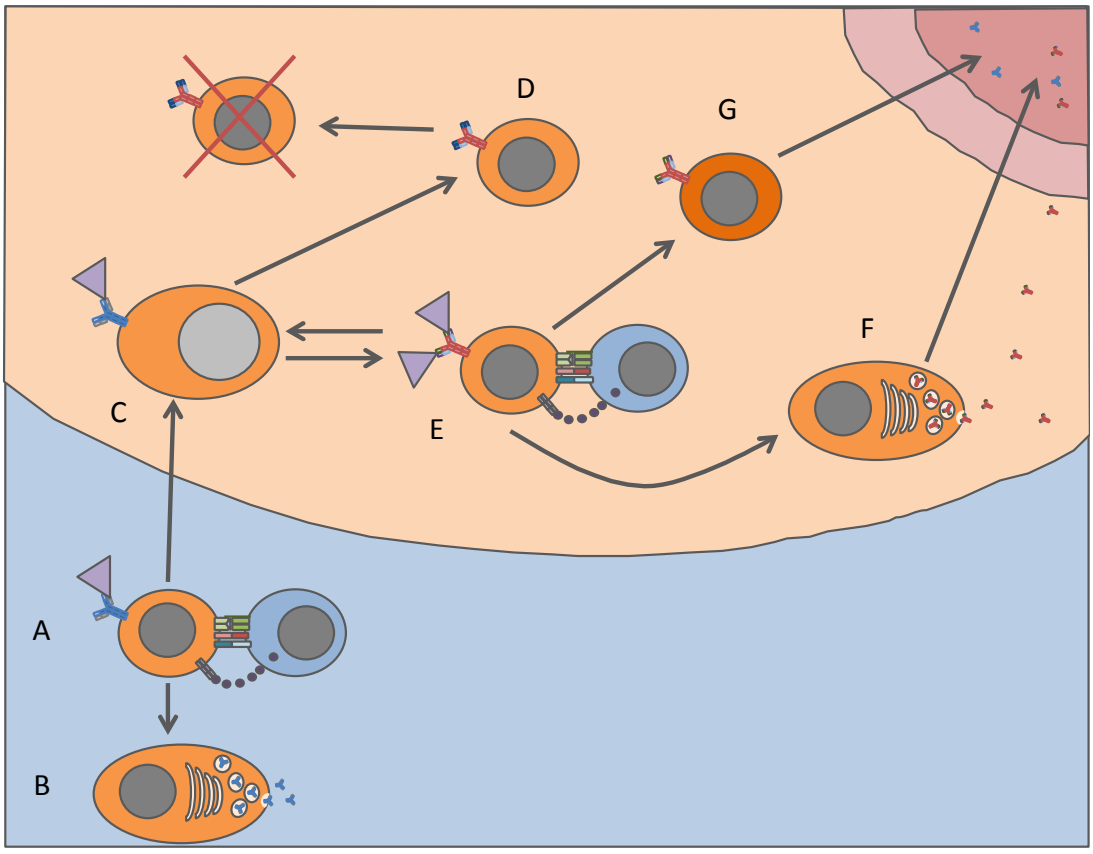

Figure 1.7 The humoral immune response.
A B cells become activated by T cells. **B** Some activated B cells develop into antigen-secreting plasma cells. **C** Activated B cells migrate to the B cell follicle, proliferate and form a germinal centre. SHM and CSR occur. **D** B cells with low-affinity B cell receptors undergo apoptosis. **E** B cells with high-affinity B cell receptors get more T cell help, proliferate and generate plasma (**F**) or memory cells (**G**).

In a first wave of activation, some of the B cells then proliferate in an extrafollicular response and develop into antigen-secreting plasma cells (Figure 1.7 A, B) (MacLennan et al., 2003). The second phase of the response is characterised by the formation of a germinal centre. The activated B cells migrate to the B cell zone and proliferate extensively (Figure 1.7 C). Simultaneously, somatic hypermutation (SHM) of the variable Ig regions and class switch recombination (CSR) occur (Figure 1.7 C, Figure 1.8) (Schmidlin et al., 2009). In both mice and humans, the enzyme activation-induced cytidine deaminase (AID) is required for these processes (Muramatsu et al., 2000; Revy et al., 2000). SHM leads to the stochastical generation of cells expressing immunoglobulins with higher affinity for the antigen (affinity maturation), which are selected for further proliferation and the generation of memory and plasma cells. The selection occurs through competition for T cell help. B cells compete with other B cells and soluble immunoglobulin for a limiting amount of antigen and cells with higher affinity BCRs take up, process and present more antigen and therefore interact with antigen-specific T cells more often (Figure 1.7 D, E) (Allen et al., 2007; Shulman et al., 2014; Y. Zhang et al., 2013).

CSR results in the genomic recombination of the IGH constant region, deleting Cμ and Cδ and replacing it by Cγ, Cε or Cα (Figure 1.8) (Kracker & Durandy, 2011). In this process, transcription of the specific switch region upstream of the C segment plays an important role (Fujieda et al., 1995; Gauchat et al., 1990; Stavnezer-Nordgren & Sirlin, 1986). The activation of promoters upstream of the switch regions is regulated by cytokines and their combination dictates which immunoglobulin class the B cell switches to (Avery et al., 2008; Gascan et al., 1991; Punnonen et al., 1993). Class switching changes the properties of the immunoglobulin. Firstly, signalling properties of IgG and IgE differ from that of IgM (Sato et al., 2007; Wakabayashi et al., 2002). Secondly, effector functions are different. IgA is, for example efficiently exported through mucosal epithelia and it triggers anti-inflammatory responses (Cerutti, 2008). Serum-IgE has a very short half-life of about two days but can be bound to high-affinity FcεRI on mast cells and basophils, which function in the defence of parasites and are mediators of atopic diseases (Moon et al., 2009; Stone et al., 2010). IgG can bind to inhibitory FcγRII, regulating B cell function, or to activating FcγRI and III to trigger macrophage endocytosis, NK cell and neutrophil activation (Anderson et al., 1990; Ravetch & Bolland, 2001; Titus et al., 1987).

The outcome of the germinal centre reaction is the generation of memory and plasma cells, which express high affinity, class-switched immunoglobulins (Figure 1.7 F, G) (Shlomchik & Weisel, 2012). Plasma cells secrete high amounts of these immunoglobulins to mediate the humoral immune response. After elimination of the antigen, apoptosis of the B cells leads to germinal centre contraction (Janeway et al.,

2001). However, long-lived plasma cells can survive in the bone marrow and continuously secrete immunoglobulins (Chu & Berek, 2013) and memory B cells can survive for decades without repeated antigenic stimulation (Yu et al., 2008). Upon repeated encounter with the antigen, a secondary immune response is mediated by these cells. They are rapidly activated and generate plasma cells, which secrete high-affinity immunoglobulin (Good & Tangye, 2007; Liu et al., 1995).

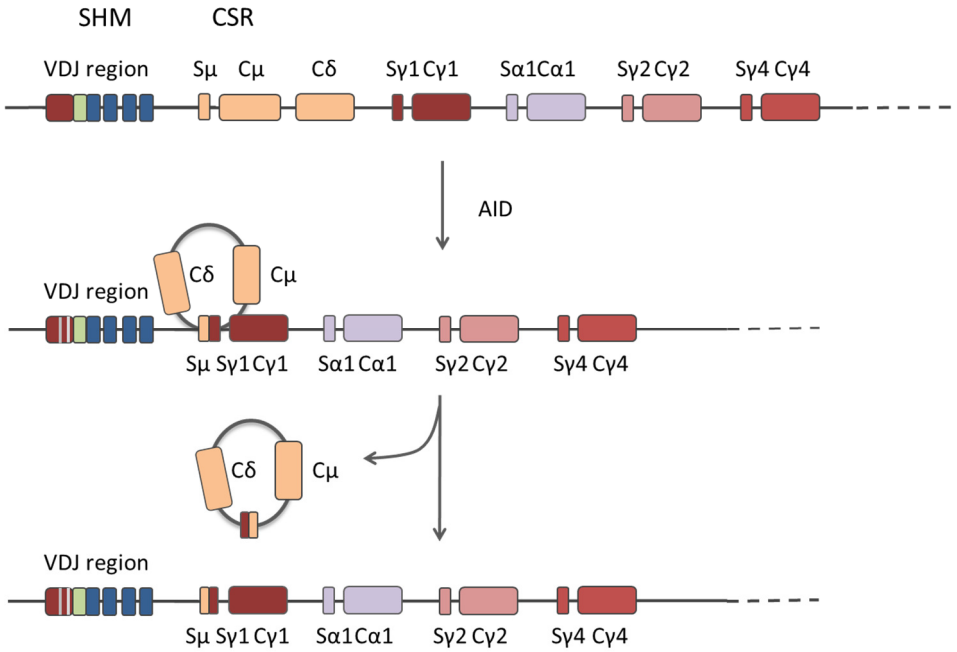

Figure 1.8 Somatic hypermutation and class switch recombination.
Somatic hypermutation and class switch recombination are both mediated by AID. SHM occurs in the VDJ region of the IGH or the VJ region of the IGL chain. CSR leads to the excision of circular DNA and religation of the switch regions (S), joining the variable with a different constant region.

B cell malignancies can arise from different stages of the germinal centre reaction, from memory or plasma cells (Alizadeh et al., 2000; Chiorazzi & Ferrarini, 2011; García-Muñoz et al., 2012). Thus, some malignancies have activated AID and are characterised by on-going somatic hypermutation, which also targets genes other than the immunoglobulin loci and can therefore generate oncogenic mutations to facilitate tumour progression (Pasqualucci et al., 2004; Pérez-Durán et al., 2007; Ramiro et al., 2004). Further, malignant cells can present with class-switched immunoglobulins or retain IgM and IgD expression (Lanasa & Weinberg, 2011; Ruminy et al., 2011). Like their normal counterparts, malignant B cells are often dependent on T cell help via CD40L stimulation for their survival (Ito et al., 2012; Os et al., 2013).

1.2.5 Self-tolerance

In the whole process of B cell development, maturation and activation, self-reactive immunoglobulins can arise. It has been shown that about 75% of the immature B cells in the bone marrow of human subjects react with auto-antigens (Wardemann et al., 2003). Therefore, a strict control system, eliminating those B cells, must be in place. In the bone marrow, autoreactive cells undergo receptor editing (rearrangement of the light chain) and if this fails to ablate autoreactivity, they are removed by apoptosis or become anergic (Goodnow et al., 1988; Melamed & Nemazee, 1997; Nemazee & Bürki, 1989). Both apoptosis and anergy can also be induced in auto-reactive cells in the peripheral lymphoid organs and even in the germinal centre (Chan et al., 2012; Goodnow et al., 1989; Russell et al., 1991). These mechanisms of immune tolerance can often be circumvented by malignant B cells, e.g. via mutations of FAS (Müschen et al., 2002) or deregulation of BCL2 proteins (Del Gaizo Moore et al., 2007), allowing for their uncontrolled proliferation and survival.

Anergic cells are unresponsive to antigenic stimulation, have a low IgM but high IgD surface expression and a reduced life span (Fulcher & Basten, 1994; Yarkoni et al., 2010). About 2.5% of the peripheral B cells in humans show an anergic phenotype and cannnot be stimulated by cross-linking of either IgM or IgD (Duty et al., 2009). However, if these cells are kept *in vitro* in culture medium over night, they recover their ability to be activated (Duty et al., 2009). This is consistent with findings in mice, showing that removal of the antigen reverses anergy (Gauld et al., 2005). In agreement with these findings, continuous occupancy of and signalling via the BCR promote inhibitory downstream effects (Brauweiler et al., 2007; Healy et al., 1997; Merrell et al., 2006; O'Neill et al., 2011). Further, anergic cells can be activated when T cell help is given (Fulcher et al., 1996). Due to the mechanism of antigen presentation to naïve T cells in the thymus, these are usually self-tolerant, so that activation of autoreactive B cells is prohibited (Yarkoni et al., 2010). In conclusion, anergy is generally induced in B cells that are stimulated via the BCR without getting a second signal from T cells. Anergy plays an important role in chronic lymphocytic leukaemia, as these cells are often autoreactive (see section 1.3.1.2). They do, however, avoid apoptosis, which usually follows the induction of anergy, and display an increased life span (Del Gaizo Moore et al., 2007; Souers et al., 2013).

1.2.6 B cell receptor signalling

B cell receptor signalling plays a major role in the survival and proliferation of many mature B cell malignancies and blocking B cell receptor signalling pathways, for example by inhibiting BTK with Ibrutinib, is a promising therapeutic strategy for the treatment of several B cell neoplasms (Niemann & Wiestner, 2013). In different malignancies, different arms of the BCR pathway play predominant roles and different mechanisms for deregulated signalling can be observed (see Section 1.3). While CLL cells display chronically active BCR signalling, often without mutations in the BCR pathway (Burger & Chiorazzi, 2013), DLBCL cells acquire a plethora of mutations that activate BCR signalling (Davis et al., 2010) and Burkitt lymphoma cells are dependent on tonic BCR signalling (Schmitz et al., 2012), which is also constitutively active in normal B cells. Therefore, the current understanding of normal B cell receptor signalling is reviewed in the next section.

1.2.6.1 Activation of upstream BCR signalling pathways

Antigen binding to the BCR results in intracellular signalling events, triggered by crosslinking of the membrane-bound immunoglobulins (Rudich et al., 1988). Depending on the strength and nature of the transmitted signal and the presence or absence of co-stimulatory signals, B cells can be activated, become anergic or even apoptotic (Matsuuchi & Gold, 2001). In resting cells, BCRs associate with both positive (e.g. CD19, CD45) and negative regulatory co-receptors (e.g. CD5, CD22, CD72) (Monroe, 2006).

Signalling is mediated by the clustering of antigen-bound receptors and their relocation to lipid rafts (P.C. Cheng et al., 1999; Sohn et al., 2006). This is believed to exclude negative co-receptors from BCR complexes to allow stable activation of BCR signalling (Monroe, 2006). Upon activation, LYN or other Src-family kinases (SFKs) phosphorylate the CD79a and CD79b immunoreceptor tyrosine-based activation motifs (ITAMs) (Clark et al., 1992; Schmitz et al., 1996; Sohn et al., 2006). To be activated and recruited to the receptor, LYN has to be dephosphorylated at a C terminal tyrosine by the phosphatase of the co-receptor CD45 (Pao & Cambier, 1997). CD79 phosphorylation leads to the recruitment of the spleen tyrosine kinase (SYK) via its tandem SH2 domains, which changes its conformation and allows for autophosphorylation and activation (Rowley et al., 1995). In a positive feedback loop, SYK then amplifies ITAM phosphorylation (Rolli et al., 2002) (Figure 1.9). It was even proposed that LYN is only capable of phosphorylating one of the ITAM tyrosine residues, resulting in low-affinity SYK recruitment, which then phosphorylates the

second tyrosine residue to stimulate its own full activation (Rolli et al., 2002). Monroe hypothesised that this can only happen after full activation of the BCR when the receptors are clustered in lipid rafts, as SYK would only then be recruited sufficiently (Monroe, 2006).

Non-ITAM tyrosine phosphorylation of CD79a Y204 leads to the recruitment of B cell linker protein (BLNK) via its SH2 domain (Engels et al., 2001; Kabak et al., 2002). This allows SYK to phosphorylate this adapter protein, which facilitates recruitment of downstream effectors, like growth factor receptor-bound protein 2 (GRB2) with son of sevenless (SOS), the VAV gauanine nucleotide exchange factors, Bruton's tyrosine kinase (BTK) and phospholipase C γ (PLCγ) via their SH2 domains (Fu et al., 1998; Ishiai et al., 1999) (Figure 1.9). Interestingly, GRB2 associates with BLNK in resting cells via its SH3 domain and interaction is increased upon BLNK phosphorylation through additional SH2 domain binding. However, only activation of the BCR leads to localisation of BLNK/GRB2-SOS to the membrane, bringing them into close proximity to their target rat sarcoma (RAS) (Fu et al., 1998).

Binding of BTK to BLNK is required for Y551 phosphorylation by SYK, which leads to its activation (Baba et al., 2001). BTK can then phosphorylate and activate PLCγ, which is necessary for most downstream signalling events (Rodriguez et al., 2001). BTK and PLCγ also have pleckstrin homology (PH) domains, which interact with phosphatidylinositol-3,4,5-trisphosphate (PIP_3) generated by phosphatidylinositol-3 kinase (PI3K). This integrates PI3K signalling into the pathway and serves to enhance and prolong membrane localisation and activation of BTK and PLCγ (Kurosaki et al., 2000) (Figure 1.9).

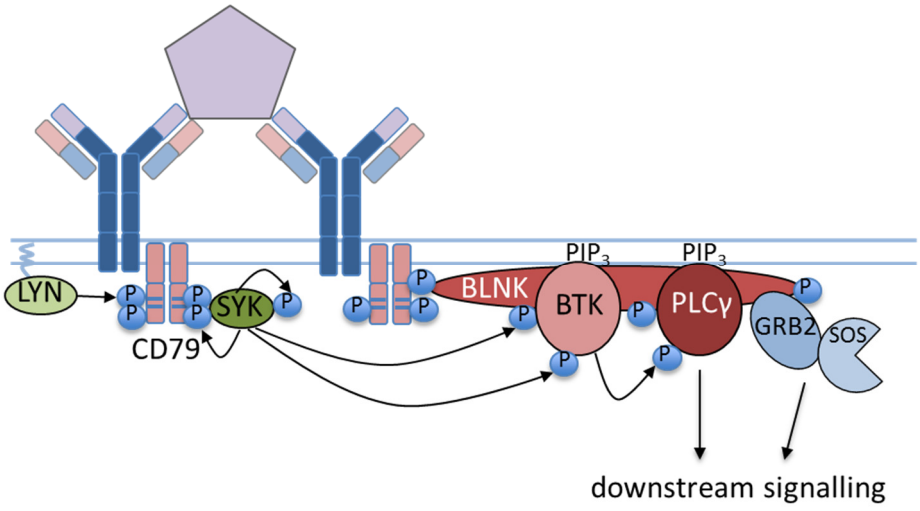

Figure 1.9 Activation of the upstream BCR signalling cascade.
Phosphorylation of CD79 leads to recruitment of SYK and BLNK, which is phosphorylated by SYK to allow for BTK, PLCγ and GRB2 recruitment. SYK reinforces CD79 phosphorylation and phosphorylates and activates BTK, which then activates PLCγ.

1.2.6.2 Calcium signalling

PLCγ catalyses the hydrolysis of phosphatidylinotisol-4,5-bisphosphate to the second messengers inositol-1,4,5-trisphosphate (IP_3) and diacylglycerol (DAG). IP_3 binds to receptors on the ER and stimulates Ca^{2+} release (Kurosaki et al., 2000). Elevated intracellular Ca^{2+} activates CaMKII (Valentine et al., 1995) and the phosphatase Calcineurin, which targets NFAT. NFAT dephoshorylation results in its nuclear translocation and activation of target gene transcription (Choi et al., 1994; Venkataraman et al., 1994) (Figure 1.10).

Further, both Ca^{2+} and DAG activate different PKC isoforms. PKCs can be divided into classical (α, β, γ), novel (δ, ε, η, θ) and atypical (ζ, λ, τ), depending on their structure and regulation. Classical PKCs are regulated by both Ca^{2+} and DAG, novel PKCs are regulated by DAG only and atypical PKCs are regulated by neither of the two (Guo et al., 2004). In B cells, different PKC isoforms have been shown to be activated downstream of the BCR: PKCβ, PKCδ, PKCε and PKCζ (Barbazuk & Gold, 1999; Leitges et al., 1996; Martin et al., 2002; Pracht et al., 2007; Ting et al., 2002). PKCη seems to play a role in pre-BCR signalling (Oda et al., 2008) and the PKC-related proteins PKCμ and PKCv can also be activated upon BCR stimulation (Matthews et al., 2003; Sidorenko et al., 1996).

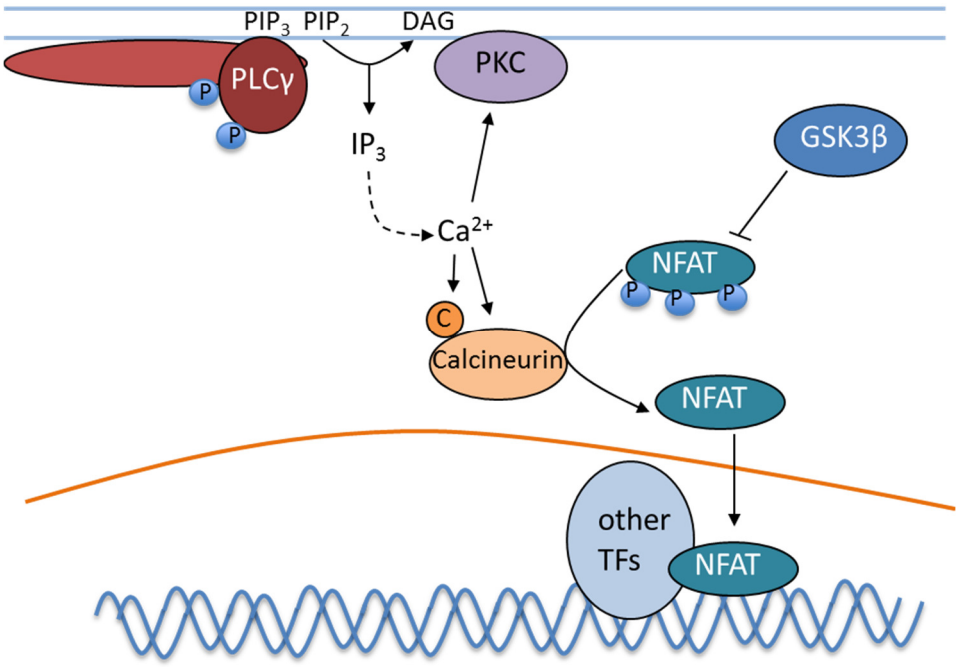

Figure 1.10 Activation of Ca^{2+}-dependent pathways.
PLCγ stimulates Ca^{2+}-dependent signalling pathways through the production of IP_3. Ca^{2+} activates Calcineurin and thus NFAT, which stimulates transcription. Ca^{2+} and DAG activate classical PKCs and trigger downstream BCR signalling.

PKCδ has been shown to play both positive and negative roles in BCR signalling. It is required for activation of cAMP response element-binding protein (CREB), which in turn is important for B cell proliferation and survival (Blois et al., 2004; Zhang et al., 2002). On the other hand, PKCδ knockout mice show enhanced production of autoreactive B cells and PKCδ loss-of-function causes B cell autoimmunity in humans (Belot et al., 2013; Kuehn et al., 2013; Mecklenbräuker et al., 2002; Miyamoto et al., 2002; Salzer et al., 2013). These effects are due to a function of PKCδ in both negative selection of immature B cells and negative regulation of BCR signalling in mature B cells. Consistently, PKCδ knockout mice show enhanced phosphorylation of CD79a and SYK upon BCR cross-linking (Limnander et al., 2014).

1.2.6.3 Activation of NFκB

At least in mice, PKCβ has essential and non-redundant functions during BCR signalling. PKCβ knockout mice show a phenotype which is comparable to BTK-deficiency: a reduction in mature B cells, a reduced response to T cell-independent antigens and no proliferative response to BCR stimulation (Leitges et al., 1996). In both primary B cells from mouse and human B cell lines, PKCβ has been shown to activate the inhibitor of nuclear factor κB (NFκB) kinase (IKK), and thus NFκB, through activation of the adapter protein caspase recruitment domain (CARD)-containing and membrane-associated guanylate kinase (MAGUK) protein (CARMA1). PKCβ phosphorylates the CARMA1 linker domain, relieving its autoinhibition and facilitating the interaction with the BCL10 CARD domain (Sommer et al., 2005). BCL10 forms a complex with mucosa-associated lymphoid tissue lymphoma translocation gene 1 (MALT1) and the E2 complex UBC13-MMS2 (Zhou et al., 2004) (Figure 1.11). The active complex contains BCL10-MALT1 oligomers (Sun et al., 2004). In T cells, both the E3 ligases mind bomb 2 (MIB2) and tumour necrosis factor (TNF) receptor-associated factor 6 (TRAF6) have been described to associate with the complex to mediate autoubiquitination and ubiquitination of target proteins (Stempin et al., 2011; Sun et al., 2004). PKCδ has been shown to inhibit CARMA1 function in a kinase-independent fashion by blocking its association with MALT1 and TRAF6 (Liu et al., 2012).

Ubiquitination of MALT1 and BCL10 have been shown to mediate interaction with the NFκB essential modulator (NEMO), the IKK inhibitory subunit (Oeckinghaus et al., 2007; Wu & Ashwell, 2008) (Figure 1.11). Then, NEMO is ubiquitinated by K63-linked ubiquitin chains, which does not lead to its degradation but is essential for sustained NFκB activation (Zhou et al., 2004). Further, autoubiquitination of the E3 ligase generates a binding site for the TGF-beta activated kinase 1 (TAK1) binding proteins 2

and 3 (TAB2/3) which form a complex with TAK1 (Kanayama et al., 2004). TAK1 is activated by autophosphorylation and can then phosphorylate and activate IKKβ (Stempin et al., 2011; Sun et al., 2004) (Figure 1.11).

Active IKKβ contributes to CARMA1 activation in a feedforward loop by phosphorylating the linker domain (Shinohara et al., 2007). Further, IKK now phosphorylates IκBα, targeting it for ubiquitination and degradation (Chen et al., 1996; Traenckner et al., 1995). NFκB can then translocate into the nucleus and activate target gene transcription (Figure 1.11), including genes encoding caspase inhibitors, like the cellular inhibitors of apoptosis (IAPs) and FLICE-like inhibitory protein (FLIP), the antiapoptotic proteins BCL2 and BCL-XL, proteins that drive proliferation, like cyclin D1/D2 and MYC, as well as cytokines like TNF, IL1, IL2, IL6, and the immunmodulators inducible nitric oxide synthase (iNOS) and cyclooxygenase 2 (COX2) (Stoffel, 2005; Tracey et al., 2005).

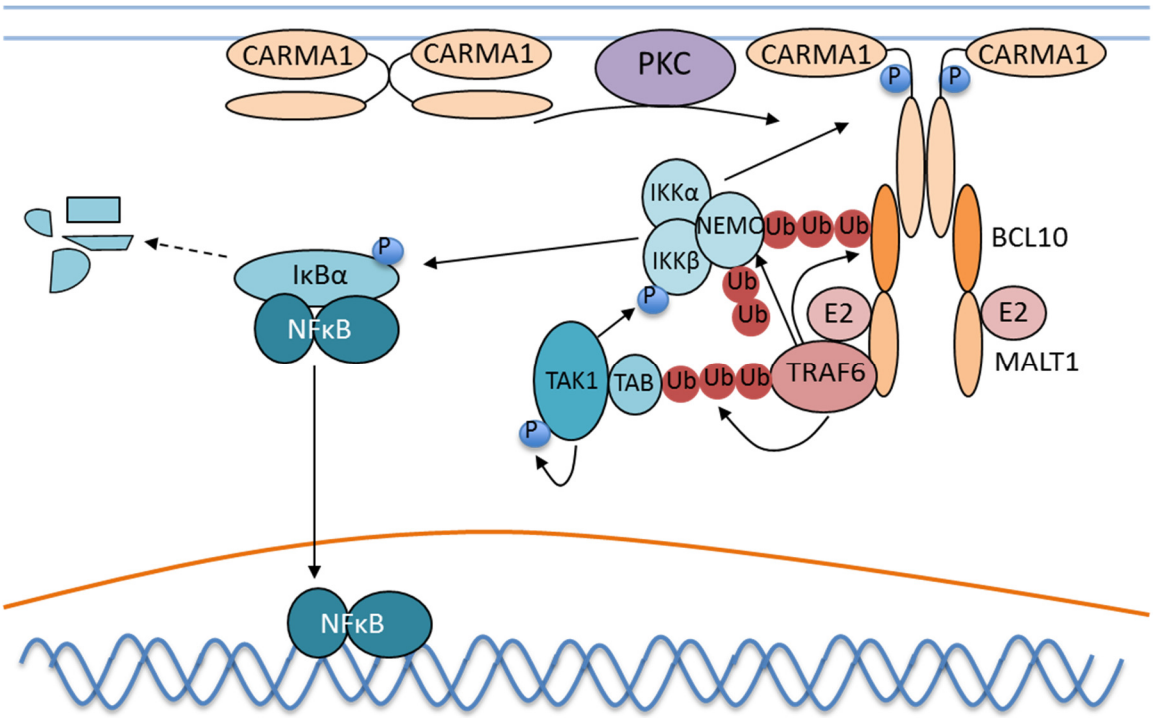

Figure 1.11 Activation of the NFκB pathway.
Activation of the NFκB transcription factor is mediated via PKC-dependent activation of CARMA1, which associates with BCL10, MALT1 and ubiquitin ligases to facilitate recruitment and activation of the IKK complex. The active IKK phosphorylates IκBα and leads to its degradation, allowing for nuclear translocation of NFκB.

1.2.6.4 Activation of the RAS/RAF/MEK/ERK pathway

Activation of the PLCγ-PKC pathway is also important for the activation of the RAS/RAF/MEK/ERK pathway. This pathway generally regulates cell adhesion and migration, cell cycle progression, cell survival and proliferation but also differentiation (Roskoski Jr., 2012). In B cells, ERK stimulates pre-B cell expansion, but is also required for their cell cycle exit and IGK rearrangement (Mandal et al., 2009; Yasuda et al., 2008). Further, ERK activity is required for the transition of immature to mature B cells and for the BCR-induced proliferation of mature B cells (Richards et al., 2001; Rowland et al., 2010; Teodorovic et al., 2014).

The activity of the guanosine triphosphatase (GTPase) RAS is regulated by binding of GTP (active) and GDP (inactive). Guanine nucleotide exchange factors (GEFs), like SOS and RAS guanine nucleotide releasing proteins (RASGRPs) stimulate exchange of GDP for GTP, whereas GTPase-activating proteins (GAPs) stimulate the RAS intrinsic GTPase. RAS-GTP activates the RAF/MEK/ERK pathway (Campbell et al., 1998). Surprisingly, GRB2-SOS recruitment to BLNK is not sufficient for RAS activation, whereas a different pathway using RASGRP3 is essential (Coughlin et al., 2005; Oh-hora et al., 2003; Roose et al., 2007). RASGRP3 is recruited to the plasma membrane by the PLCγ substrate DAG via its C1 domain (Oh-hora et al., 2003). It is then activated by T133 phosphorylation, possibly directly mediated by PKC (Zheng et al., 2005). In a positive feed forward loop, RAS-GTP allosterically activates SOS, which can then contribute to RAS activation and both RASGRPs and SOS are required for full and sustained activation of the RAF/MEK/ERK pathway (Roose et al., 2007) (Figure 1.12).

RAS-GTP recruits RAF kinases to the membrane, where they can be activated through phosphorylation and dephosphorylation events (Wellbrock et al., 2004). Both RAF1 and BRAF are expressed in B cells and both kinases are required for full activation of immediate early gene expression, while only BRAF is essential for sustained activation of ERK (Brummer et al., 2002). RAF phosphorylates two serine residues in MEK1 and MEK2 and activates them. MEKs can then phosphorylate ERK1/2 on threonine and tyrosine residues (Wellbrock et al., 2004) (Figure 1.12).

Activated ERKs phosphorylate nuclear and cytosolic substrates. In the cytosol ERKs mainly phosphorylate other kinases, like ribosomal S6 kinases (RSK1-4), mitogen and stress-activated protein kinases (MSK1/2) and MAP kinase-interacting kinases (MNK1/2) (Roskoski Jr., 2012). RSKs and MSKs phosphorylate and activate or stabilise the transcription factors CREB and FOS, respectively. (Chen et al., 1993; Deak et al., 1998; Pierrat et al., 1998). Further, RSKs have been shown to phosphorylate and inactivate glycogen synthase kinase 3β (GSK3β) (Figure 1.12),

thereby inhibiting its repressive phosphorylation of a plethora of substrates, like NFAT, JUN, cyclin D1 and the translation initiation factor eIF2B (Diehl et al., 1998; Neal & Clipstone, 2001; Nikolakaki et al., 1993; Sutherland et al., 1993; Welsh & Proud, 1993). They also promote cap-dependent translation via phosphorylation of the ribosomal protein S6 and the translation initiation factor eIF4B, which is a cofactor for the eIF4A RNA helicase (Lawson et al., 1989; Roux et al., 2007; Shahbazian et al., 2006). Moreover, RSKs can inhibit apoptosis by phosphorylating and inhibiting BCL2-associated agonist of cell death (BAD) at S112 and death-associated protein kinase (DAPK1) (Anjum et al., 2005; Bonni et al., 1999; Shimamura et al., 2000). Additionally, RSK2 and MSK1/2 are capable of phosphorylating histone H3 at serine 10 and serine 28 to regulate transcription (He et al., 2003; Sassone-Corsi et al., 1999; Soloaga et al., 2003).

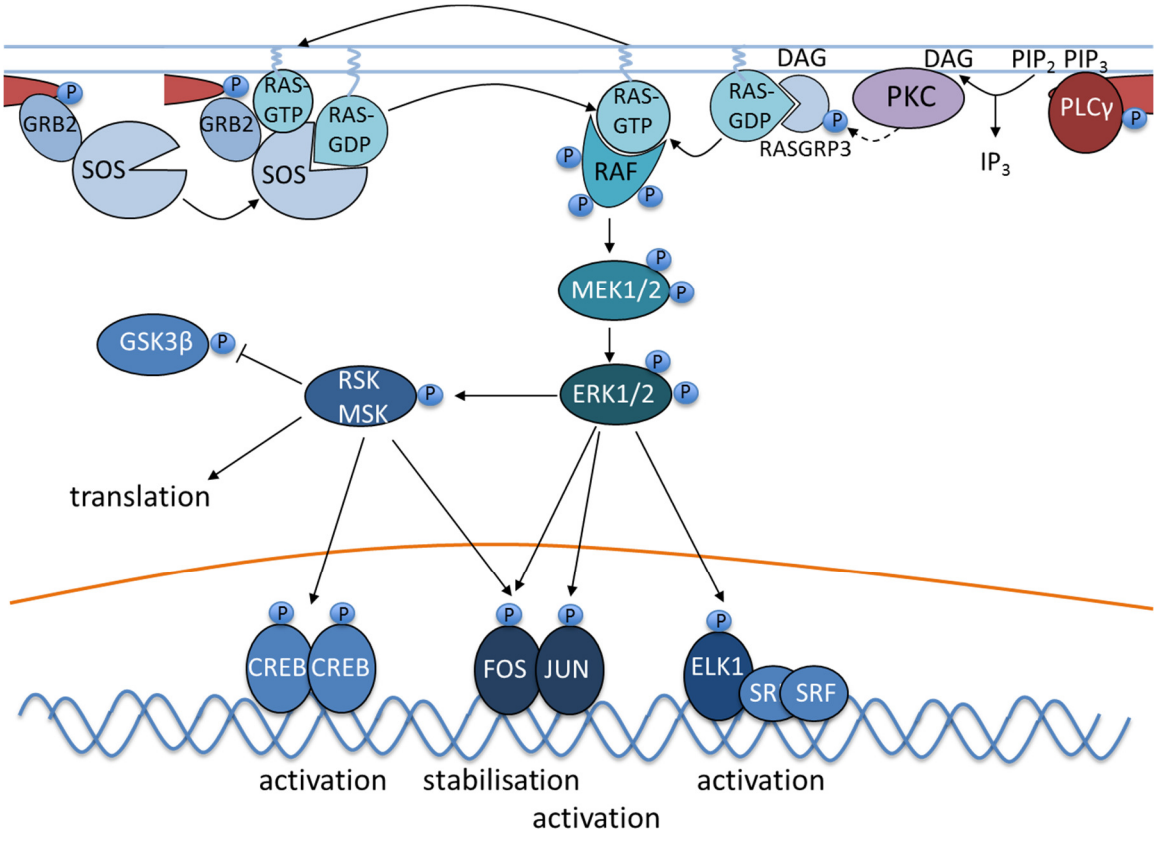

Figure 1.12 Stimulation of the RAS/RAF/MEK/ERK pathway.
Activation of the RAS/RAF/MEK/ERK pathway is predominantly mediated via RASGRP3, while SOS is subsequently activated by RAS-GTP. RAS activates RAF, which phosphorylates MEK1/2, which in turn activates ERK1/2. ERK targets RSKs and MSKs and activates transcription factors. RSKs and MSK stimulate cap-dependent translation and gene expression.

ERK1/2 can also directly phosphorylate anti-apoptotic proteins, like BCL2-interacting mediator of cell death (BIM_{EL}) (Ley et al., 2004; Luciano et al., 2003; Marani et al., 2004). Further, transcription factors of the ETS family, ELK1, ELK3 and ELK4 as well as ETS1 and ETS2 can be phosphorylated and activated by ERK1/2, which leads to the expression of immediate early genes, like *FOS*, *MYC* and *EGR1* (Ducret et al., 2000; Gille et al., 1992; Janknecht et al., 1995; Marais et al., 1993; Paumelle et al., 2002; Seidel & Graves, 2002; Yang et al., 1996; Yang et al., 1998). In addition, the activator protein 1 (AP1) transcription factors FOS and JUN can be phosphorylated by ERK1/2 and RSKs, which leads to their stabilisation or activation, respectively (Morton et al., 2003; Okazaki & Sagata, 1995) (Figure 1.12). MYC is also phosphorylated and stabilised through RAS-dependent phosphorylation, which is most likely directly mediated by ERKs (Murphy et al., 2004; Sears et al., 2000).

1.2.6.5 Activation of the PI3K/AKT pathway

Class IA PI3Ks (α, β and δ) consist of a catalytical p110 and one of five regulatory p85-family subunits, which are SH2 domain-containing adapter proteins (Limon & Fruman, 2010; Okkenhaug et al., 2007). The p85 proteins normally block p110 activity via inhibitory interactions of their SH2 domains with the p110 subunit, which are relieved when the SH2 domains bind phospho-tyrosine, leading to PI3K activation (Burke et al., 2011; X. Zhang et al., 2011).

PI3Kδ is highly expressed in B cells and plays the dominant role in BCR signalling (Bilancio et al., 2006; Clayton et al., 2002; Jou et al., 2002; Okkenhaug et al., 2002). p85 can directly bind to two phosphorylated YXXM motifs in the CD19 intracellular domain (Tuveson et al., 1993) and this binding is essential for normal B cell activation (Y. Wang et al., 2002). The phosphorylation of CD19 Y513 is directly mediated by LYN (Fujimoto et al., 2000; van Noesel et al., 1993; Roifman & Ke, 1993), but apart from Y513, Y482 phosphorylation by an as yet unknown kinase is essential for PI3K recruitment and activation (Ishiura et al., 2010) (Figure 1.13).

As mice lacking p85α have a much more severe phenotype than CD19 knockout mice, additional pathways must be in place that activate PI3K (Engel et al., 1995; Fruman et al., 1999). Indeed, PI3K can also bind to the B cell adaptor for PI3K (BCAP) (Okada et al., 2000), which is recruited to CD79a by the adaptor NCK. NCK binds the non-ITAM Y204p, which is phosphorylated in a LYN-dependent manner (Castello et al., 2013). BCAP carries proline-rich regions and is recruited by the NCK SH3 domains (Castello et al., 2013). BCAP phosphorylation by SYK and BTK generates binding sites for the p85 subunit of PI3K (Okada et al., 2000) (Figure 1.13). Knockout of both BCAP and

CD19 leads to an almost complete inhibition of PI3K activation upon CD79b cross-linking, suggesting that these two pathways are sufficient for PI3K activation (Aiba et al., 2008).

However, PI3K can also be activated via the GEF VAV. VAV1/2/3 are recruited to both CD19 and BLNK via their SH2 domains (Fu et al., 1998; O'Rourke et al., 1998), are activated through tyrosine phosphorylation by SYK or LYN (Deckert et al., 1996; Fujimoto et al., 2000) and function as RHO and RAC GEFs (Crespo et al., 1997; Movilla & Bustelo, 1999; Schuebel et al., 1998). RHO and RAC GTPases regulate cytoskeletal reorganisation and VAV has been shown to be essential for BCR internalisation (Malhotra et al., 2009). Further, RAC1-GTP directly binds to and stimulates PI3K (Inabe et al., 2002; Murga et al., 2002; Reynolds et al., 2002) (Figure 1.13).

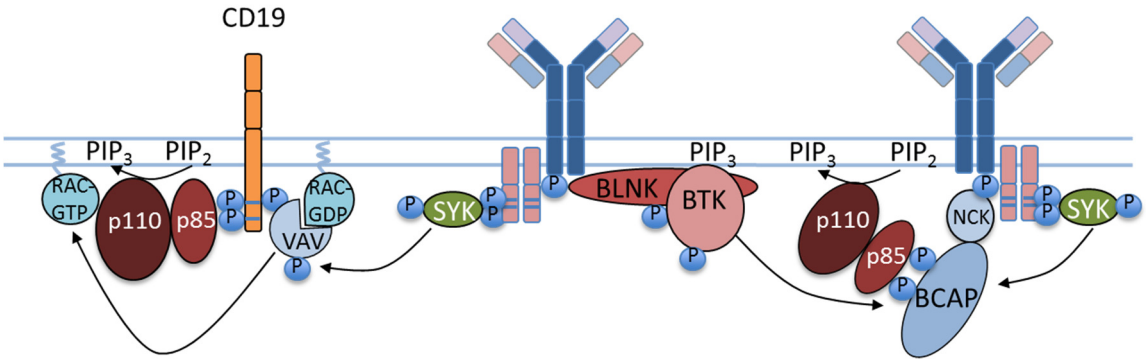

Figure 1.13 Activation of PI3K.
Activation of PI3K is mediated by different mechanisms. CD19 directly recruits and activates PI3K. Additionally, the NCK-BCAP complex, which associates with CD79, can be phosphorylated by BTK and mediate PI3K recruitment and activation. Additionally, RAC-GTP, induced by VAV, can interact with and activate PI3K.

After activation, PI3K phosphorylates PI-4,5-P_2 to generate PI-3,4,5-P_3, which serves as a docking molecule for pleckstrin homology (PH) domain-containing proteins, like BTK and PLCγ (Figure 1.13). This increases membrane recruitment and prolongs signalling via these pathways (Fruman & Limon, 2012). The best characterised PI3K signal transduction pathway leads to the activation of protein kinase B (PKB/AKT). AKT has a PH domain and binding to PIP_3 results in a conformational change, which is necessary for AKT activation by the downstream kinase PDK1 (Milburn et al., 2003). PDK1 is also recruited to PIP_3 and this recruitment is necessary for its activity towards AKT (Alessi et al., 1997; McManus et al., 2004; Stokoe et al., 1997). PDK1 phosphorylates AKT at a threonine in the activation loop (Alessi et al., 1997; Stokoe et al., 1997). A second residue in the C-terminal hydrophobic domain is phosphorylated mainly by mammalian target of rapamycin complex 2 (mTORC2), which is also directly

regulated by PIP_3 (Gan et al., 2011; Sarbassov et al., 2005) (Figure 1.14). Although this phosphorylation does not activate AKT, it increases PDK1-dependent phosphorylation. Therefore, phosphorylation of the hydrophobic domain likely precedes activation of AKT by PDK1 under physiological conditions (Scheid et al., 2002).

AKT suppresses apoptosis by targeting BAD-S136 (Datta et al., 1997) and forkhead box O (FOXO) transcription factors. AKT-mediated phosphorylation of FOXOs in the nuclear localisation sequence (NLS) leads to their nuclear export (Figure 1.14). FOXO transcription factors stimulate the expression of genes encoding for pro-apoptotic proteins, like BIM and FAS ligand (FASL), and negative cell cycle regulators, like $p21^{CIP1}$, $p27^{KIP1}$ and cyclin G2, but also genes that protect cells from environmental stress, like the DNA repair factor growth arrest and DNA damage 45 (GADD45), superoxide dismutase (MnSOD) and catalase (Greer & Brunet, 2005). Conversely, FOXO1 is also required for the expression of genes that are essential for B cell function, like RAG1, RAG2 and AID (Dengler et al., 2008). Consistently, AKT activation leads to suppression of CSR (Omori et al., 2006).

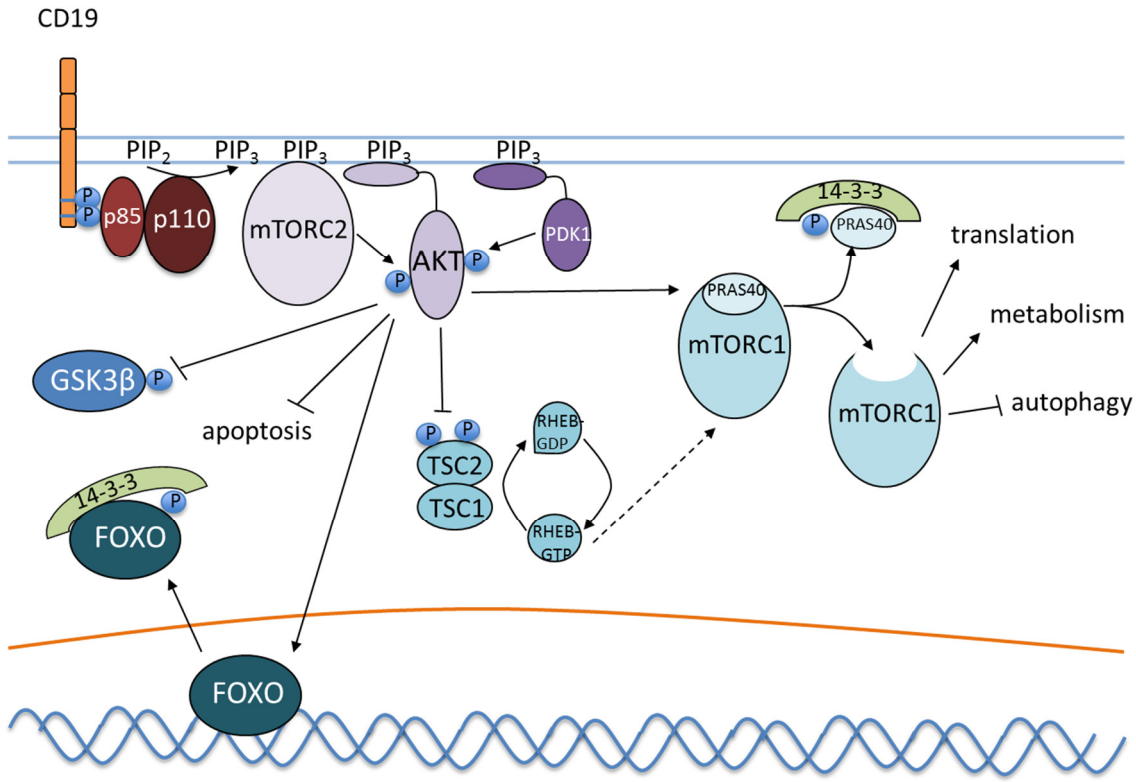

Figure 1.14 The PI3K/AKT pathway.
The production of PIP_3 leads to the activation of PDK1, mTORC2 and subsequently AKT. AKT inhibits apoptosis and stimulates cell proliferation through inhibition of GSK3β and FOXO transcription factors and the activation of mTORC1 by inhibiting the TSC complex and phosphorylating PRAS40. mTORC1 enhances cap-dependent translation and anabolic processes.

AKT also stimulates cell survival and proliferation by phosphorylating and inhibiting GSK3β (van Weeren et al., 1998) and by activating mTORC1. AKT can phosphorylate and inactivate the GAP tuberous sclerosis complex (TSC1/2), thus increasing GTP-bound RAS homolog enriched in brain (RHEB-GTP) in the cell (Dan et al., 2002; Inoki et al., 2002; Inoki et al., 2003; Manning et al., 2002; Potter et al., 2002; Tee et al., 2003). RHEB-GTP stimulates mTORC1 activity by a yet unknown mechanism (Wang & Proud, 2011). AKT also directly phosphorylates the inhibitory proline-rich AKT substrate of 40 kDa (PRAS40) subunit of mTORC1, leading to its dissociation and binding to 14-3-3 proteins (Kovacina et al., 2003; Sancak et al., 2007; Vander Haar et al., 2007) (Figure 1.14). This step is crucial for the activation of mTORC1 (Vander Haar et al., 2007).

Among others, mTORC1 regulates mRNA translation and protein synthesis through the phosphorylation of eukaryotic translation initiation factor 4E binding protein 1 (4EBP1) and ribosomal S6 kinases (S6K1/2), thereby leading to cell growth and cell cycle progression (Hay & Sonenberg, 2004; Laplante & Sabatini, 2012). Further, mTORC1 inhibits autophagy and stimulates lipid and glucose metabolism (Düvel et al., 2010; Kim et al., 2011). Particular functions for mTORC1 in B cells have not been studied in detail, but knockout of mTOR in murine B cells leads to reduced formation of germinal centres and impaired CSR because of a decrease in AID due to increased AKT activity (S. Zhang et al., 2013). Conversely, deletion of TSC1, which leads to a hyperactive mTORC1, also impairs germinal centre formation and response to T cell-dependent antigens (Benhamron & Tirosh, 2011).

1.2.6.6 Negative regulators of BCR signalling

Negative coreceptors for the BCR are FcγRIIB, Fc receptor-like (FCRL2-5), CD22, sialic acid-binding Ig-like lectin 10 (SIGLEC10), platelet/endothelial cell adhesion molecule 1 (PECAM1), leukocyte immunoglobulin-like receptor, subfamily B (LILRB1/2), leukocyte-associated Ig-like receptor 1 (LAIR1), programmed cell death 1 (PD1) and CD72 (Tsubata, 2012; Verbrugge et al., 2006). The negative coreceptors CD22 and SIGLEC10 recognise sialic acid residues, which are abundant on mammalian but not bacterial cells, possibly dampening B cell responses particularly towards self-antigens (Lanoue et al., 2002; Tsubata, 2012). FcγRIIB binds the Fc portion of IgG, thus negatively regulating B cell responses when circulating IgG levels are already high (Heyman, 2003). CD72 binds CD100, which is expressed on T cells, activated B cells and activated antigen-presenting cells. Ligand binding to CD72 inhibits its activity, therefore enhancing antigen response by B cells (Kumanogoh et al.,

2000). Generally, most of these inhibitory co-receptors recruit phosphatases, the main negative regulators of BCR signalling.

Immunoreceptor tyrosine-based inhibitory motifs (ITIMs) in negative coreceptors, like CD22, FcγRIIB and PECAM1 have been shown to be targeted by LYN (Nishizumi et al., 1998; Tourdot et al., 2013). Their phosphorylation leads to the recruitment of SH2 domain-containing phosphotyrosine phosphatases (SHP1, SHP2) or SH2 domain-containing inositol polyphosphate-5-phosphatase (SHIP) (Doody et al., 1995; Okazaki et al., 2001; Ono et al., 1996; Tridandapani et al., 1997) (Figure 1.15). SHIP can also bind to monophosphorylated CD79 in anergic B cells, where it is constitutively active and required for their phenotype (O'Neill et al., 2011). Further, SHIP is recruited by the adapter docking protein 3 (DOK3), which is constitutively localised to the plasma membrane via its PH domain and is phosphorylated by LYN upon BCR stimulation (Lemay et al., 2000). SHIP targets PIP_3, thereby inactivating the PI3K pathway and limiting activation of BTK and PLCγ (Damen et al., 1996; Nitschke, 2005). Possible SHP1/2 targets include CD79, SYK, BTK and BLNK (Adachi et al., 2001; Huang et al., 2003; Jang et al., 2014; Maeda et al., 1999; Mizuno et al., 2000; Okazaki et al., 2001) (Figure 1.15). SHP1 has also been shown to target VAV1 (Stebbins et al., 2003) and actin, leading to actin depolymerisation (Baba et al., 2003).

FcγRIIB can also activate phosphatase and tensin homolog (PTEN), an inositol polyphosphate-3-phosphatase that targets PI-3,4-P_2 and PIP_3, thereby regulating the PI3K-AKT pathway (Brown et al., 2004) (Figure 1.15). Generally, inactive PTEN is intramolecularly folded, which inhibits its membrane localisation and activity. Releasing this autoinhibition by different mechanisms activates the enzyme. This can be facilitated by enhanced membrane recruitment after phosphorylation and SUMOylation or by protein-protein interactions (J. Huang et al., 2012; Shi et al., 2012; Song et al., 2012). On the other hand, phosphorylation, acetylation and oxidation can inhibit PTEN and ubiquitination targets it for degradation (Shi et al., 2012; Song et al., 2012).

Adapter proteins can mediate phosphatase-independent inhibitory effects. DOK1 binds RASGAP and inhibits the ERK pathway (Tamir et al., 2000; Yamanashi et al., 2000) (Figure 1.15). It was first proposed that SHIP is required to recruit DOK1 to the plasma membrane (Tamir et al., 2000), but a subsequent study found that SHIP is not required for DOK1 recruitment (Phee et al., 2001). Consistently, in T cells and fibroblasts, the PH domains of DOK1 and DOK2 bind PI-5-P, PI-3,4-P_2, PI-4,5-P_2 and PI-3,4,5-P_3 and this is necessary for their membrane recruitment and function as repressors of signalling (Guittard et al., 2009; Zhao et al., 2001). DOK3 does not bind RASGAP, but associates with GRB2, which is required to attenuate SYK activation and Ca^{2+} flux (Lösing et al., 2013; Stork et al., 2007) (Figure 1.15).

Further, kinases function as negative regulators of BCR signalling. Some of the negative coreceptors recruit the C-terminal SRC kinase (CSK), which negatively regulates SFKs (Okada, 2012; Sayós et al., 2004; Verbrugge et al., 2006) and PKCβ is involved in a negative feedback loop by phosphorylating an inhibitory serine residue of BTK (Figure 1.15). Consistently, PKCβ inhibition results in an increased Ca^{2+} signal upon BCR cross-linking (Kang et al., 2001).

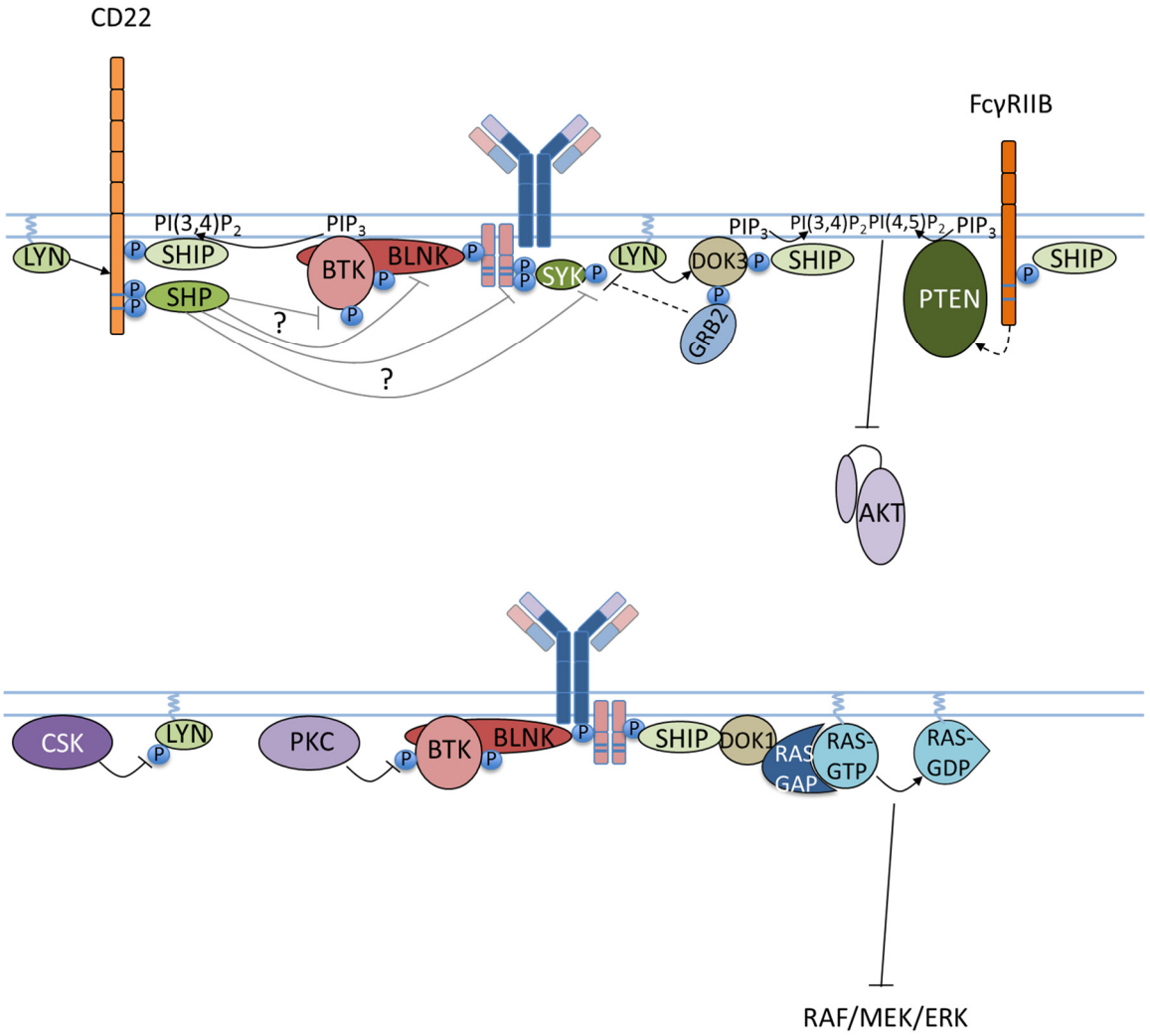

Figure 1.15 Inhibitory BCR signalling.
Negative regulation of B cell receptor signalling is mediated by inhibitory co-receptors and membrane-associated adapter proteins (DOKs). LYN-mediated phosphorylation of negative co-receptors leads to the recruitment of SHIP, which targets PIP_3, and SHP, which inhibits BTK, BLNK, CD79 and SYK. FcγRII activation stimulates PTEN, which inhibits the AKT pathway. DOK3 recruits GRB2, which attenuates SYK-signalling, DOK1 inhibits activation of RAS. CSK phosphorylates and inhibits LYN, while PKCβ negatively regulates BTK.

1.3 B cell malignancies

As mentioned earlier, malignant B cells can arise from different stages of the differentiation and maturation process. The World Health Organisation (WHO) classifies B cell malignancies into precursor and mature B cell neoplasms. Among others, mature B cell neoplasms include non-Hodgkin lymphomas (NHLs), like chronic lymphocytic leukaemia (CLL)/small lymphocytic lymphoma (SLL), marginal zone lymphomas, follicular lymphoma, mantle cell lymphoma, diffuse large B cell lymphoma (DLBCL) and Burkitt lymphoma (BL), Hodgkin lymphoma and plasma cell malignancies (myeloma, plasmacytoma) (Jaffe, 2009; Shankland et al., 2012). Of note, CLL and SLL are essentially the same disease at different stages. CLL shows peripheral blood involvement, while SLL is mainly restricted to tissue sites. Therefore, the WHO classifies CLL as an NHL (Harris et al., 1999).

In this study, the NHLs CLL, DLBCL and BL were of special interest. NHL is the fifth most common cancer in the UK and about 90% of the cases derive from B cells, the remaining 10% are T or NK cell malignancies (Shankland et al., 2012). While most NHLs are indolent diseases, DLBCL and BL are classified as aggressive lymphomas.

1.3.1 Chronic lymphocytic leukaemia (CLL)

CLL is the most common leukaemia in the Western world. Patients are diagnosed at a median age of over 70 years and about two thirds of patients are male (Catovsky et al., 1989; Shankland et al., 2012; Zhang & Kipps, 2014). Patients present with a clonal expansion of $CD5^+$ B cells in the blood and lymphoid tissues. CLL is a heterogeneous disease and can be divided into two subgroups, depending on whether the BCR is mutated (M-CLL) or unmutated (UM-CLL). The BCR is classified as unmutated when the V_H region is at least 98% identical to germ line. UM-CLL has a poor prognosis, whereas M-CLL patients have a much longer overall survival (Hamblin et al., 1999).

1.3.1.1 B cell receptor signalling in disease pathogenesis

Generally, CLL cells use stereotyped BCRs. V_H1, several V_H3 and some V_H4 alleles, usually combined with a restricted set of D and J segments, are significantly overrepresented in CLL cells compared to normal $CD5^+$ B cells (Fais et al., 1998; Messmer et al., 2004; Murray et al., 2008; Tobin et al., 2004; Widhopf II et al., 2004). The heavy chain complementarity-determining region 3 (HCDR3), which is formed by part of the V, all of the D and part of the J regions, is commonly longer in BCRs of UM-CLL patients and long HCDR3s have been associated with polyreactivity (Aguilera et

al., 2001; Murray et al., 2008). Also, HCDR3 regions of receptors using the same V_H segment in different patients are stereotyped independent of their length and mutation status of the receptor (Hervé et al., 2005; Tobin et al., 2003; Tobin et al., 2004). All these observations suggest that stimulation by common antigens plays an essential role in CLL pathogenesis.

Consistently, BCRs of most UM-CLL and some M-CLL cells are polyreactive towards autoantigens and various microbial molecules (Bröker et al., 1988; Hervé et al., 2005; Myhrinder et al., 2008; Sthoeger et al., 1989). Other monoreactive M-CLL BCRs display high affinity towards fungal antigens, which stimulate their proliferation (Hoogeboom et al., 2013). Also, CLL BCRs have recently been described to recognise regions in adjacent Ig molecules, leading to constitutive BCR cross-linking and auto-activation. This feature is independent of the mutation status but mediated by the HCDR3 region (Binder et al., 2013; Minden et al., 2012). Consistently, CLL cells do show features of constant antigen engagement *in vivo* and generally express low levels of surface IgM (Krysov et al., 2010).

In agreement with an important role for BCR signalling in disease pathogenesis, stronger responses to BCR cross-linking *in vitro* are linked with poor clinical outcome (Cesano et al., 2013; Roy et al., 2012) and several components of the BCR signalling pathway are deregulated in CLL cells. Both LYN and SYK are overexpressed and constitutively active (Buchner et al., 2009; Contri et al., 2005) and in contrast to non-malignant cells, UM-CLL cells often overexpress the SYK family kinase Zeta-chain-associated protein kinase 70 (ZAP70), which associates with CD79b and enhances signalling in response to IgM crosslinking independent of its kinase activity (L. Chen et al., 2002; Chen et al., 2008). BTK activation after BCR cross-linking is enhanced in CLL cells compared to normal B cells (Cheng et al., 2014). CLL cells also have higher levels of nuclear NFκB compared to normal B cells (Furman et al., 2000) and some patients display constitutive phosphorylation of ERK1/2 (Muzio et al., 2008). Further, the PI3K/AKT pathway is constitutively active (Ringshausen et al., 2002; Zhuang et al., 2010).

1.3.1.2 Anergy in CLL

In vivo, UM-CLL cells show a more pronounced BCR gene expression signature than M-CLL cells and *in vitro* most UM-CLL cells respond better to IgM cross-linking and show a stronger proliferative response than M-CLL cells (Guarini et al., 2008; Herishanu et al., 2011; Lanham et al., 2003). However, most cells respond to IgD and CD79 cross-linking and can recover responsiveness to IgM cross-linking after incubation *in vitro*, indicating that the underlying mechanism of unresponsiveness is anergy (Lanham et al., 2003; Mockridge et al., 2007). This is consistent with the constant antigen exposure and the resulting low surface IgM expression of CLL cells (Gauld et al., 2005; Krysov et al., 2010). Moreover, unresponsive CLL cells have been shown to have constitutively active ERK1/2 and NFAT but not AKT, features that resemble murine anergic B cells (Muzio et al., 2008).

Anergy is more often seen in M-CLL and therefore correlates with a good prognosis (Mockridge et al., 2007). However, anergy participates in CLL development as it increases the survival of CLL cells *in vitro* (Apollonio et al., 2013). This finding was surprising, as anergic cells normally have a short life span, which is linked to BIM-mediated apoptosis (Enders et al., 2003; Oliver et al., 2006). Indeed, CLL cells express high levels of BIM, but its function is counteracted by simultaneous overexpression of BCL2 and targeting BCL2 in CLL leads to rapid induction of apoptosis (Del Gaizo Moore et al., 2007; Souers et al., 2013). Further, like CLL cells, anergic B cells fail to differentiate into plasma cells and it was recently shown that anergy is also linked to the maturation defect of CLL B cells (Duckworth et al., 2014). The data indicate that the chronic nature of CLL is intricately linked to the induction of anergy in conjunction with a defect in apoptosis.

1.3.1.3 Cell of origin

The cell of origin of CLL is still a matter of on-going debate. It was believed that CLL cells might derive from naturally occurring $CD5^+$ B cells, which normally represent a minor population of B cells and might be a counterpart of murine $CD5^+$ B1 cells. They are seen as the source of natural antibodies, which are constitutively secreted, polyreactive and usually unmutated immunoglobulins (Dono et al., 2004). However, the question whether a B1 cell compartment exists in humans has still not been resolved. Consistently, CD5 can be upregulated on conventional activated B cells and is associated with anergy and receptor editing (Gagro et al., 2000; García-Muñoz et al., 2012; Hillion et al., 2005; Hippen et al., 2000; Morikawa et al., 1993; Zupo et al., 1994). CD5 functions as a co-receptor for the BCR and directly associates with it (Lankester et

al., 1994). It has been shown to be phosphorylated by LYN, to recruit SHP1 (Tibaldi et al., 2011) and to attenuate BCR-induced PLCγ activation, Ca^{2+} signalling and ERK phosphorylation (Gary-Gouy et al., 2000; Gary-Gouy, Harriague, Dalloul, et al., 2002). Conversely, CD5 seems to play a positive role in the activation of signal transducer and activator of transcription 3 (STAT3) and NFAT2 and the production of IL-10, which promotes cell survival (Garaud et al., 2011; Gary-Gouy, Harriague, Bismuth, et al., 2002).

Due to the finding that CD5 is a dynamically expressed surface molecule and does not distinguish one specific B cell subset, other hypotheses on the cell of origin were proposed. CLL cells might derive from marginal zone B cells, as these can have both mutated and unmutated BCRs, which are often polyreactive, and, like CLL cells, they display a memory phenotype (Chiorazzi & Ferrarini, 2011) (Figure 1.16 A). Alternatively, M-CLL cells might be derived from germinal centre cells that have generated an autoreactive BCR during SHM and have then become anergic, while UM-CLL cells are autoreactive, anergic pre-germinal centre cells (García-Muñoz et al., 2012) (Figure 1.16 B).

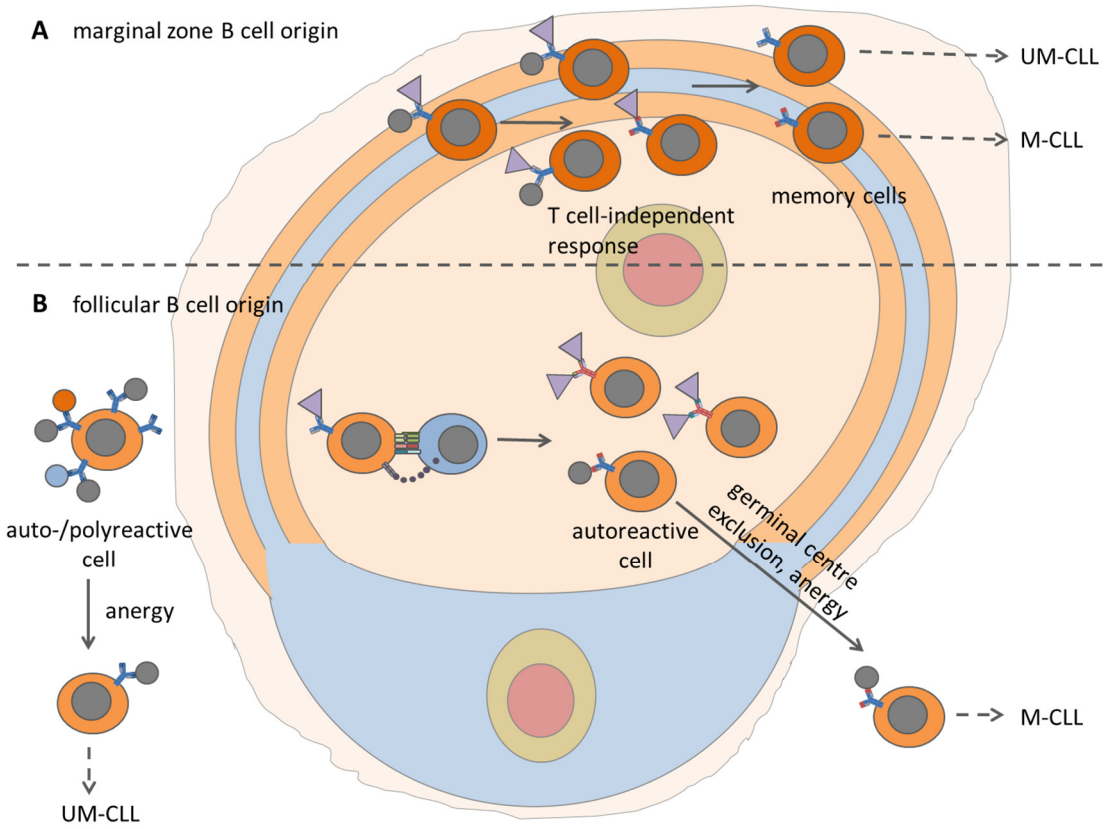

Figure 1.16 Possible cells of origin for CLL clones.
A CLL cells could be derived from marginal zone memory B cells, which are often polyreactive and can have mutated BCRs. **B** Alternatively, UM-CLL cells could be derived from pre-germinal centre B cells, which have become anergic due to autoreactivity, while M-CLL cells could be develop from germinal centre cells that have become autoreactive and anergic.

1.3.1.4 The microenvironment in disease pathogenesis

Similar to normal B cells, CLL cells depend on stimulation from other cell types like stromal cells, nurse-like cells (NLCs) and T cells for proliferation and survival (Bhattacharya et al., 2011; Burger et al., 2000; Lagneaux et al., 1998; Os et al., 2013; Patten et al., 2008). In absence of these stimuli in cell culture, CLL cells undergo spontaneous apoptosis (Burger et al., 2000; Lagneaux et al., 1998). *In vivo*, proliferation occurs at specific tissue sites, so called pseudofollicles in the lymph nodes (Donhuijsen et al., 1983; Herishanu et al., 2011). Homing to lymphoid tissues first requires transendothelial migration (TEM) and CLL cells express CCR7, the receptor for CCL21 and CCL19, which is required for TEM (Till et al., 2002). Further, CLL cells in the blood express high levels of CXCR4 and CXCR5 which allow them to home to specific areas in the lymphoid tissues, where stromal cells and NLCs produce the ligands CXCL12 and CXCL13 (Burger et al., 1999; Bürkle et al., 2007; Dürig et al., 2001; Möhle et al., 1999). These molecules do not only serve as chemoattractants but provide potent pro-survival signals as well (Burger et al., 2000; O'Hayre et al., 2010; Ticchioni et al., 2007). Binding of the chemokines leads to receptor endocytosis and BCR stimulation downmodulates the receptors, so that tissue CLL cells have low levels of CXCR4/5, which facilitates their recirculation to the blood (Burger et al., 1999; Burger et al., 2000; Bürkle et al., 2007; Calissano et al., 2011; Vlad et al., 2009). Consistently, recently stimulated, proliferating $Ki67^+$ CLL cells display lower CXCR4/5 surface expression (Bennett et al., 2007). Cells in the blood, where stimulatory signals are low or absent, then upregulate CXCR4/5 again, which allows for their remigration into lymphoid tissues (Calissano et al., 2011; Herishanu et al., 2011). These same cells also show higher levels of surface IgM, consistent with the *in vitro* findings that absence of stimulation leads to upregulation of the receptor. They are most responsive to BCR stimulation *in vitro* and most likely represent the subset of cells that can proliferate upon stimulation in the lymph node (Coelho et al., 2013) (Figure 1.17).

In total, 0.1% to 13.8% of cells in the peripheral blood are $Ki67^+$ (Damle et al., 2007) and, depending on the patient, between 0.1% and over 1% of the CLL cells are newly generated each day. As most of the patients show very little change in white blood cell counts, the proliferation must be counterbalanced by apoptosis (Messmer et al., 2005). Consistently, apoptotic cells make up 0.5% to over 10% of the CLL cells in the peripheral blood (Cheng et al., 2014). Therefore, CLL is a very dynamic disease and a shift in the balance between proliferation and apoptosis leads to either progression or regression.

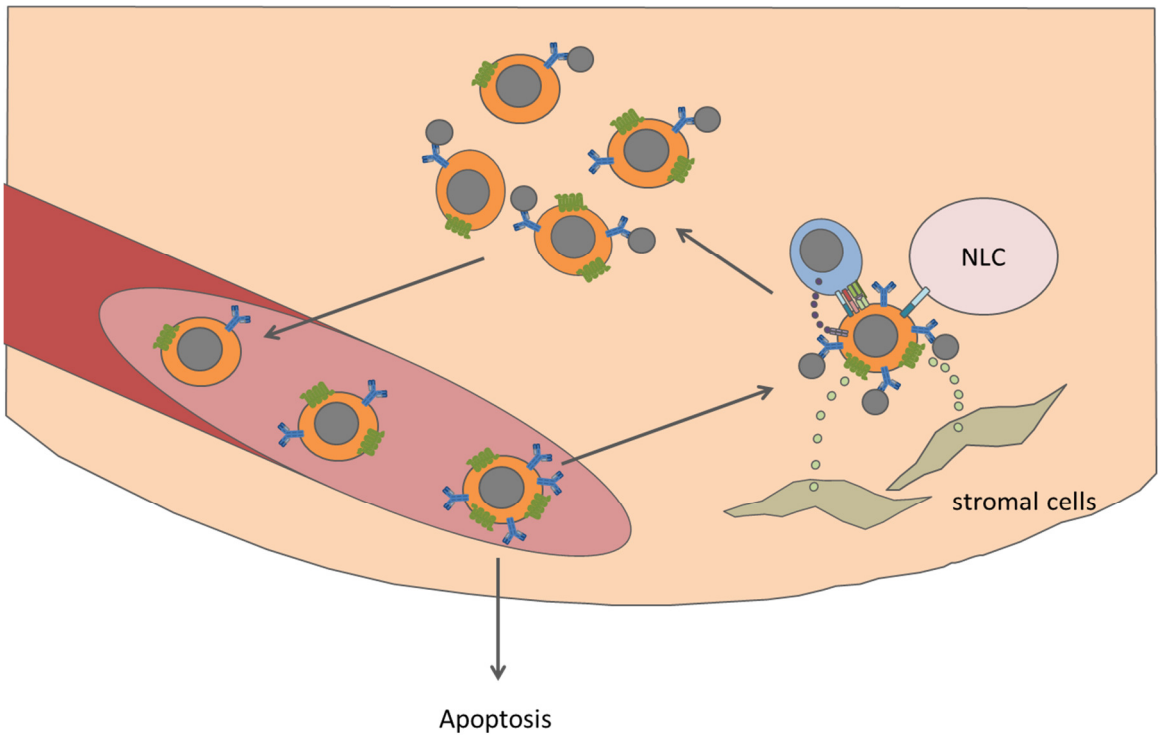

Figure 1.17 CLL cells depend on the microenvironment for proliferation.
In pseudofollicles the cells receive proliferation and survival signals from stromal, nurse-like (NLC) and T cells. Downregulation of the BCR and chemokine receptors leads to their egress into the circulation, where the lack of stimulation leads to reexpression of the receptors. Cells then either enter the tissue again or undergo apoptosis.

1.3.2 Diffuse large B cell lymphoma

DLBCL accounts for about one third of the NHL cases and is a heterogeneous disease (Shankland et al., 2012). One of the hallmarks of DLBCL is the frequent genomic aberration, which facilitates abnormal cell proliferation and survival and arises through spontaneous mutations, genomic translocation, copy number variations or aberrant somatic hypermutation (ASHM) (Bea et al., 2005; Pasqualucci et al., 2001). Most, if not all, DLBCL cases express AID and show ASHM, which recurrently targets a number of genes. ASHM requires active transcription and usually targets regions up to 2 kb downstream of the TSS (Pasqualucci et al., 2001). Apart from ASHM, AID is likely to play a role in chromosomal translocations because these are usually observed between genes that are targeted by ASHM and the switch regions of the IgH locus and their frequency correlates with AID expression levels (Lenz et al., 2007).

Depending on the gene expression profile, DLBCLs have been grouped into germinal-centre B cell-like (GCB), activated B cell-like (ABC) and type 3 DLBCL (Alizadeh et al., 2000; Rosenwald et al., 2002; Wright et al., 2003). GCB-DLBCL cells derive from activated germinal centre (GC) B cells and about 85% of the cases express BCL6 (Iqbal et al., 2007). ABC-DLBCL cells are post-GC B cells that entered plasmablastic differentiation and show an NFκB gene expression signature (Pasqualucci & Dalla-Favera, 2014; Rosenwald et al., 2002; Wright et al., 2003) (Figure 1.18). Consistently, ABC-DLBCL cell lines are dependent on chronically active BCR and NFκB signalling and knockdown of BTK, CD79, IgM or Igκ inhibits survival of these cells (Davis et al., 2010). Additionally, a number of mutations that activate the NFκB pathway have been identified in ABC-DLBCL (Boone et al., 2004; Compagno et al., 2009; Davis et al., 2010; Georg Lenz et al., 2008; Ngo et al., 2011; Shembade et al., 2010).

The classification is also predictive of disease outcome and under current standard treatment, which is a combination immunochemotherapy of rituximab, cyclophosphamide, doxorubicin, vincristine and prednisone (R-CHOP) (Habermann, 2012), GCB-DLBCL and ABC-DLBCL patients have 5-year survival rates of about 80% and 50 - 60%, respectively (Y. Huang et al., 2012; G Lenz et al., 2008; Perry et al., 2014). Interestingly, the mRNAs encoding for the kinases PIM1 and PIM2 are among the genes that are highly expressed in ABC-DLBCL but not GCB-DLBCL (Care et al., 2013; Wright et al., 2003). Both genes are NFκB targets, which explains their preferential expression in ABC-DLBCL (Asano et al., 2011; Zhu et al., 2002). Because PIM kinases have been shown to cooperate with MYC during lymphomagenesis (Allen et al., 1997; van der Lugt et al., 1995; van Lohuizen et al., 1991; Verbeek et al., 1991), they might contribute to the aggressive phenotype of ABC-DLBCL. It has already been shown in other cell types that the cooperation between PIM1 and MYC is at least in

part mediated through a direct activation of MYC-dependent transcription by PIM1 (for more details on PIM kinases see section 1.6) (J. Kim et al., 2010; Zippo et al., 2007). Therefore PIM kinases might play a role in aberrant transcriptional regulation in ABC-DLBCL. In agreement with this hypothesis, MYC is expressed in about 70% of ABC-DLBCL cases (S. Hu et al., 2013). Interestingly, both *MYC* and *PIM1* are also frequently targeted by ASHM (Khodabakhshi et al., 2012).

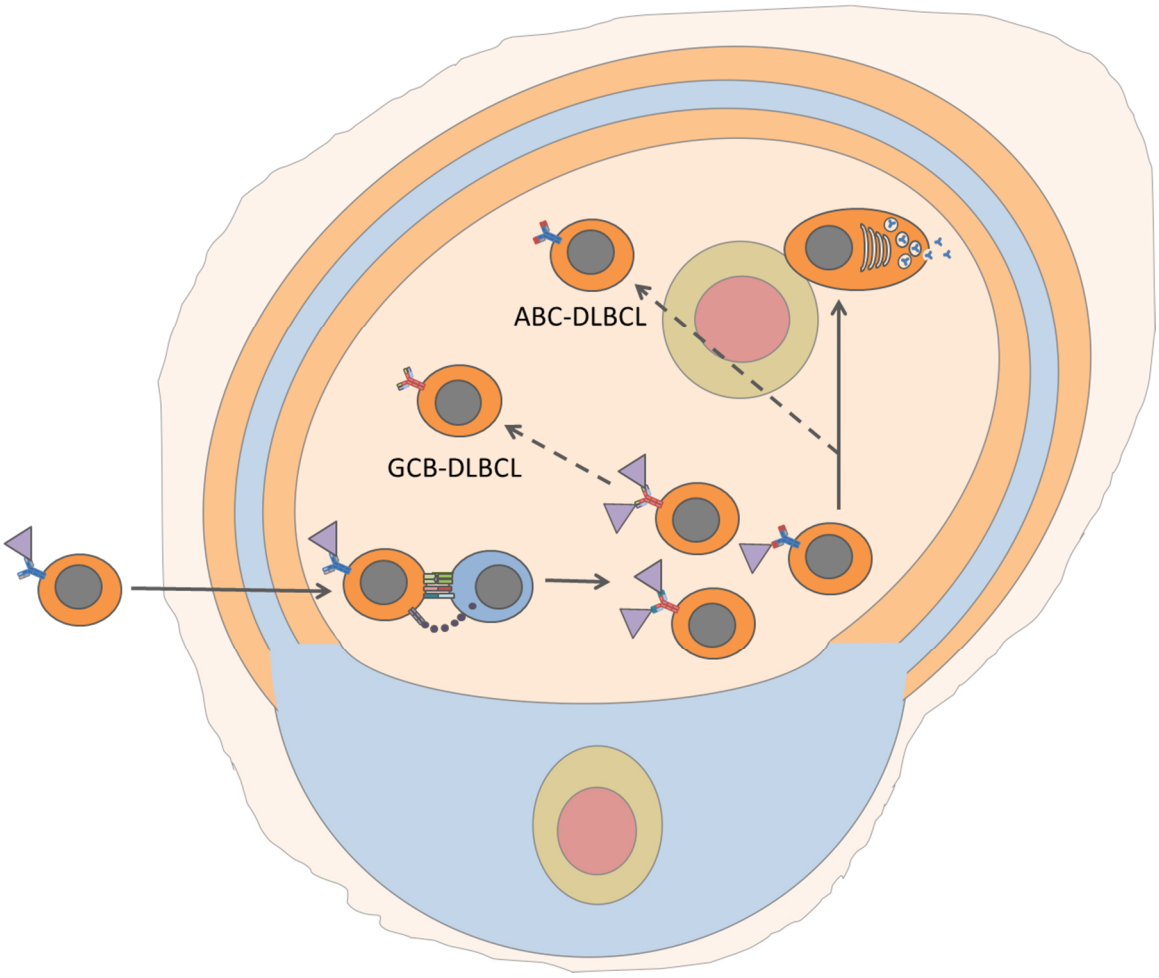

Figure 1.18 Current hypothesis for the origin of ABC- and GCB-DLBCL.
GCB-DLBCL cells are derived from activated germinal centre cells, while ABC-DLBCL cells show features of cells that entered plasmablastic differentiation.

1.3.3 Burkitt lymphoma

Burkitt lymphoma is a GC-derived malignancy and can be classified into endemic (eBL), sporadic (sBL) and immunodeficiency-associated disease (Frick et al., 2012). eBL is seen in some regions of Africa and is associated with malaria and Epstein-Barr virus (EBV) infection (Shankland et al., 2012). sBL occurs in all parts of the world and immunodeficiency-associated BL is usually linked to HIV infection (Frick et al., 2012).

Burkitt lymphoma cells depend on MYC activity for proliferation and survival (Gomez-Curet et al., 2006; Spender & Inman, 2012) and the hallmark of BL is the overexpression of MYC through a translocation of the *MYC* gene into close proximity of one of the Ig enhancers (IgH, Igκ or Igλ) (Dalla-Favera et al., 1982). As GC B cells, BL cells express AID and *MYC* is typically fused to the IgH switch region (Pasqualucci et al., 2004; Ramiro et al., 2004). *MYC* is normally repressed by BCL6 in GCs, but the BCL6 binding sites are removed through the translocation, so that expression is no longer inhibited (Dominguez-Sola et al., 2012; Schmitz et al., 2014). Consistently, the untranslocated MYC allele is usually silent (ar-Rushdi et al., 1983).

In normal cells, overexpression of MYC leads to induction of the proapoptotic protein BIM and activation of the p53 apoptotic pathway via induction of ARF (Sakamuro et al., 1995; Zindy et al., 1998). In about 70% of sBL cases, *MYC* is mutated by ASHM (Bemark & Neuberger, 2000; Schmitz et al., 2012) and most mutations occur in the N-terminal MYC box I (MBI). Two common mutations have been shown to selectively inhibit transcriptional activation of the *BIM* gene, without affecting proliferation compared to wild type MYC (Hemann et al., 2005). Further, the *BIM* promoter is hypermethylated and silenced in about 50% of patients (Richter-Larrea et al., 2010). In addition, p53 mutations occur in about 35% of BLs but rarely together with the MYC mutations that show reduced activation of *BIM* (Schmitz et al., 2012) (Figure 1.19).

1.3.3.1 Tonic BCR signalling in BL

Two thirds of BL cell lines show a reduced amount of viable cells when CD79a or SYK are knocked down, suggesting that BCR signalling is important for BL cell survival. Unlike ABC-DLBCL cells, they do not depend on NFκB but rather on PI3K/AKT activity, indicating that BL, like normal B cells, depend on tonic BCR signalling (Schmitz et al., 2012). In mice, PI3K has been shown to strongly cooperate with MYC in lymphomagenesis and to result in a Burkitt-like tumour (Sander et al., 2012).

The PI3K-AKT pathway can further be activated through PTEN inactivating mutations or PTEN downregulation through the MYC-dependent overexpression of miR17-92 (Schmitz et al., 2012). Additionally, mutations in the PI3K regulatory subunit gene

PI3KR1 were detected (Love et al., 2012). Cooperation of MYC and AKT seems to require AKT-mediated FOXO phosphorylation, because FOXO normally inhibits expression of several MYC-dependent genes (Bouchard et al., 2004). Further, FOXO directly activates *ARF* transcription, thereby inhibiting MYC-dependent lymphomagenesis (Bouchard et al., 2007). Additionally, mTORC1-mediated activation of eIF4E and the BCL2 protein MCL1 supress MYC-dependent apoptosis (S. Li et al., 2003; Mills et al., 2008) (Figure 1.19).

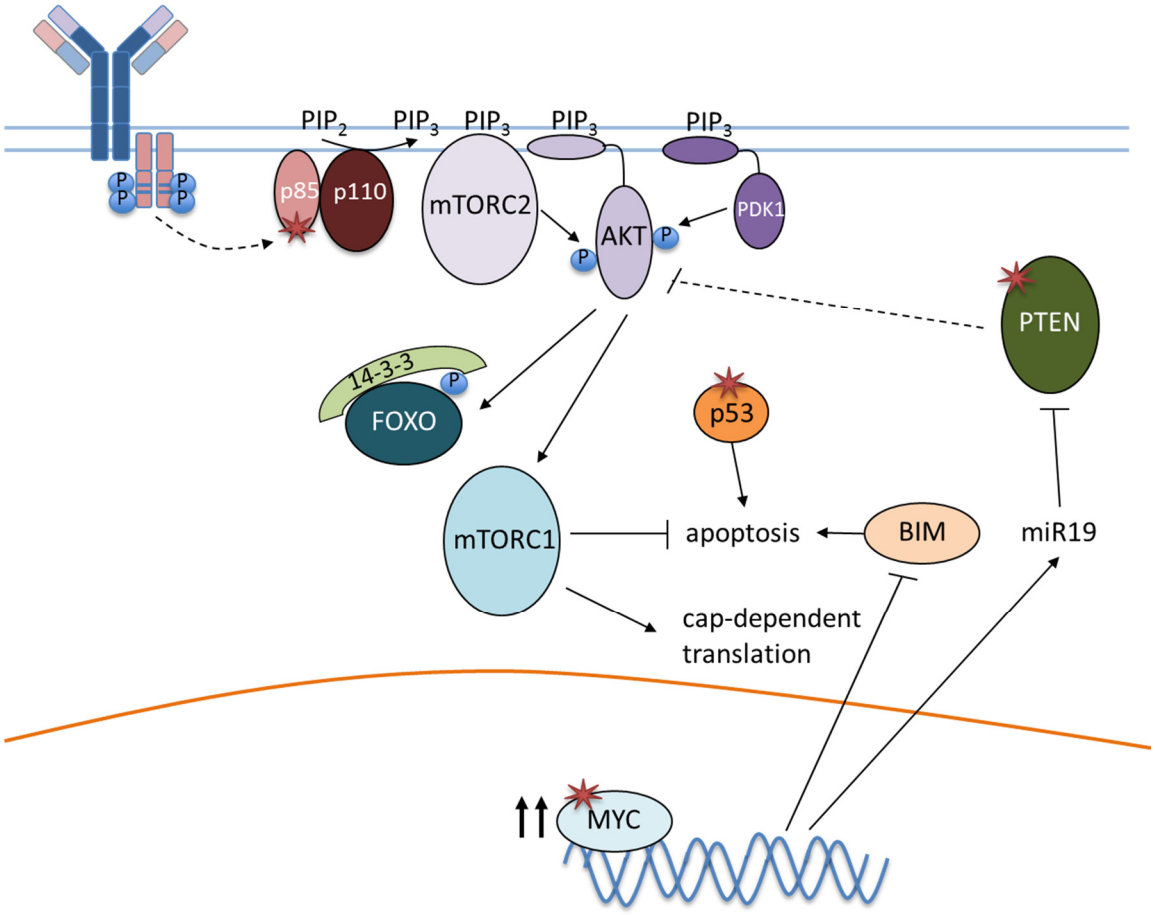

Figure 1.19 Oncogenic pathways and mutations in Burkitt lymphoma.
Frequent mutations are depicted as stars. The hallmark of BL is the overexpression of MYC, which cooperates with the PI3K pathway to drive tumour cell survival. The PI3K pathway is activated through MYC via miR19, through activation of tonic BCR signalling or through mutations in PTEN or the p85 subunit of PI3K. Moreover, apoptosis is frequently counteracted by mutations in MYC, which inhibit BIM expression or by p53 mutations

1.4 Kinase inhibitors as therapeutics and tools to study protein function

Targeting proteins with small molecule inhibitors is a developing field in cancer therapy. Some tumours are absolutely dependent on the activity of specific pathways, e.g. Burkitt lymphomas are dependent on MYC and PI3K, ABC-DLBCL and CLL are dependent on BCR signalling, so that inhibiting one of those pathways results in inhibition of tumour cell viability. Other tumours are even dependent on one specific oncogene, a mechanism called oncogene addiction (Weinstein & Joe, 2006). Most inhibitors have so far been developed against kinases, because these are intricately involved in different signal transduction pathways and inhibition of key kinases elicits a significant response (J. Zhang et al., 2009). Further, developing inhibitors for transcription factors is often unsuccessful. For example, although considerable efforts have been made, there is no specific MYC inhibitor available to date (McKeown & Bradner, 2014). Moreover, kinase inhibitors show a favourable side-effect profile because the negative effects of kinase inhibition on tumour cells can usually be circumvented in normal cells, as these are not relying on one specific pathway for their viability and normal function (J. Zhang et al., 2009).

However, one problem that arises during the treatment of cancers with kinase inhibitors, is the development of resistances through mutations, for example of BTK in Ibrutinib-treated CLL (Woyach et al., 2014), amplifications of the target, e.g. amplification of the BCR-ABL1 gene in Imatinib-treated CML (le Coutre et al., 2000) or upregulation of alternative pro-survival pathways (Engelman et al., 2007). Most kinase inhibitors were designed to specifically target certain kinases, but they are rarely specific *in vivo*, and often this unspecificity is even required for their biological activity. The BCR-ABL inhibitor Imatinib, for example, does also target the tyrosine kinase KIT and inhibition of both kinases is necessary to induce apoptosis in CML cells (Belloc et al., 2009). Therefore, it is important to understand how kinase inhibitors work in a cellular context, which exact pathways they target and which other oncogenes cooperate with the targeted protein, so that alternative drugs for treatment of resistant patients or drugs for combination therapy can be developed.

Another application kinase inhibitors can be used for, is the study of kinase functions *in vitro*. Because kinase inhibitors are often not highly specific for the targeted drug (Knight & Shokat, 2005), it is important to make use of different, structurally distinct kinase inhibitors (Martin & Arthur, 2012). Only effects elicited by all these different inhibitors are then likely to be due to inhibition of the kinase of interest.

1.4.1 Example: Treatment of CLL with inhibitors of the BCR pathway

Because CLL cells are dependent on BCR signalling for their survival and proliferation, inhibitors of several components of the BCR pathway are now being extensively tested in clinical trials. We were aiming to better understand the mechanism of action of Ibrutinib, which will be reviewed in the following section.

1.4.1.1 Ibrutinib

Ibrutinib is an inhibitor of BTK with an IC_{50} of 0.5 nM. It covalently binds to C481 in the BTK active site and blocks its catalytic activity (Honigberg et al., 2010). It also potently inhibits several other kinases (Table 1.1), of which the SFKs B lymphoid kinase (BLK), FGR, LCK, FYN and LYN, as well as the kinases CSK, JAK3 and fms-related tyrosine kinase 3 (FLT3) might have roles in CLL (Abts et al., 1991; Aoki et al., 1994; Mankaï et al., 2008). Ibrutinib inhibits cell proliferation and survival, as well as signalling via CXCR4 and migration towards CXCL12/13 *in vitro* (Chang et al., 2013; Honigberg et al., 2010; Ponader et al., 2012). This possibly explains why CLL cells in patients redistribute from the lymphoid tissues into the peripheral blood, so that Ibrutinib-treated patients present with lymphocytosis in the first weeks to months of treatment (Byrd et al., 2013; de Rooij et al., 2012).

Name	IC_{50} (nM)	Name	IC_{50} (nM)
BTK	0.5	JAK3	16.1
BLK	0.5	FRK	29.2
BMX	0.8	LCK	33.2
CSK	2.3	RET	36.5
FGR	2.3	FLT3	73
BRK	3.3	TEC	78
HCK	3.7	ABL	86
EGFR	5.6	FYN	96
YES	6.5	RIPK2	152
ERBB2	9.4	SRC	171
ITK	10.7	LYN	200

Table 1.1 Kinases targeted by Ibrutinib.
IC_{50} values for kinases inhibited by Ibrutinib as determined *in vitro* using a ^{33}P filtration binding assay with ^{33}P-ATP. Adapted from Honigberg et al., 2010.

Generally, Ibrutinib is well tolerated in patients and leads to a durable remission, even in relapsed or refractory patients (Byrd et al., 2013). It is, however, still unclear how Ibrutinib leads to remission. One study suggested that apoptosis of CLL cells in both blood and lymphoid tissues is induced by Ibrutinib (Wodarz et al., 2014), whereas a second study shows that Ibrutinib treatment does not increase apoptosis above the normal level in untreated patients (Cheng et al., 2014). In the first study, death rates of 0.5% per day were estimated on the basis of an earlier study by Messmer et al., while apoptosis was directly measured before and after treatment in the second study (Cheng et al., 2014; Messmer et al., 2005; Wodarz et al., 2014). Further, the latter study showed that Ibrutinib induces apoptosis *in vitro* only at concentrations that cannot be achieved *in vivo* (Advani et al., 2013; Cheng et al., 2014). Thus, inhibition of proliferation in conjunction with unchanged death rates seems to account for the reduction in disease burden.

Some patients have already been described to be resistant to Ibrutinib and relapsed under treatment. Out of six patients analysed by Woyach et al., four had a C481S mutation in BTK, making the inhibition of BTK by Ibrutinib reversible. One patient had an R665W mutation in PLCγ and the sixth patient presented with the BTK C481S and three PLCγ mutations (L845F, R665W and S707Y). All three PLCγ mutations led to a gain of function and neither Ca^{2+} flux nor ERK or AKT activation after IgM cross-linking were inhibited by Ibrutinib *in vitro* (Woyach et al., 2014). Therefore, it is of interest to understand the exact mechanism of action of Ibrutinib to develop new therapeutics for patients with Ibrutinib-resistant CLL. Further, this suggests that Ibrutinib should be used as a combination therapy with other drugs and understanding how Ibrutinib works, will help clinicians choose useful combination schemes.

1.4.1.1.1 Other inhibitors of the BCR pathway

Apart from Ibrutinib, other BCR pathway inhibitors are available and are studied in clinical trials for use in CLL. These are Fostamatinib, a SYK inhibitor and Idelalisib, a PI3Kδ inhibitor. Like Ibrutinib, Fostamatinib and Idelalisib inhibit BCR and chemokine signalling and cause an initial lymphocytosis (Buchner et al., 2010; Hoellenriegel et al., 2011; Robak & Robak, 2013). Both drugs are also well tolerated by patients and lead to remission (Friedberg et al., 2010; Khan et al., 2014; Wiestner, 2012).

1.5 The transcription factor MYC

As described earlier, overexpression of MYC is the hallmark of Burkitt lymphoma. Further, it is expressed in most cases of ABC-DLBCL, where it might cooperate with the kinases PIM1 and PIM2 to promote tumour cell survival or proliferation. Consistent with a role in tumourigenesis, MYC was initially discovered as the cellular homolog of the transforming gene of the avian myelocytomatosis virus (Sheiness & Bishop, 1979) and was then found to be an integration site for avian leukosis virus, which leads to its increased expression from the viral enhancer/promoter (Hayward et al., 1981; Payne et al., 1982).

Increased expression of MYC, or of the related MYCN or MYCL, is found in many kinds of tumours and can be mediate by genomic amplification, translocation, retroviral insertion or retroviral transduction (Alitalo et al., 1983; Conacci-Sorrell et al., 2014; Kohl et al., 1983; Nau et al., 1985; Schwab et al., 1983). Further, increased expression of MYC can result from the activation of upstream signal transduction pathways and the stabilisation of the MYC protein (Gregory & Hann, 2000; Salghetti et al., 1999; Sears et al., 2000). MYC overexpression is associated with poor clinical outcome (McKeown & Bradner, 2014) and MYC inhibition in mice by expressing a dominant negative MYC derivative, is effective against RAS-driven glioma and KRAS-driven lung cancer, indicating that targeting MYC is a valid therapeutic approach (Annibali et al., 2014; Soucek et al., 2013). However, because no specific MYC inhibitor could be developed to date (McKeown & Bradner, 2014), it is important to better understand the MYC signalling network and to identify drugable targets that influence MYC-dependent transcription. Consistently, is has already been shown that targeting histone deacetylase 3 (HDAC3) and enhancer of zeste homolog 2 (EZH2), which are components of a transcriptional repressive MYC complex, inhibits lymphoma growth *in vitro* and *in vivo* (X. Zhang et al., 2012). Other such targets could be the PIM kinases, whose known functions will be reviewed in chapter 1.6.

1.5.1 Structure of the MYC transcription factor

The MYC family transcription factors have an N-terminal transactivation domain, which includes the two conserved MYC boxes MBI and MBII, a middle domain with MBIII, MBIV and a proline glutamate serine threonine (PEST) domain, and a C-terminal DNA-binding and dimerization basic helix-loop-helix leucine zipper (bHLHZ) domain (Conacci-Sorrell et al., 2014) (Figure 1.20). MYC binds DNA as a heterodimer with the transcription factor MYC-associated factor X (MAX) and dimerization occurs via the HLHZ domain (Blackwood & Eisenman, 1991; Blackwood et al., 1992; Nair & Burley,

2003). MYC/MAX heterodimers bind Enhancer box (E box) elements with the consensus sequence 5'-CACGTG-3' and stimulate transcription (Amati et al., 1993; Blackwood et al., 1992; Kretzner et al., 1992). In contrast to MYC, MAX does not have a transactivation domain (Figure 1.20), which explains why MAX homodimers do not activate transcription (Amati et al., 1993; Kato et al., 1992; Kretzner et al., 1992). MAX can also form heterodimers with MNT or MXD1-4 and mediate transcriptional repression through the recruitment of SIN3A or SIN3B, which associate with histone deacetylases (HDACs) (Ayer et al., 1995; Hooker & Hurlin, 2006; Hurlin et al., 1995; Hurlin et al., 1997; Kadamb et al., 2013; Schreiber-Agus et al., 1995).

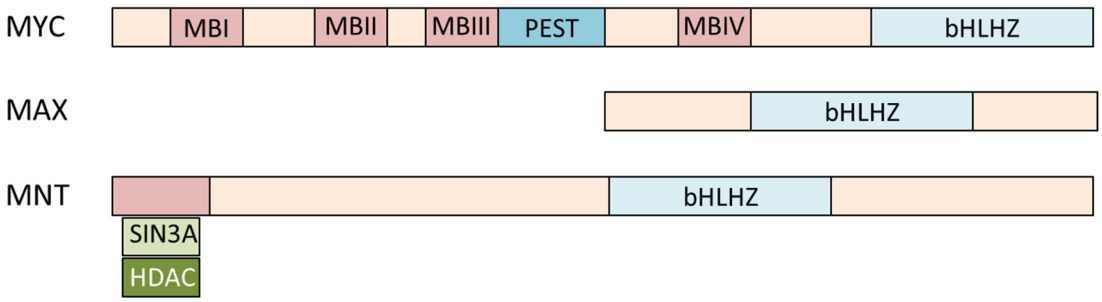

Figure 1.20 Structure of MYC, MAX and MNT.
MB = MYC box, PEST = proline, glutamate, serine, threonine-rich sequence, bHLHZ = basic helix-loop-helix leucine zipper. MAX can form heterodimers with MYC or MNTs to activate or repress transcription, respectively. Adapted from Conacci-Sorrell et al., 2014.

1.5.2 Regulation of MYC

MYC can be transcribed from different promoters, the main ones being P1 and P2, which initiate approximately 25% and 75% of transcripts, respectively (Levens, 2010; Watt et al., 1983). The functions of these different transcripts remain, however, still elusive. Transcription of the *MYC* gene is tightly regulated by most extracellular signals, including WNT, NOTCH, growth factors, TGFβ, interferons and interleukins (Levens, 2010). However, our understanding of the molecular processes behind *MYC* regulation are just beginning to be elucidated. Binding sites for a plethora of transcription factors have been identified in the *MYC* promoter and extensive cross-talk between these factors can be observed (Calo et al., 2003; C.-R. Chen et al., 2002; Duyao et al., 1990; Ghosh et al., 1999; Hiebert et al., 1989; Ho et al., 2005; Iavarone et al., 2003; Kabbout et al., 2014; Kessler et al., 1992; Mognol et al., 2012; Roussel et al., 1994; Thalmeier et al., 1989; Toualbi et al., 2006; Yagi et al., 2002; Yochum et al., 2010) (Figure 1.21).

Apart from transcriptional regulation, the *MYC* gene product is regulated at the posttranscriptional, translational and posttranslational level. The mRNA contains 3' AU-rich elements (AREs) and is bound by the decay-promoting factor tristetraprolin (TTP) (Marderosian et al., 2006). The mRNA stability is also reduced by several microRNAs, like let-7a, miR-145 and miR-34 (Cannell et al., 2010; Christoffersen et al., 2009; Sachdeva et al., 2009; Sampson et al., 2007). The *MYC* mRNA can be translated starting either from a canonical AUG or an upstream CUG codon and translation of both forms is dependent on eIF4E (Carter et al., 1999; Hann et al., 1988). Further, binding of AU-rich element binding factor 1 (AUF1) to the ARE stimulates *MYC* translation, while binding of the protein translational repression by RNA binding (TIAR) has the opposite effect (Liao et al., 2007) (Figure 1.21).

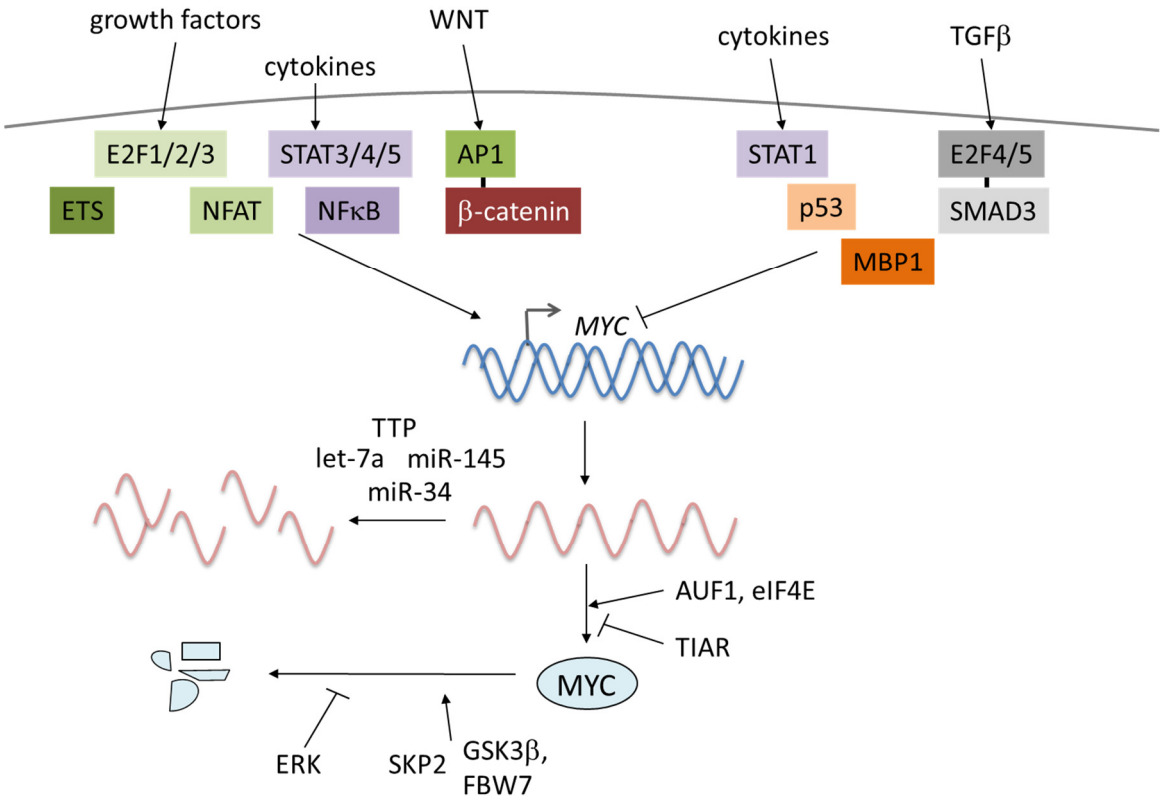

Figure 1.21 Regulation of MYC expression.
MYC transcription is regulated by a number of extracellular signals through a plethora of transcription factors. The mRNA stability is regulated by miRNAs and TTP, translation is influenced by ARE binding proteins and is cap-dependent. MYC protein stability is regulated by kinases and ubiquitin ligases. ETS = E-twenty-six oncogene homolog, E2F = Adenovirus *E2* gene promoter region binding factor, SMAD = Mothers against decapentaplegic homolog, MBP1 = MYC-binding protein 1

MYC is a very unstable protein and has a half-life of about 25 minutes (Hann & Eisenman, 1984). The MBI is essential for the regulation of MYC stability, which is increased by phosphorylation of S62 but decreased by T58 phosphorylation (Sears et al., 2000). S62 can be phosphorylated by ERK, whereas T58 is targeted by GSK3β (Sears et al., 2000). Phosphorylation of T58 does, however, only occur when S62 is already phosphorylated (Lee et al., 2008; Lutterbach & Hann, 1994; Sears et al., 2000). Dually phosphorylated MYC is bound by the E3 ligase F box and WD repeat domain containing 7 (FBW7) to be ubiquitinated and degraded (Welcker et al., 2004; Yada et al., 2004). Interestingly, T58 is often mutated in BL, which increases MYC protein stability (Bahram et al., 2000). Another protein that can regulate MYC stability is S phase kinase-associated protein 2 (SKP2) (Figure 1.21). SKP2 interacts with the MBII domain, ubiquitinates MYC and leads to its degradation. Intriguingly, it also enhances transcriptional activation by MYC (S.Y. Kim et al., 2003; von der Lehr et al., 2003). Binding of $p14^{ARF}$ to MYC inhibits SKP2-mediated ubiquitination and leads to expression of non-canonical target genes. Loss of ubiquitination is, for example, sufficient to stimulate expression of proapoptotic genes, like *BIM* (Q. Zhang et al., 2013).

1.5.3 MYC target genes and functions

MYC generally promotes cell growth and cell cycle progression, but when overexpressed, it also sensitises cells to apoptosis. Therefore, cancers overexpressing MYC always show second hit mutations that counteract its proapoptotic functions (Meyer et al., 2006).

MYC most strongly upregulates genes implicated in ribosome biogenesis, translation, RNA processing, metabolism and biosynthesis, cell cycle control and transcriptional regulation (Bretones et al., 2014; Fernandez et al., 2003; Ji et al., 2011; Jones et al., 1996; Zeller et al., 2006). MYC also directly stimulates transcription of genes for rRNAs and tRNAs by POL I and POL III and increases processing of the 45S rRNA (Gomez-Roman et al., 2003; Goodfellow et al., 2006; Kenneth et al., 2007; Poortinga et al., 2004; Schlosser et al., 2003). Consistently, MYC-repressed genes include negative cell cycle regulators like $p21^{CIP}$ and $p15^{INK4B}$ (Wang et al., 2011; Zeller et al., 2006). MYC has also been shown to have transcription independent effects on cell proliferation by directly regulating DNA replication through replication origin licensing (Dominguez-Sola et al., 2007) (Figure 1.22).

MYC stimulates apoptosis through the induction of *BIM* (Campone et al., 2011; Hemann et al., 2005) and *BAX* (Mitchell et al., 2000) and repression of *BCL2* and

BCL2L1 (encoding BCL-X_L) (Eischen et al., 2001; Maclean et al., 2003). MYC-mediated induction of the miR17-92 cluster does, however, play an important role in repressing BIM, as well as other tumour suppressors like PTEN or SIN3B (Li et al., 2014; O'Donnell et al., 2005; Xiao et al., 2008). MYC also indirectly induces $p14^{ARF}$ and thus activates the p53 pathway and *BIM* expression (Q. Zhang et al., 2013; Zindy et al., 1998). Further, MYC triggers an autoregulatory feedback loop by stimulating expression of MAX, MNT, MXD1 and MXD3 and by downregulating its own expression (Penn et al., 1990; Zeller et al., 2006) (Figure 1.22).

Although some specific MYC target genes have been described, the range of MYC functions seems to be a lot wider. Under physiological conditions, MYC is bound to approximately 10% of all known promoters, mainly with canonical 5'-CACGTG-3' E boxes, but when overexpressed it also binds to lower affinity 5'-CANNTG-3' E boxes in enhancers and to non-E box elements (Fernandez et al., 2003; Z. Li et al., 2003; Nie et al., 2012; Sabò et al., 2014; Walz et al., 2014). MYC preferentially binds to E boxes associated with CpG islands and to sites, which already show higher levels of histone acetylation, indicating that MYC is not a pioneer factor (Fernandez et al., 2003; Zeller et al., 2006). MYC binding can further enhance acetylation, but this does not necessarily increase mRNA expression (Fernandez et al., 2003). Consistently, only about 20% of MYC-associated genes are directly regulated by MYC when assessed by microarray (Nie et al., 2012; Zeller et al., 2006).

However, recent work suggests that MYC regulates all bound genes, but that conventional normalisation methods mask this effect, simply because the normalisation genes are upregulated as well. Accordingly, MYC leads to an increase in the total cellular RNA content. This is, at least in part, a transcriptional effect as MYC binding to promoters and proximity of the MYC binding site to the TSS correlate with the level of gene expression. Also, normal transcription factors bind with high affinity to target sites but a second population can be detected as background binding. MYC, however, shows a range of affinities for genomic sites with the background being inseparable from specific binding. And last, MYC/MAX globally stimulate pause release by increasing P-TEFb recruitment to all active genes (Lin et al., 2012; Nie et al., 2012; Rahl et al., 2010).

In contrast, other studies suggest that MYC does specifically up- or downregulate cancer-associated genes and that amplification of total RNA expression can occur as a secondary mechanism through transcriptional regulation by those target gene products or through mRNA stabilisation. The discrepancies between these studies seem to arise from differences in the starting levels of MYC protein and the cell types analysed. Low MYC expression prior to induction will thus lead to both amplification of all genes and

specific regulation of a subset of target genes, whereas high basal MYC levels counteract amplification of transcription and lead to a specific regulation of some genes (Sabò et al., 2014; Walz et al., 2014).

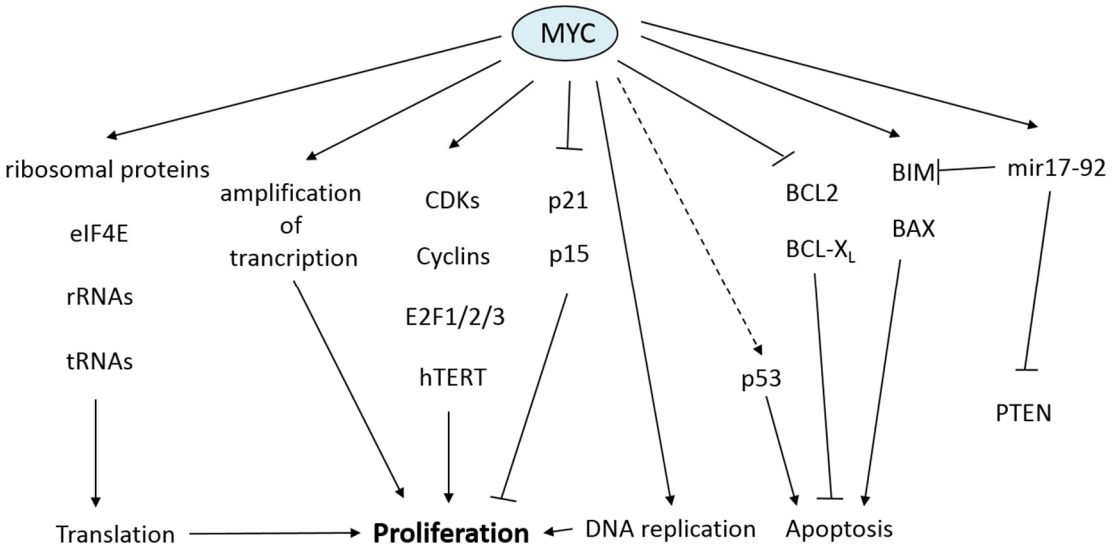

Figure 1.22 MYC target genes.
MYC targets include a number of genes that induce proliferation by enhancing translation, metabolism or cell cycle progression. MYC also directly stimulates DNA replication. However, high MYC levels sensitise cells to apoptosis by both p53-dependent and -independent pathways. CDK = Cyclin-dependent kinase, hTERT = human telomerase reverse transcriptase

1.5.4 Mechanisms of transcriptional activation by MYC

Transcriptional coactivators are mostly recruited by the MBII domain. One of these is the transformation/transcription domain-associated protein (TRRAP), which is part of several human acetyltransferase complexes (Frank et al., 2003; McMahon et al., 1998) (Figure 1.23). TRRAP recruits the 2 MDa SPT3-TAF9-GCN5 acetyltransferase (STAGA) and the 60 kDa Trans-Activator of Transcription (Tat)-interacting protein (TIP60) acetyltransferase complex for transactivation (Liu et al., 2003; McMahon et al., 2000). TRRAP is also part of the p300/CBP-associated factor (PCAF) and the GCN5-containing TATA-binding protein (TBP)-free TAFII-containing complex (TFTC), therefore also likely recruiting those complexes to MYC (Brand et al., 1999; Vassilev et al., 1998). GCN5 also directly interacts with MBI and the linker between MBI and MBII and this interaction is required for STAGA recruitment (Zhang et al., 2014). Further, MYC can directly recruit the p300 and CBP acetyltransferases to its N- or C-terminus, respectively (Faiola et al., 2005; Vervoorts et al., 2003). GCN5, TIP60, CBP and p300 have been shown to acetylate MYC. While one study showed that CBP enhances MYC stability by acetylation, another study suggests that acetylation by p300 and CBP destabilises MYC. However, their binding to MYC counteracts this effect, resulting in an

overall stabilisation of MYC (Faiola et al., 2005; Vervoorts et al., 2003). Acetylation by GCN5 and TIP60 leads to stabilisation of MYC (Patel et al., 2004). STAGA is required for transactivation by mediating histone H3 acetylation, as well as POL II and Mediator recruitment (Liu et al., 2008; Martinez et al., 2001). The TIP60 complex mediates acetylation of H4 and H2A (Ikura et al., 2000) and p300 and CBP are capable of acetylating all four core histones (Ogryzko et al., 1996).

MYC has also been shown to interact with the INI1 subunit of the SWI/SNF complex via its bHLHZ domain and functional SWI/SNF is required to activate a reporter construct (S.-W.G. Cheng et al., 1999). In addition, MYC recruits the positive transcription elongation factor b (P-TEFb), consisting of Cyclin T and CDK9, via direct binding of Cyclin T to the MBI (Eberhardy & Farnham, 2002; Kanazawa et al., 2003). Further, the kinase PIM1 binds to the MBII domain, it phosphorylates histone H3S10 and stimulates the recruitment of P-TEFb to nucleosomes (Zippo et al., 2007; Zippo et al., 2009). The transactivation domain also binds the core transcription factors TFIIH and TBP (McEwan et al., 1996). Furthermore, MYC directly stimulates POL I and POL III transcription. To facilitate POL III-dependent transcription, MYC binds TFIIIB and recruits TRRAP and GCN5 (Gomez-Roman et al., 2003; Kenneth et al., 2007) (Figure 1.23). Similarly, at POL I-dependent rDNA genes, MYC recruits components of the POL I and enhances acetylation at these sites (Grandori et al., 2005).

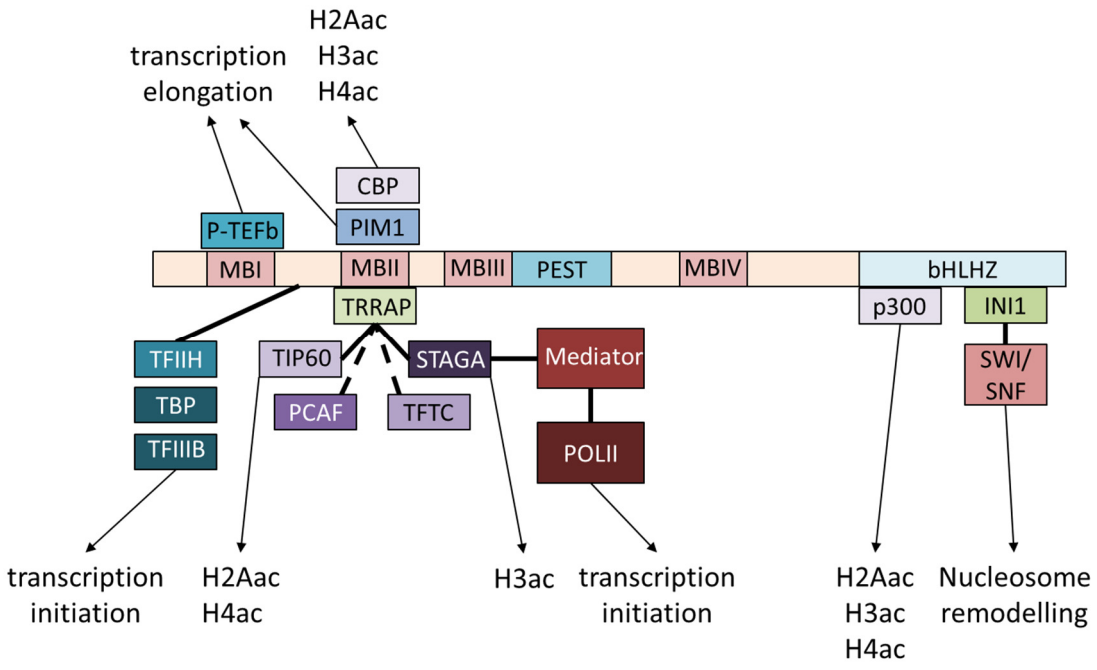

Figure 1.23 Mechanisms by which MYC can activate transcription.
MYC interacts with acetyltransferases (CBP, p300, TIP60, STAGA and possibly also PCAF and TFTC), which acetylate histones or other proteins and STAGA interacts with and recruits the Mediator. Further, MYC tethers general transcription factors, like TFIIH, TBP, TFIIIB and P-TEFb to the chromatin and it has also been shown to interact with the SWI/SNF complex.

1.5.5 Repression of transcription by MYC

A common mechanism of transcriptional repression by MYC/MAX heterodimers is their binding to other activating transcription factors, which results in the formation of a repressive complex. The transcription factor MYC-interacting Zinc-finger protein 1 (MIZ1), for example, activates the expression of genes encoding antiproliferative proteins, like $p21^{CIP}$ and $p15^{INK4B}$, but also of *BCL2* (Herold et al., 2002; Kosan et al., 2010; Seoane et al., 2001; Staller et al., 2001). MIZ1 recruits p300 and nucleophosmin (NPM1) as coactivators and binding of MYC/MAX to MIZ1 replaces these cofactors (Staller et al., 2001; Wanzel et al., 2008). Association of MYC/MAX with MIZ1 leads to the recruitment of HDACs and DNMT3A (Brenner et al., 2005; Varlakhanova et al., 2011) (Figure 1.24). In embryonic stem cells, MYC binds to 30% of MIZ1-associated genes and co-occupied genes are predominantly differentiation-associated genes. Consistently, knockdown of MYC leads to differentiation of embryonic stem (ES) cells, indicating that MYC-mediated repression of MIZ1 target genes is a general phenomenon (Varlakhanova et al., 2011). Similarly, MYC has been shown to bind to the Specificity protein 1 (SP1)-SMAD complex and to inhibit its transactivation function (Feng et al., 2002).

Apart from coactivators, the transactivation domain can also be bound by inhibitory factors, like myc modulator 1 (MM1), which binds Transcription intermediary factor 1 beta (TIF1β) to recruit the SIN3-HDAC complex (Mori et al., 1998; Satou et al., 2001). Additionally, MM1 promotes degradation of MYC, by directly interacting with the proteasome (Kimura et al., 2007). The MBIII plays an important role in MYC-mediated repression of pro-apoptotic genes by recruiting HDAC3 (Kurland & Tansey, 2008).

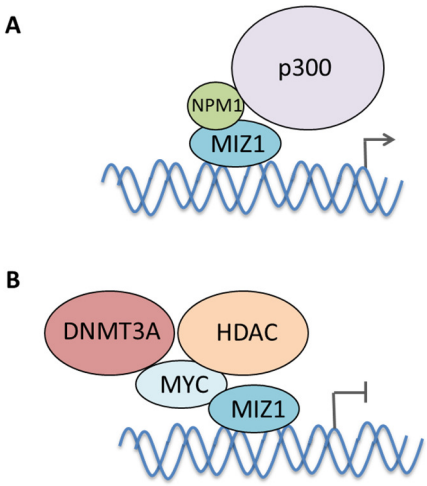

Figure 1.24 Transcriptional repression by MYC.
A MIZ1 is a transcriptional activator that induces gene expression through interactions with NPM1 and p300. **B** MYC replaces transcriptional co-activators from MIZ1 and recruits DNMT3A and HDACs to repress transcription. This process is E box-independent.

1.6 The PIM protein kinase family

Studying PIM kinases in the context of lymphoma is of great interest, because they were first described as oncogenes in both T and B cells. Moreover, both *PIM1* and *PIM2* mRNAs are part of an ABC-DLBCL gene expression profile that distinguishes this type of DLBCL from GDB-DLBCL (Alizadeh et al., 2000; Care et al., 2013; Wright et al., 2003). Further, they have been shown to cooperate with MYC, which itself is an important oncogene in lymphomagenesis (Breuer et al., 1989; Cuypers et al., 1984; van Lohuizen et al., 1989; van Lohuizen et al., 1991; Verbeek et al., 1991). In contrast to MYC, PIM kinases can be targeted therapeutically by small molecule inhibitors, a large number of which has been developed in recent years. Some of these inhibitors have already been tested at the pre-clinical stage (Burger et al., 2013; Garcia et al., 2014; Keeton et al., 2014). Therefore, it will be helpful to determine whether PIM kinases are valid therapeutic targets in DLBCL and the MYC-dependent BL.

1.6.1 PIM kinases cooperate with MYC in lymphomagenesis

The related kinases proviral integration site for Moloney murine leukaemia virus 1 (PIM1), PIM2 and PIM3 form the PIM kinase family of constitutively active serine/threonine kinases (Qian et al., 2005). All three PIM kinases are conserved in mammals, *C. elegans* expresses one PIM kinase homolog, PRK-2, and over 300 PIM kinases have been found in the zebrafish genome by computational analysis, whereas no *Drosophila* homolog is known to date (Rakshambikai et al., 2013; Zheng et al., 2011). *Pim1* and *Pim2* were initially identified as targets for the integration of Moloney murine leukaemia virus (MMLV) in murine T cell lymphoma, indicating that they function as oncogenes (Breuer et al., 1989; Cuypers et al., 1984) (Figure 1.25 A). The oncogenicity of PIM1 was confirmed in mice that express *Pim1* under control of the IGH enhancer (E_μ), which leads to specific expression in B and T cells. *Pim1* was found to be a weak oncogene, as only 5 – 10% of these mice have developed T cell lymphomas at 7 months of age (van Lohuizen et al., 1989) (Figure 1.25 B). However, if these mice are injected with MMLV after birth, lymphomas develop faster and much more frequently and, interestingly, insertion of the virus occurs either upstream of *Myc* or *Mycn* in all cases, suggesting a strong cooperation between *Myc* and *Pim1* during lymphomagenesis (van Lohuizen et al., 1989) (Figure 1.25 C).

In contrast to E_μ-*Pim1* transgenic mice, E_μ-*Myc* transgenic mice develop B cell lymphoma (Adams et al., 1985). If E_μ-*Myc* mice are injected with MMLV, 35% of insertions can be found upstream of the *Pim1* locus in B cell tumours (Figure 1.25 D) and E_μ-*Myc*/E_μ-*Pim1* double transgenic mice develop pre-B cell leukaemia prenatally,

again indicating cooperation between the two oncogenes (van Lohuizen et al., 1991; Verbeek et al., 1991) (Figure 1.25 E). Similarly, Eμ-*Mycn*/Eμ-*Pim1* and Eμ-*Mycl*/ Eμ-*Pim1* double transgenic mice develop early onset B or T cell malignancies, respectively, although the phenotype is less severe than in Eμ-*Myc*/Eμ-*Pim1* double transgenic mice (Möröy et al., 1991).

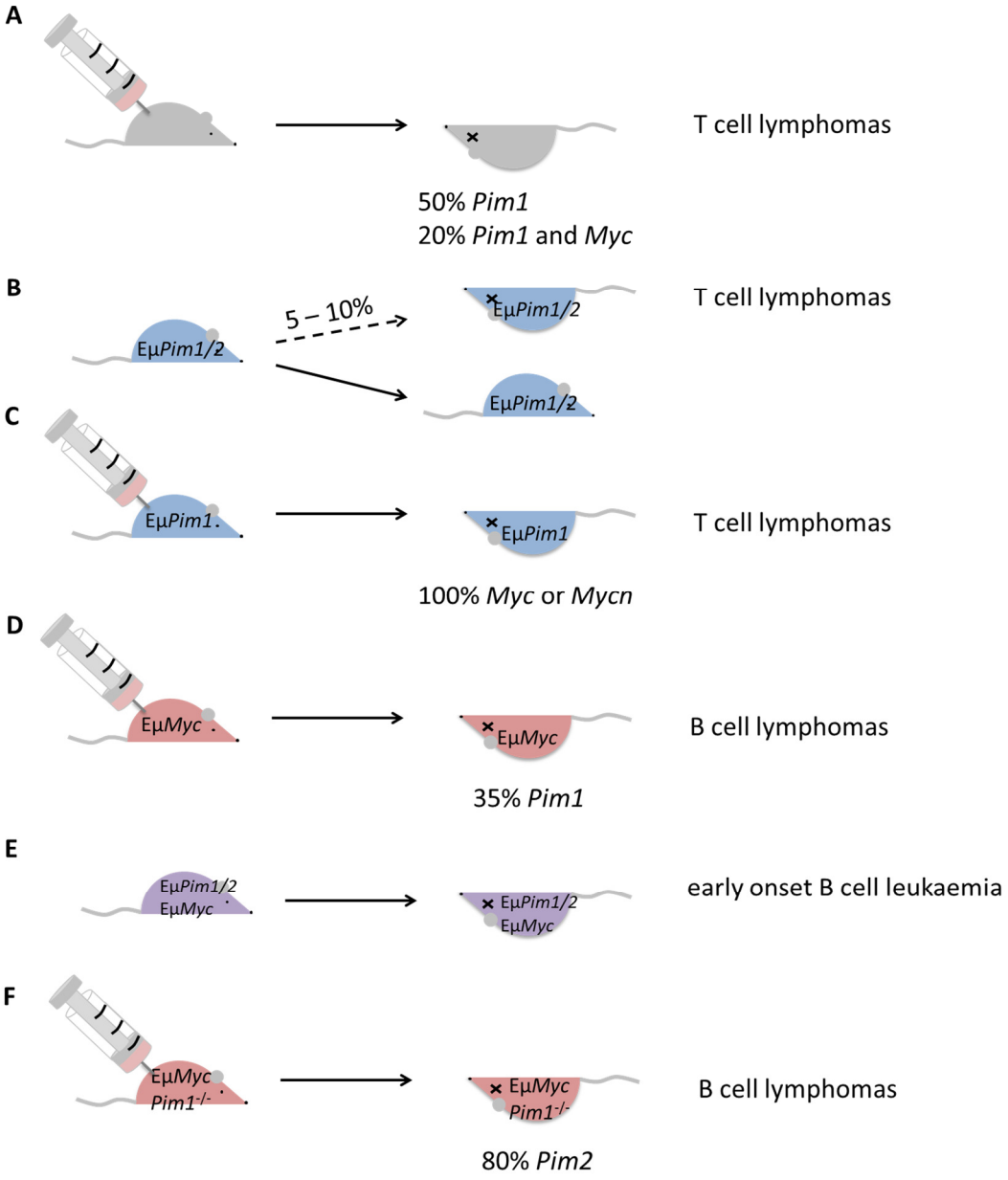

Figure 1.25 PIM kinases as oncogenes in murine lymphomas.
Early studies in mice suggest a cooperation between PIM kinases and MYC in oncogenesis. **A** MMLV-induced T cell lymphomas show insertion of the virus upstream of *Pim1* or *Pim1* and *Myc*. **B** PIM1 or PIM2 overexpression leads to lymphomagenesis with low penetrance, injection of the virus results in accelerated lymphomagenesis through insertion upstream of *Myc* or *Mycn* (**C**). **D** Injection of MMLV into MYC overexpressing mice results in tumours carrying insertions upstream of *Pim1*. **E** Overexpression of PIM1 or PIM2 and MYC induces early onset leukaemia. **F** MMLV infection of MYC overexpressing, *Pim1* knockout mice results in proviral insertion upstream of *Pim2*, indicating that PIM2 can compensate for PIM1.

E_μ-*Myc*/*Pim1*$^{-/-}$ mice infected with MMLV show proviral insertion upstream of *Pim2* in 80% of tumours, compared to only 15% in *Pim1* WT animals (van der Lugt et al., 1995) (Figure 1.25 F). Additionally, proviral insertion at the *Pim3* locus occurs in 25% of E_μ-*Myc*/*Pim1*$^{-/-}$/*Pim2*$^{-/-}$ mice, suggesting that PIM kinases can compensate for each other during lymphomagenesis (Mikkers et al., 2002). Consistently, the phenotypes of E_μ-*Pim2* mice resemble those of E_μ-*Pim1* mice. E_μ-*Pim2* mice develop T cell lymphoma with relatively long latency (Figure 1.25 B) and E_μ-*Myc*/E_μ-*Pim2* mice are born with pre-B cell leukaemia (Allen et al., 1997) (Figure 1.25 E).

1.6.2 Regulation of PIM expression

PIM kinases are widely expressed in haematopoietic, neuronal and epithelial cells of different origins, in embryonic stem cells, as well as in smooth and cardiac muscle cells and in the testis (Amson et al., 1989; Katakami et al., 2004; Konietzko et al., 1999; Muraski et al., 2007; Sorrentino et al., 1988; Stewart & Rice, 1995; Wingett et al., 1992; Zippo et al., 2004). As constitutively active enzymes, PIM kinases are mainly regulated at the expression level. Expression of PIM kinases can be induced by a variety of growth factors and cytokines through the activation of STAT1, STAT3, STAT4 and STAT5 (Lilly et al., 1992; Matikainen et al., 1999; Morcinek et al., 2002; Nosaka et al., 1999; Shirogane et al., 1999). Further, the NFκB pathway stimulates the expression of PIM kinases (Asano et al., 2011; Zhu et al., 2002). *PIM3* has been shown to be a direct MYC and ETS1 target gene (Forshell et al., 2011; Y.-Y. Li et al., 2009) (Figure 1.26).

All three *PIM* genes give rise to a single transcript, but translation initiation from non-canonical CUG codons results in expression of two PIM1 (34 kDa and 44 kDa) and three PIM2 isoforms (34 kDa, 38 kDa and 40 kDa) (Nawijn et al., 2011; Xie et al., 2006; Yan et al., 2003). The *PIM1* mRNA is destabilised by AREs in its 3'UTR (Domen et al., 1987) and binding of TTP to one of these elements enhances mRNA degradation (H.K. Kim et al., 2012; Mahat et al., 2012). Additionally, miR-1 and miR-33a have been shown to regulate *PIM1* mRNA levels (Nasser et al., 2008; Thomas et al., 2012). Translation of *PIM* mRNAs is cap-dependent and stimulated by eIF4E (Hoover et al., 1997; Schatz et al., 2011) (Figure 1.26). eIF4E also enhances nuclear export of the *PIM1* mRNA, by binding to a specific stem loop structure in the 5' UTR, called eIF4E sensitivity element (Culjkovic et al., 2006).

The PIM1 protein has a half-life of less than 5 minutes. Its activity and protein levels are negatively regulated by the prolyl isomerase PIN1 and the protein phosphatase 2A (PP2A) (Losman et al., 2003; Ma et al., 2007). Consistently, PIM1 autophosphorylates and has predicted phosphorylation sites for a large variety of kinases, but it is currently

unknown, whether PP2A targets the autophosphorylation residues or sites phosphorylated by another, unknown kinase (Bachmann et al., 2004; Brault et al., 2010). Binding of heat shock protein 90 (HSP90) stabilises PIM1, while binding of HSP70 increases its ubiquitination and proteasomal degradation (Shay et al., 2005). Hypoxia has been shown to prevent ubiquitination and degradation of PIM1 and to induce its translocation from the cytoplasm to the nucleus (Jian Chen et al., 2009) (Figure 1.26).

Although both PIM1 isoforms have comparable kinase activities *in vitro* (Saris et al., 1991), their subcellular localisations, and therefore their functions, are different. The 44 kDa PIM1L has a proline-rich domain capable of interacting with SH3 domains of membrane-associated proteins. It has been shown to bind to the Tec family kinase BMX and activate it (Xie et al., 2006). No functional differences have been described for the different PIM2 isoforms, but their half-lives range from 10 minutes for the 38 kDa isoform to more than 60 minutes for the 34 kDa isoform (Yan et al., 2003).

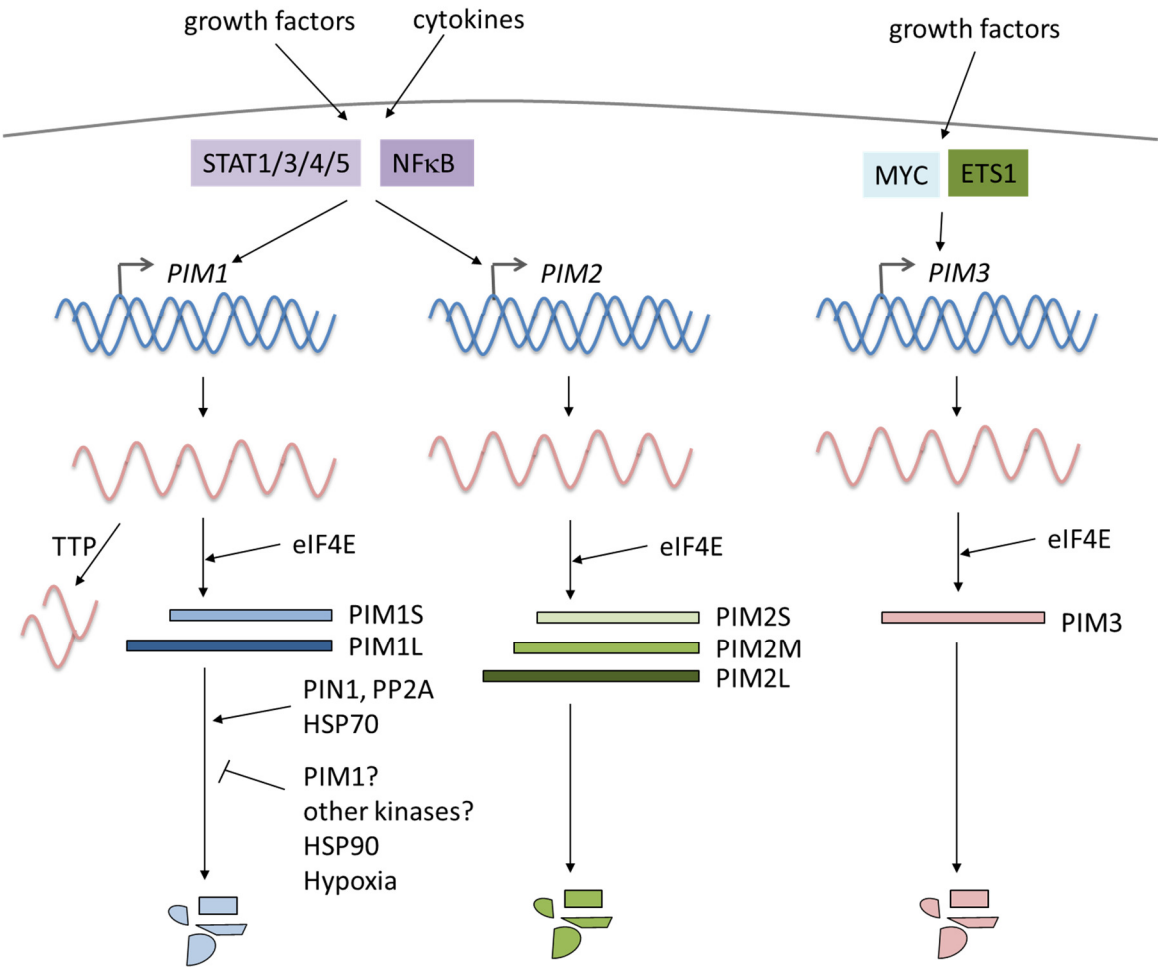

Figure 1.26 Regulation of PIM kinase expression.
The expression of *PIM1* and *PIM2* is regulated by cytokines and growth factors via STATs and NFκB. *PIM3* expression is regulated by MYC and ETS1. *PIM1* mRNA stability is reduced by TTP and translation of all mRNAs is cap-dependent. PIM1 protein stability is influenced by phosphorylation and heat shock proteins.

1.6.3 Mechanisms of PIM function

Several molecular mechanisms for the oncogenic potential of PIM kinases and for the cooperation between PIM kinases and MYC have been described. PIM1 and PIM2 can directly stabilise MYC through phosphorylating S329, which inhibits T58p and increases S62p (Y. Zhang et al., 2008). PIM1 has been shown to be recruited to the chromatin by binding to the MYC MBII and to induce gene expression through phosphorylation of histone H3S10 (Zippo et al., 2007). H3S10p leads to recruitment of 14-3-3 proteins, which serve as adaptors for the acetyl transferase MOF. MOF acetylates H4K16, which is recognised by the bromodomain containing protein 4 (BRD4), an adapter for P-TEFb. Thus, PIM1 stimulates transcriptional elongation (Zippo et al., 2009) (Figure 1.27, see section 1.7.2.1 for a description of the POL II transcription cycle). PIM1 is required for the expression of 20% of the MYC-induced genes after serum shock in HEK293 cells (Zippo et al., 2007). Consistently, PIM1 overexpression in prostate cancer cell lines enhances expression of MYC target genes (J. Kim et al., 2010) and PIM1 knockdown is sufficient to decrease proliferation, survival and tumourigenicity of MYC-overexpressing prostate cancer cells (Wang et al., 2012). PIM1 was also described to be nuclear in Burkitt lymphoma, which would allow for cooperation of PIM1 and MYC at the chromatin level (Ionov et al., 2003).

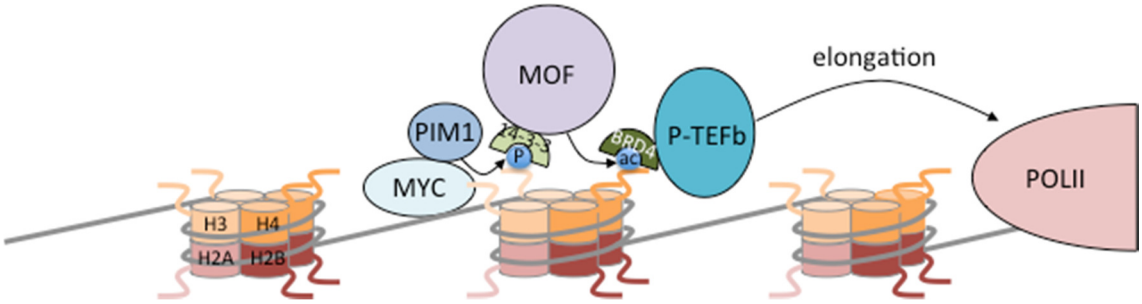

Figure 1.27 Mechanism of transcriptional activation by PIM1.
The DNA-binding transcription factor MYC recruits PIM1 to the chromatin, where it phosphorylates histone H3S10. This leads to the recruitment of 14-3-3 proteins, the acetyltransferase MOF and acetylation of H4K16. Recruitment of BRD4 and P-TEFb then triggers transcriptional elongation.

Cooperation between PIM2 and MYC requires the ability of PIM2 to stimulate the NFκB pathway via activation of the kinase COT. Blocking NFκB in MYC and PIM2 overexpressing cells induces apoptosis *in vitro* and inhibits growth in a tumour graft model (Hammerman et al., 2004). Interestingly, proviral insertion in E_{μ}-*Myc*/*Pim1*$^{-/-}$/ *Pim2*$^{-/-}$ mice occurred upstream of the *Tpl2* gene, which encodes COT, in approximately 20% of the tumours (Mikkers et al., 2002). PIM1 can also activate the NFκB pathway via TAK1 (K. Kim et al., 2010) and stabilisation of RelA/p65 through direct phosphorylation (Nihira et al., 2010) (Figure 1.28).

Further, PIM kinases have been shown to have several other MYC-independent pro-proliferative and anti-apoptotic effects. PIM1, PIM2 and PIM3 phosphorylate BAD at S112 and other sites, which leads to binding of 14-3-3 proteins and inhibits its interaction with anti-apoptotic BCL-X_L (Aho et al., 2004; Macdonald et al., 2006). PIM1 has also been shown to phosphorylate and inhibit the apoptosis signalling kinase 1 (ASK1), which results in reduced JNK and p38 MAPK phosphorylation and protects cells from H_2O_2-induced apoptosis (Gu et al., 2009) (Figure 1.28).

To stimulate cell cycle progression, PIM1 phosphorylates and inhibits MAP/microtubule affinity-regulating kinase 3 (MARK3). MARK3 phosphorylates CDC25C-S216, which leads to its cytoplasmic sequestration by 14-3-3 proteins, so that it cannot dephosphorylate and activate CDK1. Thus, inhibition of MARK3 by PIM1 leads to G2/M progression (Bachmann et al., 2004). Further, PIM1 has been shown to directly phosphorylate and activate CDC25C (Bachmann et al., 2006) and CDC25A. The latter stimulates apoptosis in Rat1 fibroblasts but is predicted to also promote G1/S and G2/M progression (Mochizuki et al., 1999). The CDK inhibitors $p21^{CIP1}$ and $p27^{KIP1}$ are also PIM1 or PIM1/2/3 targets, respectively, and phosphorylation by PIM kinases leads to their cytoplasmic localisation, which allows for G1/S transition (Morishita et al., 2008; Z. Wang et al., 2002; Zhang et al., 2007). PIM1 also stimulates $p27^{KIP1}$ degradation by phosphorylating and stabilising SKP2 (Cen et al., 2010) (Figure 1.28).

PIM kinases share several substrates with AKT and PIM2 has been shown to compensate for mTORC1 inhibition during haematopoiesis and in acute myeloid leukaemia (AML) (Hammerman et al., 2005; Tamburini et al., 2009). Consistently, treating AML cells with both a pan-PIM and an AKT inhibitor synergistically reduces cell growth and survival (Meja et al., 2014). PIM1 does, for example, phosphorylate FOXO1a, FOXO3a (Morishita et al., 2008), as well as PRAS40-T246, which leads to activation of mTORC1 (F. Zhang et al., 2009). PIM2 has been shown to stimulate phosphorylation of 4EBP1 and eIF4E (Hammerman et al., 2005; Tamburini et al., 2009). Like AKT, PIM1/2/3 can also phosphorylate and stabilise MDM2 (Hogan et al., 2008; Ionov et al., 2003) (Figure 1.28). Interestingly, stabilisation of MDM2 can also be mediated by kinase-dead PIM1 (Wood et al., 2009). Conversely, some PIM1 overexpressing cells show increased p53 (Hogan et al., 2008; Zemskova et al., 2010), which might be mediated by an enhanced interaction of phosphorylated MDM2 with $p14^{ARF}$, which inhibits degradation of p53 (Hogan et al., 2008). Therefore, PIM kinases could induce senescence or apoptosis in $p14^{ARF}$ and p53 expressing cells but have growth promoting effects in cells having no or low expression of these proteins (Zemskova et al., 2010). In this context, it is worth noting that MDM2 has functions distinct from p53 activation. It can, for example serve as a co-factor for NFκB and also stabilise PIM1 (Hogan et al., 2008; Thomasova et al., 2012).

At the chromatin, PIM1 can target proteins other than histone H3, like the splicing factor PIM-associated protein 1 (PAP1) (Maita et al., 2000; Maita et al., 2004) and the heterochromatin protein 1γ (HP1γ) (Koike et al., 2000). One study suggests that PIM1-dependent phosphorylation of HP1γ-S93 enhances its association with H3K9me3 and promotes heterochromatin formation (Jin et al., 2014). Other than MYC, PIM1 has been shown to phosphorylate and activate NFAT1 (Rainio et al., 2002), RUNX transcription factors (Aho et al., 2006), the androgen receptor (AR) (Ha et al., 2013; Linn et al., 2012) and the vitamin D receptor (VDR) (Maier et al., 2012) (Figure 1.28).

Further, migration of cells via CXCR4 is regulated by PIM1. The kinase phosphorylates the intracellular domain to facilitate proper receptor recycling and PIM1 is essential for CXCR4 surface expression. Consistently, PIM1 levels in leukaemic blasts from AML patients correlate with membrane CXCR4 (Grundler et al., 2009) and expression of all three PIM kinases correlates with CXCR4 phosphorylation in DLBCL (Brault et al., 2012). PIM kinases can also contribute to drug resistance of tumour cells. PIM1L has been shown to phosphorylate the ATP-binding cassette transporter G2 (ABCG2), promote multimerisation and substance export (Xie et al., 2008).

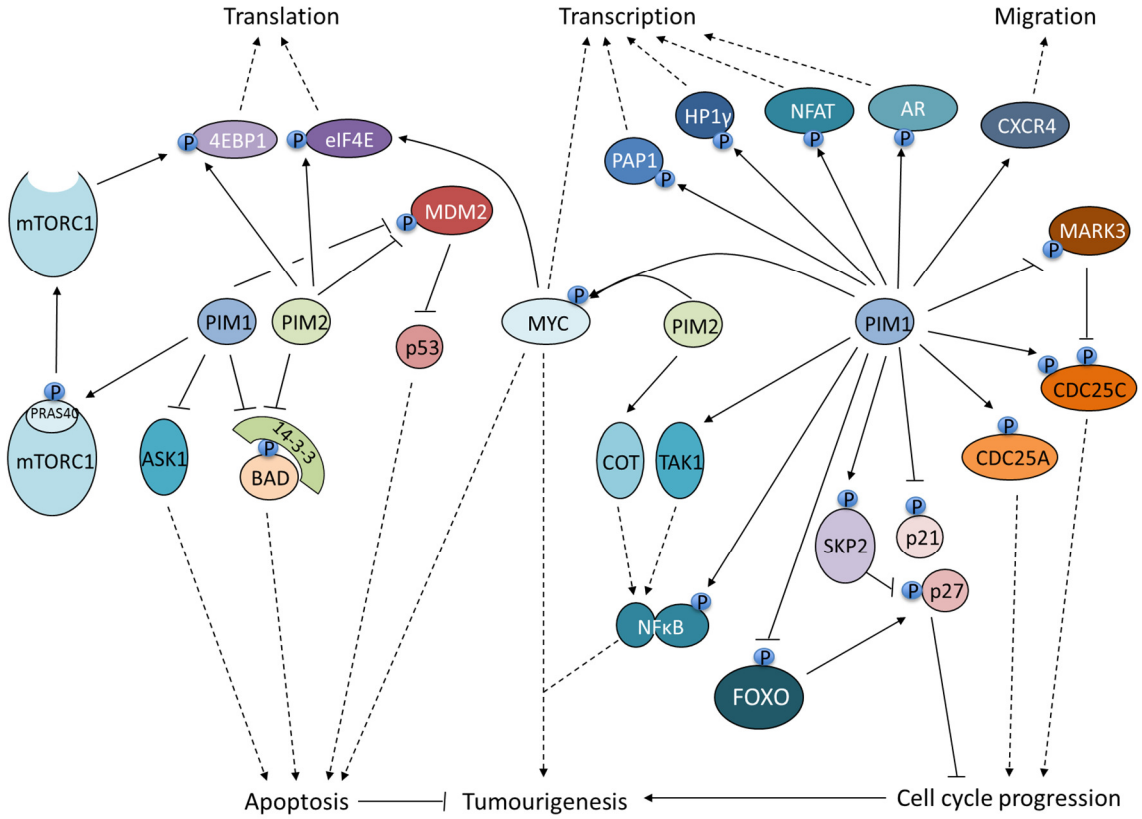

Figure 1.28 PIM kinase targets.
PIM kinases are bona fide oncogenes. They promote cell cycle progression and inhibit apoptosis via a number of different mechanisms. They enhance cap-dependent translation and influence transcription by targeting a lot of different transcription factors.

1.6.4 PIM kinases in human cancers

1.6.4.1 PIM kinases in haematological malignancies

Early studies showed that PIM1 is overexpressed in 30% of lymphoid and myeloid human leukaemias. However, no correlation with MYC overexpression was found (Amson et al., 1989). PIM2 is overexpressed in AML (Mizuki et al., 2003). Both PIM1 and PIM2 mRNAs are overexpressed in the NHLs CLL, DLBCL and mantle cell lymphoma (MCL), whereas PIM2 is also overexpressed in follicular lymphoma, MALT lymphomas, nodal marginal zone lymphomas and multiple myeloma (Cohen et al., 2004; Gómez-Abad et al., 2011). No overexpression of PIM3 is seen in NHL (Gómez-Abad et al., 2011). PIM2 expression in CLL correlates with ZAP70 expression and poor prognosis (Hüttmann et al., 2006) and PIM2/3 are required for CLL cell survival, whereas PIM1 mediates CXCR4-dependent cell migration (Decker et al., 2014). Both PIM1 and PIM2 have been shown to be upregulated upon EBV infection and to stimulate the transactivation potential of Epstein–Barr virus nuclear antigen 2 (EBNA2) (Rainio et al., 2005).

1.6.4.1.1 PIM kinases in DLBCL

PIM1 and *PIM2* mRNAs are highly expressed in ABC-DLBCL compared to GCB-DLBCL (Care et al., 2013; Wright et al., 2003). However, PIM protein-positive tumours do not differ significantly between non-GCB- and GCB-DLBCL. In one study, only 27% of ABC-DLBCL samples expressed PIM2 protein, compared to 18% for GCB-DLBCL (Gómez-Abad et al., 2011). In a second study, around 80% of both non-GCB and GCB cases were positive for PIM1, 70% of non-GCB and 55% of GCB cases were positive for PIM2 and about 55% of each were positive for PIM3 (Brault et al., 2012). It should however be noted that these studies did not differentiate between high and low PIM kinase expression. A difference between ABC- and GCB-DLBCL was observed when nuclear PIM1 was studied. 10 out of 12 cases with predominant nuclear PIM1 staining were of the non-GCB type and nuclear PIM1 was highly correlated with disease stage (Brault et al., 2012). However, no correlation between PIM and MYC expression was found. In contrast, PIM1 and PIM2 expression did correlate with activation of STATs and expression of ABCB1 (Brault et al., 2012). Nevertheless, expression of PIM1 and/or PIM2 is indicative of disease-free, disease-specific and overall survival in non-GCB-, but not GCB-DLBCL (Brault et al., 2012; Gómez-Abad et al., 2011).

As mentioned before, *PIM1* is also a target of ASHM in DLBCL, but surprisingly, 3 out of 5 mutants analysed showed reduced kinase activity and only one mutation resulted in an increase in kinase activity, suggesting that PIM1 may have kinase-independent

functions (Brault et al., 2010; Deutsch et al., 2007; Kumar et al., 2005). Consistently, inhibition of PIM kinases was moderately effective or not effective in inhibiting proliferation or inducing apoptosis in DLBCL cell lines (Brault et al., 2012; Gómez-Abad et al., 2011). Therefore, Brault et al. proposed that PIM kinases are more progression markers than bona fide therapeutical targets in DLBCL. PIM kinase inhibitors seem to be most effective in multiple myeloma, AML, MCL and CLL (Cervantes-Gomez et al., 2013; Lisa S. Chen et al., 2009; Chen et al., 2011; Decker et al., 2014; Garcia et al., 2014; Hiasa et al., 2014; Keeton et al., 2014; Q. Yang et al., 2012). As the present study was started in 2011, we were, however, unaware of the limited impact of PIM kinase inhibition on DLBCL cell survival at this time.

1.6.4.2 PIM kinases in solid tumours

Apart from haematopoietic malignancies, PIM1 is highly expressed in prostatic intraepithelial neoplasia and prostate cancer (Cibull et al., 2006; Dhanasekaran et al., 2001). MYC and PIM1 cooperate in prostate tumourigenesis and inhibition of PIM kinases in MYC-expressing cancers decreases proliferation, survival and tumourigenicity (J. Wang et al., 2010; Wang et al., 2012). PIM1 is further found highly expressed in mammary carcinoma cell lines (Gapter et al., 2006; Malinen et al., 2013), in squamous cell carcinoma (Peltola et al., 2009), pancreatic ductal adenocarcinoma (Reiser-Erkan et al., 2008), non-small cell lung cancer (Jin et al., 2012) and bladder cancer (Guo et al., 2010). Unexpectedly, PIM1 expression is associated with a good prognosis in both prostate and pancreatic carcinomas (Dhanasekaran et al., 2001; Reiser-Erkan et al., 2008).

PIM2 is associated with disease progression and invasion in prostate cancer (Dai et al., 2005) and both PIM2 and PIM3 are highly expressed in hepatocellular carcinoma (Fujii et al., 2005; Gong et al., 2009). PIM3 is further implicated in pancreatic cancer (Li et al., 2006) and progression of gastric adenocarcinoma (Zheng et al., 2008).

1.7 Chromatin and the regulation of transcription

A hallmark of cancer in general is the deregulation of gene expression (Hanahan & Weinberg, 2000; Lee & Young, 2013; Sadikovic et al., 2008). In recent years it has been increasingly recognised that gene expression is mainly regulated at the level of the chromatin, through structural organisation of genes, DNA methylation, posttranslational modifications (PTMs) of histones and transcription factors and co-factors (Berger, 2007; Li, Carey, et al., 2007). Especially DNA methylation has been extensively studied and was found to be deregulated in haematological malignancies (Galm et al., 2006; Yu, 2006). Further, inhibitors against some epigenetic modifiers, like HDACs or EZH2 have already been shown to be effective against several haematological malignancies (Bhadury et al., 2014; Duan et al., 2005; Ferreira et al., 2014; Garapaty-Rao et al., 2013; McCabe et al., 2012; X. Zhang et al., 2012). BET (bromodomain and extra terminal domain) inhibitors, which target adapter proteins that recognise histone acetylation marks, are very potent drugs against MYC-dependent lymphomas (Delmore et al., 2011). However, kinases are preferred targets for cancer therapy and they are significantly involved in the regulation of transcription downstream of signalling pathways and possibly also in the regulation of constitutively transcribed genes. Therefore, it might be important to identify chromatin-associated kinases as therapeutic targets, because they are likely contributing to the deregulated gene expression programme. PIM1 is, for example, required for the expression of 20% of MYC-regulated genes in serum-shocked HEK293 cells (Zippo et al., 2007).

Kinases do not act in isolation, but trigger the establishment of other chromatin modifications, like histone acetylation or methylation (Kim et al., 2014; Liokatis et al., 2012; Zippo et al., 2009), or structural rearrangement of the chromatin (Drobic et al., 2010). Therefore, it is also of interest to study effects of kinases on chromatin organisation and other histone modifications. Further, it might be helpful to determine which effects established kinase inhibitors have at the chromatin level to understand their mechanism of action and thus mechanisms of resistance. Altogether, a better understanding of the still elusive relationship between signalling kinases and chromatin alterations might lead to the identification of novel therapeutic targets or useful combinations of drugs.

1.7.1 Chromatin structure

Chromatin is the DNA with its associated proteins and RNAs. The role of chromatin is to package DNA to fit into the cell, to allow mitosis and meiosis, DNA repair and replication, and to control gene expression (Campos & Reinberg, 2009). The most abundant proteins in chromatin are the histones. These are small, positively charged, globular proteins with an extended N-terminal tail, which form octameres of two copies of H2A, H2B, H3 and H4 each (core histones). Approximately 146 bp of DNA are wrapped around these octameres to form nucleosomes (Luger et al., 1997; Alberts, 2008). Two nucleosomes are connected by so-called linker DNA, resulting in a “beads-on-a-string” structure (Luger et al., 2012). Further compaction of the chromatin is achieved through the linker histone H1, interactions between the nucleosomes and through non-histone proteins (Alberts, 2008; Hediger & Gasser, 2006; Luger et al., 2012) (Figure 1.29).

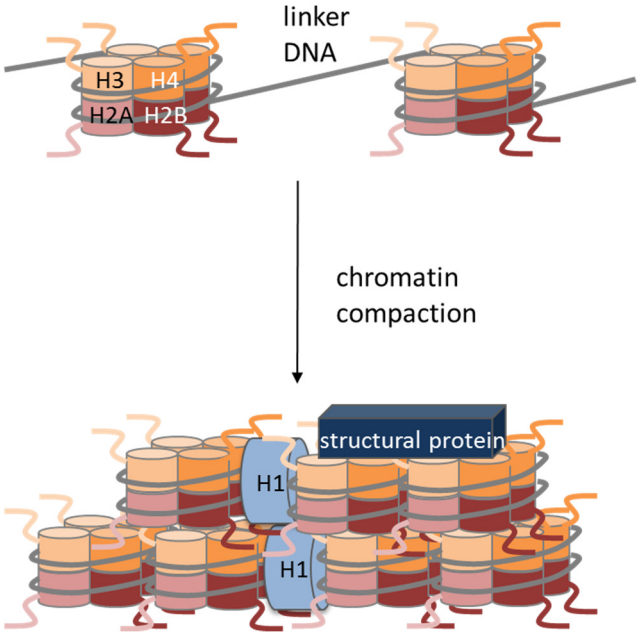

Figure 1.29 Schematic overview of open and closed chromatin structures. Chromatin compaction is mediated by histone H1 and other structural proteins.

Generally, densely packed, inactive regions are collectively called heterochromatin, while open chromatin regions are referred to as euchromatin. In recent years, it has, however, been established that there are different forms of both eu- and heterochromatin, which are characterised by different densities of chromatin packaging, differential use of histone variants, distinct posttranslational modifications of histones and binding of specific non-histone proteins and non-coding RNAs (Ernst & Kellis, 2010; Ernst et al., 2011; Julienne et al., 2013; Ram et al., 2011). In *Drosophila*, five different types of chromatin have been identified, two of which are classic

heterochromatin, characterised by the presence of either heterochromatin protein 1 (HP1) or Polycomb proteins, two are different euchromatic chromatin states and the bulk of chromatin is silent, non-HP1- or -Polycomb-associated chromatin, which is devoid of associated proteins and histone posttranslational modifications (black or "null" chromatin) (Filion et al., 2010). Similarly, in human cells, four principal chromatin states have been detected: euchromatin, Polycomb-silenced chromatin, HP1-associated heterochromatin and silent "null" chromatin (Ciabrelli & Cavalli, 2014; Julienne et al., 2013) (Table 1.2). If further subdivided, chromatin adopts specific and distinct structures at promoters, actively transcribed regions, regulatory elements, silenced and repetitive regions, like telomeres, centromeres and pericentromeric regions (Ernst & Kellis, 2010; Ernst et al., 2011; Julienne et al., 2013; Ram et al., 2011) (Figure 1.30).

Chromatin state	Euchromatin	Polycomb-silenced	Hetero-chromatin	Null chromatin
H3K4me3	++	-	-	-
H3K36me3	++	-	-	-
H3K27ac	++	-	-	-
H3K79me2	++	-	-	-
H3K9me1	++	+	-	-
H2A.Z	++	+	-	-
H4K20me1	+	+	-	-
H3K27me3	+/-	++	-	+/-
H3K9me3	+/-	+/-	++	-
POL II	++	+/-	-	-
SIN3A	++	-	-	-
CTCF	+	+	-	+/-
HP1γ	++	+/-	-	-

Table 1.2 Chromatin marks associated with the four principal chromatin states. Adapted from Julienne et al. 2013. ++ strong enrichment of mark, + enrichment of mark, +/- mark enriched at some loci, - mark not present. Coloured cells show chromatin modifications and proteins characteristic of the different chromatin states.

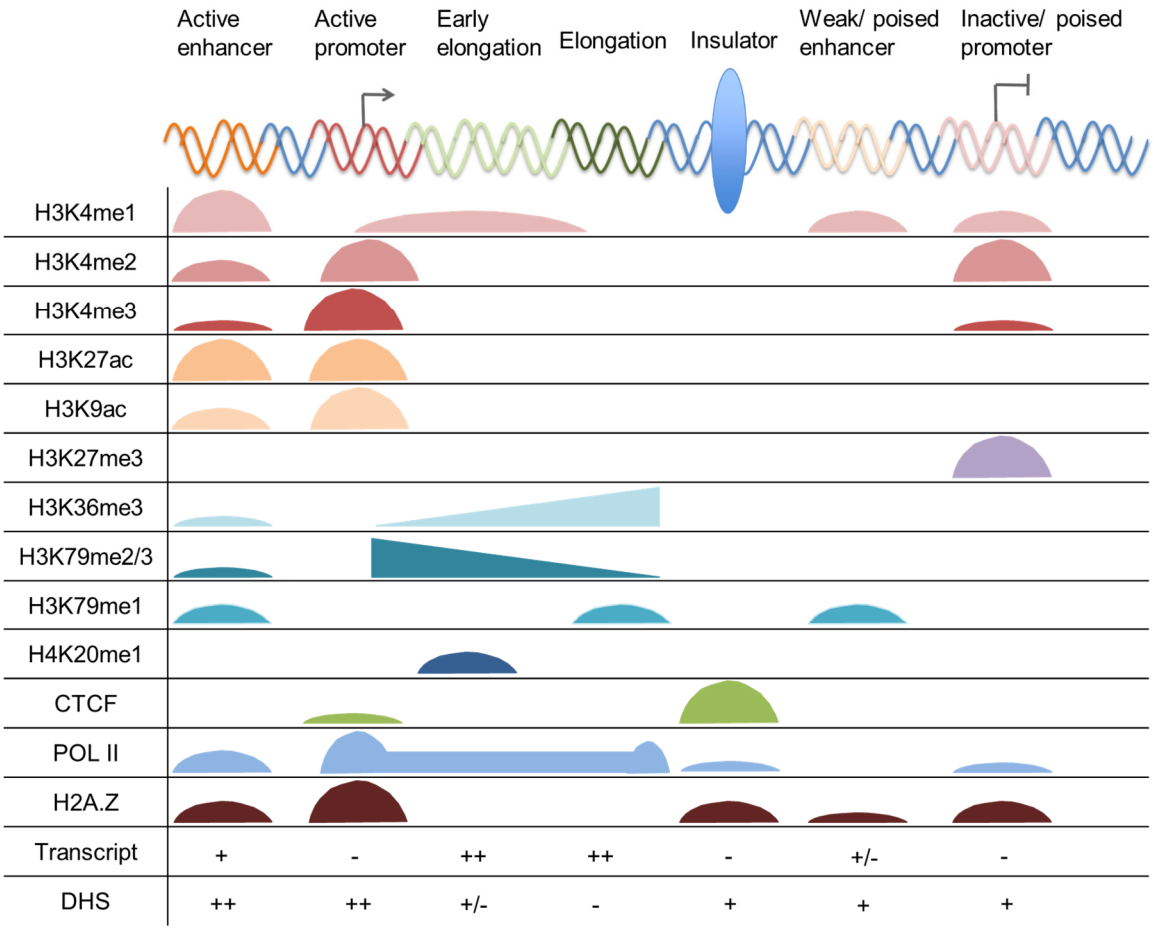

Figure 1.30 Chromatin marks and proteins associated with specific euchromatic regions.
Different combinations of chromatin modifications mark specific regions in euchromatin. These are also associated with different levels of transcription and DNase hypersensitive sites (DHS). These correlations were described by Ernst et al. 2011 and Ernst and Kellis 2010.

Further, chromatin is topologically organised in the nucleus of the cell. Inactive chromatin regions are associated with the nuclear lamina, while actively transcribed domains are localised to the centre of the nucleus (Foster & Bridger, 2005; Guelen et al., 2008). Moreover, specific microdomains have recently been identified, so called topologically associating domains (TADs). These are linear, about 1 Mb long stretches of chromatin, which fold into three-dimensional structures and are separated from each other by house-keeping genes or insulators (Ciabrelli & Cavalli, 2014; Dixon et al., 2012). The lengths of these TADs are conserved among cell types, while the intrinsic organisation can be variable, even in cells of the same type (Dixon et al., 2012; Nagano et al., 2013). Each TAD adopts one of the four principal chromatin states and genes within a TAD are usually co-regulated (Ciabrelli & Cavalli, 2014). Although intra-TAD interactions are preferred, long-range interactions between different TADs can also be observed (Nagano et al., 2013). Interactions occur between promoters and

enhancers as well as between co-regulated promoters to enhance or repress transcription (Li et al., 2012).

1.7.2 Transcription through chromatin

Chromatin is generally a repressive environment for transcription. Nucleosomes pose a barrier towards the POL II and inhibit binding of transcription factors to DNA (Petesch & Lis, 2012). Consistently, densely packed chromatin inhibits processive transcription, while open chromatin, regions with low nucleosome occupancy and high nucleosome turnover are accessible for the transcription machinery. Therefore, transcriptional regulation occurs largely at the level of nucleosomes and there is extensive cross-talk between POL II, transcription factors, histone variants, histone posttranslational modifications and chromatin remodelling complexes. For example, histone variants and histone PTMs can recruit transcription factors and chromatin remodelling complexes and together they can lead to the recruitment of the POL II. Posttranslational modifications of the POL II C-terminal domain (CTD) are required for transcription, by recruiting RNA processing enzymes (Cho et al., 1997; Ghosh et al., 2011), but also by binding enzymes that modify or remodel histones (Kizer et al., 2005; Kwon et al., 2010). Therefore, modifications of the POL II CTD during transcription, histone variants and histone PTMs are reviewed in the following sections.

1.7.2.1 The POL II transcription cycle

The largest subunit of the POL II carries an extended C-terminal domain (CTD), which consists of 52 heptad repeats with the consensus sequence Y-S-P-T-S-P-S (Egloff & Murphy, 2008). Serine, threonine and tyrosine residues in the CTD are subjected to extensive phosphorylation, which generates a CTD code (Buratowski, 2003; Heidemann et al., 2013; Komarnitsky et al., 2000).

The POL II is recruited to the chromatin in its hypophosphorylated form via interactions with general transcription factors and the Mediator. At the promoter, both S5 and S7 are phosphorylated by the TFIIH subunit CDK7 in a Mediator-dependent fashion (Boeing et al., 2010). These phosphorylation events release the POL II from the Mediator (Søgaard & Svejstrup, 2007) and S5p generates a binding platform for the capping enzyme guanylyltransferase (Cho et al., 1997; Ghosh et al., 2011) (Figure 1.31). While the POL II progresses along the gene, S5 is dephosphorylated (Tietjen et al., 2010). Several different phosphatases have been described in mammals (Hsu et al., 2014; Lehman & Dahmus, 2000; Lin et al., 2002; Thompson et al., 2006;

Washington et al., 2002; Yeo et al., 2003). S7p also peaks in the 5' region of the gene, but stays higher during transcription than S5p (Tietjen et al., 2010).

At protein-coding genes, phosphorylation of S2 occurs during elongation and peaks towards the 3' end (Tietjen et al., 2010). In the promoter region, P-TEFb mediates S2 phosphorylation, while CDK12 and CDK13 phosphorylate the elongating POL II (Bartkowiak et al., 2010). P-TEFb stimulates transcription elongation mainly through the phosphorylation of the Suppressor of Ty 5 (SPT5) subunit of DRB sensitivity-inducing factor (DSIF), an SPT4-SPT5 heterodimer (Kim & Sharp, 2001), and of the negative elongation factor (NELF) (Fujinaga et al., 2004). The NELF-DSIF complex induces pausing of the POL II 20 to 60 nt downstream of the TSS, probably via binding to nascent RNA (Kwak & Lis, 2013). P-TEFb-mediated phosphorylation of SPT5 and NELF leads to dissociation of NELF from the POL II and turns DSIF into a transcriptional activator to allow for processive elongation. DSIF and the PAF1 complex (PAF1C) bind cooperatively to the POL II and both are required for gene expression (Yexi Chen et al., 2009). S2p is essential for the recruitment of splicing and polyadenylation factors (Ahn et al., 2004; Davidson et al., 2014; Gu et al., 2013) (Figure 1.31). At the same time, efficient cleavage and polyadenylation are required for high levels of S2p (Davidson et al., 2014).

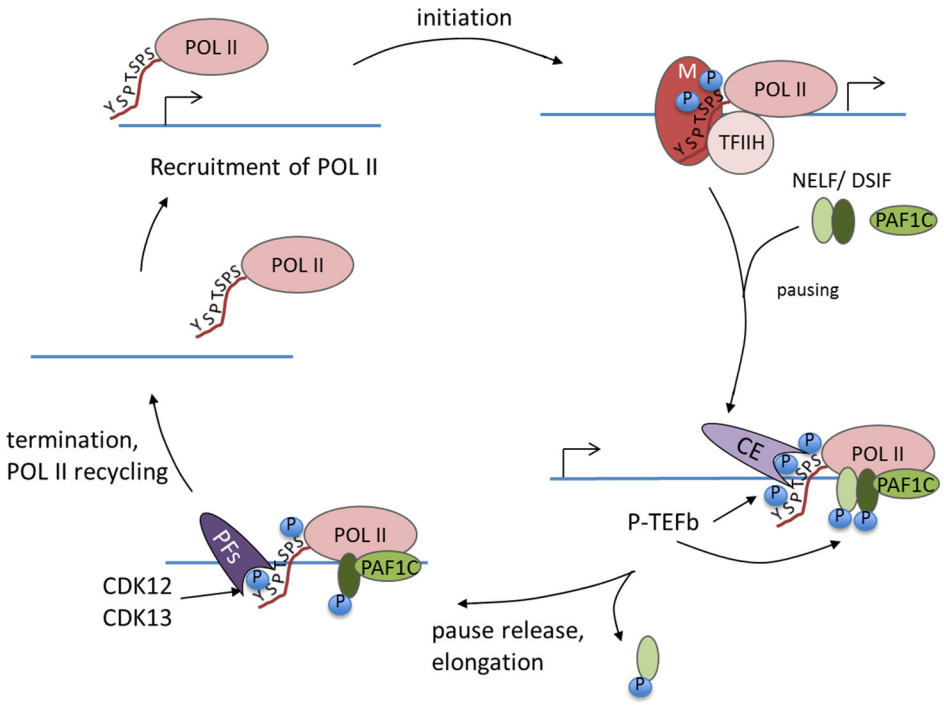

Figure 1.31 The POL II transcription cycle.
Hypophosphorylated POL II is recruited to the chromatin by the Mediator (M). Phosphorylation of the CTD S5 and S7 initiate transcription and bind the capping enzymes (CE). The NELF/DSIF complex induces pausing downstream of the TSS, which is relieved by P-TEFb. CTD S2 phosphorylation is required for the recruitment of polyadenylation factors (PFs). Phosphatases dephosphorylate the CTD and POL II is recycled.

1.7.2.2 The histone code hypothesis

Especially histone tail modifications and histone variants are predictive of different chromatin states. Enhancers are, for example, characterised by histone H3K4 monomethylation (H3K4me1) and when they are active, also by H3K27 acetylation. Core promoters are generally marked by H3K4me3 and histone acetylation, while heterochromatin is distinguished by the presence of H3K9me3 or H3K27me3 (Bernstein et al., 2005; B.E. Bernstein et al., 2006; Creyghton et al., 2010; Ernst & Kellis, 2010; Ernst et al., 2011; Heintzman et al., 2007; Heintzman et al., 2009; Mikkelsen et al., 2007; Rivera & Ren, 2013). Consistently, it had been proposed that combinations of histone post-translational modifications function as a histone code, in which marks are established sequentially or simultaneously and which is instructive for the fate of certain chromatin regions (Strahl & Allis, 2000). The marks are established by “writer” proteins and serve as docking platforms for chromatin “readers”, which often recognise distinct combinations of histone modifications. Thus, the same histone PTMs can, depending on the context, instruct different outcomes, like the activation or repression of transcription by recruiting RNA polymerases, transcription factors and co-factors or transcriptional repressors. H3K9me2/3 are, for example, associated with heterochromatin formation and recruitment of the HP1 protein (Bannister et al., 2001; Jacobs et al., 2001; Lachner et al., 2001). Phosphorylation of the adjacent H3S10 prevents HP1 binding to H3K9me2/3 (Fischle et al., 2005; Hirota et al., 2005; Papamokos et al., 2012), but can activate transcription (Winter et al., 2008).

1.7.2.3 Regulation of transcription by histone variants

As part of the histone code, histone variants, which usually differ from canonical histones by a few amino acids or extended N- or C-terminal tails, regulate transcription. In mammalian cells, the histones H1, H2A, H2B and H3 exist in several isoforms, which are associated with specific chromatin states and mediate different effector functions (Talbert & Henikoff, 2010).

1.7.2.3.1 The Histone H3.3 variant

H3.1 and H3.2 are the canonical histone H3 variants (referred to as H3), which are mainly deposited into the chromatin during DNA replication. H3.3, which differs from the canonical histone variants by 5 amino acids, can be introduced into the chromatin at any time of the cell cycle, because different histone chaperones are responsible for its deposition (Drané et al., 2010; Galvani et al., 2008; Goldberg et al., 2010; Konev et al., 2007; Tagami et al., 2004). H3.3 can be found in actively transcribed regions of the

genome and at transcription factor binding sites, but also at telomeres and pericentromeric regions (Ahmad & Henikoff, 2002; Goldberg et al., 2010; Santenard et al., 2010; Schwartz & Ahmad, 2005; Sutcliffe et al., 2009; Tagami et al., 2004; Tamura et al., 2009). Consistent with their presence in actively transcribed and regulatory regions, H3.3-containing nucleosomes are less stable than nucleosomes formed with canonical H3 and repress the formation of higher order chromatin structures (Braunschweig et al., 2009; Chen et al., 2013; Jin & Felsenfeld, 2007).

1.7.2.3.2 Histone H2A.Z

H2A can be replaced by its variant H2A.Z in promoter and pericentromeric regions (Rangasamy et al., 2003). It is integrated into the chromatin by a SWI/SNF family chromatin-remodelling enzyme, the SWR1 complex in yeast and p400 or SRCAP in humans (Gévry et al., 2007; Kobor et al., 2004; Ruhl et al., 2006). It was proposed that H2A.Z is randomly deposited throughout the genome, but that active transcription leads to the eviction of H2A.Z-containg nucleosomes and their replacement by H2A-containing nucleosomes. That explains, why H2A.Z is enriched in non-transcribed regions, like heterochromatin, but depleted from gene bodies (Hardy et al., 2009).

Knockout of H2A.Z is lethal in *Drosophila* and mice (van Daal & Elgin, 1992; Faast et al., 2001), but not in yeast. However, H2A.Z is required for the transcription of inducible genes in *S. cerevisiae* and the C-terminal portion of H2A.Z had been shown to directly interact with the POL II. H2A.Z is globally present at active and inactive promoters in yeast and facilitates stable nucleosome positioning (Guillemette et al., 2005; Raisner et al., 2005). However, upon induction of gene expression H2A.Z is removed from promoters (Adam et al., 2001; Larochelle & Gaudreau, 2003).

In *Drosophila*, H2A.Z-containing nucleosomes have been shown to pose a lower barrier to transcription than normal H2A-containing nucleosomes, probably because the H2A.Z-H2B dimer can be evicted more easily, leaving a H3-H4 tetramer that facilitates the passage of the POL II (Weber et al., 2014). Genome wide studies in human cells showed that H2A.Z is generally associated with distal regulatory elements, independent of their activation status. In contrast to yeast, it is however only associated with active or poised, but not silent, promoters. Nevertheless, like in yeast, H2A.Z-containing nucleosomes are found flanking the nucleosome-free region (NFR) (Barski et al., 2007; Hardy et al., 2009) and H2A.Z leads to stable positioning of nucleosomes around the NFR (Gévry et al., 2009). Specific recruitment of the variant histone is observed at silent promoters in humans prior to activation (Gévry et al., 2009; Hardy et al., 2009), possibly facilitated by transcription factors. Consistently, the oestrogen

receptor (ER) has been shown to directly associate with p400 (Gévry et al., 2007; Gévry et al., 2009). As H2A.Z deposition facilitates stable nucleosome positioning, transcription factor binding sites or the TATA box could be exposed, which allows for transcription initiation (Gévry et al., 2009) (Figure 1.32). H2A.Z is generally required for POL II recruitment, as is evident from global loss of POL II from the chromatin upon H2A.Z knockdown (Hardy et al., 2009). After recruitment of the POL II, H2A.Z is lost from the promoters to allow for elongation (Gévry et al., 2007; Hardy et al., 2009; John et al., 2008). Consistent with a role in POL II recruitment to promoters, the proximity of H2A.Z to the TSS correlates with POL II occupancy and with the level of gene expression in mouse brain and liver (Bargaje et al., 2012).

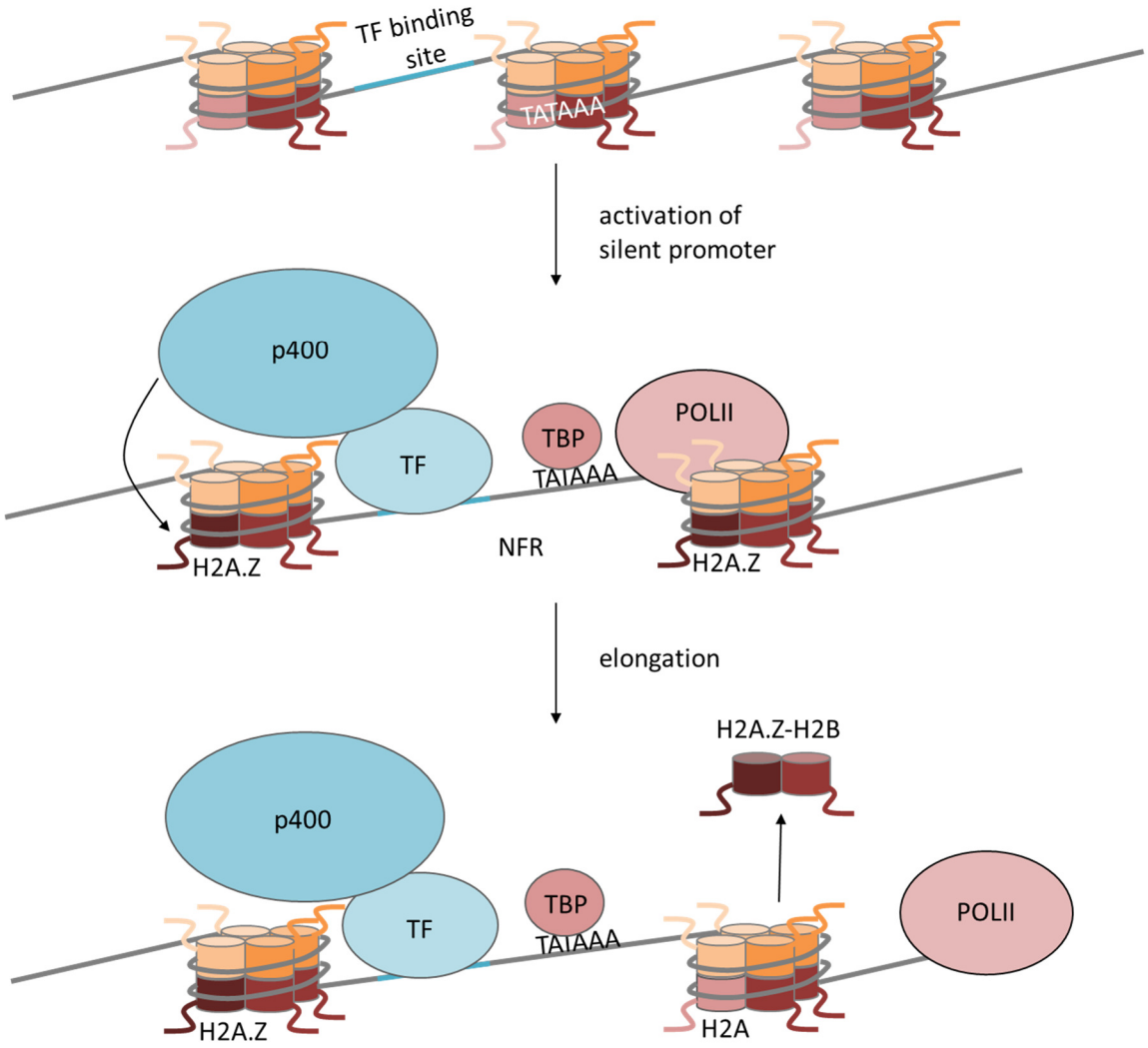

Figure 1.32 Deposition of H2A.Z at promoters.
H2A.Z is absent from silent promoters and is deposited during activation by the p400 chromatin remodelling complex. H2A.Z facilitates the stable generation of a nucleosome-free region (NFR) and is required for POL II recruitment. Upon induction of gene expression, H2A.Z is evicted.

1.7.2.4 Histone posttranslational modifications

Although histone variants are part of the histone code, it is mainly fomed by diverse PTMs of histones, especially histone tails. These modifications add another layer of complexity to the histone code. Lysines can be mono-, di- or trimethylated, acetylated, ubiquitinated or SUMOylated, arginines can be mono-, symmetrically or asymmetrically dimethylated, citrullinated or ADP-ribosylated. Glutamine residues can also be methylated. Phosphorylation of serine, threonine and tyrosine residues and N-acetylglucosaminylation of serine and threonine residues can take place. Further, proline isomerisation has been observed (Sakabe et al., 2010).

1.7.2.4.1 Histone acetylation

Acetylation of lysine residues reduces the positive charge of histones, disrupts histone-DNA interactions and is generally associated with transcriptional activation (Bannister & Kouzarides, 2011). Nuclear histone acetyltransferases (HATs) can be divided into at least three families, the GCN5-related N-acetyltransferase (GNAT), the MOZ, Ybf2, Sas2 and Tip60 (MYST) and the CBP/p300 families (Yang & Seto, 2007). HATs form large, up to several MDa, multiprotein complexes that allow them to be active *in vivo* (Allard et al., 1999; Grant et al., 1997; John et al., 2000). Acetyl moieties are removed by histone deacetylases (HDACs), which are usually part of HDAC complexes, including the SIN3A complex (Bannister & Kouzarides, 2011).

Acetylated histone residues that are widely associated with transcriptional activation are H3K9, H3K14, H3K27, H3K56, H4K5, H4K8, H4K12 and H4K16 (Smolle & Workman, 2013). Apart from fulfilling a passive function through destabilising histone-DNA interactions, acetylation marks can also directly be recognised by the bromodomains and tandem plant homeodomain (PHD) fingers of histone modification reader proteins (Dhalluin et al., 1999; Lange et al., 2008; Qiu et al., 2012; Yap & Zhou, 2010; Zeng et al., 2010).

One protein recruited to acetylated lysine residues is the $TAF_{II}250$ subunit of the TFIID, which recognises di- or tetraacetylated H4 via its double bromodomain (Jacobson et al., 2000). Other bromodomain-containing proteins are the acetyltransferases CBP, p300, GCN5 and PCAF, the chromatin remodelling enzymes SWI/SNF related, matrix associated, actin-dependent regulator 2 (SMARCA2) and SMARCA4, Mixed lineage leukaemia (MLL1) and some transcription factors (Dhalluin et al., 1999; Filippakopoulos et al., 2012; Hudson et al., 2000; Ragvin et al., 2004; Shen et al., 2007; Zeng et al., 2008) (Figure 1.33). Important acetyl lysine binding proteins are the bromodomain and extra terminal domain (BET) proteins (BRDs), a family consisting of BRD2, BRD3,

BRD4 and BRDT (Filippakopoulos et al., 2012; Shi & Vakoc, 2014). These proteins have two bromodomains and recognise dually acetylated substrates (Dey et al., 2003). They serve as adaptor proteins to recruit transcriptional regulators. BRD4 has been shown to recruit P-TEFb (Jang et al., 2005; Yang et al., 2005), the Mediator (Houzelstein et al., 2002; Jiang et al., 1998; Yang et al., 2005), the H3K36 mono- and dimethyltransferase NSD3 and the arginine demethylase Jumonji domain-containing protein (JMJD6) to facilitate transcription inititation and elongation (Rahman et al., 2011). BRD4 has also been described as an atypical protein kinase that can phosphorylate the POL II CTD S2 directly (Devaiah et al., 2012). Consistently, BRD4 has been shown to occupy promoters and enhancers genome-wide together with Mediator and POL II S2p (Lovén et al., 2013; W. Zhang et al., 2012). Recently, BET inhibitors have been developed and have been shown to be effective in inhibiting growth of Burkitt lymphoma, multiple myeloma and AML cell lines. One mechanism of action is the inhibition of transcription of *MYC* and *BCL2* (Dawson et al., 2011; Delmore et al., 2011; Mertz et al., 2011).

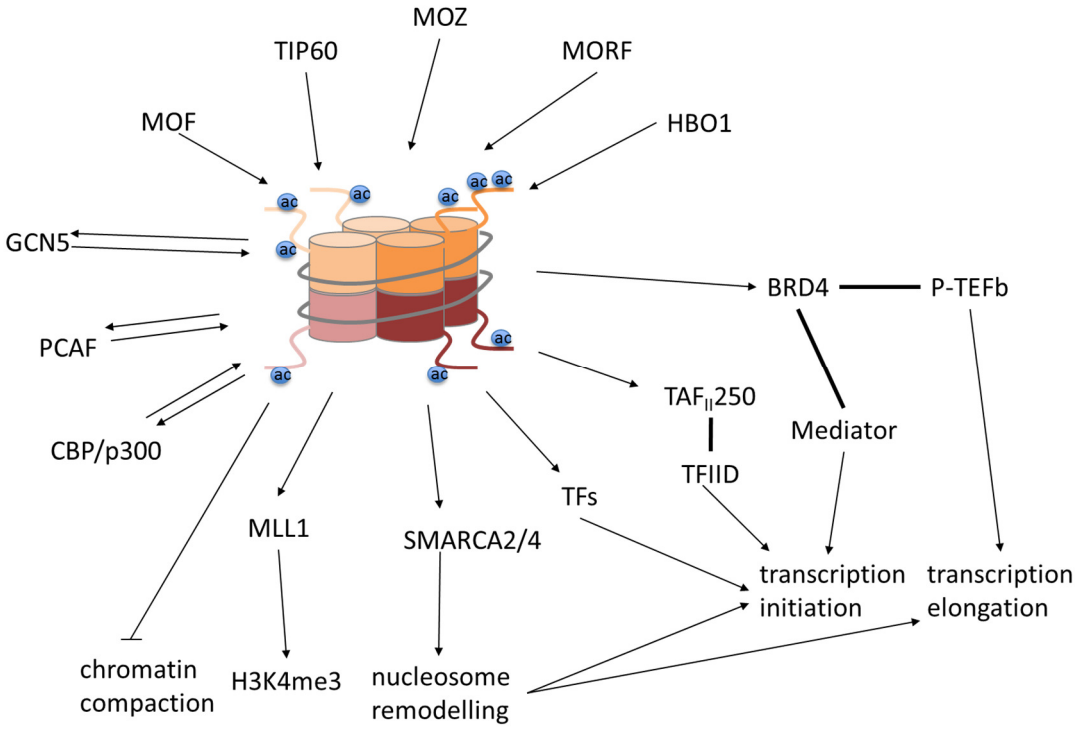

Figure 1.33 Regulation and functions of histone acetylation.
Writers of histone acetylation marks are acetyltransferases of the MYST family (MOF, TIP60, Monocytic leukaemia zinc finger protein (MOZ), MOZ-related factor (MORF) and Histone acetyltransferase bound to ORC (HBO1)), the GNAT family (GCN5, PCAF) and the p300/CBP family. These acetyltransferases are themselves readers of the acetylation marks and other reader proteins include the MLL1 methyltransferase, the SWI/SNF family proteins SMARCA2/4, BRD4 and transcription factors (TFs). Further, acetylation of histones generally counteracts chromatin compaction by changing the charge of the nucleosome.

1.7.2.4.2 Histone methylation

Methylation of lysines competes with acetylation of the same residues. Methylation does not change the charge of the histones and does thus not disrupt histone-DNA interactions (Bannister & Kouzarides, 2011). Therefore, the main purpose of methylation marks is to recruit specific proteins to stimulate or suppress transcription. Methylation occurs on several lysines, but the best-characterised are H3 lysines 4, 9, 27, 36, 79 and histone H4K20 (Tan et al., 2011; Wozniak & Strahl, 2014). These lysine methylation marks show a specific distribution along transcribed genes, at enhancers and at repressed chromatin regions.

1.7.2.4.2.1 H3K4 methylation

H3K4me2/3 are high in active core promoter regions (Bernstein et al., 2005; Koch et al., 2007), H3K4me1/2 can be found further downstream of the TSS (Koch et al., 2007) and H3K4me1 marks active or poised enhancers (Heintzman et al., 2007). In humans, six H3K4 methyltransferases, which are only functional in multiprotein complexes homologous to the yeast Set1/COMPASS (Complex proteins associated with Set1) complex, have been identified: SET domain-containing 1A (SET1A), SET1B and MML1-4 (Shilatifard, 2012). SET1A/B are responsible for the bulk of H3K4me3 in the cells (Wu et al., 2008), MLL1 and MLL2 are required for H3K4me3 only at a subset of genes (P. Wang et al., 2009) and MLL3/4 have recently been described as the major enhancer-associated monomethyltransferases (Herz et al., 2012; D. Hu et al., 2013).

Di- and trimethylation of H3K4, but not H3K4me1, through the SET1 complex are stimulated by monoubiquitination of H2BK120, which is carried out by the RAD6/BRE1 E2/E3 complex. H2Bub is found in the promoters and gene bodies of transcribed genes and, interestingly, on-going transcription is required for efficient H2B ubiquitination (Kim et al., 2009). Further, the PAF1C is required for proper H2B ubiquitination and H3K4 methylation. It binds to the POL II and serves as a docking platform for both the RAD6/BRE1 and, at least in yeast, the SET1 complex (Kim et al., 2009; Krogan et al., 2003; Ng et al., 2003; Zhu et al., 2005). In mice and humans, MLL1 has been shown to interact with the PAF1C (Milne et al., 2010; Muntean et al., 2010).

Chromatin readers recognise methylation marks through PHD fingers, chromodomains, Tudor, Bromo-adjacent homology domain (BAH), PWWP or CW domains (Wozniak & Strahl, 2014). H3K4me3 recruits several transcription activating proteins, like the TAF3 subunit of the TFIID via its PHD finger (Vermeulen et al., 2007). The efficiency of TFIID recruitment, and thus of the preinitiation complex, can therefore be fine-tuned through binding of TBP to the TATA box, through histone H4 acetylation and through H3K4me3

(Wozniak & Strahl, 2014). Other proteins recruited by H3K4me3 are the chromatin remodelling enzyme chromodomain helicase DNA-binding protein 1 (CHD1) (Lin et al., 2011), the STAGA and HBO1 HAT complexes (Hung et al., 2009; Saksouk et al., 2009; Vermeulen et al., 2010) and the Jumonji domain-containing protein 2A (JMJD2A) demethylase, which demethylates H3K9me3 and H3K36me3 (Huang et al., 2006; Kim et al., 2006). Further, in a positive feed-forward loop, SET1A/B and MLL1 complexes are recruited by H3K4me3 (Eberl et al., 2013; Milne et al., 2010; Z. Wang et al., 2010). H3K4me1 at enhancers is specifically read by the TIP60 HAT (Jeong et al., 2011). Other proteins, including the DNA methyltransferases DNMT3A and DNMT3B specifically bind to H3 that is unmethylated on K4 and their binding is inhibited by H3K4me2/3 (Ooi et al., 2007; Yingying Zhang et al., 2010). Under certain conditions, H3K4me3 can also lead to recruitment of transcriptional repressors. The SIN3A-HDAC1 complex is recruited to H3K4me3 after genotoxic stress (Shi et al., 2006) (Figure 1.34).

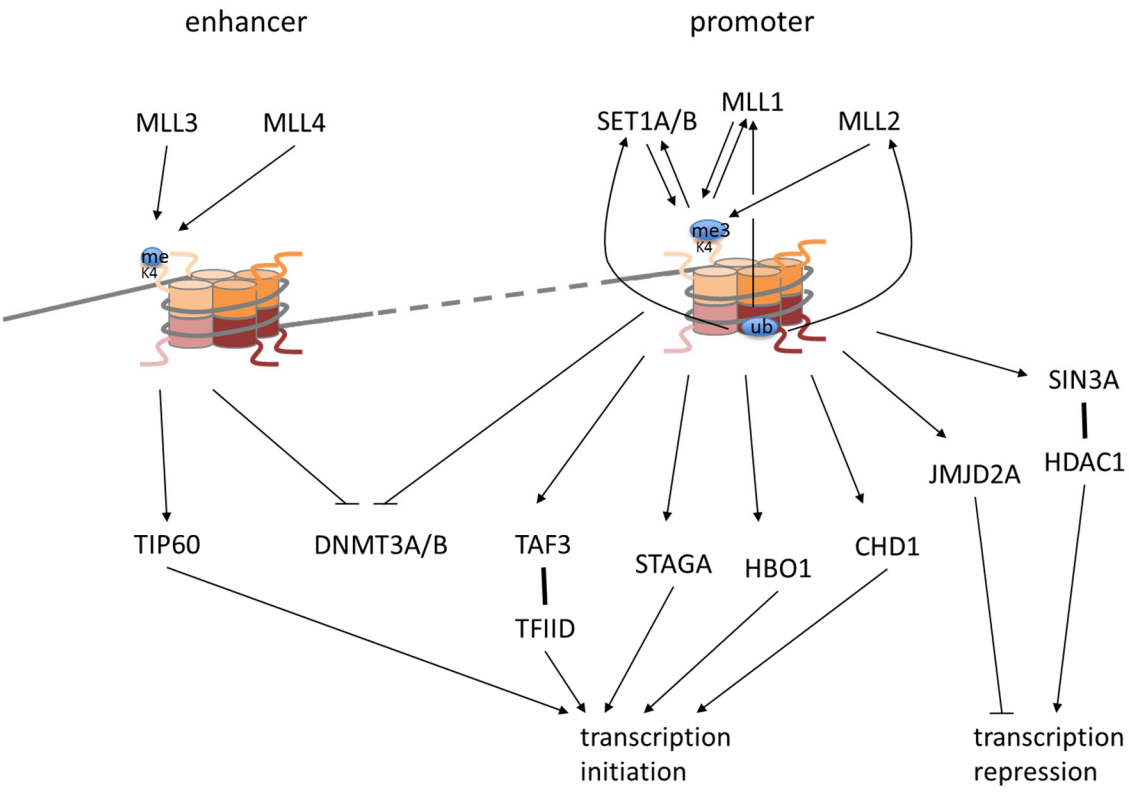

Figure 1.34 Regulation and functions of H3K4 methylation.
In humans, MLL3 and MLL4 mainly mediate H3K4me1 at enhancers, while SET1A/B, MLL1 and MLL2 mediate H3K4me3. H3K4me3 is enhanced by H2Bub. Proteins that interact with H3K4me3 are TFIID, acetyltransferases (STAGA, HBO1), the chromatin remodeller CHD1 and the demethylase JMJD2A. Generally, H3K4me3 mediates transcriptional activation, but under some conditions the SIN3A-HDAC complex can also be recruited to this mark. H3K4me1 interacts with TIP60.

1.7.2.4.2.2 H3K36 methylation

H3K36me1/2 are enriched in the 5' regions of actively transcribed genes, whereas H3K36me2/3 are higher towards the 3' end (Bannister et al., 2005; Lucio-Eterovic et al., 2010). Among others, nuclear receptor-binding SET domain proteins (NSD1/2/3) are H3K36 mono- and dimethyltransferases, whereas SET domain-containing 2 (SETD2) is a trimethyltransferase (Edmunds et al., 2008; Y. Li et al., 2009; Qiao et al., 2011; Wagner & Carpenter, 2012).

At least in yeast, the SETD2 homolog Set2 has been shown to interact with the POL II CTD that is phosphorylated on both S2 and S5 and this interaction is important for H3K36 methylation. The interaction domain is conserved in human SETD2, making it plausible that SETD2 also interacts with the POL II (Kizer et al., 2005). Further, recruitment of SETD2 to genes is increased by splicing and consistently, H3K36me3 is highest along intron-containing genes and increases over spliced exons (de Almeida et al., 2011). Conversely, H3K36me3 has also been associated with alternative splicing by recruiting proteins that suppress splice site usage (Luco et al., 2011).

In both yeast and humans, H3K36 methylation promotes the establishment of repressive chromatin to inhibit aberrant transcription initiation (Carvalho et al., 2013). H3K36me3 leads to the recruitment of the Rpd3S HDAC complex in yeast, maintaining the gene body in a hypoacetylated state to repress cryptic initiation from intragenic promoters (Carrozza et al., 2005; Joshi & Struhl, 2005; Keogh et al., 2005; Li, Gogol, et al., 2007). The homologous PF1-MRG15-SIN3B-HDAC1 complex in humans is targeted to both H3K4me3- and H3K36me3-containing nucleosomes and can thus be found directly downstream of the TSS but not throughout the transcribed region. Consistently, it regulates the level of transcription but not aberrant transcription initiation (Jelinic et al., 2011). In humans, deacetylation of the coding region is most likely mediated by HDAC6, which directly interacts with the POL II CTD (Z. Wang et al., 2009).

During transcription elongation, nucleosomes are disassembled and removal of the H2A-H2B dimer is sufficient to allow for the passage of the POL II (Belotserkovskaya et al., 2003). H3K36me3 mediates the recruitment of the histone chaperone facilitates transcription (FACT) complex, which is crucial for both the removal and the reestablishment of H2A-H2B dimers in the wake of POL II transcription (Carvalho et al., 2013). Consistently, H3K36me3 inhibits the interaction of histone chaperones with H3 in yeast, conserving the H3-H4 tetramer but allowing for exchange of the H2B-H2A dimers (Venkatesh et al., 2012). Therefore, H3K36me3 both facilitates transcription elongation and inhibits cryptic transcription initiation (Carvalho et al., 2013). Further, H3K36me3 recruits DNMT3A via its PWWP domain (Dhayalan et al., 2010).

Conversely, H3K36me3 can also recruit transcriptional activators, like the acetyltransferase MOZ (Vezzoli et al., 2010) (Figure 1.35).

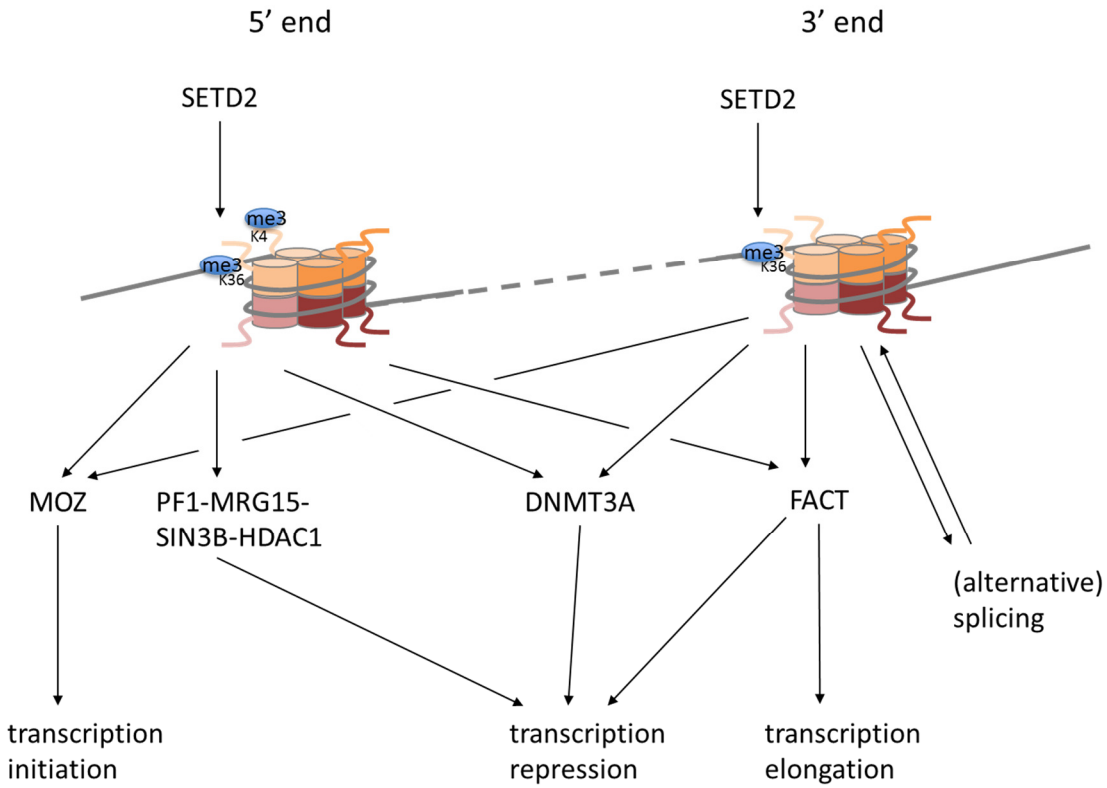

Figure 1.35 Deposition and effector functions of H3K36me3.
Trimethylation of H3K36 is mediated by SETD2. At the 5' end of genes, where H3K4me3 is also present, a HDAC1-containing complex is recruited, to mediate transcriptional repression. H3K36me3 alone is sufficient to recruit the transcriptional activator MOZ, the histone chaperone FACT, which both activates elongation and represses cryptic transcription initiation, and the transcriptional repressor DNMT3A. H3K36me3 also mediates alternative splicing and, reciprocally, its establishment is regulated by splicing.

1.7.2.4.2.3 H3K9 methylation and HP1 proteins

Methylation marks that are traditionally associated with silent chromatin are H3K9me3, H3K27me3 and H4K20me3. Methyltransferases for H3K9 are histone H3K9 methyltransferase 3 (G9A) (Tachibana et al., 2001), G9A-like protein (GLP) (Ogawa et al., 2002), SET domain-containing B1 (SETDB1) (Schultz et al., 2002), PR domain containing 2 (PRDM2) (K.-C. Kim et al., 2003), suppressor of variegation 3-9 homolog 1 (SUV39H1) (Rea et al., 2000) and SUV93H2 (O'Carroll et al., 2000). Demethylases belong to the Jumonji domain-containing histone demethylase (JHDM2/KDM3) (Yamane et al., 2006), JMJD2/KDM4 (Cloos et al., 2006; Fodor et al., 2006; Klose et al., 2006; Whetstine et al., 2006) and KDM8 families (Horton et al., 2010; Krishnan et al., 2011; Loenarz et al., 2010).

The best-studied H3K9me3 interacting proteins are the heterochromatin proteins HP1α, HP1β and HP1γ. They recognise H3K9me3 with their chromodomain (Bannister et al., 2001; Jacobs et al., 2001; Lachner et al., 2001) and dimerise via their chromoshadow domain (Brasher et al., 2000; Cowieson et al., 2000). Further, the dimeric chromoshadow domain interacts with other proteins, like SUV39H1 and SUV420H2, which methylates H4K20 (Souza et al., 2009; Yamamoto & Sonoda, 2003) (Figure 1.36). While HP1α and HP1β are mainly associated with constitutive heterochromatin (Minc et al., 1999), HP1γ can be found in both eu- and heterochromatin (Minc et al., 2000).

The exact mechanisms for heterochromatin formation are not yet clear. HP1 proteins associate with the chromatin in a dynamic fashion and this dynamic interaction is required for chromatin condensation (Cheutin et al., 2003; Festenstein et al., 2003). SUV39H1, in contrast, seems to stably bind heterochromatic regions. Therefore, it was proposed that SUV39H1 recruits HP1 to heterochromatin via direct protein-protein interactions and H3K9 methylation (Krouwels et al., 2005). This hypothesis is supported by experiments in mouse ES cells expressing a SUV39H1 mutant deficient for HP1 interaction. In these cells, SUV39H1 was recruited to pericentromeric regions but HP1 and SUV420H recruitment were impaired (Muramatsu et al., 2013). HP1 and SUV93H1 also interact with DNMT1 and DNMT3A (Fuks et al., 2003) and the methyl CpG-binding protein 2 (MeCP2) interacts with and recruits HP1, reinforcing heterochromatin formation (Agarwal et al., 2007). Further, non-coding RNAs (ncRNAs) are implicated in the establishment of heterochromatin (Bouzinba-Segard et al., 2006; Deng et al., 2009; Pal-Bhadra et al., 2004) (Figure 1.36).

H3K9me2/3 and HP1γ-S83p are also associated with the body of actively transcribed, euchromatic genes and HP1γ directly interacts with the POL II CTD, when it is phosphorylated at S2 or S5 (Lomberk et al., 2006; Vakoc et al., 2005). *Drosophila*

HP1c interacts with the FACT complex and recruits it to the elongating POL II (Kwon et al., 2010). Further, HP1γ promotes inclusion of alternative exons by slowing down the POL II, which allows for binding of the spliceosome to weak splice sites, and by binding to the nascent mRNA (Saint-André et al., 2011). In addition, HP1 proteins are also associated with gene repression. Transcription factors can recruit SUV39H1 or G9A and HP1 to mediate chromatin compaction (Xiaoping Chen et al., 2009; Lee et al., 2010; Lomberk et al., 2012; Nielsen et al., 2001; Yahi et al., 2008). However, at least in *Drosophila*, some genes which are transcribed in a heterochromatin environment, require HP1 proteins for their expression (Lu et al., 2000).

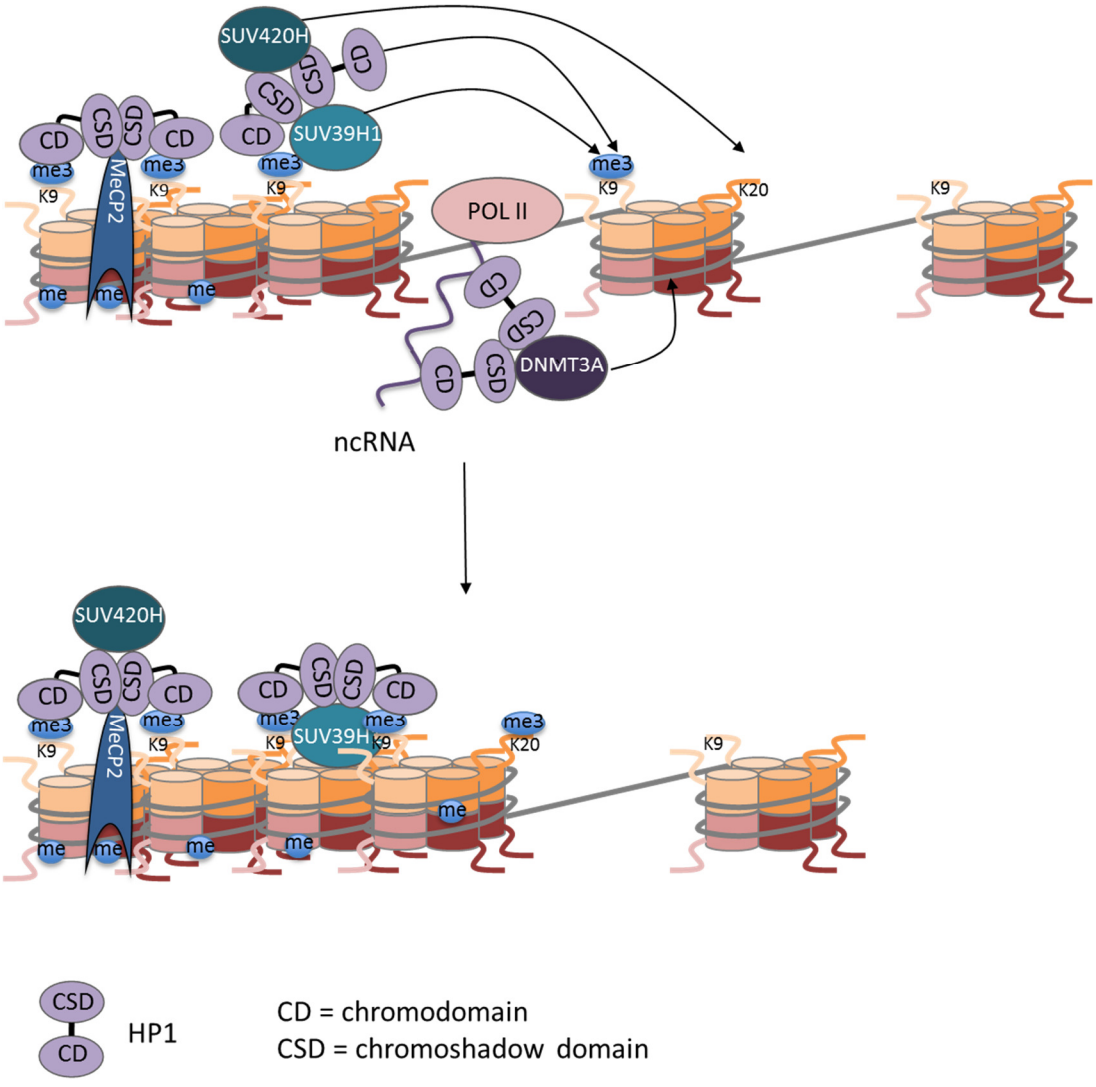

Figure 1.36 Heterochromatin formation.
Mechanisms implicated in heterochromatin formation are the recruitment of HP1 proteins by H3K9me3, SUV39H1, MeCP2 and ncRNAs. Conversely, HP1 also recruits DNMT3A and SUV20H to reinforce heterochromatin formation. Interaction of HP1 with the chromatin is very dynamic.

1.7.2.4.2.4 H3K27 methylation and Polycomb complexes

Mono-, di- and trimethylation of H3K27 is mediated by enhancer of zeste homolog 1 (EZH1) and EZH2, which are part of the Polycomb repressive complex 2 (PRC2) (Ferrari et al., 2014; Shen et al., 2008). H3K27me3 is associated with transcriptional silencing. It serves as a docking site for the PRC1 (E. Bernstein et al., 2006; Cao et al., 2002; Fischle et al., 2003; Kaustov et al., 2011; Min et al., 2003), which contains the ubiquitin E3 ligase RING1 and mediates H2AK119 ubiquitination (Cao et al., 2005; Wang et al., 2004). PRC1 mediates chromatin compaction and gene repression, which is dependent on H2Aub at some genes but not others (Endoh et al., 2012; Francis et al., 2004). In a positive feedforward loop, H2Aub leads to further PRC2 recruitment (Kalb et al., 2014).

It is only incompletely understood, how PRC2 is initially recruited to the DNA, but binding to unmethylated CpG islands, recruitment by transcription factors and the involvement of ncRNAs have been described (Arnold et al., 2013; Dietrich et al., 2012; Herranz et al., 2008; Kanhere et al., 2010; Ku et al., 2008; Lynch et al., 2012; Mendenhall et al., 2010; Rinn et al., 2007; Tanay et al., 2007; Zhao et al., 2008). In a feedforward loop, PRC2 also binds to H3K27me3 (Margueron et al., 2009). Intriguingly, recent studies suggest that PRCs do not initiate gene silencing but are recruited to already silenced loci, probably to reinforce and maintain silencing (Hosogane et al., 2013; Riising et al., 2014; Yuan et al., 2012). Many PRC targets are poised genes, which are marked by both H3K4me3 and H3K27me3 (Pan et al., 2007; Zhao et al., 2007). They are occupied by S5 phosphorylated POL II and can be rapidly activated (Brookes et al., 2012).

1.7.2.4.3 Histone phosphorylation

Especially H3S10 and H3S28 phosphorylation are associated with rapid transcriptional activation upon stimulation with growth factors, cytokines or after stress (Mahadevan et al., 1991; Sawicka et al., 2014; Yamamoto et al., 2003). Histone phosphorylation is involved in the regulation of gene expression by extracellular signals. Many signalling kinases can translocate into the nucleus and phosphorylate chromatin-associated proteins, like histones, transcription factors, the POL II or structural proteins to regulate gene expression (Baek, 2011; Koike et al., 2000; Tee et al., 2014). Phosphorylation of H3S10 by Aurora A and B, of H3T11 by Zipper-associated protein kinase (ZIPK) and phosphorylation of H3S28 were initially linked to mitosis and meiosis (Crosio et al., 2002; Goto et al., 1999; Gurley et al., 1978; Paulson & Taylor, 1982; Preuss et al., 2003; Wang et al., 2006; Wei et al., 1998). Later, these marks have also been associated with rapid transcriptional activation and H3S10 is phosphorylated in apoptotic cells (Park & Kim, 2012).

1.7.2.4.3.1 Phosphorylation of H3S10 and H3S28

Kinases known to target H3S10 are PIM1 (Zippo et al., 2007), IKKα (Anest et al., 2003; Yamamoto et al., 2003), CDK8 (Meyer et al., 2008), MSK1/2 (Soloaga et al., 2003; Strelkov & Davie, 2002; Thomson et al., 1999), JNK (Tiwari et al., 2012), PKA (DeManno et al., 1999) and COT (Choi et al., 2008). MSK1/2 also phosphorylate H3S28 (Soloaga et al., 2003; Zhong et al., 2001) (Figure 1.37). The kinases are usually recruited by transcription factors. MSK1/2 can be recruited by ELK1 (Hsu et al., 2013; H.-M. Zhang et al., 2008), the progesterone receptor (Vicent et al., 2006) and NFκB (Vermeulen et al., 2003). PIM1 is recruited by MYC (Zippo et al., 2007), IKKα binds to NFκB (Anest et al., 2003), JNK is recruited by NF-YA (Tiwari et al., 2012) or the ER (Sun et al., 2012) and CDK8 is part of a specific Mediator (Wang et al., 2001).

Phosphorylation of either S10 or S28 lead to gene activation. Consistently, tethering MSK1 to target genes is sufficient for the activation of transcription (Lau & Cheung, 2011) and H3S28p can also stimulate POL III-mediated transcription (Q. Zhang et al., 2011). Although MSK1/2 can phosphorylate both H3S10 and H3S28, these modifications do not occur together on the same nucleosome or even the same promoter region *in vivo* (Drobic et al., 2010; Dunn & Davie, 2005; Dyson et al., 2005). Interestingly, different stimuli can lead to the recruitment of distinct kinases to the same promoters to mediate transcriptional activation. For example, MSK1/2 lead to H3S10 phosphorylation in response to growth factors, but they are dispensable for phosphorylation of H3 at the same promoters in response to TNF stimulation (Duncan et al., 2006).

Nucleosomes which contain phosphorylated H3 are hyperacetylated (Barratt et al., 1994) and both acetylation and phosphorylation of the same histone tail are required for efficient gene activation (Clayton et al., 2000; Hauser et al., 2002; Soloaga et al., 2003). Consistently, yeast Gcn5 has been shown to preferentially acetylate histone H3 that is phosphorylated on S10 (Cheung et al., 2000; Lo et al., 2000), while MSK1, on the other hand, does not prefer acetylated substrates (Liokatis et al., 2012). Further, IKKα-mediated H3S10 phosphorylation is required for subsequent H3K14 acetylation by CBP (Yamamoto et al., 2003) and CDK8-Mediator can be found in a complex with TRRAP/GCN5L to mediate phosphoacetylation of H3 and activate transcription (Meyer et al., 2008). Further, phosphorylation of H3 by MSK1 stimulates H4K12 but not H4K16 acetylation (Lau & Cheung, 2012), whereas PIM1-mediated H3S10 phosphorylation stimulates H4K16 but not H4K12 acetylation (Zippo et al., 2009). H3 phosphorylation by MSK1/2 can also lead to the inhibition of deacetylation, for example by displacing the SIN3A-HDAC2 complex from the HDAC1 promoter (Sawicka et al., 2014).

H3S10p and H3S28p can be recognised by several members of the 14-3-3 adapter protein family, which bind substrates as homo- or heterodimers (Keum et al., 2012; Macdonald et al., 2005; Walter et al., 2008). While H3S28p is strongly bound, binding to H3S10p is weak and requires concomitant acetylation of K9 or K14, with S10pK14ac being the best substrate (Macdonald et al., 2005; Walter et al., 2008; Winter et al., 2008). 14-3-3 proteins are essential for phosphorylation-dependent induction of gene expression and knockdown of 14-3-3 is sufficient to inhibit expression of the HDAC1 gene, without affecting phosphoacetylation (Winter et al., 2008). 14-3-3ε has been shown to bind the CDK9 subunit of P-TEFb to facilitate POL II S2 phosphorylation and pause release (Keum et al., 2012). Similarly, 14-3-3ζ can recruit the MOF acetyl transferase to PIM1-phopshorylated enhancer regions, which leads to the recruitment of P-TEFb (Zippo et al., 2009). 14-3-3 proteins and MSK1 also form a multiprotein complex with the SWI/SNF chromatin remodeller, recruiting it to immediate early genes (Drobic et al., 2010). The 14-3-3ε/ζ heterodimer can recruit the H3K4 methyltransferase SET and MYND domain-containing 3 (SMYD3) and the p52 subunit of TFIIH to activate transcription (Li et al., 2011) (Figure 1.37).

Interestingly, H3S10pK14ac and H3K9me2S10pK14ac are equally good substrate for 14-3-3 proteins, suggesting that phosphoacetylation of the H3 tail can override inhibitory K9 methylation to activate gene expression (Winter et al., 2008). Moreover, H3S10p mediates dissociation of repressive HP1 proteins from H3K9me2/3 (Fischle et al., 2005; Hirota et al., 2005; Papamokos et al., 2012). While most studies suggest that S10p is sufficient for the dissociation, one study claims that both S10p and K14ac have to be present (Mateescu et al., 2004). Further, H3K9me3S10p is present at Polycomb-regulated genes in conjunction with H3K27me3. The K9me3S10p double modification

reduces binding of PRCs and paused POL II to the promoters and mediates stable gene repression in differentiated cells (Sabbattini et al., 2014). Furthermore, H3S28p can trigger the release of PRC from promoters, facilitate H3K27 acetylation and gene activation (Gehani et al., 2010; Lau & Cheung, 2011).

Phosphatases for H3S10p include MAP kinase phosphatase 1 (MKP1), which preferentially binds H3 when it is phosphoacetylated (Gadewal et al., 2013; Kinney et al., 2009), protein phosphatase 1 (PP1) (Qian et al., 2011) and PP2A (Simboeck et al., 2010). PP1 can also target H3S28p (Qian et al., 2011) (Figure 1.37).

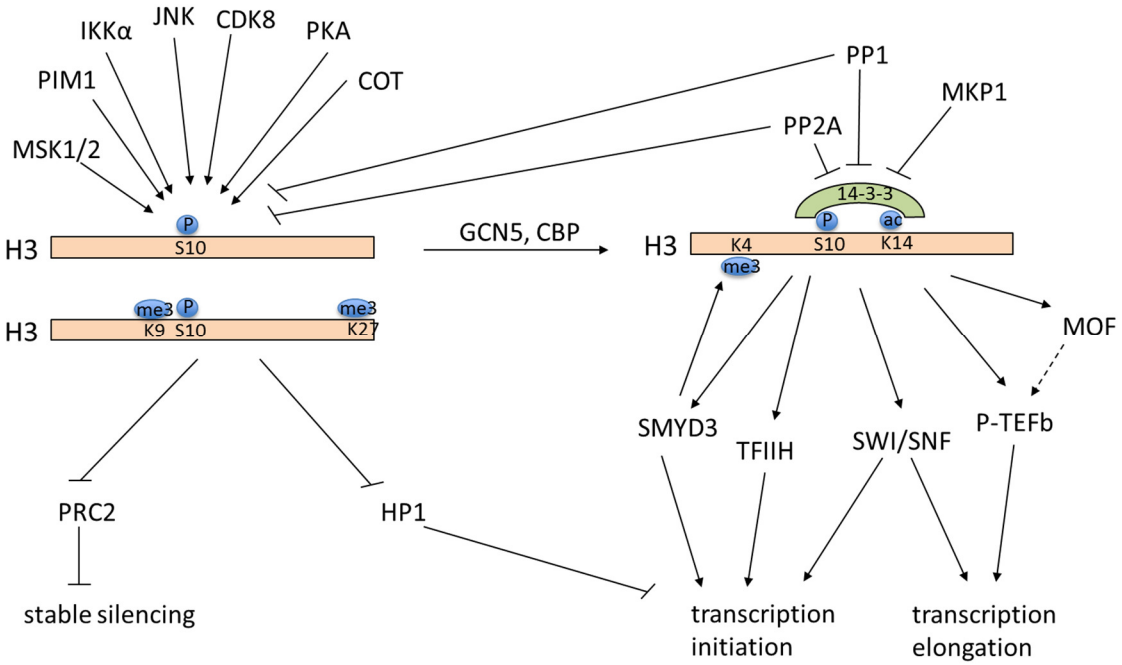

Figure 1.37 Kinases that mediate H3S10 phosphorylation and target proteins. Several kinases, like MSK1/2, PIM1, IKKα, JNK, CDK8, PKA and COT phosphorylate H3S10. Simultaneous acetylation of H3K14 leads to the recruitment of 14-3-3 proteins, which serve as adaptors for TFIIH, the H3K4 methyltransferase SMYD3, the nucleosome remodelling complex SWI/SNF and P-TEFb, either directly or via MOF, acetylation of H4 and the BRD4 adapter protein. These effectors stimulate transcriptional initiation or elongation. Further, H3S10p leads to displacement of HP1 and the double H3K9me3S10p mark displaces PRC2 from repressed promoters, leading to stable gene silencing.

1.7.2.4.3.2 Other histone phosphorylation marks

Effects of histone phosphorylation marks other than H3S10p on transcription have hardly been studied and are only poorly understood. Intriguingly, apart from H3S10, both RSK2 and MSK1 have been shown to phosphorylate histone H2AS1, which inhibits transcription (Postnikov et al., 2006; Zhang et al., 2004).

Further, the H3.3-specific S31 can be phosphorylated. One kinase which mediates H3.3S31 phosphorylation is IKKα. IKKα can bind to the POL II CTD S2p and S5p and travel with the POL II along the gene to mediate intragenic H3.3S31 phosphorylation. HP1γ facilitates IKKα loading from the CTD onto the chromatin and inhibits H3S10 phosphorylation by IKKα, which explains the preferential S31 phosphorylation within the gene body (Thorne et al., 2012). However, the function of H3.3S31p is not yet clear.

Upon androgen receptor (AR) activation, protein kinase C-related kinase 1 (PRK1) is recruited and phosphorylates H3T11. This stimulates JMJD2 to demethylate H3K9me3 and promotes POL II S5 phosphorylation (Metzger et al., 2008). Further, H3T11p is bound by the WDR5 subunit of the MLL1 complex, which leads to an increase in H3K4me3 (Kim et al., 2014). Subsequently, PKCα and PKCβ can phosphorylate H3T6, which blocks demethylation of H3K4me1/2 but not H3K9me1/2 by LSD1 at androgen receptor target genes (Metzger et al., 2010) (Figure 1.38). Pyruvate kinase M2 (PKM2) has been shown to phosphorylate H3T11 upon EGF receptor activation and lead to activation of *MYC* and *CCND1* expression (W. Yang et al., 2012)

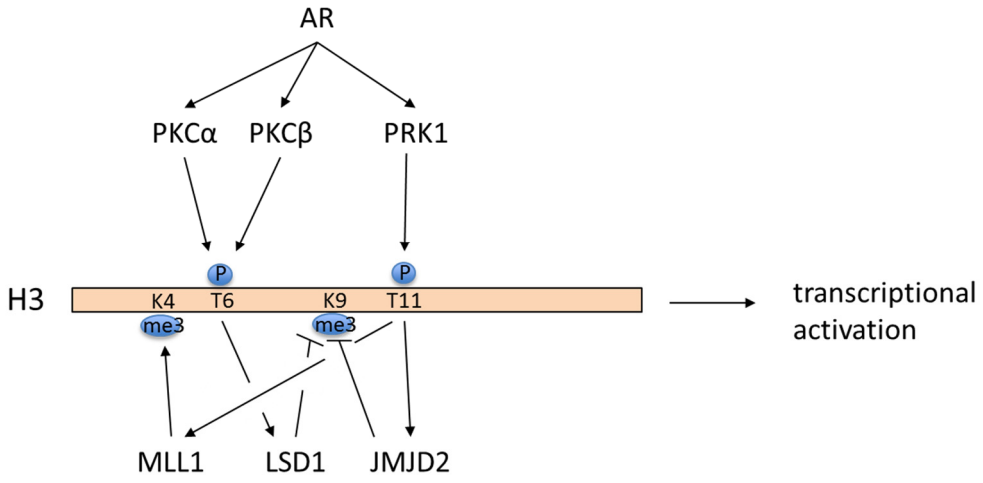

Figure 1.38 Histone H3T6 and T11 phosphorylation at AR-target genes.
Histone H3T6 or H3T11 phosphorylation by PKCs or PRK1, respectively, lead to transcriptional activation at androgen receptor target genes. H3T11p stimulates JMJD2 to demethylate K9 and recruits MLL1 to trimethylate K4. H3T6p inhibits LSD1-mediated K4 demethylation but stimulates its activity towards K9me1/2.

2 Aims and Objectives

The overall aim of this work was to analyse the effects of signalling kinases and their inhibition on chromatin structure and transcription in B cell lymphoma and leukaemia. Kinase inhibitors are now widely studied for the therapeutic use in haematopoietic malignancies and kinases affect key pathways, which are important for malignant transformation. Deregulation of these pathways results in aberrant gene expression programmes, which ultimately drive malignant transformation. Because gene expression is regulated at the chromatin level, identifying kinases, which mediate their oncogenic effects via the regulation of chromatin structure by phosphorylating histone and non-histone proteins, is of particular interest. Further, the chromatin structure is indicative of the activation status of a gene and thus the phenotype of a tumour. Therefore, global chromatin analysis could be an important tool to assess tumour stage and response to treatment.

In the first part of this study, functions of PIM kinases in DLBCL and BL were assessed. High *PIM1* and *PIM2* mRNA expression are a distinguishing factor of the more agressive ABC-DLBCL vs. GCB-DLBCL (Care et al., 2013; Wright et al., 2003). Consistent with a function in transcriptional regulation, PIM1 can be nuclear in DLBCL and BL and this is associated with progressive disease (Brault et al., 2012; Ionov et al., 2003). Further, PIM1 has been shown to associate with MYC, to phosphorylate histone H3S10 and to promote transcriptional elongation (Zippo et al., 2007; Zippo et al., 2009). Therefore, our aim was to assess the potential therapeutic value of PIM kinases in B cell lymphoma. In particular, we wanted to clarify, whether PIM kinases are important for the viability of DLBCL and BL cell lines, whether they mediate MYC-dependent gene expression in these cells and whether their effect on viability is correlated with their effect on transcriptional regulation.

In the second part of this study, the effects of Ibrutinib on the chromatin structure in CLL cells were analysed. Although Ibrutinib is already used in clinical trials for the treatment of haematological malignancies, little is known about its mechanism of action. It is hypothesised that it inhibits BCR signalling by blocking BTK (Honigberg et al., 2010). Because some patients already developed Ibrutinib resistances (Woyach et al., 2014), understanding which key pathways and chromatin-mediated effects are altered downstream of the BCR in Ibrutinib-treated cells is of vital importance to identify useful combination therapies and possibly novel drugable targets. Therefore, our aim was to identify BCR signalling-dependent chromatin changes, which are altered by Ibrutinib treatment. Histone phosphorylation, methylation and acetylation, as well as the use of histone variants, were analysed. Further, we wanted to globally assess the effects of Ibrutinib on histone modifications *in vitro* to facilitate the development of a tool for the analysis of drug response *in vivo* in patients.

3 Materials and Methods

3.1 Materials

3.1.1 Chemicals, solutions, consumables

Product	Manufacturer
0.2 ml PCR tubes	Fisher Scientific, Loughborough, UK
1.5 ml and 0.5 ml tubes	Eppendorf, Hamburg, Germany
10 x Trypsin-EDTA	Life Technologies, Carlsbad, US
100 x Penicillin/Streptomycin (pen/strep)	Life Technologies, Carlsbad, US
100 x proteinase inhibitor cocktail (PIC, P8340)	Sigma Aldrich, Dorset, UK
100 x TE	Sigma Aldrich, Dorset, UK
15 ml and 50 ml tubes	Corning Incorporated, Corning, NY, US
16% Formaldehyde	Fisher Scientific, Loughborough, UK
2 x ReddyMix PCR Master Mix	Fisher Scientific, Loughborough, UK
5 mg/ml glycogen	Life Technologies, Carlsbad, US
50 x TAE	Severn Biotech, Kidderminster, UK
Agencourt AMPure XP	Beckman Coulter, High Wycombe, UK
Amaxa® Cell Line Nucleofector® Kit V	Lonza Group Ltd, Basel, Switzerland
Amersham Hyperfilm™ ECL	GE Healthcare, Little Chalfont, UK
Axygen 96 well PCR Microplate clear, PCR-96-C	Corning Incorporated, Corning, NY, US
AZD1208	Active Biochemicals, Maplewood, NJ, US
Bradford reagent	Bio-Rad, Hertfordshire, UK
Buffers P1, P2, P3	QIAGEN, Manchester, UK
Cell culture consumable	Corning Incorporated, Corning, NY, US
Cryotubes	Sarstedt, Leicester, UK
D1000 Screen Tapes, sample buffer and ladder for 2200 TapeStation	Agilent Technologies, Stockport, UK
DAPK inhibitor	Merck Millipore, Nottingham, UK
dATP, dCTP, dGTP, dTTP	Promega, Southampton, UK
DNA Clean &Concentrator™-5 Kit	Zymo Research, Freiburg, Germany
Dulbecco's Modified Eagle Medium (DMEM)	Sigma Aldrich, Dorset, UK
Dynabeads® Protein G	Life Technologies, Carlsbad, US

EDTA tubes	Greiner Bio-One, Stonehouse, UK
Electroporation cuvettes	Cell Projects, Maidstone, UK
Ethidium bromide solution, 10 mg/ml	Bio-Rad, Hertfordshire, UK
FACS tubes	BD Biosciences, Oxford, UK
Foetal calf serum (FCS)	GE Healthcare, Little Chalfont, UK
Freezing container	Agilent Technologies, Stockport, UK
Gel Loading Dye, Blue (6 x)	New England Biolabs, Hitchin, UK
Gö6983	Merck Millipore, Nottingham, UK
GoTaq® qPCR Master Mix	Promega, Southampton, UK
HyClone™ water	Fisher Scientific, Loughborough, UK
Ibrutinib	Pharmacyclics, Sunnyvale, CA, US
Iscove's Modified Dulbecco's Medium (IMDM)	Sigma Aldrich, Dorset, UK
Lymphoprep™	Axis-Shield, Dundee, UK
MicroPlex Library Preparation™ kit	Diagenode, Seraing (Ougrée), Belgium
MMLV Reverse Transcriptase and buffer	Life Technologies, Carlsbad, US
PageRuler™ Prestained Protein Ladder	Fisher Scientific, Loughborough, UK
Phosphate buffered saline (PBS)	Sigma Aldrich, Dorset, UK
Phusion® high-fidelity polymerase and buffers	New England Biolabs, Hitchin, UK
PIM1/2 inhibitor VI	Merck Millipore, Nottingham, UK
PKCβ inhibitor	Merck Millipore, Nottingham, UK
Platinum® Pfx DNA polymerase and buffer	Life Technologies, Carlsbad, US
Polyvinylidene fluoride (PVDF) membrane, Amersham Hybond-P	GE Healthcare, Little Chalfont, UK
Proteinase K	Roche, Burgess Hill, UK
Puromycin	Sigma Aldrich, Dorset, UK
QIAGEN Plasmid Maxi Prep	QIAGEN, Manchester, UK
QIAquick Gel Extraction Kit	QIAGEN, Manchester, UK
QIAquick PCR Purification Kit	QIAGEN, Manchester, UK
Quant-iT™ Broad-Range DNA Assay Kit	Life Technologies, Carlsbad, US
Quercetagetin	Merck Millipore, Nottingham, UK
Random Primers, 3 µg/µl	Life Technologies, Carlsbad, US
Restriction endonucleases, buffers and 100x BSA	New England Biolabs, Hitchin, UK
RNase A (1 mg/ml)	Life Technologies, Carlsbad, US
RNaseOut	Life Technologies, Carlsbad, US

RPMI-1640	Sigma Aldrich, Dorset, UK
RQ1 RNAse-free DNAse and buffer	Promega, Southampton, UK
RSK inhibitor II	Merck Millipore, Nottingham, UK
SMI4a	Enzo Life Sciences, Exeter, UK
SuperSignal West Pico Enhanced Chemiluminescent Substrate/ SuperSignal West Femto Enhanced Chemiluminescent Substrate	Fisher Scientific, Loughborough, UK
T4 DNA ligase and buffer	New England Biolabs, Hitchin, UK
Taq DNA Polymerase and buffers	Life Technologies, Carlsbad, US
TRIzol®	Life Technologies, Carlsbad, US
Trypan Blue solution	Sigma Aldrich, Dorset, UK
U0126	Merck Millipore, Nottingham, UK

3.1.2 Equipment

Product	**Manufacturer**
2200 TapeStation	Agilent Technologies, Stockport, UK
ABI 7500 and ABI 7900HT	Life Technologies, Carlsbad, US
Amaxa™ Nucleofector™	Lonza Group Ltd, Basel, Switzerland
BD™ LSRII Flow Cytometer	BD Biosciences, Oxford, UK
Bioruptor®	Diagenode, Seraing (Ougrée), Belgium
Centrifuge 5415D	Eppendorf, Cambridge, UK
Centrifuge 5810R	Eppendorf, Cambridge, UK
FLUOStar GALAXY	BMG Labtech, Aylesbury, UK
Gel Doc™ XR	Bio-Rad, Hertfordshire, UK
Gene Pulser® II	Bio-Rad, Hertfordshire, UK
Heat block QBD2	Grant Instruments, Cambridge, UK
HiSeq® 2000 System	Illumina, Little Chesterford, UK
Konica SRX-101A	Konica Minolta Business Solutions (UK) Ltd, Basildon, UK
Micromix5	Euro/DPC, Gwynedd, UK
Mini-PROTEAN® System	Bio-Rad, Hertfordshire, UK
Mithras LB940 plate reader	Berthold technologies, Bad Wildbad, Germany
NanoDrop 1000	Fisher Scientific, Loughborough, UK
PTC-200 PCR cycler	M J Research Inc., Watertown, MA, US
T3000 Thermocycler	Biometr, Göttingen, Germany

Vortex mixer	Bibby Scientific, Stone, UK

3.1.3 Buffers

All chemicals were purchased from Sigma Aldrich, unless otherwise stated.

Name	**Ingredients**
10 x Annealing Buffer	300 mM HEPES-KOH, pH 7.4 1 M Potassium Acetate (KAc) 20 mM Magensium Acetate ($MgAc_2$)
10 x Running Buffer	0.25 M Tris-HCl, pH 8.6 1.9 M Glycine 1% Sodium dodecyl sulfate (SDS)
10% acrylamide separating gel	6.7 ml 30% acrylamide-bisacrylamide (29:1) solution (Severn Biotech, Kidderminster, UK) 8.3 ml dH_2O 5 ml 4 x Lower Buffer 50 µl 25% ammonium persulfate (APS) 20 µl Tetramethylethylendiamin (TEMED)
12.5% acrylamide separating gel	8.3 ml 30% acrylamide-bisacrylamide (29:1) solution 6.7 ml dH_2O 5 ml 4 x Lower Buffer 50 µl 25% APS 20 µl TEMED

2 x IP Buffer	50 mM Tris-HCl, pH 8 4 mM Ethylenediaminetetraacetic acid (EDTA) 300 mM NaCl (VWR International, Lutterworth, UK) 2% Triton X-100 0.4% SDS (Bio-Rad, Hertfordshire, UK) 0.1 x proteinase inhibitor cocktail (PIC) 2 µM Phenylmethylsulfonyl fluoride (PMSF) 0.5 mM NaF 2 mM $NaVO_3$
4 x Lower Buffer	1.5 M Tris-HCl, pH 8.8 0.4% SDS
4 x SDS Sample Buffer (SSB)	0.35 M Tris pH 6.8 30% glycerol 10% SDS 0.6 M Dithiotreitol (DTT) 0.012% bromophenol blue
Acrylamide stacking gel	0.8 ml 30% acrylamide-bisacrylamide (29:1) solution 3.6 ml dH_2O 1.5 ml Upper Buffer 50 µl 25% APS 20 µl TEMED
Buffer A	10 mM HEPES pH 8 10 mM EDTA 0.5 mM Ethyleneglycol tetraacetic acid (EGTA) 0.25% Triton X-100 0.1 x PIC 2 µM PMSF 0.5 mM NaF 2 mM $NaVO_3$

Buffer B	10 mM HEPES pH 8 200 mM NaCl 1 mM EDTA 0.5 mM EGTA 0.01% Triton X-100 0.1 x PIC 2 µM PMSF 0.5 mM NaF 2 mM $NaVO_3$
Elution Buffer	1% SDS 100 mM $NaHCO_3$
Glycerol Buffer	10 mM Tris-HCl, pH 7.4 0.1 mM EDTA 5 mM $MgAc_2$ 10% glycerol 0.1 x PIC 2 µM PMSF 0.5 mM NaF 2 mM $NaVO_3$
Hypotonic cell lysis buffer HCLB-300/ -500	20 mM HEPES, pH 7.5 0.5 mM KCl 1.5 mM $MgCl_2$ 0.5 mM DTT 0.5% Triton X-100 10% glycerol 300 or 500 mM NaCl 0.1 x PIC 2 µM PMSF 0.5 mM NaF 2 mM $NaVO_3$

LiCl Buffer	10 mM Tris-HCl pH 8 250 mM LiCl 0.5% NP40 0.5% Na deoxycholate 1 mM EDTA 0.1 x PIC 2 µM PMSF 0.5 mM NaF 2 mM $NaVO_3$
PBS-NP40	0.1% NP40 in PBS 0.1 x PIC 2 µM PMSF 0.5 mM NaF 2 mM $NaVO_3$
Propidium iodide (PI) staining solution	100 µg/ml PI in PBS 0.6% NP40 1 mg/ml RNase A
Proteinase K suspension	50 mg/ml Proteinase K in 50% glycerol 50% 1 x TE
RF1	75 mM KCl 50 mM KAc 50 mM $MnCl_2$ 10 mM $CaCl_2$ 15% glycerol pH 5.8
RF2	10 mM 3-(N-morpholino)propansulfonic acid (MOPS) 10 mM KCl 75 mM $CaCl_2$ 15% glycerol pH 6.8

RIPA	10 mM Tris-HCl 1 mM EDTA 0.5 mM EGTA 140 mM NaCl 0.1% SDS 1% Triton X-100 0.1% Na deoxycholate 1 x PIC 2 µM PMSF 1 mM DTT 0.5 mM NaF 2 mM $NaVO_3$
TBST	50 mM Tris-HCl pH 7.6 150 mM NaCl 0.1% Tween-20
Transfer Buffer	25 mM Tris-HCl, pH 8.3 192 mM Glycine 20% Methanol
Upper Buffer	0.5 M Tris-HCl, pH 6.8 0.4% SDS
Washing Buffer 1	20 mM Tris-HCl pH 8 2 mM EDTA 1% Triton X-100, 0.1% SDS 150 mM NaCl 0.1 x PIC 2 µM PMSF 0.5 mM NaF 2 mM $NaVO_3$
Washing Buffer 2	20 mM Tris-HCl pH 8 2 mM EDTA 1% Triton X-100 0.1% SDS 500 mM NaCl 0.1 x PIC 2 µM PMSF 0.5 mM NaF 2 mM $NaVO_3$

3.1.4 Antibodies

Antibody	Company	Application
$F(ab')_2$ fragment goat anti-human IgM (109-006-129)	Jackson ImmunoResearch, West Grove, PA, US	BCR stimulation
$F(ab')_2$ fragment goat anti-human IgM and IgG (109-006-127)	Jackson ImmunoResearch, West Grove, PA, US	BCR stimulation
mouse anti-flag M2 (F1804)	Sigma Aldrich, Dorset, UK	ChIP
mouse anti-Histone H2BK120ub (05-1312)	Merck Millipore, Nottingham, UK	ChIP
mouse anti-POL II CTD (ab817)	Abcam, Cambridge, UK	ChIP
mouse anti-β-actin (A1978)	Sigma Aldrich, Dorset, UK	Western blot, 1:100,000 in TBST with 5% milk
rabbit anti-BAD (9239)	Cell Signaling Technology, Leiden, The Netherlands	Western blot, 1:1,000 in TBST with 5% milk
rabbit anti-BADS112p (5284)	Cell Signaling Technology, Leiden, The Netherlands	Western blot, 1:1,000 in TBST with 5% BSA
rabbit anti-H2A.Z (ab4174)	Abcam, Cambridge, UK	ChIP
rabbit anti-H3K9ac (39917)	Active Motif, La Hulpe, Belgium	ChIP
rabbit anti-Histone H3 (ab1791)	Abcam, Cambridge, UK	Western blot, 1:100,000 in TBST with 5% milk ChIP, IP
rabbit anti-Histone H3.3S31p (ab92628)	Abcam, Cambridge, UK	Western blot, 1:3,000 in TBST with 5% BSA ChIP
rabbit anti-Histone H3K27me3 (07-449)	Merck Millipore, Nottingham, UK	ChIP

rabbit anti-Histone H3K4me3 (04-745)	Merck Millipore, Nottingham, UK	ChIP
rabbit anti-Histone H3K9acS10p (ab12181)	Abcam, Cambridge, UK	Western blot, 1:3,000 in TBST with 5% BSA ChIP
rabbit anti-Histone H3S10p (060570)	Merck Millipore, Nottingham, UK	ChIP
rabbit anti-Histone H3T11p (ab5168)	Abcam, Cambridge, UK	Western blot, 1:10,000 in TBST with 5% BSA ChIP
rabbit anti-Histone H3T3p (04-746)	Merck Millipore, Nottingham, UK	Western blot, 1:3,000 in TBST with 5% BSA ChIP
rabbit anti-Histone H3T6p (ab14102)	Abcam, Cambridge, UK	Western blot, 1:1,000 in TBST with 5% BSA ChIP
rabbit anti-HPRT (FL-218)	Santa Cruz Biotechnology, Dallas, TX, US	Western blot, 1:3,000 in TBST with 5% BSA
rabbit anti-MYC (sc-764)	Santa Cruz Biotechnology, Dallas, TX, US	Western blot, 1:3,000 in TBST with 5% BSA ChIP
rabbit anti-PIM1 (2907)	Cell Signaling Technology, Leiden, The Netherlands	Western blot, 1:500 in TBST with 5% milk
rabbit anti-PIM1 (A300-313A)	Bethyl Laboratories, Montgomery, TX, US	ChIP, IP
rabbit anti-POL II CTD S2p (ab5095)	Abcam, Cambridge, UK	Western blot, 1:10,000 in TBST with 5% BSA ChIP
rabbit anti-POL II CTD S5p (ab5131)	Abcam, Cambridge, UK	ChIP

rabbit anti-ZIPK (AHP490)	AbD Serotec, Kidlington, UK	Western blot, 1:10,000 in TBST with 5% milk ChIP, IP
rat anti-PIM2 (61159)	Active Motif, La Hulpe, Belgium	Western blot, 1:3,000 in TBST with 5% BSA
goat anti-rabbit IgG HRP (111-035-003)	Jackson ImmunoResearch, West Grove, PA, US	WB, 1:10,000
goat anti-rat IgG HRP (18-4818-82)	eBioscience, Hatfield, UK	WB, 1:10,000
mouse anti-rabbit IgG, light chain-specific, HRP (211-032-171)	Jackson ImmunoResearch, West Grove, PA, US	WB, 1:10,000
normal rabbit IgG (sc-2027)	Santa Cruz Biotechnology, Dallas, TX, US	IP
rabbit anti-mouse IgG HRP (315-035-003)	Jackson ImmunoResearch, West Grove, PA, US	WB, 1:10,000

3.1.5 Primers and oligonucleotides

Primers were designed using primer BLAST (Ye et al., 2012). Some changes to the standard setting were made: primers were designed with an optimal length of 22 nt, the maximal PCR product length was set to 150bp, the maximal melting temperature difference was 1°C and, when possible, the maximal GC content in the most 3' 5 nt was 2. Primers were synthesised by Sigma Aldrich.

Name	Sequence 5' → 3'
3xflag-EGFP-EcoRI F	ATATGAATTCATGGATTACAAGGATGACGACGATAA GGATTACAAGGATGACGACGATAAGGATTACAA GGATGACGACGATAAGGTGAGCAAGGGCGAGGAGCT
3xflag-EGFP-NotI R	ATATGCGGCCGCTTACTTGTACAGCTCGTCCA

3xflag-PIM1-EcoRI F	ATATGAATTCATGGATTACAAGGATGACGACGATAA GGATTACAAGGATGACGACGATAAGGATTACAA GGATGACGACGATAAGGTCTTGTCCAAAATCAACTC
3xflag-PIM1-NotI R	ATATGCGGCCGCCTATTTGCTGGGCCCCGGCG
ARID3A F	ATGGCCCTGGTGGCCGATGA
ARID3A R	CGGCTTTCGGAGGCTTGGCT
BCL2 F	ATGTGTGTGGAGAGCGTCAA
BCL2 R	GCCGGTTCAGGTACTCAGTC
BCL2A1 +0.1 F	CTACGCACGAAAGTGACTAGGA
BCL2A1 +0.1 R	GATACATGGAGGCTGGTGGAAT
BCL2A1 +10.4 F	TAATTTCTTGGGTCTGGCTGGA
BCL2A1 +10.4 R	CACACCTGAAAGGGTCTACCG
BCL2A1 F	ACAATCACACACCTATGCTGGT
BCL2A1 R	TCATCCAGCCAGATTTAGGTTCA
CCND2 -0.2 F	AGCTTGCGTCACCGCTT
CCND2 -0.2 R	GTCCTCCCCTTAAAACTGGTCT
CCND2 +31.6 F	CCAGCAGTCCTCAGAATGGAAT
CCND2 +31.6 R	TGACTTGTACCGCCATAACACA
CCND2 F	GTCGATGATCGCAACTGGAAGT
CCND2 R	AATCCACGTCTGTGTTGGTGAT
CCR6 F	CTGTGGTGTGTGAGAAGGAAGT
CCR6 R	ACATAGTGAAGGACGACGCATT
CCR7 F	CCTCCCTCCATCGTTTTCTTCA
CCR7 R	AGGGGATGAGTGTGCTTTTAGG
CD40 F	TGAGTGACTGCACAGAGTTCAC
CD40 R	TAGGTTGGGGTCGCAGTATTTG
CDC25B F	CACCGAGAGCTGATTGGAGATT
CDC25B R	ACCATCGTTTCTGGTGAGATGT

CTCF site 1 F	GGCCCAGGACTCCACGTTCAGA
CTCF site 1 R	GCCCTCTGGTGTTTGGCAGCAA
CTCF site 3 F	CACCCAGCAGAGGGCCCAGATA
CTCF site 3 R	CCCTTCGCCTTCTCTCCAGCCA
CXCR4 F	GCACATCATGGTTGGCCTTATC
CXCR4 R	GAGTGTGACAGCTTGGAGATGA
CXCR5 F	CACCCTACCACATCGTCATCTT
CXCR5 R	TTCAGCTTGCAGGTATTGTCCA
DUSP2 -0.3 F	CTAAAGGGGGACCTGCATCTG
DUSP2 -0.3 R	GACTAAGGGAAGGGAAGGTGTT
DUSP2 +2.4 F	GGAAGTGATGGGTGTGTCATGT
DUSP2 +2.4 R	AAATAATTTTCCAGCGCCAGCA
DUSP2 +3.1 F	CATTTGGAGTGTCATCCAGCCA
DUSP2 +3.1 R	ACAGACCACGGACAGATCCTTA
DUSP2 +4.2 F	AGGAGTGAGGTTGATCTGATGT
DUSP2 +4.2 R	CCAGCCGTTATGAGTGTCCAT
DUSP2 F	TACTTCCTGCGAGGAGGCTT
DUSP2 R	GGCTGGTTTTGTCCCCTGTT
DUSP4 +0.2 F	GACCGGCAAAAATACACGGGA
DUSP4 +0.2 R	GGAGGAGAGTGTGTTTACGAGA
DUSP4 +17.7 F	TCAACCACTTCTGGCTTGGTTA
DUSP4 +17.7 R	GTTCTTTCCTCCCCTTCCAAGT
DUSP4 F	ATCACGGCTCTGTTGAATGTCT
DUSP4 R	ATGTCGGCCTTGTGGTTATCTT
EGR1 -0.1 F	GCCATATTAGGGCTTCCTGCTT
EGR1 -0.1 R	GATCCGCCTCTATTTGAAGGGT
EGR1 -0.85 F	TACAGTGTCCCAAGAACCAAGT
EGR1 -0.85 R	CGATCTATGGCACGGTGTCTTT

EGR1 -6.1 F	CCTGGGGTAGGAGCAGAACT
EGR1 -6.1 R	TGTCACACTTTCCGACTGACTT
EGR1 +2.2 F	CTGCGACATCTGTGGAAGAAAG
EGR1 +2.2 R	GCCGCAAGTGGATCTTGGTAT
EGR1 +3.8 F	GCTGCGATTGGGTATGTGTTTC
EGR1 +3.8 R	AGAAAACCTCACAGCCCTCAAT
EGR1 F	ACAAAAGTGTTGTGGCCTCTTC
EGR1 R	GTGGCCGGGGATGGATAAGA
FOSL1 -37 F	CGGGGATCAAAGATGAAGAA
FOSL1 -37 R	TGGGGAGCAGATAGCTGAGT
FOSL1 +1.15 F	GCCCTCGATCCCTTTGCCGAATG
FOSL1 +1.15 R	AGGAAATGGGCACCTGCAGCCT
FOSL1 F	CGAAGGCCTTGTGAACAGAT
FOSL1 R	GAAGTCGGTCAGTTCCTTCCT
GAPDH F	ACAGTCAGCCGCATCTTCTT
GAPDH R	ACGACCAAATCCGTTGACTC
GNL3 -0.5 F	AGGCCCTGAGCAACGGAGGAA
GNL3 -0.5 R	GCGCACTACGGGTCGGAAACTC
GNL3 -3.5 F	CCTGCCCAACTGCCCCCTAGTC
GNL3 -3.5 R	GGGGGAGGGTGTTTTCCAGACCT
GNL3 -6.5 F	TCCTGCTTGGGCCTGGTGTTGA
GNL3 -6.5 R	GCTACCTCCCCTTCCAGCAGTGT
GNL3 +0.1 F	CCAGCGGAGGCAGGTTGATGTG
GNL3 +0.1 R	TGGCTGCAGCAACTTCCAGACG
GNL3 +0.4 F	TTAACCGCGCGGGCTCATTCTG
GNL3 +0.4 R	CAGCTCTCACCTGGGCCAGTCT
GNL3 +3.5 F	GCCTCCGATGTTGTCCTAGAGGTGTT
GNL3 +3.5 R	TCCCCACTGCCTAGCACTGTCTC

GNL3 +5 F	TGGGCTCTGGAGCCTGATTGCT
GNL3 +5 R	AGCATTCTTCTTTGCCTTCACACGCT
GNL3 +9 F	CCAAGGTGGCGGACATTCCACA
GNL3 +9 R	AGCAGAACCCTGGCTGGTAGCAT
GNL3 F	GGCAGGTTGATGTGTTTGTG
GNL3 R	TATGGCAGGTCATGCGTTTA
ID2 -1.4 F	GGAAGGCCCTCCGCAAACTTCT
ID2 -1.4 R	TGACAGCTATGCGCCCCATGAC
ID2 -1.7 F	AGGCTCGAACTGTGGGAGGACT
ID2 -1.7 R	CTGCCTGCGACTCTGTCCCTGA
ID2 F	ATCCCCCAGAACAAGAAGGT
ID2 R	GGTGATGCAGGCTGACAATA
LYN F	CAGCAAGGGAAGGTGCTAAG
LYN R	TTCCAAAGGACCACACATCA
MYC +0.1 F	TGCCTCTCGCTGGAATTACTAC
MYC +0.1 R	GAGGGATCGCGCTGAGTATAAA
MYC +5.5 F	CAGGAAGCATCTTAGAACCTCCA
MYC +5.5 R	GAGGGTGGTCTTAAGAAAGGCA
MYC F (B cell lines)	GTAGTGGAAAACCAGCAGCC
MYC F (CLL)	GGAGGGATCGCGCTGAGTATAA
MYC R (B cell lines)	CTCGTCGCAGTAGAAATACGG
MYC R (CLL)	TGCCTCTCGCTGGAATTACTACA
NCL F	GCTTGGCTTCTTCTGGACTCAT
NCL R	CCATTTTCTTGGGGTCACCTTG
NPM1 -7 F	GAGAGTGGCACACTTCATCTCCAT
NPM1 -7 R	GAGGTCTGAAAGGGTAGGTCATCA
NPM1 +1 F	GCCTGCTTGTTGGAGCGGGTAGA
NPM1 +1 R	GCCGAAGCACGCGAGGTAAGTC

NPM1 +2 F	TCATTCTGCTTTGCCCTCTGGTAGC
NPM1 +2 R	TTTGTCGGCCTTTAGTTCACAACCTGT
NPM1 +24 F	CAGTTCTGTGCCGTTTTCCTTGGGA
NPM1 +24 R	TACACGCCCAAAGCAGCAAGCA
NPM1 +4 F	GGGGCTGGTGCAAAGGATGAGT
NPM1 +4 R	GCAGCAGAAGCCCCCATGTTCA
PIM1 F	CAGGCAGAGGGTCTCTTCAG
PIM1 R	TCCATGGATGGTTCTGGATT
PIM2 F	GCCTGGCCCCCAAACCTTCTTC
PIM2 R	GGGGTACATCCTCGGCTGGTGT
PPP6C F	TGGAAATGCTAATGCCTGGAGA
PPP6C R	TTCCTGATTCCGTTCGATGGTT
PRDX1 F	AGTGATTGGTGCTTCTGTGGAT
PRDX1 R	CCCCATAATCCTGAGCAATGGT
SEPX1 -0.3 F	CGCGGAAAGGCTGCATGACCTC
SEPX1 -0.3 R	CGCGAATCCGTAGGGTCGTGTC
SEPX1 F	TGTCGTTCTGCAGCTTCTTC
SEPX1 R	ATAGCCACACTTGGCACACA
shMYC F	CGGTCCTGAGACAGATCAGCAACAACTC GAGTTGTTGCTGATCTGTCTCAGGTTTTTG
shMYC R	AATTCAAAAACCTGAGACAGATCAGCAACAACTC GAGTTGTTGCTGATCTGTCTCAGGACCGGTAC
shPIM1 1196	TGCTGTTGACAGTGAGCGAGCAGAGGGTCTCTTCAGAAT GTAGTGAAGCCACAGATGTACATTCTGAAGAGACCCTCTG CCTGCCTACTGCCTCGGA
shPIM1 1600	TGCTGTTGACAGTGAGCGATCTCTTCTTCTCATAGGTGTC TAGTGAAGCCACAGATGTAGACACCTATGAGAAGAAGAG AGTGCCTACTGCCTCGGA

shPIM1 2138	TGCTGTTGACAGTGAGCGCACAGTTGGCATGGTAGTATA CTAGTGAAGCCACAGATGTAGTATACTACCATGCCAACT GTATGCCTACTGCCTCGGA
shPIM1_1 F	CCGGACATCCTTATCGACCTCAATCCTC GAGGATTGAGGTCGATAAGGATGTTTTTTG
shPIM1_1 R	AATTCAAAAAACATCCTTATCGACCTCAATCCTC GAGGATTGAGGTCGATAAGGATGT
shPIM1_2 F	CCGGCATCCGCGTCTCCGACAACTTCTC GAGAAGTTGTCGGAGACGCGGATGTTTTTTG
shPIM1_2 R	AATTCAAAAAACATCCGCGTCTCCGACAACTTCTC GAGAAGTTGTCGGAGACGCGGATG
shPIM2 1600	TGCTGTTGACAGTGAGCGCCCACACAAACTTAGTTCATAT TAGTGAAGCCACAGATGTAATATGAACTAAGTTTGTGTGG TTGCCTACTGCCTCGGA
shPIM2 664	TGCTGTTGACAGTGAGCGAGCCCAGGATCTCTTTGACTA TTAGTGAAGCCACAGATGTAATAGTCAAAGAGATCCTGG GCGTGCCTACTGCCTCGGA
shPIM2 881	TGCTGTTGACAGTGAGCGCACACTGACTTTGATGGGACA ATAGTGAAGCCACAGATGTATTGTCCCATCAAAGTCAGTG TATGCCTACTGCCTCGGA
shPIM2_1 F	CCGGGATGAACCCTACACTGACTTTCTC GAGAAAGTCAGTGTAGGGTTCATCTTTTTG
shPIM2_1 R	AATTCAAAAAGATGAACCCTACACTGACTTTCTC GAGAAAGTCAGTGTAGGGTTCATC
shPIM2_2 F	CCGGCCAGGATCTCTTTGACTATATCTC GAGATATAGTCAAAGAGATCCTGGTTTTTG
shPIM2_2 R	AATTCAAAAACCAGGATCTCTTTGACTATATCTC GAGATATAGTCAAAGAGATCCTGG

SM2C F	GATGGCTGCTCGAGAAGGTATATTGCTGTTGACAGTGAGCG
SM2C R	GTCTAGAGGAATTCCGAGGCAGTAGGCA
SNORD19 F	TGGGTGAGGTACGAGGAAACAGT
SNORD19 R	GGCTTTGCTGAGATCAGAGTTGGAT
SNORD19B F	GGTTGAAATATGATGAGTGTACAAA
SNORD19B R	CTGGCTGAAATCAGAGTTGGA
SNORD69 F	GTGAAGCAAATGATGATAAACTGGA
SNORD69 R	AGCTCAGGGTTGGATTGAACAG
TBP F	TGCTCACCCACCAACAATTTAG
TBP R	TCTGGGTTTGATCATTCTGTAGATTAA
TLR10 F	GCTAACAACACACCCTTGGAAC
TLR10 R	GCAAGCACCTGAAGACAGAATC

3.1.6 Plasmids

3.1.6.1 pCMV6-XL4-PIM1

The pCMV6-XL4-PIM1 construct was purchased from OriGene (Cambridge Bioscience, Cambridge, UK). The GenBank accession number for the pCMV6-XL4 parental plasmid is AF067196. For an overview of the plasmid structure, see Figure 3.1. The full-length PIM1 cDNA was cloned between the two NotI restriction sites.

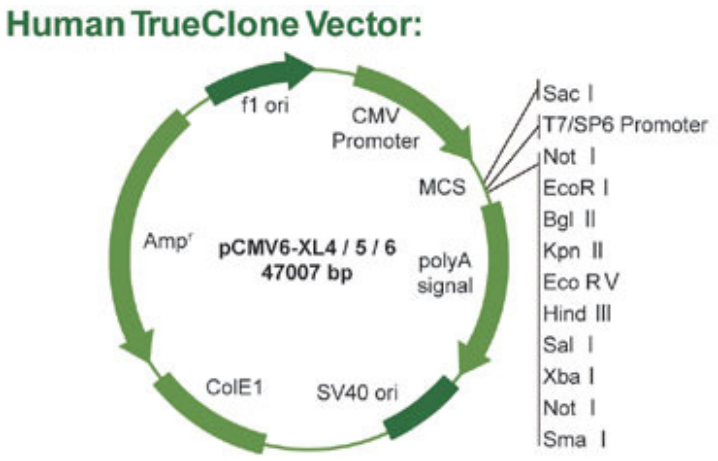

Figure 3.1 Map of pCMV6-XL4 (from OriGene).
MCS = multi cloning site, ColE1 = Colicin E1, Amp^r = ampicillin resistance

3.1.6.2 pCMV-SPORT6

The pCMV-SPORT6 vector (Life Technologies, Figure 3.2) was a kind gift from Justin Gillespie. It was used for cloning 3 x flag-tagged-PIM1 and -PIM1-KD between the NotI and EcoRI sites.

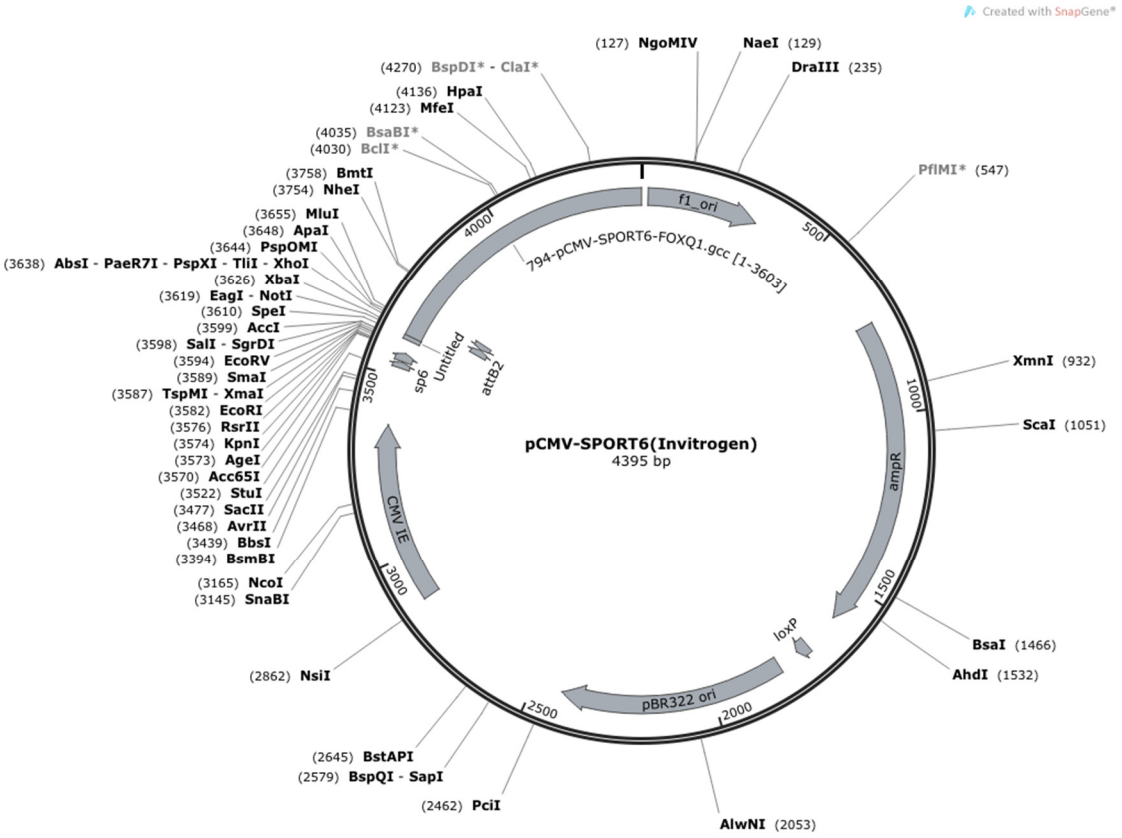

Figure 3.2 Map of pCMV-SPORT6 (from GenBank).
CMV 1E = CMV promoter

3.1.6.3 pMSCV-miR30

pMSCV-miR30 (Figure 3.3) was a kind gift from Peter Laslo and was used for cloning of PIM1 and PIM2 shRNAs for transient transfection. The shRNAs were cloned between the XhoI and EcoRI sites.

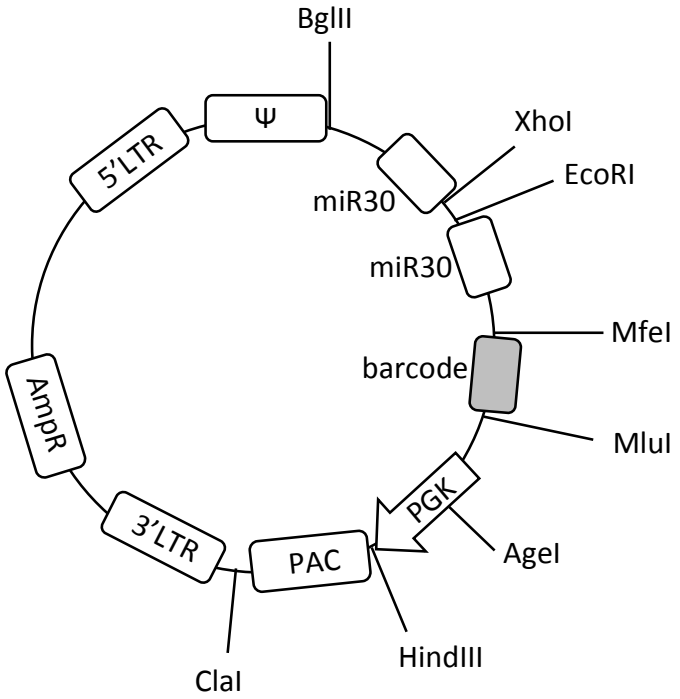

Figure 3.3 Map of the pMSCV-miR30 vector.
Ψ = viral packaging signal, PGK = murine phosphoglycerate kinase promoter, PAC = Puromycin N-acetyltransferase, LTR = long terminal repeat

3.1.6.4 pLKO_IPTG_3xLacO

The pLKO_IPTG_3xLacO-shLuc vector was purchased from Sigma Aldrich. The parental vector map is shown in Figure 3.4. The luciferase shRNA (shLuc) was inserted between the AgeI and EcoRI sites, destroying the AgeI site. Therefore, shMYC was cloned between the KpnI and EcoRI sites, reconstituting the AgeI site, to allow for cloning of shPIM1_1, shPIM1_2, shPIM2_1 and shPIM2_2 between the AgeI and EcoRI sites.

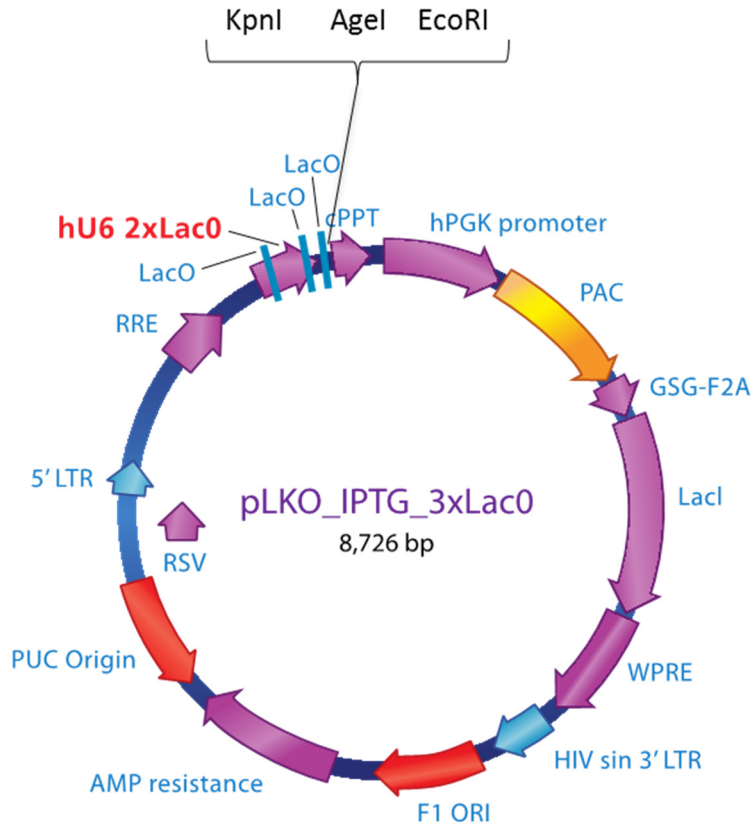

Figure 3.4 Map of pLKO_IPTG_3xLacO (adapted from Sigma Aldrich).
RRE = Rev response element, hU6 = human U6 promoter, LacO = Lac operator, cPPT = central polypurine tract, GSG-F2A = Glycine-Serine-Glycine fused to 2A peptide from foot-and-mouth disease virus (FMDV), LacI = Lac inhibitor, WPRE = Woodchuck hepatitis virus posttranscriptional regulatory element, HIV sin 3' LTR = HIV self-inactivating 3' LTR, RSV = respiratory syncytial virus promoter

3.2 Methods

3.2.1 Patient samples

Samples from CLL patients were anonymised clinical blood waste samples. Ethical approval was granted by the NHS Research Ethics Committee (reference numbers 04/Q1205/178, 04/Q1205/125 and 14/WS/0098). No samples were taken specifically for this study and informed consent was not required. Samples were taken in EDTA tubes.

3.2.1.1 Isolation of peripheral blood mononuclear cells (PBMCs)

Due to logistic requirements, samples were stored in the EDTA tubes at 4°C over night, obtained the next day and processed immediately. Blood was diluted 1:2 in phosphate-buffered saline (PBS) and carefully layered over a sucrose density gradient (Lymphoprep^{TM}). After centrifugation at 200 x g for 20 min (acceleration reduced to 60%, brake off), the different blood cell types had separated (see Figure 3.5). PBMCs were then recovered with a Pasteur pipette, transferred into a new tube and washed twice with PBS. Although I was studying CLL B cells, no specific B cell enrichment step was performed, as PBMCs from CLL patients are mainly B cells (in a study with 11 patients conducted by Bonyhadi et al. 85.5% ± 8.1% of PBMCs were B cells (Bonyhadi et al., 2005)). Cells were counted and plated into T25 flasks at appropriate densities or were frozen.

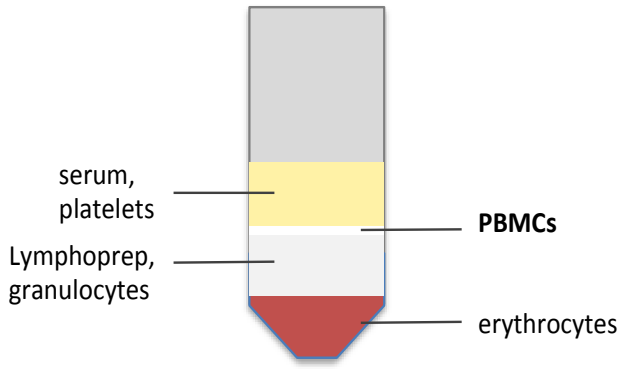

Figure 3.5 Cell separation after use of Lymphoprep^{TM}.

3.2.2 Cell culture

3.2.2.1 Maintenance of cell lines

All cells were cultured at 37°C and 5% CO_2. HEK293 cells were cultured in DMEM with 10% FCS and pen/strep. OCI-Ly3 and OCI-Ly10 cells (ATCC) were maintained in IMDM substituted with 20% FCS and pen/strep at densities of 0.5 – 1 x 10^6 cells/ml. OCI-Ly19, SUDHL6, Raji, Ramos (ATCC), murine L cells stably expressing CD40L (CD40L cells) and M210B4 cells were cultured in RPMI-1640 with 10% FCS and pen/strep. OCI-Ly19 and SUDHL6 cells were maintained at 0.5 – 1.0 x 10^6 cells/ml and Raji and Ramos cells were cultured at 0.1 – 1.0 x 10^6 cells/ml. All suspension cells were spun down at 100 x g for 10 min at room temperature once a week prior to splitting to remove cell debris. CD40L cells were first generated and described by Garrone et al. (Garrone et al., 1995) and were a kind gift from Sean Diehl.

HEK293, CD40L and M210B4 cells were cultured to 80% density, then the medium was removed, the cells were washed with PBS and treated with 0.5 x Trypsin-EDTA for 10 minutes at 37°C. The reaction was stopped with 10 ml fresh culture medium. The cells were washed off the flask and transferred into 50 ml tubes. They were then sedimented by centrifugation at 300 x g for 5 min, resuspended in fresh culture medium, split 1:5 for HEK293 and 1:10 for CD40L and M210B4 cells and seeded into new culture flasks. When used as feeders for CLL cells, CD40L and M210B4 cells were irradiated with a total dose of 50 Gy for 50 minutes. M210B4 cells were directly seeded into tissue culture flasks, while CD40L cells were frozen down and thawed as required. CLL cells were cultured with or without feeder cells in RPMI-1640 with 10% FCS and pen/strep at densities of 0.1 x 10^7 cells/ml with and 0.5 x 10^7 cells without feeder cells.

3.2.2.2 Cell counting

Depending on the observed cell density, cells in culture medium were diluted 1:5 to 1:50 in Trypan Blue solution. 20 µl of this suspension were applied to a haemocytometer and all four large squares were counted (Figure 3.6). To obtain the cell number per ml, the following formula was used:

$$cell\ number/ml = \ average\ cell\ number/large\ square * 10^4 * dilution\ factor$$

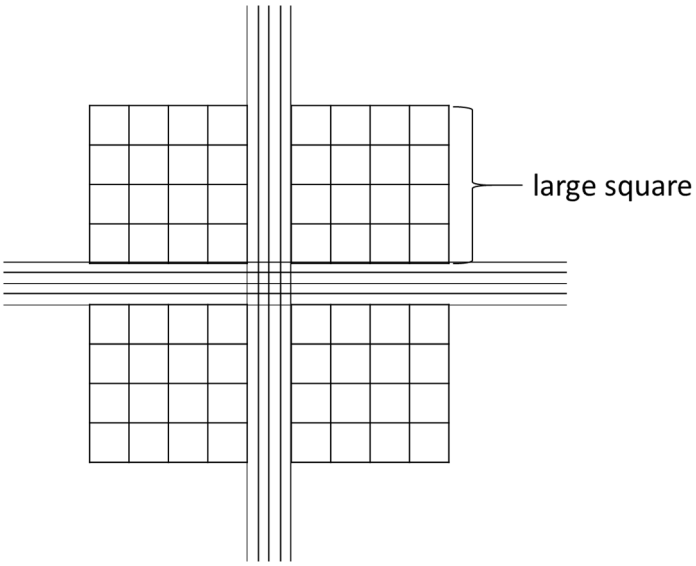

Figure 3.6 Schematic representation of the counting area of a haemocytometer.

3.2.2.3 MTT assay

The MTT assay measures mitochondrial integrity, which can be used as a measure of cell viability. MTT has a yellow colour, but is converted into a purple formazan product in viable/metabolically active cells. The accumulation of the product can be detected by measuring the absorbance of the sample at around 570 nm (Riss et al., 2004).

For the assay, 90 µl of cell suspension were transferred into duplicate wells of 96 well plates. For the standard curve, cells were counted using a haemocytometer and 5 µl, 10 µl, 20 µl, 50 µl, 60 µl and 90 µl of this suspension, made up to 90 µl with culture medium, were also measured in duplicate. As controls, 90 µl culture medium, and culture medium with DMSO or the inhibitors tested, were used. 10 µl MTT (50 mg/ml) were added to each well and mixed well on a plate shaker. The plate was then incubated at 37°C and 5% CO_2, controlled every hour for MTT turnover and after 3 to 6 h, when formation the formazan product became visible, the formation of the product was measured. The plate was centrifuged at 3,200 x g for 5 minutes to sediment

suspension cells and free formazan product. Then, 50 µl of the medium were removed from each well and the formazan product was solubilised by adding 100 µl DMSO. The plate was mixed well on a plate shaker and after a 5 minute incubation, the absorbances at 570 nm and 630 nm were measured, using the Mithras LB940 plate reader. The analysis was then done using Microsoft Excel. First, the absorbance at 570 nm was corrected by the absorbance at 630 nm.

$$A_{corr} = A_{570} - A_{630}$$

Then, the average of the two duplicates was taken and subtracted by the corrected absorbance of medium with DMSO or the appropriate inhibitor.

$$A_{final} = A(sample)_{corr} - A(control)_{corr}$$

The A_{final} values of the standards were then plotted against the cell numbers to generate a standard curve. Linear regression was used to fit a curve. From that, the cell numbers in the samples could be calculated. For long-term experiments, cells were split to maintain appropriate cell densities and calculated cell numbers were multiplied by the dilution factor of the cell suspension.

3.2.2.4 Freezing of cells

Exponentially growing cells were collected by centrifugation and resuspended in cold 90% FCS and 10% DMSO at a density of 10^6 cells/ml for cell lines and 10 x 10^7 cells/ml for CLL cells. 1 ml of the suspension was transferred into cryotubes and stored into a freezing container at -80°C for at least 24 h. The tubes were then transferred into the liquid nitrogen storage tank.

3.2.2.5 Treatment of lymphoma cell lines with PIM inhibitors

OCI-Ly3, OCI-Ly10, SUDHL6, OCI-Ly19, Raji and Ramos cells were treated with different PIM kinase inhibitors. The cells were seeded into appropriate tissue culture flasks or plates on the day of, or the day before the experiment and then treated with 40 µM SMI4a, 40 µM Quercetagetin, 40 µM PIM1/2 inhibitor VI, 1 to 10 µM AZD1208 or DMSO (control) for desired times. The medium was changed every second day and cells were either counted using a haemocytometer or cell vitality was measured using the MTT assay. Alternatively, RNA or protein were prepared.

In vitro, using 0.1 µM ATP and BAD as a substrate, SMI4a has an IC_{50} of 24 nM for PIM1 and of 100 nM for PIM2 (Xia et al., 2009). The IC_{50} for proliferation of PC3 prostate cancer cells was found to be 17 µM (Xia et al., 2009). Using BAD as a

substrate and 10 µM ATP, the IC_{50} of Quercetagetin was found to be 340 nM for PIM1 and 3.45 µM for PIM2 and the IC_{50} for p-BAD in RWPE2 prostate cancer cells is 5.55 µM (Holder et al., 2007). The IC_{50} for PIM1/2 inhibitor VI (SMI16a) was determined using 0.1 µM ATP and BAD as a substrate as being 150 nM for PIM1 and 20 nM for PIM2. Its IC_{50} for proliferation of PC3 prostate cancer cells was found to be 48 µM (Xia et al., 2009).

AZD1208 is a potent PIM kinase inhibitor that shows an IC_{50} for p-BAD in a cellular assay in U2OS cells of 10 nM for PIM1, 151 nM for PIM2 and 102 nM for PIM3. Tested against 442 kinases at a concentration of 1 µM, PIM kinases were inhibited most strongly and only 13 other kinases were inhibited by 50% or more. However, affinity of AZD1208 was at least 43-fold higher for PIM kinases than for all those other kinases. Growth of AZD1208-sensitive AML cell lines was inhibited at AZD1208 concentrations lower than 1 µM (Keeton et al., 2014).

3.2.2.6 Treatment of Raji cells with DRB

5,6-Dichloro-1-β-D-ribofuranosylbenzimidazole (DRB) is an inhibitor of transcription elongation. It targets the CDK9 subunit of P-TEFb and leads to a rapid loss of elongating POL II and promoter-bound CTD-S2-phosphorylated POL II (Baumli et al., 2010).

Raji cells were cultured in complete medium and then treated with 100 µM DRB for 1 h or were left untreated. Chromatin was either harvested directly after DRB treatment or the cells were released from transcriptional inhibition. For that purpose, the cells were washed twice with PBS, taken up in fresh medium and cultured until chromatin was prepared.

3.2.2.7 Serum starvation and release of Raji cells

Raji cells were cultured in normal growth medium for two to three days and then serum starved. The cells were sedimented by centrifugation at 300 x g for 5 min, then washed three times in sterile PBS and resuspended in RPMI-1640 with 0.5% FCS and pen/strep. They were cultured for up to 4 h and then FCS was added to result in a final concentration of 10% FCS. To monitor RNA and protein expression, aliquots of cells were harvested at different times.

3.2.2.8 Stimulation of Raji cells via the BCR or with PMA

Raji cells were seeded in tissue culture flasks in normal medium and the next day they were stimulated with 10 µg/ml anti-IgM/anti-IgG or 100 ng/ml PMA for 0 to 24 h. Protein or RNA were prepared at different time points.

3.2.2.9 Serum shock of HEK293 cells

HEK293 cells were cultured in 6-well plates in full medium to about 50% confluence. They were then either left untreated or treated over night with 40 µM SMI4a, Quercetagetin, PIM1/2 inhibitor VI or equivalent amounts of DMSO. The next day, serum shock was performed by adding 1 ml FCS, resulting in a total concentration of 33% FCS. RNA was harvested at the desired time points.

3.2.2.10 Stimulation of the B cell receptor on CLL cells

CLL cells were kept in culture medium for 16 h to 48 h to facilitate reexpression of the B cell receptor. Then they were treated with either 1 µM Ibrutinib, 0.2 to 10 µM PKCβ inhibitor, 20 µM DAPK inhibitor, 10 µM U0126, 1 µM Gö6983, 10 µM RSK inhibitor II or equivalent amounts of DMSO for 2 h. Afterwards, cells were either harvested (0 h anti-IgM) or treated with 10 µg/ml goat anti-human IgM for 10 min up to 24 h. Chromatin, RNA and protein were harvested for further analyses.

PKCβ inhibitor (CAS 257879-35-9) is a potent ATP-competitive inhibitor for $PKC\beta_I$ (IC_{50} = 21 nM) and $PKC\beta_{II}$ (IC_{50} = 5 nM). It inhibits PKCα with an IC_{50} of 331 nM, PKCε with an IC_{50} of 2.8 µM and PKCγ with an IC_{50} of > 1 µM (Tanaka et al., 2004). In two further screens, this inhibitor was, however, just as potent against RSK1-4 as it is against PKCβ and it also targeted PKCθ and PKCη (Anastassiadis et al., 2011; Gao et al., 2013).

Gö6983 (CAS 133053-19-7) is an ATP-competitive PKC inhibitor (PKCα and PKCβ IC_{50} = 7nM, PKCγ IC_{50} = 6 nM, PKCδ IC_{50} = 10 nM, PKCζ IC_{50} = 60 nM) (Gschwendt et al., 1996). In two other screens, it also potently inhibited PKCε, η and θ and it inhibited RSK1/2/3/4 with similar efficiencies to PKCs (Anastassiadis et al., 2011; Gao et al., 2013).

U0126 (CAS 109511-58-2) non-competitively inhibits MEK1/2 with IC_{50} values of 72 nM or 58 nM, respectively, in a kinase assay using 40 µM ATP. Using 10 to 20 µM ATP, the IC_{50} values for Abl, Cdk2, Cdk4, ERK, JNK, MEKK, MKK3, MKK4, MKK6 and PKC are more than 10 µM. U0126 almost completely inhibits ERK1/2 phosphorylation in COS7 cells at a concentration of 10 µM (Favata et al., 1998).

RSK inh II (CAS 501437-28-1) is an ATP-competitive inhibitor that targets RSK1/2/3/4 with IC_{50} < 31 nM in kinase assays using 100 µM ATP. It does not target PKCβ, but has moderate activity towards PKCα, GSK3β, CDK2 and CK1 and strongly inhibits PLK1 and Aurora B at approximate K_m concentration of ATP. The IC_{50} for inhibition of RSK1/2 in HEK293 cells is 1 µM (Sapkota et al., 2007).

At 10 µM ATP, DAPK inhibitor shows IC_{50} values of 69 and 225 nM against DAPK1 and DAPK3, respectively. Of the other kinases tested at apparent K_m concentration of ATP, it only significantly inhibited p70S6K (see Table 3.1) (Okamoto et al., 2009).

no inhibition at 10 µM				**IC_{50} > 10 µM**		**1 µM < IC_{50} < 10 µM**
ABL	Erk1	MARK1	PKCζ	CK1δ	FGFR1	p70S6K
AKT1	FLT3	MAPKAPK2	PKD2	DYRK1α	KDR	
AKT2	FYN	MET	PKGα	ERK2	SGK1	
AMPK	GSK3β	MSK1	PRAK			
AurA	HGK	MST2	ROCK2			
BTK	IGF1R	p38α	RSK1			
CAMK2	INSR	PAK2	SRC			
CAMK4	IRAK4	PIM2	SYK			
CDK2	LCK	PKA	c-TAK1			
CHK1/2	LYN	PKCβ2	c-Raf			

Table 3.1 Other kinases targeted by DAPK inhibitor (adapted from Okamoto et al., 2009).

3.2.2.11 Transient transfection of lymphoma cell lines

Raji cells were transfected using the Amaxa™ Nucleofector™ as indicated by the manufacturer. Briefly, 10^7 Raji cells were suspended in 100 µl complete Nucleofector Solution V, 10 µg plasmid DNA were added and the cells were subjected to nucleofection, using programme M-013. Immediately after, cells were suspended in 500 µl pre-warmed culture medium and transferred into appropriate cell culture flasks.

SUDHL6 cells were transfected using the Gene Pulser® II. 5 x 10^6 cells were suspended in 500 µl RPMI-1640, mixed with 10 µg DNA and transferred into a pre-chilled electroporation cuvette. Electroporation was performed at 200 V or 260 V and 1000 µF. Cells were then taken up in pre-warmed medium and transferred into appropriate culture flasks.

3.2.2.12 Generation of stably transfected cell lines

3.2.2.12.1 Testing the sensitivity of Raji cells towards puromycin

2 x 10^5 Raji cells were seeded into 6 well plates and left untreated or were treated with 1 µg/ml, 2.5 µg/ml, 5 µg/ml, 7.5 µg/ml or 10 µg/ml puromycin in triplicate, respectively. The medium with puromycin was renewed after two days and the effects on cell vitality were monitored over four days. 1 µg/ml puromycin was found to effectively induce cell death and this concentration was used in future experiments.

3.2.2.12.2 Selection of stably pLKO_IPTG_3xLacO-shRNA transfected single cell clones

Raji cells were transfected as for transient expression of the gene product and kept in T25 flasks. 24 h after transfection, cells were treated with 1 µg/ml puromycin. The medium was changed twice a week and after 10 days, a limiting dilution was performed. Cells were counted, diluted to cell concentrations of 20 cells/100 µl, 10 cells/100 µl, 5 cells/100 µl and 1 cell/100 µl and plated into 96 well plates as shown in Figure 3.7.

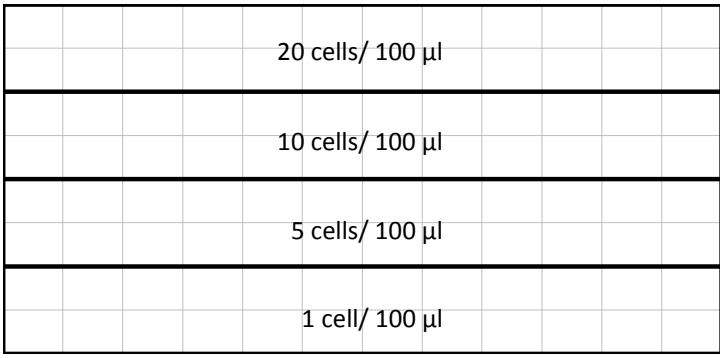

Figure 3.7 Plate layout for selection of stable, single cell clones by limiting dilution.

Wells were checked for presence of single cells 24 h later and these wells were expanded. Evaporated medium was replaced with puromycin-containing medium twice a week. Expanded, single cell-derived colonies were transferred into 48-, then 24-, 12- and 6-well plates. An aliquot was then tested for efficient knockdown, while the rest of the cells were expanded further and frozen down.

3.2.2.12.3 Induction of shRNA expression

Stably transfected Raji cells were seeded into appropriate tissue culture dishes and left untreated or were treated with 5 mM IPTG in normal culture medium. The medium with IPTG was renewed every second day and the cells were counted or RNA, protein or chromatin were harvested after two to ten days.

3.2.2.13 Cell cycle synchronisation

3.2.2.13.1 Thymidine/nocodazole block

A thymidine/nocodazole block used to synchronise cells in M phase as described by Whitfield et al. (Whitfield et al., 2000). Thymidine blocks DNA replication by inhibiting the generation of dCDP (Van Potter, 1963; Reichard et al., 1960) and nocodazole inhibits microtubule polymerisation (Zieve et al., 1980).

Raji cells were grown in normal growth medium to a density of about 0.8 x 10^6 cells/ml. They were then treated with 2 mM thymidine for 24 h, to block cell cycle progression in S phase. Subsequently, the cells were sedimented by centrifugation at 300 x g for 5 min, washed twice with PBS and resuspended in normal growth medium to allow for progression through S and G2 phase. 3 h later, 100 ng/ml nocodazole were added for 12 h to block cell cycle progression in M phase. Afterwards, the cells were washed twice with PBS and released into normal growth medium. Cell cycle progression was monitored using flow cytometry and RNA and chromatin were prepared at different time points.

3.2.2.13.2 Analysis of cell cycle progression by flow cytometry

To assess the cell cycle synchronisation, cellular DNA was stained with propidium iodide (PI). In G0/G1 phase, cells have half the DNA content of cells in M phase, therefore they are stained half as brightly. This difference can be measured by flow cytometry.

Synchronised cells were sedimented by centrifugation at 200 x g, washed twice with PBS, resuspended in 100 µl PBS and then fixed with 5 ml 70% ethanol. The fixed cells were stored at 4°C for up to a few days. On the day of analysis, the ethanol was removed by sedimenting the cells at 500 x g for 10 min. Afterwards, the cells were washed twice in PBS and transferred into FACS tubes between the two washes. The cell pellet was taken up in 50 µl staining solution and incubated on ice in the dark for at least 45 min. The cells were then suspended in 400 µl PBS and analysed on a BD

LSRII flow cytometer. The intensity of the PI staining was measured using an excitation wavelength of 488 nm and detecting emission in the PE channel at 562–588 nm.

Cells were first gated on forward and side scatter to exclude apoptotic cells (Figure 3.8 A). Then cells were gated for positive PI staining by plotting forward scatter values against PI (Figure 3.8 B) and then only single cells (no duplets, triplets etc.) were included in the analysis by gating on the height and area of the PI signal (Figure 3.8 C).

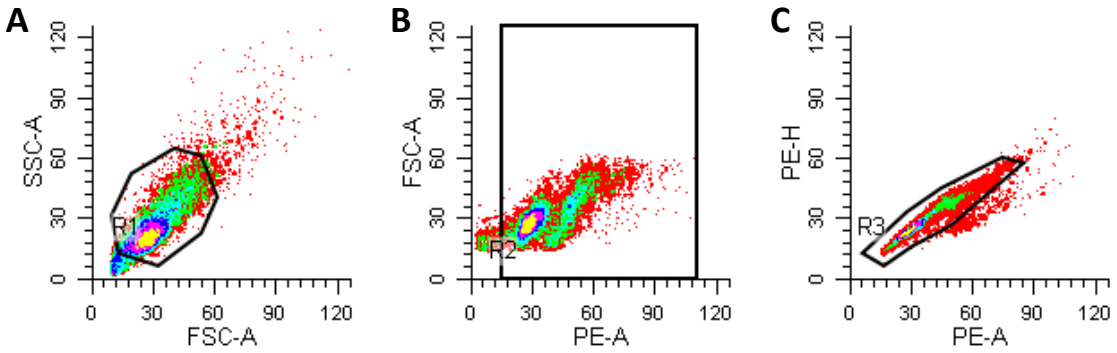

Figure 3.8 Gating strategy for cell cycle analysis using PI.

These cells were then further analysed for the cell cycle stage using the ModFit software (Verity Software House). Briefly, the PE area histogram was plotted and the G1 peak centre was defined. The G2/M peak was set at about twice the value of the G1 peak and the widths of the peaks were adjusted to match the shape of the histogram. The software then calculated percentages of cells in the different cell cycle stages.

3.2.3 Molecular cloning

3.2.3.1 PCR amplification of DNA inserts

PIM1 and PIM2 shRNAs for cloning into pMSCV-miR30 were amplified from oligonucleotides using the ReddyMix PCR Master Mix. Per reaction, 12 µl ReddyMix were combined with 11 µl HyClone™ water, 1 µl 10 µM SCV2 for and rev and 1 µl 1 µM shRNA oligonucleotide. The PCR was done under the following conditions:

95°C	5 min	1 x
95°C	30 s	30 x
54°C	30 s	
68°C	30 s	
68°C	10 min	1 x

DNA coding for PIM1S and kinase dead PIM1S (PIM1-KD) was amplified from pCMV5-flag-PIM1 and -PIM1-KD vectors, which were a kind gift from Andrew MacDonald (Macdonald et al., 2006). Kinase-dead PIM1 carries a mutation, which converts the aspartate in the DFG motif into an alanine (D186A). This region is part of the ATP-binding pocket (Kumar et al., 2005). The primers used were partly complementary to *PIM1*, but the 5' primer had a 3 x flag overhang and a NotI restriction site, whereas the 3' primer had an EcoRI restriction overhang (see section 3.1.5). The amplification was tested both with Pfx and Phusion DNA polymerases, but a product was obtained from the reaction with Phusion polymerase only.

For the PCR with Pfx polymerase, 18 µl HyClone™ water, 3.75 µl 10 x Pfx buffer, 0.75 µl 25 mM dNTPs, 0.5 µl 50 mM $MgSO_4$, 0.75 µl 10 µM primer mix PIM1S for and rev, 10 ng pCMV5-flag-PIM1 or -PIM1-KD and 0.4 µl Pfx polymerase were mixed. The PCR was done using the following conditions:

94°C	5 min	1 x
94°C	15 s	5 x
50°C	30 s	
68°C	1 min	

94°C	15 s	30 x
60°C	30 s	
68°C	1 min	
4°C	hold	

For the PCR with Phusion polymerase, the following was combined in a 0.5 ml tube: 12.4 µl HyClone™ water, 4 µl 5 x HF buffer, 0.2 µl 25 mM dNTPs, 10 µM primers PIM1S for and rev, 10 ng pCMV5-flag-PIM1 or -PIM1-KD and 0.2 µl Phusion. The PCR was run under the following conditions:

98°C	30 s	1 x
98°C	10 s	5 x
50°C	30 s	
72°C	30 s	
98°C	10 s	30 x
60°C	30 s	
72°C	30 s	
72°C	10 min	1 x
4°C	hold	

The PCR products were then analysed on a 1% agarose gel and purified using the QIAquick PCR Purification Kit, eluting with 20 µl elution buffer.

3.2.3.2 Agarose gel electrophoresis

1% agarose gels were prepared by boiling 1 g agarose in 100 ml 1 x TAE buffer until dissolved. The solution was then allowed to cool to about 60°C, then 10 µl Ethidiumbromide solution (10 mg/ml) were added and the gel was cast. After gelling of the agarose, the gel was transferred into a tank filled with 1 x TAE, DNA samples in gel loading dye and DNA ladder were loaded and the gel was run at 50 V until the desired separation was achieved. Then, the DNA was visualised using the Gel Doc™ XR.

3.2.3.3 Annealing of shRNAs

For cloning of shRNAs into pLKO_IPTG_3xLacO, validated MISSION® shRNAs (Sigma Aldrich) were customised and ordered as two complementary oligonucleotides. The annealed oligonucleotides carry a 5' AgeI-complementary overhang, a 3' EcoRI cohesive overhang and a 21 nt long target sequence, separated from the complementary siRNA sequence by a 6 nt linker (Figure 3.9). The customisation included the addition of a G or C in forward and reverse oligonucleotides, behind the poly-T tract or before the poly-A tract, respectively, to retain the EcoRI site after ligation of the shRNA into the vector. The MYC shRNA was designed specifically for cloning into the pLKO_IPTG_3xLacO-shLuc vector, in which the AgeI site had been destroyed. Therefore, the shMYC oligonucleotides were cloned between the KpnI and EcoRI sites. They were designed to reintroduce the original vector sequence and allow for cloning of the other shRNAs between the AgeI and EcoRI sites.

AgeI overhang	target sequence	linker	siRNA	EcoRI overhang

5'-CCGGACATCCTTATCGACCTCAATCCTCGAGGATTGAGGTCGATAAGGATGTTTTTTG-3'
3'-TGTAGGAATAGCTGGAGTTAGGAGCTCCTAACTCCAGCTATTCCTACAAAAAACTTAA-5'

Figure 3.9 shRNA oligonucleotides after annealing.

For annealing of the purchased oligonucleotides, 9 µl 100 µM sense oligonucleotide, 9 µl 100 µM antisense oligonucleotide and 2 µl 10 x annealing buffer were combined and incubated in a PCR machine under the following conditions:

95°C, 78°C, 74°C, 70°C, 67°C, 63°C, 60°C, 56°C, 53°C, 50°C, 48°C, 46°C, 44°C, 42°C, 40°C, 39°C, 37°C, 36°C, 35°C, 34°C, 33°C, 32°C, 31°C	5 min each
30°C, 28°C, 26°C, 24°C, 22°C, 20°C	10 min each

The annealing reaction was then diluted 50 x with HyClone™ water and ligated into the pLKO_IPTG_3xLacO vector.

3.2.3.4 Restriction digest of vectors and DNA inserts

To insert oligonucleotides into the vector, both the vector and the PCR products have to be digested with restriction endonucleases. 6 µg of the vector or 10 µl PCR product, 2 µl buffer, 2 µl 10 x BSA and 1 µl of each restriction enzyme were mixed with water to make up 20 µl. The reaction was incubated at 37°C for 1 to 4 h, depending on the enzymes used.

pLKO_IPTG_3xLacO-shLuc was digested with KpnI and EcoRI in NEBuffer 1 and pLKO_IPTG_3xLacO-shMYC was digested with AgeI and EcoRI in NEBuffer 4. pCMV-SPORT6 and 3 x flag-PIM1S and -PIM1S-KD were digested with EcoRI and NotI in NEBuffer 4. pMSCV-miR30 and the shRNAs for cloning into this vector were digested with EcoRI and XhoI in NEBuffer 2. Subsequently, the reaction was analysed on a 1% agarose gel. The digested vector was then cut out of the gel and purified using the QIAquick Gel Extraction Kit, eluting with 20 µl elution buffer. The digested PCR products were purified using the QIAquick PCR Purification Kit. Finally, DNA concentrations were measured using the NanoDrop™ spectrometer.

3.2.3.5 Ligation of vector and insert

For the ligation of vectors with the respective insert, 50 ng of cut vector were mixed with the appropriate amount of insert, 1 µl 10 x T4 DNA ligase buffer, 1 µl T4 DNA ligase and HyClone™ water to 10 µl.

The amount of insert needed was calculated using the following formula:

$$amount(insert) = \frac{size(insert) * amount(vector)}{size(vector)} * insert/vector\ ration$$

The reaction was incubated at room temperature for 16 h and then directly used for transformation of *E.coli* DH5α.

3.2.3.6 Generation of chemically competent *E. coli*

E. coli DH5α were grown at 37°C over night in 5 ml LB medium and then transferred into 100 ml LB medium to be grown to an OD_{600} of 0.4 to 0.5. The culture was then cooled to 4°C and the bacteria were sedimented by centrifugation at 3,200 x g and 4°C for 15 min. The pellet was resuspended in 30 ml RF1, incubated on ice for 2 min and spun down by centrifugation at 3,200 x g at 4°C for 15 min. Now, the pellet was taken up in 8 ml RF2, incubated on ice for 15 min and then the suspension was frozen in methanol/dry ice as 100 µl aliquots. Competent cells were stored at -80°C.

3.2.3.7 Transformation of chemically competent *E.coli*

Competent *E.coli* DH5α were carefully thawed on ice and mixed with all of the ligation reaction or 100 pg of pure vector. They were then incubated on ice for 20 min, heat shocked at 42°C for 1 min and cooled on ice. Afterwards, all of the cells transformed with ligation reactions were plated on LB agar plates with 100 µg/ml ampicillin, whereas only 10 µl of the plasmid-transformed cells were plated. The plates were then incubated at 37°C over night.

3.2.3.8 Colony PCR

E.coli colonies from ligation reactions were transferred into 100 µl LB medium in 1.5 ml tubes and incubated shaking at 37°C for 4 h. Then, 1 µl of this mix was used for a control PCR to check presence of the insert in the vector.

1 µl bacterial culture was mixed with 15.7 µl water, 2 µl 10 x PCR buffer without $MgCl_2$, 0.5 µl 50 mM $MgCl_2$, 0.16 µl 25 mM dNTPs, 2 µl 50 µM primer mix and 0.3 µl Taq Polymerase. The PCR was run under the following conditions:

94°C	5 min	1 x
94°C	15 s	30 x
60°C	30 s	
72°C	1 min/kb	
72°C	5 min	1 x
4°C	hold	

The products were then analysed on a 1% agarose gel and colonies showing only one PCR product of the right size were inoculated for miniprep. For shRNA cloning, no colony PCR was performed, the clones were directly subjected to minipreps and control digested.

3.2.3.9 Miniprep

Plasmids were isolated from bacteria using the alkaline lysis method. Briefly, cells are first resuspended in a Glucose-Tris-EDTA buffer containing RNase, are then lysed with 0.2 M NaOH/1% SDS and the suspension is neutralised with a potassium acetate solution (Engebrecht & Brent, 2001), which leads to precipitation of genomic DNA,

proteins and high molecular weight RNAs (Bimboim & Doly, 1979). After removal of the precipitated molecules, the plasmid can be precipitated using Isopropanol.

For the plasmid preparation, *E.coli* colonies were transferred into 5 ml LB with 100 µg/ml ampicillin and cultured at 37°C shaking over night. The next day, 3 ml of the suspension were transferred into a new tube and sedimented by centrifugation at 10,000 x g for 5 min. The pellet was thoroughly resuspended in 300 µl buffer P1, then 300 µl P2 were added and the tube was inverted 6 to 8 times. After a 2 minute incubation at room temperature, 300 µl cold P3 were added. The suspension was incubated on ice for 5 min, then centrifuged for 10 min at 16,100 x g and 4°C. 800 µl of the supernatant were transferred to a new tube and 560 µl of isopropanol were added. The samples were mixed by inverting, the DNA was precipitated by centrifugation at 16,100 x g for 30 min at 4°C and the pellet was washed with 1 ml 70% ethanol. After another centrifugation at 16,100 x g and 4°C for 10 min, the pellet was air dried and resuspended in 20 µl 1 x TE.

The DNA concentration was measured and the plasmid was used for a control digestion. pCMV-SPORT6-PIM1S/-PIM1S-KD were digested with the same restriction endonucleases used for cloning, pMSCV-miR30-shRNA plasmids were digested with BglII and HindIII in NEBuffer 2, which results in excision of a 900 bp fragment. The pLKO_IPTG_3xLacO-shRNA plasmids were cut with EcoRI and NotI in NEBuffer 4 and AgeI and NotI in NEBuffer 4. NotI and EcoRI should cut a fragment of about 1200 bp out of the vector, while the AgeI site was destroyed during cloning, leading to a vector cut only by NotI in the second reaction. For pLKO_IPTG_3xLacO-shMYC, both reactions result in a fragment of about 1200 bp. The resulting fragments were analysed on a gel and if they matched the expected fragment sizes, the plasmid was sent for sequencing to Source Bioscience, Nottingham, UK. The sequenced insert was compared to the reference sequence using BLASTN (http://blast.ncbi.nlm.nih.gov/Blast.cgi) and if the two sequences matched, the bacterial colony carrying the plasmid was used for maxiprep.

3.2.3.10 Maxiprep

To obtain DNA, which is clean enough for transfection into mammalian cell lines, the plasmid had to be purified further and large-scale preparations of the plasmid were carried out using the QIAGEN Plasmid Maxi Kit according to the manufacturer's recommendations. 5 µl *E.coli* culture containing the plasmid (rest from miniprep) were transferred into 5 ml of LB with 100 µg/ml ampicillin and incubated for 8 h at 37°C shaking. This starting culture was then used to inoculate a 500 ml over night culture,

which was subjected to maxiprep. The resulting DNA pellet was resuspended in 50 to 100 µl of 1 x TE. After measuring the DNA concentration using the NanoDrop™, the plasmid DNA was stored at -20°C.

3.2.4 Protein analysis

3.2.4.1 Preparation of protein lysates

Suspension cells were collected by centrifugation at 300 x g for 5 min at room temperature, resuspended in 1 ml PBS, transferred into a 1.5 ml tube and pelleted by centrifugation at 16.100 x g for 10 s. The pellet was resuspended in an appropriate amount of RIPA buffer (20 – 50 µl). Samples were then stored at -80°C until used.

3.2.4.2 Bradford protein assay

For protein samples generated from cell lines, a Bradford protein assay was used to measure protein concentrations in the sample. Bradford reagent was diluted 1:5 in dH_2O and 1-2 µl of protein lysate were mixed with 500 µl of diluted reagent. For the standard curve, a 1 µg/µl BSA solution was prepared and 0 µg, 2 µg, 4 µg, 6 µg, 8 µg or 10 µg were added to 500 µl of diluted Bradford reagent. The absorbance of the samples at 595 nm was then measured in 150 µl duplicates using the Mithras plate reader. The analysis was done using Microsoft Excel. The standard curve was generated by plotting the absorbance against the amount of BSA used. From that, the protein concentrations of the samples could be calculated.

3.2.4.3 Nuclear-cytoplasmic fractionation

Nuclear-cytoplasmic fractionation was done using the Rapid, Efficient and Practical (REAP) method as described by Suzuki et al. (Suzuki et al., 2010). Briefly, cells were sedimented by centrifugation at 300 x g for 5 min, the cell pellet was resuspended in 1 ml cold PBS and transferred into a 1.5 ml tube. The cells were sedimented by centrifugation at 16,100 x g for 10 s at 4°C and washed two more times with cold PBS. Then, the cells were lysed in 100 µl cold PBS-NP40 by carefully pipetting five to six times. The nuclei were immediately sedimented by centrifugation at 16,100 x g for 10 s at 4°C and the supernatant was removed as the cytoplasmic fraction. The nuclei were washed twice in PBS-NP40 and sedimented each time by centrifugation at 16,100 x g for 10 s at 4°C. Finally, the nuclei were taken up in 100 µl PBS-NP40 and 33 µl 4 x SSB. Nuclear and cytoplasmic fractions were stored at -80°C. Prior to SDS-

Polyacrylamide gel electrophoresis (SDS-PAGE), nuclear lysates were sonicated for 5 min using the Bioruptor at high power, 30 s on, 30 s off.

3.2.4.4 Immunoprecipitation

The primary antibody used for immunoprecipitation was bound to Dynabeads Protein G. To this end, 20 µl Dynabead suspension were mixed with 200 µl PBS-NP40. The beads were separated from the supernatant using a magnet and washed once more with PBS-NP40, before they were resuspended in 200 µl PBS-NP40 and 4.8 µg of the appropriate antibody were added. The suspension was then incubated at 4°C rotating for 2 h.

In the meantime, about 2 x 10^7 cells were sedimented by centrifugation, washed once with PBS and lysed in cold PBS-NP40. If histones were to be analysed, the cell suspension was then sonicated for 5 min using the Bioruptor at high power, 30 s on, 30 s off, otherwise the lysate was immediately used for immunoprecipitation.

The beads with the bound primary antibody were washed once with 200 µl PBS-NP40 and then incubated with the lysate from 5 x 10^6 to 10^7 cells in 100 µl PBS-NP40 for 2 h at 4°C rotating. Afterwards, the supernatant was removed and the beads were washed once with PBS-NP40, once or twice with HCLB-300 and once or twice with HCLB-500. Then, the bound proteins were eluted with 30 µl PBS-NP40 and 10 µl 4 x SSB by heating the suspension at 65°C for 10 min and flicking the tube every 2 to 3 min. The eluate was then transferred to a new tube, stored at -80°C and analysed by SDS-PAGE and western blotting.

3.2.4.5 SDS-PAGE

Polyacrylamide gels were cast using the Mini-PROTEAN® gel stand. For the cell lines, 20 µg to 40 µg of protein or protein lysate from 2 x 10^5 CLL cells were combined with an appropriate amount of dH_2O and 4 x SSB. The CLL samples were then subjected to a 5 minute sonication at high setting, 30 s on, 30 s off. Samples were denatured at 95°C for at least five minutes. Subsequently, the samples and 5 µl protein ladder were loaded and the gels were run at 30 to 50 mA/gel in 1 x running buffer until the desired separation was achieved.

3.2.4.6 Western blotting

After separating proteins on an SDS-polyacrylamide gel, western blotting was performed using a PVDF membrane, which was activated in methanol and then washed with transfer buffer. Four sheets of filter paper and the gel were equilibrated in transfer buffer for 5 min until the transfer sandwich was assembled as shown in Figure 3.10.

Figure 3.10 Assembly of the transfer sandwich.
For western blotting, the acrylamide gel and the membrane were placed between filter papers so that the membrane faces the anode.

The blotting was performed at 4°C in a tank filled with 1 x transfer buffer for 1.5 h at 300 mA with constant stirring. After the blotting, the membrane was washed in TBST, blocked with 5% milk or 5% BSA in 1 x TBST for at least 30 min, washed again and incubated with the primary antibody against the protein of interest over night. Afterwards, the membrane was washed three times 10 min with 1 x TBST and then incubated with the appropriate secondary antibody diluted in 5% milk or 5% BSA in 1 x TBST, respectively. After a 1 h incubation at room temperature, the membrane was washed three times ten minutes in 1 x TBST and treated with HRP substrate for 5 min. Then, the membrane was exposed to a chemiluminescence film (Amersham Hyperfilm™ ECL), which was developed using the Konica SRX-101A developer.

3.2.5 RNA analysis

3.2.5.1 Preparation of total RNA

Total RNA was prepared from 0.5 - 2 x 10^6 cells using TRIzol® according to the manufacturer's recommendations. The RNA pellet was redissolved in 16.5 µl HyClone™ water, 2 µl 10 x DNase buffer, 1 µl DNase and 0.5 µl RNaseOut and incubated at 37°C for 30 min to digest contaminating genomic DNA. Afterwards, 0.5 ml TRIzol® were added and the RNA was extracted again. The dry RNA pellet was taken up in 10 - 20 µl of HyClone™ water and dissolved at 55°C for 10 min. After that, the RNA concentration was determined using the NanoDrop™ spectrophotometer and the RNA was stored at -80°C.

3.2.5.2 Measuring RNA and DNA concentrations

To determine the concentration of DNA or RNA in solution, the NanoDrop™ spectrophotometer was used. DNA and RNA concentrations were determined by measuring the absorbance of the sample at 260 nm and normalising to the absorbance at 340 nm, using the following formulas:

$$c_{DNA} = (A_{260} - A_{340}) * 50 \frac{ng}{ml}$$

$$c_{RNA} = (A_{260} - A_{340}) * 40 \frac{ng}{ml}$$

Further, the ratio between absorbance at 260 nm and 280 nm was calculated as a measure of purity:

$$purity \rightarrow \frac{(A_{260} - A_{340})}{(A_{280} - A_{340})} = 1.8\ for\ pure\ DNA, 2.0\ for\ pure\ RNA$$

RNA samples with lower values were still used for cDNA synthesis, but results were analysed more carefully. Similarly, DNA with lower values was still used for cloning and transfection.

3.2.5.3 cDNA synthesis

For the cDNA synthesis, 0.5 - 1 µg of RNA were mixed with HyClone™ water and 1 µl diluted random primers (1 µM) to a final volume of 14 µl and incubated at 70°C for 5 min. Hereafter, the mixture was chilled on ice and 4 µl 5 x FS buffer, 1 µl MMLV reverse transcriptase, 0.5 µl RNaseOut and 0.5 µl 25 mM dNTPs were added. The cDNA synthesis was performed at 37°C for 1 h, followed by a denaturation at 95°C. The cDNA was diluted 1:5 in 1 x TE and stored at -20°C.

3.2.5.4 qPCR

For real-time qPCR, cDNA was diluted 1:10, genomic DNA (gDNA) from ChIP experiments 1:5 or 1:50 (input samples) in HyClone™ water. For the standard curve, aliquots of all cDNA or ChIP input samples used in the experiment were mixed and diluted 1:5 for cDNA or 1:20 for ChIP inputs. A 1:5 dilution series was made, with the lowest concentrated sample being 1:625 or 1:2500 diluted, respectively. The PCR reaction was carried out in duplicate in clear 96- or 384-well plates. For each well 5 µl diluted DNA, 5 µl GoTaq® qPCR Master Mix and 0.02 µl primer mix (500 µM forward and reverse primer) were combined. If the PCR was run using the ABI 7900HT, 0.05 µl CXR dye were also added to each sample. A sample with HyClone™ water instead of

DNA was used as a negative control. The qPCR was run in an ABI 7500 for 96 well plates or ABI 7900HT real-time cycler for 384 well plates under the following conditions:

50°C	2 min	1 x
95°C	10 min	1 x
95°C	15 s	40 x
60°C	1 min	

The amplification was followed by a melting curve analysis from 60°C to 95°C to ensure the specificity of the amplification. Only samples, for which the melting curve had only one peak with high amplitude were included in the analysis (Figure 3.11).

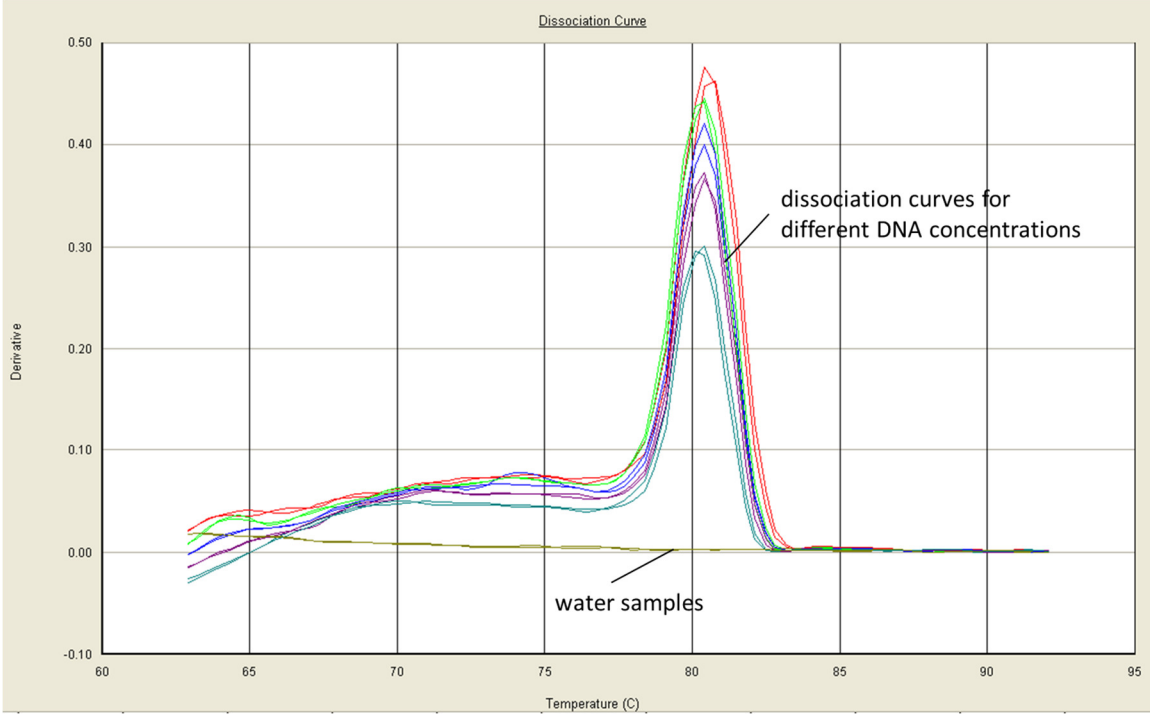

Figure 3.11 Example dissociation curves for a 1:5 dilution series of input DNA and a water control sample.

Ct values were calculated individually for each primer pair to make sure that the threshold was set in the exponential phase of the reaction. The final analysis was carried out in Microsoft Excel, using the efficiency-corrected ΔΔCt method (Pfaffl, 2001). The standard curve was generated by plotting the Ct values against the relative amounts of DNA in the individual samples. Linear regression was performed and the

efficiency (E) of the amplification was calculated using the slope (a) of the curve in the following formula:

$$E = 10^{-1/a}$$

An efficiency of 2 means that the DNA was exactly doubled in every PCR cycle, E < 2 means that it was less than doubled and E > 2 means that it was more than doubled. Then, the amount of DNA in the samples was calculated relative to a control sample using the following formula:

$$relative\ amount\ of\ DNA = \frac{\frac{(E_{target})^{-Ct_{target,sample}}}{(E_{target})^{-Ct_{target,control}}}}{\frac{(E_{reference})^{-Ct_{reference,sample}}}{(E_{reference})^{-Ct_{reference,control}}}}$$

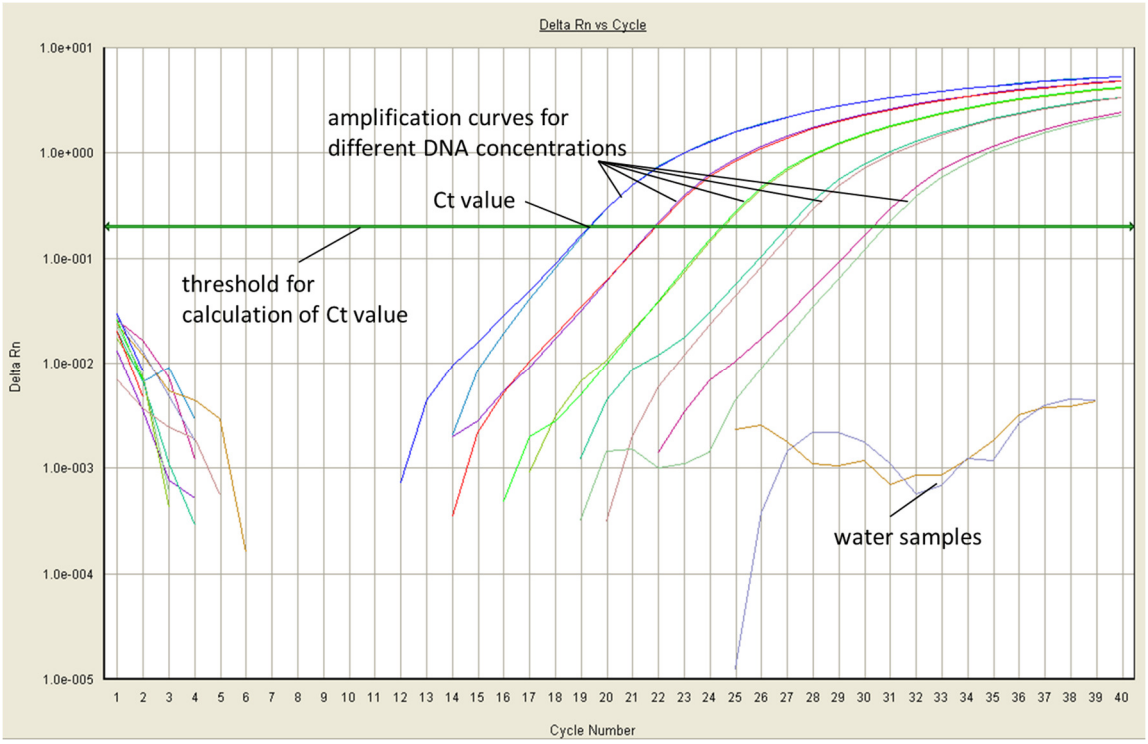

Figure 3.12 Example amplification curves for a 1:5 dilution series of input DNA and a water control sample.
The Ct values were set in the exponential phase of the amplification.

3.2.6 Chromatin analysis

To detect protein-DNA interactions, chromatin immunoprecipitation (CHIP) was used. Figure 3.13 shows a brief overview of the procedure.

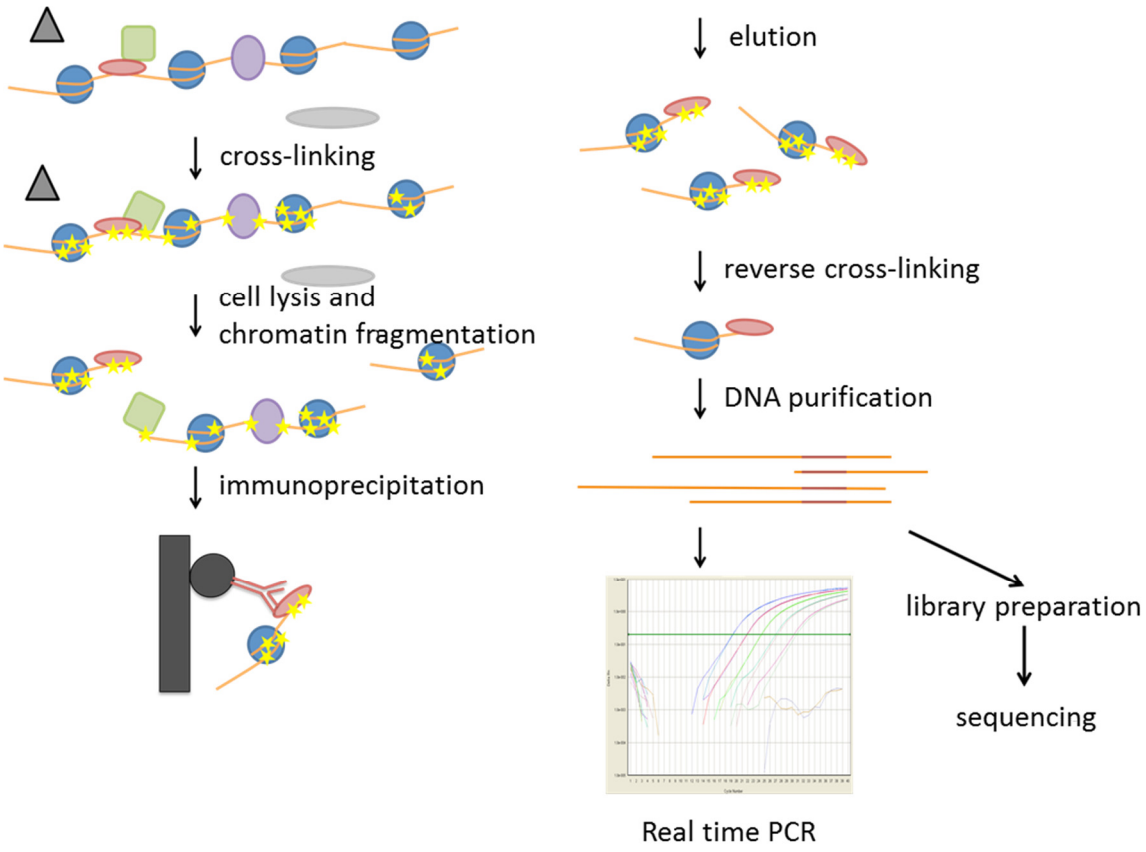

Figure 3.13 Chromatin immunoprecipitation (ChIP).
After cross-linking the DNA and its associated proteins, cells are lysed and the chromatin is fragmented. Application of an antibody coupled to magnetic beads leads to precipitation of the protein of interest and its associated DNA. After elution of the complex from the beads, the cross-linking is reversed, the DNA is purified and subsequently analysed by real-time qPCR. Alternatively, a library can be generated and sequenced.

3.2.6.1 Preparation of chromatin

Cells in culture medium were treated with formaldehyde at a final concentration of 1.5% for 10 min at room temperature with gentle agitation. The cells were then scraped off the tissue culture flask, transferred into 50 ml tubes and sedimented by centrifugation at 800 x g for 5 min. Cell lines were washed three times with 10 ml PBS, whereas CLL cells were resuspended in 1 ml PBS and transferred into 1.5 ml tubes. They were washed twice by spinning for 10 s at 16,100 x g and resuspending in PBS.

Subsequently, the cells were resuspended in 10 ml or 1 ml buffer A, respectively, and incubated at 4°C for 10 min on a rotating wheel. Sedimentation of the nuclei was done by centrifugation at 800 x g for 5 min (cell lines) or 16.100 x g for 10 s (CLL cells). The supernatant was discarded and the nuclei were resuspended in 10 ml or 1 ml buffer B, respectively. After a 10 min incubation at 4°C on a rotating wheel, the nuclei were again sedimented and resuspended in 100 µl glycerol buffer/2 x 10^7 cells. The suspension was then either frozen at -80°C and thawed later for sonication (cell lines) or directly subjected to sonication (CLL cells).

3.2.6.2 Chromatin sonication

The nuclei in glycerol buffer were mixed with an equal amount of 2 x IP buffer and sonicated using the Bioruptor sonicator. For each cell line and for the primary CLL cells, sonication conditions were optimised by testing different sonication times and analysing samples on a 1% agarose gel. Samples for analysis were treated like input samples and run on a gel after the 4 h incubation with proteinase K (see section 3.2.6.3). Sonication was satisfactory, when the bulk of the fragments was seen between 200 and 1000 bp. The chromatin of the lymphoma cell lines was sonicated for 2 x 15 min on high power, with 30 s on, 30 s off. The CLL chromatin was sonicated for 2 x 10 min on high power, with 30 s on, 30 s off. After the first cycle, the tubes were inverted a couple of times to guarantee optimal chromatin shearing. Subsequently, cell debris was removed by centrifugation at 5,900 x g for 5 min and the supernatant was transferred to a new tube. The chromatin was then either frozen at -80°C for up to a few days or directly used for ChIP.

3.2.6.3 Chromatin immunoprecipitation (ChIP)

For the chromatin precipitation, 10 µl of Dynabeads Protein G were washed twice with 100 µl 1 x IP buffer, using a magnet. The beads were then resuspended in 100 µl 1 x IP buffer and 2.4 µg of the desired antibody were added. Binding of the antibody to the Protein G was achieved during a two hour incubation at 4°C on a rotating wheel. Afterwards, the beads were washed once with 1 x IP buffer. The sheared chromatin was diluted in 1 x IP buffer, so that 100 µl of the suspension contained the chromatin of 2 x 10^6 to 2 x 10^7 cells, depending on the antibody used. The beads were then resuspended with 100 µl of this chromatin suspension and incubated for 2 h at 4°C on a rotating wheel. 10 - 20 µl of chromatin suspension were kept as an input sample.

In the next step, the beads were washed once with 100 µl each of washing buffer 1, washing buffer 2, LiCl buffer and twice with 100 µl 1 x TE. They were then

resuspended in 50 µl freshly prepared elution buffer and incubated at 65°C for 4 h. Simultaneously, the input samples were mixed with 1 µl 10 µg/µl RNase A and incubated at 37°C for 30 min. Next, 1 µl 50 µg/µl Proteinase K were added and the samples were incubated at 65°C for 4 h. Afterwards, the eluates and the inputs were transferred into a 96-well plate. Elution buffer was added to the input samples to make up 50 µl and all samples were subjected to DNA purification.

3.2.6.4 DNA purification

3.2.6.4.1 Purification using AMPure beads

If ChIP samples were used for qPCR, 90 µl of AMPure bead suspension were added to 50 µl of DNA sample. The samples were mixed by inversion, incubated at room temperature for 5 min and the beads were separated from the supernatant using a magnet. The supernatant was discarded and, on the magnet, the beads were washed twice with freshly prepared 70% ethanol without disturbing the pellet. The beads were then air-dried for 5 min and the DNA was eluted with 33 µl of 1 x TE. The DNA was now used for qPCR (see section 3.2.5.4).

3.2.6.4.2 Purification using phenol-chloroform precipitation

If ChIP samples were prepared for library generation and sequencing, the DNA was purified using phenol-chloroform precipitation. 50 µl of DNA were mixed with 150 µl freshly prepared 3:1 phenol-chloroform and vortexed for 10 s. The samples were centrifuged at 15,000 x g for 5 min at room temperature, the upper aqueous layer was transferred to a fresh tube and mixed with 150 µl chloroform. The mixture was again vortexed for 10 s, spun at 15,000 x g for 5 min at room temperature and the upper aqueous layer was transferred into a fresh tube. Then, 4 ml 5 mg/ml glycogen, followed by 250 µl ice cold 100% ethanol were added. After gentle mixing, the samples were incubated at -20°C for 30 min. After that, the DNA was pelleted by a 15 minute centrifugation at 15,000 x g and 4°C. The pellet was washed with 250 µl freshly prepared ice cold 70% ethanol, pelleted again by centrifugation at 15,000 x g and 4°C for 15 min and the supernatant was removed. After another 2 min centrifugation to remove all residual ethanol, the pellet was air dried and then incubated in 20 µl 0.1 x TE at 37°C for 45 min to resuspend the DNA. The samples were then stored at 4°C for up to a few days.

3.2.6.5 Analysis of ChIP-qPCR data

qPCR data were normalised as described in section 3.2.5.4. In formula 1), the input samples served as controls, and an invariant genomic region was used as the reference.

$$1)\ relative\ amount\ of\ DNA = \frac{\frac{(E_{target})^{-Ct_{target,sample}}}{(E_{target})^{-Ct_{target,control}}}}{\frac{(E_{reference})^{-Ct_{reference,sample}}}{(E_{reference})^{-Ct_{reference,control}}}}$$

3.2.6.6 Library preparation for ChIP-sequencing (ChIP-seq)

Before library preparation, the quality of the ChIP was assessed by qPCR using an aliquot of the sample.

3.2.6.6.1 DNA quantification

For the DNA quantification, the Quant-iT DNA assay kit (LifeTechnologies) was used according to the manufacturer's recommendations. The DNA staining solution was prepared by diluting the DNA dye 1:200 in the required amount of dilution buffer. Then, a black 96-well plate was set up as shown in Figure 3.14. 2 µl of each sample and each standard were diluted in 198 µl DNA staining solution. As the DNA concentrations in the samples were very low, the standards were diluted 1:10 in DNA staining solution to generate a standard curve in the range of the sample DNA concentrations. The samples were mixed by briefly shaking the plate on a plate shaker. Then, the fluorescence of the samples was measured with an excitation wave length of 485 nm and the emission was detected at 520 nm using a FLUOStar GALAXY fluorometer.

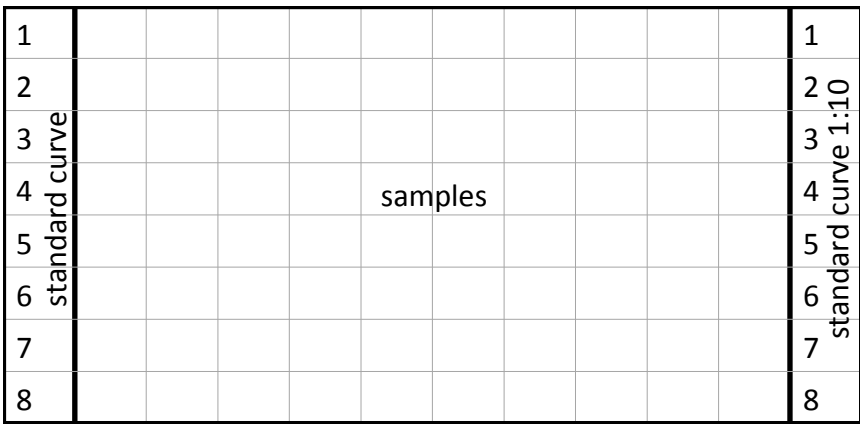

Figure 3.14 Set up of DNA quantification assay

The analysis was done by the FLUOstar software. The standard curve was calculated using the 1:10 diluted standards by plotting the fluorescence units against the DNA concentrations and performing a linear regression. Using the equation calculated for the standard curve, the DNA concentrations in the samples could be determined.

3.2.6.6.2 Library generation

1 to 10 ng of DNA were used to prepare ChIP-seq libraries using the MicroPlex Library Preparation kit (Diagenode), following the manufacturer's recommendations. 10 µl of (diluted) DNA sample were mixed with 2 µl Template Preparation Buffer and 1 µl Template Preparation Enzyme. After a brief centrifugation, the samples were incubated in a thermal cycler at 22°C for 25 min, then at 55°C for 20 min, followed by 22°C for up to 10 min. The liquid was collected at the bottom of the tube by centrifugation and 1 µl of each Library Synthesis Buffer and Library Synthesis Enzyme were added. The samples were mixed thoroughly, briefly centrifuged and incubated in a thermal cycler at 22°C for 40 min and then kept at 4°C for up to 30 min. After another centrifugation step, the library was amplified. For this purpose, 8 µl nuclease-free water, 48.5 µl Library Amplification Buffer and 1.5 µl Library Amplification Enzyme were added. The samples were mixed by pipetting, before 2 µl of the indexing reagents were combined with the samples.

As the Illumina sequencer uses a red laser to sequence A/C and a green laser to sequence G/T, it is important to combine indices for multiplexing so that every position gives a signal in both channels (Table 3.2).

A T C A C G C G A T G T T T A G G C T G A C C A A C A G T G G C C A A T	A T C A C G C G A T G T T T A G G C T A G C T T G G C T A C C T T G T A
not okay → position 3 only red!	okay → both colours in all positions

Table 3.2 Examples of acceptable and not acceptable combinations of indices for Illumina sequencing.

The samples were then spun down and the DNA was amplified in a thermal cycler using the following programme:

72°C	3 min	1 x
85°C	2 min	1 x
98°C	2 min	1 x
98°C	20 s	4 x
67°C	20 s	
72°C	40 s	
98°C	20 s	15 – 18 x, depending on the amount of starting material
72°C	50 s	
4°C	hold	

The quality of the library was then analysed using the TapeStation. If no prominent band between 200 to 400 bp was detected, the sample was immediately subjected to further amplification cycles, using the following conditions:

98°C	20 s	2 – 3 x
72°C	50 s	
4°C	hold	

Subsequently, the library was again analysed on the TapeStation. If the prominent band at 200 to 400 bp was detected, the library was then size-selected using AMPure beads.

3.2.6.6.3 Analysis of the library using the TapeStation

The buffer, ladder and Screen Tape were equilibrated at room temperature for 30 min. Then, 3 µl of sample buffer were pipette-mixed with 1 µl of ladder or 1 µl of library DNA in an 8-well strip. The strip, a Screen Tape and loading tips were placed in the TapeStation and the run was started. The analysis was performed using the TapeStation analysis software.

3.2.6.6.4 Library size selection using AMPure beads

The library samples were transferred into 1.5 ml tubes, made up to 100 µl with 0.1 x TE and mixed with 80 µl AMPure bead suspension. The mix was then vortexed, incubated at room temperature for 5 min and the beads were separated from the supernatant using a magnet. The beads have bound large, the supernatant contains shorter DNA fragments. The supernatant was transferred into a new 1.5 ml tube and combined with 20 µl AMPure beads, which bind the shorter DNA fragments. The mix was again vortexed, incubated for 5 min and then the beads were sedimented using a magnet. The supernatant was discarded and, on the magnet, the beads were washed twice with freshly prepared 80% ethanol without disturbing the pellet. After air-drying the beads, the DNA was eluted with 20 µl 0.1 x TE. The size-selected library was once more analysed using the TapeStation. A successful purification leads to an enrichment of fragments between 200 and 400 bp and a loss of any larger DNA fragments. If necessary, the size selection was repeated. The concentration of the size-selected library was measured using the Quant-iT DNA analysis kit.

3.2.6.6.5 Sequencing of the library

Six of the amplified, size-selected libraries were combined, when possible at equal concentrations, to a final concentration of 2 ng/µl. If necessary, the pool was concentrated using the DNA Clean & Concentrator Kit according to the manufacturers recommendations. The DNA was eluted with 10 µl 0.1 x TE. The sequencing was performed by the Next Generation Sequencing Facility of the University of Leeds using the Illumina HiSeq 2000 sequencer in rapid mode according to the manufacturer's instructions.

3.2.6.7 Data analysis of ChIP-seq data

The analysis of the sequencing raw data was done by Matthew Care. Briefly, the reads were trimmed to remove adapters and low confidence regions using a python script. Low confidence regions were defined as regions spanning four nucleotides with an average Phred quality score < 20, which is less than 99% accuracy. The reads were trimmed down to such regions. Trimmed reads were then aligned to the hg19 human genome assembly using Bowtie2 and the 'very sensitive' setting (Langmead & Salzberg, 2012). The resulting SAM file was converted into a BAM file, using a cut-off for the mapping quality score of 20, which reflects a minimum 99% confidence that the read was aligned correctly. The BAM files were analysed for peaks using GEM

(Genome wide Event finding and Motif discovery) with a quality score of 1. Here the quality score is $q = -\log_{10}(FDR)$, which means one in 10 peaks might be false.

Further, the BAM files were converted into BED files and fragment length was estimated using MaSC (mappability-sensitive cross-correlation) (Ramachandran et al., 2013). The reads were then extended to the estimated fragment length and a BED file, scaled to reads per million, was generated. This was converted to a coverage file using the UCSC genomeCoverageBed tool and then to a BigWig file using UCSC bedGraphToBigWig, which was visualised using the UCSC genome browser (http://genome.ucsc.edu/) (Kent et al., 2002). Peaks were annotated using V19 of Gencode or the latest RefSeq annotation.

All further analysis was carried out by myself. The peak data were used for a motif analysis with MEME ChIP (Machanick & Bailey, 2011). As the data were available only as genomic intervals, the sequences for the chromosomal peak regions had to be retrieved using the Galaxy function “Extract Genomic DNA” (Blankenberg et al., 2001; Giardine et al., 2005; Goecks et al., 2010). The resulting FASTA file was entered into MEME ChIP, compared versus the Jolma2013, JASPAR CORE and UniProbe Mouse motif databases and the top motifs detected by MEME and CentriMo were analysed further.

The sequences in which CTCF motifs were detected were extracted, uploaded to Galaxy and converted into interval files. As CTCF motifs from 3 different sources (Jolma 2013, JASPAR CORE and MEME *de novo* motif) were used, three mostly overlapping, but partly distinct datasets were generated. Consequently, these datasets were fused using the “Join two Datasets” function, converted into a BED file and intersected with available ChIP-seq peak data for CTCF in GM12878 cells (UCSC accession wgEncodeEH000029). Further, all peak sequences were compared to publicly available H3K27ac and STAT3 ChIP-seq peaks from GM12878 cells (UCSC accessions wgEncodeEH000030 and wgEncodeEH001811).

4 PIM kinases in transcriptional regulation in B cell lymphoma

Signalling kinases play an important role in transcriptional regulation by phosphorylating histone and non-histone proteins. PIM1 has been shown to associate with MYC, to phosphorylate histone H3S10 and to promote transcriptional elongation (Zippo et al., 2007; Zippo et al., 2009). Another H3S10 kinase, IKKα, associates with NFκB (Anest et al., 2003; Yamamoto et al., 2003), phosphorylates HP1γ and H3.3S31p and binds to the phosphorylated POL II CTD to travel with the elongating POL II (Thorne et al., 2012) (Figure 4.1). As kinases often have redundant functions at different genes or in response to different stimuli (Duncan et al., 2006) and as PIM1 can also target HP1γ (Koike et al., 2000), we hypothesised that at MYC-dependent genes, PIM kinases might function like IKKα at NFκB target genes. It has been extensively shown that PIM2 can compensate for PIM1 knockout (Allen et al., 1997; van der Lugt et al., 1995) and that PIM1 and PIM2 share several substrates, so that we hypothesised that PIM2 might also be recruited to MYC and stimulate transcriptional elongation.

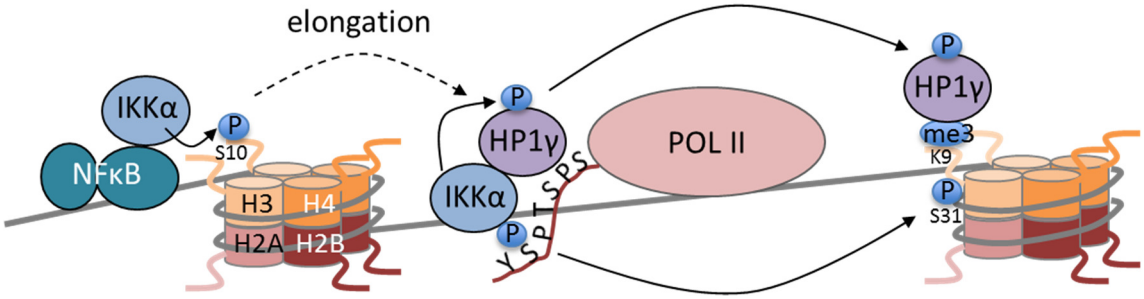

Figure 4.1 IKKα travels with the elongating POL II and phosphorylates H3.3S31. IKKα binds to NFκB at the promoters of target genes, where it phosphorylates H3S10 and promotes transcriptional elongation. It also binds to the POL II CTD and travels with the elongating POL II. HP1γ, which is also bound to the CTD independent of IKKα, is phosphorylated by the latter and then loaded onto H3K9me3. It inhibits IKKα-mediated phosphorylation of H3S10, but stimulates H3.3S31 phosphorylation. Because PIM1 also stimulates elongation by phosphorylating H3S10 and also phosphorylates HP1γ, it might mimic the other functions of IKKα as well.

PIM1 has been shown to be nuclear in DLBCL and BL and this is associated with progressive disease (Brault et al., 2012; Ionov et al., 2003). Further, high *PIM1* and *PIM2* mRNA expression are a distinguishing factor of ABC-DLBCL vs. GCB-DLBCL (Care et al., 2013; Wright et al., 2003). Therefore, MYC-dependent activation of

transcription by PIM kinases might play a role in survival of lymphoma cells and in disease progression. This part of the thesis aims to answer the following questions:

1. Does PIM kinase inhibition reduce the viability of B cell lymphoma cell lines?
2. Does PIM1 regulate MYC-dependent gene expression in BCL cell lines? And does it mimic the functions of IKKα at NFκB target genes?
3. Is the effect of PIM kinase inhibition on viability due to a change in MYC-dependent transcription?
4. Do PIM kinases have other functions at the chromatin level?

4.1 Expression of PIM kinases in BCL cell lines

First, expression of PIM kinases was assessed in the cytoplasm and nucleus of six different lymphoma cell lines (Figure 4.2). OCI-Ly3 and OCI-Ly10 are ABC-DLBCL cell lines, SUDHL6 and OCI-Ly19 are GCB-DLBCL cell lines and Raji and Ramos are BL cell lines. While Raji cells are EBV-transformed, Ramos cells are EBV-negative.

Both the 34 and 44 kDa PIM1 isoforms can be detected by western blot. Further, in the nucleus, the antibody detected a 50 kDa protein of unknown identity, which might be a ubiquitinated or otherwise modified PIM1 variant. The PIM2 antibody also detects all three PIM2 isoforms of 34, 38 and 40 kDa. As expected, both ABC-DLBCL cell lines expressed high levels of PIM1 and PIM2 protein. Also consistent with the literature (Rainio et al., 2005), Raji BL cells showed high expression of PIM1, but lower PIM2 levels, whereas non-EBV-transformed Ramos cells expressed lower levels of both PIM1 and PIM2. GCB-DLBCL cells had the lowest amounts of PIM1 and PIM2, the 34 kDa PIM1 variant and PIM2 being completely undetectable in OCI-Ly19 cells (Figure 4.2 A). However, the kinases were detected mostly in the cytoplasmic compartment and nuclear PIM1 and PIM2 were only visible after longer exposure of the film (Figure 4.2 A). Comparable MYC expression was seen in all cell lines and its localisation was mainly nuclear (Figure 4.2 A). However, a substantial amount of MYC was also detected in the cytoplasm. This is in agreement with a previous study showing that MYC is present in both nucleus and cytoplasm of both BL and DLBCL cells (Ruzinova et al., 2010).

Similarly, mRNA expression of *PIM1* was higher in OCI-Ly3 and Raji than in Ramos and SUDHL6 cells. Of note, *PIM1* levels were variable between experiments. Also consistent with the protein data, *PIM2* mRNA expression was highest in OCI-Ly3, lower in the BL cell lines and lowest in SUDHL6 cells (Figure 4.2 B).

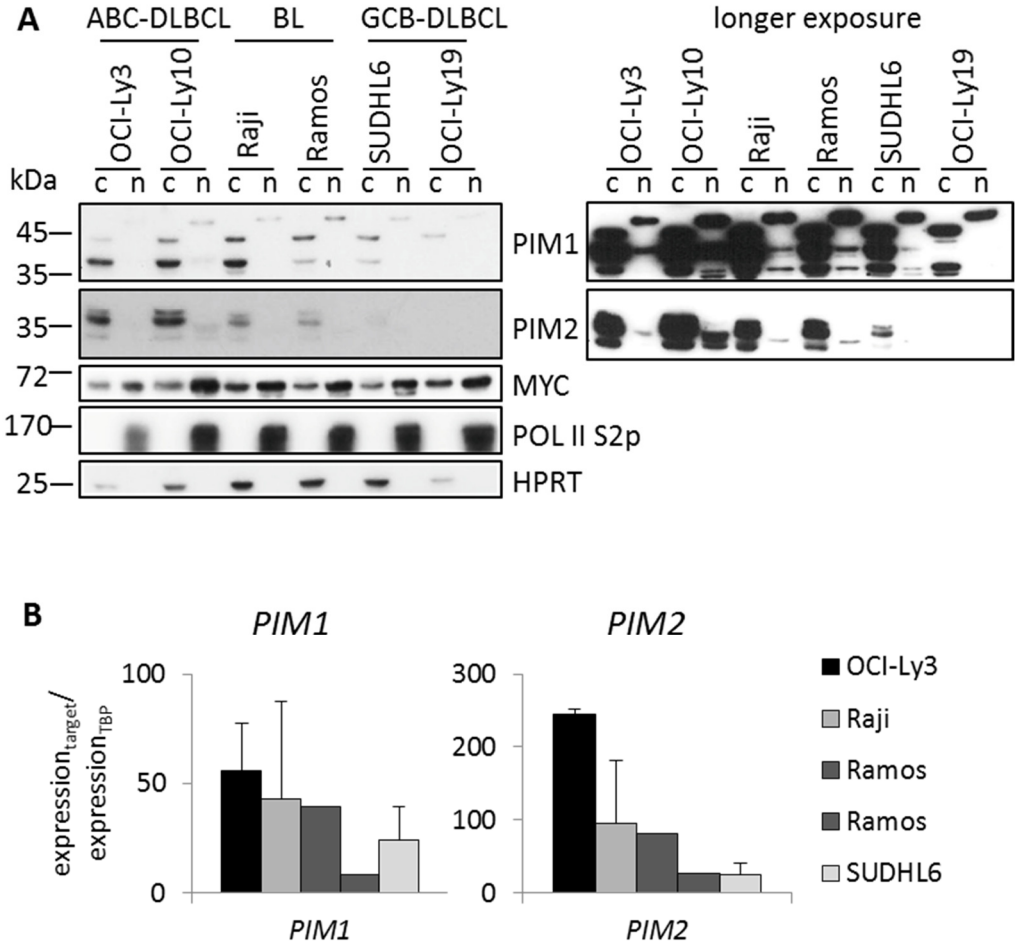

Figure 4.2 Expression of PIM kinases in B cell lymphoma cell lines.
A Protein expression of PIM kinases was assessed in different BCL cell lines by western blot after nuclear-cytoplasmic fractionation (c = cytoplasm, n = nucleus). The data are representative of three independent experiments. PIM kinases were mainly cytoplasmic, while MYC predominantly localised to the nucleus in all cell lines tested. **B** mRNA expression of *PIM1* and *PIM2* was measured by RT-qPCR and is shown relative to *TBP* expression. Means and sd of three to five independent experiments are plotted for OCI-Ly3, Raji and SUDHL6 cells. For Ramos cells, the results of two independent experiments are shown. Expression levels were variable between experiments, but expression of both *PIM1* and *PIM2* were on average highest in OCI-Ly3 and Raji cells.

4.2 PIM1 expression under different conditions

Because PIM1 expression was generally quite low, very variable between experiments and because PIM1 has been shown to be inducible by serum, certain stressors, like oxidative stress and exposure to cytotoxic agents (Katakami et al., 2004; Zemskova et al., 2008; Zippo et al., 2007), as well as by activation of STATs and NFκB (Asano et al., 2011; Lilly et al., 1992; Matikainen et al., 1999; Morcinek et al., 2002; Nosaka et al., 1999; Shirogane et al., 1999; Zhu et al., 2002), induction of PIM kinases in response to different stimuli was assessed in Raji cells.

First, expression of PIM kinases and MYC was monitored after serum starvation and release into normal medium. PIM1 was inducible by serum starvation, with maximum protein levels being reached after 1 h. Protein levels then decreased to or below baseline at 4 h starvation. Release into normal medium resulted in PIM1 induction in 2 out of 4 experiments, whereas PIM1 protein levels remained low in the other 2 experiments. Surprisingly, MYC expression remained high after serum starvation and was reduced after release into normal medium in two out of three experiments (Figure 4.3 A). At the mRNA level, *PIM1* and *PIM2* expression were also increased after 1 h starvation and reduced at later time points (Figure 4.3 B). However, PIM1 protein induction was a lot stronger, suggesting that PIM1 expression was also regulated at the posttranscriptional and/or -translational level. *MYC* mRNA expression was also induced after serum starvation (Figure 4.3 C). When PIM1 levels were monitored over 24 h after medium change, maximum protein levels were also reached at 1 h and remained high (Figure 4.3 D).

Further, because PIM kinase expression is stimulated via STATs and NFκB, we reasoned that stimulation of the BCR might induce expression of PIM1. However, while *MYC* mRNA levels increased upon BCR stimulation in Raji cells, *PIM1* and *PIM2* levels decreased (Figure 4.4 A, B, C). This effect was not restricted to Raji cells, as BCR-stimulated CLL cells also downregulated *PIM1* (Figure 4.4 D). Similarly, phorbol-12-myristate-13-acetate (PMA) treatment, which activates PKC and thus NFκB, did not induce PIM1 or PIM2 protein expression (Figure 4.4 E).

This indicates that PIM1 and MYC expression are induced by certain stressors, like starvation. Interestingly, however, PIM1 expression was also responsive to addition of fresh medium but not to B cell receptor or PMA stimulation. Thus, PIM1 is acutely sensitive to serum-levels but not to the tested growth factors in Raji cells.

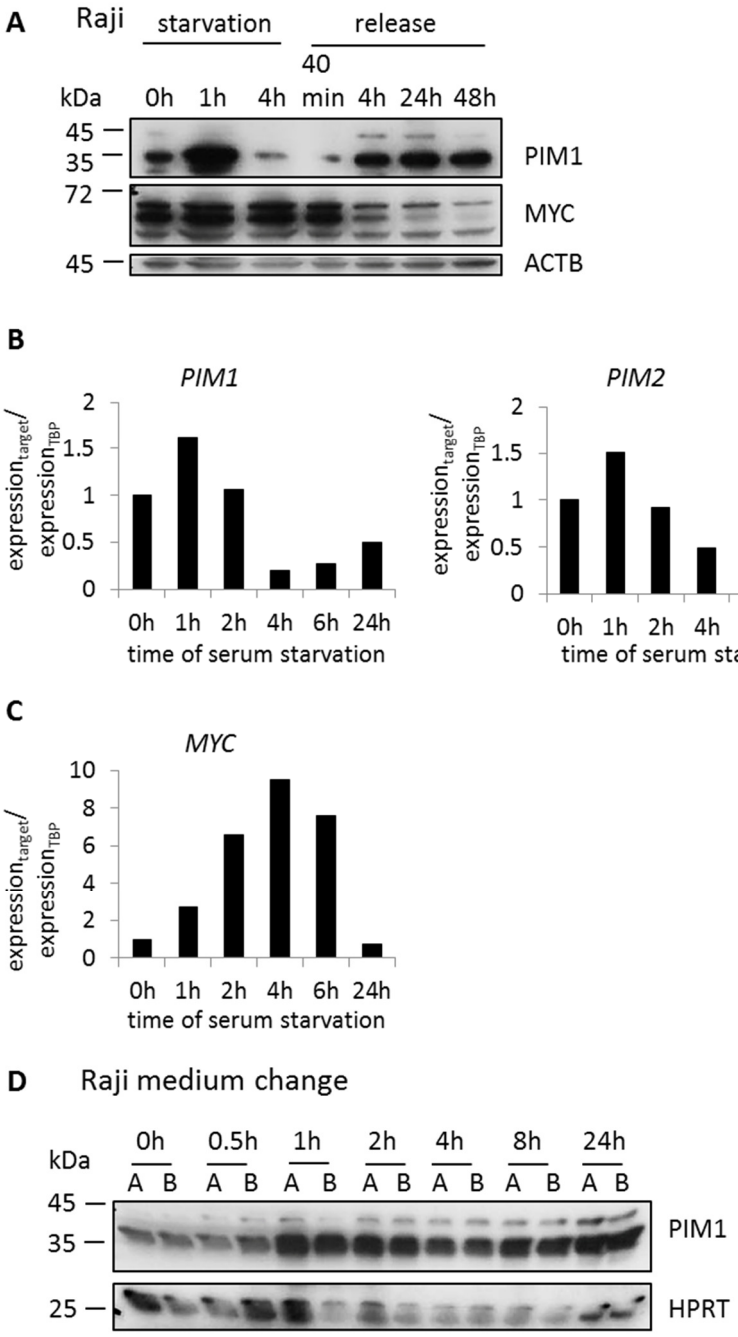

Figure 4.3 Regulation of PIM kinase expression by different serum levels.
A Raji cells were serum starved in 0.5% FCS for 0 h to 4 h and then released into normal growth medium. The western blot shown is representative of four independent experiments for PIM1 and three independent experiments for MYC. PIM1 expression was induced in the first hour after serum starvation, but decreased afterwards. Release from starvation led to induction of PIM1 in two out of four experiments, but PIM1 levels remained low in the other two. MYC protein was not reduced by starvation, but by release into normal growth medium. **B**, **C** Raji cells were serum starved in 0.5% FCS and mRNA levels were assessed by RT-qPCR. One experiment was conducted. Like the protein, *PIM1* and *PIM2* mRNAs were induced immediately after starvation and decreased at 4 to 24 h. *MYC* mRNA was also induced upon starvation and peaked at 4 h. **D** Culture medium of Raji cells was changed and PIM1 protein expression was evaluated before and after medium change. The western blot shown is representative of three independent experiments. PIM1 expression was induced 1 h after the medium change and remained elevated up to 24 h later.

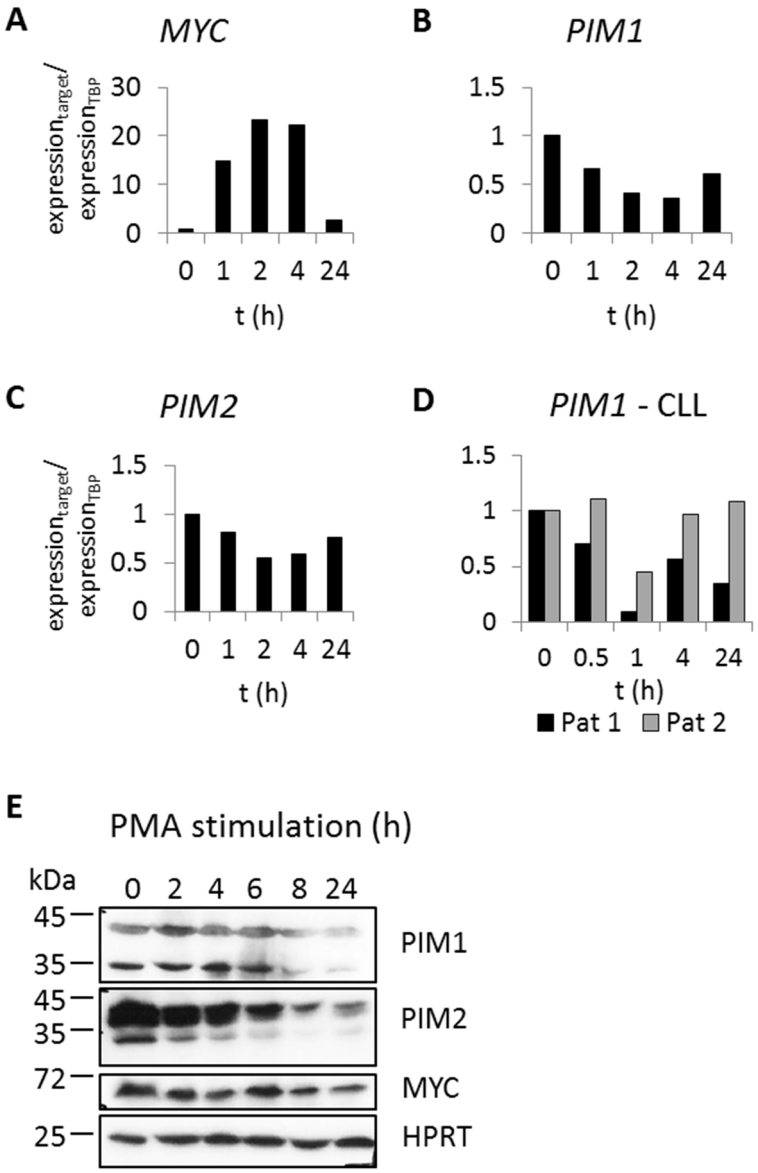

Figure 4.4 Regulation of PIM kinase expression by different stimuli.

A, **B**, **C** Raji cells were stimulated with 10 µg/ml anti-IgM/anti-IgG and expression of *MYC*, *PIM1* and *PIM2* mRNA was measured. One experiment conducted in duplicate wells of a 6-well plate is shown. Data are normalised to TBP expression and untreated cells. While *MYC* was induced after BCR cross-linking, both *PIM1* and *PIM2* were downregulated. **D** CLL cells were stimulated with 10 µg/ml anti-IgM and *PIM1* mRNA expression was assessed. The results from two different patients are shown. Like in the Raji cell line, the *PIM1* mRNA is decreased in patients 1 h after BCR cross-linking. **E** Raji cells were treated with 100 ng/ml PMA for indicated times. Protein was prepared and analysed by western blot. PMA did not induce the expression of PIM1, PIM2 or MYC but led to a downregulation of both PIM1 and PIM2 after 8 and 24 h.

4.3 Treatment of BCL cell lines with PIM kinase inhibitors

In order to test the potential role of PIM kinases in cell viability, two structurally similar kinase inhibitors, SMI4a, and PIM1/2 inhibitor VI (inh VI), and another structurally distinct inhibitor, Quercetagetin, were used as an initial strategy. First, Raji, Ramos, OCI-Ly3 and OCI-Ly10 cells were treated with the PIM kinase inhibitor SMI4a at a concentration of 40 µM (Figure 4.5). At least three experiments were carried out until day 3 in Raji cells or until day 4 in OCI-Ly3 and OCI-Ly10 cells. In Ramos cells, only two experiments were done. In each cell line, one experiment was done until day 9 or 10, respectively, to assess whether the effect of SMI4a would persist over longer times. In all cell lines, SMI4a caused a reduction in cell viability. While DMSO-treated cells grew exponentially, SMI4a-treated cells showed hardly any increase in cell number, even after nine or ten days (Figure 4.5).

Also, when relative cell numbers of different independent experiments were combined, cell numbers were significantly reduced in SMI4a-treated compared to DMSO-treated Raji cells on days 2 and 3 (Figure 4.5 A). Cell number was also greatly reduced in Ramos cells (Figure 4.5 B). No significant difference between SMI4a- and DMSO-treated OCI-Ly10 cells on days 2 and 4 (n = 3) was observed, mainly because the drug effect was very variable between experiments (Figure 4.5 C). In SMI4a-treated OCI-Ly3 cells, however, cell number was significantly decreased on day 4 (Figure 4.5 D).

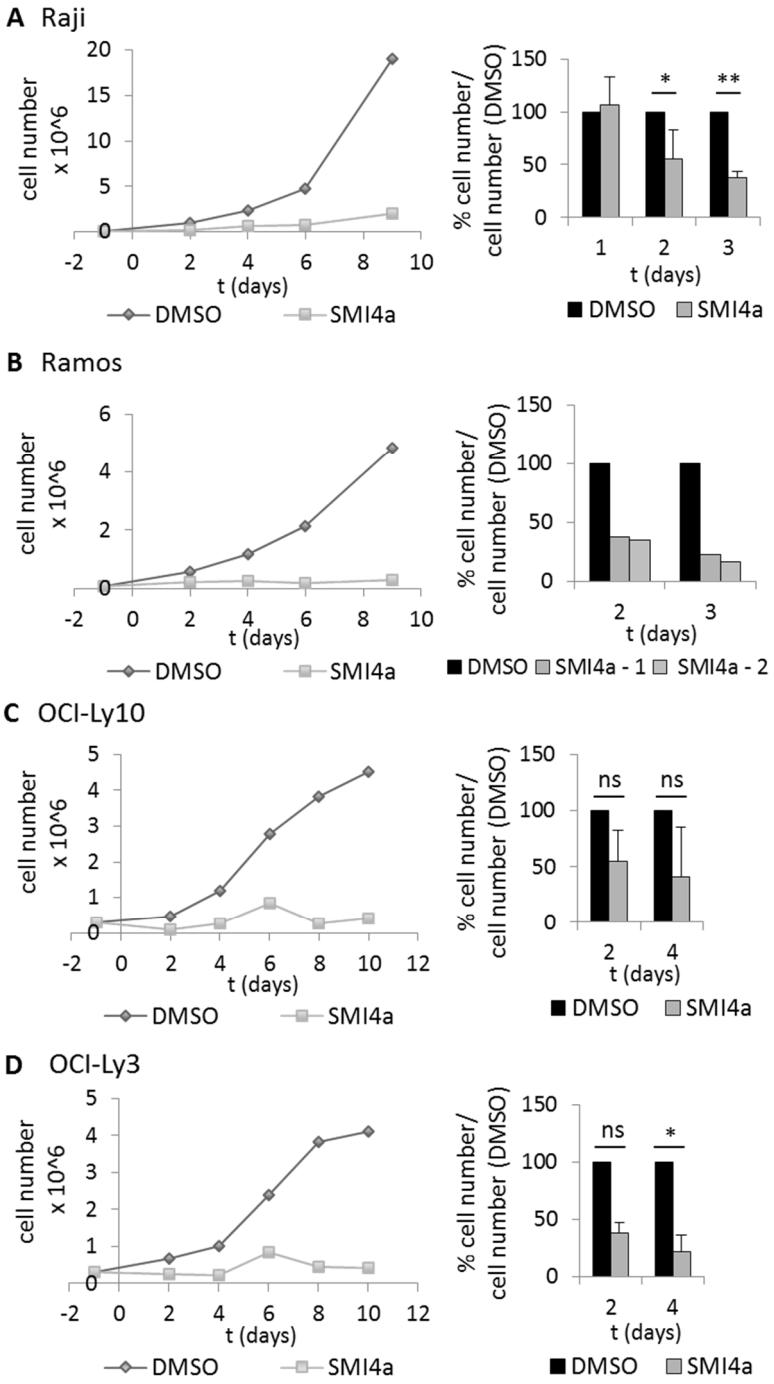

Figure 4.5 Effects of SMI4a on cell number of B cell lymphoma cell lines.
For each experiment Raji (**A**), Ramos (**B**), OCI-Ly10 (**C**) and OCI-Ly3 (**D**) cells were seeded into duplicate wells of 6-well plates on day -1, treated with DMSO or 40 µM SMI4a from day 0 for up to 10 days. The medium was renewed every second day and cells were counted using the MTT assay or a haemocytometer. Left: For the growth curves, the means of technical duplicates of one representative experiment are shown for each cell line. SMI4a strongly reduced cell numbers in all four cell lines tested. Right: Cell numbers relative to DMSO are shown. For Ramos cells, the results of two independent experiments are plotted. For the other cell lines means and sd of at least three independent experiments are depicted. Student's t-test was carried out: ns = not significant, * $p < 0.05$, ** $p < 0.01$. SMI4a significantly reduced the cell number in Raji and OCI-Ly3 cells, whereas a trend towards reduction was observed in OCI-Ly10 cells, which did not reach significance. Similarly, cell number was reduced in Ramos cells in both experiments compared to DMSO-treated controls.

For each cell line, one experiment was conducted in duplicate wells using two other PIM kinase inhibitors: Quercetagetin and inh VI. At concentrations of 40 µM, both Quercetagetin and inh VI prevented an increase in cell number in the Raji and Ramos BL cell lines over a time course of three days (Figure 4.6 A). However, Quercetagetin was not effective in OCI-Ly3 and OCI-Ly10 cells and inh VI reduced cell number only on days three and four (Figure 4.6 B).

As a control, PIM1/2-low SUDHL6 and OCI-Ly19 cells were also treated with all three inhibitors (one experiment in duplicate wells). The cell number was reduced in inhibitor-treated SUDHL6 and OCI-Ly19 cells compared to DMSO-treated cells on days 3 and 4 (Figure 4.6 C). Surprisingly, Quercetagetin was very toxic for OCI-Ly19 cells. As these cells do not express any detectable PIM1 or PIM2 (Figure 4.2 A), the effect was most likely not mediated via PIM kinase inhibition. Consistent with this, Quercetagetin has been shown to inhibit a plethora of other kinases that may promote cell proliferation and survival, like DYRK1A, DYRK2, DYRK3, AKT2, RSK2, TAK1, YES1 and Aurora B with similar efficiency to PIM kinases (http://www.kinase-screen.mrc.ac.uk, see appendix).

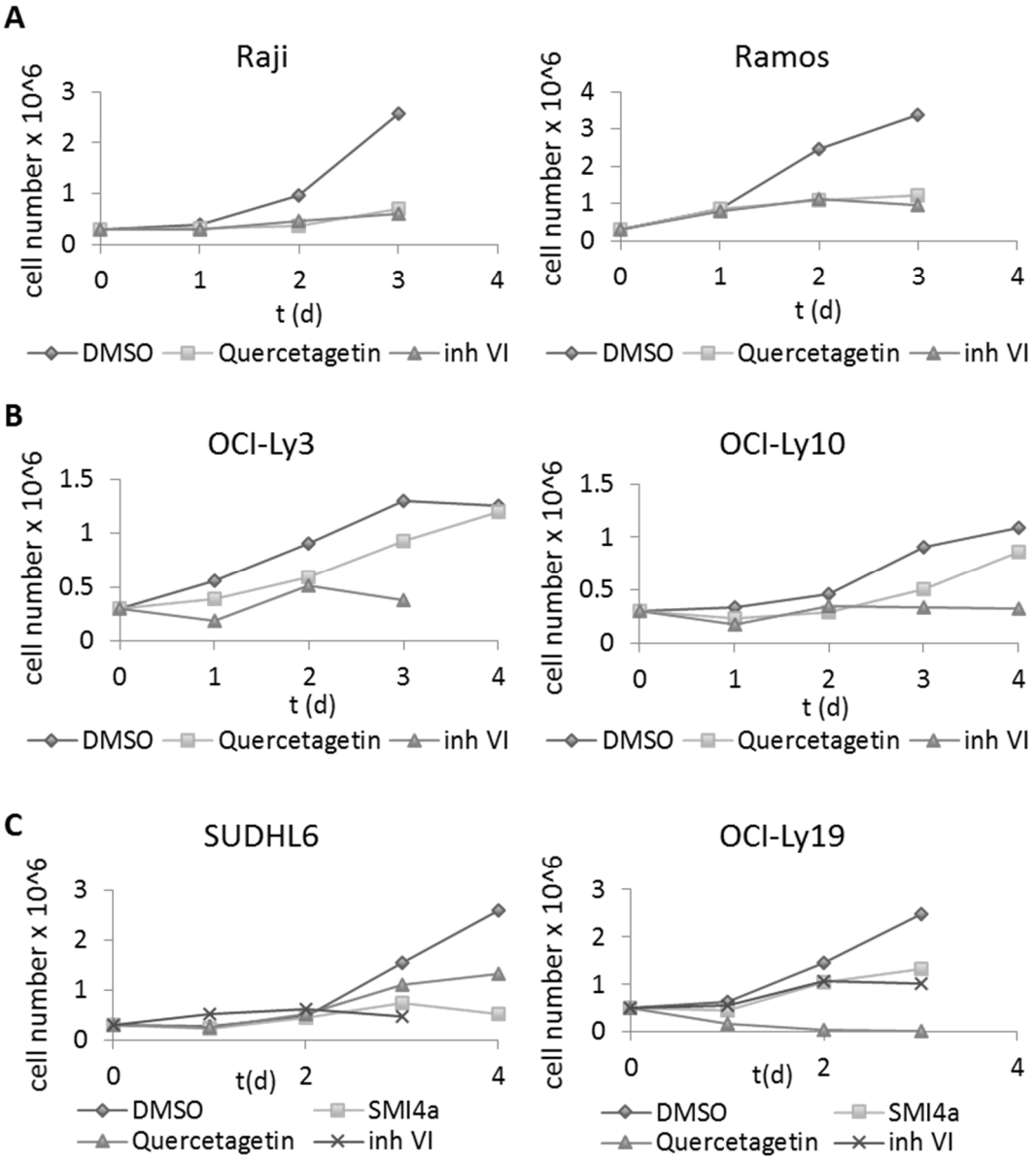

Figure 4.6 Effects of different PIM kinase inhibitors on cell number of B cell lymphoma cell lines.

For each experiment Raji, Ramos (**A**), OCI-Ly3 and OCI-Ly10 (**B**) cells were seeded into duplicate wells of 6-well plates and treated with DMSO, 40 µM Quercetagetin or 40 µM inh VI for up to 4 days without refeeding. Cells were counted using Trypan blue staining and a haemocytometer. Means of technical duplicates of one experiment are shown. While inh VI effectively decreased cell numbers in all four cell lines, Quercetagetin treatment had no effect on the two ABC-DLBCL cell lines. **C** SUDHL6 and OCI-Ly19 cells were plated into duplicate wells of 6-well plates and treated with DMSO, 40 µM SMI4a, 40 µM Quercetagetin or 40 µM inh VI for up to 4 days without renewal of the medium. Cells were counted using Trypan blue staining and a haemocytometer. The means and sd of two independent experiments are plotted for DMSO-treated SUDHL6 cells. For all other conditions, the means of technical duplicates of one experiment are shown. All three inhibitors affected cell viability in SUDHL6 and OCI-Ly19 cells, with Quercetagetin being very toxic for OCI-Ly19 cells.

4.4 Analysis of PIM1 and MYC occupancy at different promoter or enhancer regions in Raji and Ramos cells

PIM1 has been shown to promote elongation at MYC-dependent genes and it is highly expressed in ABC-DLBCL and BL. As especially nuclear PIM1 is associated with a poor prognosis in DLBCL and mediates oncogenic effects in BL, we predicted that PIM1 might be involved in the regulation of transcriptional elongation in lymphoma. Further, we hypothesised that, at MYC-dependent genes, PIM1 might mimic the effects of IKKα at NFκB target genes (see Figure 4.1).

To test these hypotheses, we sought to identify possible PIM1 target genes in lymphoma cell lines. The ABC-DLBCL metaprofile generated by Care et al. identified PIM1 and PIM2 among the top 20 genes associated with ABC-DLBCL (Care et al., 2013). Therefore, it seemed plausible that other genes associated with the ABC profile in this study might be transcriptionally regulated by PIM kinases. For further analyses we picked the known oncogenes guanine nucleotide binding protein-like 3 (*GNL3*), AT-rich interactive domain 3A (*ARID3A*), *LYN* and B cell CLL/lymphoma 2 (*BCL2*), as well as the cell surface marker *CD44* and the methionine sulfoxide reductase B1 gene (*MSRB1*, *SEPX1*). Of those, *GNL3* and *SEPX1* have known E box elements in their promoters. Initially, ChIP was performed to identify directly PIM1-bound genes.

4.4.1 Optimising ChIP conditions

For the ChIP experiments, chromatin sonication was optimised in Raji cells (Figure 4.7 A). 2 x 15 minutes sonication was found to give a good spread of DNA fragment lengths (200 – 1000 bp), when chromatin was cross-linked with 1.5% formaldehyde for 10 min.

Then the PIM1 antibody used for ChIP (rabbit anti-PIM1, Bethyl Laboratories) was tested, as there were no publications available confirming its specificity in ChIP experiments. As shown in Figure 4.7 B and C, the antibody selectively precipitates the 34 kDa, but not the 44 kDa PIM1 isoform from both Raji cell extract and formaldehyde cross-linked chromatin. However, under the conditions used, no co-precipitation of MYC was detected (Figure 4.7 B). Further, the antibody was specific for PIM1 and did not precipitate PIM2 (Figure 4.7 B). To further confirm specificity of the antibody, ChIP after PIM1 overexpression was performed. However, hardly any ChIP signal was detected in several experiments, which might be due to the mass of non-chromatin-bound PIM1 blocking the antibody. Only PIM1 knockdown finally confirmed that the antibody specifically precipitates PIM1, because the ChIP signal was significantly

reduced in knockdown cells (Figure 5.16). In conclusion, the antibody can be used for ChIP and it precipitates PIM1 cross-linked to chromatin.

4.4.2 Identification of PIM1 and MYC target genes

ChIP-qPCR was used to identify PIM1 and MYC binding sites in target genes. The presence of these proteins at the known E box elements in *GNL3* (*GNL3* +0.1, *GNL3* +0.4) and *SEPX1* (*SEPX1* -0.3) was analysed. Further, Zippo et al. described regions upstream of the *ID2* (*ID2* -1.4, *ID2* -1.7) and within the *FOSL1* gene (*FOSL1* +1.15) to be occupied by PIM1 and MYC, which were also assessed in the present study (Zippo et al., 2007). The *FOSL1* -37 region served as a negative control, *NPM1* +1 was a positive control as it is a known MYC-bound site in BL cell lines (Seitz et al., 2011).

ChIP-qPCR showed that both PIM1 and MYC bound to the *GNL3* promoter and the *NPM1* intronic enhancer in both Raji and Ramos cells (Figure 4.7 D). While no binding was observed at any of the other regions tested in Raji cells, some PIM1 binding could also be detected at the *ID2* and *FOSL1* regions in Ramos cells, but without a concomitant MYC signal. MYC and PIM1 were not detected at the *SEPX1* E box, although POL II was bound there. A POL II signal was also seen at the PIM1- and MYC-bound regions of the *GNL3* and *NPM1* genes (Figure 4.7 D).

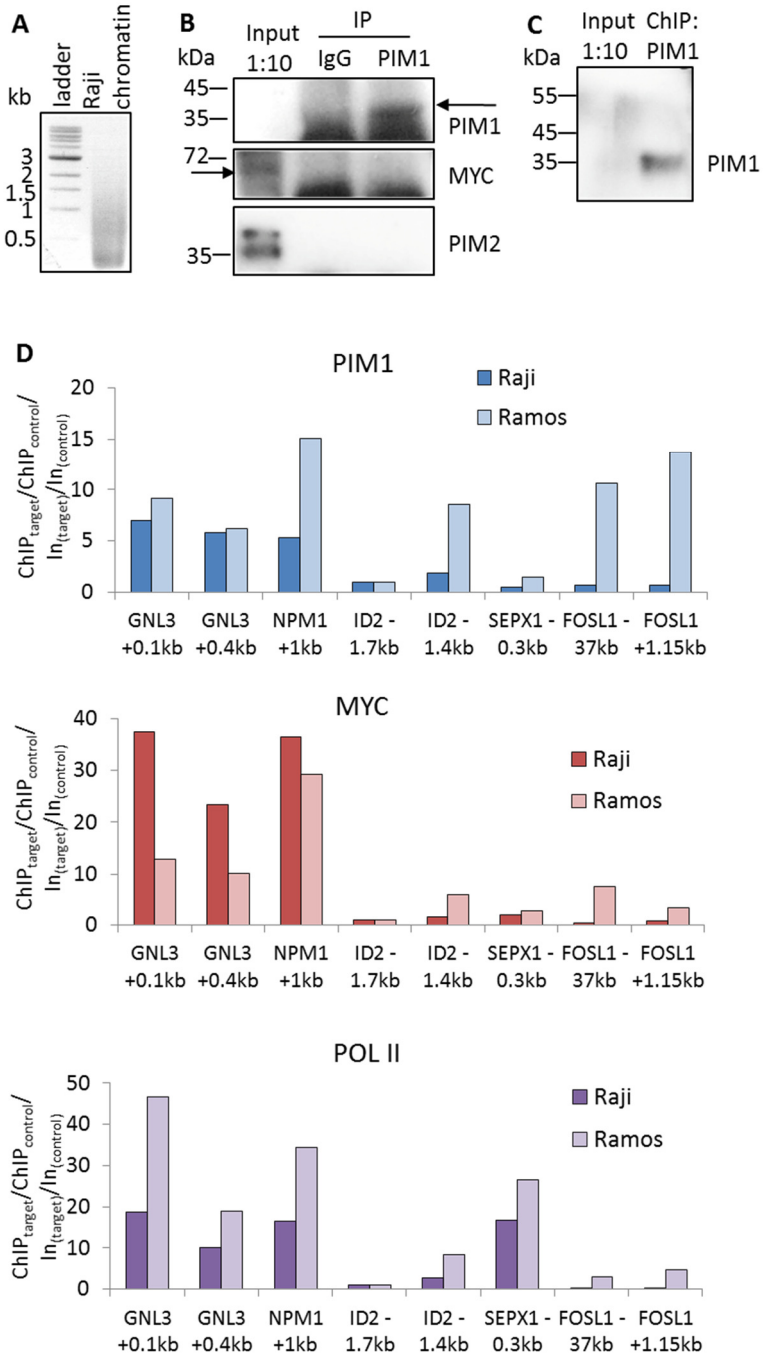

Figure 4.7 Identification of MYC and PIM1-bound chromatin regions.
A Raji chromatin was sonicated for 2 x 15 min and analysed on a 1% agarose gel. The chromatin nicely spread between 200 and 1000 bp. **B** Raji lysate was immunoprecipitated with either rabbit IgG or a PIM1 antibody, showing that the antibody specifically precipitates PIM1. The results are representative of two independent experiments. **C** ChIP was done using chromatin from Raji cells and the eluate was subjected to western blotting. This confirms that the antibody precipitates PIM1 even when it is formaldehyde cross-linked to chromatin. **D** ChIP-qPCR was performed using the PIM1, MYC and POL II CTD antibodies. qPCR was done with primer pairs close to different E box elements or the *FOSL1* -37 kb control region. Results are normalised to input and the *ID2* -1.4 kb region. For Raji cells, the means of technical duplicates are shown, whereas the result of one experiment is presented for Ramos cells. MYC and PIM1 were bound to the *NPM1* enhancer and *GNL3* promoter (*NPM1* +1, *GNL3* +0.1, *GNL3* +0.4) in both cell lines, where POL II was also detected.

4.5 Detailed analysis of the *NPM1* and *GNL3* genes by ChIP

4.5.1 *GNL3* and *NPM1* displayed an active gene signature

As both PIM1 and MYC were bound to the *GNL3* and *NPM1* genes, we sought to analyse these further with respect to the distributions of PIM1, MYC and POL II, as well as histone modification patterns at these genes. Because PIM1 can, like IKKα, phosphorylate H3S10 and HP1γ and promote transcriptional elongation, it might also share other substrates and functions with IKKα. Consequently, the starting hypothesis was that PIM1 occupancy at the *GNL3* gene might be similar to that of IKKα at the murine *Tnf* gene after LPS stimulation. IKKα binds to the elongating POL II and can be found enriched at the NFκB binding site, in the gene body and at the 3' region of the *Tnf* gene after activation (Thorne et al., 2012; Witham et al., 2013). Further, IKKα phosphorylates H3.3S31 in the gene body (Thorne et al., 2012), so that we anticipated a similar function for PIM1 and hypothesised that H3.3S31 might be phosphorylated along the *NPM1* and *GNL3* genes. To test these assumptions, primers were designed over the whole lengths of both genes and ChIP was performed with different antibodies.

For *NPM1*, ChIP was done using chromatin from both Raji and Ramos cells (Figure 4.8). PIM1 was mainly bound to the +1 kb E-box-containing region of the gene in both cell types, but could also be found enriched in the gene body more than in upstream regions of the *NPM1* gene, matching the POL II profile (Figure 4.8 A, C). Yet, no PIM1 peak was seen at the 3' end of the gene (*NPM1* +24). Similarly, MYC was only bound to the +1 kb E-box-containing region of the *NPM1* gene in both cell lines (Figure 4.8 B). Total POL II was also enriched around the +1 kb region and decreased over the length of the gene (Figure 4.8 C).

A similar pattern was seen at the *GNL3* gene in both Raji and OCI-Ly10 cells. PIM1 peaked at the +0.1 kb E-box-containing site and its signal declined with distance from this region (Figure 4.9 A). Again, no peak was detected at the 3' end of the gene (*GNL3* +9). MYC was also only bound to the +0.1 kb region of the *GNL3* gene in both cell lines (Figure 4.9 B). Any signal detected in other regions was most likely due to the close proximity of the -0.5 kb and +0.4 kb primer pairs to the binding site at +0.1 kb. Total POL II was enriched both in the upstream and downstream promoter regions (-0.5 kb to +0.1 kb) (Figure 4.9 C).

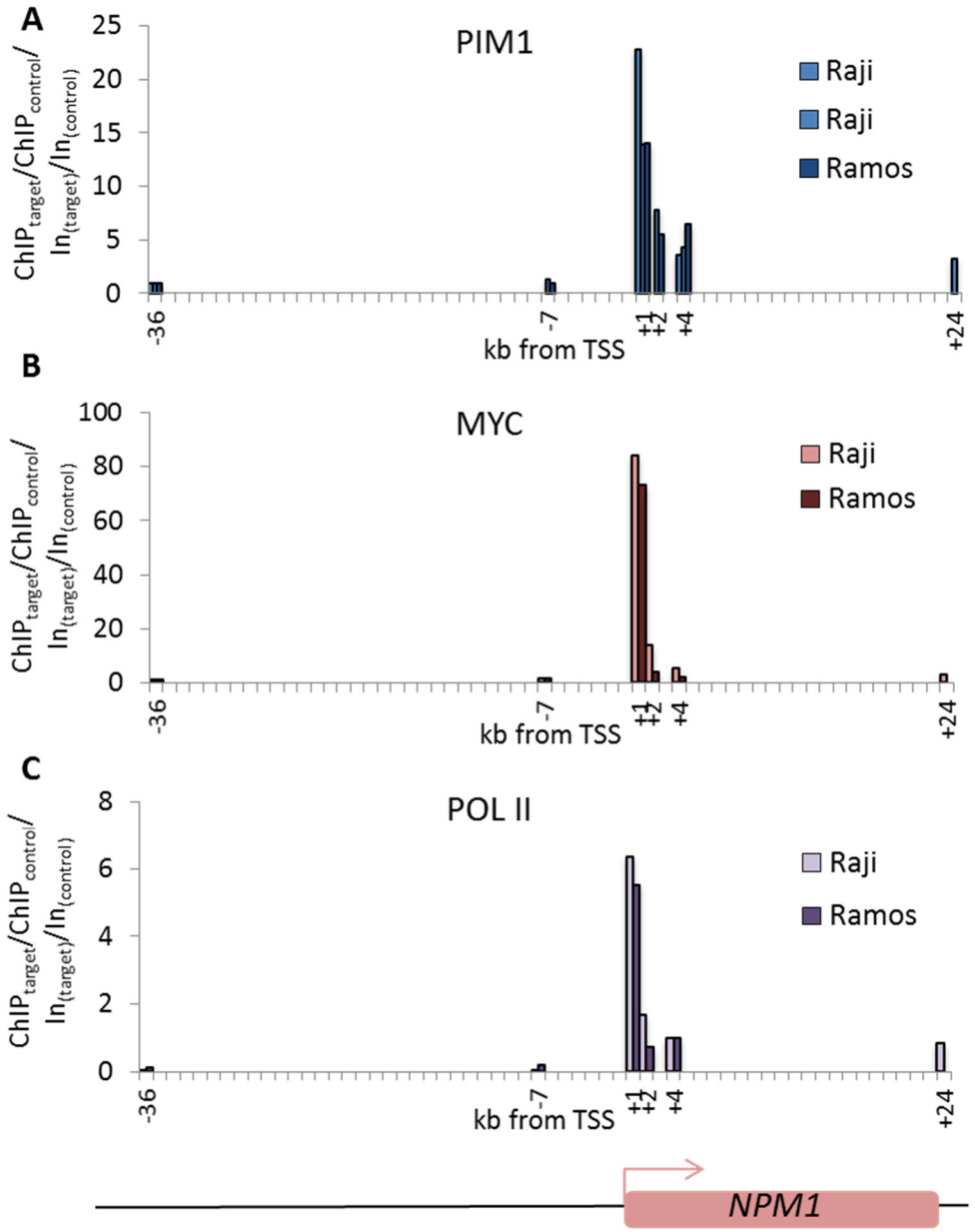

Figure 4.8 PIM1, MYC and POL II occupancy of the *NPM1* gene.
ChIP was performed in Raji and Ramos cells with antibodies against PIM1 (**A**), MYC (**B**) and POL II CTD (**C**). Primer pairs in different regions of the *NPM1* gene were used for qPCR. **A** qPCR results are normalised to input and the *NPM1* -36 kb region. For some regions in Raji cells, two independent experiments were performed, whereas only one experiment was done in Ramos cells. **B** qPCR results are shown normalised to input and the *NPM1* -36 kb region. Results of one experiment are shown for each cell line. **C** Results are normalised to input and the +4 kb region of the *NPM1* gene. One experiment was performed in each cell line. PIM1 and POL II show overlapping profiles for the *NPM1* gene in both cell lines, while MYC binding is restricted to the *NPM1* +1 kb site.

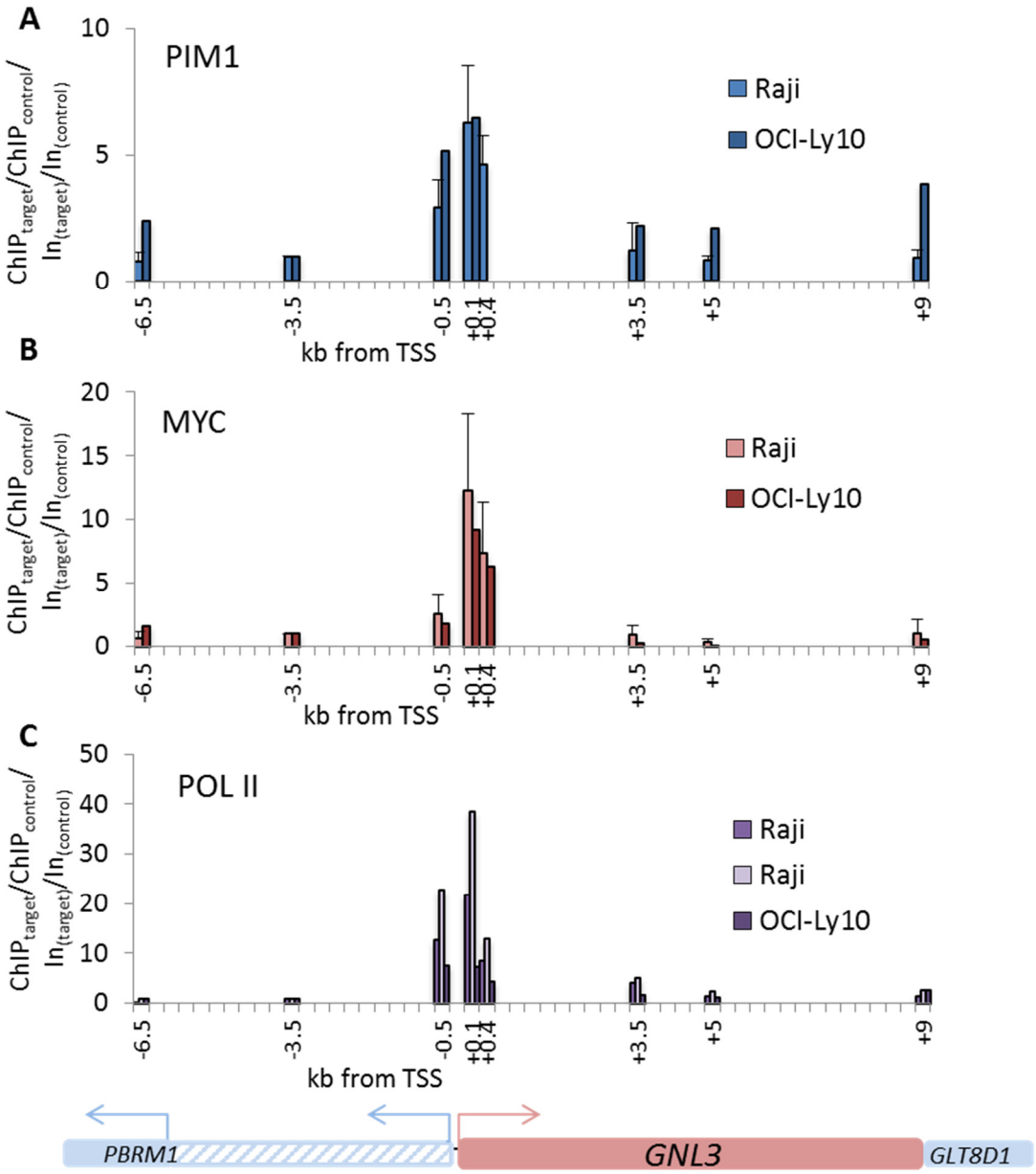

Figure 4.9 PIM1, MYC and POL II occupancy of the *GNL3* gene.
ChIP was carried out using chromatin from Raji and OCI-Ly10 cells and antibodies against PIM1 (**A**), MYC (**B**) or POL II CTD (**C**). Eluted gDNA was then subjected to qPCR using primer pairs in different regions of the *GNL3* gene. **A** qPCR results were normalised to input and the *GNL3* -3.5 kb region. For Raji cells, means and sd of six independent experiments are shown and one experiment was done in OCI-Ly10 cells. **B** Results are shown normalised to input and the *GNL3* -3.5 kb region. Means and sd of five independent experiments are shown for Raji cells, whereas one experiment was carried out in OCI-Ly10 cells. **C** Results are normalised to input and the *GNL3* -3.5 kb region. Two independent experiments are shown for Raji cells, one experiment was done in OCI-Ly10 cells. PIM1, MYC and POL II show similar profiles along the *GNL3* gene and peak in the *GNL3* +0.1 kb region.

Next, to further analyse the transcriptional activity of the *NPM1* and *GNL3* genes, the distributions of different phosphorylated forms of POL II were analysed at these genes in Raji cells. ChIP was done for both the initiating (CTD S5p) and the elongating form of POL II (CTD S2p). As expected, POL II S5p peaked in the promoter region and around the PIM1/MYC-binding sites at both genes (Figure 4.10 A, C). In contrast, POL II S2p increased downstream of the promoter at *NPM1* +4 kb and *GNL3* +3.5 kb and remained high in the 3' regions, which is expected for actively transcribing genes (Figure 4.10 B, D).

The presence of different histone PTMs, which are indicative of actively transcribed genes, was also analysed at the *NPM1* and *GNL3* genes in Raji cells. ChIP for histone H3S10p was done because it is known to be targeted by PIM1 and to promote transcriptional elongation. H3.3S31p was analysed because it is targeted by IKKα and might be phosphorylated by PIM1 and histone H2BK120ub (H2Bub) was assessed as a mark for actively transcribed genes.

As shown in Figure 4.11 A and Figure 4.12 A, H3 does not display any significant enrichments or depletions along the *NPM1* or *GNL3* genes. It was surprising at first that H3S10p was not detected around the PIM1 binding region in both genes, but only further downstream at *NPM1* +4 kb and *GNL3* +3.5 kb (Figure 4.11 B, Figure 4.12 B). Previous work on this mark in our group had, however, shown that the antibody is unable to recognise H3S10p when the adjacent K9 is also modified. Therefore, the ChIP was repeated with an antibody recognising the dual H3K9acS10p mark, which could be readily detected around the PIM1-binding site of the *GNL3* gene (Figure 4.12 C). Therefore, at the *GNL3* gene, H3S10p was mainly present on histone tails that were also modified at the K9 residue. Interestingly, some enrichment for the H3.3S31p mark could also be detected around the PIM1 binding site at both the *NPM1* and *GNL3* genes (Figure 4.11 C, Figure 4.12 D). As expected, H2Bub, a mark of actively transcribing genes, was also detected towards the 5' end of both the *NPM1* and *GNL3* genes (Figure 4.11 D, Figure 4.12 E).

In conclusion, PIM1 and MYC show overlapping binding at both genes. Marks of actively transcribed genes were detected (POL II S2p, H2Bub) and H3 phosphorylation marks, which could be a result of PIM1 activity, were present around the PIM1-binding site, especially at the *GNL3* gene.

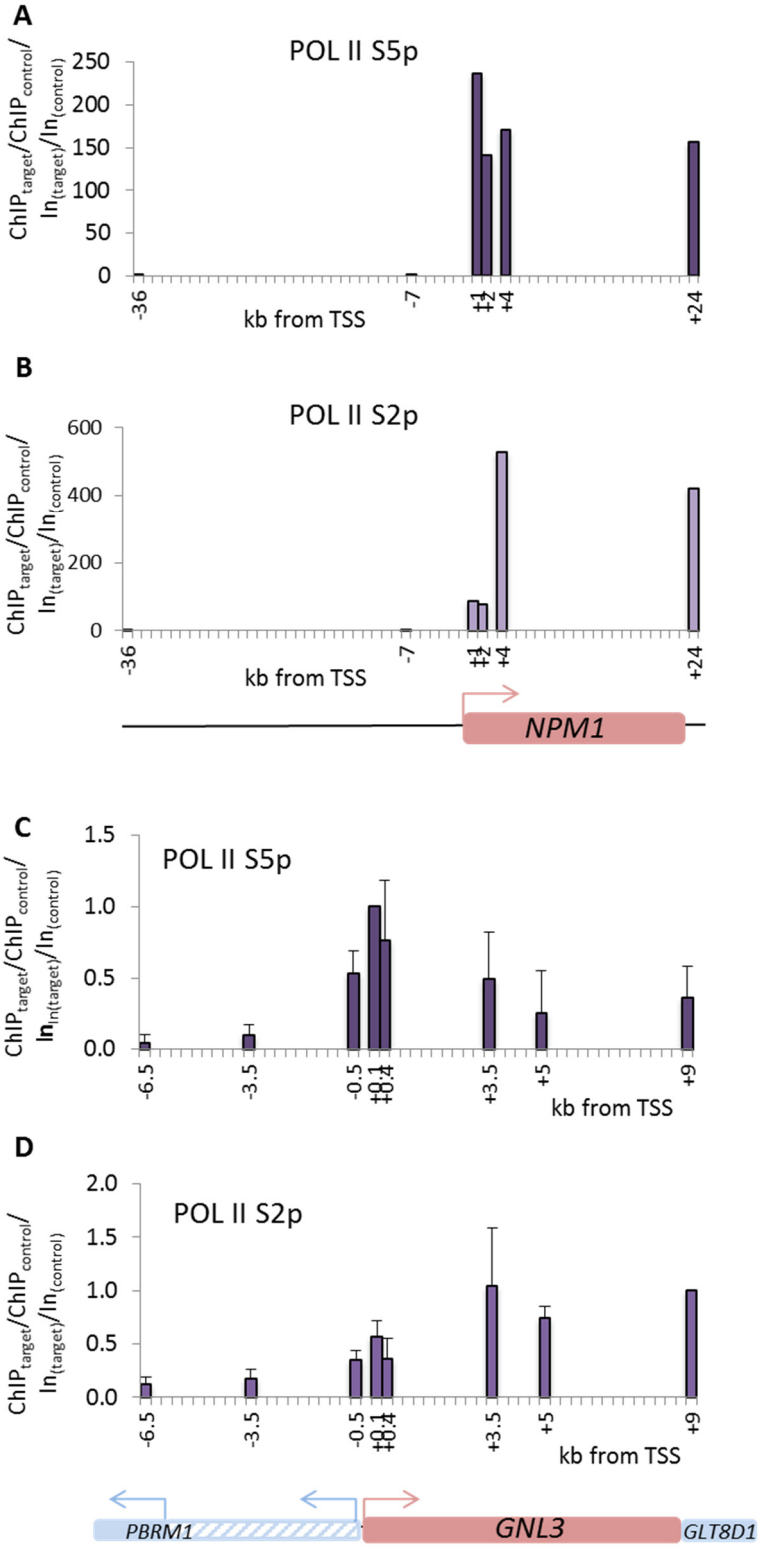

Figure 4.10 POL II S5p and S2p occupancy of the *NPM1* and *GNL3* genes. Raji chromatin was used for ChIP with anti-POL II S5p (**A**, **C**) and S2p antibodies (**B**, **D**). Eluted gDNA was then subjected to qPCR with primer pairs spanning different regions of the *NPM1* and *GNL3* genes. **A**, **B** Results of one experiment are shown normalised to input and the *NPM1* -36 kb region. **C**, **D** Means and sd of five independent experiments are shown normalised to input and the +0.1 kb (**C**) or +9 kb region (**D**). Both genes display the POL II signature of actively transcribed genes, with POL II S2p being detected in the gene body and at the 3' end.

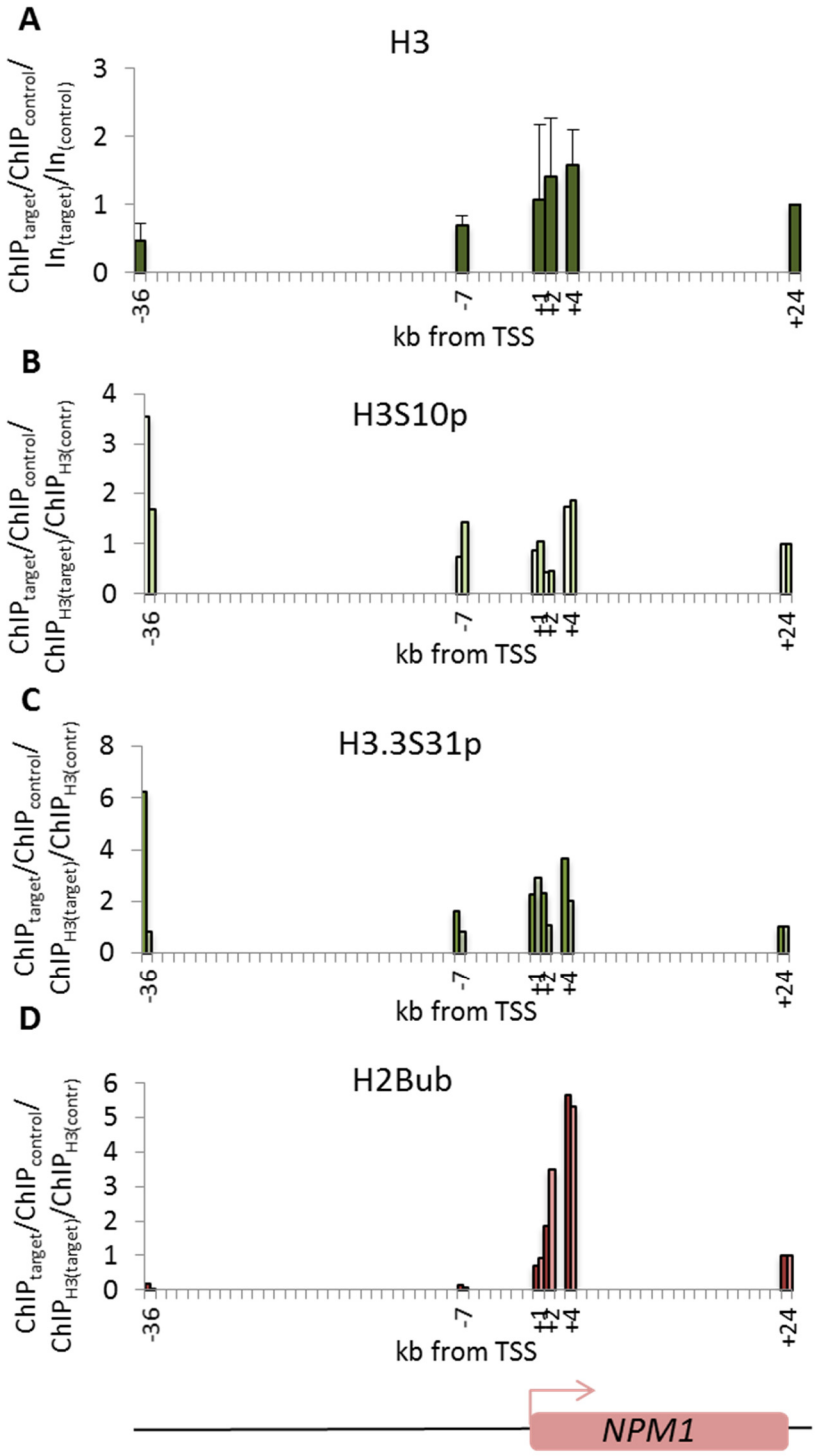

Figure 4.11 Analysis of different histone modifications at the *NPM1* gene.
ChIP was carried out using chromatin from Raji cells and antibodies against H3 (**A**), H3S10p (**B**), H3.3S31p (**C**) and H2Bub (**D**). **A** The means and sd of three independent experiments are shown normalised to input and the +24 kb region. **B**-**D** Two independent experiments are plotted normalised to H3 and the +24 kb region. A trend towards increased H3S10p was detected downstream of the PIM1 binding site, while H3.3S31p tended to be higher around the PIM1 binding site (*NPM1* +1 kb). H2Bub was enriched downstream of the TSS in the gene body, as would be expected for an actively transcribed gene.

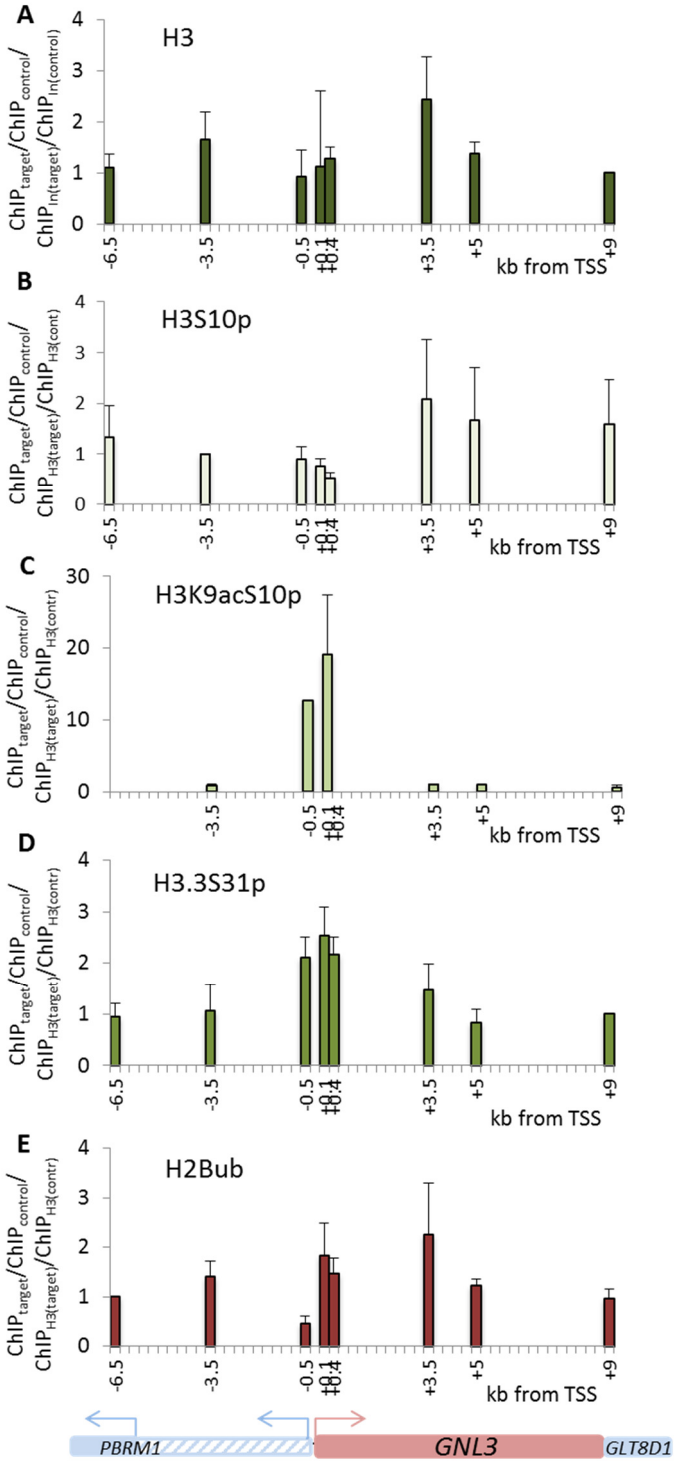

Figure 4.12 Analysis of different histone modifications at the *GNL3* gene. Chromatin from Raji cells was used for ChIP with antibodies against H3 (**A**), H3S10p (**B**), H3K9acS10p (**C**), H3.3S31p (**D**) and H2Bub (**E**). **A** The means and sd of five independent experiments are shown normalised to input and the +9 kb region. **B**, **C**, **D** Results are presented as means and sd of three independent experiments and are normalised to H3 and the -3.5 kb region of *GNL3*. **E** Results, plotted as means and sd of three independent experiments, are normalised to H3 and the -6.5 kb region. While H3S10p showed a moderate increase downstream of the PIM1 binding site, H3K9acS10p and H3.3S31p peaked around the promoter region. Both S10 and S31 might be targeted by PIM1 in this area. A trend towards increased H2Bub was detected downstream of the promoter, indicating that *GNL3* is actively transcribed.

4.5.2 Inhibition of transcription led to increased binding of PIM1 to the *GNL3* promoter

As described earlier, Thorne et al. discovered that IKKα binds to the POL II CTD preferentially when it is phosphorylated on S2. IKKα is then loaded onto the chromatin, which requires its binding to HP1γ. Because PIM1 can also bind HP1γ, we reasoned that PIM1 might also interact with the POL II CTD. Consistently, PIM1 occupancy was detected further into the 5' regions of the *NPM1* and *GNL3* genes, whereas MYC was more restricted to its binding site (Figure 4.8 A, B, Figure 4.9 A, B). In the case of IKKα, treatment with the transcription elongation inhibitor 5,6-Dichloro-1-β-D-ribofuranosylbenzimidazole (DRB) inhibited its enrichment at the *Tnf* gene after LPS treatment (Thorne et al., 2012). The question was therefore, whether a similar mechanism could be observed for PIM1 at the *GNL3* gene.

As shown in Figure 4.13 A, POL II was efficiently depleted from the gene body and at the 3' end of *GNL3* after 1 h of DRB treatment (compare w/o DRB to DRB), indicating an effective block of transcription elongation. At the same time, PIM1 occupancy increased in the promoter region, but did not change in the gene body or at the 3'end of the gene (Figure 4.13 B). Therefore, active elongation was not required for PIM1 binding to the *GNL3* gene. In contrast, active transcription might lead to a dynamic turnover of PIM1 at the *GNL3* +0.1 region.

This is very different to the observation made for IKKα at the *Tnf* gene, where DRB resulted in decreased recruitment to the chromatin. Hence, the role of PIM1 at the *GNL3* gene is most likely different from the role of IKKα at the *Tnf* gene after LPS stimulation. This could be explained by the different transcriptional activities. Whereas the *GNL3* gene is constitutively expressed, *Tnf* is normally silent but shows rapid induction kinetics. Therefore, the rates of transcription and the requirements for chromatin remodelling will be very different at both genes, so that distinct mechanisms of transcriptional regulation have to be in place. Additionally, the increased recruitment of PIM1 to its binding site upon transcriptional stalling and its induction by certain stressors (see section 4.2), might implicate this protein in the transcriptional stress response pathway.

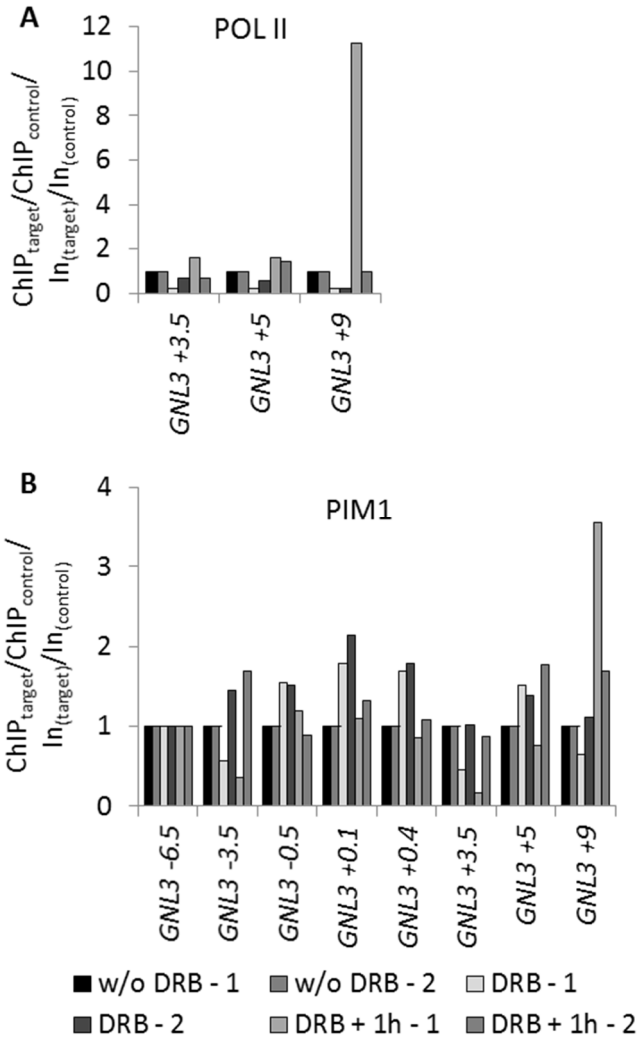

Figure 4.13 Effects of DRB on PIM1 levels at the *GNL3* gene.
Raji cells were left untreated (w/o DRB) or were treated with DRB for 1 h (DRB), then washed extensively and released in fresh medium for 1 h (DRB + 1h). ChIP was performed with anti-POL II (**A**) or anti-PIM1 (**B**). Two independent experiments are shown. While POL II was depleted from the gene body, there was a trend towards increased binding of PIM1 in the promoter region of *GNL3*.

5 *GNL3* as a transcriptional target of PIM1 and MYC

5.1 The *GNL3* oncogene as a possible PIM1-regulated gene

Several studies have described the GNL3 protein (also called nucleostemin) as an oncoprotein, which shows high expression in stem and tumour cells (Beekman et al., 2006; Lin et al., 2010; Liu et al., 2004; Yaghoobi et al., 2005). It can promote cell proliferation and survival in both p53-dependent and -independent ways (Jafarnejad et al., 2008; Lo et al., 2014; Ma & Pederson, 2007; Meng et al., 2008; Nikpour et al., 2009; Rahmati et al., 2014; Romanova et al., 2009). *GNL3* had been shown to be a direct transcriptional target of MYC and *Gnl3* haploinsufficiency is sufficient to inhibit MYC-dependent lymphomagenesis in mice (Zwolinska et al., 2011), making this gene an important contributor to MYC-dependent tumourigenesis. Strikingly, cardiomyocyte-specific overexpression of PIM1 in mice leads to upregulation of GNL3 (Siddiqi et al., 2008). As PIM1 binds to the *GNL3* promoter (see sections 4.4, 4.5), this upregulation might be caused by a direct effect of PIM1 on *GNL3* transcription.

Additionally, *GNL3* is a host gene for three intronic small nucleolar RNAs (snoRNAs): SNORD19, SNORD19B and SNORD69 (Figure 5.1). Depending on sequence conservation, snoRNAs are grouped into two classes: box C/D snoRNAs (like SNORD69, SNORD19 and SNORD19B) and box H/ACA snoRNAs (Balakin et al., 1996). Their canonical function is to guide modification of rRNAs, tRNAs and small nuclear RNAs (snRNAs) (Bratkovič & Rogelj, 2011; Kiss, 2002). While C/D box snoRNAs guide 2'-O-ribose methylation, H/ACA box snoRNAs guide pseudouridylation (Kiss, 2002). However, many snoRNAs are complementary to mRNAs and especially box C/D snoRNAs can have miRNA-like functions or even regulate alternative splicing (Brameier et al., 2011; Kishore & Stamm, 2006; Kishore et al., 2010). These properties make snoRNAs potentially oncogenic, so that it could be important to study their regulation in the context of lymphoma. Processing of snoRNAs can occur via a splicing-dependent or a splicing-independent pathway (Hirose & Steitz, 2001; Hirose et al., 2003; Hirose et al., 2006). As PIM1 modulates the activity of HP1γ (Koike et al., 2000), which has in turn been shown to regulate splicing (Saint-André et al., 2011), it is conceivable that PIM kinases might regulate processing of these snoRNAs. One can also imagine that PIM kinases could regulate the splicing-independent processing of these small RNAs. Accordingly, *GNL3* seems to be an essential, possibly PIM-regulated oncogene, so that, in the following, this study focussed on the regulation of the *GNL3* gene and its intronic snoRNAs.

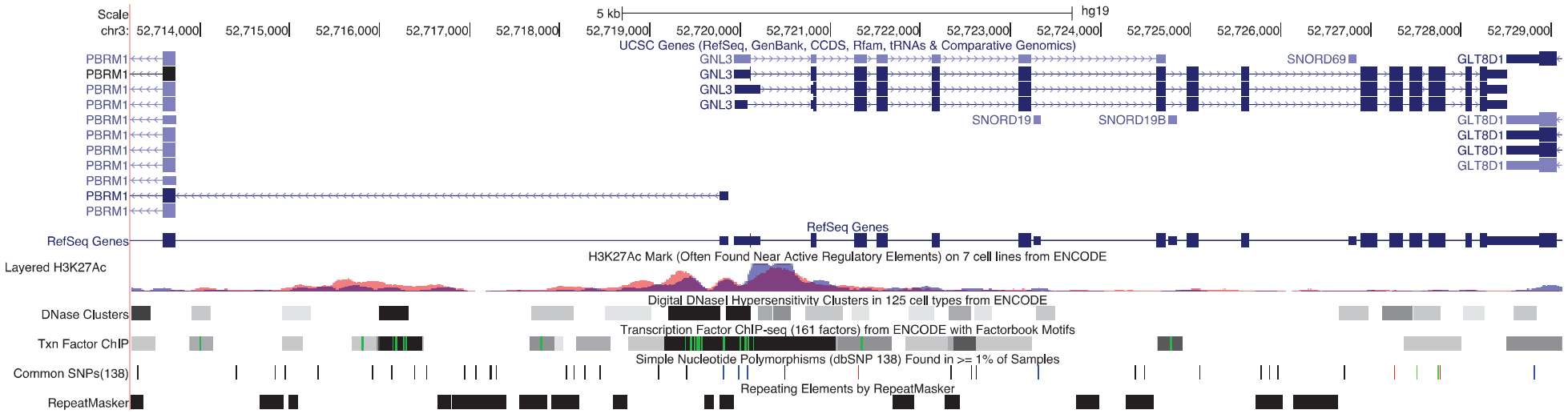

Figure 5.1 The GNL3 gene locus with intronic snoRNAs and the neighbouring genes PBRM1 and GLT8D1 (http://genome.ucsc.edu/). The ChIP-seq tracks for H3K27ac in the lymphoblastoid GM12878 (red) cell line and the K562 acute myeloid leukaemia cell line (blue) are shown. Further, DNase hypersensitive sites and transcription factor ChIP signals are displayed (Kent et al., 2002; Rosenbloom et al., 2013).

5.2 Expression of *GNL3*, SNORD69, SNORD19 and SNORD19B in different BCL cell lines

First, expression of *GNL3*, SNORD69, SNORD19 and SNORD19B was assessed by real time RT-PCR in OCI-Ly3, Raji, Ramos and SUDHL6 cells (Figure 5.3 A). snoRNA expression was normalised to hnRNA expression, as the primers will also amplify the *GNL3* hnRNA and that way, a specific increase in snoRNAs over primary transcript can be detected (Figure 5.2).

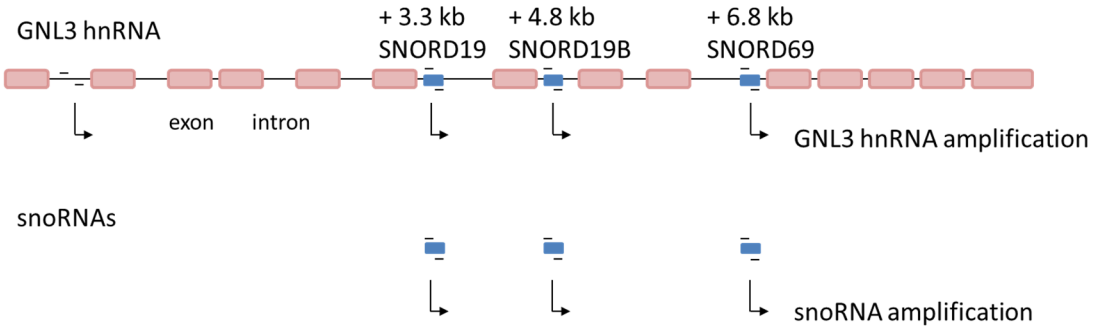

Figure 5.2 Amplification of GNL3 hnRNA and snoRNAs by the snoRNA primers.
To specifically measure the increase in snoRNAs, their expression was normalised to that of an amplicon that is only present in the primary transcript.

GNL3 mRNA levels were variable between experiments, but average expression of *GNL3* was similar in all four cell lines and did therefore not correlate with the average PIM1 or PIM2 expression levels (compare Figure 5.3 A with Figure 4.2). Especially in OCI-Ly3 and SUDHL6 cells, SNORD69 expression levels also varied between experiments (Figure 5.3 A). However, there was again no correlation between average PIM1 or PIM2 and snoRNA expression levels in the different cell lines.

Yet, when the expression of the *GNL3* mRNA was compared to that of *PIM1* in different experiments done in the same cell line, there was a significant correlation between their expression levels in both OCI-Ly3 and Raji, but not SUDHL6 cells (Figure 5.3 B). No significant correlations were observed for SNORD69, SNORD19 or SNORD19B. However, a trend towards negative correlation between *PIM1* and SNORD69 or SNORD19B and a trend towards positive correlation between *PIM1* and SNORD19 expression were seen (Figure 5.3 C - E). In conjunction with the observed binding of PIM1 to the *GNL3* promoter, these data suggest a direct link between *PIM1* and *GNL3* expression, which might be due to a direct regulation of

GNL3 by PIM kinases. Further, both genes might be regulated by the same upstream factors and both mechanisms are not mutually exclusive.

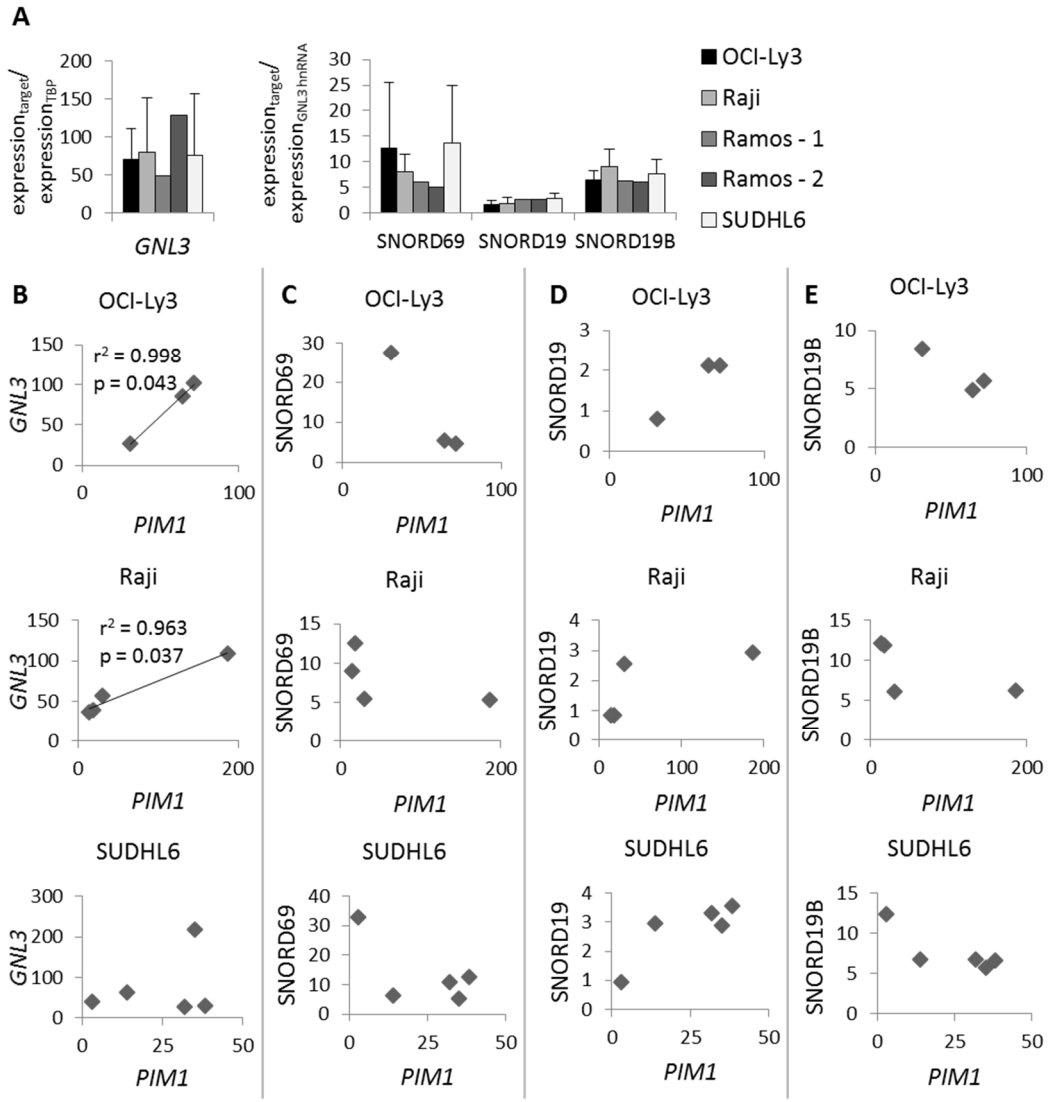

Figure 5.3 Expression of GNL3 and intronic snoRNAs in B cell lymphoma cell lines.

A Expression of *GNL3* and its intronic snoRNAs was assessed by RT-qPCR. Results were normalised to *TBP* or *GNL3* hnRNA, respectively. The means and sd of n experiments are plotted, with n = 3 for OCI-Ly3, n = 4 for Raji and n = 5 for SUDHL6. Results of two independent experiments are plotted for Ramos cells. Expression levels of *GNL3* and the snoRNAs were variable between experiments conducted in the same cell line, but were on average similar between different cell lines. **B** - **E** Normalised expression levels of *GNL3*, SNORD69, SNORD19 and SNORD19B were plotted against *PIM1* expression levels in OCI-Ly3, Raji and SUDHL6 cell lines. Linear regression was performed to analyse the correlation between *GNL3* and *PIM1* expression. p values were calculated using a free software (Soper DS, 2014) and the trend line is only depicted for $p < 0.05$. A positive correlation between *PIM1* and *GNL3* expression levels was seen in OCI-Ly3 and Raji cells. There was a trend towards a positive correlation in SUDHL6 cells and between SNORD19 and *PIM1* in all cell lines. Conversely, a trend towards negative correlation between *PIM1* and SNORD69 or SNORD19B was seen.

5.3 Effects of potential PIM kinase inhibitors on the expression of possible PIM1 target genes

The data so far indicate that PIM kinases might directly regulate *GNL3* expression. Thus, the influence of PIM kinase inhibition on *GNL3* mRNA and hnRNA as well as SNORD69, SNORD19 and SNORD19B levels was determined. hnRNA expression was assessed as a more direct readout of transcription to avoid effects of mRNA stability that might mask changes in transcription. The mRNA levels of the other possible PIM target genes -– *LYN*, *SEPX1*, *ARID3A*, *BCL2* and *CD44* – were also measured, because on the basis of the ChIP-qPCR data, it was not possible to exclude binding of PIM1 and MYC to promoter or enhancer regions of these genes. Therefore, PIM kinases might still directly regulate their transcription.

Raji, Ramos, OCI-Ly3, SUDHL6 and OCI-Ly19 cells were treated with SMI4a, inh VI, Quercetagetin or equivalent amounts of DMSO for 2 h to 24 h. Short periods of drug treatment were chosen, so that the outcome observed would be direct and not caused by secondary effects. Yet, no changes in *GNL3* mRNA or hnRNA expression were observed, even after 11 h or 24 h of inhibitor treatment in Raji, Ramos, OCI-Ly3 or SUDHL6 cells using any of the three inhibitors (Figure 5.4). Similarly, expression of the intronic snoRNAs did not change significantly after SMI4a or inh VI treatment in any of the four cell lines (Figure 5.5). *LYN*, *SEPX1*, *ARID3A* and *BCL2* expression was also mostly unchanged, but showed a trend towards increased expression in Raji cells (Figure 5.6, Figure 5.7 A, B). Ramos cells did not express detectable levels of *BCL2.* Similarly, *CD44* was only expressed in OCI-Ly3 and OCI-Ly19 cells, but mRNA levels were unchanged after PIM inhibitor treatment (Figure 5.7 C). OCI-Ly19 was the only cell line, in which *GNL3*, *LYN*, *SEPX1* and *BCL2* were strongly downregulated 4 h and 6 h after treatment with Quercetagetin. This was, however, most likely not due to PIM inhibition, as these cells did not express detectable PIM1 or PIM2 levels (Figure 4.2 A), but due to off-target effects and the strong toxic effect of Quercetagetin on OCI-Ly19 cells. In conclusion, short-term inhibition of PIM kinases did not inhibit expression of possible PIM target genes in BCL cell lines.

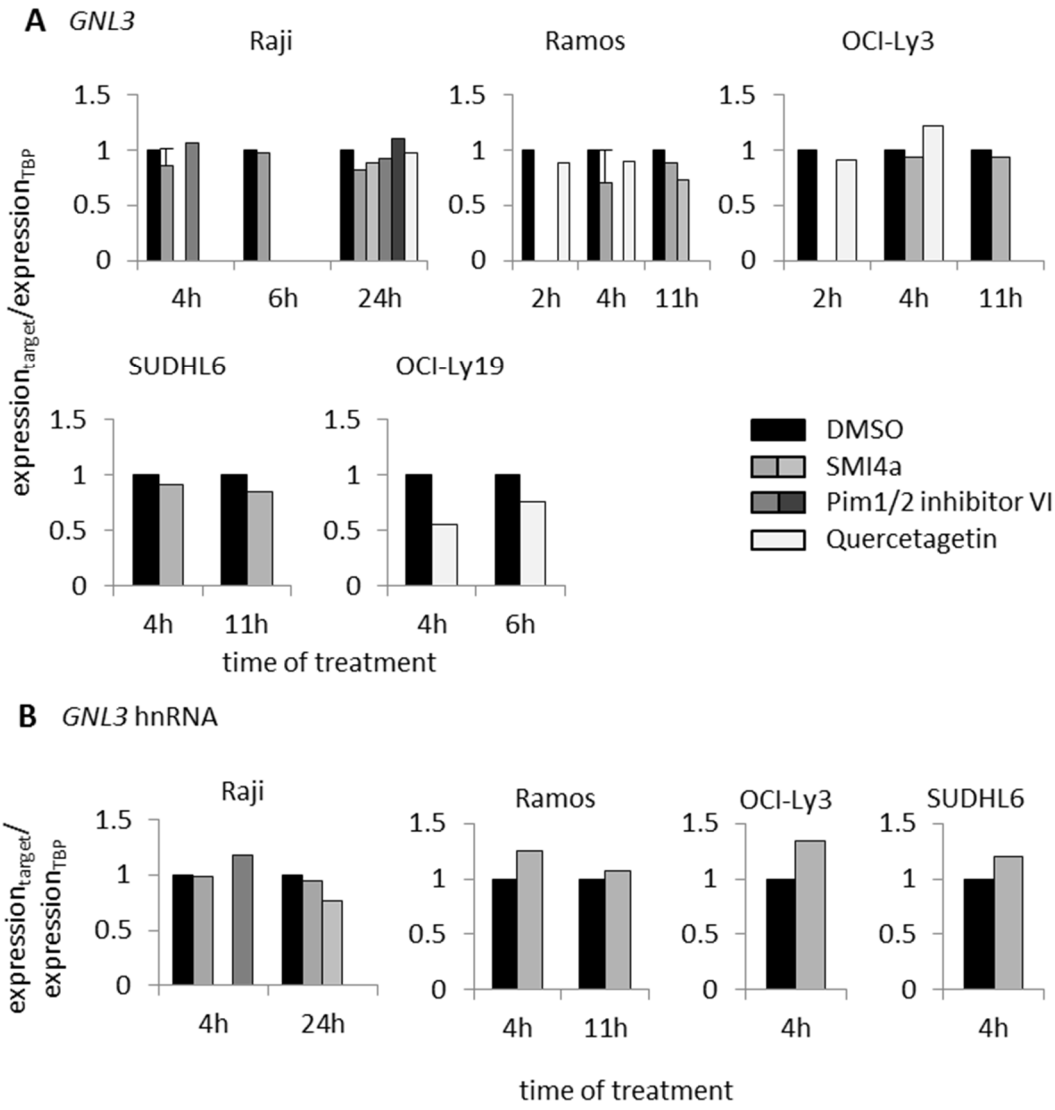

Figure 5.4 Effects of PIM kinase inhibitors on *GNL3* expression.
The cells were plated in triplicate wells of 6-well plates and treated with DMSO, 40 μM SMI4a, 40 μM inh VI or 40 μM Quercetagetin for indicated times. Expression of *GNL3* mRNA (**A**) and hnRNA (**B**) was analysed by RT-qPCR. The data are shown as means of one experiment conducted in triplicate wells or means and sd of three independent experiments carried out in triplicate wells each (Raji and Ramos SMI4a, 4 h). *GNL3* hnRNA expression was measured using the *GNL3* +0.4 kb intronic primer. Expression was normalised to that of *TBP* and DMSO-treated cells. No effect of the inhibitors on *GNL3* mRNA or hnRNA expression was detected in Raji, Ramos, OCI-LY3 or SUDHL6 cells, while the *GNL3* mRNA was decreased in OCI-Ly19 cells.

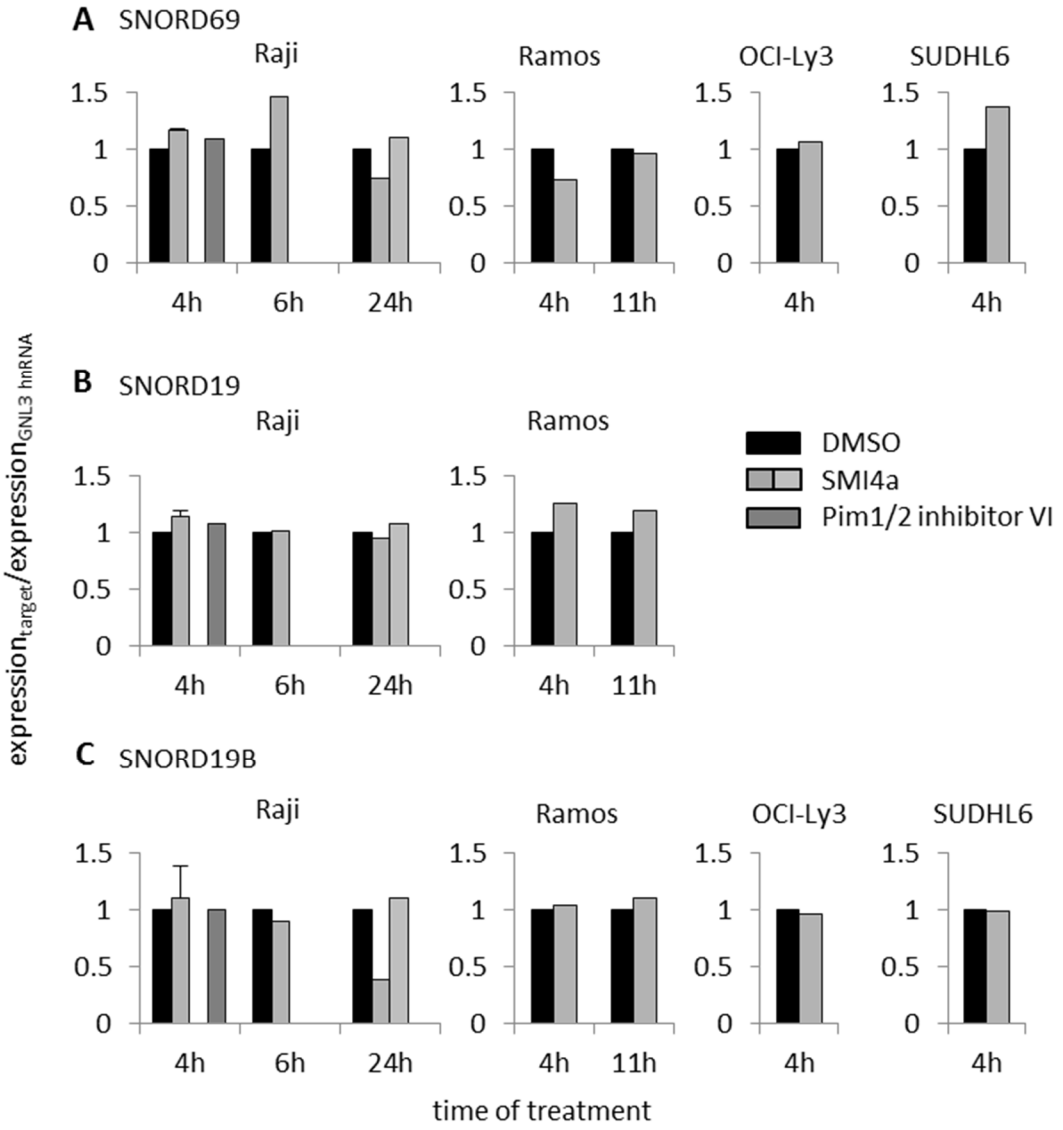

Figure 5.5 Effects of PIM kinase inhibitors on snoRNA expression.
The cells were plated in triplicate wells of 6-well plates and treated with DMSO, 40 μM SMI4a or 40 μM inh VI for indicated times. Expression of SNORD69 (**A**), SNORD19 (**B**) and SNORD19B (**C**) was analysed by RT-qPCR. The data are shown as means of one experiment conducted in triplicate wells or means and sd of three independent experiments carried out in triplicate wells each (Raji 4 h SMI4a). Results are normalised to *GNL3* hnRNA expression and to expression in DMSO-treated cells. Neither treatment of the cells with SMI4a nor inhibitor VI led to a change in snoRNA expression in any of the cell lines tested.

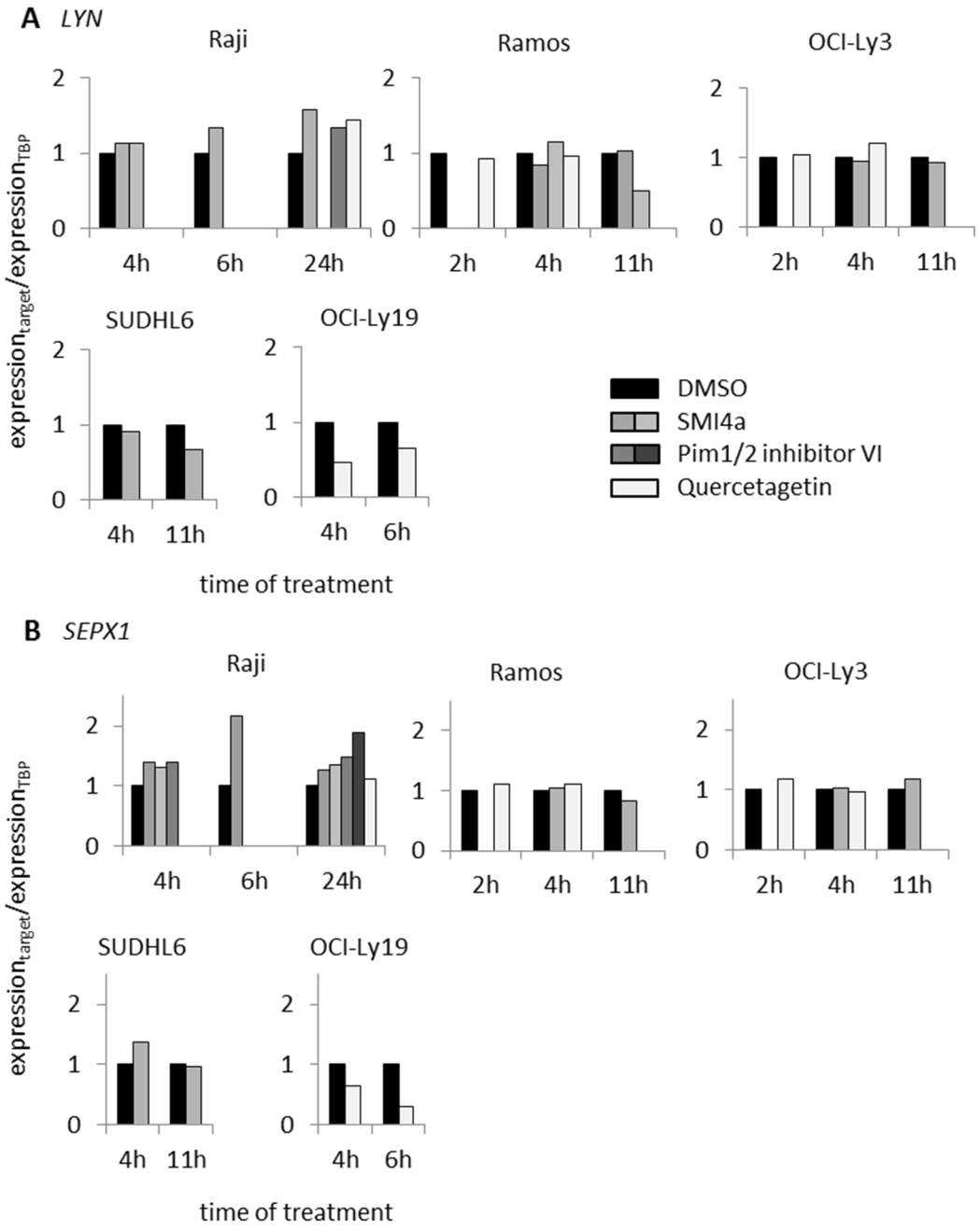

Figure 5.6 Effects of PIM kinase inhibitors on *LYN* and *SEPX1* expression. The cells were plated in triplicate wells of 6-well plates and treated with DMSO, 40 μM SMI4a, 40 μM inh VI or 40 μM Quercetagetin for indicated times. *LYN* (**A**) and *SEPX1* (**B**) mRNA levels were measured by RT-qPCR. The data are shown as means of one experiment conducted in triplicate wells. Expression was normalised to that of *TBP* and DMSO-treated cells. *LYN* showed a trend towards increase in inhibitor-treated Raji cells after 24 h, but its expression levels were unaltered at any other time point or in the other cell lines. In OCI-Ly19 cells, a decrease in *LYN* expression was observed. *SEPX1* expression also tended to increase in Raji cells after 6 and 24 h of inhibitor treatment, whereas it was unaltered in Ramos, OCI-Ly3 and SUDHL6 cells and was decreased in OCI-Ly19 cells.

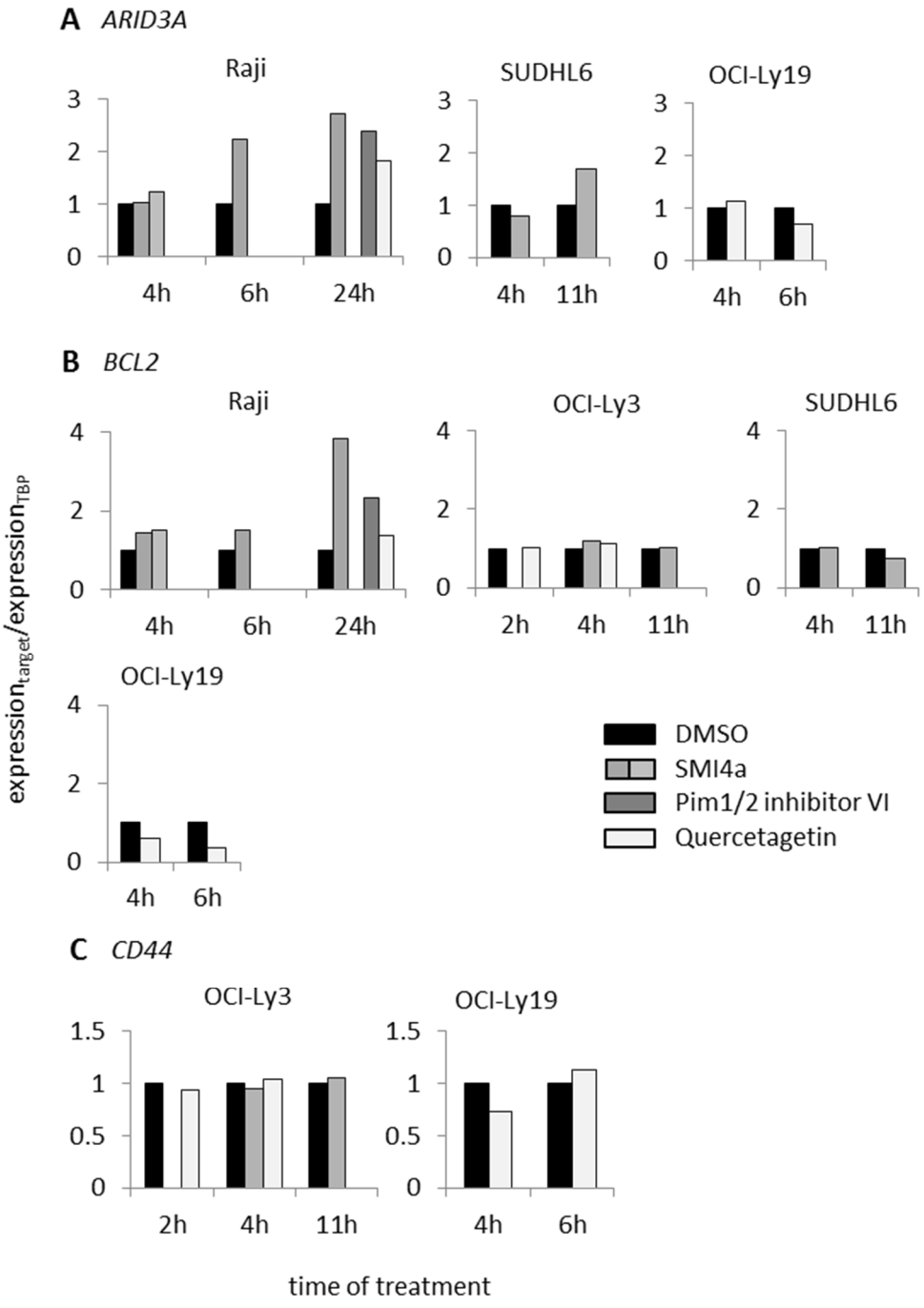

Figure 5.7 Effects of PIM kinase inhibitors on *ARID3A*, *BCL2* and *CD44* expression.

The cells were plated in triplicate wells of 6-well plates and treated with DMSO, 40 µM SMI4a, 40 µM inh VI or 40 µM Quercetagetin for indicated times. *ARID3A* (**A**), *BCL2* (**B**) and *CD44* (**C**) expression levels were measured by RT-qPCR. The data are shown as means of one experiment conducted in triplicate wells. Results are normalised to *TBP* and to expression in DMSO-treated cells. Expression of *ARID3A* and *BCL2* showed a trend towards increase in Raji cells after 6 and 24 h of inhibitor treatment, whereas it remained unaltered in the other cell lines. *BCL2* even decreased in OCI-Ly19 cells. *CD44* expression was unchanged in OCI-Ly3 and OCI-Ly19 cells after inhibitor treatment.

Because PIM kinase inhibition did not alter the expression of any of the possible target genes in BCL cells, the effect of the inhibitors on known PIM target genes was tested. PIM1 had been shown to be essential for the serum-induced stimulation of *ID2* and *FOSL1* expression in HEK293 cells (Zippo et al., 2007). Therefore, this experiment was reproduced and the effect of the three inhibitors on this response was analysed. After serum shock, only upregulation of *FOSL1*, but not *ID2*, was seen in our cells (Figure 5.8 A). Surprisingly, this induction was not inhibited when cells were treated with any of the three inhibitors over night before the serum shock (Figure 5.8 B). Therefore, the inhibitors might not be effective enough to prevent PIM-dependent gene expression and in the following, overexpression and knockdown of PIM kinases were used to evaluate their functions regarding the regulation of gene expression.

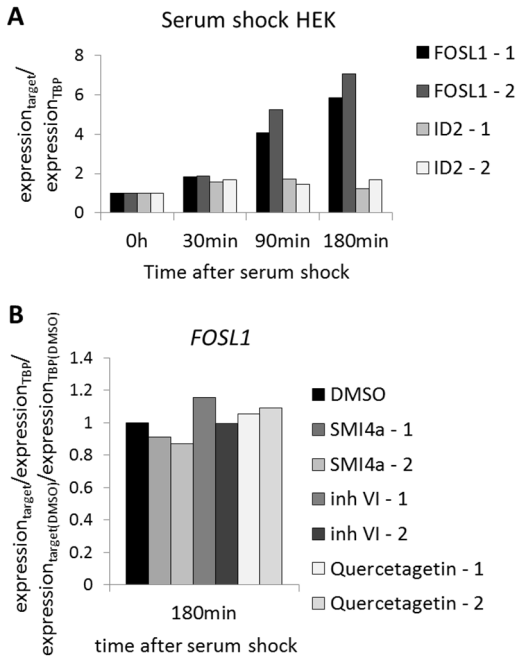

Figure 5.8 Effect of PIM kinase inhibitors on serum-induced *FOSL1* expression in HEK293 cells.
A HEK293 cells were serum shocked with 33% FCS and gene expression was analysed by RT-qPCR. Results were normalised to *TBP* and expression before serum shock (0 min). Two independent experiments conducted in triplicate wells of 6-well plates are shown. While *FOSL1* was induced 90 and 180 min after serum shock, *ID2* was not. **B** HEK293 cells were treated with DMSO, SMI4a, inh VI or Quercetagetin overnight and then serum shocked with 33% FCS for 180 min. Gene expression was assessed by RT-qPCR and normalised to *TBP* and DMSO-treated cells. Two independent experiments conducted in triplicate wells of 6-well plates are shown. None of the inhibitors tested blocked the induction of *FOSL1*, although this induction had previously been described as PIM1-dependent (Zippo et al., 2007). Therefore, we questioned whether the inhibitors were targeting PIM1 at all.

5.4 PIM1 overexpression did not alter *GNL3* or snoRNA expression

First, Raji and SUDHL6 cells were transfected with the pCMV6-XL4-PIM1 vector and PIM1 expression levels were analysed by western blot or qPCR. These two cell lines were chosen, because they express different levels of endogenous PIM1 and might therefore show different phenotypes upon PIM1 overexpression. As the transfected construct contains the full length PIM1 cDNA, including 5' and 3' UTRs, overexpression of both the 34 kDa and 44 kDa PIM1 isoforms was seen (Figure 5.9 A). 48 h after transfection, cells were harvested in TRIzol, RNA was prepared and expression was measured by RT-qPCR. The experiment was repeated twice in Raji cells and four times in SUDHL6 cells with variable outcomes (Figure 5.9 C, E). Although, relative *PIM1* expression levels, as measured by qPCR, were always higher than in untransfected cells, *GNL3* and *GNL3* hnRNA were either up- or downregulated (Figure 5.9 D, experiments 1 and 2, Figure 5.9 F). The amount of *PIM1* overexpression did not correlate with the level of *GNL3* expression, suggesting that overexpression of full-length *PIM1* did not directly affect *GNL3* expression.

Further, SNORD69, SNORD19 and SNORD19B expression levels were unaltered (Figure 5.9 C, E). The only highly significant change was a consistent downregulation of the *PIM2* mRNA in SUDHL6 cells and a trend towards downregulation in Raji cells (Figure 5.9 C, E). As PIM1 and PIM2 have several shared substrates and PIM2 has been shown to compensate for PIM1 knockout during lymphomagenesis (van der Lugt et al., 1995), it can be anticipated that overexpression of PIM1 might lead to downregulation of PIM2. Therefore, *PIM2* downregulation served as a positive control for effective PIM1 overexpression (Figure 5.9 C, E).

The PIM1 transcript is unstable due to AU-rich elements in the 3' UTR (H.K. Kim et al., 2012), which might inhibit high level PIM1 protein expression. Therefore, a 3xflag-tagged construct, containing the coding DNA sequence (CDS) only, was cloned into pCMV-SPORT6 and overexpressed in Raji cells. Furthermore, a kinase-dead variant, carrying a D186A mutation, was cloned and overexpressed as a control. Western blot confirmed that both constructs were overexpressed and localised to the nucleus and cytoplasm (Figure 5.9 B). However, the kinase-dead variant seemed to be unstable. Although sufficient overexpression of PIM1 was

achieved compared to pGL2-transfected control cells, *GNL3* and *GNL3* hnRNA expression levels were unaltered (Figure 5.9 D, experiment 3).

In conclusion, there was no evidence for a direct regulation of *GNL3* by PIM1 from the overexpression experiments. However, PIM1 is recruited to the DNA by MYC, which might be a limiting factor. ChIP after PIM1 overexpression, using either the PIM1 or flag antibodies, did not pull down enough gDNA to be detected by qPCR, which might be due to the saturation of the antibody by non-chromatin bound, overexpressed PIM1. Alternatively, cell numbers might have been too low due to the observed toxicity of the transient transfection. Therefore, although overexpressed PIM1 was nuclear, it could not be established whether it was also binding to DNA. If it is not recruited to the *GNL3* promoter, this might explain why no regulation of *GNL3* or snoRNA expression was observed in PIM1 overexpressing cells. For those reasons, we next attempted to knock down PIM kinases and MYC in Raji cells.

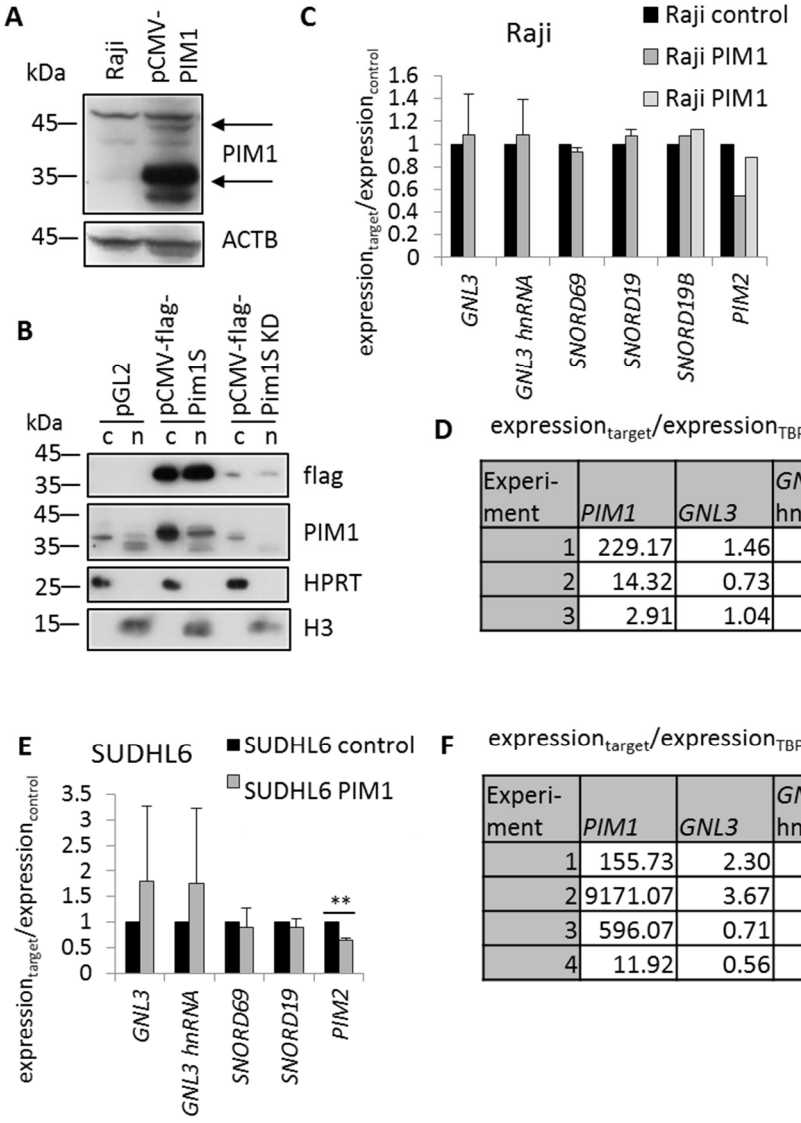

Experiment	*PIM1*	*GNL3*	*GNL3* hnRNA
1	229.17	1.46	1.34
2	14.32	0.73	0.72
3	2.91	1.04	1.17

Experiment	*PIM1*	*GNL3*	*GNL3* hnRNA
1	155.73	2.30	2.07
2	9171.07	3.67	3.71
3	596.07	0.71	0.70
4	11.92	0.56	0.58

Figure 5.9 Effects of PIM1 overexpression on *GNL3* and snoRNA expression. **A** Overexpression of full-length PIM1 in pCMV6-XL4 in Raji cells. The blot shown is representative of three independent experiments. **B** Overexpression of 3xflag-PIM1 and kinase-dead 3xflag-PIM1 in pCMV-SPORT in Raji cells. Western blot was done after nuclear-cytoplasmic fractionation. **C** RT-qPCR results of *GNL3*, SNORD69, SNORD19, SNORD19B and *PIM2* expression in Raji cells. The means and sd of three experiments conducted in triplicate wells of 6-well plates are shown for *GNL3*, *GNL3* hnRNA, SNORD69 and SNORD19. Two independent experiments conducted in triplicate wells of 6-well plates are shown for SNORD19B and *PIM2*. Results were normalised to *TBP* or *GNL3* hnRNA and control-transfected cells. **D** Relative amounts of *PIM1* or *GNL3* expression in Raji cells in different experiments. **E** Expression levels of *GNL3*, the snoRNAs and *PIM2* in SUDHL6 after PIM1 overexpression. The qPCR results are normalised to mock or control transfected cells and *TBP* or *GNL3* hnRNA. The means and sd of at least three independent experiments conducted in triplicate wells of 6-well plates are plotted. ** $p < 0.01$ as determined by Student's t test. **F** Relative amounts of *PIM1* or *GNL3* expression in different experiments in SUDHL6 cells. In conclusion, PIM1 overexpression did not influence *GNL3* or snoRNA expression in Raji or SUDHL6 cells, while it induced a decrease in *PIM2* mRNA levels.

5.5 Knockdown of MYC and PIM kinases

Because the ChIP after PIM1 overexpression was not successful, we could not conclusively determine whether overexpressed PIM1 was recruited to the *GNL3* promoter and whether it regulates *GNL3* transcription or not. Our hypothesis was that the amount of endogenous PIM1 might be sufficient to drive maximum expression of *GNL3* and that an increase in the PIM1 levels, through overexpression, cannot further elevate *GNL3* transcription. Therefore, an effect on *GNL3* expression might only be observed after knockdown of PIM kinases.

First, a transient transfection approach was chosen to knock down PIM1 or PIM2. Three shRNAs against PIM1 and three shRNAs against PIM2 were cloned into the pMSCV-miR30 vector and transiently transfected into Raji cells. However, transfection efficiency was too low to achieve a detectable knockdown. Further, transfection of these shRNAs into HEK293 cells did not result in knockdown of PIM1 or PIM2. Therefore, we decided to generate cells that were stably transfected with PIM1 or PIM2 shRNAs. Evidence from the literature suggested that knockdown of target proteins in Raji cells works best, when the shRNA is not expressed in a miR30 context, but as a classic shRNA from a U6 promoter (Lebbink et al., 2011). Further, an inducible system was preferred in this study, as knockdown of PIM kinases was expected to reduce cell viability, so that the generation of stable clones would be impossible when the shRNA is expressed constitutively. Hence, the pLKO_IPTG_3xLacO vector and validated shRNAs against PIM1 (shPIM1_1, shPIM1_2), PIM2 (shPIM2_1, shPIM2_2) and MYC (shMYC) were chosen and transfected into Raji cells.

After a first attempt to generate stable knockdown cells from a mixed population failed, single cell clones were selected, expanded and tested for efficient knockdown. shRNA expression was induced with 5 mM IPTG. Only shPIM1_1 and shPIM2_1 clones showed knockdown of PIM1 or PIM2, respectively, whereas the other two PIM shRNAs were not effective. Also, PIM1/2 double knockdown clones were generated. Of note, these often lost the ability to knock down PIM1 after about two weeks in culture, but retained their ability to knock down PIM2. The clones used in this study were: shMYC clones 2 and 4, shPIM1_1 clones 1B, 2B and 4B, shPIM2_1 clones 1, 4 and 8 and the double knockdown clones shPIM1_1/2_1 clones 6 and 8.

5.5.1 Knockdowns of MYC, PIM1 or PIM2 differentially affected Raji cell viability

First, the effect of PIM1, PIM2 or MYC knockdown on the viability of Raji cells was assessed over a time of ten days. Cell number and protein expression of IPTG-treated cells were compared to untreated cells. Knockdown of PIM1 was seen in IPTG-treated cells from day 4 onwards (Figure 5.10 A), while expression of PIM2 and MYC was unchanged. However, no effect on cell viability was detected when knockdown cells were compared to their untreated counterpart (Figure 5.10 B, Figure 5.11 A). The experiment was conducted twice with shPIM1_1 clone 2B and once with shPIM1_1 clone 4B and although the latter showed a more efficient knockdown, the outcome on viability was the same. Therefore, PIM1 is either dispensable for Raji cell viability or the residual low amount of PIM1 is sufficient to fulfil its essential cellular functions.

Knockdown of PIM2 was more efficient than PIM1 knockdown and occurred from day 2 onwards (Figure 5.10 C). Interestingly, a moderate upregulation of MYC was seen after knockdown. Cell viability was significantly reduced on day 8 and day 10 in these cells (Figure 5.10 D, Figure 5.11 B), suggesting that, in Raji cells, PIM2 plays a more important role than PIM1. Results were comparable between different clones, the experiment was done once with each of the shPIM2_1 clones (1, 4 and 8). MYC knockdown was very efficient (Figure 5.10 E) and resulted in a rapid loss of cell viability compared to untreated cells (Figure 5.10 F, Figure 5.11 C). This was expected, as BL cells are known to be obligatory dependent on MYC function. As Raji cells did, however, grow independent of the level of PIM1, the knockdown results favour a model, in which PIM1 is dispensable for MYC-dependent transcription in these cells under normal growth conditions.

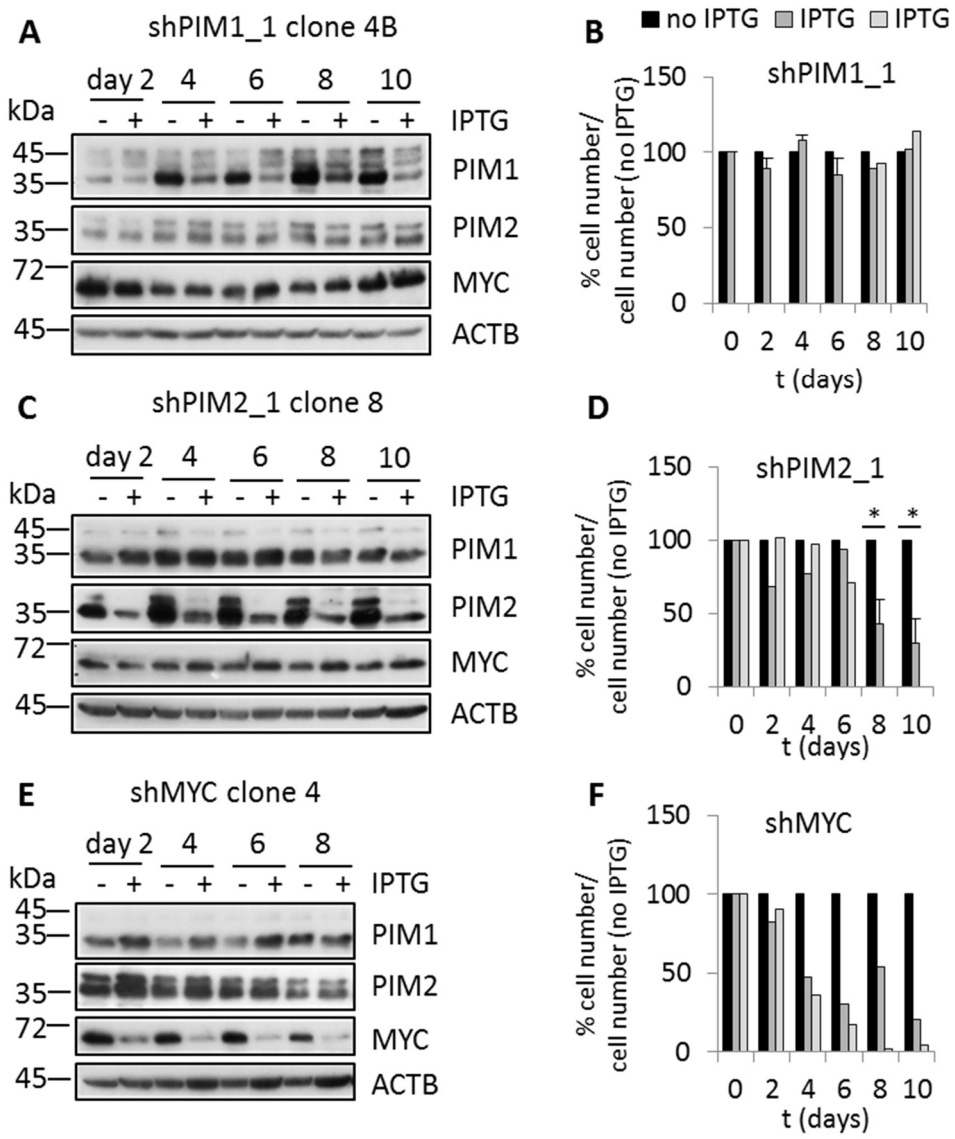

Figure 5.10 Consequences of PIM1, PIM2 or MYC knockdown for the number of Raji cells.

A, **C**, **E** Western blots showing knockdown of PIM1, PIM2 and MYC after treatment with 5 mM IPTG in one representative clone each. **B**, **D**, **F** Cell numbers, as determined by MTT assay, of untreated and IPTG-treated cells were normalised to untreated cells. The means and sd of three independent experiments conducted in duplicate wells of six-well plates are shown for shPIM1_1 days 0 to 6 and shPIM2_1 days 8 and 10. For all other time points the results of two independendent experiments are plotted individually. Knockdown of PIM1 did not reduce Raji cell number compared to control cells, whereas knockdown of PIM2 showed an effect on cell number on days 8 and 10 and MYC knockdown cells showed a trend towards a reduction in cell number already on day 4.

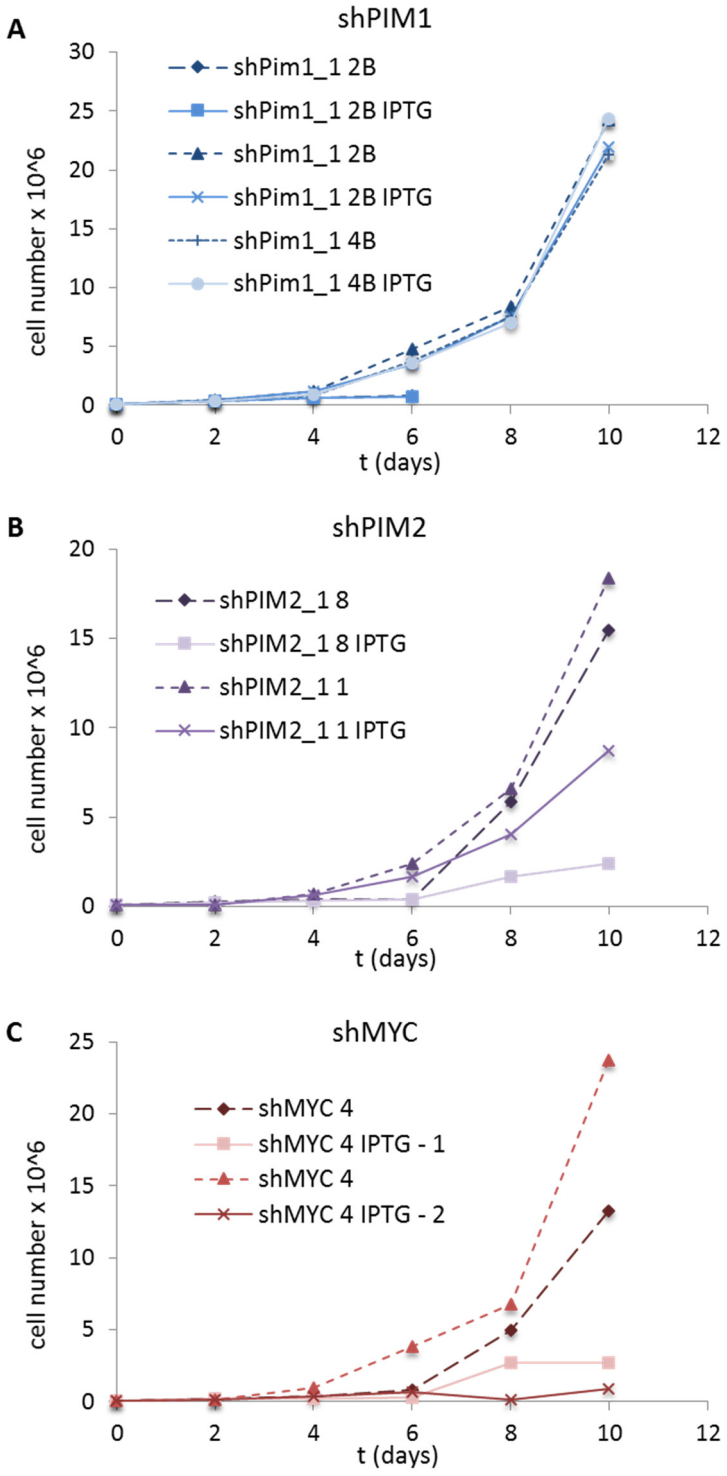

Figure 5.11 Growth curves of different knockdown clones.
Stably transfected Raji cell clones were seeded into duplicate wells of 6-well plates and treated with 5 mM IPTG or were left untreated. Cell numbers were determined every second day using an MTT assay. **A** Three experiments were done with different shPIM1 clones, but cell viability was unaffected by PIM1 knockdown in any of these experiments. **B** Two experiments were done with different shPIM2_1 clones and in both, cell number was strongly reduced in IPTG-treated compared to untreated cells on days 8 and 10. **C** Two experiments were done with the shMYC clone 4 and cell number was strongly reduced in IPTG-treated cells.

5.5.2 Knockdowns of MYC, PIM1 or PIM2 did not alter *GNL3* or snoRNA expression

Next, the effects of PIM1, PIM2, PIM1/2 double and MYC knockdowns on the expression of *GNL3* and its snoRNAs were analysed. PIM1 knockdown in three different clones (2B, 1B, 4B), which showed different levels of protein knockdown (Figure 5.12 A, B), did not result in any significant change in *GNL3* or *GNL3* hnRNA expression (Figure 5.12 E). Also, the *PIM1* mRNA was only slightly reduced, probably due to a compensatory upregulation of *PIM1* transcription (Figure 5.12 C), and *PIM2* and *MYC* expression were unaffected (Figure 5.12 C, D). The shPIM2_1 clones 1 and 4 both showed strong reduction in PIM2 expression on both protein and mRNA level (Figure 5.13 A, B). However, no consistent changes in expression of *PIM1*, *MYC*, *GNL3* or *GNL3* hnRNA were seen (Figure 5.13 B). Because PIM kinases have very similar functions and substrates, it is possible that knockdown of only PIM1 or PIM2 is not sufficient to see effects on the *GNL3* expression levels. Therefore, PIM1/2 double knockdown was used to investigate this idea. But, although both PIM1 and PIM2 were knocked down efficiently (Figure 5.14 A), only a very mild effect on *GNL3* mRNA and no effect on *GNL3* hnRNA expression were observed (Figure 5.14 B).

MYC might recruit other cofactors that allow for efficient transcription to occur. Thus, two shMYC clones with different knockdown efficiencies were analysed (Figure 5.15 A). As shown in Figure 5.10 and Figure 5.11, MYC knockdown was sufficient to inhibit cell growth. It was therefore very surprising not to see any effect on *GNL3*, *GNL3* hnRNA, SNORD69, SNORD19 or SNORD19B expression (Figure 5.15 B). Yet, MYC knockdown did have an effect: a compensatory upregulation of *MYC*, *PIM1* and *PIM2* mRNAs was detected (Figure 5.15 B). In conclusion, although PIM1 and MYC were bound to the *GNL3* promoter, there was no evidence that they regulated *GNL3* expression under normal growth conditions.

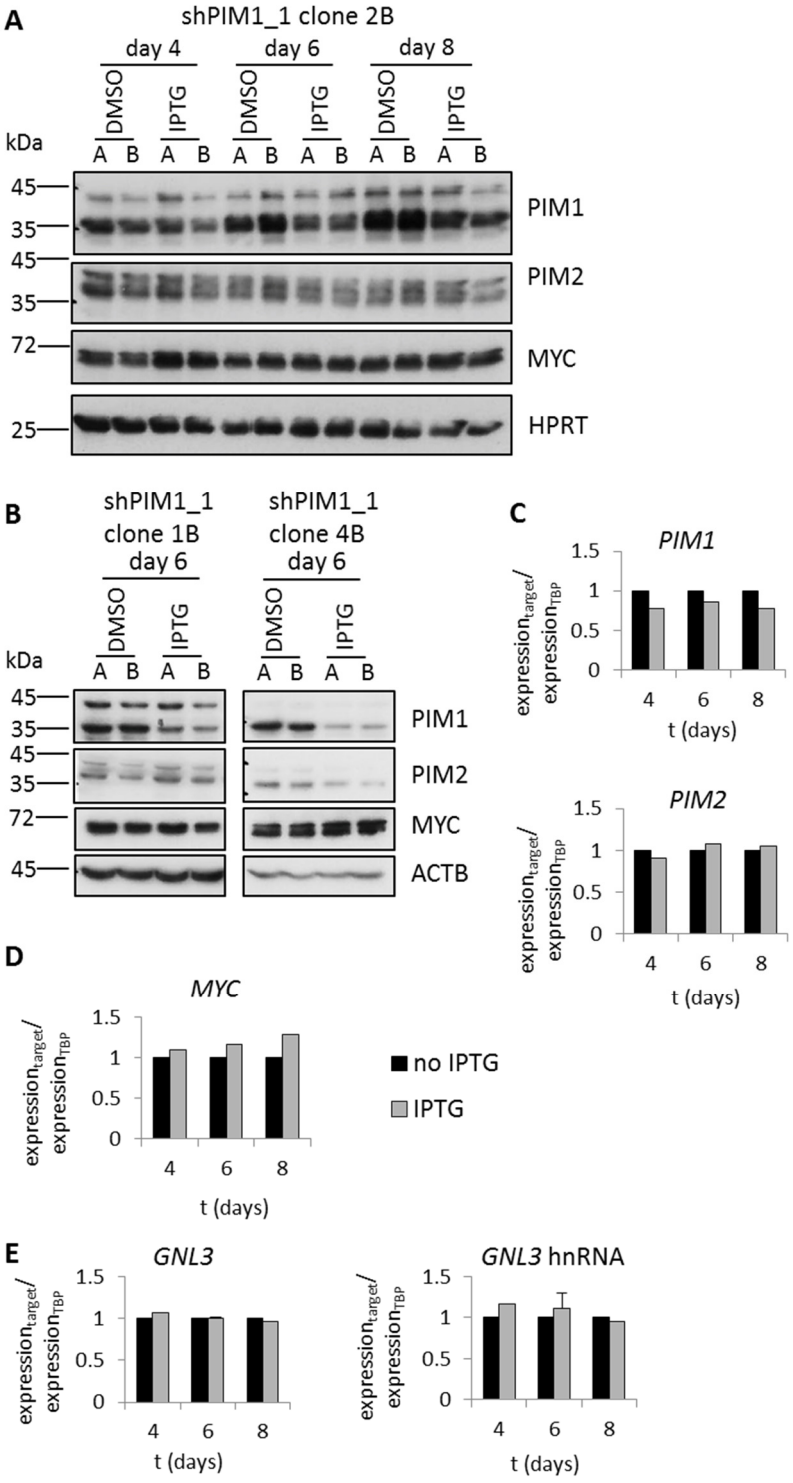

Figure 5.12 Effects of PIM1 knockdown on *GNL3* expression.

A, **B** Western blots showing knockdown of PIM1 after treatment with 5 mM IPTG for indicated times in different clones. A and B are technical duplicates from different wells of 6-well plates. **C**, **D** Expression of *PIM1*, *PIM2* and *MYC* in cells in **A**. Averages of technical duplicates are shown and qPCR results are normalised to *TBP* and non-IPTG-treated cells. **E** Expression of *GNL3* mRNA and hnRNA. Averages of technical duplicates, and for day 6 means and sd of the three different clones in **A** and **B** are shown. Results are normalised to *TBP* and untreated cells. Although PIM1 was knocked down, this did not result in any changes in *GNL3* mRNA or hnRNA expression.

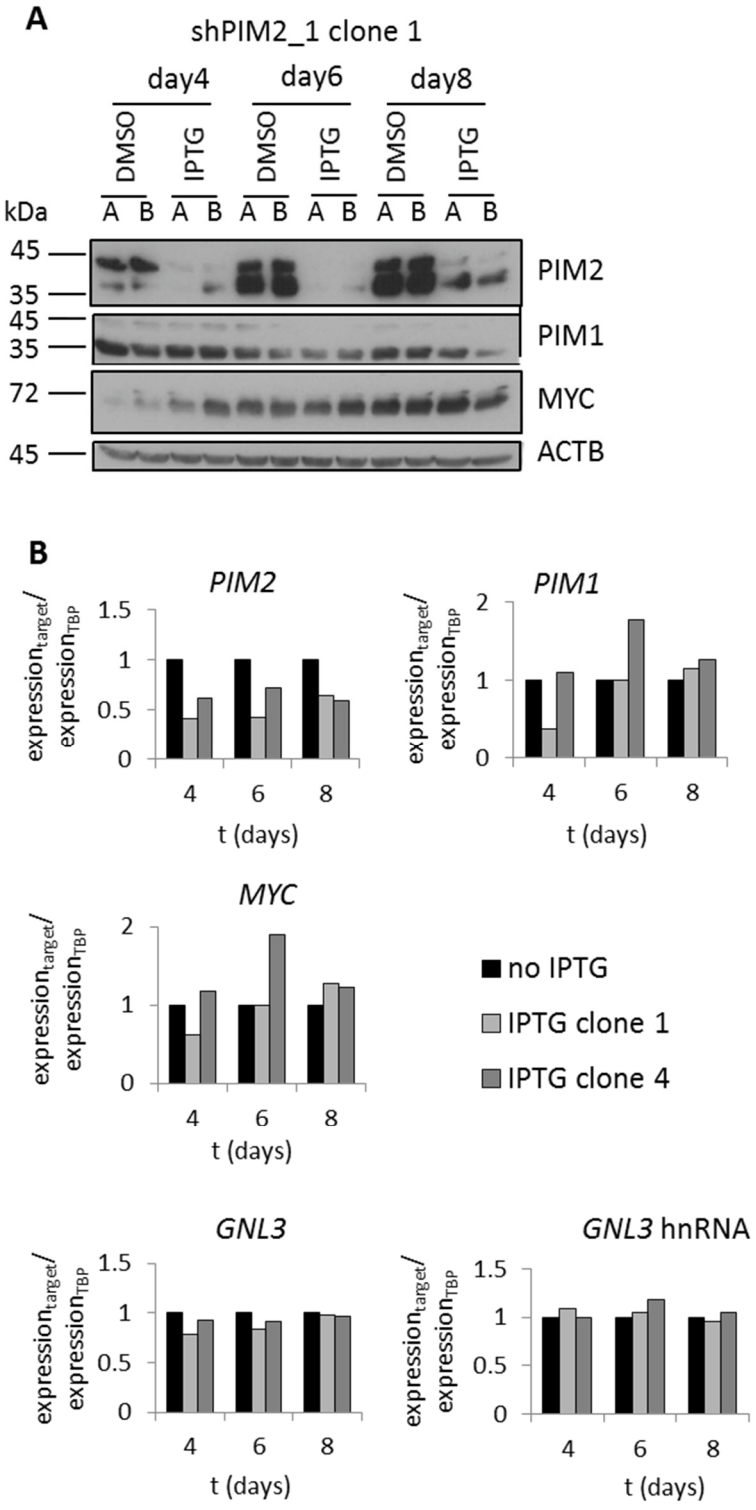

Figure 5.13 Influence of PIM2 knockdown on *GNL3* expression.
A Western blot showing PIM2 knockdown. The blot is representative of two different shPIM2_1 clones. **B** Expression of *PIM2*, *PIM1*, *MYC*, *GNL3* and *GNL3* hnRNA was measured by qPCR. Two independent experiments, conducted in duplicate wells of 6-well plates, are graphed. The results were normalised to *TBP* and non-IPTG-treated cells. Although PIM2 knockdown was very efficient on both the protein and mRNA level, no change in *GNL3* mRNA or hnRNA expression was seen.

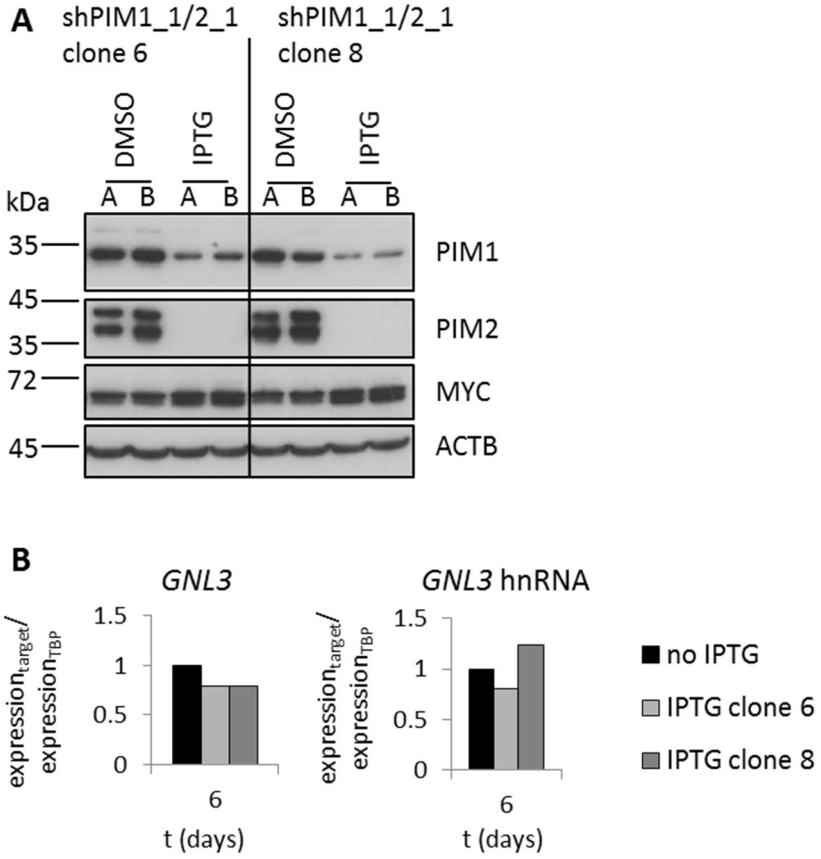

Figure 5.14 Effect of PIM1/2 double knockdown on *GNL3* expression.
A Western blot confirming knockdown of both PIM1 and PIM2 in shPIM1/2 double knockdown clones. A and B are technical duplicates from different wells of 6-well plates. **B** Expression of *GNL3* and *GNL3* hnRNA after double knockdown as determined by qPCR. Two independent experiments, carried out in duplicate wells of 6-well plates each, are depicted. The expression was normalised to that of *TBP* and non-IPTG-treated cells. Double knockdown was very efficient but only a small trend towards reduction of *GNL3* expression and no change in hnRNA levels could be observed.

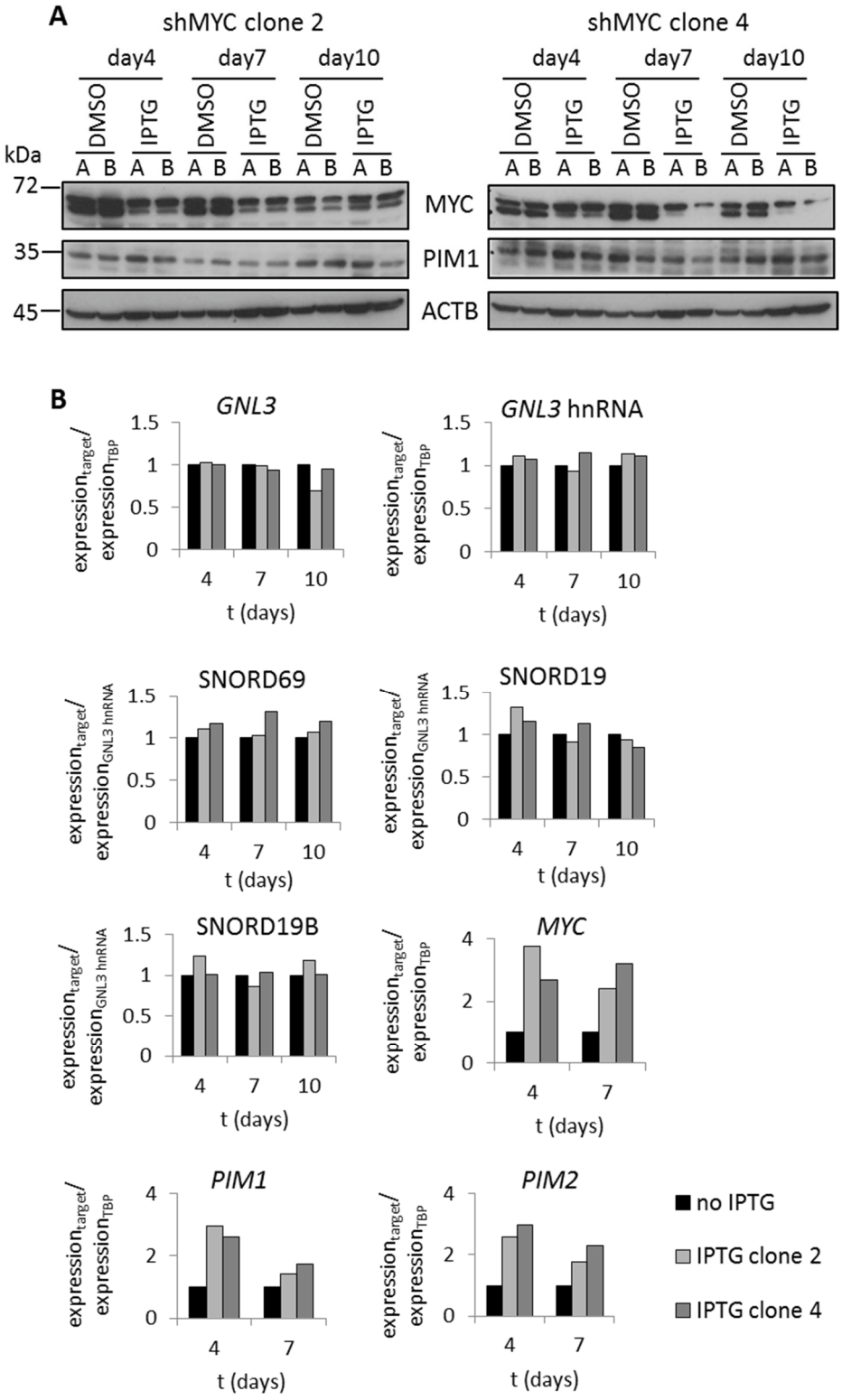

Figure 5.15 Influence of MYC knockdown on *GNL3* expression.
A Western blots showing knockdown of MYC in two different single cell-derived clones. A and B are cells from duplicate wells of 6-well plates. **B** RNA expression is plotted normalised to *TBP* or *GNL3* hnRNA and non-IPTG-treated cells. Results from the two independent clones in **A** are shown. Although MYC knockdown was efficient and strongly reduced cell viability, it did not affect *GNL3* mRNA or hnRNA levels or the expression of the intronic snoRNAs.

5.5.3 PIM1, PIM2, PIM1/2 double and MYC knockdown altered protein binding to the *GNL3* promoter

Because no change in *GNL3* or snoRNA expression was detected, we asked whether the knockdowns were sufficient to reduce binding of PIM1 and MYC to the *GNL3* promoter. ChIP confirmed that knockdown of PIM1 significantly reduced its binding to the *GNL3* promoter compared to non-IPTG-treated cells (Figure 5.16 A). Interestingly, PIM2 knockdown led to an increase in PIM1 recruitment, suggesting an inhibitory function of PIM2 (Figure 5.16 A). As expected, PIM1/2 double knockdown also decreased PIM1 binding to the *GNL3* promoter. But surprisingly, MYC knockdown had no effect on the presence of PIM1 at the *GNL3* +0.1 site, although MYC was reduced in this region (Figure 5.16 A, B). This suggests that PIM1 can be recruited to the chromatin independent of MYC. In the reciprocal experiment, knockdown of the PIM kinases did not alter MYC occupancy at the *GNL3* promoter (Figure 5.16 B).

No significant change in H3K9acS10p was seen in any of the conditions tested, although there was a trend towards increase after PIM2 knockdown, consistent with the increased binding of PIM1, and a trend towards decrease in MYC knockdown cells (Figure 5.16 C). This suggests that another kinase distinct from PIM1 and PIM2 can replace PIM1 to phosphorylate H3S10 in PIM1 and PIM1/2 double knockdown cells. As a marker for active elongation, POL II S2p was also analysed (Figure 5.16 D). Its presence in the promoter region and at the 3' end of *GNL3* was largely unaltered; only knockdown of MYC led to a slight reduction in POL II S2p at

Figure 5.16 Effects of PIM1, PIM2, PIM1/2 double and MYC knockdown on protein occupancy of the *GNL3* promoter.
ChIP was performed in untreated or IPTG-treated pLKO-shRNA-transfected cells. Antibodies against PIM1 (**A**), MYC (**B**), H3K9acS10p (**C**) or POL II S2p (**D**) were used. The results are normalised to input and control regions (*GNL3* -3.5 and *GNL3* +9 for PIM1 and MYC (**A**, **B**), CTCF1 for H3K9acS10p (**C**) and CTCF1 and *GNL3* -3.5 for POL II S2p (**D**)) and plotted relative to untreated cells. Means and sd of three independent experiments are shown for shPIM1_1 and shPIM2_1, one experiment was done for shPIM1_1/2_1 and two independent experiments are plotted for shMYC. For n = 3 experiments, two-tailed Student's t test was performed: * $p < 0.05$. PIM1 binding to the *GNL3* promoter was reduced in PIM1 knockdown cells, but increased in PIM2 and one of the MYC knockdowns. MYC binding to the promoter was largely unaffected by PIM kinase knockdown, but tended to be reduced by about 50% after MYC knockdown. However, H3K9acS10p was mostly unaltered in all the knockdown cells, a trend towards increased H3K9acS10p was only observed after PIM2 knockdown. Similarly, POL II S2p occupancy was unchanged in knockdown cells. A trend towards reduced POL II S2p occupancy was only observed in MYC knockdown cells at the *GNL3* +9 kb region.

the 3' end. This did, however, not result in any change in *GNL3* expression (Figure 5.15 B).

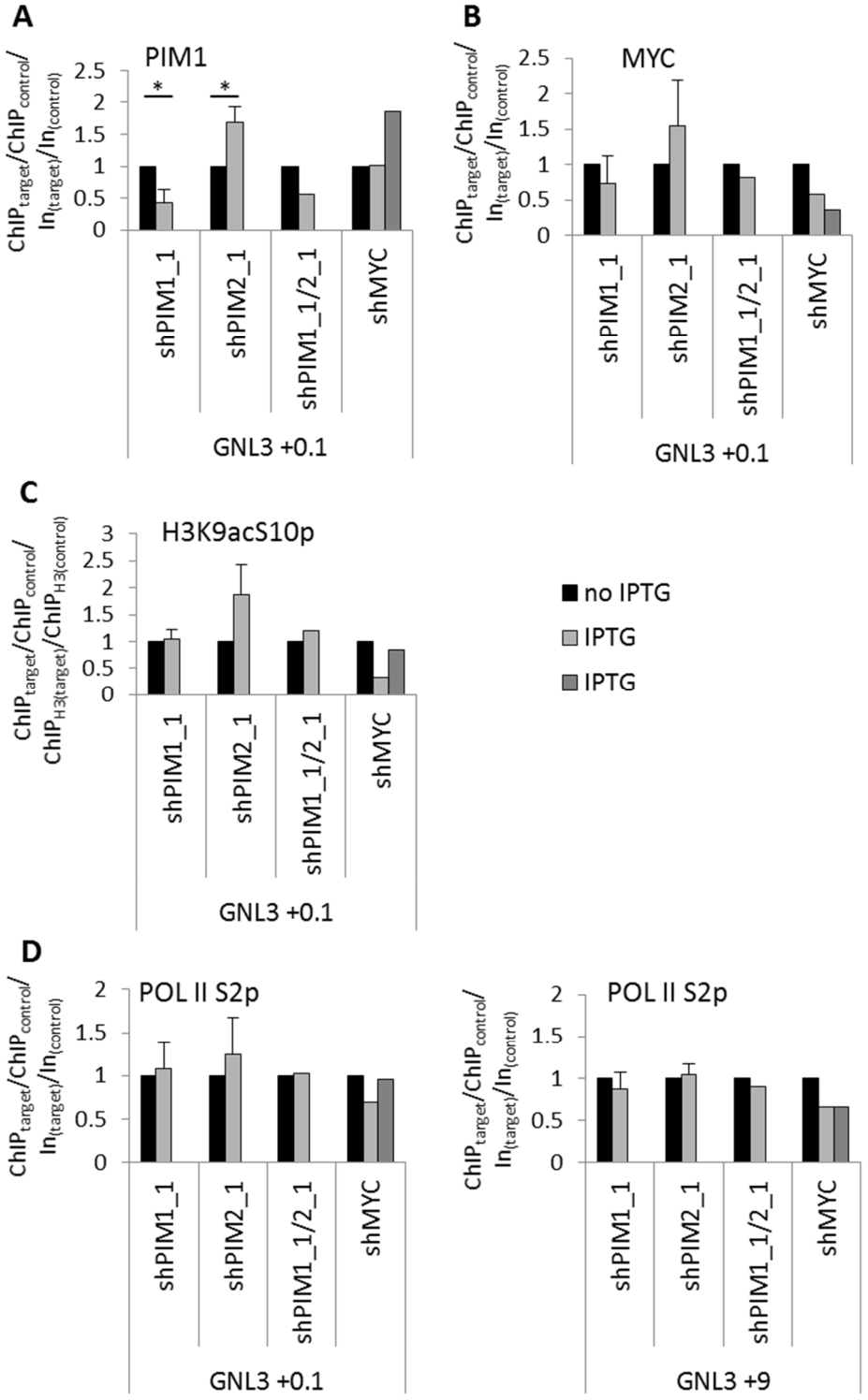

5.6 The pan-PIM kinase inhibitor AZD1208

The previous experiments suggested that PIM1 knockdown alone does not affect viability of Raji cells. It was, however, difficult to maintain double PIM1/2 knockdown cells over a prolonged period of time, so that I was unable to assess the effect of the double knockdown on cell viability. Further, the effect of specific PIM kinase inhibition on the ABC-DLBCL cell lines was still of interest, but the PIM kinase inhibitors used in section 4.3 and 5.3 were probably not specifically targeting PIM kinases and it was unclear, whether they exerted their effects on cell viability via PIM kinase inhibition. Consistently, SMI4a inhibited BAD phosphorylation only in OCI-Ly3, but not in Raji, Ramos or OCI-Ly10 cells (Figure 5.17).

Therefore, a novel and more potent pan-PIM kinase inhibitor, AZD1208, was used to study the effect of pan-PIM kinase inhibition on cell viability, gene expression and chromatin structure at the *GNL3* gene. Importantly, this inhibitor has been extensively tested against a panel of 442 kinases, and at a concentration of 1 µM only 13 other kinases were inhibited 50% or more, but the affinity of the inhibitor to PIM kinases was at least 43-fold greater than to any other kinase (Keeton et al., 2014).

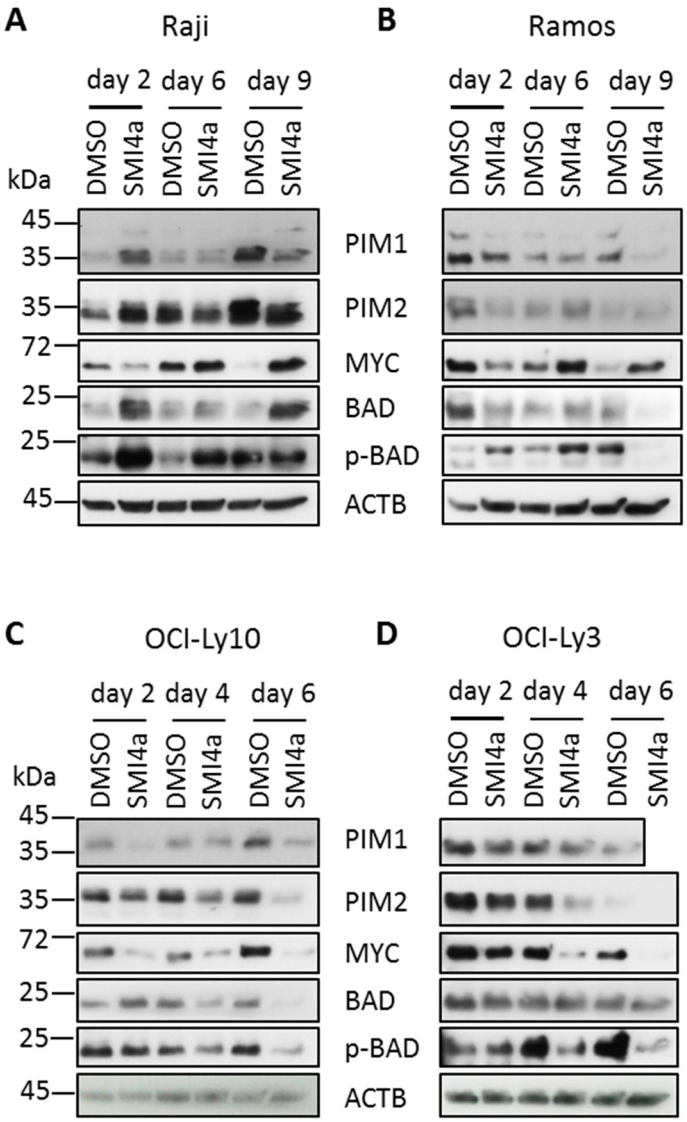

Figure 5.17 Effects of SMI4a on protein expression and BAD phosphorylation in B cell lymphoma cell lines.

Raji (**A**), Ramos (**B**), OCI-Ly10 (**C**) and OCI-Ly3 (**D**) cells were cultured in T25 flasks and treated with DMSO or 40 μM SMI4a. Protein samples were harvested at indicated times. SMI4a did not influence BAD-S112 phosphorylation in Raji, Ramos or OCI-Ly10 cells. Only OCI-Ly3 cells showed reduced pBAD.

5.6.1 AZD1208 had only minor effects on cell viability

First, Raji, Ramos, OCI-Ly3 and OCI-Ly10 cells were treated with different concentrations of AZD1208 (1 µM to 10 µM) or DMSO, respectively, and cell number was assessed over a time of six days. Interestingly, Raji and Ramos cells were mostly resistant to the drug (Figure 5.18 A, B), an inhibition of cell growth was seen in Ramos cells at 10 µM AZD1208 in one experiment only. Similarly, OCI-Ly3 cells showed a moderate reduction in cell number at 5 µM and 10 µM AZD1208 and only OCI-Ly10 cells displayed a reduced cell number already at 1 µM AZD1208 (Figure 5.18 C, D).

Surprisingly, PIM kinases were already strongly inhibited in all cell lines at 1 µM AZD1208, as assessed by BAD-S112 phosphorylation (p-BAD) (Figure 5.19 A, B). This observation does not match the hypothesis that PIM kinase activity is required for the proliferation or survival of lymphoma cells. In Raji, OCI-Ly3 and OCI-Ly10 cells, an upregulation or stabilisation of BAD was also seen at higher AZD1208 concentrations (Figure 5.19 A, B). Further, a compensatory upregulation or stabilisation of PIM1 and PIM2 could be observed in all four cell lines (Figure 5.19 A, C). MYC levels were also higher in inhibitor-treated compared to DMSO-treated cells.

These experiments show that both BL cell lines could grow independently of PIM kinase activity, although they had a strong requirement for MYC activity to survive. Therefore, PIM kinase activity does not seem to be essential for MYC-dependent transcription in general in these cells. Thus, although OCI-Ly3 and OCI-Ly10 cells were slightly more sensitive towards PIM kinase inhibition, this is most likely not due to its effects on transcription but on its other cellular targets.

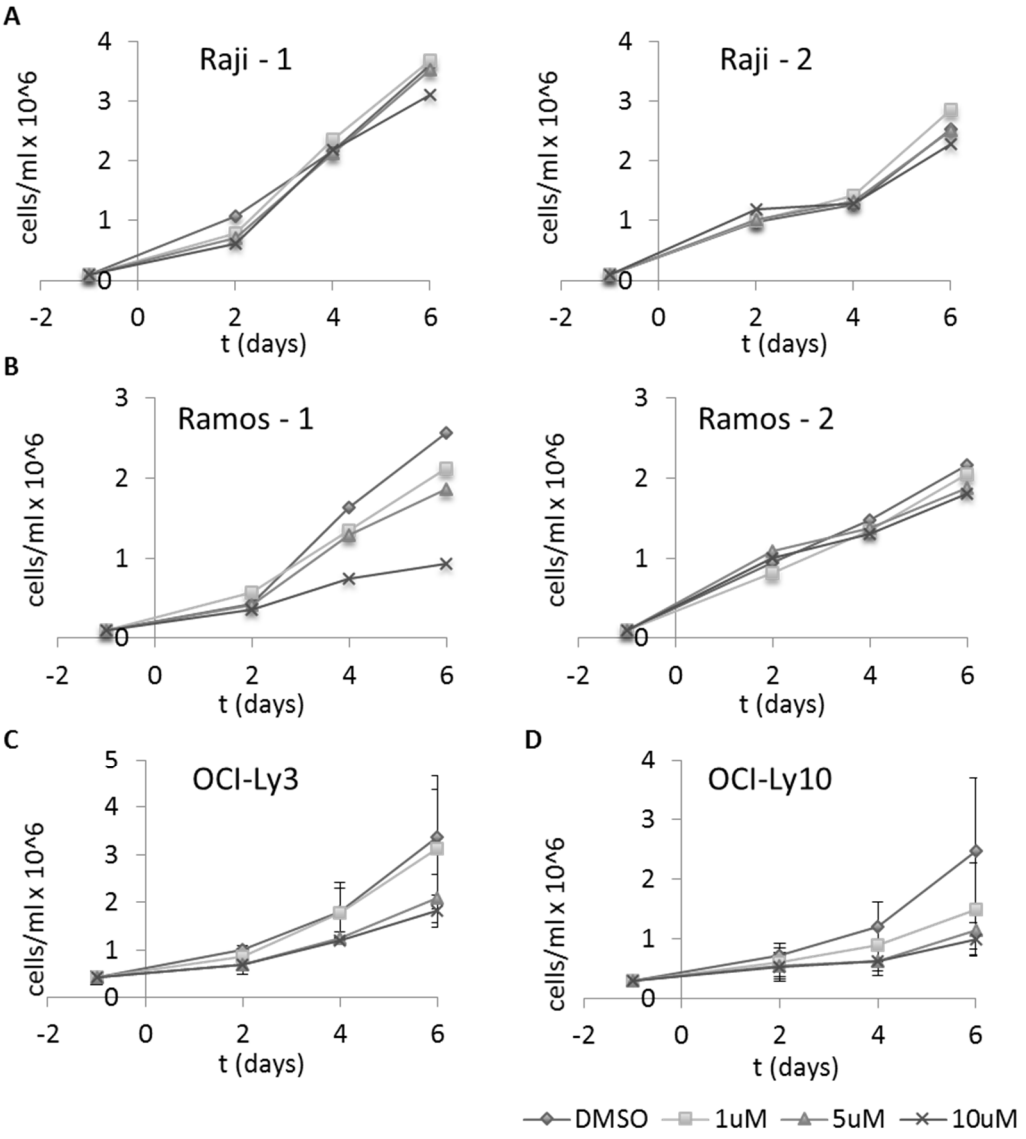

Figure 5.18 Consequences of AZD1208 treatment for the proliferation of B cell lymhoma lines.

A - **D** Cells were seeded into duplicate wells of 6-well plates and treated with DMSO, 1 µM, 5 µM or 10 µM AZD1208 for indicated times. The medium was replaced every second day and cell number was measured by MTT assay. For Raji (**A**) and Ramos (**B**), two independent experiments conducted in duplicate wells of 6-well plates are shown and for OCI-Ly3 (**C**) and OCI-Ly10 (**D**) the means and sd of three independent experiments, conducted in duplicate wells of six-well plates, are plotted. While AZD1208 did not affect Raji cell viability, high concentrations of AZD1208 affected Ramos cells in one experiment but not the other. OCI-Ly3 cell number was reduced by 5 µM and 10 µM AZD1208, and only OCI-Ly10 cells were sensitive to 1 µM AZD1208.

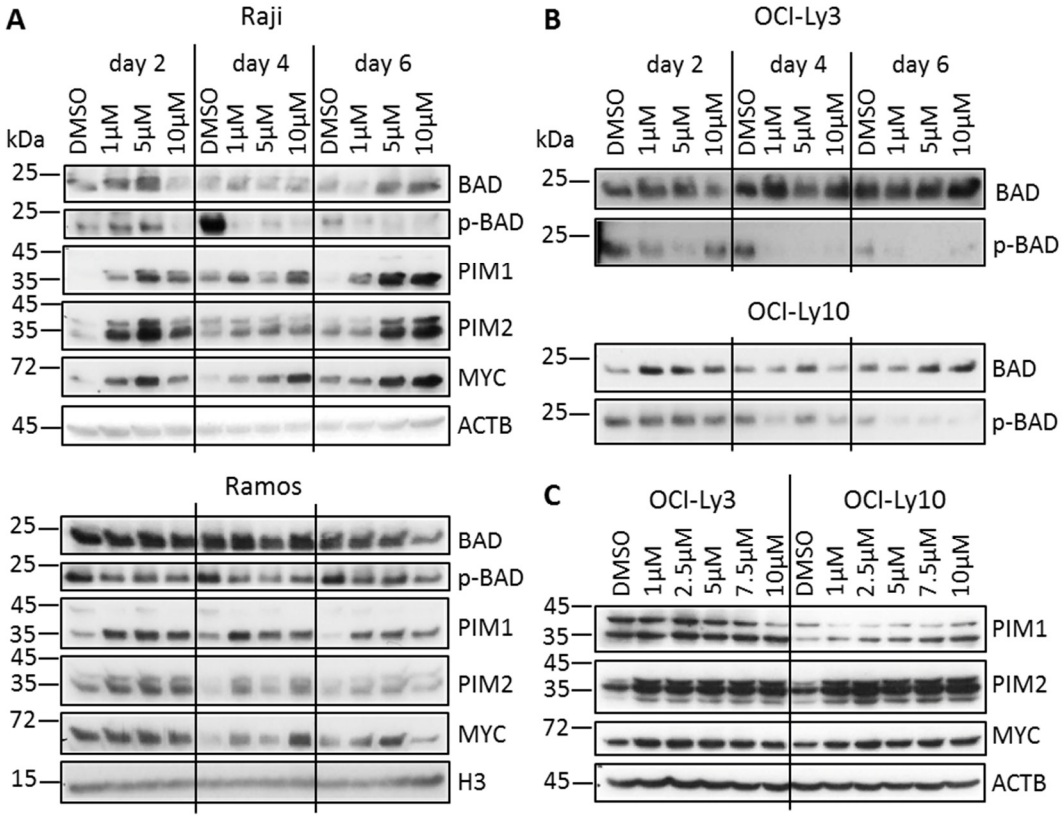

Figure 5.19 Consequences of AZD1208 treatment for protein expression and BAD phosphorylation in different BCL cell lines.

A, **B** Cells were seeded into T25 flasks and treated with DMSO, 1 µM, 5 µM or 10 µM AZD1208 for indicated times. The medium was replaced every second day. Aliquots were harvested and analysed by western blot. **C** Cells were seeded into T25 flasks and treated with 1 µM, 2.5 µM, 5 µM, 7.5 µM or 10 µM AZD1208 or a respective amount of DMSO for three days. Then, protein expression was evaluated by western blot. 1 µM AZD1208 inhibited BAD phosphorylation in all cell lines tested. Further, PIM1, PIM2 and MYC expression were elevated, which is indicative of efficient PIM kinase inhibition

5.6.2 AZD1208 did not affect *GNL3* expression in Raji cells

Because PIM kinase inhibition did not affect viability of the Raji BL cell line, we predicted that gene expression would also be unaffected. Therefore, expression of the *GNL3* gene was assessed in Raji cells after treatment with 1 µM, 5 µM or 10 µM AZD1208 for one, three or seven days. As expected, *GNL3* and *GNL3* hnRNA expression were unchanged, only DMSO-treated cells showed higher *GNL3* mRNA levels on day seven, without a change in hnRNA (Figure 5.20 A, B). Therefore, PIM kinase inhibition did not affect transcription of the *GNL3* gene. Similarly, SNORD69 and SNORD19 expression levels were unaltered (Figure 5.20 C, D).

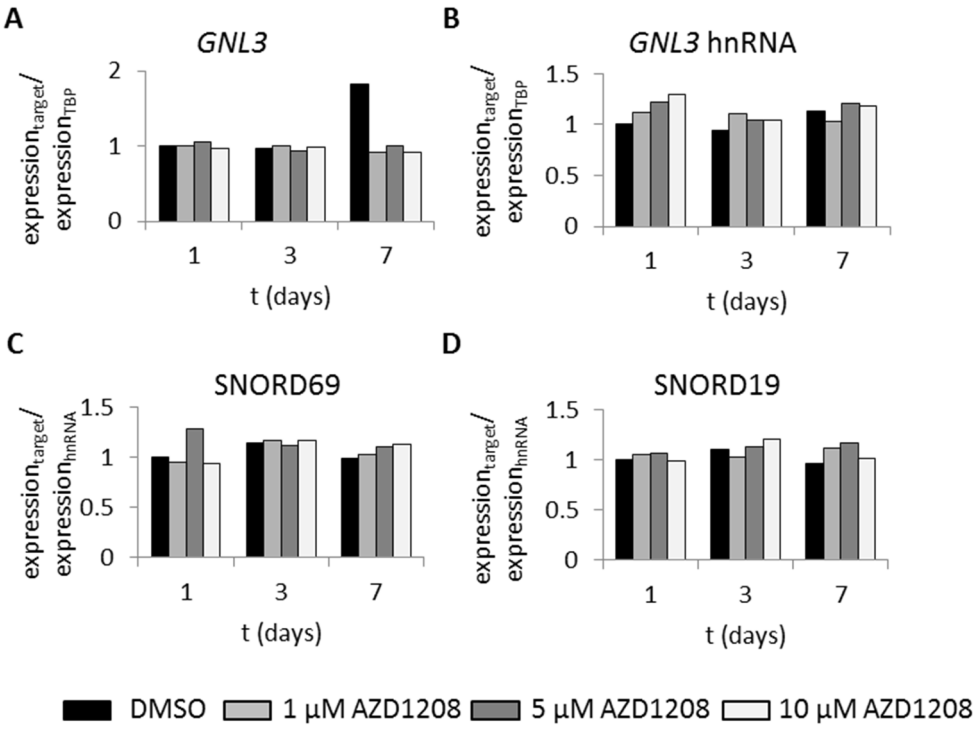

Figure 5.20 Effects of AZD1208 on the expression of *GNL3* and snoRNAs. Raji cells were plated in duplicate wells of 6-well plates and treated with 1 µM, 5 µM or 10 µM AZD1208 for indicated times. The medium was changed every day. RNA expression was measured by RT-qPCR and normalised to *TBP* (**A**, **B**) or *GNL3* hnRNA (**C**, **D**) and DMSO-treated cells on day 1. The results of one experiment are plotted. As expected, the expression of *GNL3* mRNA and hnRNA, SNORD69 and SNORD19 were unaffected by AZD1208 treatment.

5.6.3 AZD1208 affected PIM1, MYC and H3K9acS10p occupancy at the *GNL3* gene

Although PIM kinase activity was dispensable for survival of Raji BL cells and for the expression of *GNL3*, we were interested to see, whether chromatin structure at the *GNL3* gene was affected regardless. Therefore, Raji cells were treated with 5 µM AZD1208 for one, three or seven days. ChIP results showed that both PIM1 and MYC were stabilised at the *GNL3* promoter on day 1 of treatment (Figure 5.21 A, B). This might indicate that PIM kinase activity is required for its turnover at the *GNL3* promoter. AZD1208 might stabilize the PIM1 protein, which would correlate with the increased PIM1 and PIM2 protein levels in AZD-treated cells (Figure 5.19 A). The increased presence of MYC might be a consequence of the increased PIM1 binding at the promoter or might also be a result of MYC stabilisation or upregulation after AZD1208 treatment (Figure 5.19 A). However, no increased binding was seen on days 3 and 7 (Figure 5.21 A, B), although total PIM1 and MYC proteins were still elevated (Figure 5.19 A).

In contrast to PIM1 knockdown cells (Figure 5.16 C), H3K9acS10p was reduced after AZD1208 treatment (Figure 5.21 C). This could be explained by the presence of inactive PIM1 at the promoter, which prevents the recruitment of an alternative H3S10 kinase. Unexpectedly, the reduced H3K9acS10p did not result in lower transcription (Figure 5.20). When POL II S2p occupancy at the promoter and the 3' end of the GNL3 gene was investigated, no significant change could be seen (Figure 5.21 D). There was, however, a trend towards increase on day 7, which was not correlated with a change in expression of the gene (Figure 5.20). These data confirm that H3K9acS10p levels do not correlate closely with transcriptional activity of the *GNL3* gene or POL II S2 phosphorylation.

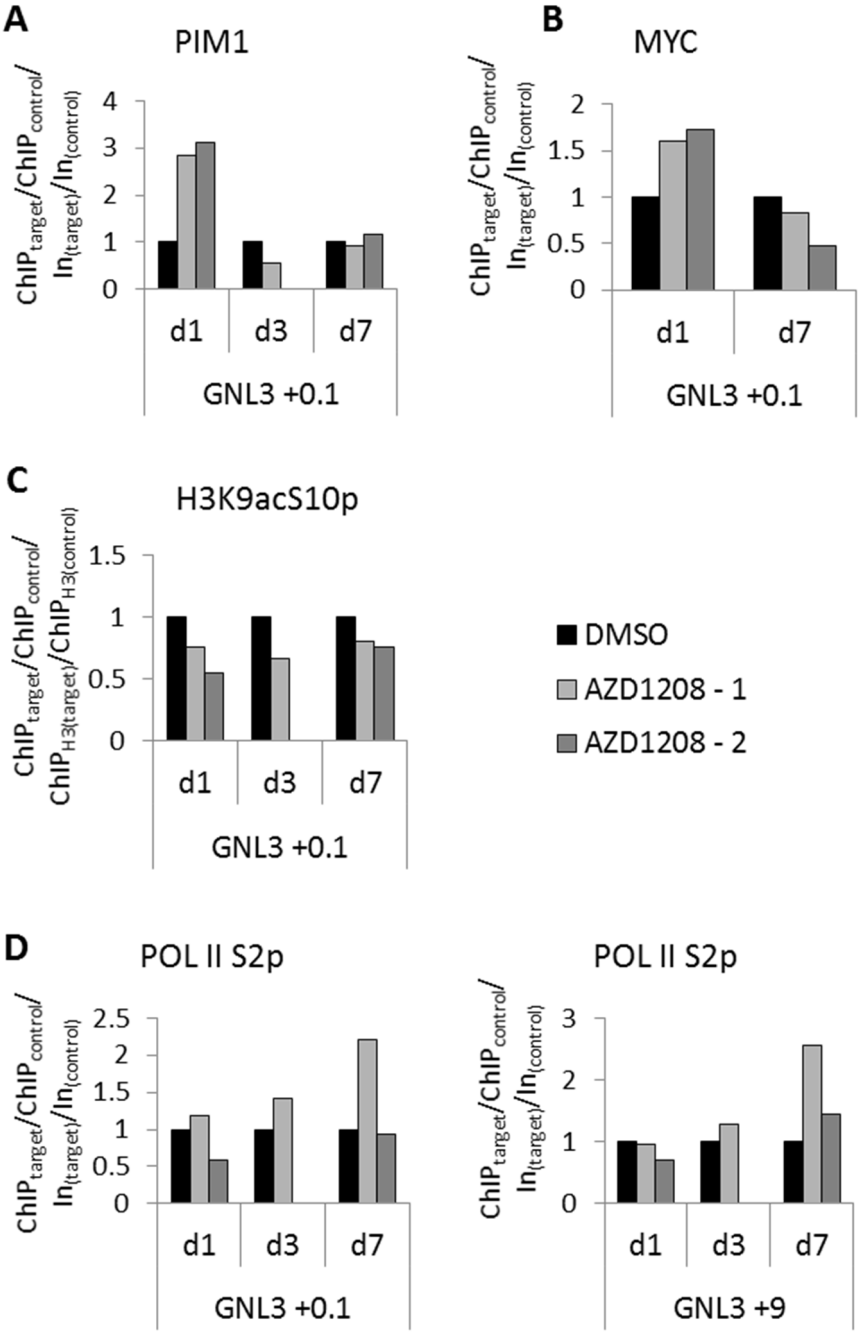

Figure 5.21 Effects of AZD1208 on chromatin structure of the *GNL3* gene. ChIP was performed in Raji cells after AZD1208 treatment. The cells were plated on day -1, treated with 5 μM AZD1208 or DMSO from day 0 for 1, 3 or 7 days. ChIP was done with antibodies against PIM1 (**A**), MYC (**B**), H3K9acS10p (**C**) or POL II S2p (**D**). Results are normalised to input or H3 and control regions (CTCF1 and CTCF3 for PIM1, MYC and POL II S2p, CTCF3 and *GNL3* +9 for H3K9acS10p) and DMSO-treated cells. Two independent experiments are shown for days 1 and 7, the result of one experiment is plotted for day 3. Both PIM1 and MYC tended to be elevated at the *GNL3* promoter on the first day of AZD1208 treatment but were decreased again on days 3 and 7. We observed a trend towards decrease in H3K9acS10p at the promoter and variable changes in POL II S2p, with a trend towards increased POL II S2p at the *GNL3* +9 kb region on day 7.

5.7 MYC and PIM1 might be implicated in the regulation of DNA replication at the *GNL3* promoter

Although PIM1 and MYC were bound to the *GNL3* promoter and influenced H3K9acS10p, they did not alter *GNL3* expression. However, MYC is implicated in the regulation of DNA replication and regulates licensing of some replication origins independent of transcription. It mainly acts as an origin activating protein in G1 phase (Dominguez-Sola et al., 2007; Swarnalatha et al., 2012). Further, 14-3-3 proteins are required for initiation of DNA replication in *S. cerevisiae* (Yahyaoui & Zannis-Hadjopoulos, 2009). 14-3-3 proteins can be recruited to the chromatin by H3S10p and PIM1 might play a role here. Moreover, the MYST family acetyltransferase HBO1 is required for replication origin licensing (Iizuka et al., 2006). Because PIM1 regulates the recruitment of another MYST family member – MOF – to stimulate transcriptional elongation, it might also regulate HBO1 recruitment. Interestingly, origins of replication often overlap with active promoters, but it is important that transcription and replication are temporally separated (Meryet-Figuiere et al., 2014). Therefore, MYC and PIM1 might regulate DNA replication and the separation of DNA replication and transcripton at the *GNL3* promoter.

To test this hypothesis, Raji cells were synchronised in M phase using a thymidine/nocodazole block and then released to progress through the cell cycle. PI-staining and flow cytometry were applied to determine the cell cycle stage. A high proportion of unsynchronised Raji cells were in S phase (Figure 5.22 A), whereas thymidine/nocodazole-synchronised cells were arrested in M phase (Figure 5.22 B). 4 h after release, cells had progressed into G1 phase (Figure 5.22 C), 8 h after release they were mostly in G1 and early S phase (Figure 5.22 D) and after 12 h, the majority of cells had entered S phase (Figure 5.22 E).

Then, ChIP was performed on synchronised cells to assess the recruitment of MYC and PIM1 to the *GNL3* promoter region. Interestingly, in one experiment more than twice as much MYC as in G1 phase was bound to the promoter in G1/early S phase cells and the level was reduced again during S phase (Figure 5.23 A). In the same experiment, PIM1 binding to the promoter was increased in G1/early S phase cells and decreased during S phase (Figure 5.23 B). Intriguingly, no change in H3K9acS10p was seen (Figure 5.23 C) but POL II S2p decreased at the 3' end of the *GNL3* gene when cells progressed into S phase (Figure 5.23 D). Surprisingly,

however, no decrease in *GNL3*, SNORD69 or SNORD19 expression was observed while the cells progressed through the cell cycle (Figure 5.23 E).

The increase in MYC and PIM1 binding to the *GNL3* promoter in G1/S phase cells suggests a cell cycle-dependent function of these proteins, which might be the regulation of DNA replication or the coordination of DNA replication and transcription.

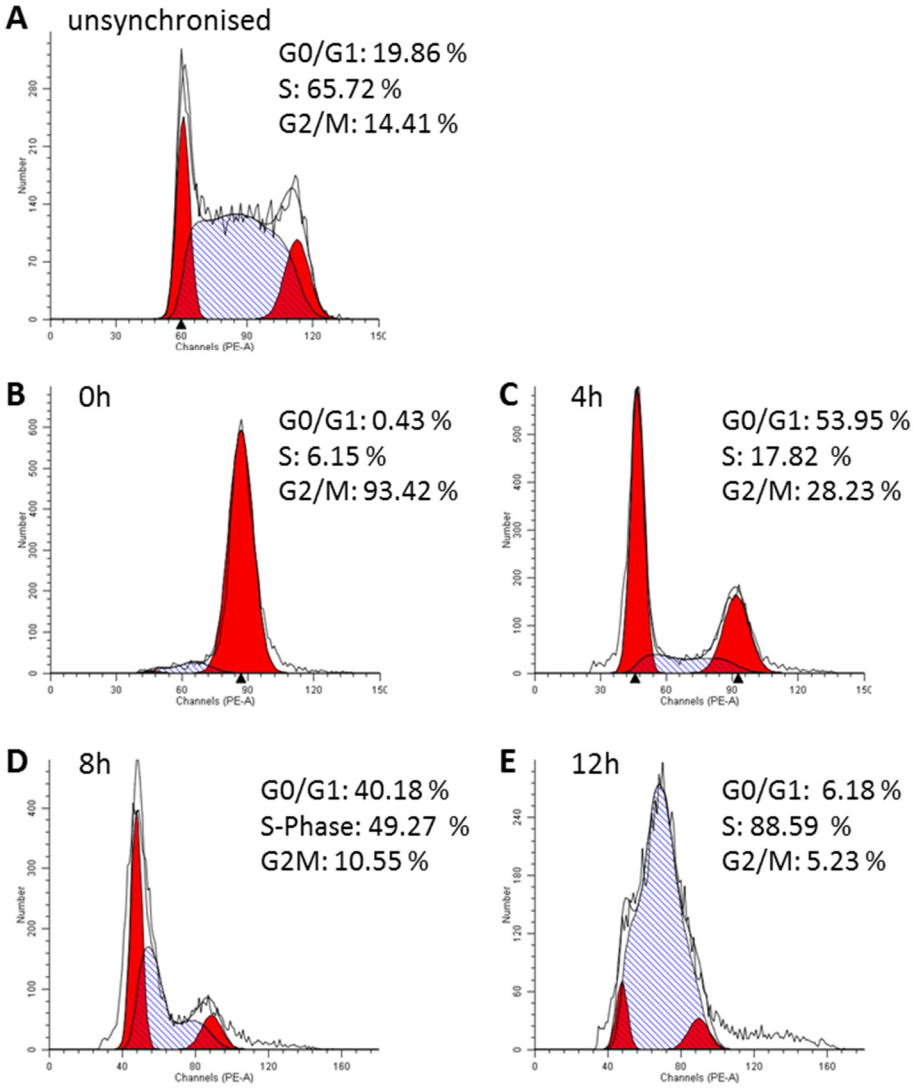

Figure 5.22 Analysis of cell cycle synchronisation by thymidine/nocodazole in Raji cells.
Raji cells were cultured in T125 flasks and synchronised in M phase of the cell cycle using a thymidine/nocodazole block. PI-staining and FACS were applied to monitor progression through the cell cycle. ModFit was used to make the graphs and calculate percentages of cells in different cell cycle phases. The results shown are representative of two independent experiments. **A** Exponentially growing, unsynchronised Raji cells were mainly in S phase **B** Raji cells after synchronisation with thymidine/nocodazole. The cell cycle was blocked in M phase **C** Raji cells 4 h after release from thymidine/nocodazole block. Cells rogressed into G1 phase. **D** Raji cells 8 h after release from thymidine/nocodazole block. The cell progressed into late G1/early S phase. **E** Raji cells 12 h after release from thymidine/nocodazole block were mainly in S phase.

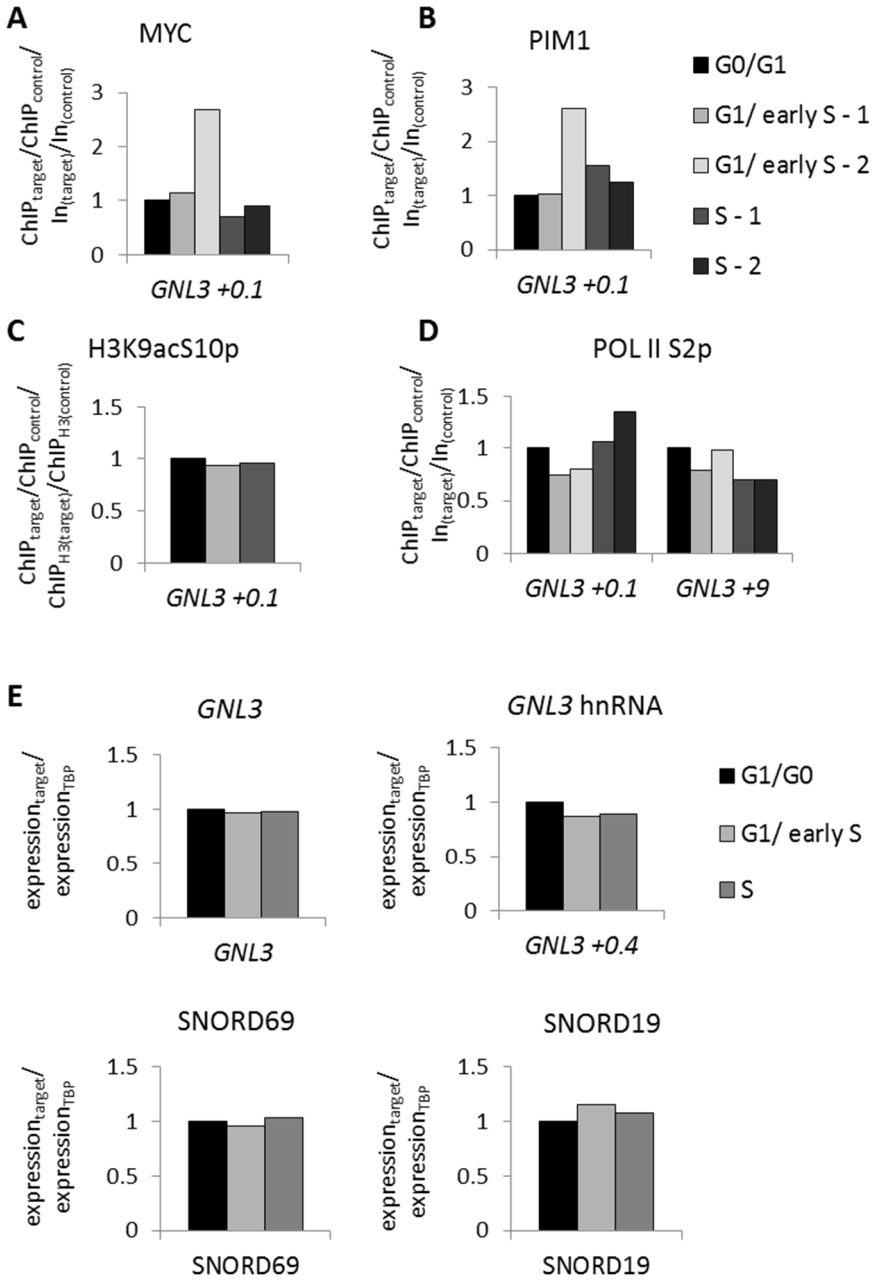

Figure 5.23 Effects of the cell cycle phase on the chromatin structure of the *GNL3* gene and its expression.

Raji cells were synchronised using a thymidine/nocodazole block and then released into the cell cycle. After 4 h (G0/G1 phase), 8 h (G1/S phase) and 12 h (S phase) chromatin was prepared and used for ChIP with anti-MYC (**A**), anti-PIM1 (**B**), anti-H3K9acS10p (**C**) or anti-POL II S2p (**D**) antibodies. Results are normalised to input (**A**, **B**, **D**) or total H3 (**C**), the CTCF1 control region and G0/G1 phase cells. Two independent experiments are shown in **A**, **B** and **D**, one experiment is plotted in **C**. MYC and PIM1 binding to the *GNL3* promoter was increased in G1/early S phase in one experiment. This did, however, not correlate with transcriptional activation, as POL II S2p was unchanged. **E** RNA expression was measured in synchronised cells using RT-qPCR. Results of one experiment are shown. Expression of *GNL3*, SNORD69 and SNORD19 did not change while cells progressed through G1 and S phase.

6 Gene expression in CLL cells and effects of Ibrutinib

The irreversible BTK inhibitor Ibrutinib is a novel drug, which is currently being trialled for the treatment of CLL and other haematological malignancies and it has been shown to be effective in relapsed and refractory CLL (Advani et al., 2013; Byrd et al., 2013). Early studies have indicated that Ibrutinib has a reduced toxicity profile compared to standard CLL therapy with high response rates (Byrd et al., 2013; O'Brien et al., 2014). However, its mechanism of action is unclear.

As Ibrutinib targets BTK, it is expected to block BCR signalling and most downstream effects of the BCR signalling pathway, e.g. the activation of PLCγ, and thus Ca^{2+} signalling, PKCs, NFκB and ERK1/2. While knowledge about downstream signal transduction pathways is extensive, little is known about alterations at the chromatin level in response to BCR signalling in normal as well as CLL B cells. Therefore, we aim to study the chromatin structure at BCR target genes in CLL cells before and after BCR cross-linking and to elucidate possible effects of Ibrutinib.

The focus of this study was laid on histone phosphorylation marks, because these are transient (half-life 20 to 30 min (Jackson et al., 1975)), rapidly changing, signalling-induced marks, which have been shown to result in transcriptional activation of target genes. In addition, several of the signalling kinases downstream of the BCR-signalling pathway, such as MSK1/2 or PKCβ, have been shown to directly target histones. Target genes are likely to be important survival and proliferation genes, as BCR signalling is vitally important for CLL. By identifying key pathways, which lead to histone phosphorylation, the understanding of Ibrutinib's mechanism of action is improved and it might be possible to identify novel drug targets, inhibitors for which could be used in combination with Ibrutinib or in Ibrutinib-resistant patients.

In addition, we wanted to analyse more stable histone PTMs, like methylation and acetylation marks, as these provide information about the long-term activation status of a gene. If Ibrutinib treatment leads to changes in these marks, they could later also be analysed in samples from patients, which are treated with Ibrutinib and serve as predictive markers for drug response and drug resistance.

The aims of this part of the study were

1. To test genes, which are activated upon BCR signalling in CLL cells and to assess the effect of Ibrutinib on expression of these genes.

2. To identify histone phosphorylation marks, which change at BCR target genes upon BCR signalling and to study the effect of Ibrutinib on these marks.
3. To identify signalling pathways which are essential for histone phosphorylation.
4. To study the effects of Ibrutinib on both activating and inhibitory histone methylation and acetylation marks at BCR target genes.

6.1 Gene expression of CLL cells co-cultured with CD40L or M210B4 cells

CLL cell proliferation and survival are dependent on the microenvironment. This microenvironment can be partially reproduced *in vitro* by co-culturing PBMCs from CLL patients with CD40L or M210B4 cells. While M210B4 is a murine stromal cell line, CD40L cells are murine L cells expressing human CD40L. Therefore, it was expected that CD40L cells would stimulate pro-proliferative gene expression in CLL cells. To amplify cDNA from human PBMCs only, qPCR primers were designed to specifically bind to the human but not the murine sequence. Genes analysed were chosen on the basis of differentially expressed genes in anti-IgM-stimulated vs. -unstimulated CLL cells identified by Guarini et al., as our main aim was to study the effects of Ibrutinib on BCR signalling (Guarini et al., 2008).

Expression of cyclin D2 (*CCND2*), *MYC*, dual-specificity phosphatase 4 (*DUSP4*), BCL2-related protein A1 (*BCL2A1*), chemokine (C-C motif) receptor 7 (*CCR7*), peroxiredoxin 1 (*PRDX1*) and nucleolin (*NCL*) was stimulated by CD40L but not M210B4 co-culture. In contrast, *CDC25B* was strongly downregulated in cells co-cultured with CD40L cells. *DUSP2* expression was enhanced in PBMCs co-cultured with either CD40L or M210B4. Early growth response 1 (*EGR1*) was unchanged in all but one patient, when PBMCs were cultured on M210B4 cells, while Toll-like receptor 10 (*TLR10*) expression was unaltered (Figure 6.1).

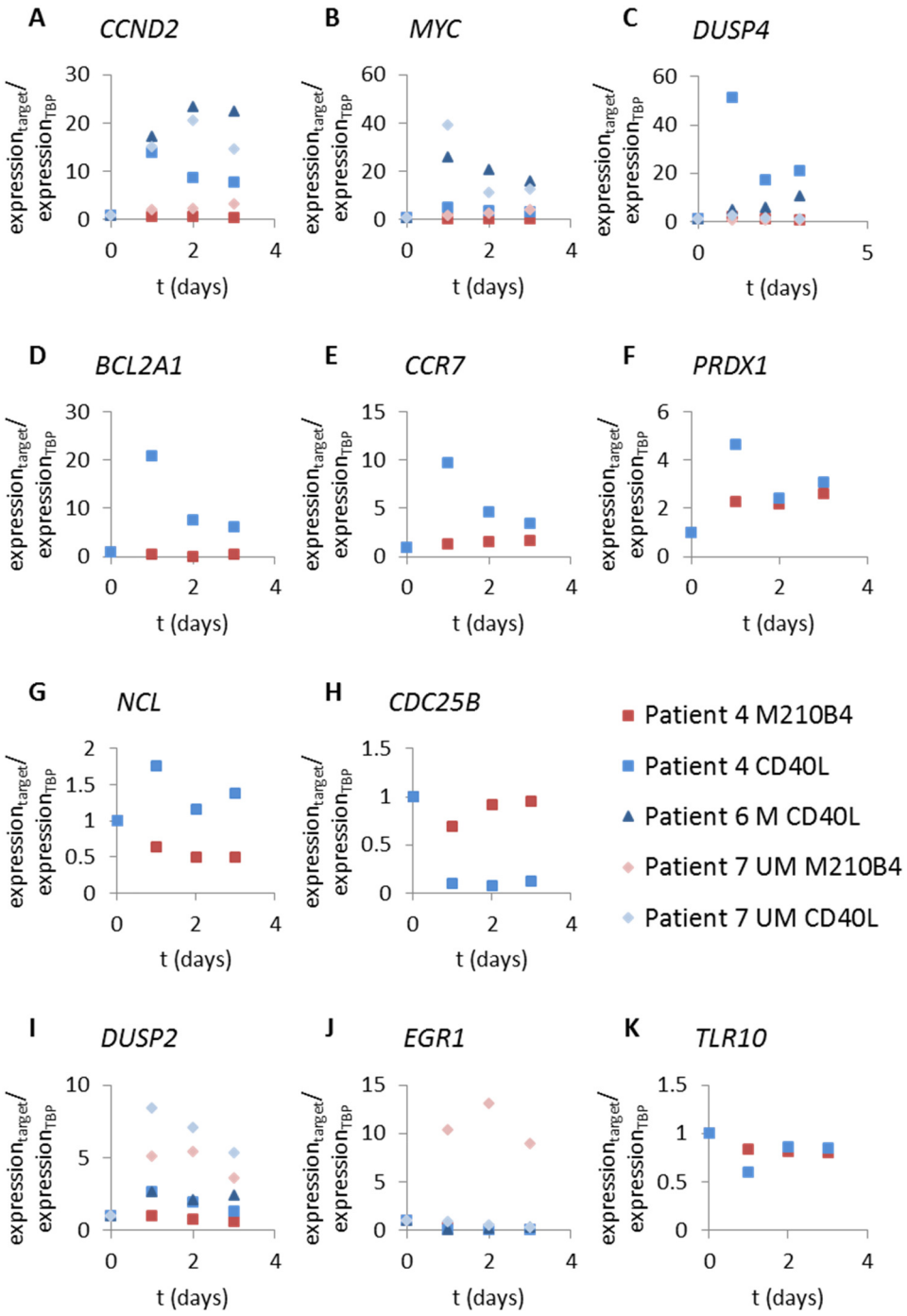

Figure 6.1 Influence of CD40L and M210B4 cells on gene expression in CLL cells.

CD40L and M210B4 cells were seeded into 6-well plates. The day after, CLL cells were added and co-cultured for up to three days. RNA was prepared and gene expression was analysed by RT-qPCR using the indicated primers. The results are shown normalised to *TBP* and expression in unstimulated cells (day 0). Cells from the same patient are depicted using the same symbol, M = mutated CLL, UM = unmutated CLL. Stimulation via CD40 increased the expression of *CCND2*, *MYC*, *DUSP4*, *BCL2A1*, *CCR7*, *PRDX1* and *NCL*, while expression of *CDC25B* was strongly decreased. *DUSP2* expression was enhanced in PBMCs co-cultured with either CD40L or M210B4 and *EGR1* was upregulated in one patient when cells were co-cultured with M210B4.

6.2 BCR stimulation and effects of Ibrutinib

6.2.1 Gene expression in CLL cells after BCR stimulation

Because CLL cells are especially dependent on BCR signalling, we next assessed the effect of BCR stimulation on the gene expression in patient cells. Further, half the cells were treated with Ibrutinib to evaluate how Ibrutinib influences gene expression. It was anticipated that Ibrutinib would block activation of most downstream target genes, as it is believed to inhibit the key BCR signalling pathways. Although the initial plan was to keep CLL cells in co-culture with M210B4 or CD40L cells, it was tested whether CLL cells would survive a few days in culture at high densities without feeder cells, as was described by Schulz et al. (Schulz et al., 2011). Indeed, CLL cells from most patients survived at cell densities of 5 x 10^6 PBMCs/ml for a few days in culture. Therefore, BCR stimulation experiments were done with cells cultured without feeder cells, to prevent activation of BCR-independent signalling pathways.

After BCR stimulation, CLL cells rapidly upregulated expression of *EGR1* and *DUSP2* within 30 min. *MYC* mRNA levels increased after 1 to 4 h, whereas *DUSP4* and *CCND2* were induced after 4 h. Expression of *BCL2A1*, *PRDX1*, *NCL*, *CDC25B* and *TLR10* was largely unaltered, while *PIM1* and *CXCR4* expression decreased. Changes in *CXCR5*, *CCR6* and *CCR7* expression levels were variable and patient-dependent. Induction or repression of all the genes tested were blocked when cells were pre-treated with 1 µM Ibrutinib for 2 h (Figure 6.2). Interestingly, genes induced by BCR stimulation were different from those induced by CD40L. *CCND2*, *MYC*, *DUSP4* and *BCL2A1* were, for example, induced a lot stronger by CD40 activation, whereas *CDC25B* was not downregulated by BCR activation. Both pathways seem to complement each other, explaining why both stimulation via the BCR and CD40L are required for B cell proliferation *in vivo*.

Figure 6.2 Effects of BCR stimulation and Ibrutinib on gene expression in CLL cells.
PBMCs were cultured in RPMI-1640 over night, treated with DMSO or Ibrutinib for 2 h and then stimulated with anti-IgM. RNA was prepared at indicated time points and gene expression was analysed by qPCR. Cells from the same patient are depicted using the same symbols. *EGR1* and *DUSP2* expression were strongly increased 30 min after BCR cross-linking. *MYC* expression peaked 1 to 4 h after cross-linking and *DUSP4* and *CCND2* were upregulated after 4 h. *PIM1* was transiently downregulated, while *CXCR4* expression was inhibited even 24 h after BCR activation.

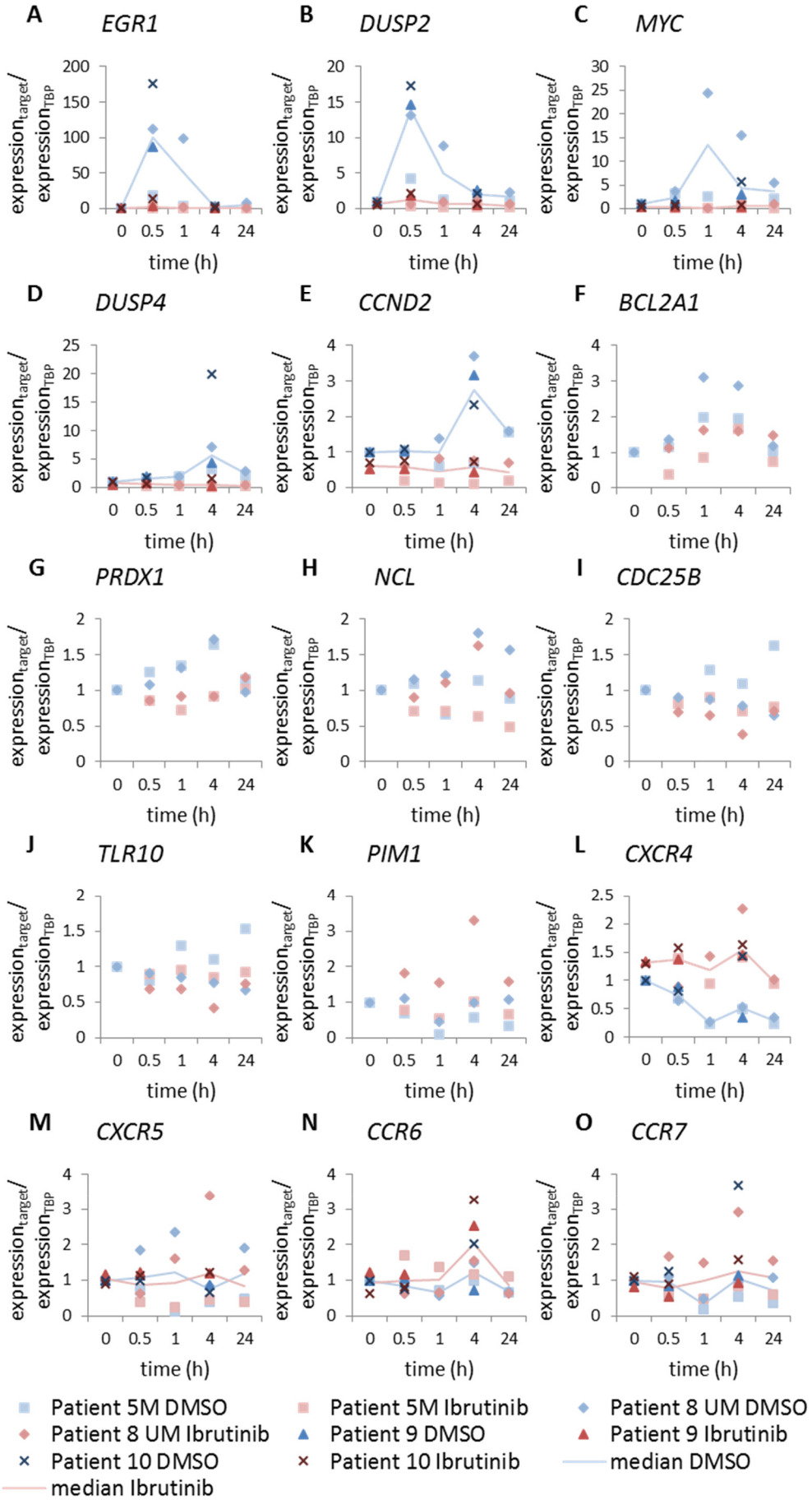
A
EGR1
B
DUSP2
C
MYC
D
DUSP4
E
CCND2
F
BCL2A1
G
PRDX1
H
NCL
I
CDC25B
J
TLR10
K
PIM1
L
CXCR4
M
CXCR5
N
CCR6
O
CCR7
expression target/ expression TBP
time (h)
0 0.5 1 4 24
Patient 5M DMSO
Patient 5M Ibrutinib
Patient 8 UM DMSO
Patient 8 UM Ibrutinib
Patient 9 DMSO
Patient 9 Ibrutinib
Patient 10 DMSO
Patient 10 Ibrutinib
median DMSO
median Ibrutinib

6.2.2 Effects of BCR stimulation and Ibrutinib treatment on global histone phosphorylation

Histone phosphorylation downstream of the BCR was of particular interest, as these PTMs are especially found at a large number of inducible genes and mediate their expression. Phosphorylation of H3S10 and H3S28 has been associated with induction of gene expression downstream of diverse growth factors and cytokines in response to activation of the ERK1/2, p38 MAPK or NFκB pathways (Duncan et al., 2006; Healy et al., 2012; Soloaga et al., 2003; Zippo et al., 2007). However, few studies so far concentrated on histone phosphorylation marks other than H3S10 and histone phosphorylation downstream of the BCR has, to our knowledge, never been studied before. Therefore, it was initially assessed which histone phosphorylation marks increase globally in CLL cells after activation of the BCR.

The phosphorylation of H3T3, T6, T11, S10 in conjunction with K9 acetylation, and H3.3S31 was analysed in anti-IgM-stimulated PBMCs from four different CLL patients. While H3T3p, H3T6p, H3T11p and H3.3S31p were variable and changes were not obviously associated with BCR stimulation, H3K9acS10p was induced in all four patients after 30 min of BCR activation when cells were pre-treated with DMSO and Ibrutinib clearly inhibited this induction (Figure 6.3). Different patients showed different levels of H3K9acS10p induction. These differences were most likely due to differences in the amount of pre-activation of the cells. CLL is a very heterogeneous disease and different patients show different percentages of activated, proliferating cells in their blood and also different strengths of chronic signalling. As a consequence, strongly activated or strongly chronically signalling cells express less surface IgM and can therefore hardly be activated further, which would result in weak induction of H3K9acS10p. Weakly chronically signalling cells are much more susceptible to IgM cross-linking, which would correlate with a stronger increase in H3K9acS10p.

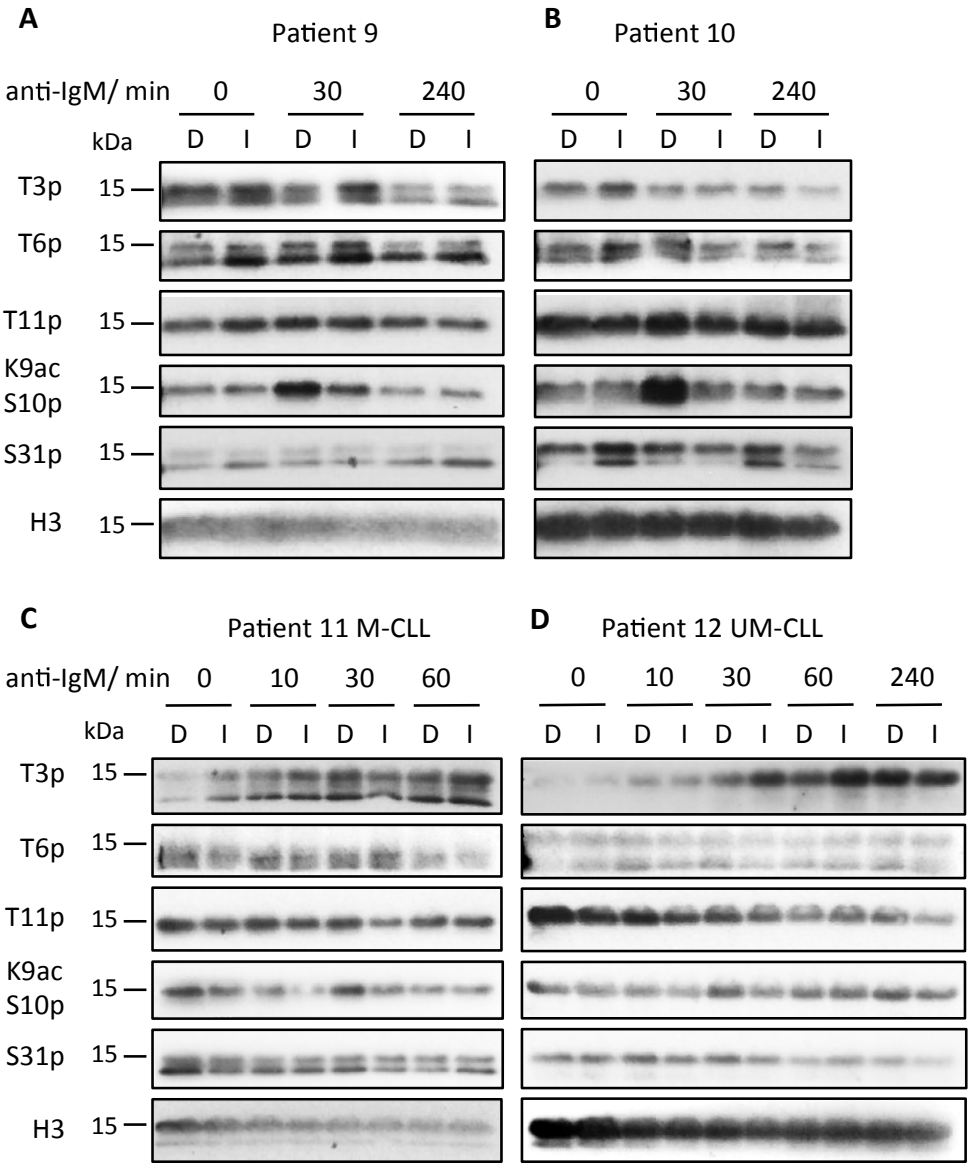

Figure 6.3 Effects of BCR stimulation and Ibrutinib on histone phosphorylation in CLL cells.
PBMCs were cultured in RPMI-1640 over night, treated with DMSO (D) or Ibrutinib (I) for 2 h and then stimulated with anti-IgM. The different histone H3 phospho-modifications were analysed by western blot. H3K9acS10p was induced in all patients after 30 min anti-IgM stimulation. This was inhibited, when the cells were pre-treated with Ibrutinib.

6.2.3 Effects of BCR stimulation and Ibrutinib treatment on gene-specific histone phosphorylation

Although most of the histone H3 phospho-modifications did not change at the global level, they might be induced or repressed locally at distinct promoter or enhancer regions. Therefore, the presence of these marks at BCR regulated genes was determined by ChIP. Initially, presence of the different marks was assessed both in the 5' and the 3' regions of the genes, because for most of these marks, their distribution along active genes was unknown and H3.3S31p has been shown to be enriched along the gene body of the active murine *Tnf* gene (Thorne et al., 2012). Therefore, some other phosphorylation marks might be found along the gene body or at the 3' end. The genes analysed were *EGR1*, *DUSP2*, *MYC*, *DUSP4* and *CCND2*, as these were induced after BCR stimulation.

At the *EGR1* gene, histone H3 occupancy was lower in DMSO-treated compared to Ibrutinib-treated cells 30 min to 1 h after anti-IgM stimulation at the promoter (*EGR1* -0.1) and 30 min after anti-IgM stimulation also in the 3' region (*EGR1* +3.8). In the 3' region, histone H3 occupancy increased in DMSO-treated cells after 4 h of stimulation, which might reflect a reinforcement of gene silencing and might inhibit aberrant transcription (Figure 6.4). An increase in H3K9acS10p was seen in DMSO-treated cells at 30 min anti-IgM-stimulation in the promoter region (*EGR1* -0.85, *EGR1* -0.1), which was inhibited in Ibrutinib-treated cells. However, after 1 h anti-IgM treatment, both Ibrutinib- and DMSO-treated cells showed comparable enrichment of H3K9acS10p in the *EGR1* -0.1 region (Figure 6.5). Induction of both H3T6p and H3T11p mirrored the induction kinetics of the *EGR1* gene. They were elevated along the whole gene after 30 min of anti-IgM stimulation only in cells pre-treated with DMSO and after 1 h, both marks had decreased back to baseline (Figure 6.6, Figure 6.7). No induction of H3T6p and H3T11p was seen in Ibrutinib-treated cells.

In the *DUSP2* +2.4 region, H3 occupancy was lower in DMSO- than in Ibrutinib-treated cells after 30 min of anti-IgM stimulation but no difference was seen in the 5' region (*DUSP2* -0.3) (Figure 6.8 A). H3K9acS10p was very variable between patients but mostly, no significant difference between DMSO- and Ibrutinib-treated cells was seen (Figure 6.8 B). Similar to the *EGR1* gene, H3T6p and H3T11p matched the induction kinetics of the *DUSP2* gene. They were increased in the *DUSP2* +2.4 region after 30 min of anti-IgM stimulation in DMSO- but not Ibrutinib-treated cells and decreased to baseline after 1 h of BCR activation (Figure 6.9).

At the other three genes tested, H3 occupancy was not decreased in DMSO-treated compared to Ibrutinib-treated cells (Figure 6.10 A, Figure 6.12 A, Figure 6.14 A). At the *DUSP4* gene, there was even a tendency towards higher H3 occupancy in DMSO-treated cells after 4 h of BCR activation (Figure 6.12 A), which is the time point, when expression of the *DUSP4* gene was seen (Figure 6.2 D). At the *MYC* gene, H3K9acS10p increased in the promoter region after 1 h of anti-IgM treatment in DMSO-treated cells (Figure 6.10 B), which matched the induction of *MYC* expression (Figure 6.2 C). At the *DUSP4* and the *CCND2* promoters, H3K9acS10p was not significantly increased at any time point. At the 3' ends of both genes, the variation seen seemed to be background precipitation, as the precipitated DNA was amplified by qPCR with Ct values around the background level (Figure 6.12 B, Figure 6.14 B). Furthermore, no BCR signalling-induced increase in H3T6p or H3T11p was seen at the *MYC*, *DUSP4* or *CCND2* genes (Figure 6.11, Figure 6.13, Figure 6.15). No enrichment of H3T3p, H3.3S31p or IKKα was detected in any of the regions tested.

In conclusion, H3 occupancy decreased upon activation at early genes (*EGR1*, *DUSP2*), but not at later activated genes. This possibly reflects the rate of transcription, which must be especially high at the *EGR1* gene, as it is induced 100 fold on average, and lower at later activated genes, like *MYC*, *DUSP4* and *CCND2*. Higher transcription rates result in enhanced removal of nucleosomes to allow for the passage of POL II. Although H3K9acS10p increased globally after BCR crosslinking, this mark was generally very variable in the regions analysed and its induction was not completely blocked by Ibrutinib. Further, induction of this mark only partially matched the induction kinetics of the studied genes. However, other genes might be more dependent on H3K9acS10p for their expression and it will be interesting to identify such genes in future studies. The most interesting marks to study further were H3T6p and H3T11p. They were specifically induced at the early genes *EGR1* and *DUSP2* with kinetics mirroring the mRNA expression. Further, their induction was completely blocked when cells were pre-treated with Ibrutinib. Thus, H3T6p and H3T11p might be important for expression of *EGR1* and *DUSP2* and possibly other genes.

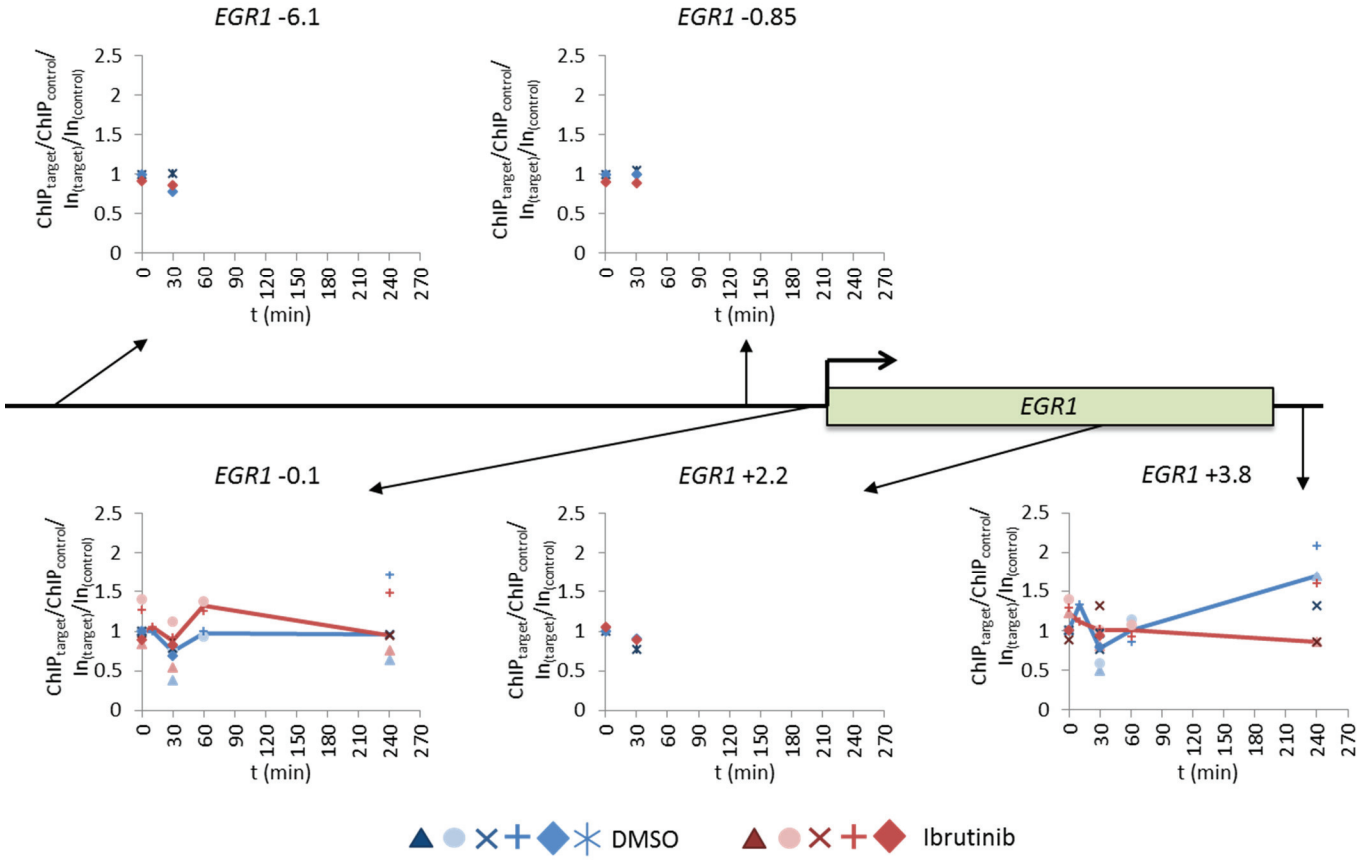

Figure 6.4 Effects of BCR stimulation and Ibrutinib on H3 occupancy at the *EGR1* gene.

PBMCs were cultured in RPMI-1640 over night, treated with DMSO or Ibrutinib for 2 h and then stimulated with anti-IgM. Histone H3 occupancy at different regions along the *EGR1* gene was analysed by ChIP at different time points after anti-IgM stimulation. ChIP results were normalised to input, the CTCF1 control region and DMSO-treated cells at 0 h. The same symbols are used for cells from the same patients and for n ≥ 3 the median is displayed as a line. Especially in the *EGR1* promoter, H3 occupancy is reduced in DMSO- compared to Ibrutinib-treated cells after BCR cross-linking.

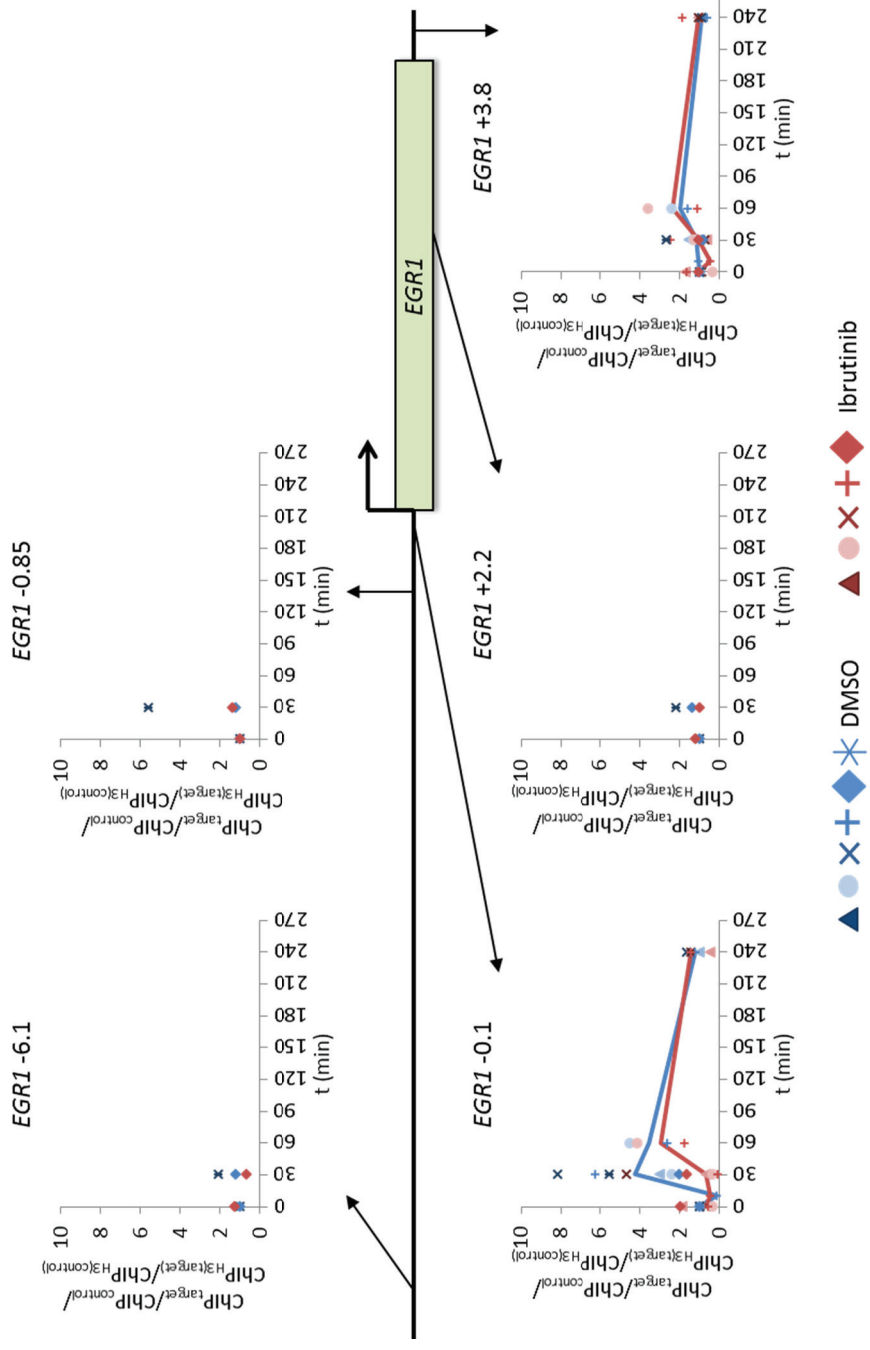

Figure 6.5 Effects of BCR stimulation and Ibrutinib on H3K9acS10p along the *EGR1* gene.
PBMCs were cultured in RPMI-1640 over night, treated with DMSO or Ibrutinib for 2 h and then stimulated with anti-IgM. Histone H3K9acS10p at different regions along the *EGR1* gene was analysed by ChIP at different time points after anti-IgM stimulation. ChIP results were normalised to H3, the CTCF1 control region and DMSO-treated cells at 0 h. The same symbols are used for cells from the same patients and for n ≥ 3 the median is displayed as a line. H3K9acS10p increased in the *EGR1* promoter region (*EGR1* -0.85, *EGR1* -0.1) in DMSO-treated cells 30 min after BCR cross-linking, but this was not completely inhibited by Ibrutinib.

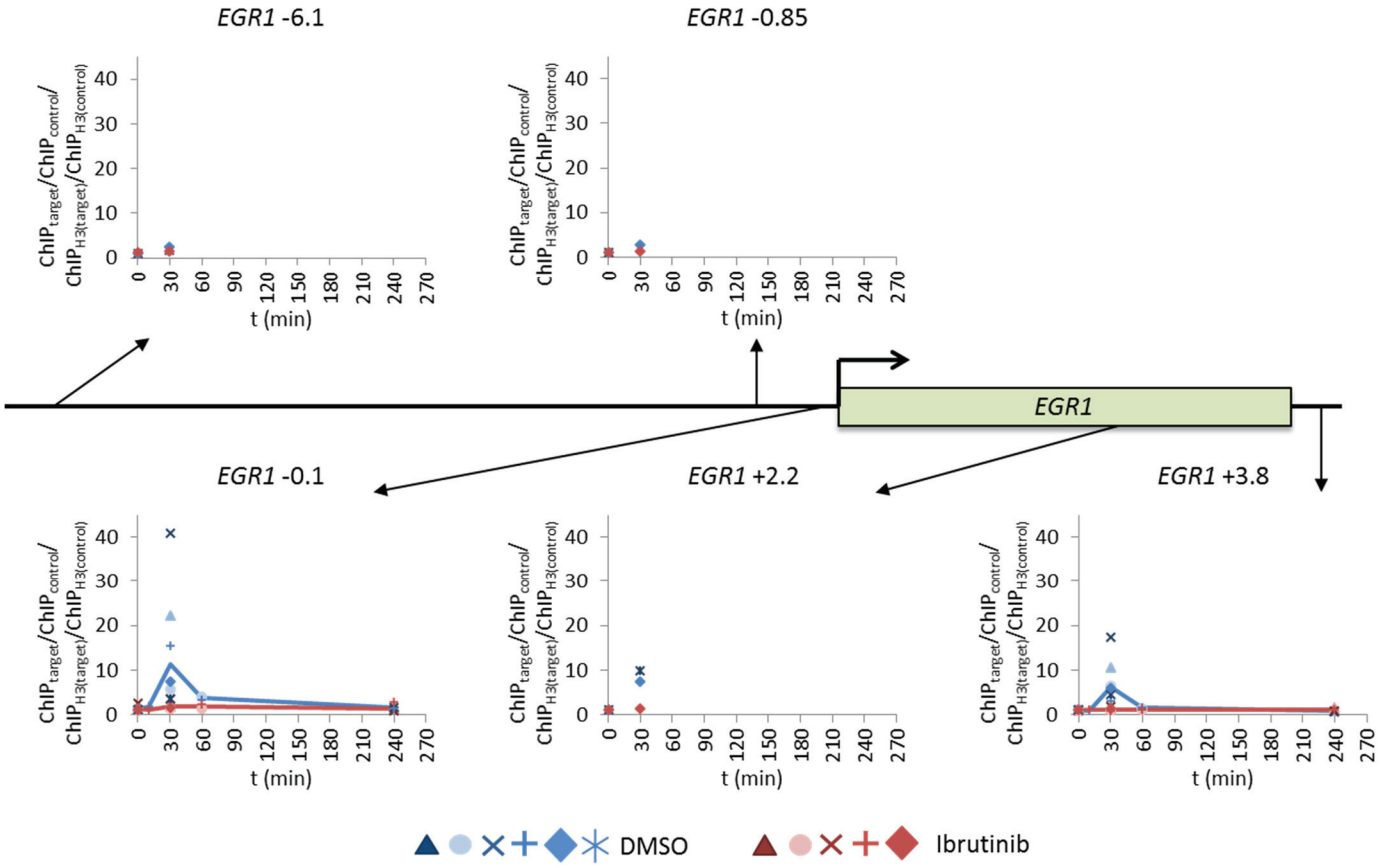

Figure 6.6 Analysis of H3T6p along the *EGR1* gene after BCR cross-linking without or with Ibrutinib.

PBMCs were cultured in RPMI-1640 over night, treated with DMSO or Ibrutinib for 2 h and then stimulated with anti-IgM. Histone H3T6p at different regions along the *EGR1* gene was analysed by ChIP at different time points after anti-IgM stimulation. ChIP results were normalised to H3, the CTCF1 control region and DMSO-treated cells at 0 h. The same symbols are used for cells from the same patients and for n ≥ 3 the median is displayed as a line. 30 min after anti-IgM treatment, H3T6p is increased along the length of the *EGR1* gene and this increase is blocked by Ibrutinib.

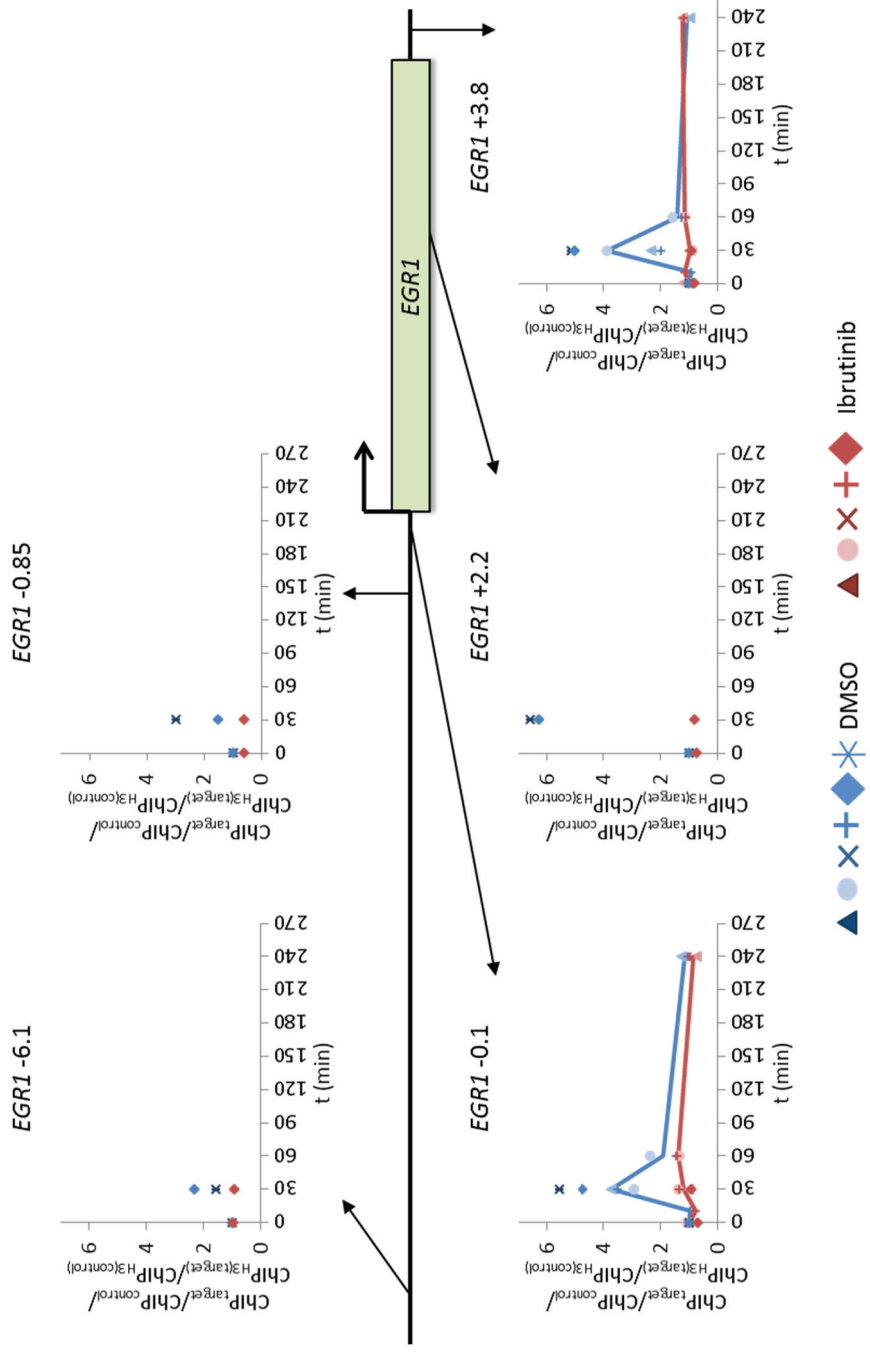

Figure 6.7 Effects of BCR cross-linking and Ibrutinib on H3T11p along the *EGR1* gene.
PBMCs were cultured in RPMI-1640 over night, treated with DMSO or Ibrutinib for 2 h and then stimulated with anti-IgM. Histone H3T11p at different regions along the *EGR1* gene was analysed by ChIP at different time points after anti-IgM stimulation. ChIP results were normalised to H3, the CTCF1 control region and DMSO-treated cells at 0 h. The same symbols are used for cells from the same patients and for n ≥ 3 the median is displayed as a line. H3T11p is increased along the whole EGR1 gene 30 min after BCR cross-linking in DMSO-, but not in Ibrutinib-treated cells.

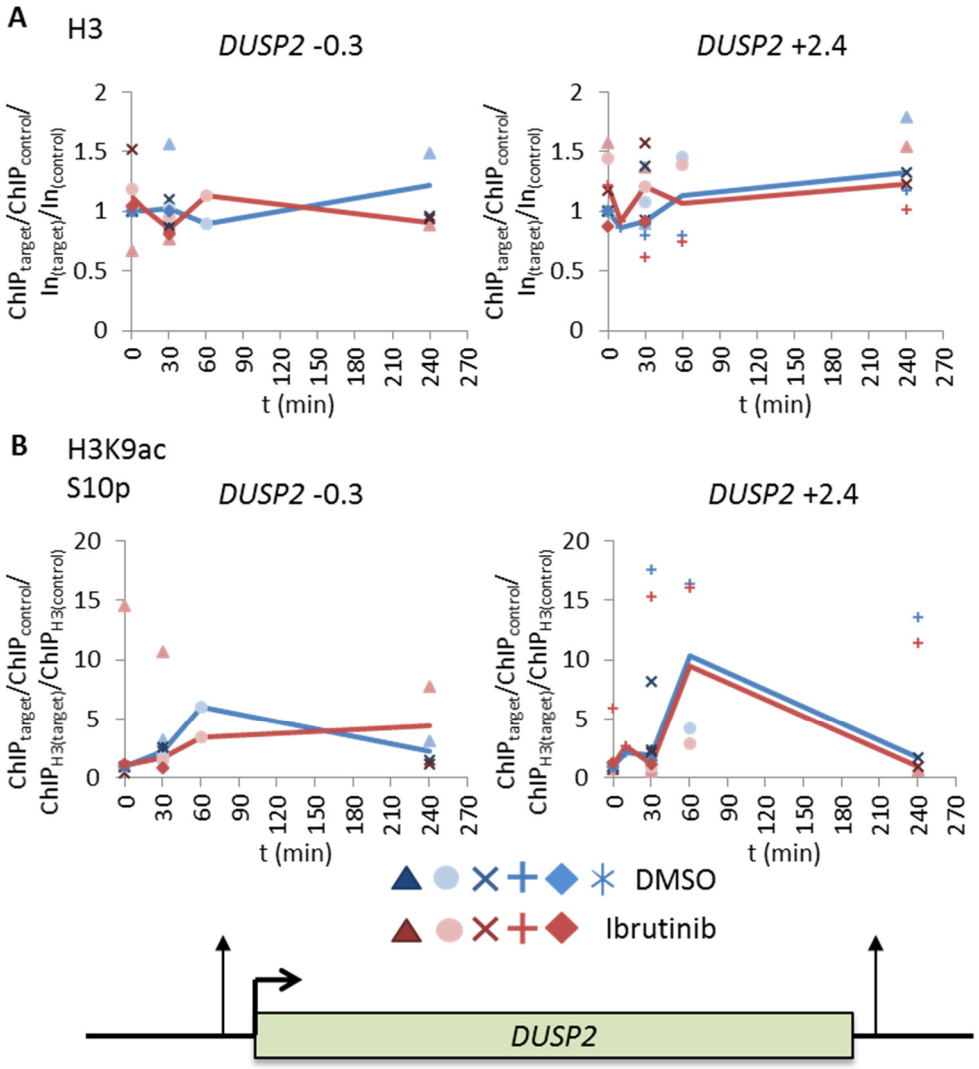

Figure 6.8 Analysis of H3 and H3K9acS10p at the *DUSP2* gene after BCR cross-linking without or with Ibrutinib.
PBMCs were cultured in RPMI-1640 over night, treated with DMSO or Ibrutinib for 2 h and then stimulated with anti-IgM. Histone H3 (**A**) or H3K9acS10p (**B**) at different regions along the *DUSP2* gene were analysed by ChIP at different time points after anti-IgM stimulation. ChIP results were normalised to input (**A**) or H3 (**B**), the CTCF1 control region and DMSO-treated cells at 0 h. The same symbols are used for cells from the same patients and the median is displayed as a line. H3 occupancy in the DUSP2 +2.4 region was lower in DMSO-treated cells than in Ibrutinib-treated cells at 30 min anti-IgM stimulation. H3K9acS10p was induced in this region and the induction was similar in Ibrutinib- and DMSO-treated cells.

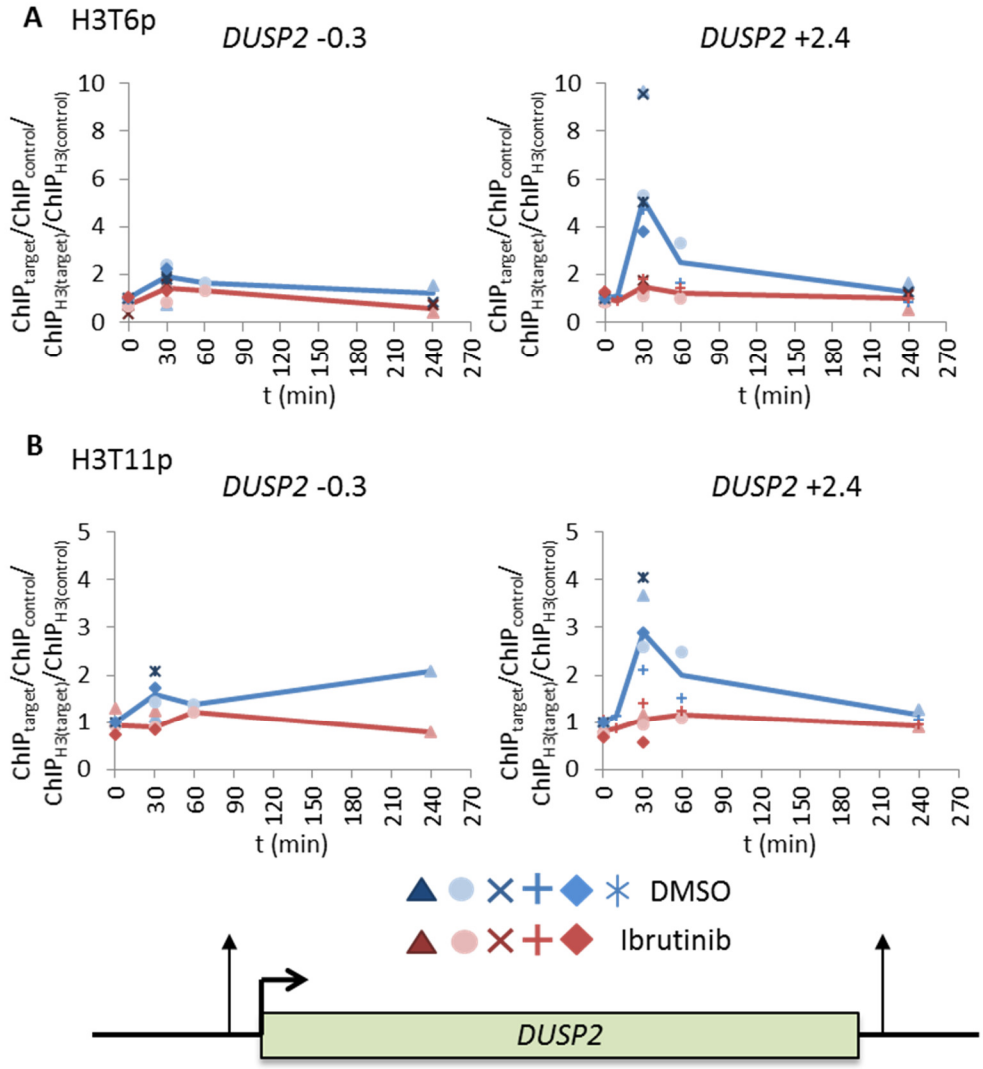

Figure 6.9 Effects of BCR cross-linking and Ibrutinib on H3T6p and H3T11p at the *DUSP2* gene.

PBMCs were cultured in RPMI-1640 over night, treated with DMSO or Ibrutinib for 2 h and then stimulated with anti-IgM. Histone H3T6p (**A**) or H3T11p (**B**) at different regions along the *DUSP2* gene were analysed by ChIP at different time points after anti-IgM stimulation. ChIP results were normalised to H3, the CTCF1 control region and DMSO-treated cells at 0 h. The same symbols are used for cells from the same patients and the median is displayed as a line. Both H3T6p and H3T11p increased in the DUSP2 +2.4 region after BCR cross-linking and this induction was blocked by Ibrutinib.

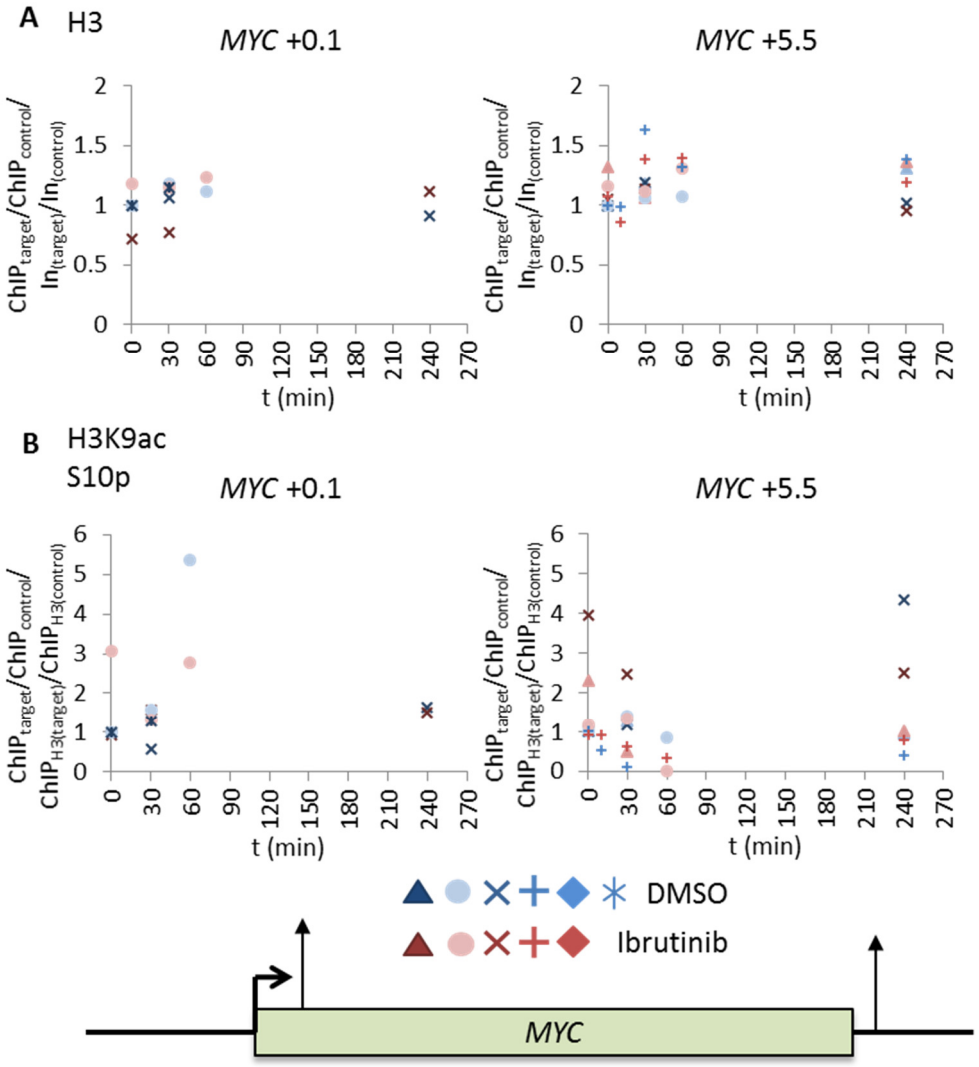

Figure 6.10 Influence of BCR cross-linking and Ibrutinib on H3 and H3K9acS10p occupancy of the *MYC* gene.
PBMCs were cultured in RPMI-1640 over night, treated with DMSO or Ibrutinib for 2 h and then stimulated with anti-IgM. Histone H3 (**A**) or H3K9acS10p (**B**) at different regions along the *MYC* gene were analysed by ChIP at different time points after anti-IgM stimulation. ChIP results were normalised to input (**A**) or H3 (**B**), the CTCF1 control region and DMSO-treated cells at 0 h. The same symbols are used for cells from the same patients. No differences in H3 occupancy were seen at the 5' or 3' end of the MYC gene between Ibrutinib and DMSO-treated cells. In the one patient tested, H3K9acS10p was increased in the MYC promoter region 1 h after anti-IgM stimulation and Ibrutinib partially inhibited this effect.

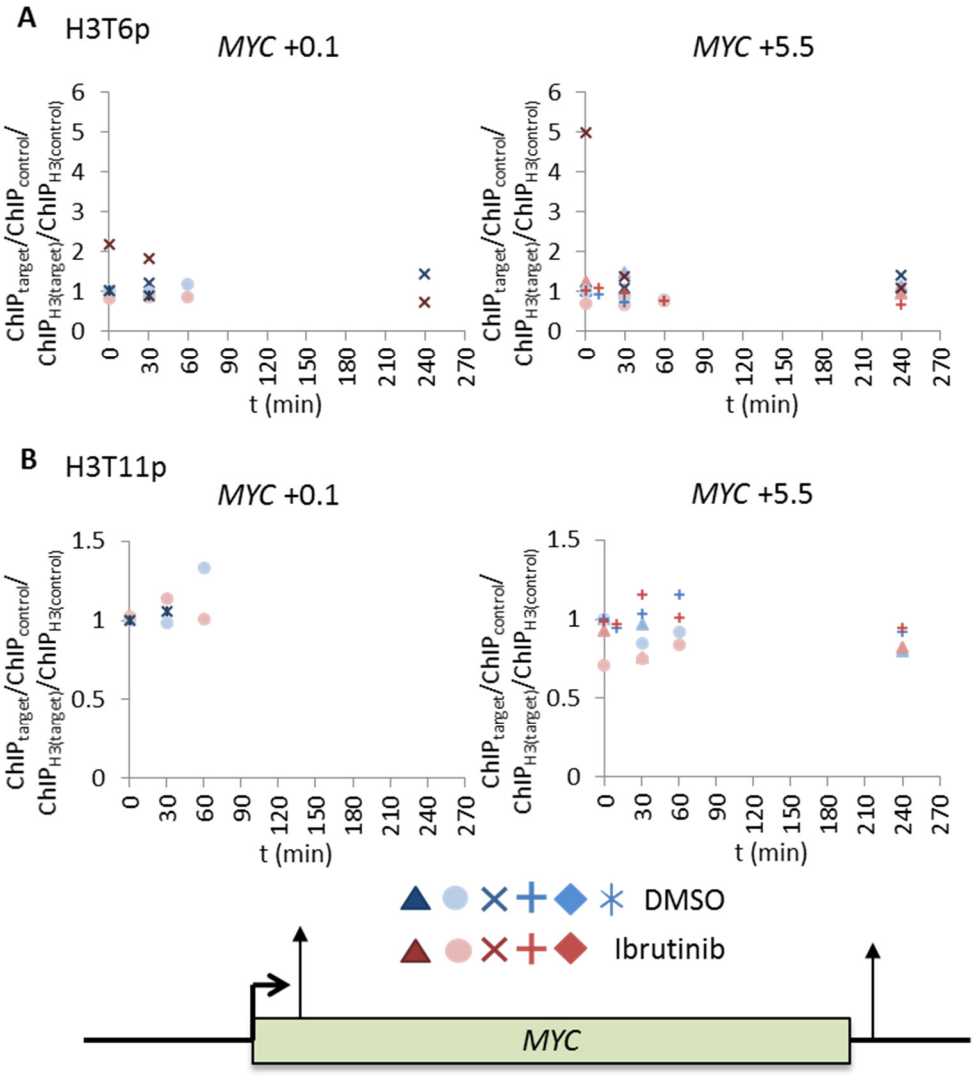

Figure 6.11 Effects of BCR cross-linking and Ibrutinib on H3T6p and H3T11p at the *MYC* gene.
PBMCs were cultured in RPMI-1640 over night, treated with DMSO or Ibrutinib for 2 h and then stimulated with anti-IgM. Histone H3T6p (**A**) or H3T11p (**B**) at different regions along the *MYC* gene were analysed by ChIP at different time points after anti-IgM stimulation. ChIP results were normalised to H3, the CTCF1 control region and DMSO-treated cells at 0 h. The same symbols are used for cells from the same patients. No induction of H3T6p or H3T11p was seen after BCR cross-linking.

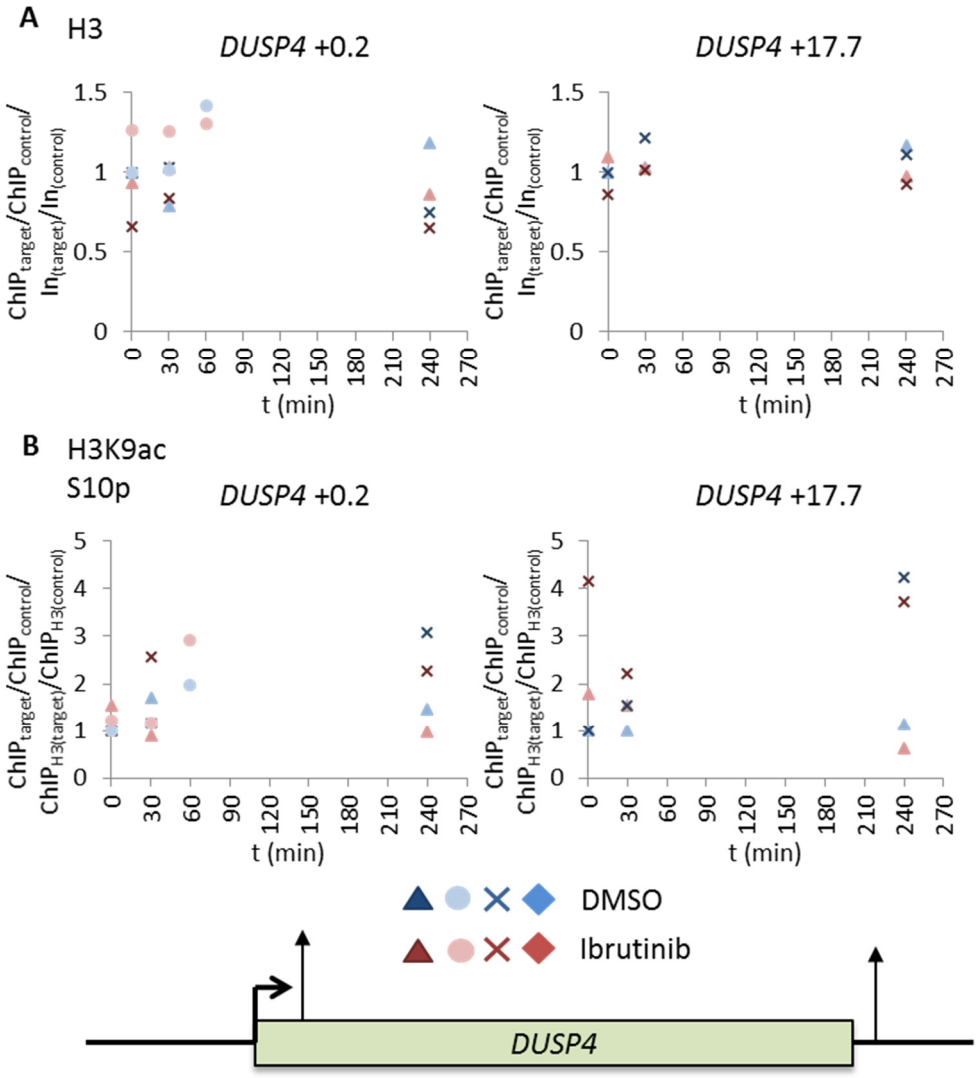

Figure 6.12 Analysis of H3 and H3K9acS10p occupancy at the *DUSP4* gene after BCR cross-linking without and with Ibutinib.
PBMCs were cultured in RPMI-1640 over night, treated with DMSO or Ibrutinib for 2 h and then stimulated with anti-IgM. Histone H3 (**A**) or H3K9acS10p (**B**) at different regions along the *DUSP4* gene were analysed by ChIP at different time points after anti-IgM stimulation. ChIP results were normalised to input (**A**) or H3 (**B**), the CTCF1 control region and DMSO-treated cells at 0 h. The same symbols are used for cells from the same patients. H3 occupancy was not different between DMSO- or Ibrutinib-pretreated cells and H3K9acS10p was not induced at the late activated *DUSP4* gene.

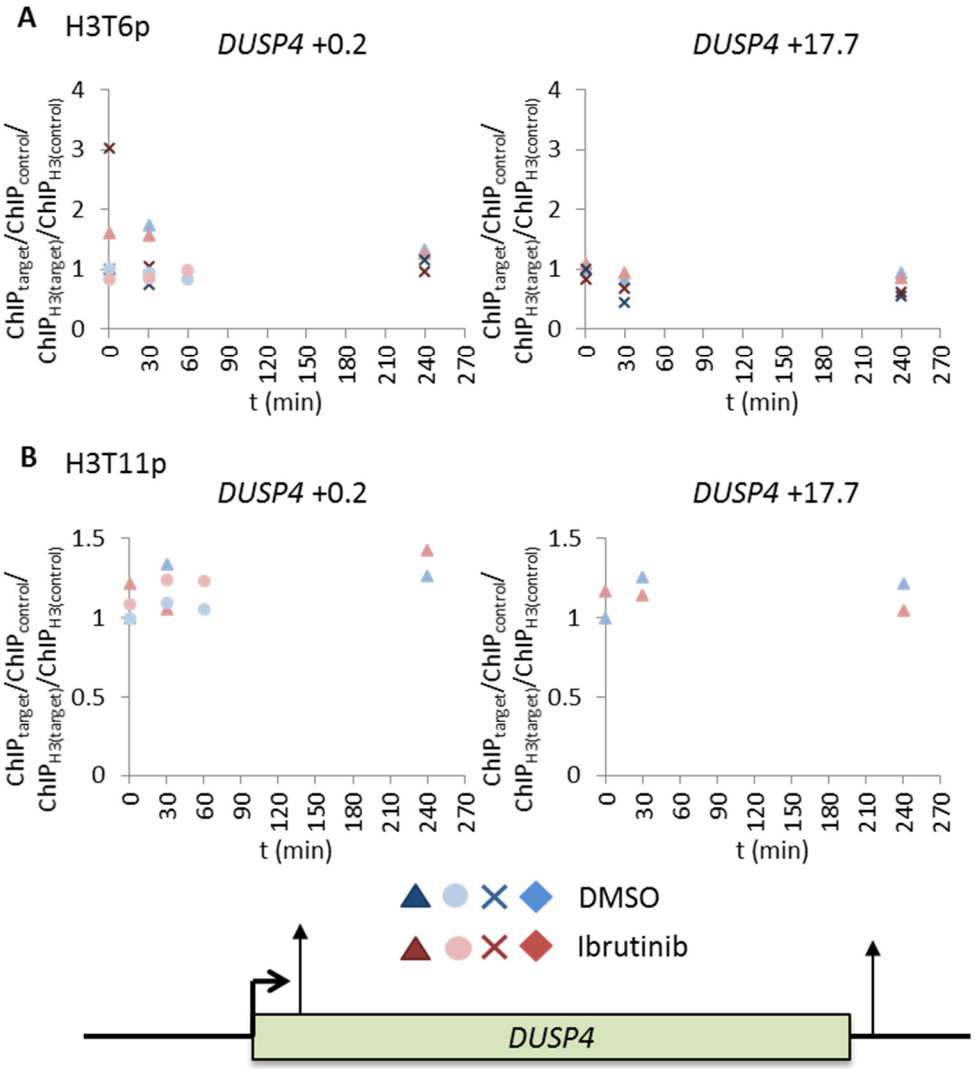

Figure 6.13 Effects of BCR cross-linking and Ibrutinib on H3T6p and H3T11p at the *DUSP4* gene.
PBMCs were cultured in RPMI-1640 over night, treated with DMSO or Ibrutinib for 2 h and then stimulated with anti-IgM. Histone H3T6p (**A**) or H3T11p (**B**) at different regions along the *DUSP4* gene were analysed by ChIP at different time points after anti-IgM stimulation. ChIP results were normalised to H3, the CTCF1 control region and DMSO-treated cells at 0 h. The same symbols are used for cells from the same patients. No induction of H3T6p or H3T11p was observed at any of the time points.

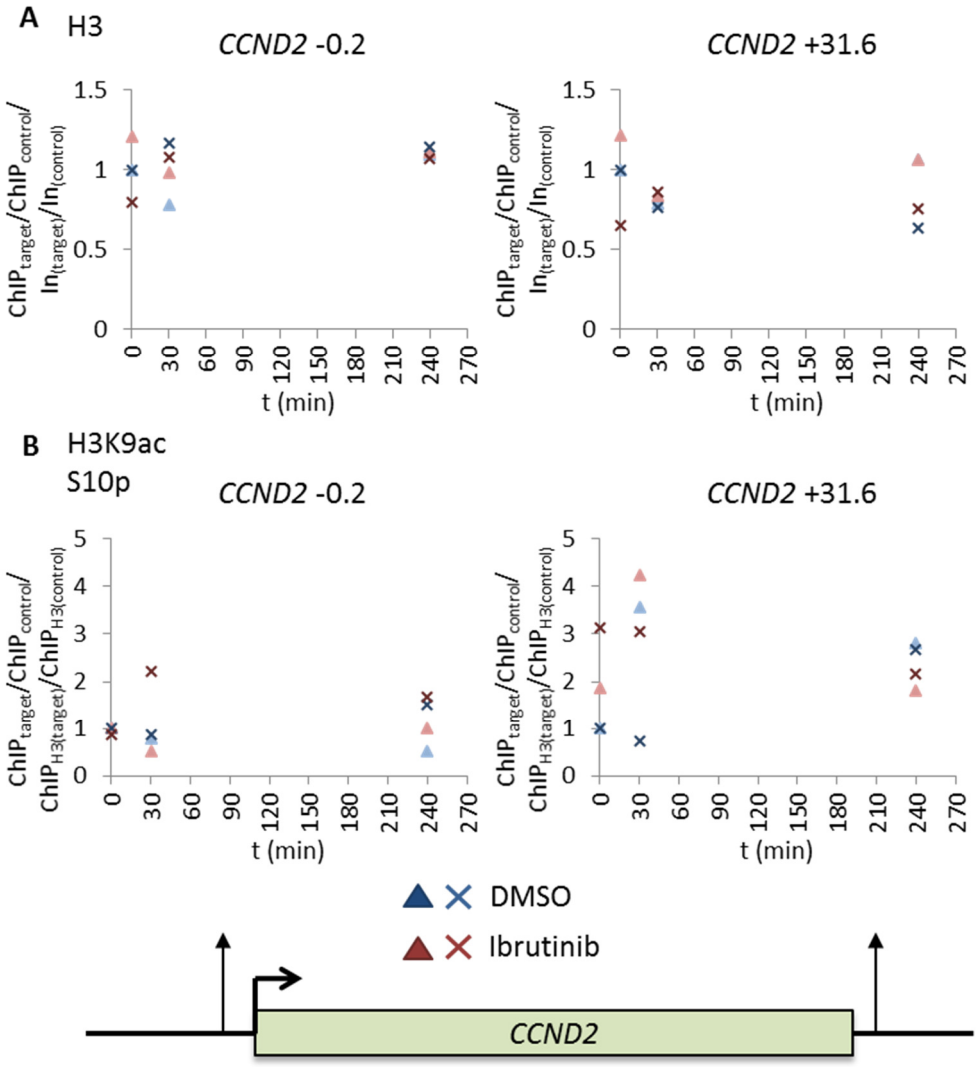

Figure 6.14 Influence of BCR cross-linking and Ibrutinib-treatment on H3 and H3K9acS10p at the *CCND2* gene.
PBMCs were cultured in RPMI-1640 over night, treated with DMSO or Ibrutinib for 2 h and then stimulated with anti-IgM. Histone H3 (**A**) or H3K9acS10p (**B**) at different regions along the *CCND2* gene were analysed by ChIP at different time points after anti-IgM stimulation. ChIP results were normalised to input (**A**) or H3 (**B**), the CTCF1 control region and DMSO-treated cells at 0 h. The same symbols are used for cells from the same patients. There was no difference in H3 occupancy at the *CCND2* gene between Ibrutinib- and DMSO-pretreated cells up to 4 h after BCR cross-linking. Further, H3K9acS10p was not induced.

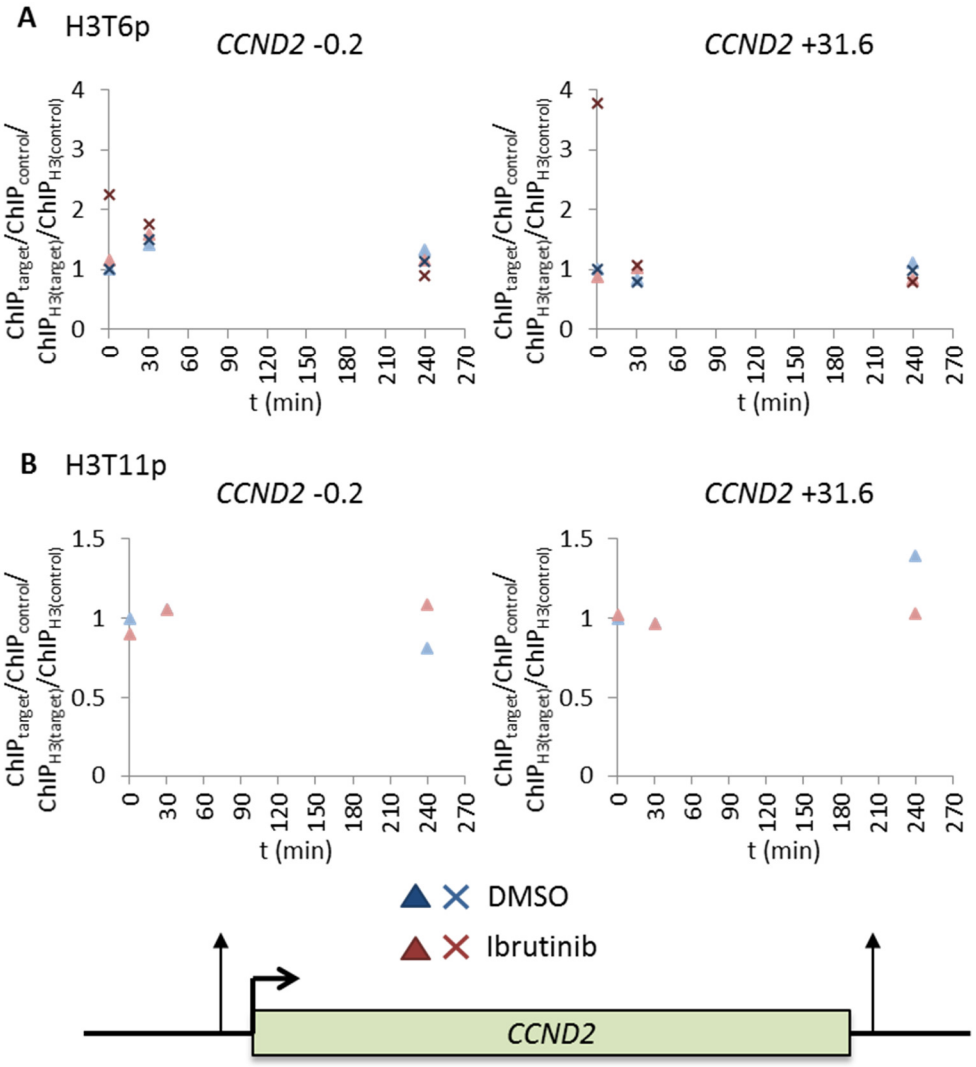

Figure 6.15 Analysis of H3T6p and H3T11p at the *CCND2* gene in response to BCR cross-linking and Ibrutinib treatment.
PBMCs were cultured in RPMI-1640 over night, treated with DMSO or Ibrutinib for 2 h and then stimulated with anti-IgM. Histone H3T6p (**A**) or H3T11p (**B**) at different regions along the *CCND2* gene were analysed by ChIP at different time points after anti-IgM stimulation. ChIP results were normalised to H3, the CTCF1 control region and DMSO-treated cells at 0 h. The same symbols are used for cells from the same patients. No induction of H3T6p or H3T11p was detected after BCR cross-linking.

6.2.4 Effects of BCR stimulation and Ibrutinib treatment on POL II

Phosphorylation of histone H3T6 and H3T11 has been shown to induce transcription at AR-dependent genes and H3S10p stimulates POL II S2 phosphorylation and transcriptional elongation. Therefore, the effects of BCR stimulation and Ibrutinib treatment on POL II and POL II S2p occupancy at the induced genes was analysed next. It was anticipated that BCR stimulation might increase recruitment of POL II, reduce pausing and increase elongating POL II, while Ibrutinib treatment would block these effects.

Generally, the effects of BCR stimulation on POL II recruitment were variable between patients. One patient (Pat 15) showed a strong increase in POL II occupancy, another patient (Pat 34) showed a moderate increase and a third patient (Pat 25) displayed hardly any further POL II recruitment upon BCR stimulation (Figure 6.16 blue bars). This probably reflects the differing basal activation of BCR signalling and possibly also different levels of activation of gene expression. However, no matter by how much POL II increased along the *EGR1*, *DUSP2*, *MYC* or *DUSP4* genes, Ibrutinib did not strongly affect POL II levels (Figure 6.16, compare blue bars (DMSO) to red bars (Ibrutinib)).

Similarly, POL II S2p induction was inhibited in patient 34 at the *EGR1* gene but was not completely blocked, as would have been expected because of the complete block in expression of *EGR1*. Further, POL II S2p was increased in patient 25 at the *EGR1* and *DUSP2* genes and the *MYC* promoter after 30 min of anti-IgM treatment, which might represent paused or stalled POL II. At the *DUSP4* gene, no increase in POL II S2p was seen compared to unstimulated, DMSO-treated cells, which was expected, as the gene was only induced at later time points (Figure 6.17).

Thus, although Ibrutinib blocks gene expression downstream of the BCR, it does not completely inhibit induction of transcription and elongation, but might instead inhibit processive elongation, release of stalled POL II, processing of the transcript or proper termination, so that some primary transcripts might be produced, which do, however, never develop into mature mRNAs and were therefore not detected by our RT-qPCR analysis.

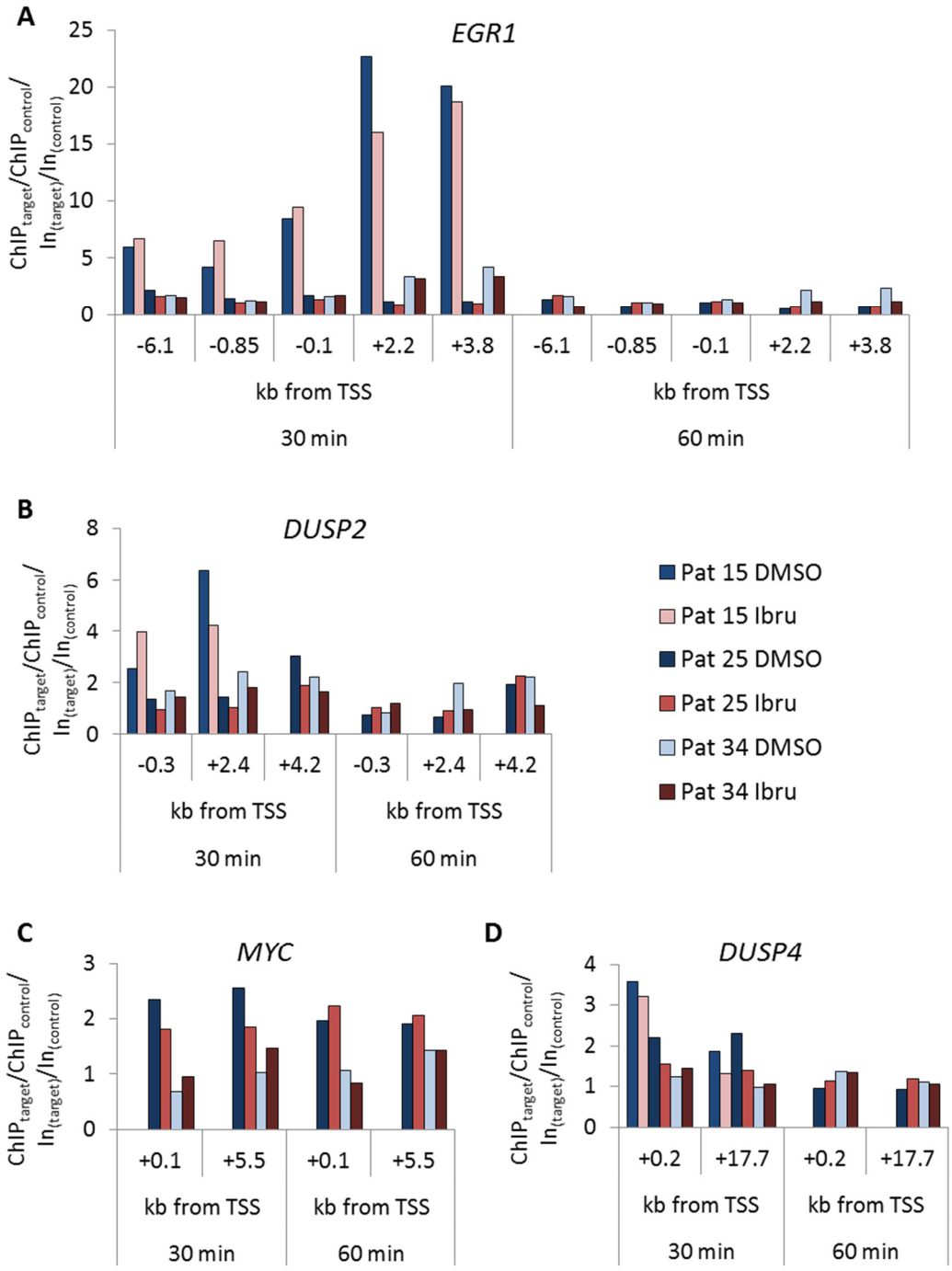

Figure 6.16 Assessment of POL II occupancy at different genes after BCR cross-linking without and with Ibrutinib.
PBMCs were cultured in RPMI-1640 over night, treated with DMSO or Ibrutinib for 2 h and then stimulated with anti-IgM. POL II occupancy at different regions along the *EGR1* (**A**), *DUSP2* (**B**), *MYC* (**C**) and *DUSP4* (**D**) genes was analysed by ChIP. Results were normalised to input, the CTCF1 and CTCF3 control regions and DMSO-treated cells at 0 h. DMSO-treated cells are depicted in blue, Ibrutinib-treated cells in red. Samples from the same patient are shown next to each other. For patient 15, not all time points and regions were analysed. It could be shown that Ibrutinib treatment did not strongly affect POL II recruitment and occupancy at the *EGR1*, *DUSP2*, *MYC* and *DUSP4* genes after BCR cross-linking.

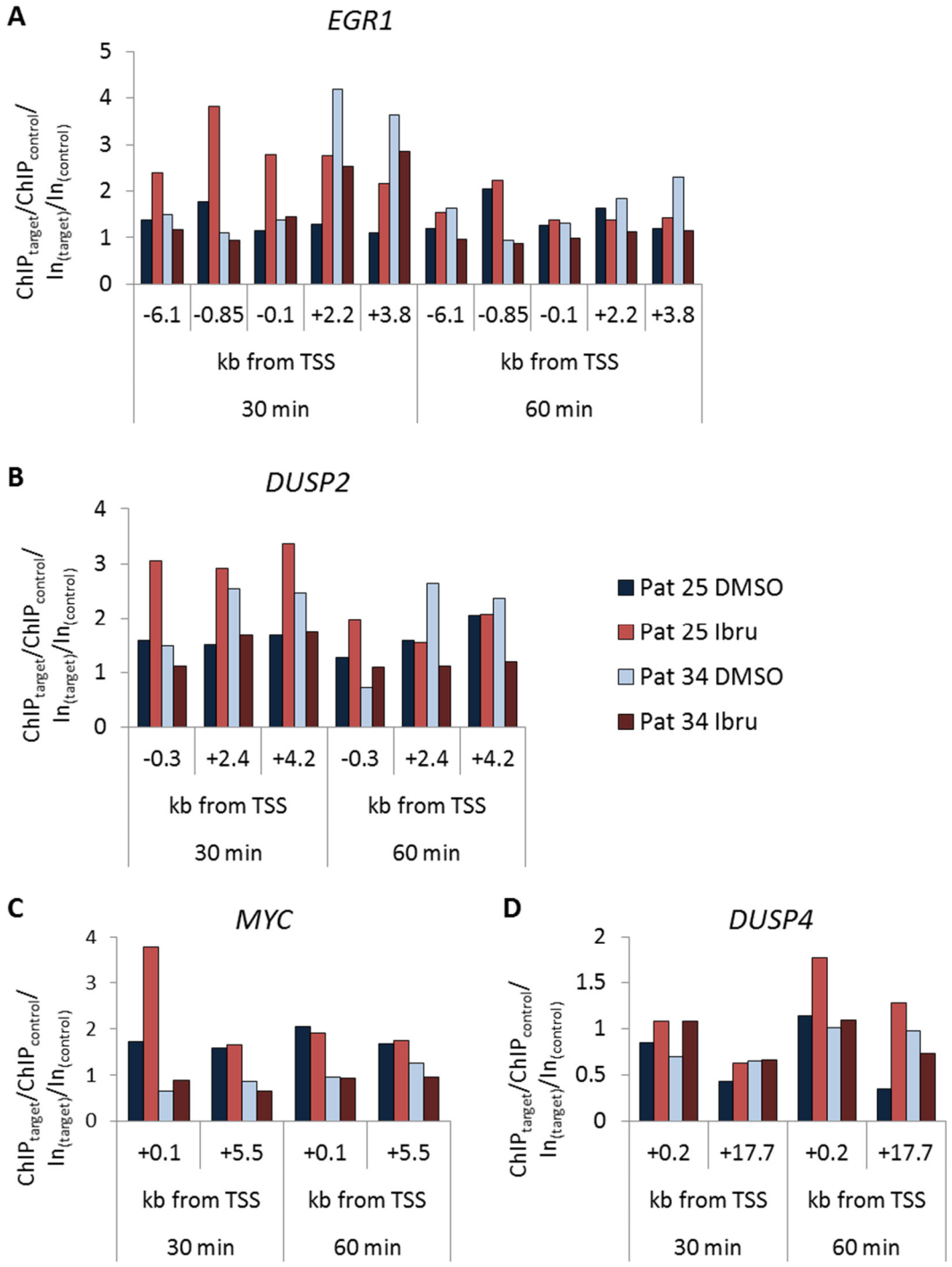

Figure 6.17 Effects of BCR cross-linking and Ibrutinib on the presence of POL II S2p at different genes.

PBMCs were cultured in RPMI-1640 over night, treated with DMSO or Ibrutinib for 2 h and then stimulated with anti-IgM. POL II S2p occupancy at different regions along the *EGR1* (**A**), *DUSP2* (**B**), *MYC* (**C**) and *DUSP4* (**D**) genes were analysed by ChIP. Results were normalised to input, the CTCF1 and CTCF3 control regions and DMSO-treated cells at 0 h. DMSO-treated cells are depicted in blue, Ibrutinib-treated cells in red. Samples from the same patient are shown next to each other. Surprisingly, Ibrutinib only partially decreased POL II S2p along the *EGR1* and *DUSP2* genes after BCR cross-linking.

6.2.5 Effects of BCR stimulation and Ibrutinib on H3 methylation and acetylation marks and the incorporation of H2A.Z

It has so far been shown that Ibrutinib can inhibit the phosphorylation of certain histone H3 residues downstream of the BCR and that this correlates with gene expression. Because histone phosphorylation marks are mostly unstable and rapidly changing marks, it would be difficult to analyse them in patient samples or to use them as predictors of drug response or resistance in clinical trials. Therefore, we were also interested in the effect of Ibrutinib on more stable chromatin modifications, like histone methylation, acetylation or the use of histone variants. These alterations in the chromatin structure are also indicative of a gene's activation status. H3K4me3 marks promoters of active genes or genes that had recently been activated, as well as genes that are poised for activation. H3K9ac is a mark for active genes. The H2A.Z histone variant is present at genes which can become activated and is decreased both in active and repressed genes. H3K27me3 marks genes, which are repressed or, when it is found together with H3K4me3, genes that are poised for activation.

To analyse effects of Ibrutinib treatment on these chromatin modifications *in vitro*, CLL cells were first cultured overnight, then they were treated with DMSO or Ibrutinib and stimulated with anti-IgM for up to 24 h, before the medium was changed to fresh, DMSO- or inhibitor-containing medium. The cells were cultured under these conditions for up to 5 days and the medium with DMSO or Ibrutinib was renewed daily.

On average, H3K4me3 levels were unchanged in DMSO-treated CLL cells after anti-IgM stimulation in all the regions analysed (Figure 6.18). However, there were some patient-to-patient variations; in some patients H3K4me3 was slightly increased, in others it was decreased upon BCR stimulation. This might be due to differences in basal BCR signalling levels. In contrast, H3K4me3 levels were elevated in Ibrutinib-treated cells before anti-IgM stimulation and H3K4me3 was further induced 30 min after BCR cross-linking in the *EGR1*, *DUSP2* and *DUSP4* promoters, but not in the distal *EGR1* -6.1 region or at the *MYC* promoter (Figure 6.18). At later time points (1 h, 4 h, 24 h), H3K4me3 levels decreased to baseline in Ibrutinib-treated cells and after 3 to 5 days (72 – 120 h) of Ibrutinib treatment, H3K4me3 was reduced in all the regions tested.

The puzzling observation that Ibrutinib increased H3K4me3 in the promoter regions before and after 30 min anti-IgM stimulation, could be explained through a reduction in histone turnover. In DMSO-treated CLL cells, which chronically signal via the

BCR, an equilibrium might exist between histone turnover, which would remove H3K4me3-carrying nucleosomes from the promoters, and H3K4 methylation. In agreement, nucleosomes are constantly turned over at inducible promoters in yeast (Cairns, 2009; Rufiange et al., 2007). Ibrutinib might selectively block histone turnover without influencing H3K4 methyltransferases, which would lead to the increased levels of H3K4me3 in the promoter regions. Further, although Ibrutinib is predicted to block BCR signalling, it does not seem to completely inhibit promoter activation at BCR target genes, as BCR stimulation was capable of enhancing H3K4me3 after 30 min. By some regulatory mechanism, possibly because inhibitory BCR signalling, e.g. via SHIP or SHP1, is not blocked by Ibrutinib, H3K4me3 levels were downregulated to equilibrium levels after BCR stimulation. Long-term Ibrutinib treatment decreased H3K4me3, most likely because chronic BCR signalling, and thus the maintenance of H3K4 methylation, were blocked.

In contrast to H3K4me3, H3K9ac increased in DMSO-treated cells at the *EGR1* and the *DUSP2* promoters after BCR stimulation and this induction was only marginally inhibited by Ibrutinib treatment. These data suggest again that Ibrutinib does not completely block promoter activation downstream of the BCR. After 24 h, however, H3K9ac was reduced in Ibrutinib-treated cells at both the *EGR1* and *DUSP2* promoters. At the *MYC* and *DUSP4* promoters, H3K9ac levels were mostly unchanged in both DMSO- and Ibrutinib-treated CLL cells (Figure 6.19).

H2A.Z occupancy of the promoter regions was largely unaltered after BCR stimulation in both DMSO- and Ibrutinib-treated CLL cells. Only in patient 18, H2A.Z was integrated into the *EGR1*, *DUSP2* and *MYC* promoter chromatin upon BCR stimulation in both DMSO- and Ibrutinib-treated cells (Figure 6.20). As H2A.Z is present in promoters that are just being activated or that have been activated previously, the increase in H2A.Z might indicate that the cells had not been pre-activated as much as the other patients' cells and therefore incorporated more H2A.Z into the promoter in order to activate gene expression. When the gene is actually expressed, H2A.Z is removed again, explaining the drop in H2A.Z levels after 1 to 24 h of BCR activation. Interestingly, the same patient displayed a large increase in H2A.Z occupancy 3 days (72 h) after BCR stimulation in DMSO- but not Ibrutinib-treated cells, possibly reflecting the previous activation of gene expression and the establishment of an "expression memory". Consistently, patient 29 also showed a slight increase in H2A.Z occupancy at the *EGR1* and *MYC* promoters in DMSO-treated cells on day 3 (72 h). On day 5 (120 h), however, H2A.Z levels had dropped in both patients, probably due to the lack of stimulation (Figure 6.20).

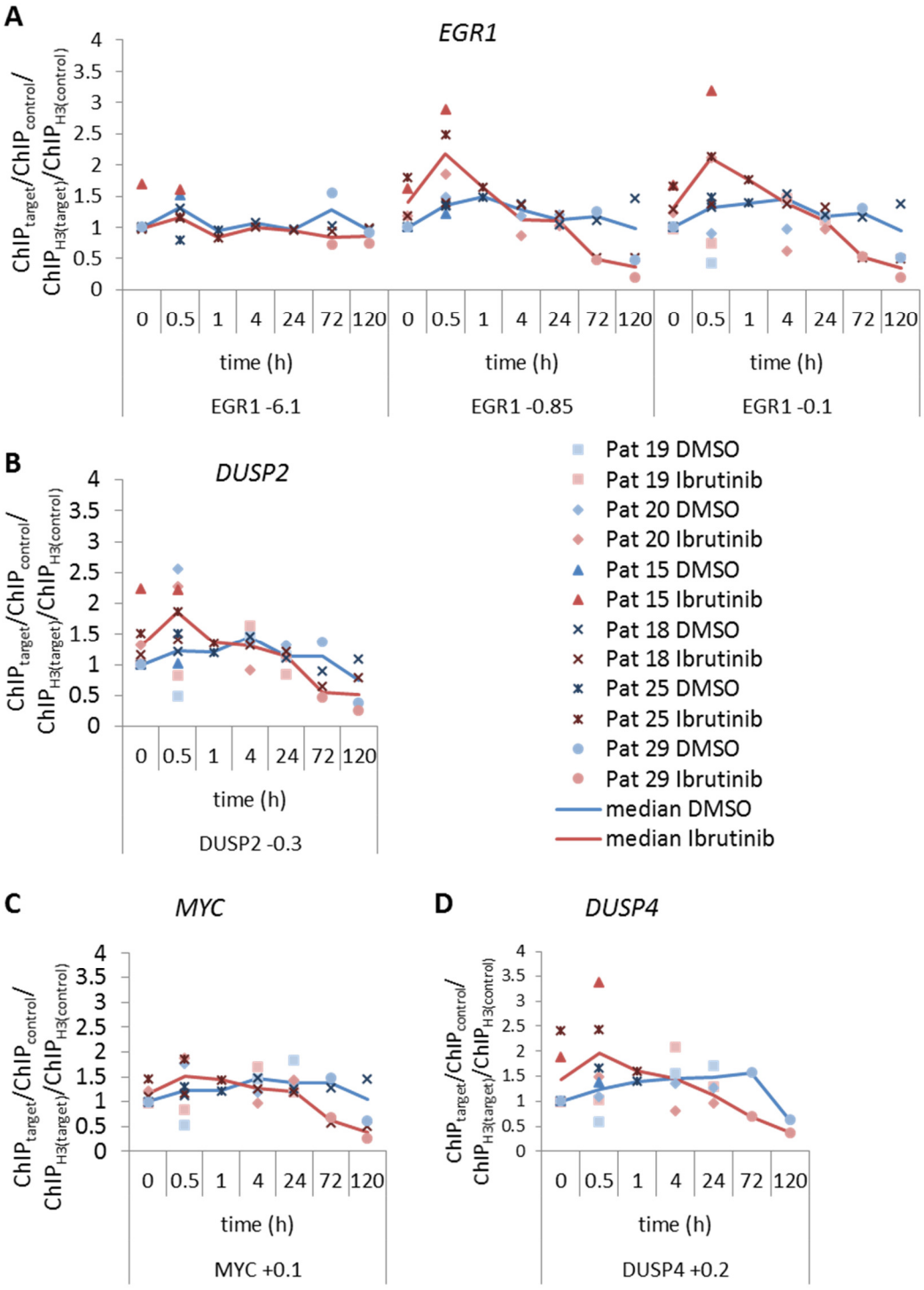

Figure 6.18 Analysis of H3K4me3 at different time points after BCR cross-linking without and with Ibrutinib.
PBMCs were cultured in RPMI-1640 over night, treated with DMSO or Ibrutinib for 2 h and then stimulated with anti-IgM. H3K4me3 levels at the promoters of *EGR1* (**A**), *DUSP2* (**B**), *MYC* (**C**) and *DUSP4* (**D**) were analysed by ChIP. Results were normalised to input, the CTCF1 and CTCF3 control regions and unstimulated, DMSO-treated cells. Median H3K4me3 levels are displayed as a line. Cells pretreated with Ibrutinib showed an increase in H3K4me3 at the promoters of *EGR1*, *DUSP2*, *MYC* and *DUSP4* before and 30 min after BCR cross-linking. In contrast, long-term Ibrutinib treatment (72 h – 120 h) led to a decrease in H3K4me3 in the same regions.

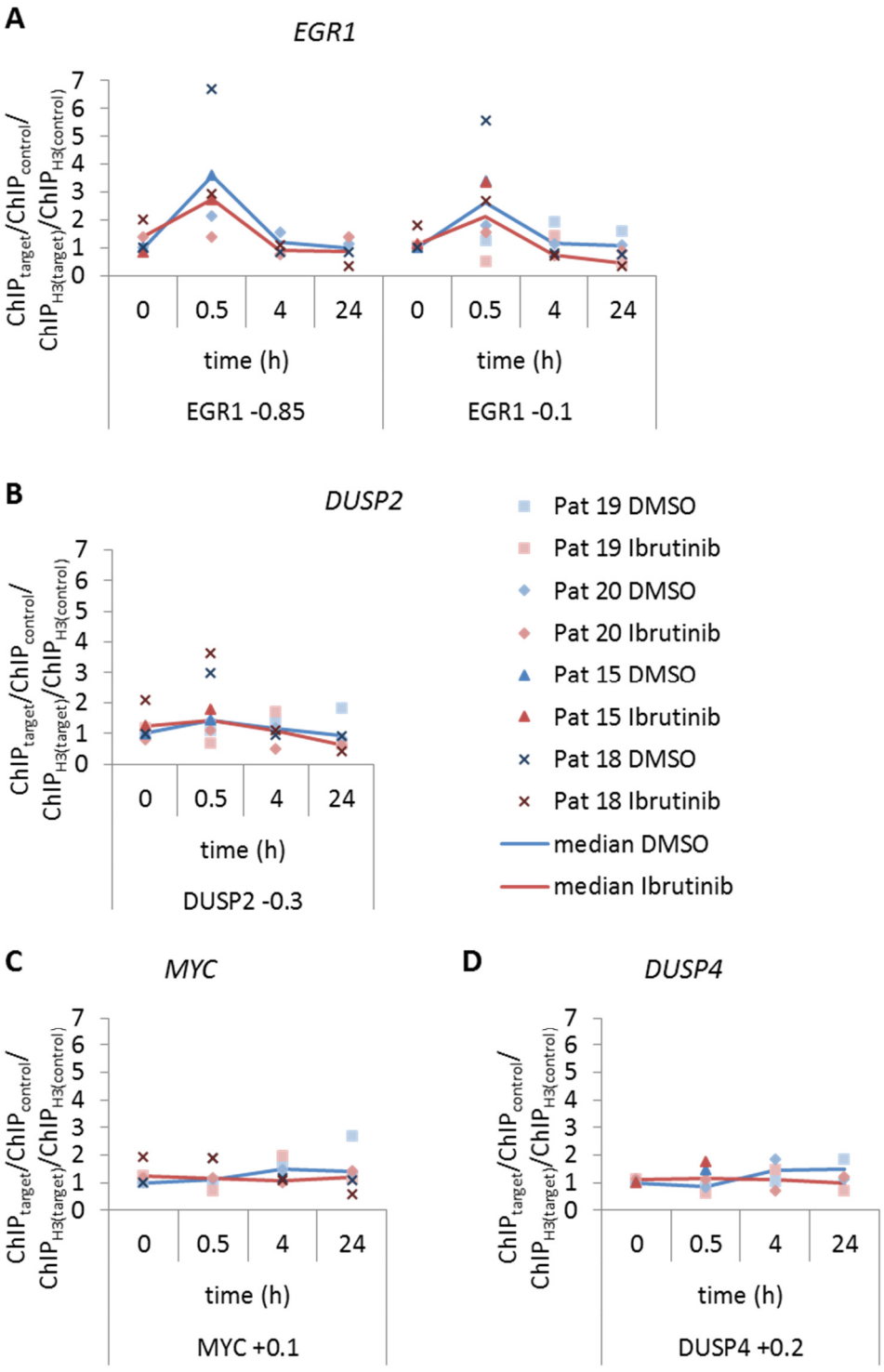

Figure 6.19 Effects of Ibrutinib on H3K9ac at different genes after BCR stimulation.

PBMCs were cultured in RPMI-1640 over night, treated with DMSO or Ibrutinib for 2 h and then stimulated with anti-IgM. H3K9ac levels at the promoters of *EGR1* (**A**), *DUSP2* (**B**), *MYC* (**C**) and *DUSP4* (**D**) were analysed by ChIP. Results were normalised to input, the CTCF1 and CTCF3 control regions and unstimulated, DMSO-treated cells. Median H3K9ac levels are displayed as a line. Ibrutinib did not block the BCR signalling-induced increase in H3K9ac at the *EGR1* and *DUSP2* genes, but led to a decrease in H3K9ac after 24 h compared to DMSO.

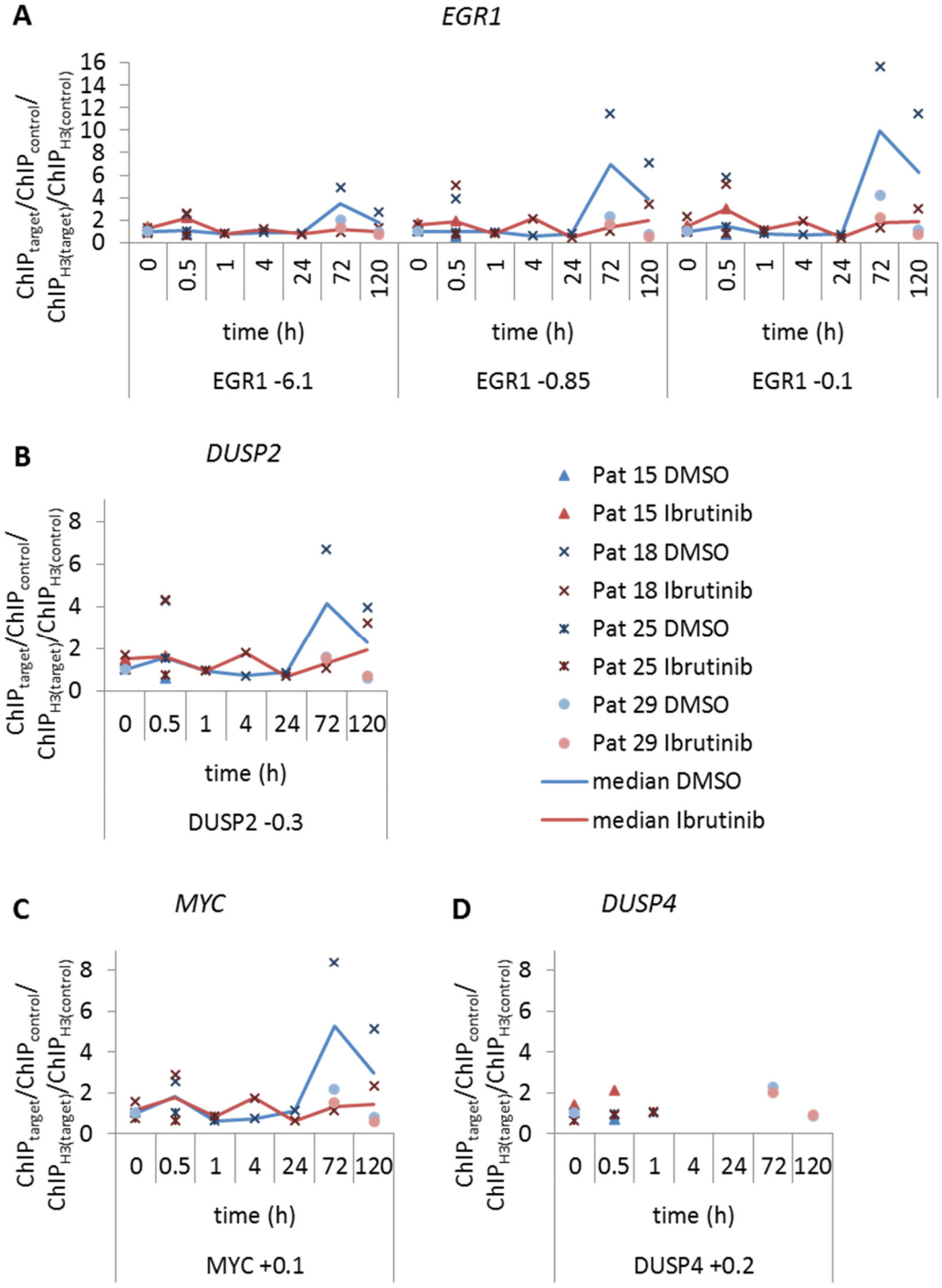

Figure 6.20 Influence of BCR cross-linking and Ibrutinib on H2A.Z occupancy at different genes.
PBMCs were cultured in RPMI-1640 over night, treated with DMSO or Ibrutinib for 2 h and then stimulated with anti-IgM. H2A.Z levels at the promoters of *EGR1* (**A**), *DUSP2* (**B**), *MYC* (**C**) and *DUSP4* (**D**) were analysed by ChIP. Results were normalised to input, the CTCF1 and CTCF3 control regions and unstimulated, DMSO-treated cells. Median H2A.Z levels are displayed as a line. Ibrutinib did not inhibit H2A.Z incorporation 30 min after BCR cross-linking compared to DMSO-treated cells, but it blocked the later peak in H2A.Z incorporation 72 h after BCR cross-linking.

Next, the inhibitory H3K27me3 mark was analysed at the *EGR1*, *DUSP2* and *MYC* promoters. H3K27me3 levels were generally very low in these regions and were only increased after 72 h and 120 h of treatment. In the *EGR1* -0.85 region, Ibrutinib treatment led to an increase in H3K27me3 in cells of one patient, but not the other, while both DMSO- and Ibrutinib-treated cells showed an increase in H3K27me3 in the *EGR1* -0.1 region. At the *DUSP2* promoter, H3K27me3 was increased only in Ibrutinib-treated cells and no increase in H3K27me3 was seen at the *MYC* promoter (Figure 6.21).

In summary, Ibrutinib does not seem to block BCR-induced promoter activation, including POL II recruitment, in general. However, because no induction of mRNA expression of any of the BCR target genes was seen, Ibrutinib treatment does most likely block a different step in the transcription process, for example pause release, processive transcriptional elongation and/or mRNA processing. It might, for example, inhibit full activation of gene expression by blocking histone turnover and H3T6 and H3T11 phosphorylation.

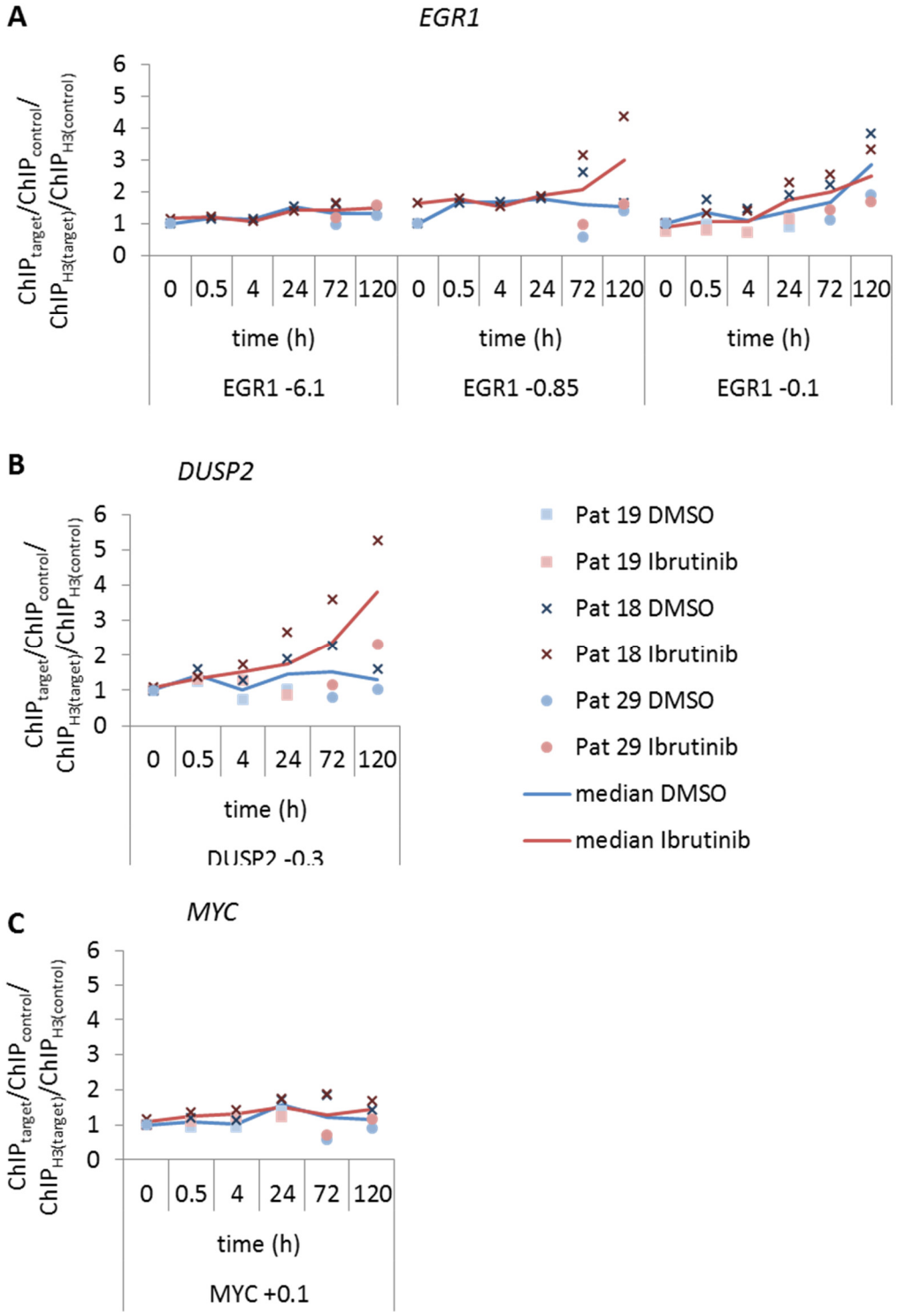

Figure 6.21 Analysis of H3K27me3 after BCR cross-linking with and without Ibrutinib at different genes.
PBMCs were cultured in RPMI-1640 over night, treated with DMSO or Ibrutinib for 2 h and then stimulated with anti-IgM. H3K27me3 levels at the promoters of *EGR1* (**A**), *DUSP2* (**B**) and *MYC* (**C**) were analysed by ChIP. Results were normalised to input, the CTCF1 and CTCF3 control regions and unstimulated, DMSO-treated cells. Median H3K27me3 levels are displayed as a line. Ibrutinib treated cells showed a trend towards increased H3K27me3 72 h and 120 h after anti-IgM stimulation, especially at the *DUSP2* promoter.

7 Identification of signalling pathways leading to H3T6 and H3T11 phosphorylation

We next wanted to identify signalling pathways or kinases that are required for the phosphorylation of H3T6p and H3T11p downstream of the BCR. The induction of both marks correlated well with the induction of gene expression, e.g. they were not induced in Ibrutinib-treated cells, and both marks were found along the whole *EGR1* and *DUSP2* genes, so that they might be important mediators of transcriptional elongation. Consistently, Ibrutinib did not seem to block transcription initiation, including POL II recruitment, H3K9 acetylation and H2A.Z incorporation, at the studied genes, but did block generation of mature mRNAs, possibly by blocking processive elongation. Although we hypothesised that this might be mediated by H3T6 and H3T11 phosphorylation, we could not exclude effects of other histone marks. By specifically inhibiting H3T6 and/or H3T11 phosphorylation, for example by targeting the kinase directly phosphorylating these residues, the essential effects of these marks on transcription initiation and elongation could be elucidated. If H3T6p and H3T11p turn out to be important mediators of gene expression downstream of the BCR, essential downstream pathways might be targeted therapeutically together with BTK or in Ibrutinib-resistant patients.

7.1 PKCβ as a candidate kinase

We first chose a candidate approach to identify the kinase or pathway responsible for H3T6 and H3T11 phosphorylation. As described earlier, PKCβ had been shown to phosphorylate H3T6 at androgen receptor-dependent genes and to stimulate transcription (Metzger et al., 2010). As PKCβ also plays an essential role downstream of the BCR, it seemed plausible that PKCβ might be the kinase targeting H3T6 and possibly H3T11 in CLL cells.

To test this hypothesis, PBMCs of one patient were initially treated with 200 nM PKCβ inhibitor or with Ibrutinib and expression of *EGR1*, *DUSP2*, *MYC* and *CXCR4* were analysed. Further, H3T6p and H3T11p at the *EGR1* gene were assessed by ChIP. No significant difference in expression of *EGR1*, *MYC* or *CXCR4* mRNA levels were seen between DMSO- or PKCβ inhibitor-treated cells, while Ibrutinib reduced expression of *EGR1* and *MYC* or inhibited repression of *CXCR4* after anti-IgM stimulation, respectively. Expression of *DUSP2* was reduced to the same level

in Ibrutinib- and PKCβ inhibitor-treated cells only after 60 min anti-IgM stimulation. Further, H3T6p and H3T11p levels at the *EGR1* gene were unaltered (Figure 7.1).

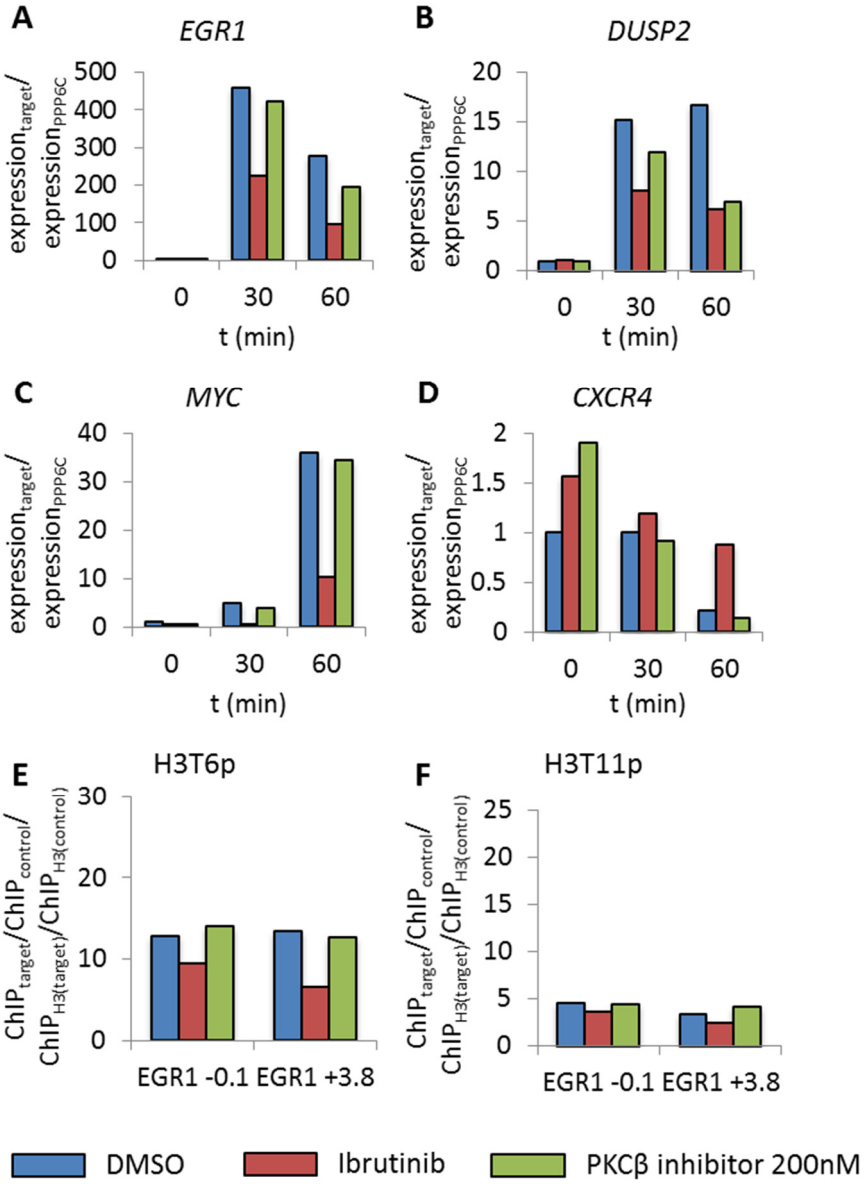

Figure 7.1 Effects of PKCβ inhibition on gene expression as well as H3T6p and H3T11p at the *EGR1* gene.
PBMCs of one patient were cultured in RPMI-1640 over night, treated with DMSO, 1 µM Ibrutinib or 200 nM PKCβ inhibitor for 2 h and then stimulated with anti-IgM. **A**-**D** RNA was harvested and gene expression was analysed by RT-qPCR. Data are normalised to *PPP6C* expression and expression in unstimulated, DMSO-treated cells. Inhibition of PKCβ did not result in decreased expression of *EGR1* or *MYC*, while *DUSP2* expression was only reduced 60 min after BCR cross-linking compared to DMSO-treated cells. The inhibitor did also not affect the downregulation of *CXCR4*. **E**, **F** Chromatin was prepared before and after 30 min anti-IgM stimulation and the *EGR1* gene was analysed for H3T6p and H3T11p by ChIP-qPCR. The data are normalised to H3, the CTCF1 control region and H3T6p or H3T11p in DMSO-treated, unstimulated cells. H3T6p and H3T11p were unaltered in PKCβ inhibitor-treated compared to DMSO-treated cells

To ensure that PKCβ was sufficiently inhibited, higher concentrations of the inhibitor (1 µM,10 µM and 1 µM overnight) were applied to PBMCs of two other patients. Again, expression of both *EGR1* and *DUSP2* did not differ significantly between DMSO- and PKCβ inhibitor-treated cells, while Ibrutinib inhibited induction of both genes (Figure 7.2 A, B). Further, when H3T6p and H3T11p at the *EGR1* gene were analysed, a trend towards increased phosphorylation was seen (Figure 7.2 C, D). From these experiments, it was concluded that PKCβ does not directly target H3T6 and H3T11 in CLL cells. It might rather have an inhibitory function on BCR signalling by phosphorylating and inhibiting BTK, which would explain why H3T6p and H3T11p are slightly increased after PKCβ inhibitor treatment.

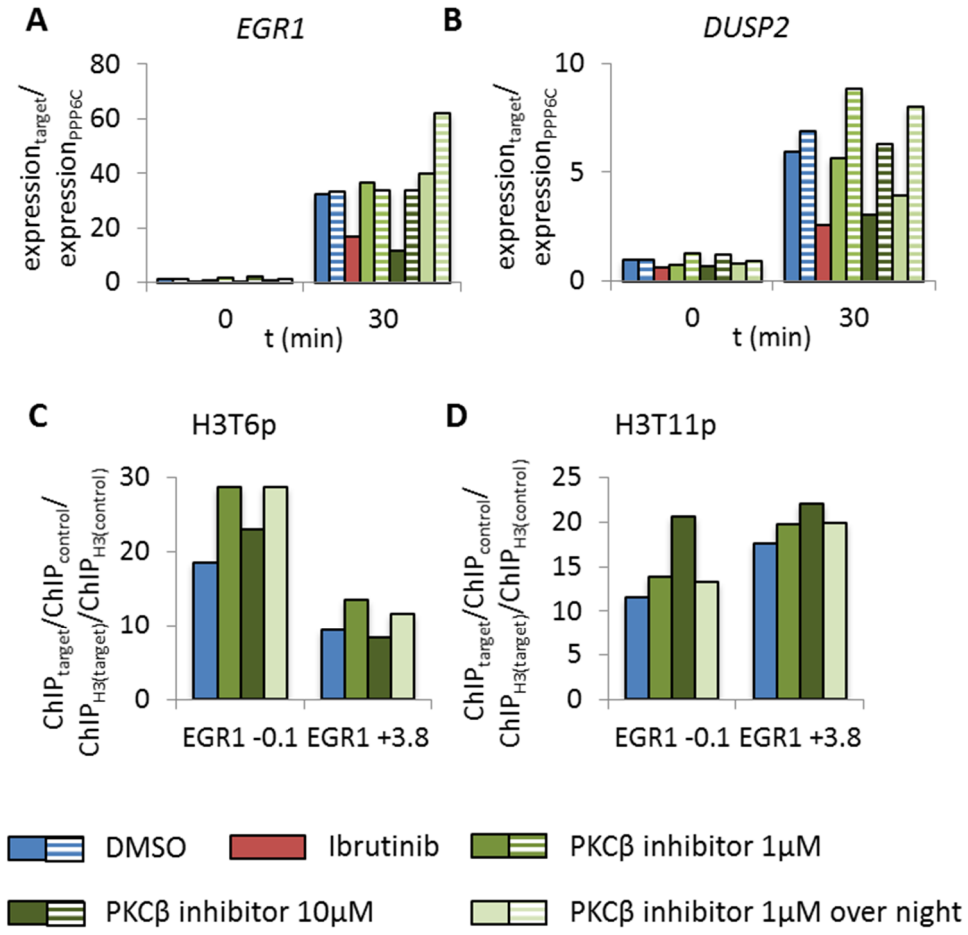

Figure 7.2 Consequences of high-dose PKCβ inhibitor treatment for the expression of *EGR1* and *DUSP2*, as well as for H3T6p and H3T11p at the *EGR1* gene.

PBMCs of two patients were cultured in RPMI-1640 over night and treated with DMSO, 1 µM Ibrutinib, 1 µM or 10 µM PKCβ inhibitor for 2 h the next day or they were directly incubated with 1 µM PKCβ inhibitor overnight. Inhibitor-treated cells were then stimulated with anti-IgM. **A**, **B** RNA was harvested and gene expression was analysed by RT-qPCR. Data are normalised to PPP6C expression and expression in unstimulated, DMSO-treated cells. The results from two different patients are shown. High doses of the PKCβ inhibitor were not sufficient to consistently inhibit the expression of *EGR1* and *DUSP2* after BCR stimulation. **C**, **D** From one of the patients, chromatin was prepared and the *EGR1* gene was analysed for H3T6p and H3T11p by ChIP-qPCR. The data are normalised to H3, the CTCF1 control region and H3T6p or H3T11p in DMSO-treated, unstimulated cells. PKCβ inhibitor-treated cells tended to show higher levels of H3T6p and H3T11p than DMSO-treated cells, indicating that PKCβ does not directly target these residues downstream of the BCR.

7.2 Identification of other candidate kinases for H3T6 and H3T11

As PKCβ was most likely not the kinase targeting H3T6 and H3T11 downstream of the BCR signalling pathway and was also not involved in the pathway leading to H3T6 and H3T11 phosphorylation, I sought to identify other possible kinases targeting H3T6 and/or H3T11. To this end, a kinase prediction was performed using the freely available software GPS 2.1 (Xue et al., 2008) and the H3 N-terminal tail as input sequence. Among the kinases predicted to phosphorylate H3T6 and H3T11 were the kinases listed in Table 7.1.

H3T6		H3T11	
Kinase	Score	Kinase	Score
MEK2	4	PKCa	2.873
PKCa	5.284	PKCg	2.8
PKCb	4.125	RSK1	3
PKCg	2.2	RSK2	3.222
PKCd	2.435	ZIPK	6.889
PKCt	5.25		
PKCz	3.462		
RSK2	4.111		
ZIPK	4.056		

Table 7.1 Kinases predicted by GPS 2.1 (Xue et al., 2008) to phosphorylate H3T6 and H3T11.

Among these kinases MEK2, RSK1/2 and PKCs are known downstream elements of the BCR signalling pathway. Consequently, inhibitors targeting these kinases were tested for their ability to inhibit expression of *EGR1* and *DUSP2* and phosphorylation of H3T6 and H3T11 along these genes. The inhibitors used were Gö6983, a pan-PKC inhibitor, RSK inhibitor II, a pan-RSK inhibitor, and U0126, a MEK1/2 inhibitor. All three inhibitors tested did not significantly inhibit the induction of *EGR1* or *DUSP2* expression after 30 and 90 min anti-IgM stimulation (Student's t test $p > 0.15$) (Figure 7.3 A, Figure 7.4 A).

PBMCs from two of the patients were also analysed by ChIP (Figure 7.3, Figure 7.4). The induction of H3T6p was reduced at the *EGR1* gene when the cells were pre-treated with Gö6983 or RSK inh II, but not when MEK1/2 were inhibited (Figure 7.3 D, E), whereas induction of H3T6p at the *DUSP2* +2.4 region was only reduced by Gö6983 (Figure 7.4 D, E). In one patient, the increase in H3T11p was reduced by all inhibitors (Figure 7.3 F, Figure 7.4 F), but only Gö6983 pre-treatment led to inhibition of H3T11p induction in both patients (Figure 7.3 F, G, Figure 7.4 F, G). However, the induction of H3T11p in the second patient was on average very weak and it did not reach more than 2-fold induction at most *EGR1* regions or at the *DUSP2* gene, so that the observed inhibitor effects were also weak. From these experiments, it was concluded that PKCs and/or RSKs are likely involved in the upstream signalling to induce H3T6 or H3T11 phosphorylation, but are not directly targeting these residues in CLL cells. Further, other signalling pathways are expected to play a role, as the phosphorylation of H3T6 and H3T11 was not inhibited as strongly as after Ibrutinib treatment.

Figure 7.3 Influence of different kinase inhibitors on the expression of *EGR1* and on H3T6p and H3T11p at the *EGR1* gene.
PBMCs of CLL patients were cultured for 16 to 48 h and then treated with DMSO, 1 µM Ibrutinib, 1 µM Gö6983, 10 µM RSK inhibitor II or 10 µM U0126 for 2 h, before the BCR was cross-linked. **A** Expression of *EGR1* was assessed and the means and sd of at least three independent experiments from different patients are shown normalised to *TBP* and to the induction of *EGR1* mRNA expression in DMSO-treated cells after 30 min. ** $p < 0.01$, ns = not significant in Student's t test. None of the inhibitors, other than Ibrutinib, did significantly block induction of *EGR1*. **B** - **G** ChIP was performed before and after 30 min anti-IgM stimulation using primers along the *EGR1* gene and antibodies against H3 (**B**, **C**), H3T6p (**D**, **E**) or H3T11p (**F**, **G**). ChIP results after 30 min anti-IgM stimulation are plotted. Results of two representative patient are shown normalised to input (**B, C**) or H3 (**D-G**), the CTCF1 and CTCF3 control regions and unstimulated, DMSO-treated cells. Ibrutinib was the most effective inhibitor leading to an increase in H3 occupancy and inhibition of H3T6p and H3T11p. Gö6983 also reduced H3T6 and H3T11 phosphorylation in both patients, while RSK inhibitor II only affected H3T6p. U0126 did not alter H3T6p and H3T11p induction.

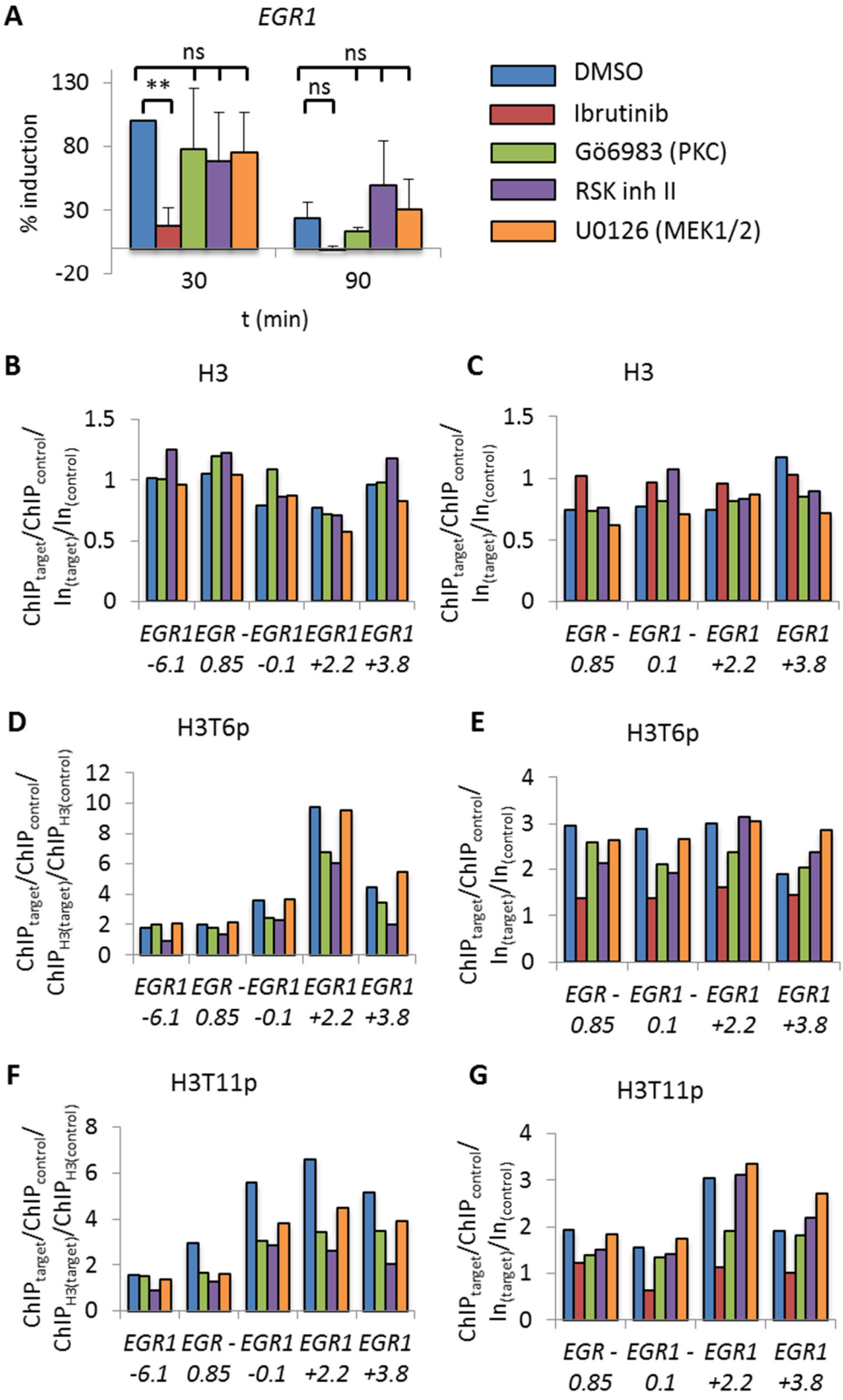
A
EGR1
ns
ns
ns
**
130
80
30
-20
% induction
30
90
t (min)
DMSO
Ibrutinib
Gö6983 (PKC)
RSK inh II
U0126 (MEK1/2)
B
H3
C
H3
ChIP target/ChIP control / In (target)/In (control)
1.5
1
0.5
0
EGR1 -6.1
EGR 0.85
-EGR1 -0.1
EGR1 +2.2
EGR1 +3.8
D
H3T6p
E
H3T6p
ChIP target/ChIP control / ChIP H3(target)/ChIP H3(control)
12
10
8
6
4
2
0
F
H3T11p
G
H3T11p
3
EGR - 0.85
EGR1 - 0.1

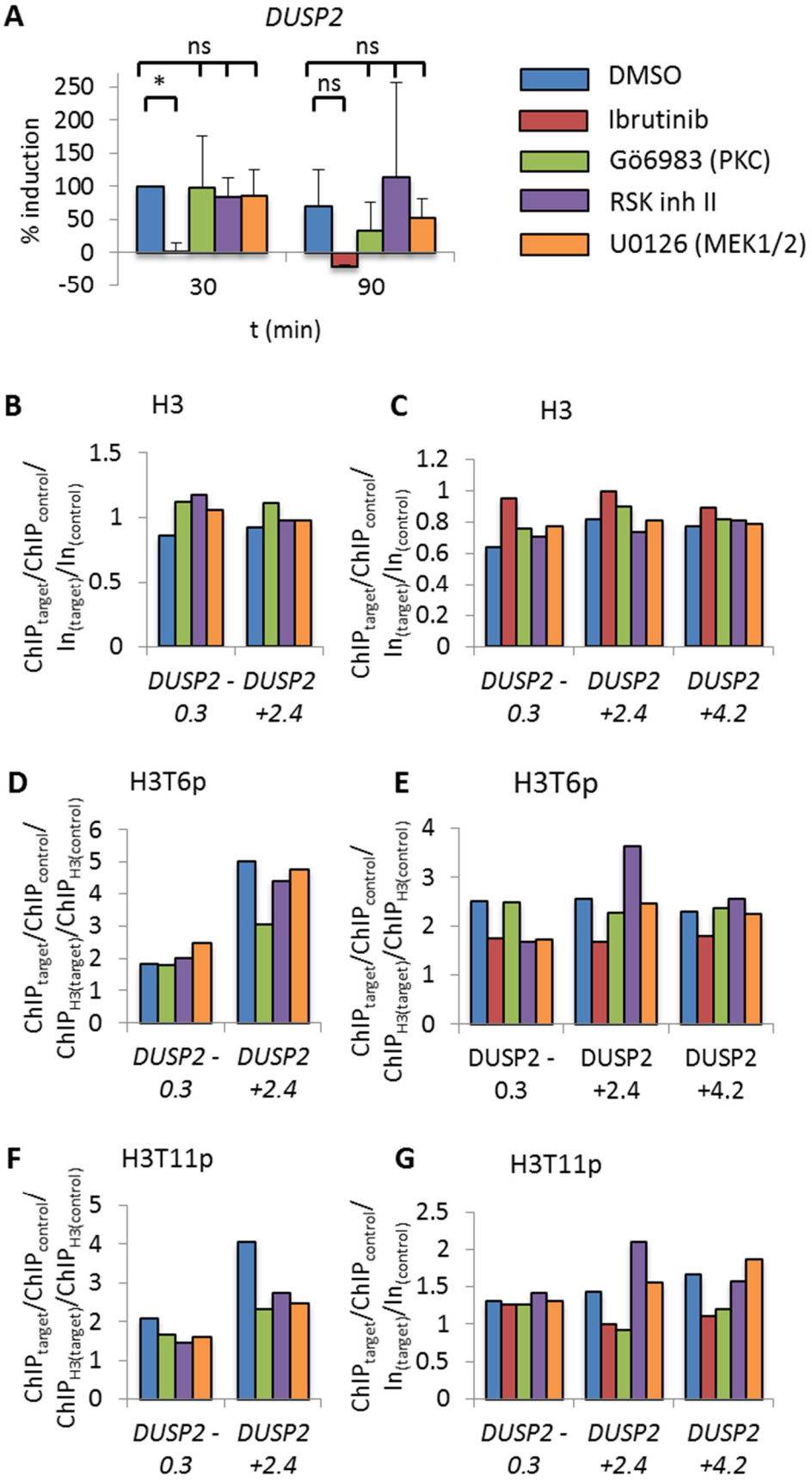
A
DUSP2
ns
ns
*
ns
250
200
150
100
50
0
-50
% induction
30
90
t (min)
DMSO
Ibrutinib
Gö6983 (PKC)
RSK inh II
U0126 (MEK1/2)
B
H3
ChIP target/ChIP control/ In (target)/In (control)
1.5
1
0.5
0
DUSP2 - 0.3
DUSP2 +2.4
C
H3
1.2
1
0.8
0.6
0.4
0.2
0
DUSP2 - 0.3
DUSP2 +2.4
DUSP2 +4.2
D
H3T6p
ChIP target/ChIP control/ ChIP H3(target)/ChIP H3(control)
6
5
4
3
2
1
0
DUSP2 - 0.3
DUSP2 +2.4
E
H3T6p
4
3
2
1
0
DUSP2 - 0.3
DUSP2 +2.4
DUSP2 +4.2
F
H3T11p
5
4
3
2
1
0
DUSP2 - 0.3
DUSP2 +2.4
G
H3T11p
2.5
2
1.5
1
0.5
0
DUSP2 - 0.3
DUSP2 +2.4
DUSP2 +4.2

Figure 7.4 Effect of different kinase inhibitors on the expression of *DUSP2* and on H3T6p and H3T11p at the *DUSP2* gene.
PBMCs of CLL patients were cultured for 16 to 48 h and then treated with DMSO, 1 µM Ibrutinib, 1 µM Gö6983, 10 µM RSK inhibitor II or 10 µM U0126 for 2 h. They were subsequently stimulated with anti-IgM. **A** Expression of *DUSP2* was assessed and the means and sd of at least three independent experiments from different patients are shown normalised to *TBP* and to the induction of *DUSP2* mRNA expression in DMSO-treated cells after 30 min. * $p < 0.05$, ns = not significant in Student's t test. Only Ibrutinib did significantly block expression of DUSP2, while the other inhibitors did not inhibit its induction compared to DMSO-pretreated cells. **B** - **F** ChIP was performed before and after 30 min anti-IgM stimulation using primers along the *DUSP2* gene and antibodies against H3 (**B**, **C**), H3T6p (**D**, **E**) or H3T11p (**F, G**). ChIP results after 30 min anti-IgM stimulation are plotted. Results from two different patients are shown normalised to input (**B, C**) or H3 (**D**-**G**), the CTCF1 and CTCF3 control regions and unstimulated, DMSO-treated cells. None of the inhibitors mimicked Ibrutinib's effect on H3 occupancy after BCR cross-linking. Gö6983 did, however, inhibit H3T6p in one patient, but not the other and decreased H3T11p in both patients. RSK inh II and U0126 led to a decrease in H3T11p in the first patient only, but were not effective in the second patient.

Surprisingly, however, treatment of CLL cells with high concentrations of the PKCβ inhibitor or with Gö6983 led to a global, BCR stimulation-independent reduction in H3T11p and an inhibition of H3K9acS10p induction upon BCR stimulation (Figure 7.5). Therefore, a kinase inhibited by both drugs directly or indirectly mediated the global phosphorylation of H3T11, possibly at centromeric regions, but it was not directly responsible for BCR-induced H3T11 phosphorylation. The inhibition of H3K9acS10p upon BCR stimulation is probably due to inhibition of BCR downstream signal transduction pathways.

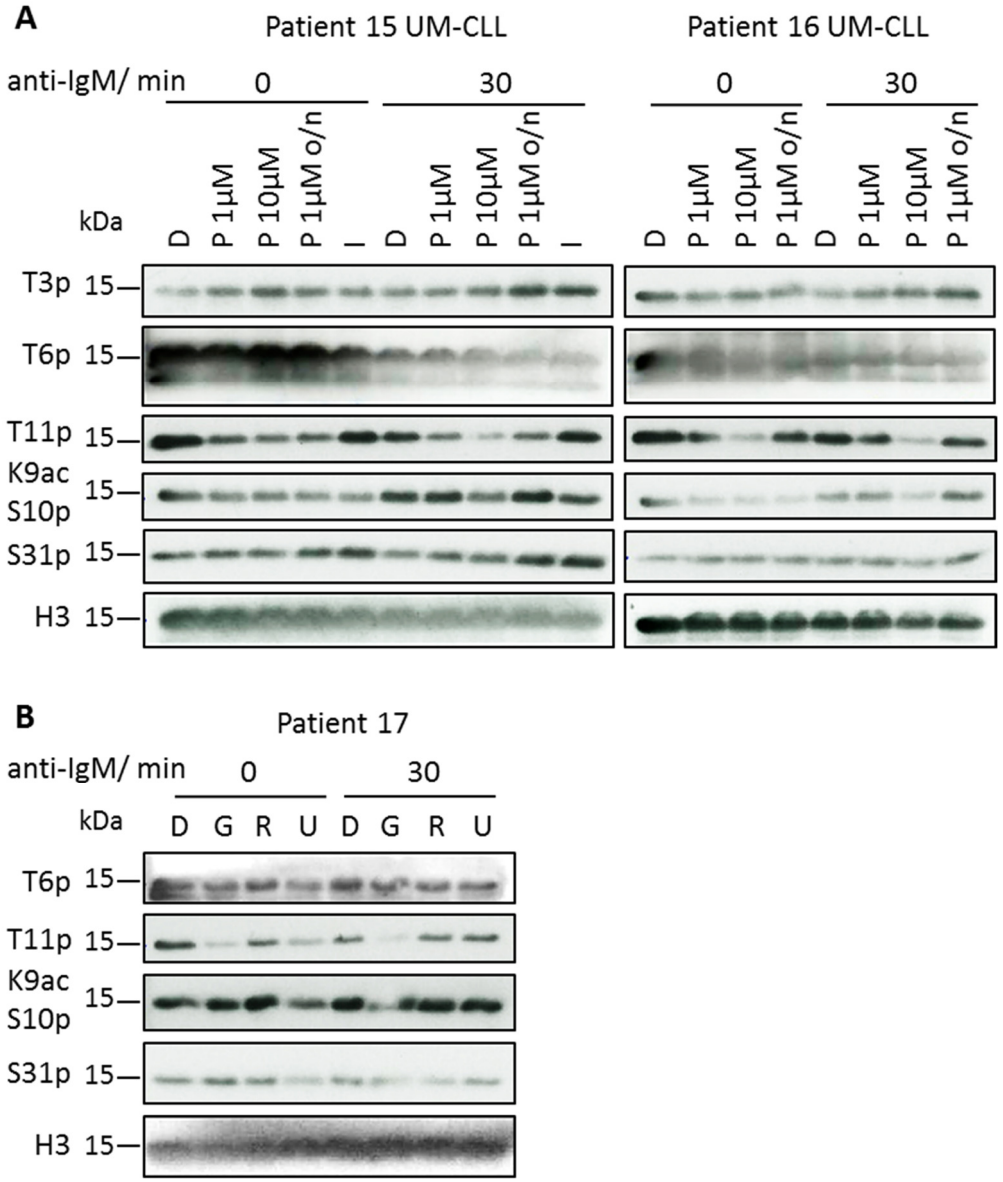

Figure 7.5 Effect of different kinase inhibitors on global histone phosphorylation in CLL cells.

A PBMCs of two patients were cultured in RPMI-1640 over night and then treated with DMSO (D), 1 µM Ibrutinib (I), 1 µM or 10 µM PKCβ inhibitor (P) for 2 h or they were directly incubated with 1 µM PKCβ inhibitor overnight (P o/n). Inhibitor-treated cells were subsequently stimulated with anti-IgM. **B** PBMCs were cultured in RPMI-1640 overnight, treated with DMSO (D), 1 µM Gö6983 (G), 10 µM RSK inhibitor II (R) or 10 µM U0126 (U) for 2 h and were then stimulated with anti-IgM. Western blot was performed with antibodies against the different histone H3 phospho-modifications. High doses of the PKCβ inhibitor and Gö6983 led to a decrease in global H3T11p even before BCR cross-linking, indicating that a kinase targeted by both inhibitors is required to maintain H3T11 phosphorylation. Both inhibitors also blocked the BCR signalling-induced increase in H3K9acS10p.

7.3 Zipper-interacting protein kinase (ZIPK) as a candidate kinase for H3T6 and H3T11

All kinases tested so far did not directly target H3T6 or H3T11. However, among the kinases predicted by GPS 2.1, ZIPK (also known as death-associated protein kinase 3, DAPK3, or DAP-like kinase (DLK)) was the kinase with the highest score for H3T11 and was also predicted to phosphorylate H3T6 (see Table 7.1). ZIPK belongs to the death-associated protein kinase family together with DAPK1, DAPK2 (DRP1), death-associated protein kinase related protein 1 (DRAK1) and DRAK2. Interestingly, a splice variant of DRP1 has been detected, which resembles ZIPK (Shoval et al., 2011). ZIPK is activated by phosphorylation and autophosphorylation. The active ZIPK is an oligomeric protein and it oligomerises via its leucine zipper and kinase domains (Graves et al., 2005).

However, ZIPK has mostly been associated with cell death signalling and tumour suppression (Bi et al., 2009; Brognard et al., 2011; Kawai et al., 2003; Kocher et al., 2014 p. 2003; Kögel et al., 2003; Wu et al., 2010). It is believed to mediate its effects on cell death primarily through autophagy by phosphorylating myosin light chain and thus linking autophagy proteins to cytoskeletal reorganisation (Murata-Hori et al., 1999; Murata-Hori et al., 2001; Tang et al., 2011). Consistently, no cleavage of caspase 3 or poly-(ADP-ribose) polymerase (PARP) are seen in ZIPK overexpressing cells (Shani et al., 2004).

When overexpressed in HeLa cells, human ZIPK shows a predominantly cytoplasmic localisation (Murata-Hori et al., 2001) and phosphorylation of T299 triggers its nuclear export (Graves et al., 2005). Conversely, deletion of the leucine zipper leads to nuclear retention of the kinase (Graves et al., 2005). Interestingly, a splice variant lacking the leucine zipper has been described (Takamoto et al., 2006). One kinase that can phosphorylate T299 is DAPK1 and both DAPK1 and ZIPK synergistically induce apoptosis upon overexpression (Shani et al., 2004). In contrast, murine ZIPK lacks the T299 residue and is consequently localised predominantly in the nucleus, is associated with chromatin and has been shown to phosphorylate histones (Kögel et al., 1998; Weitzel et al., 2011), specifically histone H3T11 at centromeres during mitosis (Preuss et al., 2003).

In mice and rats, diffuse nuclear localisation of ZIPK is associated with cell survival, while localisation to the cytoplasm through interaction with prostate apoptosis response 4 (PAR4) or within nuclear bodies is required for ZIPK-mediated apoptosis (Kawai et al., 2003; Kögel et al., 1999; G. Page et al., 1999). As PAR4

interacts with the actin cytoskeleton and leads to stress fibre formation, it was proposed that PAR4 recruits ZIPK to actin bundles, where it can activate myosin and induce apoptosis (Vetterkind et al., 2005). However, human ZIPK fails to interact with PAR4 (Shoval et al., 2007).

Nevertheless, nuclear localisation of ZIPK might also inhibit its proapoptotic effects in humans, as mutations in the leucine zipper domain lead to nuclear localisation of the enzyme and reduce induction of apoptosis while increasing kinase activity (Graves et al., 2005). Moreover, the stimulation of apoptosis seems to be cell type-specific, as ZIPK also stimulates contraction of smooth and cardiac muscle cells by inhibiting myosin light chain phosphatase and by phosphorylating the myosin light chain (Chang et al., 2010; Haystead, 2005; Komatsu & Ikebe, 2014; MacDonald et al., 2001; Moffat et al., 2011; Niiro & Ikebe, 2001). Further, ZIPK also induces proliferation of smooth muscle cells (Usui et al., 2014) and is required for migration of fibroblasts (Komatsu & Ikebe, 2004).

ZIPK is activated in cells stimulated with IL-6 and the IL-6 family cytokine leukaemia inhibitory factor (LIF) (Sato et al., 2006). It can interact with RHOD-GTP, which inhibits stress fibre and focal adhesion formation (Nehru et al., 2013), but it is also activated by Rho kinase 1 (ROCK1) (Hagerty et al., 2007). It stabilises the cell cycle regulator p21 and activates MDM2 (Burch et al., 2004; Zhou et al., 2001). Further, ZIPK has been shown to bind and phosphorylate STAT3 (Sato et al., 2005) and to bind the AR to stimulate its ubiquitination by MDM2, which enhances transactivation and degradation (Felten et al., 2013; Leister et al., 2008). Both murine and human ZIPK bind the activating transcription factor 4 (ATF4) (Kawai et al., 1998; Shoval et al., 2011) and murine ZIPK has been shown to bind apoptosis antagonising transcription factor (AATF) (G Page et al., 1999), as well as the rat homolog of the *S.pombe* splicing factor CDC5 (CDC5L) (Engemann et al., 2002).

7.3.1 Effects of ZIPK inhibition on gene expression, H3T6 and H3T11 phosphorylation

Although ZIPK has, to our knowledge, never been described as a kinase downstream of the BCR signalling pathway, it had already been shown to associate with chromatin, to phosphorylate H3T11 and to be capable of binding to several transcription factors. Further, ZIPK is overexpressed in CLL compared to normal B cells (Marina et al., 2010), but it might not function as a cell death-inducing kinase, because DAPK1 is downregulated in CLL cells through epigenetic silencing (Raval et al., 2007), so that the synergy between both kinases is abrogated. Therefore, we assessed the effects of ZIPK inhibition on the expression of *EGR1* and *DUSP2* and on histone phosphorylation at these genes.

Treatment of CLL cells with DAPK inhibitor, which targets both ZIPK and DAPK1, resulted in reduced induction of both *EGR1* and *DUSP2* upon BCR activation, which was comparable to the effect of Ibrutinib (Figure 7.6 A, Figure 7.7 A). Similarly, the induction of H3T6 and H3T11 phosphorylation at the *EGR1* and *DUSP2* genes was inhibited to the same extent as in Ibrutinib-treated cells, indicating that ZIPK might be the kinase directly targeting H3T6 and H3T11 in response to BCR stimulation in CLL cells (Figure 7.6 D - G, Figure 7.7 D - F). One representative ChIP is shown (Figure 7.6 B, D, F, Figure 7.7 B, D, F) and then the means and standard deviations of the fold occupancy or induction relative to DMSO-treated cells of three patients are displayed (Figure 7.6 C, E, G, Figure 7.7 C, E). Only data points showing at least a twofold induction over unstimulated, DMSO-treated cells were used for this analysis. For H3T11p at the DUSP2 gene, only one patient fulfilled these criteria, so that no average induction was calculated.

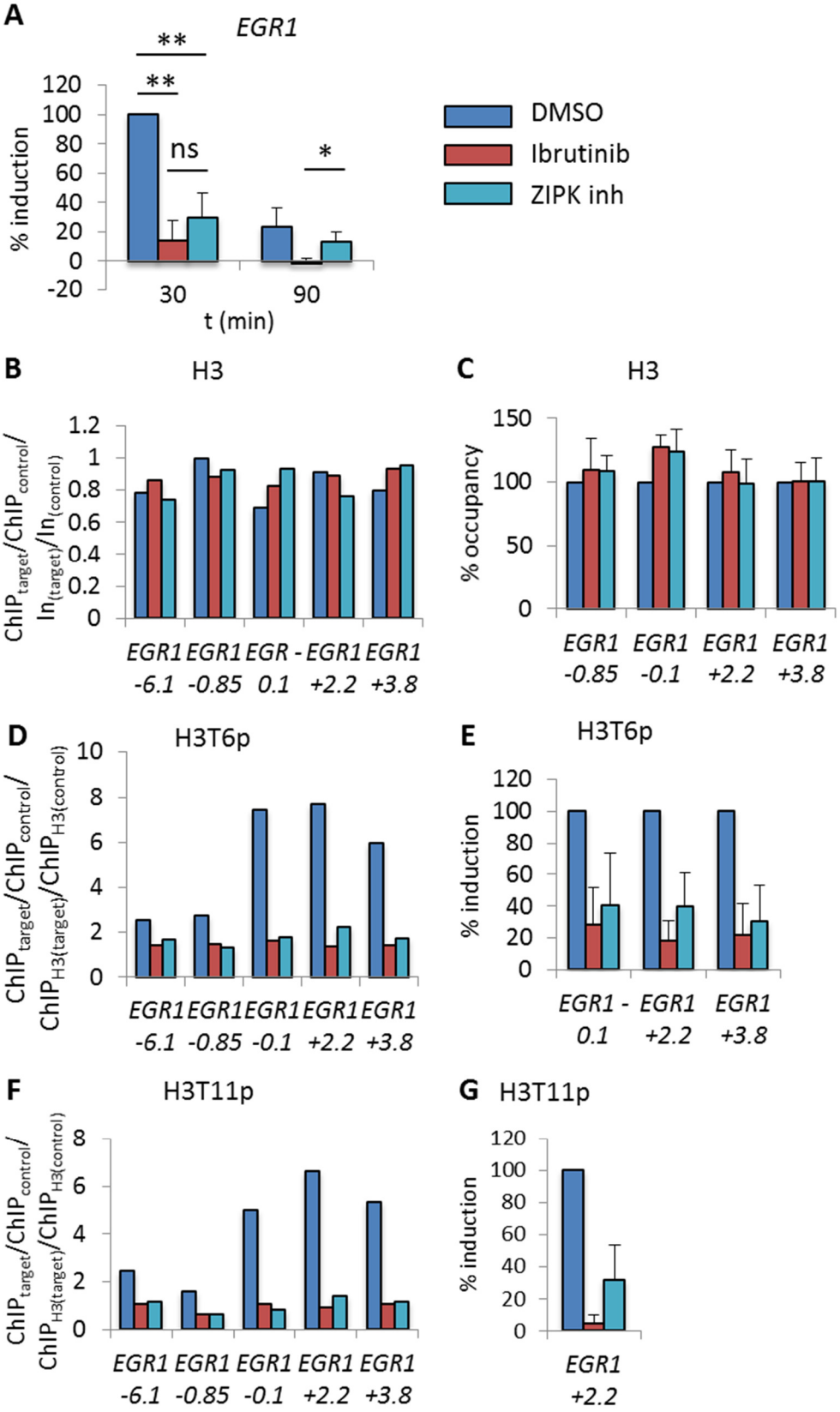
A
EGR1
**
**
ns
*
% induction
120
100
80
60
40
20
0
-20
30
90
t (min)
DMSO
Ibrutinib
ZIPK inh
B
H3
ChIP target/ChIP control/ In (target)/In (control)
1.2
1
0.8
0.6
0.4
0.2
0
EGR1 -6.1
EGR1 -0.85
EGR - 0.1
EGR1 +2.2
EGR1 +3.8
C
H3
% occupancy
150
100
50
0
EGR1 -0.85
EGR1 -0.1
EGR1 +2.2
EGR1 +3.8
D
H3T6p
ChIP target/ChIP control/ ChIP H3(target)/ChIP H3(control)
10
8
6
4
2
0
EGR1 -6.1
EGR1 -0.85
EGR1 -0.1
EGR1 +2.2
EGR1 +3.8
E
H3T6p
% induction
120
100
80
60
40
20
0
EGR1 - 0.1
EGR1 +2.2
EGR1 +3.8
F
H3T11p
ChIP target/ChIP control/ ChIP H3(target)/ChIP H3(control)
8
6
4
2
0
EGR1 -6.1
EGR1 -0.85
EGR1 -0.1
EGR1 +2.2
EGR1 +3.8
G
H3T11p
% induction
120
100
80
60
40
20
0
EGR1 +2.2

Figure 7.6 ZIPK inhibition affects the expression of *EGR1* and H3T6p and T11p.

PBMCs of CLL patients were cultured for 16 to 48 h and then treated with DMSO, 1 µM Ibrutinib or 20 µM DAPK inhibitor for 2 h. They were subsequently stimulated with anti-IgM. **A** Expression of *EGR1* was assessed and the means and sd of at least three independent experiments from different patients are shown normalised to TBP and to the induction of *EGR1* mRNA expression in DMSO-treated cells after 30 min. * $p < 0.05$, ** $p < 0.01$, ns = not significant in Student's t test. Ibrutinib and DAPK inhibitor showed a similar efficiency in inhibiting expression of *EGR1* 30 min after activation of BCR signalling. **B** - **G** ChIP was performed before and after 30 min anti-IgM stimulation using primers along the *EGR1* gene and antibodies against H3 (**B**, **C**), H3T6p (**D**, **E**) or H3T11p (**F**, **G**). ChIP results after 30 min anti-IgM stimulation are plotted. **B**, **D**, **F** Results of one representative patient are shown normalised to input (**B**) or H3 (**D**, **F**), the CTCF1 and CTCF3 control regions and unstimulated, DMSO-treated cells. **C**, **E**, **G** The occupancy of H3 or the induction of H3T6p or H3T11p are shown normalised to DMSO-treated cells after 30 min anti-IgM stimulation. The means and sd of three independent experiments from different patients are plotted. Only data points that showed more than two fold induction over unstimulated cells were used for the analysis. Inhibition of ZIPK was as effective as Ibrutinib in blocking H3T6p and H3T11p at the *EGR1* gene.

Figure 7.7 Effects of ZIPK inhibition on *DUSP2* expression and H3T6p and H3T11p at the *DUSP2* gene.

PBMCs of CLL patients were cultured for 16 to 48 h and then treated with DMSO, 1 µM Ibrutinib or 20 µM DAPK inhibitor for 2 h. They were subsequently stimulated with anti-IgM. **A** Expression of *DUSP2* was assessed and the means and sd of at least three independent experiments from different patients are shown normalised to TBP and to the induction of *DUSP2* mRNA expression in DMSO-treated cells after 30 min. ** $p < 0.01$, ns = not significant in Student's t test. DAPK inhibitor and Ibrutnib both showed similar efficiencies for the inhibition of DUSP2 expression. **B** - **F** ChIP was performed before and after 30 min anti-IgM stimulation using primers along the *DUSP2* gene and antibodies against H3 (**B**, **C**), H3T6p (**D**, **E**) or H3T11p (**F**). ChIP results after 30 min anti-IgM stimulation are plotted. **B**, **D**, **F** Results of one representative patient are shown normalised to input (**B**) or H3 (**D**, **F**), the CTCF1 and CTCF3 control regions and unstimulated, DMSO-treated cells. **C**, **E** The occupancy of H3 or the induction of H3T6p are shown normalised to DMSO-treated cells after 30 min anti-IgM stimulation. The means and sd of three independent experiments from different patients are plotted. Only data points that showed more than two fold induction over unstimulated cells were used for the analysis. DAPK inhibitor reduced the induction of H3T6p and H3T11p at the DUSP2 gene to a similar level to Ibrutinib.

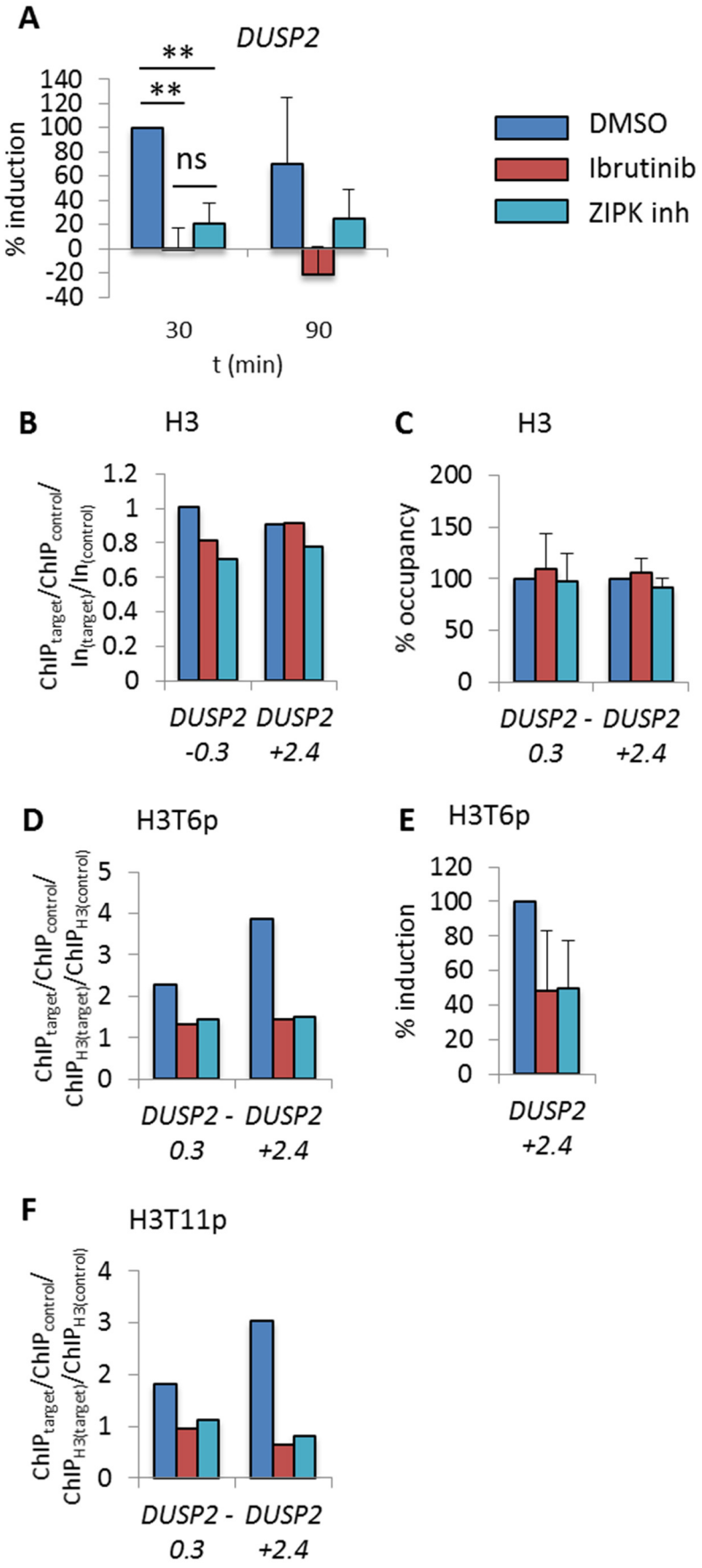
A
DUSP2
**
**
ns
% induction
140
120
100
80
60
40
20
0
-20
-40
30
90
t (min)
DMSO
Ibrutinib
ZIPK inh
B
H3
ChIP target/ChIP control/ In (target)/In (control)
1.2
1
0.8
0.6
0.4
0.2
0
DUSP2 -0.3
DUSP2 +2.4
C
H3
% occupancy
200
150
100
50
0
DUSP2 - 0.3
DUSP2 +2.4
D
H3T6p
ChIP target/ChIP control/ ChIP H3(target)/ChIP H3(control)
5
4
3
2
1
0
DUSP2 - 0.3
DUSP2 +2.4
E
H3T6p
% induction
120
100
80
60
40
20
0
DUSP2 +2.4
F
H3T11p
ChIP target/ChIP control/ ChIP H3(target)/ChIP H3(control)
4
3
2
1
0
DUSP2 - 0.3
DUSP2 +2.4

7.3.2 Expression of ZIPK and subcellular localisation in CLL cells

Because ZIPK is a promising candidate kinase for phosphorylation of H3T6 and H3T11, it was next investigated whether BCR signalling could induce expression or nuclear translocation of ZIPK. To this end, CLL cells of two different patients were treated with different inhibitors and stimulated with anti-IgM. However, protein levels of ZIPK did not change upon inhibitor treatment or BCR stimulation (Figure 7.8 A, B). PBMCs from another two patients were stimulated with anti-IgM and subjected to nuclear-cytoplasmic fractionation. ZIPK was localised to both the cytoplasm and the nucleus in cells from both patients and nuclear translocation was not induced after activation of BCR signalling (Figure 7.8 C). However, these experiments do not exclude that ZIPK might become activated by phosphorylation, which was not assessed in this study.

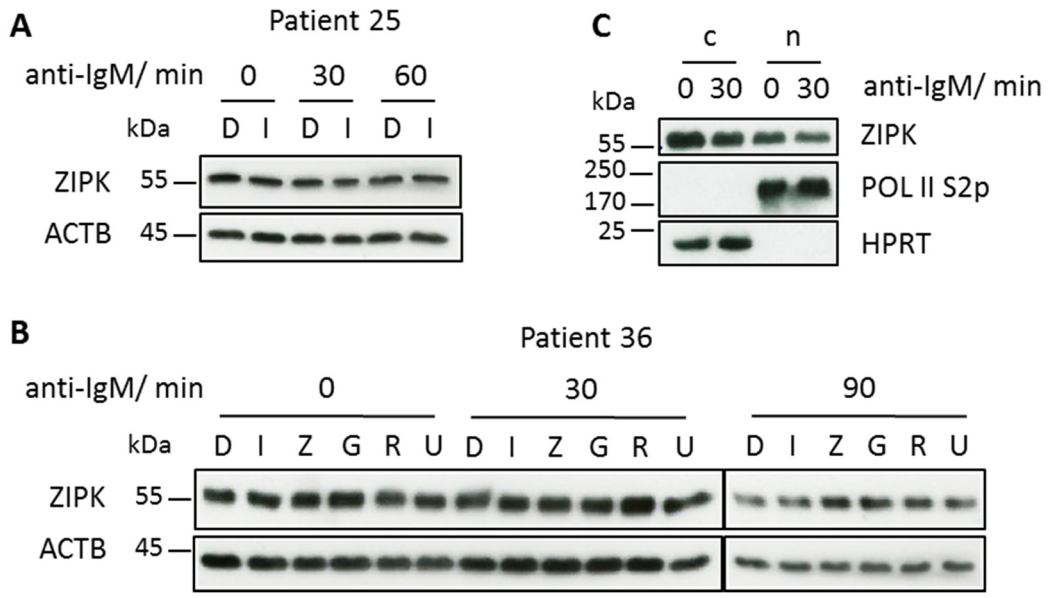

Figure 7.8 Expression of ZIPK in CLL cells in response to BCR signalling and treatment with different inhibitors.
A, **B** PBMCs were treated with DMSO (D), 1 µM Ibrutinib (I), 20 µM DAPK inhibitor (Z), 1 µM Gö6983 (G), 10 µM RSK inhibitor II (R) or 10 µM U0126 (U) for 2 h and then harvested or stimulated with anti-IgM. Protein lysates were prepared and used for western blot. Inhibitor treatment did not affect total levels of ZIPK. However, activating phosphorylation of ZIPK might be altered. **C** PBMCs were left unstimulated or were stimulated with anti-IgM and subjected to nuclear-cytoplasmic fractionation. The western blot shown is representative of two independent experiments. ZIPK was present in both the cytoplasm and the nucleus of CLL cells from both patients before and after stimulation with anti-IgM.

7.4 Analysis of global H3T11 phosphorylation by ChIP-seq

Inhibition of ZIPK led to both the loss of H3T6p and H3T11p and to inhibition of expression of *EGR1* and *DUSP2*. Therefore, H3T11p and H3T6p seemed to be closely associated with activation of gene expression downstream of the BCR. Induction of H3T6p and H3T11p had so far only been detected at the *EGR1* and *DUSP2* genes, but other regions, which were not analysed by ChIP-qPCR, might also be marked by these PTMs. Further, global H3T11 phosphorylation was also detected independent of BCR-stimulation and treatment of CLL cells with PKC inhibitors globally decreased this mark without influencing BCR-induced H3T11 phosphorylation.

Therefore, we wanted to establish, whether H3T6p and H3T11p were globally associated with active genes before BCR cross-linking and/or with genes that became activated downstream of the BCR. Consistently, it was hypothesised that Ibrutinib would inhibit BCR-induced H3T6 and H3T11 phosphorylation. As a first approach, we focussed on H3T11p, because this mark seemed to be more closely associated with gene expression. In one patient, Gö6983, RSK inhibitor II and U0126 all reduced the induction of *EGR1* and *DUSP2* and also H3T11 phosphorylation at these genes, while U0126 did not inhibit H3T6 phosphorylation. Samples of two patients were used for ChIP-seq and they were treated as displayed in Table 7.2.

Unfortunately, although the induction of H3T11 phosphorylation at the *EGR1* and *DUSP2* genes was confirmed by ChIP-qPCR before using the DNA for library preparation, only the input samples and CLL_1 H3T11p_DMSO_0 gave good sequencing results. 3853 peaks were called in the CLL_1 H3T11p_DMSO_0 sample, while only 198 peaks were detected in the CLL_1 H3T11p_DMSO_30 sample and no peaks could be called in any of the other samples, which was most likely due to low amounts of DNA used for library preparation. Therefore, the analysis was mostly restricted to the CLL_1 H3T11p_DMSO_0 sample.

Sample	Drug	Time of anti-IgM stimulation
CLL_1 Input_DMSO_0	**DMSO**	**0 h**
CLL_1 Input_DMSO_30	**DMSO**	**30 min**
CLL_1 Input_Ibrutinib_30	Ibrutinib	30 min
CLL_1 H3T11p_DMSO_0	**DMSO**	**0 h**
CLL_1 H3T11p_DMSO_30	**DMSO**	**30 min**
CLL_1 H3T11p _Ibrutinib_30	Ibrutinib	30 min
CLL_2 Input_DMSO_0	DMSO	0 h
CLL_2 Input_DMSO_30	DMSO	30 min
CLL_2 Input_Ibrutinib_30	Ibrutinib	30 min
CLL_2 H3T11p_DMSO_0	DMSO	0 h
CLL_2 H3T11p_DMSO_30	DMSO	30 min
CLL_2 H3T11p _Ibrutinib_30	Ibrutinib	30 min

Table 7.2 Samples used for ChIP-seq.
Only the samples printed in bold gave good sequencing results and were used for further analysis.

43 or 51.5% of the peaks before or after anti-IgM treatment, respectively, were detected in intragenic regions, about 40% were found in intergenic regions and 15% or 10% were detected in promoters. The distribution of peaks between the different genomic regions was largely unaltered before and after anti-IgM stimulation (Figure 7.9). However, due to the poor quality of the 30 min sample, the analysis will need to be repeated to confirm the results.

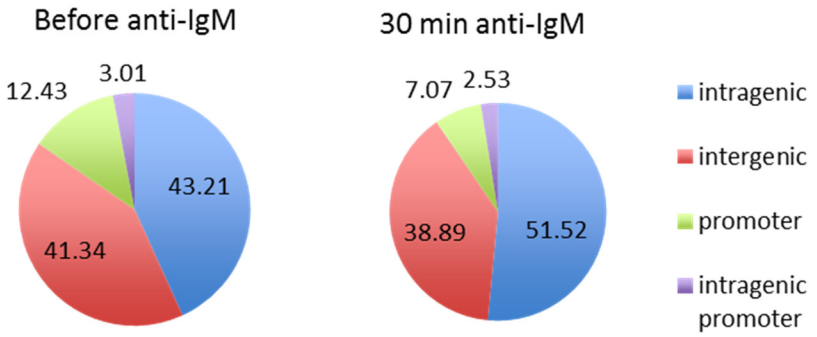

Figure 7.9 Distribution of ChIP-seq peaks annotated using the latest Ref-Seq annotation in the CLL_1 H3T11p_DMSO_0 and CLL_1 H3T11p_DMSO_30 samples.

Then, both the CLL_1 H3T11p_DMSO_0 and CLL_1 H3T11p_DMSO_30 peak sequences were used for a motif analysis with MEME-ChIP, comparing them against the JASPAR CORE and the Jolma vertebrate databases (Machanick & Bailey, 2011). 31% of the peaks in the CLL_1 H3T11p_DMSO_0 overlapped with CTCF motifs with very high confidence, while no CTCF motif was found in the CLL_1 H3T11p_DMSO_30 peaks. The CTCF consensus motif from the Jolma database and the detected motif are shown in Figure 7.10 A. Further, CentriMo analysis showed that the CTCF motif is very strongly centrally enriched in the peak sequences (Figure 7.10 B). As H3, and thus the H3T11p mark, is part of the nucleosome, it was hypothesised that the H3T11p-carrying nucleosome actually blocks binding of CTCF to these sites. Therefore, the sequences for all the peaks containing a CTCF motif were extracted and compared to CTCF ChIP-seq data from GM12878, which is an EBV-transformed lymphoblastoid cell line. In this cell line, 80% of our CTCF motif-containing peaks would overlap with actual CTCF binding sites. Consequently, if CTCF binding sites are conserved in CLL cells, 24% of the H3T11p peaks overlap with CTCF and the nucleosome would not block CTCF binding to the chromatin.

The second motif discovered with high confidence in 66% of the CLL_1 H3T11p_DMSO_0 peaks and in over 80% of the CLL_1 H3T11p_DMSO_30 peaks is an ETS factor motif (SPI1, SPIC, SPIB). The consensus and detected motifs are shown in Figure 7.10 C. ETS factor motifs were not as strongly centrally enriched in the CLL_1 H3T11p_DMSO_0 peaks as CTCF motifs (Figure 7.10 D). Further, 50% of the CLL_1 H3T11p_DMSO_0 peaks overlap with E boxes (Figure 7.10 E) and 25% of the peak sequences have a ZIC consensus binding site (CCCCCCGGGGGGG) (Figure 7.10 F), both of which are also centrally enriched.

In conclusion, H3T11p seemed to generally overlap with regulatory regions in CLL cells. Indeed, when CLL_1 H3T11p_DMSO_0 peaks were compared to the H3K27ac track of GM12878 cells, over 50% overlapped with this mark and only 10% of the peaks overlapped with both H3K27ac and CTCF, indicating that there might be two different groups of H3T11 phosphorylated regions, those that overlap with active regulatory elements, and those that overlap with structural sites.

Because ZIPK has been shown to bind to STAT3, which is constitutively active in CLL cells and is also activated downstream of the BCR (Hazan-Halevy et al., 2010; Rozovski et al., 2014), CLL_1 H3T11p_DMSO_0 peak data were also compared to STAT3 ChIP-seq peaks from GM12878 cells and it was found that 30% of the CLL H3T11p peaks overlap with STAT3 sites.

A few example ChIP-seq peaks are shown in Figure 7.11, Figure 7.12 and Figure 7.13. Although only a few strong peaks could be called in the CLL_1 H3T11p_DMSO_30 data set, some interesting results could be obtained. For example, a new H3T11p peak occurred in the *CDK14* intragenic alternative promoter 30 min after BCR stimulation, which might indicate activation of *CDK14* expression (Figure 7.11). CDK14 is a cyclin-dependent kinase, which associates with CCND3 and promotes cell cycle progression at the G1/M border (Shu et al., 2007). Another H3T11p peak was only seen in unstimulated cells and overlapped with a PU.1 binding site in GM12878 cells. Both peaks were found in H3K27 acetylated, regulatory regions (Figure 7.11).

In Figure 7.12, a constitutive H3T11p peak is shown within the *TNFRSF17* gene, which encodes for a BAFF-R that is constitutively expressed on CLL cells (Endo et al., 2007). This peak also overlaps with H3K27ac and a PU.1 site. Upstream of the *SYK* gene, a H3T11p peak that overlaps with a CTCF-site but not with H3K27ac in GM12878 cells, was detected in unstimulated CLL cells. Furthermore, two more peaks were seen in the *SYK* intragenic promoter, overlapping with H3K27ac (Figure 7.13).

More H3T11p peaks were detected around other genes associated with normal B and CLL cells. Peaks in the *TLR4* and the *BLNK* promoter and enhancer were present in both CLL_1 H3T11p_DMSO_0 and _30, peaks near the *CD5*, *LYN* and *CXCR4* genes were called in CLL_1 H3T11p_DMSO_0 only.

In summary, H3T11p was generally associated with active promoters and enhancers, as well as structural chromatin regions in CLL cells, both before and after BCR stimulation.

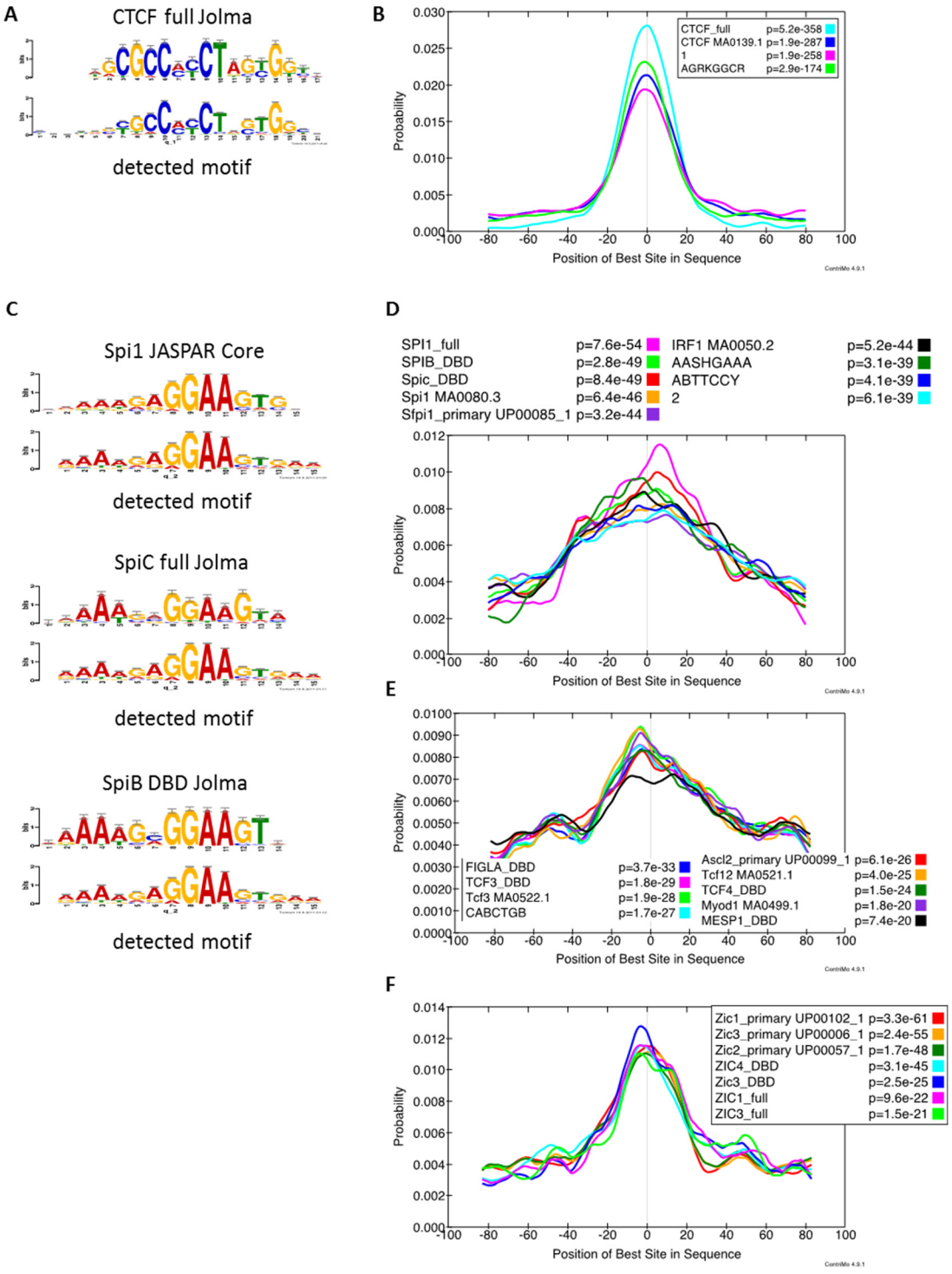

Figure 7.10 Motifs predicted by MEME-ChIP to be enriched in the peak data from CLL_1 H3T11p_DMSO_0.

A The consensus CTCF motif aligned with the motif detected in the peak sequences. **B** CentriMo plot showing central enrichment of the CTCF motif in the peak sequences. The CTCF motif was the motif detected with the lowest p-value, which is the probability to randomly find this motif enriched in any set of sequences. **C** The consensus SPI1, SPIC and SPIB motifs aligned with the motif detected in the peak sequences. **D**, **E**, **F** CentriMo plots showing central enrichment of the ETS, E box and ZIC motifs in the peak sequences.

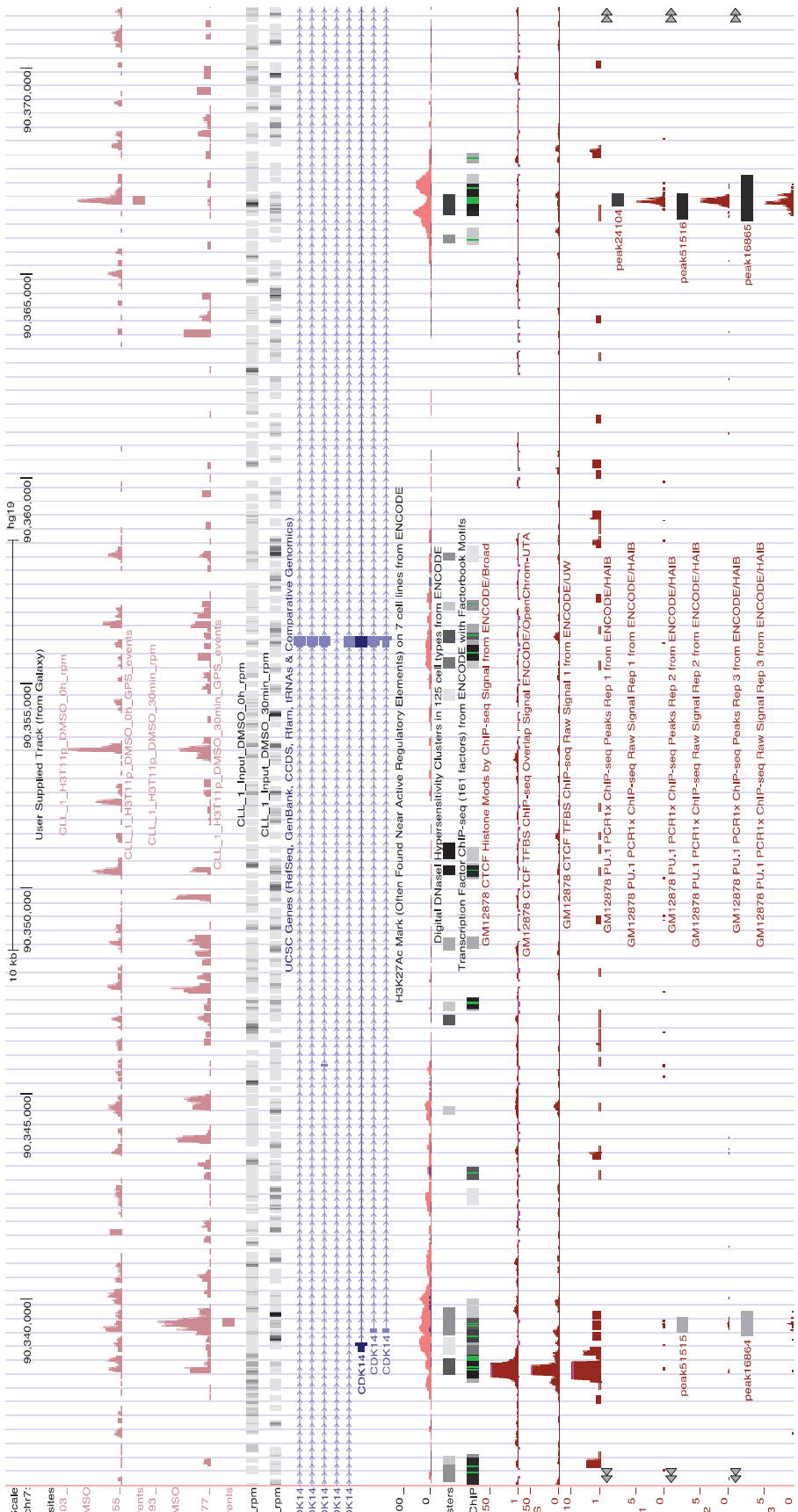

Figure 7.11 UCSC genome browser track of the *CDK14* gene.
ChIP-seq peaks for H3T11 before (top) and after 30 min anti-IgM stimulation (second from top) are shown. Below the two tracks, the inputs are displayed. Then, annotations for the CDK14 gene from different sources and H3K27ac marks in GM12878 (pink) and K562 cells (purple), followed by DNase hypersensitive sites and transcription factor ChIP-seq results are shown. The bottom six tracks are GM12878 ChIP-seq tracks for CTCF and PU.1 (SPI1). A specific H3T11p peak was detected in the *CDK14* promoter only after BCR cross-linking. Before cross-linking, a H3T11p peak was detected within the gene, overlapping with a putative PU.1 site.

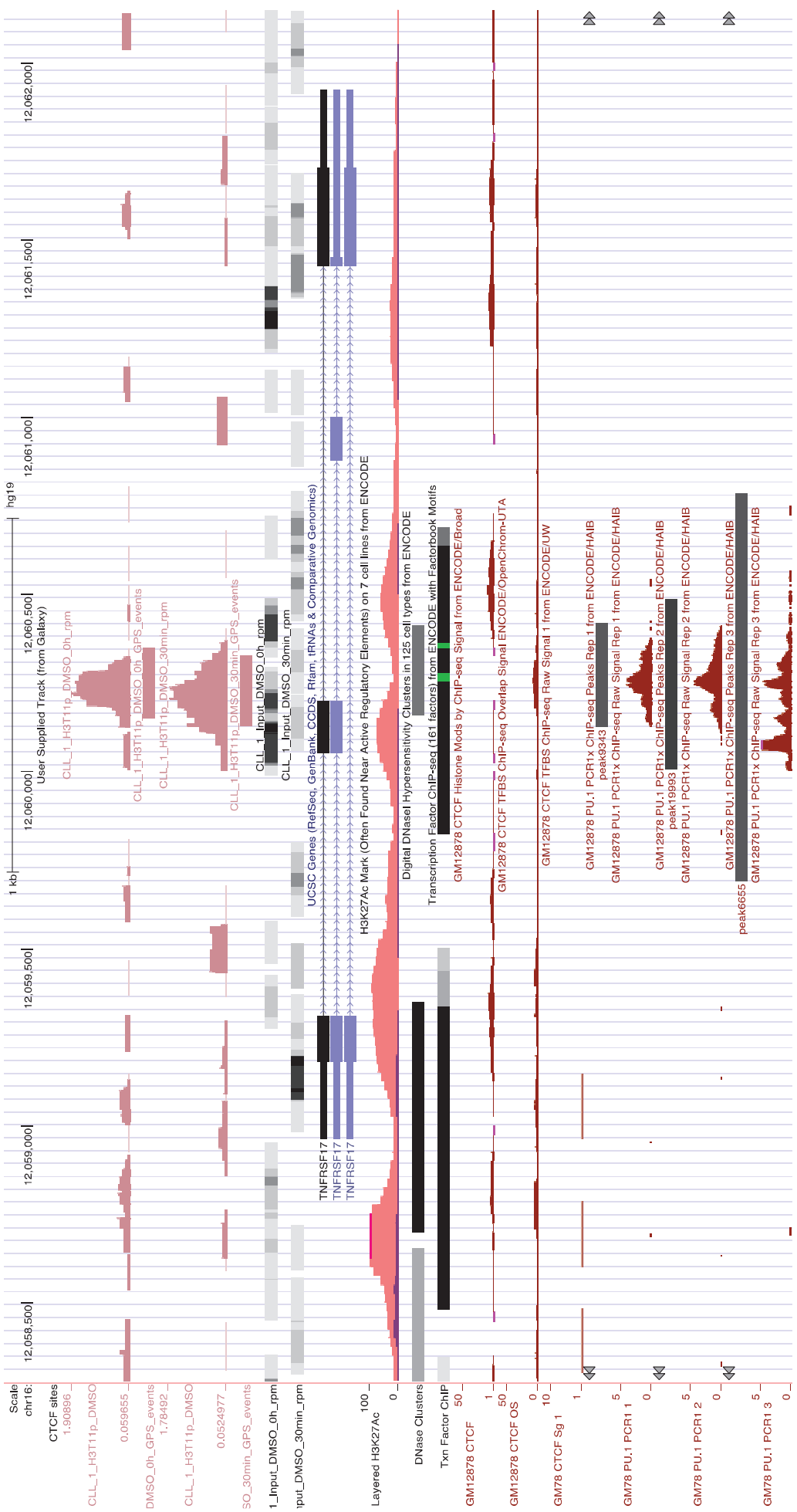

Figure 7.12 UCSC genome browser track of the *TNFRSF17* gene.
The tracks are the same as in Figure 7.11. A constitutive H3T11p peak can be seen in the *TNFRSF17* gene, overlapping with a PU.1 site.

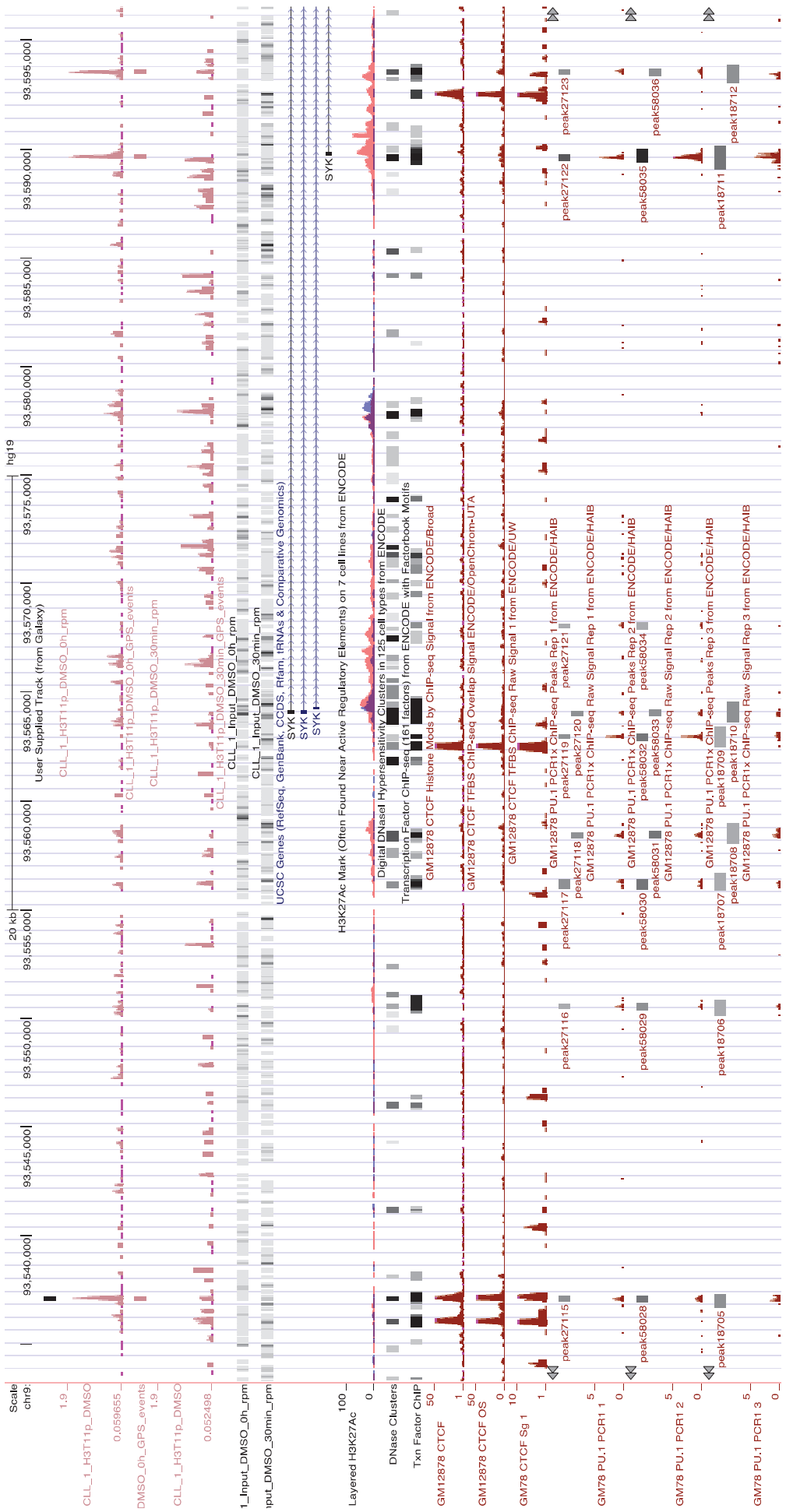

Figure 7.13 UCSC genome browser track of the *SYK* gene.
The tracks are the same as in 7.11. One H3T11p peak was detected in unstimulated cells upstream of the *SYK* gene, overlapping with a CTCF site. Two more peaks were called in a downstream promoter region, one of which overlapped with a PU.1 binding site.

8 Discussion

8.1 PIM kinases in DLBCL and BL

8.1.1 Summary of main results

Consistent with the literature (Brault et al., 2012; Gómez-Abad et al., 2011), PIM kinase inhibition was found to only marginally affect the viability of ABC-DLBCL cell lines. Further, the MYC-dependent Burkitt lymphoma cell lines were capable of growing independent of PIM kinase activity. Only knockdown of PIM2 decreased proliferation of Raji cells.

PIM1 and MYC were bound to the *GNL3* promoter and the H3K9acS10p mark was present in this region as assessed by ChIP. However, inhibition of PIM kinases, overexpression of PIM1 or knockdown of PIM1 and/or PIM2 did not alter expression of *GNL3*, although changes in PIM1 and H3K9acS10p occupancy at the promoter could be observed.

However, PIM kinases might be implicated in stress response pathways, as PIM1 was upregulated after both serum shock and serum starvation and was elevated at the *GNL3* promoter after DRB treatment. Consistently, both PIM1 and PIM2 have been shown previously, to be involved in different stress response pathways (Jian Chen et al., 2009; Zemskova et al., 2008; Zirkin et al., 2013).

8.1.2 PIM kinase inhibition alone did not efficiently reduce the viability of DLBCL and BL cell lines *in vitro*

The small molecule inhibitors SMI4a and inh VI efficiently inhibited viability of the two Burkitt lymphoma, the two ABC-DLBCL and the two GCB-DLBCL cell lines *in vitro*. Quercetagetin additionally reduced the viability of the Raji, Ramos, OCI-Ly19 and SUDHL6 cell lines. However, the reduced viability is possibly due to inhibition of several kinases and might be independent of PIM kinase inhibition. First, OCI-Ly19 cells did not express detectable levels of PIM1 and PIM2, but viability was as strongly or even more strongly inhibited as in the other cell lines. Second, all three inhibitors have been described to target several kinases other than PIM1/2/3, which might also be important for lymphoma cell survival. Quercetagetin does, for example, inhibit JNK and PI3K (Baek et al., 2013), as well as Aurora A, B and C, which leads to mitotic arrest and to induction of apoptosis (Jung et al., 2014). Other kinases, which might play a role in lymphoma cell survival and are inhibited by

Quercetagetin, include DYRK1A, DYRK2, DYRK3, AKT2, RSK2, TAK1 and YES1 (http://www.kinase-screen.mrc.ac.uk, see appendix). SMI4a and inh VI (also called SMI16a) are structurally similar inhibitors and both are also active against DYRK1A (Xia et al., 2009), which does for example phosphorylate and inhibit GSK3β (W.-J. Song et al., 2014), so that it might have oncogenic potential. Further, both inhibitors are structurally very similar to potent PI3K inhibitors (Pinson et al., 2011), making it plausible that PI3K is also inhibited by SMI4a and inh VI. Because BL cells are dependent on PI3K activity (Schmitz et al., 2012), inhibition of PI3K might be the reason for the strong inhibition of BL cell viability by SMI4a and inh VI. Inhibition of other kinases is very likely, because all inhibitors were used at very high concentrations of 40 μM, while SMI4a and inh VI have IC_{50} values of less than 150 nM for both PIM1 and PIM2. In keeping with such an off-target effect, BAD-S112 phosphorylation, which is a major target of PIM kinases, was inhibited in OCI-Ly3, but not in Raji, Ramos and OCI-Ly10 cells until day 6 of treatment. Further, none of the inhibitors blocked the induction of the *FOSL1* gene in HEK293 cells after serum shock, which had been described by Zippo et al. to be a PIM1-dependent effect. The main target of these inhibitors might therefore not be PIM1. In support of this, a potent and seemingly more selective inhibitor of PIM kinases, AZD1208, did not significantly reduce the viability of BL or ABC-DLBLC cell lines. AZD1208 has been extensively tested against a panel of 442 kinases and inhibited only 13 kinases other than PIM1/2/3 by 50% or more, but was still at least 43-fold selective for PIM kinases (Keeton et al., 2014). In the study by Keeton et al., AZD1208-sensitive cell lines showed increased apoptosis already at 1 μM AZD1208 (Keeton et al., 2014). At this concentration none of the cell lines tested in our study displayed reduced viability, while AZD1208 efficiently inhibited BAD-S112 phosphorylation in the two BL and the two ABC-DLBCL cell lines. In agreement with a previous study, in which pan-PIM kinase inhibition led to stabilisation of PIM3 (Z. Guo et al., 2014), efficient inhibition of PIM kinases also led to a stabilisation of PIM1 and PIM2 in our study. Of note, SMI4a treatment did not stabilise PIM1 or PIM2. In conclusion, inhibition of PIM kinases alone does not seem to inhibit the viability of BL and DLBCL cell lines.

However, the effect of PIM kinase inhibition on BL and DLBCL cells has so far, in this and other studies (Brault et al., 2012; Gómez-Abad et al., 2011), only been assessed *in vitro*. PIM kinases might be more important for cell growth and survival under *in vivo* conditions, when suboptimal and changing levels of growth and survival factors are present, when cells encounter oxidative stress or nutrient deprivation. I could show that PIM1 is induced in the Raji BL cell line both by serum

starvation and by serum shock and its levels were also altered after simply changing the culture medium. However, this seems to be more a stress response than a response to growth factors, as stimulation of pro-survival pathways by BCR cross-linking or PMA treatment did not lead to upregulation of PIM kinases. Therefore, PIM kinase levels seemed to be very sensitive to any environmental change. This is in keeping with previous studies showing that PIM kinases are induced by several stressors, like DNA damage in U2OS osteosarcoma and in neuronal cells (Yi Zhang et al., 2010; Zirkin et al., 2013), oxidative stress in cardiomyocytes (Borillo et al., 2010) and hypoxia in pancreatic cancer (J. Chen et al., 2009; Reiser-Erkan et al., 2008). Inhibition or knockdown of PIM kinases renders cells more sensitive to these stress conditions, so that PIM kinase inhibition might enhance apoptotsis of BL or DLBCL cells *in vivo* (Jian Chen et al., 2009; Zirkin et al., 2013; Hsu et al., 2012). Further, PIM kinases induce resistance of cells to chemotherapy and knockdown or inhibition of these proteins sensitises cells to apoptosis induced by chemotherapeutic agents, like Docetaxel (Zemskova et al., 2008), Paclitaxel (Hsu et al., 2012) or Cytarabine (Kelly et al., 2012). Therefore, PIM kinase inhibition might still be a valid therapeutic strategy in combination with other chemotherapeutic drugs *in vivo*. Combined inhibition of PIM kinases and the AKT pathway has been suggested as a promising therapeutic strategy for the treatment of AML (Meja et al., 2014) and might also be effective against prostate cancer (Toren & Zoubeidi, 2013). These findings are reinforced by a study showing that targeting cap-dependent translation, which is activated by both the AKT and PIM pathways is a valid therapeutic approach in B cell lymphoma (Schatz et al., 2011). Therefore, combination therapy with an AKT and a PIM kinase inhibitor should also be evaluated in BL and DLBCL.

Apart from PIM kinase inhibition, knockdown of PIM1 did not inhibit Raji cell viability, while PIM2 knockdown reduced cell numbers after several days. One could argue that PIM2 might be the more important kinase for Burkitt lymphoma cell proliferation and survival. PIM2 is more frequently overexpressed in different haematological malignancies than PIM1 and is more significantly associated with the activation of oncogenic pathways (Gómez-Abad et al., 2011). However, only inhibition of all PIM kinases effectively induced apoptosis of BCL cell lines in the study by Gómez-Abad et al. In my study, the knockdown of PIM2 was more efficient than that of PIM1, so that a dose-effect might play a role. If a certain amount of PIM kinases is present in the cell, no phenotypic effect can be observed. However, if the levels fall beneath a certain threshold, cell viability would be affected. Because pan-PIM kinase inhibition did not significantly reduce cell viability, although it clearly

abrogated PIM activity as assessed by BAD phosphorylation, it can be hypothesised that PIM kinases might have kinase-independent functions in DLBCL and BL. This is in agreement with findings by Hogan et al. and Wood et al., showing that overexpression of kinase-dead PIM1 can mimic some functions of active PIM1 (Hogan et al., 2008; Wood et al., 2009). Further, PIM1 is recurrently targeted by aberrant somatic hypermutation in DLBCL, but out of 5 mutant proteins analysed, only one showed increased kinase activity, while three mutants were significantly less active than the wildtype protein (Kumar et al., 2005), which also indicates that PIM kinases might have kinase-independent functions in lymphomagenesis. Alternatively, their expression could be maintained as a result of increased NFκB activity in ABC-DLBCL, although the protein itself is redundant. Thus, PIM kinases might just be “messengers” of the level of NFκB or STAT activity in these cells, without having any vital function in tumour cell proliferation or survival. This is in agreement with the findings by Brault et al. that PIM kinase expression correlates with active STAT3 and STAT5 and their hypothesis that PIM kinases are progression markers, but not bona fide therapeutic targets in DLBCL (Brault et al., 2012).

The efficient inhibition of cell viability by PIM2 knockdown but not by pan-PIM inhibition could also be interpreted as PIM2-mediated inhibition of PIM1. PIM1 binding to the *GNL3* promoter and H3K9acS10p in this region were increased in PIM2 knockdown cells, which might be a consequence of direct competition, or it might indicate other antagonistic functions of PIM1 and PIM2. PIM2 could, for example, inhibit nuclear translocation of PIM1 or inhibit association of PIM1 with the chromatin. This would mean that PIM1 has anti-tumour effects in BL, which would be counteracted by PIM2, because knockdown of PIM2 decreased cell viability, while knockdown of PIM1 alone or inhibition of both kinases with AZD1208 did not. This theory would also be in agreement with the reduced kinase activity of somatically hypermutated PIM1 in DLBCL. Furthermore, activation of the BCR led to an unexpected reduction in PIM1 mRNA expression in the Raji cell line as well as in primary B cells from CLL patients. Similarly, PMA treatment led to a reduction in PIM protein expression. Signalling via the BCR is supposed to enhance proliferation and survival of B cells, indicating that PIM1 might indeed inhibit B cell proliferation and survival, at least in response to certain stimuli or under certain environmental conditions. These findings are in apparent disagreement with PIM kinases being potent oncogenes in murine B and T cell lymphomas. However, expression of PIM kinases is associated with a good prognosis in prostate and pancreatic adenocarcinomas (Dhanasekaran et al., 2001; Reiser-Erkan et al., 2008) and

overexpression of PIM kinases has been associated with the induction of apoptosis in rat fibroblasts (Mochizuki et al., 1999) and with increased p53 levels (Hogan et al., 2008; Zemskova et al., 2010). A recent study implicates PIM1 in the induction of cellular senescence through the formation of heterochromatin, which suppress pro-proliferative genes (Jin et al., 2014). Therefore, its functions, like those of most oncogenes, might depend on the status of a cell, the cell type and the presence, absence or activation of other proteins.

In conclusion, PIM kinases do not seem to be useful exclusive targets for the treatment of DLBCL or BL. Pan-PIM kinase inhibitors might, however, be effective *in vivo* and in combination with DNA-damaging chemotherapeutics or AKT pathway inhibitors, but this remains to be evaluated.

8.1.3 PIM kinases might be dispensable for MYC-dependent gene expression in unstressed Raji cells

I have shown that MYC and PIM1 bind to the *GNL3* promoter and the *NPM1* enhancer in Raji, Ramos and OCI-LY10 cells. Both genes also displayed an active gene signature in Raji cells. They showed increased occupancy of POL II S2p towards the 3' end and they were marked by H2Bub. Further, high levels of total and S5 phosphorylated POL II, possibly representing paused POL II, were found in the 5' regions of the gene, overlapping with the MYC and PIM1 binding sites, matching the finding that MYC and PIM1 are important for pause release and elongation but not initiation of transcription (Eberhardy & Farnham, 2002; Zippo et al., 2009; Zippo et al., 2007). At the *GNL3* promoter, the dual H3K9acS10p mark was also detected, while the single H3S10p mark was mostly absent at both genes.

GNL3 had been described before as a MYC-regulated gene in murine B cells and has been shown to be essential for MYC-induced tumourigenesis *in vitro* in rat fibroblasts and human colon cancer cells and *in vivo* in MYC transgenic mice (Zwolinska et al., 2011). I could, however, not confirm a direct regulation of *GNL3* expression or expression of its three intronic snoRNAs by MYC in the Raji cell line. Knockdown of MYC decreased its binding to the *GNL3* promoter, but did not affect expression of the *GNL3* gene or the snoRNAs. The discrepancies between the two studies might arise from the different cell types and the different approaches used. Zwolinska et al. overexpressd MYC and saw an increase in *GNL3* expression, which might be due to MYC occupying novel binding sites in *GNL3* enhancers. Alternatively, the effect on *GNL3* expression might be indirect, through MYC

upregulating other transcription factors that then influence *GNL3* expression. Knockdown of MYC, however, might not influence *GNL3* expression, because only a low level of MYC might be required to facilitate *GNL3* expression or because other transcription factors present at the *GNL3* promoter maintain its expression independent of MYC. A study on 59 different transcription factors conducted by Cusanovich et al. also showed that genes that are bound by a transcription factor do mostly not change their expression upon knockdown of this factor (Cusanovich et al., 2014). These sites were called non-functional sites. However, transcription factor binding sites around 10 kb of the TSS were assigned to each gene, without actual knowledge about the real target gene. Consistently, MYC and PIM1 might be bound to the *GNL3* promoter but might influence the expression of another gene, for example the *PBRM1* gene, which has a promoter overlapping with the *GNL3* promoter. Alternatively, the *GNL3* promoter region might be a long-distance enhancer for another gene, which could be regulated by MYC. In support of this hypothesis, promoters have been shown to interact with each other, even over long distances, and to influence each other's expression (Li et al., 2012). Another possibility is that changes in *GNL3* expression were not detected, because all expressed genes might have been downregulated in Raji cells, in agreement with recent findings that MYC amplifies expression of all genes (Lin et al., 2012; Nie et al., 2012; Rahl et al., 2010). Normalisation of *GNL3* expression to that of another gene would therefore mask the reduction in its expression. Further, the reduction in MYC binding to the promoter did not affect recruitment of PIM1 or H3K9acS10p in this region, making it possible that PIM1 might be recruited in a MYC-independent fashion to maintain expression. For example, one of the other MYC family proteins, MYCN or MYCL, might occupy the E box element in absence of MYC and recruit PIM1. Alternatively, since PIM1 recruitment to the promoter was very low as assessed by ChIP-qPCR, even low MYC levels may suffice. Therefore, PIM1 but not MYC might be the limiting factor for complex formation between the two proteins.

Overexpression of PIM1, knockdown of PIM1, PIM2 or PIM1 and PIM2 or inhibition of PIM kinases using SMI4a, inh VI, Quercetagetin or AZD1208 did also not show any effect on *GNL3* and intronic snoRNA expression. Consistently, *PIM1* expression in the different lymphoma cell lines did not correlate with *GNL3* expression. While *PIM1* and *PIM2* mRNA levels were variable, the levels of *GNL3* and the snoRNAs were similar between the different BL and DLBCL cell lines. However, levels of nuclear PIM1 were very low in all the cell lines, which might be the reason for the similar *GNL3* expression levels. Overexpressed PIM1

translocates to the nucleus, but I could not determine, whether it is bound to the *GNL3* promoter, because all attempts to perform ChIP in PIM1-overexpressing cells failed. Nevertheless, overexpression of PIM1 led to a downregulation of PIM2 expression, indicating that the overexpressed protein is functional. This suggests that *GNL3* might not be a PIM1-regulated gene in non-stimulated and -stressed Raji and SUDHL6 cells.

Binding of PIM1 to the promoter decreased after knockdown, but H3K9acS10p was unaffected, which might indicate that PIM1 is not responsible for H3S10 phosphorylation at the *GNL3* promoter. However, treatment of Raji cells with AZD1208 increased total PIM1 and chromatin-associated PIM1 at the *GNL3* promoter but reduced H3K9acS10p in this region. Furthermore knockdown of PIM2 led to an increased recruitment of PIM1 and a concomitant increase in H3K9acS10p, which was not seen in PIM1/2 double knockdown cells. Together these observations support the argument that PIM1 is indeed one of the kinases phosphorylating H3S10 at the *GNL3* promoter. The lack of effect of PIM1 and the PIM1/2 double knockdown on H3K9acS10p levels could be explained by MYC or another transcription factor recruiting a different H3S10 kinase in the absence of PIM1. Following AZD1208 treatment, the presence of inactive PIM1 at the promoter would block the recruitment of the alternative kinase. Because the PIM1/2 double knockdown did not reduce phosphorylation of H3S10, PIM2 is most likely not the alternative H3S10 kinase. Alternatively, the remaining PIM1 at the GNL3 promoter might be sufficient to mediate H3S10 phosphorylation or feedback regulation might reduce the activity of phosphatases for H3S10 and thus maintain H3S10p levels, although kinase activity is reduced. Consistent with such a model, the H3S10 phosphatase MKP1 has been shown to preferentially bind histone H3 that is phosphoacetylated (Gadewal et al., 2013).

The experiments after PIM2 knockdown and AZD1208 treatment showed that the H3K9acS10p levels at the *GNL3* promoter did not correlate well with *GNL3* expression. S10 phosphorylation might be important for the induction of gene expression, but once a gene is active, this chromatin mark might be dispensable. H3S10 phosphorylation is usually a very transient mark (Barth & Imhof, 2010; Jackson et al., 1975), which only appears in the promoters of inducible genes after stimulation of cells with growth factors, cytokines or after exposure to stress (Li et al., 2001; Mahadevan et al., 1991; Soloaga et al., 2003; Yamamoto et al., 2003; Zippo et al., 2007). This mark might lead to the establishment of other chromatin marks, the recruitment of transcription factors and other chromatin-bound proteins, which could form a stable complex at promoter or enhancer regions without the

need for prolonged maintenance of the H3S10p mark. The gene would then continue to be in an active state, independent of the presence of PIM kinases and the H3S10p mark. Several histone marks are only established upon transcription of a gene because the modifying enzymes are recruited to the transcribing POL II or require the presence of other transcription-associated histone marks for their efficient establishment. Examples of such marks include H2Bub, which requires ongoing transcription to be deposited (Kim et al., 2009), H3K4me3, which is stimulated by H2Bub (Kim et al., 2009; Milne et al., 2010; Muntean et al., 2010), H3K36me3, because SETD2 most likely interacts with the elongating POL II (Kizer et al., 2005) and H3K79me3, because the enzyme DOT1L also interacts with the elongating POL II and is stimulated by H2Bub (S.-K. Kim et al., 2012; McGinty et al., 2008; McGinty et al., 2009). These methylation marks are then capable of recruiting transcription factors or chromatin modifiers to activate transcription independent of H3 phosphorylation. Indeed, recruitment of BRD4 and thus P-TEFb, which has so far been shown to be the main function of PIM1-mediated H3S10p, can be generally mediated by acetylated histones (Dey et al., 2003) and transcription factors, like NFκB (Huang et al., 2009), indicating that H3S10p is not obligatory for this function.

PIM1 also seems to be dispensable for global regulation of MYC-dependent genes in unstressed cells. MYC knockdown efficiently and rapidly reduced Raji cell viability, confirming that these cells are dependent on MYC. However, knockdown of PIM1 or inhibition of PIM kinases had no such effect, although PIM1 had been shown to be required for the expression of 20% of the MYC-regulated genes in HEK293 cells 120 min after serum shock (Zippo et al., 2007). The results from our study show that PIM kinase activity seems to be dispensable for the maintenance of expression of MYC-dependent genes under stable environmental conditions. However, because PIM1 is generally induced under cellular stress conditions, it might be possible that “switching on” new genes requires its activity, which would match the findings of Zippo et al., as well as our findings that expression of the *GNL3* gene was maintained at a constant level in unstressed Raji cells, independent of the presence of MYC, PIM1 or the level of H3K9acS10p at the promoter. This is in agreement with the very low nuclear levels of both PIM1 and PIM2 in all six B cell lymphoma cell lines used in this study. After stimulation of cells with growth factors, or when cells are exposed to stress conditions, nuclear translocation of PIM kinases might be induced to facilitate the induction of gene expression. Consistent with this, it has been shown that irradiation or stimulation

with EGF induced nuclear translocation of PIM1 in squamocellular cancer cells (Peltola et al., 2009).

Therefore, the small effect of AZD1208 on the viability of ABC-DLBCL cell lines is most likely also independent of the inhibition of MYC-mediated transcription, but dependent on other cellular activities of PIM kinases. Indeed, PIM kinases have been shown to target a plethora of substrates, including cell cycle and apoptosis regulators, other transcription factors and the cap-dependent translation machinery. Moreover, several studies have shown already that expression of PIM kinases does not correlate with MYC in DLBCL (Brault et al., 2012) or lymphoid and myeloid leukaemias (Amson et al., 1989).

In summary, it seems that PIM kinases are not required for MYC-dependent transcription under steady-state conditions. Consistently, H3K9acS10p might not be required to maintain transcription at already active genes, like *GNL3*, but might be essential to activate the expression of repressed genes. Therefore, PIM kinases could play a role in lymphoma development and maintenance under conditions, where changes in gene expression are required.

8.1.4 PIM1 and MYC might have transcription-independent functions at the *GNL3* gene

Although PIM1 and MYC do not regulate *GNL3* expression under our experimental conditions, they are bound to the *GNL3* promoter and it is therefore likely that they fulfil some function in this region. It was first hypothesised that PIM1 might, like IKKα bind to the POL II CTD and travel with the elongating POL II along the gene. IKKα had been shown to phosphorylate HP1γ and to be loaded from the POL II CTD onto the chromatin in an HP1γ-dependent fashion. HP1γ would then inhibit IKKα-dependent H3S10 phosphorylation but stimulate its activity towards H3.3S31 (Thorne et al., 2012). However, several lines of evidence indicate that PIM1 does not travel with the elongating POL II. First, in contrast to IKKα, PIM1 was mainly associated with the promoter and not the 3' region of the *GNL3* and *NPM1* genes. This could, however, also be a result of the relatively low transcription rate of the *GNL3* gene as compared to the murine *Tnf* gene, so that sufficient amounts of PIM1 could just not be detected in the gene body. Second, both H3K9acS10p and the possible PIM1 target H3.3S31p were only associated with the *GNL3* and *NPM1* promoter regions and not the 3' end. And third, association of PIM1 with the *GNL3* gene was independent of transcriptional elongation, as assessed after DRB

treatment. Quite the contrary, PIM1 association with the promoter region increased when elongation was inhibited. PIM1 might therefore be recruited to the chromatin upon stalling of the polymerase and function in the transcriptional stress response. PIM1 might, in contrast to IKKα, associate with the S5-phosphorylated POL II, but it could also be recruited completely independent of the polymerase. As mentioned before, *GNL3* and *Tnf* are kinetically very different genes. While the former is a housekeeping gene, which is constitutively active, the latter is rapidly and strongly induced upon stimulation of macrophages with LPS. Thus, the requirement for nucleosome remodelling and histone turnover are likely to be very different at both genes and IKKα-mediated H3.3S31 phosphorylation might play a role in these processes. It has, for example been shown that ZMYND11 binds H3.3K36me3 and critically recognises the S31 residue (Qin & Min, 2014; Wen et al., 2014). ZMYND11 represses elongation (Wen et al., 2014) and regulates splicing, stimulating intron inclusion (R. Guo et al., 2014). One can imagine that phosphorylation of the H3.3S31 site would change the binding of ZMYND11 to H3.3K36me3, possibly inhibiting its recruitment and allowing for the high elongation rate necessary for LPS-induced *Tnf* expression, which is not necessary at the *GNL3* gene.

Further, MYC has been shown to regulate the induction of DNA replication independent of its effects on transcription (Dominguez-Sola et al., 2007). MYC does not participate in the recruitment of the origin recognition complex, but mediates origin licensing (Swarnalatha et al., 2012). Of note, origins of replication often overlap with TSS of coding and non-coding genes (Dellino et al., 2013). After synchronisation of Raji cells using a thymidine-nocodazole block, MYC was recruited to the *GNL3* promoter in a cell cycle-dependent fashion. Its recruitment peaked in late G1/early S phase, when origin-licensing takes place (Machida et al., 2005), and association of PIM1 with the chromatin was also high in late G1 and throughout S phase. It might therefore be possible that MYC and PIM1 regulate DNA replication from the *GNL3* promoter. They could coordinate the expression of *GNL3* and DNA replication throughout the cell cycle by inhibiting replication from the *GNL3* promoter, which would be in agreement with the observed constant expression of *GNL3* during S phase. Transcription and DNA replication are temporally separate in S phase, with early replicating genes being transcribed late in S phase and late replicating genes being transcribed early (Meryet-Figuiere et al., 2014). This separation needs to be tightly regulated, as head-on collisions between POL II and the DNA polymerase lead to recombination events (Prado & Aguilera, 2005). In this context, it had been shown that a stress-activated kinase in

yeast inhibits DNA replication upon osmotic stress, when transcription is required (Duch et al., 2013). PIM1 might have a similar role at the *GNL3* gene. Alternatively, MYC and PIM1 might activate replication from the *GNL3* promoter. This is consistent with a known function of yeast 14-3-3 proteins in replication (Yahyaoui & Zannis-Hadjopoulos, 2009). PIM1 might phosphorylate H3S10 or other target proteins and facilitate the recruitment of 14-3-3 proteins and thus DNA replication. However, the activation of too many origins, for example after MYC overexpression, results in DNA damage and the occurrence of γ-H2A.X (Dominguez-Sola et al., 2007). Interestingly, PIM1 and PIM2 have been implicated in DNA repair and the removal of γ-H2A.X foci (Hsu et al., 2012; Zirkin et al., 2013). They might therefore contribute to MYC-induced transformation by resolving MYC-induced replication stress.

8.1.5 Limitations of the study and future directions

One limitation was that the study was conducted *in vitro* in cell lines. As mentioned earlier, effects of PIM kinase inhibition under physiological, non-optimal conditions might have a different effect on survival and proliferation of lymphoma cells. Further, stable knockdown cells were generated only from EBV-transformed Raji cells and it is possible that knockdown of PIM kinases might have a different effect on the viability of other, non-EBV transformed Burkitt lymphoma or ABC-DLBCL cell lines. In the future, it would be interesting to see, whether PIM kinase inhibition is useful as a combination therapy together with other kinase inhibitors, for example PI3K inhibitors, or together with DNA-damaging agents. However, it seems that most PIM kinase inhibitors, which have been used so far, target multiple kinases and the results of our study indicate that PIM kinases are not the main targets. It is therefore difficult to determine, which effects on cell viability are actually mediated by PIM kinases and which are due to the inhibition of other targets.

Effects of PIM kinases on MYC-dependent transcription should in the future be studied in an inducible system, because H3S10 phosphorylation does not seem to be important for the regulation of constitutively expressed genes, but mainly for the activation of immediate gene expression in response to external stimuli (Li et al., 2001; Mahadevan et al., 1991; Soloaga et al., 2003; Yamamoto et al., 2003; Zippo et al., 2007). Therefore, it is not surprising that PIM kinases did not affect MYC-dependent transcription in general in exponentially growing, unstimulated cells. I tried to induce PIM kinase expression in Raji cells by a defined stimulus, but neither BCR cross-linking, nor PMA treatment led to an induction of PIM1.

Another difficulty encountered during this study was that three of the four PIM1 antibodies tested, were not specific for PIM1 and did not even detect the endogenous protein in western blot. Further, validation of the antibody used for ChIP was very tedious, because it bound to multiple proteins as assessed by western blot and it was not clear, whether PIM1 was one of those. The antibody did, however, precipitate PIM1 in both conventional IP and ChIP experiments, but because any manipulation of PIM kinases did not alter expression of *GNL3*, we were concerned about its specificity. It was unclear, whether the protein associated with the *GNL3* promoter was actually PIM1 or another, unknown protein. There was no known positive control region available to compare the signal to, because the only known PIM1 target regions upstream of the *FOSL1* and *ID2* genes were not bound by PIM1 in non-induced cells, consistent with the absence of *FOSL1* and *ID2* expression in Raji cells. Moreover, none of the other antibodies, especially not the antibody that very specifically detected PIM1 in western blots, precipitated PIM1 from this region. Further, because ChIP after PIM1 overexpression did not work, only generation of the stable knockdown cell lines finally confirmed that PIM1 was specifically bound to the *GNL3* promoter, because knockdown of PIM1 led to a decrease in the ChIP signal in that region.

Overall, due to its sensitivity to environmental changes, the limited availability of specific antibodies and the unspecific targeting of most PIM inhibitors, PIM1 turned out to be quite difficult to study. Further, the use B cell lymphoma cell lines made the application of overexpression and knockdown systems very challenging, as these cells could not be efficiently transiently transfected using the methods available to us. Therefore, stable cell lines had to be generated to facilitate the analysis of PIM kinase function in these cells.

In the future, it would be interesting to study other effects and functions of PIM kinases. I could, for example, show that PIM1 was acutely and strongly induced by serum starvation in Raji cells, which might be required to regulate a metabolic switch and to minimise ROS production in starved cells. This is important for tumour cells, which are frequently exposed to altering environmental conditions and to nutrient deprivation. In agreement with this hypothesis, it has recently been shown that PIM kinases stimulate glucose uptake and the expression of glycolytic enzymes in hepatocellular carcinoma and in mouse embryonic fibroblasts (MEFs) (Leung et al., 2015; J.H. Song et al., 2014). Further, PIM triple ko (TKO) MEFs showed an increased ROS production and a decrease in metabolites of the pentose-phosphate pathway (PPP), as well as in mitochondrial oxidative phosphorylation, indicating that PIM kinases are intricately linked to metabolic

regulation in cells (J.H. Song et al., 2014). PIM kinases might regulate an analogous pathway to MAPK14/p38α or be involved in this pathway. MAPK14 is activated in starved HeLa cells, where it stimulates glucose uptake and the PPP to facilitate the generation of NADPH and thus inhbit ROS accumulation, autophagy and cell death (Desideri et al., 2014). Therefore, it could be very interesting to study PIM kinase functions in starvation.

Moreover, I could show that *PIM1* mRNA expression decreases after cross-linking of the BCR. It would be very interesting to study the exact mechanism of regulation of PIM1 in this context, the effects on PIM protein levels and the involvement of PIM kinases in BCR signalling. In contrast to BCR signalling, knockdown of MYC or inhibition of PIM kinases increased PIM1 and PIM2 expression. Further, knockdown or inhibition of PIM kinases led to an increase in MYC protein expression, while PIM1 overexpression decreased the expression of PIM2. This indicates, that MYC, PIM1 and PIM2 expression levels are regulated by each other through negative feedback loops and it might be important to understand such regulatory pathways. Therefore, future studies could focus on the regulation of PIM kinase and MYC expression and their interdependence under different conditions.

And last, I could show that binding of PIM1 to the *GNL3* promoter increases after inhibition of transcriptional elongation with DRB, after treatment of cells with AZD1208 and after knockdown of PIM2. This indicates that active transcription and PIM kinase activity might be required to mediate a dynamic turnover of PIM1 at its binding sites. Future studies should investigate the mechanisms of PIM1 recruitment and binding to the cromatin and its chromatin-associated functions, as well as its possible regulation by PIM2.

8.2 Effects of Ibrutinib and inhibitors of the BCR pathway on the chromatin structure in CLL cells

8.2.1 Summary of the main results

Cross-linking of the BCR on CLL cells led to the induction or repression of several different genes with different kinetics and all changes were inhibited in Ibrutinib-pre-treated cells. Globally, H3K9acS10p was induced in DMSO- but not Ibrutinib-treated cells 30 min after BCR cross-linking. Locally, at the genes studied in this work, it was difficult to detect H3K9acS10p and when it was present, its induction was not consistently inhibited by Ibrutinib. However, especially H3T6 and H3T11 phosphorylation correlated well with the induction kinetics of the early genes *EGR1* and *DUSP2* and the induction of these two histone marks was completely inhibited in Ibrutinib-treated cells. A promising candidate kinase for the phosphorylation of the two threonine residues downstream of the BCR is ZIPK. Another kinase, which was inhibited by high levels of the PKCβ inhibitor and by Gö6983, mediated constitutive, but not inducible, H3T11 phosphorylation. Indeed, H3T11p was globally associated with active regulatory and structural chromatin elements already before cross-linking of the BCR.

In contrast to histone phosphorylation, POL II recruitment, POL II S2p occupancy, H3K4 methylation, H3K9 acetylation and H2A.Z incorporation were largely unaltered in Ibrutinib-treated cells upon BCR stimulation at the genes analysed. This indicates that activation of the promoter and transcription initiation are mediated through a BCR-downstream pathway that is not blocked by Ibrutinib. In contrast, Ibrutinib seems to inhibit processive transcriptional elongation, it might influence nucleosome turnover and probably the release of stalled POL II. H3K4me3, H3K9ac and H2A.Z levels at the studied promoters were reduced after longer Ibrutinib treatment, probably because the genes were chronically inactivated. Further, H3K27me3 was increased in Ibrutinib-treated cells after 3 to 5 days at some of the promoters analysed.

8.2.2 Ibrutinib inhibited expression of BCR-induced genes, without preventing all the BCR-induced chromatin changes

Induction of all tested genes, which were increased in CLL cells upon BCR cross-linking, was inhibited, when the cells were pre-treated with Ibrutinib. In parallel with this, expression of downregulated genes was maintained after Ibrutinib-treatment.

These results were expected, because Ibrutinib is predicted to inhibit most of the BCR downstream signal transduction pathways through the covalent inhibition of BTK. However, we found that many of the BCR-induced changes to the chromatin were not affected by Ibrutinib treatment, indicating that BCR signalling is actually only partially inhibited.

Ibrutinib inhibited the BCR-induced decrease in H3 occupancy at both the *EGR1* and *DUSP2* genes. This might be a consequence of its inhibition of transcription or might be causal for its effect on transcription. In agreement with a direct role for transcription in nucleosome exchange, inhibition of POL II elongation in *Drosophila* decreases nucleosome turnover (Teves & Henikoff, 2011). On the other hand, nucleosome remodelling complexes, like the SWI/SNF complex, can specifically activate the transcription of some genes by remodelling nucleosomes (Armstrong et al., 1998; Bakshi et al., 2010; Sun et al., 2009). Thus, by mediating the inhibition of nucleosome remodelling enzymes, Ibrutinib might inhibit nucleosome removal and affect transcription. Both hypotheses would also be in agreement with BCR stimulation not having a detectable effect on nucleosome removal from the *MYC*, *DUSP4* and *CCND2* genes. The transcription rates at all three genes are most likely lower than those at the *EGR1* and *DUSP2* genes, which would lead to lower nucleosome turnover. Alternatively, only the two early genes might depend on nucleosome remodelling complexes for their activation, while *MYC*, *DUSP4* and *CCND2* might not.

Globally, Ibrutinib inhibited the BCR-induced increase in H3K9acS10p. However, locally, at the promoters analysed, H3K9acS10p was not strongly induced. This might be due to the regions analysed not being targeted by H3S10 phosphorylation or because signalling-induced H3S10 phosphorylation is a very transient mark (Barth & Imhof, 2010; Jackson et al., 1975) and occurred mainly outside the time window analysed in this study. ChIP-sequencing at different time points after BCR stimulation might give insight into the local dynamics of H3K9acS10p in different regions. Furthermore, even when induction of H3K9acS10p was seen, Ibrutinib did not completely inhibit this induction. H3S10 phosphorylation at some promoters might be regulated by a pathway, which is not inhibited by Ibrutinib. Consistent with this, RSKs, which are putative H3S10 kinases (Sassone-Corsi et al., 1999), can be activated downstream of the BCR in a SYK-dependent but LYN- and MAPK-independent manner (Li et al., 1997). However, the global H3S10 phosphorylation was inhibited by Ibrutinib, indicating that it blocks the main S10-targeting pathways. Such discrepancies between global and local changes of histone modifications have also been observed after HDAC inhibitor treatment. Although global histone

acetylation is strongly increased, levels in promoters of differentially expressed genes hardly change (Boudadi et al., 2013; Halsall et al., 2012).

H3T6p and H3T11p were not consistently altered at the global level after BCR cross-linking in either DMSO- or Ibrutinib-pre-treated CLL cells. However, locally, at the *EGR1* and *DUSP2* genes, both marks were strongly induced 30 min after BCR cross-linking and this induction was completely blocked by Ibrutinib. Only these two early genes, but not *MYC*, *DUSP4* or *CCND2* showed an increase in H3T6 and H3T11 phosphorylation. Therefore, only a small number of genes might be targeted by H3T6 and H3T11 phosphorylation, explaining why no global increase in the two marks was detected. A difference between the global and local change in histone phosphorylation marks is not uncommon. An even more extreme difference between global and local changes can be seen in *Drosophila* cells after heat shock. While global histone phosphorylation decreases, the heat shock loci display increased phosphorylation (Nowak & Corces, 2000). Interestingly, both H3T6 and H3T11 phosphorylation were not restricted to the promoter regions. They were found along the whole length of the *EGR1* and mostly at the 3' end of the *DUSP2* gene. This is typical for chromatin marks, which are associated with elongation, like H3K36me3 (Bannister et al., 2005). Therefore, we hypothesised that these phosphorylation marks somehow contribute to proper transcription elongation at highly expressed immediate early genes, but are dispensable at later activated genes. It is, however, unclear whether H3T6 and H3T11 phosphorylation precede elongation, whether on-going elongation leads to the establishment of the marks, or whether a combination of both occurs. Presence of H3T11p might inhibit gene body acetylation and thus aberrant transcription initiation, as acetylation of H3K14 by yeast Gcn5 is inhibited, when H3T11 is phosphorylated (Liokatis et al., 2012). These proposed functions for H3T6p and H3T11p are in contrast to the functions described for H3T6 and H3T11 phosphorylation at androgen receptor target genes. Here, they contribute to transcription initiation by enhancing H3K9 demethylation and H3K4 methylation (Kim et al., 2014; Metzger et al., 2010; Metzger et al., 2008). Consistent with a different role of these two phosphorylation marks at the *EGR1* and *DUSP2* genes, no increase in H3K4me3 was seen in their promoter regions.

Intriguingly, Ibrutinib treatment did not inhibit POL II recruitment to the *EGR1* and *DUSP2* genes, indicating that transcription initiation is not inhibited by Ibrutinib. It was surprising, however, that total POL II in the gene body and at the 3' end was also unaltered and that elongation, as assessed by the presence of POL II S2p at the 3' end of the genes, was not completely blocked, because generation of the mature mRNAs was completely inhibited. Therefore, the polymerase is either

unproductive because it fails to associate with RNA processing enzymes or its processivity is very low. When assessed by ChIP, many highly processive transcription complexes can result in the same signal as few low processive enzymes. To assess the actual transcription rate, individual POL II complexes would need to be analysed, for example by fluorescence microscopy. We did not assess other posttranslational modifications of the POL II CTD, so that other modifications, which are required for proper transcription, like T4, S5 or S7 phosphorylation (Chapman et al., 2007; Heidemann et al., 2013; Hintermair et al., 2012; Hsin et al., 2011), might be altered after Ibrutinib treatment, leading to the observed phenotype.

Consistent with an alteration of transcriptional elongation but not initiation by Ibrutinib, H3K4me3, H3K9ac and H2A.Z incorporation into the promoter were not inhibited in Ibrutinib-treated CLL cells after cross-linking of the BCR. H3K4me3 was on average unaltered in the promoter regions of *EGR1*, *DUSP2*, and *DUSP4* in DMSO-treated cells upon BCR-stimulation, while it increased in Ibrutinib-treated cells. The levels of H3K4me3 in promoters were increased in Ibrutinib-treated cells even before anti-IgM addition. At least in yeast, inducible promoters display high nucleosome turnover (Cairns, 2009; Rufiange et al., 2007) and we hypothesised that the same happens in B cells. Ibrutinib might block this dynamic nucleosome exchange and thus lead to an apparent increase in H3K4me3. Further, H3K4 methylation upon BCR stimulation seems to be mediated by a BCR-downstream pathway, which is not inhibited in Ibrutinib-treated cells, because H3K4me3 further increased in promoter regions 30 min after BCR stimulation. Due to the enhanced histone turnover after BCR cross-linking, as measured by a decrease in total H3, no increase in H3K4me3 would be seen in DMSO-pre-treated cells, even if H3K4 trimethylation was induced. Interestingly, this Ibrutinib-mediated increase in H3K4me3 also happened at the *DUSP4* promoter, although the gene is only activated 4 h after BCR cross-linking, indicating that the promoter might be poised for later activation already at early time points.

Also surprisingly, H3K9ac was generally increased at the *EGR1* and the *DUSP2* promoters independent of the presence or absence of Ibrutinib. Again, Ibrutinib did not seem to influence the pathway activating the H3K9 acetyltransferase. Unlike H3K4me3, no increase in H3K9ac was seen at the *DUSP4* promoter, indicating that this mark correlates with direct transcriptional activation. Further, H2A.Z, which marks promoters that can be rapidly activated as well as promoters that had been recently active (Gévry et al., 2009; Hardy et al., 2009), was incorporated into the *EGR1* and *DUSP2* promoters after 30 min of BCR activation in one patient and this

was not inhibited by Ibrutinib. This incorporation occurred in one patient only, possibly because the cells from this patient had not been strongly activated before, so that the promoters were devoid of H2A.Z, while cells of the other patients had possibly been recently stimulated and had established a H2A.Z-dependent “expression memory” at these promoters. The same patient showed a huge increase in H2A.Z in the *EGR1, DUSP2* and *MYC* promoter regions 3 days after BCR stimulation, indicating the establishment of an expression memory. This memory function of H2A.Z had before also been described in yeast, where recently inactivated genes incorporate H2A.Z, which allows for their rapid reactivation (Brickner et al., 2007). However, the formation of an expression memory is inhibited by Ibrutinib, consistent with its inhibition of gene expression after BCR stimulation. The other patient analysed on days 3 and 5 showed a lower increase in H2A.Z, which was also inhibited by Ibrutinib, consistent with an already established memory before anti-IgM stimulation.

Long-term Ibrutinib treatment led to a decrease in H3K4me3 and H3K9ac in the promoter regions of all the genes analysed. On-going transcription, which is possibly maintained at a low level due to chronic BCR signalling, is required to deposit both marks (Kim et al., 2009; Rybtsova et al., 2007). Chronic signalling and low-level transcription are, however, thought to be inhibited by Ibrutinib, so that the renewal of H3K4me3 and H3K9ac would be blocked. Transcriptional inactivity of the loci also explains the increase in H3K27me3, especially at the *DUSP2* promoter. It was recently proposed that PRCs are generally recruited to inactive CpG islands (Riising et al., 2014) and a CpG island has been described 5’ of the *DUSP2* gene, explaining the strong increase in H3K27me3 upon inactivation of the gene (Gasco et al., 2008).

In conclusion, Ibrutinib mainly blocked processive elongation of the genes studied, but did not inhibit transcription initiation. This defect in elongation might be mediated by the loss of H3T6 and H3T11 phosphorylation, two marks which were found in the gene body of the *EGR1* and *DUSP2* genes. How promoter activation after BCR cross-linking was maintained in Ibrutinib-treated cells is unclear, because the main kinase targeted by Ibrutinib, BTK, is supposedly required for full activation of most downstream signalling pathways. However, although BTK mutant mice only develop low numbers of peripheral B cells, these show impaired, but not absent, PI3K and Ca^{2+} signalling (Rigley et al., 1989). Consistently, kinase-inactive BTK can function as an adapter molecule and is capable of partially inducing NFκB and B cell survival in mice (Middendorp et al., 2003). Therefore, it is possible that some pathways can be activated in Ibrutinib-treated cells, but that only activation of both

BTK activity-dependent and -independent pathways is sufficient to trigger the full activation of transcription as well as B cell proliferation and survival.

8.2.3 Inhibition of most BTK downstream pathways was not sufficient to block transcriptional activation of the *EGR1* and *DUSP2* genes

Because H3T6p and H3T11p seemed to be the main histone modifications mediating Ibrutinib-dependent inhibition of gene expression downstream of the BCR, we sought to identify signalling kinases that facilitate the establishment of these marks. Although PKCβ had been shown to phosphorylate H3T6 at androgen-dependent genes (Metzger et al., 2010), it did not mediate phosphorylation of this residue in response to BCR cross-linking. In contrast, CLL cells showed a trend towards higher H3T6 and H3T11 phosphorylation after BCR cross-linking when PKCβ was inhibited. Consistently, PKCβ negatively regulates BTK and inhibition of PKCβ has been shown to lead to enhanced calcium signalling in murine B cells (Kang et al., 2001). PKCβ not being the kinase targeting H3T6 in B cells also argues for a different function of these marks at BCR-dependent compared to AR-dependent genes.

Similarly, pan-PKC, RSK and MEK1/2 inhibitors did not inhibit expression of *EGR1* and *DUSP2*, although they partially inhibited H3T6 and/or H3T11 phosphorylation. Patient-to-patient variations were observed, and on average, inhibition of MEK1/2 had no effect on either phosphorylation mark, indicating that the kinase responsible for H3T6 and/or H3T11 phosphorylation might be downstream of PKCs or RSKs. However, these kinases were not the kinases directly responsible for H3T6 and H3T11 phosphorylation upon induction of BCR signalling, because phosphorylation was only partially inhibited. Therefore, there must also be a different pathway activating H3T6 and H3T11 phosphorylation. These marks might be deposited in a PI3K/AKT-dependent way or through an as yet unidentified pathway. Further, a kinase inhibited by high concentrations of the PKCβ inhibitor and by the pan-PKC inhibitor was responsible for the mass of H3T11 phosphorylation in unstimulated cells. This kinase might be a PKC or another unknown kinase targeted by those inhibitors. H3T11 phosphorylation in unstimulated cells might be associated with constitutively active genes, which would be in agreement with our ChIP-seq data, which show that H3T11p is constitutively associated with active regulatory elements and genes that would be expected to be active in B cells. Alternatively, PKC

inhibitor-targeted H3T11p might be associated with heterochromatin, as H3T11p has been shown to be deposited at centromeric heterochromatin (Preuss et al., 2003). Signalling cascades other than the BCR pathways might signal through PKCs to mediate H3T11p. In this context, H3S10 phosphorylation can, for example, be mediated by different kinases in response to different stimuli (Duncan et al., 2006).

In conclusion, none of the inhibitors tested is sufficient to repress immediate early gene expression downstream of the BCR and none of the pathways influenced is the sole pathway activating H3T6 and T11 phosphorylation. However, in resting cells, and possibly in response to different stimuli, H3T11 phosphorylation was mediated by a kinase targeted by the PKC inhibitor. Therefore, two distinct and independent pools of H3T11p seem to exist in B cells, one constitutive and one inducible, which are regulated by different pathways.

8.2.4 ZIPK might be the kinase directly targeting H3T6 and H3T11 downstream of the BCR

ZIPK was the top kinase predicted by GPS2.1 to be targeting H3T11 and treating CLL cells with an inhibitor against DAPK1 and ZIPK inhibited BCR-induced expression of *EGR1* and *DUSP2* and H3T6 and H3T11 phosphorylation as strongly as Ibrutinib. Because DAPK1 is usually repressed in CLL cells through methylation of the promoter (Raval et al., 2007), the effects of the inhibitor are most likely mediated through inhibition of ZIPK. Although ZIPK had been described mainly as an apoptosis-inducing kinase so far, its expression in CLL cells is higher than in normal B cells (Bojarska-Junak et al., 2011), arguing for a tumour promoting function. Consistently, it stimulates proliferation of smooth muscle cells (Usui et al., 2014) and is required for migration of fibroblasts (Komatsu & Ikebe, 2004). Further, its pro-apoptotic effects seem to depend on cytoplasmic localisation and overexpression. In CLL cells, however, ZIPK can be found both in the cytoplasm and the nucleus and this might be sufficient to stimulate its pro-proliferative activity. ZIPK synergistically induces apoptosis together with DAPK1 (Shani et al., 2004), but because the latter is repressed in CLL cells, ZIPK-mediated apoptosis might be suppressed. Further, ZIPK had been described before to interact with a number of transcription factors, and had been shown to activate AR-dependent transcription (Felten et al., 2013; Leister et al., 2008; Sato et al., 2005; Shoval et al., 2011), making it plausible that it activates transcription downstream of the BCR. Moreover, ZIPK had been shown to interact with STAT3, which is constitutively active in CLL

cells as well as activated downstream of the BCR (Hazan-Halevy et al., 2010; Sato et al., 2005). Importantly, ZIPK had been described as a H3T11 kinase before, it phosphorylates this residue in centromeric regions during mitosis (Preuss et al., 2003). It is therefore likely that ZIPK phosphorylates H3T11 downstream of the BCR. At the time of writing, it was, however, unclear whether ZIPK mediates H3T11 phosphorylation only at a few loci, or whether it globally phosphorylates H3T11. In the future, ChIP using a ZIPK antibody, as well as ChIP-seq after ZIPK inhibition and knockdown will clarify this question.

In summary, ZIPK is a good candidate kinase for the induced phosphorylation of H3T6 and H3T11 downstream of the BCR. It might be recruited by different transcription factors or might be constitutively associated with the chromatin, as has been shown for murine ZIPK (Kögel et al., 1998), and become activated in a gene-specific manner after BCR cross-linking.

8.2.5 H3T11p was globally associated with active regulatory elements

ChIP-seq showed that H3T11p was globally associated with active regulatory elements before BCR cross-linking. Unfortunately, we cannot draw any conclusions from the ChIP-seq data 30 min after BCR activation, because the quality of the data was poor and only a very small number of peaks could be called.

H3T11p was found associated with either CTCF sites or active regulatory regions. H3T11p seems to be a mark positively associated with transcription, because it was found in the vicinity of genes, which are actively transcribed in CLL cells, like *CD5*, *SYK*, *LYN*, *BLNK* and *CXCR4*. Consistent with a role for ZIPK in mediating H3T11 phosphorylation at CTCF sites, it has been shown to associate with the cohesin subunit RAD21 (Panigrahi et al., 2012), which in turn associates with CTCF (Parelho et al., 2008). Further, ZIPK binds to several transcription factors, and one of those, STAT3, is constitutively active in CLL cells. Interestingly, about 30% of the detected constitutive H3T11p peaks overlap with STAT3 peaks from GM12878 cells. However, most of the H3T11p might be mediated by another kinase, because treatment of CLL cells with a PKC inhibitor reduced global H3T11 phosphorylation. Nevertheless, this kinase might be upstream of ZIPK in resting CLL cells and another pathway might stimulate ZIPK upon BCR cross-linking, explaining why treatment of the cells with Gö6983 did not block BCR-induced H3T11 phosphorylation.

8.2.6 Limitations of the study and future directions

The main limitation of this study was the use of an *in vitro* system to culture CLL cells. While multiple signal transduction pathways and signalling molecules contribute to the activation of the cell *in vivo*, we restricted our analysis to cross-linking of the BCR only. *In vivo*, this cross-linking is usually accompanied by activation of several co-receptors, for example CD19 by complement (Carroll & Isenman, 2012). Further, IgD and IgM are normally both activated, while we restricted our system to IgM cross-linking, mainly because IgD cross-linking has been shown to trigger different outcomes to IgM cross-linking and to enhance apoptosis of CLL cells (Kim & Reth, 1995; Tavolaro et al., 2013). Therefore, effects of Ibrutinib and ZIPK inhibition on transcription could be different *in vivo*.

A complication of this study was the heterogeneity of CLL as a disease. Patients responded very differently to anti-IgM cross-linking and the response was not correlated with any obvious clinical feature, for example the mutation status of the BCR, although other studies show that UM-CLL cells respond better to IgM cross-linking *in vitro* than M-CLL cells (Guarini et al., 2008). To make consistent conclusions, more samples will need to be analysed in the future. Due to time constraints, only 3 to 5 patients were analysed per experiment so far.

Another limitation was that protein functions were mainly analysed using inhibitors. These are, however, rarely specific, so that is not absolutely certain whether the enzyme intended to be targeted is really the enzyme mediating the observed effects. In the future, other, structurally different inhibitors should be used as a control. Knockdown experiments could serve as good controls as well. Primary B cells are, however, very hard to transfect and viral transduction will possibly need to be used. Optimisation of viral transduction could therefore be an important tool for future studies. Moreover, ChIP-seq experiments, looking at H3T6p, H3T11p and ZIPK will provide helpful information about chromatin association of the kinase and the degree of co-localisation of ZIPK and these histone phospho-modifications. Motif analyses might also be useful to identify transcription factors likely recruiting ZIPK. Further, effects of ZIPK inhibition on the viability of CLL cells will be analysed *in vitro*, to assess whether ZIPK might be a useful therapeutic target in CLL.

9 Bibliography

Abbas, A.K. et al. 1985. Antigen presentation by hapten-specific B lymphocytes. II. Specificity and properties of antigen-presenting B lymphocytes, and function of immunoglobulin receptors. *The Journal of Immunology*. **135**(3),pp.1661–1667.

Abts, H. et al. 1991. Human chronic lymphocytic leukemia cells regularly express mRNAs of the protooncogenes lck and c-fgr. *Leukemia Research*. **15**(11),pp.987–997.

Adachi, T. et al. 2001. SHP-1 Requires Inhibitory Co-receptors to Down-modulate B Cell Antigen Receptor-mediated Phosphorylation of Cellular Substrates. *Journal of Biological Chemistry*. **276**(28),pp.26648–26655.

Adam, M. et al. 2001. H2A.Z Is Required for Global Chromatin Integrity and for Recruitment of RNA Polymerase II under Specific Conditions. *Molecular and Cellular Biology*. **21**(18),pp.6270–6279.

Adams, J.M. et al. 1985. The c-myc oncogene driven by immunoglobulin enhancers induces lymphoid malignancy in transgenic mice. *Nature*. **318**(6046),pp.533–538.

Advani, R.H. et al. 2013. Bruton Tyrosine Kinase Inhibitor Ibrutinib (PCI-32765) Has Significant Activity in Patients With Relapsed/Refractory B-Cell Malignancies. *Journal of Clinical Oncology*. **31**(1),pp.88–94.

Agarwal, N. et al. 2007. MeCP2 interacts with HP1 and modulates its heterochromatin association during myogenic differentiation. *Nucleic Acids Research*. **35**(16),pp.5402–5408.

Aguilera, I. et al. 2001. Molecular structure of eight human autoreactive monoclonal antibodies. *Immunology*. **102**(3),pp.273–280.

Ahmad, K. and Henikoff, S. 2002. The histone variant H3.3 marks active chromatin by replication-independent nucleosome assembly. *Molecular Cell*. **9**(6),pp.1191–1200.

Ahn, S.H. et al. 2004. Phosphorylation of serine 2 within the RNA polymerase II C-terminal domain couples transcription and 3' end processing. *Molecular Cell*. **13**(1),pp.67–76.

Aho, T.L.T. et al. 2006. Pim-1 kinase phosphorylates RUNX family transcription factors and enhances their activity. *BMC cell biology*. **7**,p.21.

Aho, T.L.T. et al. 2004. Pim-1 kinase promotes inactivation of the pro-apoptotic Bad protein by phosphorylating it on the Ser112 gatekeeper site. *FEBS letters*. **571**(1-3),pp.43–49.

Aiba, Y. et al. 2008. Regulation of B-cell development by BCAP and CD19 through their binding to phosphoinositide 3-kinase. *Blood*. **111**(3),pp.1497–1503.

Alberts, B. 2008. *Molecular biology of the cell* 5th ed. New York: Garland Science.

Alessi, D.R. et al. 1997. Characterization of a 3-phosphoinositide-dependent protein kinase which phosphorylates and activates protein kinase Bα. *Current Biology*. **7**(4),pp.261–269.

Alitalo, K. et al. 1983. Homogeneously staining chromosomal regions contain amplified copies of an abundantly expressed cellular oncogene (c-myc) in malignant neuroendocrine cells from a human colon carcinoma. *Proceedings of the National Academy of Sciences*. **80**(6),pp.1707–1711.

Alizadeh, A.A. et al. 2000. Distinct types of diffuse large B-cell lymphoma identified by gene expression profiling. *Nature*. **403**(6769),pp.503–511.

Allard, S. et al. 1999. NuA4, an essential transcription adaptor/histone H4 acetyltransferase complex containing Esa1p and the ATM-related cofactor Tra1p. *The EMBO journal*. **18**(18),pp.5108–5119.

Allen, C.D.C. et al. 2007. Imaging of Germinal Center Selection Events During Affinity Maturation. *Science*. **315**(5811),pp.528–531.

Allen, J.D. et al. 1997. Pim-2 transgene induces lymphoid tumors, exhibiting potent synergy with c-myc. *Oncogene*. **15**(10),pp.1133–1141.

De Almeida, S.F. et al. 2011. Splicing enhances recruitment of methyltransferase HYPB/Setd2 and methylation of histone H3 Lys36. *Nature structural & molecular biology*. **18**(9),pp.977–983.

Amati, B. et al. 1993. Oncogenic activity of the c-Myc protein requires dimerization with Max. *Cell*. **72**(2),pp.233–245.

Amson, R. et al. 1989. The human protooncogene product p33pim is expressed during fetal hematopoiesis and in diverse leukemias. *Proceedings of the National Academy of Sciences of the United States of America*. **86**(22),pp.8857–8861.

Anastassiadis, T. et al. 2011. Comprehensive assay of kinase catalytic activity reveals features of kinase inhibitor selectivity. *Nature Biotechnology*. **29**(11),pp.1039–1045.

Anderson, C.L. et al. 1990. Phagocytosis mediated by three distinct Fc gamma receptor classes on human leukocytes. *The Journal of Experimental Medicine*. **171**(4),pp.1333–1345.

Anest, V. et al. 2003. A nucleosomal function for IκB kinase-α in NF-κB-dependent gene expression. *Nature*. **423**(6940),pp.659–663.

Anjum, R. et al. 2005. The tumor suppressor DAP kinase is a target of RSK-mediated survival signaling. *Current biology: CB*. **15**(19),pp.1762–1767.

Annibali, D. et al. 2014. Myc inhibition is effective against glioma and reveals a role for Myc in proficient mitosis. *Nature Communications*. **5**,p.4632.

Aoki, Y. et al. 1994. Tyrosine phosphorylation of Blk and Fyn Src homology 2 domain-binding proteins occurs in response to antigen-receptor ligation in B cells and constitutively in pre-B cells. *Proceedings of the National Academy of Sciences of the United States of America*. **91**(10),pp.4204–4208.

Apollonio, B. et al. 2013. Targeting B-cell anergy in chronic lymphocytic leukemia. *Blood*. **121**(19),pp.3879–3888.

Armstrong, J.A. et al. 1998. A SWI/SNF-related chromatin remodeling complex, E-RC1, is required for tissue-specific transcriptional regulation by EKLF in vitro. *Cell*. **95**(1),pp.93–104.

Arnold, P. et al. 2013. Modeling of epigenome dynamics identifies transcription factors that mediate Polycomb targeting. *Genome Research*. **23**(1),pp.60–73.

Asano, J. et al. 2011. The serine/threonine kinase Pim-2 is a novel anti-apoptotic mediator in myeloma cells. *Leukemia*. **25**(7),pp.1182–1188.

Avery, D.T. et al. 2008. IL-21-induced isotype switching to IgG and IgA by human naive B cells is differentially regulated by IL-4. *Journal of Immunology (Baltimore, Md.: 1950)*. **181**(3),pp.1767–1779.

Ayer, D.E. et al. 1995. Mad-max transcriptional repression is mediated by ternary complex formation with mammalian homologs of yeast repressor Sin3. *Cell*. **80**(5),pp.767–776.

Baba, T. et al. 2003. Actin tyrosine dephosphorylation by the Src homology 1-containing protein tyrosine phosphatase is essential for actin depolymerization after membrane IgM cross-linking. *Journal of Immunology (Baltimore, Md.: 1950)*. **170**(7),pp.3762–3768.

Baba, Y. et al. 2001. BLNK mediates Syk-dependent Btk activation. *Proceedings of the National Academy of Sciences of the United States of America*. **98**(5),pp.2582–2586.

Bachmann, M. et al. 2006. The oncogenic serine/threonine kinase Pim-1 directly phosphorylates and activates the G2/M specific phosphatase Cdc25C. *The international journal of biochemistry & cell biology*. **38**(3),pp.430–443.

Bachmann, M. et al. 2004. The oncogenic serine/threonine kinase Pim-1 phosphorylates and inhibits the activity of Cdc25C-associated kinase 1 (C-

TAK1): a novel role for Pim-1 at the G2/M cell cycle checkpoint. *The Journal of biological chemistry*. **279**(46),pp.48319–48328.
Baek, S. et al. 2013. Structural and functional analysis of the natural JNK1 inhibitor quercetagetin. *Journal of Molecular Biology*. **425**(2),pp.411–423.
Baek, S.H. 2011. When signaling kinases meet histones and histone modifiers in the nucleus. *Molecular Cell*. **42**(3),pp.274–284.
Bahram, F. et al. 2000. c-Myc hot spot mutations in lymphomas result in inefficient ubiquitination and decreased proteasome-mediated turnover. *Blood*. **95**(6),pp.2104–2110.
Bakshi, R. et al. 2010. The human SWI/SNF complex associates with RUNX1 to control transcription of hematopoietic target genes. *Journal of Cellular Physiology*. **225**(2),pp.569–576.
Balakin, A.G. et al. 1996. The RNA World of the Nucleolus: Two Major Families of Small RNAs Defined by Different Box Elements with Related Functions. *Cell*. **86**(5),pp.823–834.
Bannister, A.J. et al. 2001. Selective recognition of methylated lysine 9 on histone H3 by the HP1 chromo domain. *Nature*. **410**(6824),pp.120–124.
Bannister, A.J. et al. 2005. Spatial distribution of di- and tri-methyl lysine 36 of histone H3 at active genes. *The Journal of Biological Chemistry*. **280**(18),pp.17732–17736.
Bannister, A.J. and Kouzarides, T. 2011. Regulation of chromatin by histone modifications. *Cell Research*. **21**(3),pp.381–395.
Barbazuk, S.M. and Gold, M.R. 1999. Protein kinase C-delta is a target of B-cell antigen receptor signaling. *Immunology Letters*. **69**(2),pp.259–267.
Bargaje, R. et al. 2012. Proximity of H2A.Z containing nucleosome to the transcription start site influences gene expression levels in the mammalian liver and brain. *Nucleic Acids Research*. **40**(18),pp.8965–8978.
Barratt, M.J. et al. 1994. Mitogen-stimulated phosphorylation of histone H3 is targeted to a small hyperacetylation-sensitive fraction. *Proceedings of the National Academy of Sciences of the United States of America*. **91**(11),pp.4781–4785.
Barski, A. et al. 2007. High-Resolution Profiling of Histone Methylations in the Human Genome. *Cell*. **129**(4),pp.823–837.
Barth, T.K. and Imhof, A. 2010. Fast signals and slow marks: the dynamics of histone modifications. *Trends in Biochemical Sciences*. **35**(11),pp.618–626.
Bartkowiak, B. et al. 2010. CDK12 is a transcription elongation-associated CTD kinase, the metazoan ortholog of yeast Ctk1. *Genes & Development*. **24**(20),pp.2303–2316.
Baumli, S. et al. 2010. Halogen Bonds Form the Basis for Selective P-TEFb Inhibition by DRB. *Chemistry & Biology*. **17**(9),pp.931–936.
Bea, S. et al. 2005. Diffuse large B-cell lymphoma subgroups have distinct genetic profiles that influence tumor biology and improve gene-expression-based survival prediction. *Blood*. **106**(9),pp.3183–3190.
Beekman, C. et al. 2006. Evolutionarily conserved role of nucleostemin: controlling proliferation of stem/progenitor cells during early vertebrate development. *Molecular and Cellular Biology*. **26**(24),pp.9291–9301.
Belloc, F. et al. 2009. The stem cell factor-c-KIT pathway must be inhibited to enable apoptosis induced by BCR-ABL inhibitors in chronic myelogenous leukemia cells. *Leukemia*. **23**(4),pp.679–685.
Belot, A. et al. 2013. Protein kinase cδ deficiency causes mendelian systemic lupus erythematosus with B cell-defective apoptosis and hyperproliferation. *Arthritis and Rheumatism*. **65**(8),pp.2161–2171.
Belotserkovskaya, R. et al. 2003. FACT facilitates transcription-dependent nucleosome alteration. *Science (New York, N.Y.)*. **301**(5636),pp.1090–1093.

Bemark, M. and Neuberger, M.S. 2000. The c-MYC allele that is translocated into the IgH locus undergoes constitutive hypermutation in a Burkitt's lymphoma line. *Oncogene*. **19**(30),pp.3404–3410.

Benhamron, S. and Tirosh, B. 2011. Direct activation of mTOR in B lymphocytes confers impairment in B-cell maturation andloss of marginal zone B cells. *European Journal of Immunology*. **41**(8),pp.2390–2396.

Bennett, F. et al. 2007. B-cell chronic lymphocytic leukaemia cells show specific changes in membrane protein expression during different stages of cell cycle. *British Journal of Haematology*. **139**(4),pp.600–604.

Berger, S.L. 2007. The complex language of chromatin regulation during transcription. *Nature*. **447**(7143),pp.407–412.

Bernstein, B.E. et al. 2006. A Bivalent Chromatin Structure Marks Key Developmental Genes in Embryonic Stem Cells. *Cell*. **125**(2),pp.315–326.

Bernstein, B.E. et al. 2005. Genomic Maps and Comparative Analysis of Histone Modifications in Human and Mouse. *Cell*. **120**(2),pp.169–181.

Bernstein, E. et al. 2006. Mouse polycomb proteins bind differentially to methylated histone H3 and RNA and are enriched in facultative heterochromatin. *Molecular and Cellular Biology*. **26**(7),pp.2560–2569.

Bhadury, J. et al. 2014. BET and HDAC inhibitors induce similar genes and biological effects and synergize to kill in Myc-induced murine lymphoma. *Proceedings of the National Academy of Sciences of the United States of America*. **111**(26),pp.E2721–2730.

Bhattacharya, N. et al. 2011. Nurse-like cells show deregulated expression of genes involved in immunocompetence. *British Journal of Haematology*. **154**(3),pp.349–356.

Bi, J. et al. 2009. Downregulation of ZIP kinase is associated with tumor invasion, metastasis and poor prognosis in gastric cancer. *International Journal of Cancer. Journal International Du Cancer*. **124**(7),pp.1587–1593.

Bilancio, A. et al. 2006. Key role of the p110delta isoform of PI3K in B-cell antigen and IL-4 receptor signaling: comparative analysis of genetic and pharmacologic interference with p110delta function in B cells. *Blood*. **107**(2),pp.642–650.

Bimboim, H.C. and Doly, J. 1979. A rapid alkaline extraction procedure for screening recombinant plasmid DNA. *Nucleic Acids Research*. **7**(6),pp.1513–1523.

Binder, M. et al. 2013. CLL B-cell receptors can recognize themselves: alternative epitopes and structural clues for autostimulatory mechanisms in CLL. *Blood*. **121**(1),pp.239–241.

Blackwood, E.M. et al. 1992. Myc and Max associate in vivo. *Genes & Development*. **6**(1),pp.71–80.

Blackwood, E.M. and Eisenman, R.N. 1991. Max: a helix-loop-helix zipper protein that forms a sequence-specific DNA-binding complex with Myc. *Science (New York, N.Y.)*. **251**(4998),pp.1211–1217.

Blankenberg, D. et al. 2001. Galaxy: A Web-Based Genome Analysis Tool for Experimentalists *In*: *Current Protocols in Molecular Biology*. John Wiley & Sons, Inc.

Blois, J.T. et al. 2004. B cell receptor-induced cAMP-response element-binding protein activation in B lymphocytes requires novel protein kinase Cdelta. *The Journal of Biological Chemistry*. **279**(29),pp.30123–30132.

Boeing, S. et al. 2010. RNA Polymerase II C-terminal Heptarepeat Domain Ser-7 Phosphorylation Is Established in a Mediator-dependent Fashion. *Journal of Biological Chemistry*. **285**(1),pp.188–196.

Boekel, E. ten et al. 1998. Precursor B Cells Showing H Chain Allelic Inclusion Display Allelic Exclusion at the Level of Pre-B Cell Receptor Surface Expression. *Immunity*. **8**(2),pp.199–207.

Bojarska-Junak, A. et al. 2011. Assessment of the pathway of apoptosis involving PAR-4, DAXX and ZIPK proteins in CLL patients and its relationship with the principal prognostic factors. *Folia histochemica et cytobiologica / Polish Academy of Sciences, Polish Histochemical and Cytochemical Society*. **49**(1),pp.98–103.

Bonni, A. et al. 1999. Cell Survival Promoted by the Ras-MAPK Signaling Pathway by Transcription-Dependent and -Independent Mechanisms. *Science*. **286**(5443),pp.1358–1362.

Bonyhadi, M. et al. 2005. In vitro engagement of CD3 and CD28 corrects T cell defects in chronic lymphocytic leukemia. *Journal of Immunology (Baltimore, Md.: 1950)*. **174**(4),pp.2366–2375.

Boone, D.L. et al. 2004. The ubiquitin-modifying enzyme A20 is required for termination of Toll-like receptor responses. *Nature Immunology*. **5**(10),pp.1052–1060.

Borillo, G.A. et al. 2010. Pim-1 kinase protects mitochondrial integrity in cardiomyocytes. *Circulation Research*. **106**(7),pp.1265–1274.

Bouchard, C. et al. 2007. FoxO transcription factors suppress Myc-driven lymphomagenesis via direct activation of Arf. *Genes & Development*. **21**(21),pp.2775–2787.

Bouchard, C. et al. 2004. Myc-induced proliferation and transformation require Akt-mediated phosphorylation of FoxO proteins. *The EMBO journal*. **23**(14),pp.2830–2840.

Boudadi, E. et al. 2013. The histone deacetylase inhibitor sodium valproate causes limited transcriptional change in mouse embryonic stem cells but selectively overrides Polycomb-mediated Hoxb silencing. *Epigenetics & Chromatin*. **6**(1),p.11.

Bouzinba-Segard, H. et al. 2006. Accumulation of small murine minor satellite transcripts leads to impaired centromeric architecture and function. *Proceedings of the National Academy of Sciences of the United States of America*. **103**(23),pp.8709–8714.

Brameier, M. et al. 2011. Human box C/D snoRNAs with miRNA like functions: expanding the range of regulatory RNAs. *Nucleic acids research*. **39**(2),pp.675–686.

Brand, M. et al. 1999. Identification of TATA-binding Protein-free TAFII-containing Complex Subunits Suggests a Role in Nucleosome Acetylation and Signal Transduction. *Journal of Biological Chemistry*. **274**(26),pp.18285–18289.

Brasher, S.V. et al. 2000. The structure of mouse HP1 suggests a unique mode of single peptide recognition by the shadow chromo domain dimer. *The EMBO journal*. **19**(7),pp.1587–1597.

Bratkovič, T. and Rogelj, B. 2011. Biology and applications of small nucleolar RNAs. *Cellular and Molecular Life Sciences: CMLS*. **68**(23),pp.3843–3851.

Brault, L. et al. 2012. PIM kinases are progression markers and emerging therapeutic targets in diffuse large B-cell lymphoma. *British journal of cancer*.

Brault, L. et al. 2010. PIM serine/threonine kinases in the pathogenesis and therapy of hematologic malignancies and solid cancers. *Haematologica*. **95**(6),pp.1004–1015.

Braunschweig, U. et al. 2009. Histone H1 binding is inhibited by histone variant H3.3. *The EMBO Journal*. **28**(23),pp.3635–3645.

Brauweiler, A. et al. 2007. Cutting Edge: Acute and chronic exposure of immature B cells to antigen leads to impaired homing and SHIP1-dependent reduction in stromal cell-derived factor-1 responsiveness. *Journal of Immunology (Baltimore, Md.: 1950)*. **178**(6),pp.3353–3357.

Brenner, C. et al. 2005. Myc represses transcription through recruitment of DNA methyltransferase corepressor. *The EMBO journal*. **24**(2),pp.336–346.

Bretones, G. et al. 2014. Myc and cell cycle control. *Biochimica et Biophysica Acta (BBA) - Gene Regulatory Mechanisms*.

Breuer, M.L. et al. 1989. Evidence for the involvement of pim-2, a new common proviral insertion site, in progression of lymphomas. *The EMBO journal*. **8**(3),pp.743–748.

Brickner, D.G. et al. 2007. H2A.Z-mediated localization of genes at the nuclear periphery confers epigenetic memory of previous transcriptional state. *PLoS biology*. **5**(4),p.e81.

Brognard, J. et al. 2011. Cancer-associated loss-of-function mutations implicate DAPK3 as a tumor-suppressing kinase. *Cancer Research*. **71**(8),pp.3152–3161.

Bröker, B.M. et al. 1988. Chronic lymphocytic leukemic (CLL) cells secrete multispecific autoantibodies. *Journal of Autoimmunity*. **1**(5),pp.469–481.

Brookes, E. et al. 2012. Polycomb associates genome-wide with a specific RNA polymerase II variant, and regulates metabolic genes in ESCs. *Cell Stem Cell*. **10**(2),pp.157–170.

Brown, K.S. et al. 2004. FcγRIIb-mediated negative regulation of BCR signalling is associated with the recruitment of the MAPkinase-phosphatase, Pac-1, and the 3′-inositol phosphatase, PTEN. *Cellular Signalling*. **16**(1),pp.71–80.

Brummer, T. et al. 2002. Inducible gene deletion reveals different roles for B-Raf and Raf-1 in B-cell antigen receptor signalling. *The EMBO Journal*. **21**(21),pp.5611–5622.

Buchner, M. et al. 2010. Spleen tyrosine kinase inhibition prevents chemokine- and integrin-mediated stromal protective effects in chronic lymphocytic leukemia. *Blood*. **115**(22),pp.4497–4506.

Buchner, M. et al. 2009. Spleen Tyrosine Kinase Is Overexpressed and Represents a Potential Therapeutic Target in Chronic Lymphocytic Leukemia. *Cancer Research*. **69**(13),pp.5424–5432.

Buratowski, S. 2003. The CTD code. *Nature Structural & Molecular Biology*. **10**(9),pp.679–680.

Burch, L.R. et al. 2004. Phage-peptide display identifies the interferon-responsive, death-activated protein kinase family as a novel modifier of MDM2 and p21WAF1. *Journal of Molecular Biology*. **337**(1),pp.115–128.

Burger, J.A. et al. 2000. Blood-derived nurse-like cells protect chronic lymphocytic leukemia B cells from spontaneous apoptosis through stromal cell-derived factor-1. *Blood*. **96**(8),pp.2655–2663.

Burger, J.A. et al. 1999. Chronic lymphocytic leukemia B cells express functional CXCR4 chemokine receptors that mediate spontaneous migration beneath bone marrow stromal cells. *Blood*. **94**(11),pp.3658–3667.

Burger, J.A. and Chiorazzi, N. 2013. B cell receptor signaling in chronic lymphocytic leukemia. *Trends in Immunology*. **34**(12),pp.592–601.

Burger, M.T. et al. 2013. Structure Guided Optimization, in Vitro Activity, and in Vivo Activity of Pan-PIM Kinase Inhibitors. *ACS Medicinal Chemistry Letters*. **4**(12),pp.1193–1197.

Burg, M. van der et al. 2001. Ordered recombination of immunoglobulin light chain genes occurs at the IGK locus but seems less strict at theIGL locus. *Blood*. **97**(4),pp.1001–1008.

Burke, J.E. et al. 2011. Dynamics of the Phosphoinositide 3-Kinase p110δ Interaction with p85α and Membranes Reveals Aspects of Regulation Distinct from p110α. *Structure*. **19**(8),pp.1127–1137.

Bürkle, A. et al. 2007. Overexpression of the CXCR5 chemokine receptor, and its ligand, CXCL13 in B-cell chronic lymphocytic leukemia. *Blood*. **110**(9),pp.3316–3325.

Byrd, J.C. et al. 2013. Targeting BTK with ibrutinib in relapsed chronic lymphocytic leukemia. *The New England Journal of Medicine*. **369**(1),pp.32–42.

Cairns, B.R. 2009. The logic of chromatin architecture and remodelling at promoters. *Nature*. **461**(7261),pp.193–198.

Calissano, C. et al. 2011. Intraclonal complexity in chronic lymphocytic leukemia: fractions enriched in recently born/divided and older/quiescent cells. *Molecular Medicine (Cambridge, Mass.)*. **17**(11-12),pp.1374–1382.

Calo, V. et al. 2003. STAT proteins: From normal control of cellular events to tumorigenesis. *Journal of Cellular Physiology*. **197**(2),pp.157–168.

Campbell, S. et al. 1998. Increasing complexity of Ras signaling. *, Published online: 17 September 1998*. **17**(11).

Campone, M. et al. 2011. c-Myc dependent expression of pro-apoptotic Bim renders HER2-overexpressing breast cancer cells dependent on anti-apoptotic Mcl-1. *Molecular Cancer*. **10**,p.110.

Campos, E.I. and Reinberg, D. 2009. Histones: annotating chromatin. *Annual review of genetics*. **43**,pp.559–599.

Cannell, I.G. et al. 2010. p38 MAPK/MK2-mediated induction of miR-34c following DNA damage prevents Myc-dependent DNA replication. *Proceedings of the National Academy of Sciences*. **107**(12),pp.5375–5380.

Cao, R. et al. 2005. Role of Bmi-1 and Ring1A in H2A ubiquitylation and Hox gene silencing. *Molecular Cell*. **20**(6),pp.845–854.

Cao, R. et al. 2002. Role of histone H3 lysine 27 methylation in Polycomb-group silencing. *Science (New York, N.Y.)*. **298**(5595),pp.1039–1043.

Care, M.A. et al. 2013. A Microarray Platform-Independent Classification Tool for Cell of Origin Class Allows Comparative Analysis of Gene Expression in Diffuse Large B-cell Lymphoma. *PLoS ONE*. **8**(2),p.e55895.

Carroll, M.C. and Isenman, D.E. 2012. Regulation of Humoral Immunity by Complement. *Immunity*. **37**(2),pp.199–207.

Carrozza, M.J. et al. 2005. Histone H3 methylation by Set2 directs deacetylation of coding regions by Rpd3S to suppress spurious intragenic transcription. *Cell*. **123**(4),pp.581–592.

Carter, P.S. et al. 1999. Differential expression of Myc1 and Myc2 isoforms in cells transformed by eIF4E: evidence for internal ribosome repositioning in the human c-myc 5'UTR. *Oncogene*. **18**(30),pp.4326–4335.

Carvalho, S. et al. 2013. Histone methyltransferase SETD2 coordinates FACT recruitment with nucleosome dynamics during transcription. *Nucleic Acids Research*. **41**(5),pp.2881–2893.

Castello, A. et al. 2013. Nck-mediated recruitment of BCAP to the BCR regulates the PI(3)K-Akt pathway in B cells. *Nature Immunology*. **14**(9),pp.966–975.

Catovsky, D. et al. 1989. Prognostic factors in chronic lymphocytic leukaemia: the importance of age, sex and response to treatment in survival. A report from the MRC CLL 1 trial. MRC Working Party on Leukaemia in Adults. *British Journal of Haematology*. **72**(2),pp.141–149.

Cen, B. et al. 2010. Regulation of Skp2 levels by the Pim-1 protein kinase. *The Journal of Biological Chemistry*. **285**(38),pp.29128–29137.

Cerutti, A. 2008. The regulation of IgA class switching. *Nature reviews. Immunology*. **8**(6),pp.421–434.

Cervantes-Gomez, F. et al. 2013. Biological effects of the Pim kinase inhibitor, SGI-1776, in multiple myeloma. *Clinical Lymphoma, Myeloma & Leukemia*. **13 Suppl 2**,pp.S317–329.

Cesano, A. et al. 2013. Association between B-cell receptor responsiveness and disease progression in B-cell chronic lymphocytic leukemia: results from single cell network profiling studies. *Haematologica*. **98**(4),pp.626–634.

Chang, A.N. et al. 2010. Cardiac myosin is a substrate for zipper-interacting protein kinase (ZIPK). *The Journal of Biological Chemistry*. **285**(8),pp.5122–5126.

Chang, B.Y. et al. 2013. Egress of CD19(+)CD5(+) cells into peripheral blood following treatment with the Bruton tyrosine kinase inhibitor ibrutinib in mantle cell lymphoma patients. *Blood*. **122**(14),pp.2412–2424.

Chan, T.D. et al. 2012. Elimination of germinal-center-derived self-reactive B cells is governed by the location and concentration of self-antigen. *Immunity*. **37**(5),pp.893–904.

Chapman, R.D. et al. 2007. Transcribing RNA polymerase II is phosphorylated at CTD residue serine-7. *Science (New York, N.Y.)*. **318**(5857),pp.1780–1782.

Chen, C.-R. et al. 2002. E2F4/5 and p107 as Smad Cofactors Linking the TGFβ Receptor to c-myc Repression. *Cell*. **110**(1),pp.19–32.

Cheng, P.C. et al. 1999. A Role for Lipid Rafts in B Cell Antigen Receptor Signaling and Antigen Targeting. *The Journal of Experimental Medicine*. **190**(11),pp.1549–1560.

Cheng, S. et al. 2014. BTK inhibition targets in vivo CLL proliferation through its effects on B-cell receptor signaling activity. *Leukemia*. **28**(3),pp.649–657.

Cheng, S.-W.G. et al. 1999. c-MYC interacts with INI1/hSNF5 and requires the SWI/SNF complex for transactivation function. *Nature Genetics*. **22**(1),pp.102–105.

Chen, J. et al. 2009. Hypoxia-mediated up-regulation of Pim-1 contributes to solid tumor formation. *The American Journal of Pathology*. **175**(1),pp.400–411.

Chen, J. et al. 2009. Pim-1 plays a pivotal role in hypoxia-induced chemoresistance. *Oncogene*. **28**(28),pp.2581–2592.

Chen, L. et al. 2002. Expression of ZAP-70 is associated with increased B-cell receptor signaling in chronic lymphocytic leukemia. *Blood*. **100**(13),pp.4609–4614.

Chen, L. et al. 2008. ZAP-70 enhances IgM signaling independent of its kinase activity in chronic lymphocytic leukemia. *Blood*. **111**(5),pp.2685–2692.

Chen, L.S. et al. 2011. Mechanisms of cytotoxicity to Pim kinase inhibitor, SGI-1776, in acute myeloid leukemia. *Blood*. **118**(3),pp.693–702.

Chen, L.S. et al. 2009. Pim kinase inhibitor, SGI-1776, induces apoptosis in chronic lymphocytic leukemia cells. *Blood*. **114**(19),pp.4150–4157.

Chen, P. et al. 2013. H3.3 actively marks enhancers and primes gene transcription via opening higher-ordered chromatin. *Genes & Development*. **27**(19),pp.2109–2124.

Chen, R.H. et al. 1993. Phosphorylation of the c-Fos transrepression domain by mitogen-activated protein kinase and 90-kDa ribosomal S6 kinase. *Proceedings of the National Academy of Sciences of the United States of America*. **90**(23),pp.10952–10956.

Chen, X. et al. 2009. The NF-kappaB factor RelB and histone H3 lysine methyltransferase G9a directly interact to generate epigenetic silencing in endotoxin tolerance. *The Journal of Biological Chemistry*. **284**(41),pp.27857–27865.

Chen, Y. et al. 2009. DSIF, the Paf1 complex, and Tat-SF1 have nonredundant, cooperative roles in RNA polymerase II elongation. *Genes & Development*. **23**(23),pp.2765–2777.

Chen, Z.J. et al. 1996. Site-Specific Phosphorylation of IκBα by a Novel Ubiquitination-Dependent Protein Kinase Activity. *Cell*. **84**(6),pp.853–862.

Cheung, P. et al. 2000. Synergistic Coupling of Histone H3 Phosphorylation and Acetylation in Response to Epidermal Growth Factor Stimulation. *Molecular Cell*. **5**(6),pp.905–915.

Cheutin, T. et al. 2003. Maintenance of Stable Heterochromatin Domains by Dynamic HP1 Binding. *Science*. **299**(5607),pp.721–725.

Chiorazzi, N. and Ferrarini, M. 2011. Cellular origin(s) of chronic lymphocytic leukemia: cautionary notes and additional considerations and possibilities. *Blood*. **117**(6),pp.1781–1791.

Cho, E.-J. et al. 1997. mRNA capping enzyme is recruited to the transcription complex by phosphorylation of the RNA polymerase II carboxy-terminal domain. *Genes & Development*. **11**(24),pp.3319–3326.

Choi, H.S. et al. 2008. Cot, a novel kinase of histone H3, induces cellular transformation through up-regulation of c-fos transcriptional activity. *FASEB journal: official publication of the Federation of American Societies for Experimental Biology*. **22**(1),pp.113–126.

Choi, M.S.K. et al. 1994. Induction of NF-AT in normal B lymphocytes by anti-immunoglobulin or CD40 ligand in conjunction with IL-4. *Immunity*. **1**(3),pp.179–187.

Christoffersen, N.R. et al. 2009. p53-independent upregulation of miR-34a during oncogene-induced senescence represses MYC. *Cell Death & Differentiation*. **17**(2),pp.236–245.

Chu, V.T. and Berek, C. 2013. The establishment of the plasma cell survival niche in the bone marrow. *Immunological Reviews*. **251**(1),pp.177–188.

Ciabrelli, F. and Cavalli, G. 2014. Chromatin-Driven Behavior of Topologically Associating Domains. *Journal of Molecular Biology*.

Cibull, T.L. et al. 2006. Overexpression of Pim-1 during progression of prostatic adenocarcinoma. *Journal of Clinical Pathology*. **59**(3),pp.285–288.

Clark, M.R. et al. 1992. The B cell antigen receptor complex: association of Ig-alpha and Ig-beta with distinct cytoplasmic effectors. *Science*. **258**(5079),pp.123–126.

Clayton, A.L. et al. 2000. Phosphoacetylation of histone H3 on c-fos- and c-jun-associated nucleosomes upon gene activation. *The EMBO Journal*. **19**(14),pp.3714–3726.

Clayton, E. et al. 2002. A crucial role for the p110delta subunit of phosphatidylinositol 3-kinase in B cell development and activation. *The Journal of Experimental Medicine*. **196**(6),pp.753–763.

Cloos, P.A.C. et al. 2006. The putative oncogene GASC1 demethylates tri- and dimethylated lysine 9 on histone H3. *Nature*. **442**(7100),pp.307–311.

Coelho, V. et al. 2013. Identification in CLL of circulating intraclonal subgroups with varying B-cell receptor expression and function. *Blood*. **122**(15),pp.2664–2672.

Cohen, A.M. et al. 2004. Increased Expression of the hPim-2 Gene In Human Chronic lymphocytic Leukemia and Non-Hodgkin Lymphoma. *Leukemia & Lymphoma*. **45**(5),pp.951–955.

Compagno, M. et al. 2009. Mutations of multiple genes cause deregulation of NF-kappaB in diffuse large B-cell lymphoma. *Nature*. **459**(7247),pp.717–721.

Conacci-Sorrell, M. et al. 2014. An Overview of MYC and Its Interactome. *Cold Spring Harbor Perspectives in Medicine*. **4**(1),p.a014357.

Contri, A. et al. 2005. Chronic lymphocytic leukemia B cells contain anomalous Lyn tyrosine kinase, a putative contribution to defective apoptosis. *The Journal of Clinical Investigation*. **115**(2),pp.369–378.

Cook, G.P. and Tomlinson, I.M. 1995. The human immunoglobulin VH repertoire. *Immunology Today*. **16**(5),pp.237–242.

Coughlin, J.J. et al. 2005. RasGRP1 and RasGRP3 Regulate B Cell Proliferation by Facilitating B Cell Receptor-Ras Signaling. *The Journal of Immunology*. **175**(11),pp.7179–7184.

Le Coutre, P. et al. 2000. Induction of resistance to the Abelson inhibitor STI571 in human leukemic cells through gene amplification. *Blood*. **95**(5),pp.1758–1766.

Cowieson, N.P. et al. 2000. Dimerisation of a chromo shadow domain and distinctions from the chromodomain as revealed by structural analysis. *Current biology: CB*. **10**(9),pp.517–525.

Crespo, P. et al. 1997. Phosphotyrosine-dependent activation of Rac-1 GDP/GTP exchange by the vav proto-oncogene product. *Nature*. **385**(6612),pp.169–172.

Creyghton, M.P. et al. 2010. Histone H3K27ac separates active from poised enhancers and predicts developmental state. *Proceedings of the National*

Academy of Sciences of the United States of America. **107**(50),pp.21931–21936.

Crosio, C. et al. 2002. Mitotic phosphorylation of histone H3: spatio-temporal regulation by mammalian Aurora kinases. *Molecular and Cellular Biology*. **22**(3),pp.874–885.

Culjkovic, B. et al. 2006. eIF4E is a central node of an RNA regulon that governs cellular proliferation. *The Journal of Cell Biology*. **175**(3),pp.415–426.

Cusanovich, D.A. et al. 2014. The Functional Consequences of Variation in Transcription Factor Binding. *PLoS Genet*. **10**(3),p.e1004226.

Cuypers, H.T. et al. 1984. Murine leukemia virus-induced T-cell lymphomagenesis: integration of proviruses in a distinct chromosomal region. *Cell*. **37**(1),pp.141–150.

Van Daal, A. and Elgin, S.C. 1992. A histone variant, H2AvD, is essential in Drosophila melanogaster. *Molecular Biology of the Cell*. **3**(6),pp.593–602.

Dai, H. et al. 2005. Pim-2 upregulation: biological implications associated with disease progression and perinueral invasion in prostate cancer. *The Prostate*. **65**(3),pp.276–286.

Dalla-Favera, R. et al. 1982. Human c-myc onc gene is located on the region of chromosome 8 that is translocated in Burkitt lymphoma cells. *Proceedings of the National Academy of Sciences of the United States of America*. **79**(24),pp.7824–7827.

Damen, J.E. et al. 1996. The 145-kDa protein induced to associate with Shc by multiple cytokines is an inositol tetraphosphate and phosphatidylinositol 3,4,5-triphosphate 5-phosphatase. *Proceedings of the National Academy of Sciences of the United States of America*. **93**(4),pp.1689–1693.

Damle, N.K. et al. 1991. Direct helper T cell-induced B cell differentiation involves interaction between T cell antigen CD28 and B cell activation antigen B7. *European Journal of Immunology*. **21**(5),pp.1277–1282.

Damle, R.N. et al. 2007. CD38 expression labels an activated subset within chronic lymphocytic leukemia clones enriched in proliferating B cells. *Blood*. **110**(9),pp.3352–3359.

Dan, H.C. et al. 2002. Phosphatidylinositol 3-Kinase/Akt Pathway Regulates Tuberous Sclerosis Tumor Suppressor Complex by Phosphorylation of Tuberin. *Journal of Biological Chemistry*. **277**(38),pp.35364–35370.

Darzentas, N. and Stamatopoulos, K. 2013. Stereotyped B cell receptors in B cell leukemias and lymphomas. *Methods in Molecular Biology (Clifton, N.J.)*. **971**,pp.135–148.

Datta, S.R. et al. 1997. Akt Phosphorylation of BAD Couples Survival Signals to the Cell-Intrinsic Death Machinery. *Cell*. **91**(2),pp.231–241.

Davidson, L. et al. 2014. 3' end formation of pre-mRNA and phosphorylation of Ser2 on the RNA polymerase II CTD are reciprocally coupled in human cells. *Genes & Development*. **28**(4),pp.342–356.

Davis, R.E. et al. 2010. Chronic active B-cell-receptor signalling in diffuse large B-cell lymphoma. *Nature*. **463**(7277),pp.88–92.

Dawson, M.A. et al. 2011. Inhibition of BET recruitment to chromatin as an effective treatment for MLL-fusion leukaemia. *Nature*. **478**(7370),pp.529–533.

Deak, M. et al. 1998. Mitogen- and stress-activated protein kinase-1 (MSK1) is directly activated by MAPK and SAPK2/p38, and may mediate activation of CREB. *The EMBO journal*. **17**(15),pp.4426–4441.

Decker, S. et al. 2014. PIM Kinases Are Essential for Chronic Lymphocytic Leukemia Cell Survival (PIM2/3) and CXCR4-Mediated Microenvironmental Interactions (PIM1). *Molecular cancer therapeutics*. **13**(5),pp.1231–1245.

Deckert, M. et al. 1996. Functional and physical interactions of Syk family kinases with the Vav proto-oncogene product. *Immunity*. **5**(6),pp.591–604.

Dellino, G.I. et al. 2013. Genome-wide mapping of human DNA-replication origins: levels of transcription at ORC1 sites regulate origin selection and replication timing. *Genome research*. **23**(1),pp.1–11.
Delmore, J.E. et al. 2011. BET Bromodomain Inhibition as a Therapeutic Strategy to Target c-Myc. *Cell*. **146**(6),pp.904–917.
DeManno, D.A. et al. 1999. Follicle-Stimulating Hormone Promotes Histone H3 Phosphorylation on Serine-10. *Molecular Endocrinology*. **13**(1),pp.91–105.
Dengler, H.S. et al. 2008. Distinct functions for the transcription factor Foxo1 at various stages of B cell differentiation. *Nature Immunology*. **9**(12),pp.1388–1398.
Deng, Z. et al. 2009. TERRA RNA binding to TRF2 facilitates heterochromatin formation and ORC recruitment at telomeres. *Molecular Cell*. **35**(4),pp.403–413.
Desideri, E. et al. 2014. MAPK14/p38α-dependent modulation of glucose metabolism affects ROS levels and autophagy during starvation. *Autophagy*. **10**(9),pp.1652–1665.
Deutsch, A.J.A. et al. 2007. MALT lymphoma and extranodal diffuse large B-cell lymphoma are targeted by aberrant somatic hypermutation. *Blood*. **109**(8),pp.3500–3504.
Devaiah, B.N. et al. 2012. BRD4 is an atypical kinase that phosphorylates Serine2 of the RNA Polymerase II carboxy-terminal domain. *Proceedings of the National Academy of Sciences*. **109**(18),pp.6927–6932.
Dey, A. et al. 2003. The double bromodomain protein Brd4 binds to acetylated chromatin during interphase and mitosis. *Proceedings of the National Academy of Sciences*. **100**(15),pp.8758–8763.
Dhalluin, C. et al. 1999. Structure and ligand of a histone acetyltransferase bromodomain. *Nature*. **399**(6735),pp.491–496.
Dhanasekaran, S.M. et al. 2001. Delineation of prognostic biomarkers in prostate cancer. *Nature*. **412**(6849),pp.822–826.
Dhayalan, A. et al. 2010. The Dnmt3a PWWP Domain Reads Histone 3 Lysine 36 Trimethylation and Guides DNA Methylation. *Journal of Biological Chemistry*. **285**(34),pp.26114–26120.
Diehl, J.A. et al. 1998. Glycogen synthase kinase-3beta regulates cyclin D1 proteolysis and subcellular localization. *Genes & Development*. **12**(22),pp.3499–3511.
Dietrich, N. et al. 2012. REST-mediated recruitment of polycomb repressor complexes in mammalian cells. *PLoS genetics*. **8**(3),p.e1002494.
Dixon, J.R. et al. 2012. Topological domains in mammalian genomes identified by analysis of chromatin interactions. *Nature*. **485**(7398),pp.376–380.
Domen, J. et al. 1987. Comparison of the human and mouse PIM-1 cDNAs: nucleotide sequence and immunological identification of the in vitro synthesized PIM-1 protein. *Oncogene Research*. **1**(1),pp.103–112.
Dominguez-Sola, D. et al. 2007. Non-transcriptional control of DNA replication by c-Myc. *Nature*. **448**(7152),pp.445–451.
Dominguez-Sola, D. et al. 2012. The proto-oncogene MYC is required for selection in the germinal center and cyclic reentry. *Nature Immunology*. **13**(11),pp.1083–1091.
Van Dongen, J.J.M. et al. 2003. Design and standardization of PCR primers and protocols for detection of clonal immunoglobulin and T-cell receptor gene recombinations in suspect lymphoproliferations: Report of the BIOMED-2 Concerted Action BMH4-CT98-3936. *Leukemia*. **17**(12),pp.2257–2317.
Donhuijsen, K. et al. 1983. [Pseudofollicles in chronic lymphatic leukemia]. *Zentralblatt Für Allgemeine Pathologie U. Pathologische Anatomie*. **127**(1-2),pp.109–118.
Dono, M. et al. 2004. The CD5+ B-cell. *The international journal of biochemistry & cell biology*. **36**(11),pp.2105–2111.

Doody, G.M. et al. 1995. A role in B cell activation for CD22 and the protein tyrosine phosphatase SHP. *Science (New York, N.Y.)*. **269**(5221),pp.242–244.

Drané, P. et al. 2010. The death-associated protein DAXX is a novel histone chaperone involved in the replication-independent deposition of H3.3. *Genes & Development*. **24**(12),pp.1253–1265.

Drobic, B. et al. 2010. Promoter chromatin remodeling of immediate-early genes is mediated through H3 phosphorylation at either serine 28 or 10 by the MSK1 multi-protein complex. *Nucleic Acids Research*. **38**(10),pp.3196–3208.

Duan, H. et al. 2005. Histone deacetylase inhibitors down-regulate bcl-2 expression and induce apoptosis in t(14;18) lymphomas. *Molecular and Cellular Biology*. **25**(5),pp.1608–1619.

Duch, A. et al. 2013. Coordinated control of replication and transcription by a SAPK protects genomic integrity. *Nature*. **493**(7430),pp.116–119.

Duckworth, A. et al. 2014. Variable induction of PRDM1 and differentiation in chronic lymphocytic leukemia is associated with anergy. *Blood*. **123**(21),pp.3277–3285.

Ducret, C. et al. 2000. The ternary complex factor Net contains two distinct elements that mediate different responses to MAP kinase signalling cascades. *Oncogene*. **19**(44),pp.5063–5072.

Duncan, E.A. et al. 2006. The Kinases MSK1 and MSK2 Are Required for Epidermal Growth Factor-induced, but Not Tumor Necrosis Factor-induced, Histone H3 Ser10 Phosphorylation. *Journal of Biological Chemistry*. **281**(18),pp.12521–12525.

Dunn, K.L. and Davie, J.R. 2005. Stimulation of the Ras-MAPK pathway leads to independent phosphorylation of histone H3 on serine 10 and 28. *Oncogene*. **24**(21),pp.3492–3502.

Dürig, J. et al. 2001. Differential expression of chemokine receptors in B cell malignancies. *Leukemia*. **15**(5),pp.752–756.

Duty, J.A. et al. 2009. Functional anergy in a subpopulation of naive B cells from healthy humans that express autoreactive immunoglobulin receptors. *The Journal of Experimental Medicine*. **206**(1),pp.139–151.

Düvel, K. et al. 2010. Activation of a metabolic gene regulatory network downstream of mTOR complex 1. *Molecular Cell*. **39**(2),pp.171–183.

Duyao, M.P. et al. 1990. Interaction of an NF-kappa B-like factor with a site upstream of the c-myc promoter. *Proceedings of the National Academy of Sciences of the United States of America*. **87**(12),pp.4727–4731.

Dyson, M.H. et al. 2005. MAP kinase-mediated phosphorylation of distinct pools of histone H3 at S10 or S28 via mitogen- and stress-activated kinase 1/2. *Journal of Cell Science*. **118**(10),pp.2247–2259.

Early, P. et al. 1980. An immunoglobulin heavy chain variable region gene is generated from three segments of DNA: VH, D and JH. *Cell*. **19**(4),pp.981–992.

Eberhardy, S.R. and Farnham, P.J. 2002. Myc recruits P-TEFb to mediate the final step in the transcriptional activation of the cad promoter. *The Journal of biological chemistry*. **277**(42),pp.40156–40162.

Eberl, H.C. et al. 2013. A Map of General and Specialized Chromatin Readers in Mouse Tissues Generated by Label-free Interaction Proteomics. *Molecular Cell*. **49**(2),pp.368–378.

Edmunds, J.W. et al. 2008. Dynamic histone H3 methylation during gene induction: HYPB/Setd2 mediates all H3K36 trimethylation. *The EMBO journal*. **27**(2),pp.406–420.

Egloff, S. and Murphy, S. 2008. Cracking the RNA polymerase II CTD code. *Trends in Genetics: TIG*. **24**(6),pp.280–288.

Eischen, C.M. et al. 2001. Bcl-2 is an apoptotic target suppressed by both c-Myc and E2F-1. *Oncogene*. **20**(48),pp.6983–6993.

Enders, A. et al. 2003. Loss of the Pro-Apoptotic BH3-only Bcl-2 Family Member Bim Inhibits BCR Stimulation–induced Apoptosis and Deletion of Autoreactive B Cells. *The Journal of Experimental Medicine*. **198**(7),pp.1119–1126.

Endoh, M. et al. 2012. Histone H2A mono-ubiquitination is a crucial step to mediate PRC1-dependent repression of developmental genes to maintain ES cell identity. *PLoS genetics*. **8**(7),p.e1002774.

Endo, T. et al. 2007. BAFF and APRIL support chronic lymphocytic leukemia B-cell survival through activation of the canonical NF-κB pathway. *Blood*. **109**(2),pp.703–710.

Engebrecht, J. and Brent, R. 2001. Preparation of plasmid DNA. *Current Protocols in Protein Science / Editorial Board, John E. Coligan ... [et Al.]*. **Appendix 4**,p.Appendix 4C.

Engelman, J.A. et al. 2007. MET Amplification Leads to Gefitinib Resistance in Lung Cancer by Activating ERBB3 Signaling. *Science*. **316**(5827),pp.1039–1043.

Engel, P. et al. 1995. Abnormal B lymphocyte delevopment, activation, and differentiation in mice that lack or overexpress the CD19 signal transduction molecule. *Immunity*. **3**(1),pp.39–50.

Engels, N. et al. 2001. Association of SLP-65/BLNK with the B cell antigen receptor through a non-ITAM tyrosine of Ig-alpha. *European Journal of Immunology*. **31**(7),pp.2126–2134.

Ernst, J. et al. 2011. Mapping and analysis of chromatin state dynamics in nine human cell types. *Nature*. **473**(7345),pp.43–49.

Ernst, J. and Kellis, M. 2010. Discovery and characterization of chromatin states for systematic annotation of the human genome. *Nature Biotechnology*. **28**(8),pp.817–825.

Ettinger, R. et al. 2005. IL-21 induces differentiation of human naive and memory B cells into antibody-secreting plasma cells. *Journal of Immunology (Baltimore, Md.: 1950)*. **175**(12),pp.7867–7879.

Faast, R. et al. 2001. Histone variant H2A.Z is required for early mammalian development. *Current Biology*. **11**(15),pp.1183–1187.

Faiola, F. et al. 2005. Dual Regulation of c-Myc by p300 via Acetylation-Dependent Control of Myc Protein Turnover and Coactivation of Myc-Induced Transcription. *Molecular and Cellular Biology*. **25**(23),pp.10220–10234.

Fais, F. et al. 1998. Chronic lymphocytic leukemia B cells express restricted sets of mutated and unmutated antigen receptors. *Journal of Clinical Investigation*. **102**(8),pp.1515–1525.

Favata, M.F. et al. 1998. Identification of a novel inhibitor of mitogen-activated protein kinase kinase. *The Journal of Biological Chemistry*. **273**(29),pp.18623–18632.

Felten, A. et al. 2013. Zipper-interacting protein kinase is involved in regulation of ubiquitination of the androgen receptor, thereby contributing to dynamic transcription complex assembly. *Oncogene*. **32**(41),pp.4981–4988.

Feng, X.-H. et al. 2002. Direct Interaction of c-Myc with Smad2 and Smad3 to Inhibit TGF-β-Mediated Induction of the CDK Inhibitor p15Ink4B. *Molecular Cell*. **9**(1),pp.133–143.

Fernandez, P.C. et al. 2003. Genomic targets of the human c-Myc protein. *Genes & Development*. **17**(9),pp.1115–1129.

Ferrari, K.J. et al. 2014. Polycomb-Dependent H3K27me1 and H3K27me2 Regulate Active Transcription and Enhancer Fidelity. *Molecular Cell*. **53**(1),pp.49–62.

Ferreira, A.C. dos S. et al. 2014. Histone deacetylase inhibitor prevents cell growth in Burkitt's lymphoma by regulating PI3K/Akt pathways and leads to upregulation of miR-143, miR-145, and miR-101. *Annals of Hematology*. **93**(6),pp.983–993.

Festenstein, R. et al. 2003. Modulation of Heterochromatin Protein 1 Dynamics in Primary Mammalian Cells. *Science*. **299**(5607),pp.719–721.

Filion, G.J. et al. 2010. Systematic protein location mapping reveals five principal chromatin types in Drosophila cells. *Cell*. **143**(2),pp.212–224.

Filippakopoulos, P. et al. 2012. Histone Recognition and Large-Scale Structural Analysis of the Human Bromodomain Family. *Cell*. **149**(1),pp.214–231.

Fischle, W. et al. 2003. Molecular basis for the discrimination of repressive methyl-lysine marks in histone H3 by Polycomb and HP1 chromodomains. *Genes & Development*. **17**(15),pp.1870–1881.

Fischle, W. et al. 2005. Regulation of HP1-chromatin binding by histone H3 methylation and phosphorylation. *Nature*. **438**(7071),pp.1116–1122.

Fodor, B.D. et al. 2006. Jmjd2b antagonizes H3K9 trimethylation at pericentric heterochromatin in mammalian cells. *Genes & Development*. **20**(12),pp.1557–1562.

Forshell, L.P. et al. 2011. The direct Myc target Pim3 cooperates with other Pim kinases in supporting viability of Myc-induced B-cell lymphomas. *Oncotarget*. **2**(6),pp.448–460.

Foster, H.A. and Bridger, J.M. 2005. The genome and the nucleus: a marriage made by evolution. *Chromosoma*. **114**(4),pp.212–229.

Francis, N.J. et al. 2004. Chromatin compaction by a polycomb group protein complex. *Science (New York, N.Y.)*. **306**(5701),pp.1574–1577.

Frank, S.R. et al. 2003. MYC recruits the TIP60 histone acetyltransferase complex to chromatin. *EMBO reports*. **4**(6),pp.575–580.

Frick, M. et al. 2012. New insights into the biology of molecular subtypes of diffuse large B-cell lymphoma and Burkitt lymphoma. *Best Practice & Research Clinical Haematology*. **25**(1),pp.3–12.

Friedberg, J.W. et al. 2010. Inhibition of Syk with fostamatinib disodium has significant clinical activity in non-Hodgkin lymphoma and chronic lymphocytic leukemia. *Blood*. **115**(13),pp.2578–2585.

Fruman, D.A. et al. 1999. Impaired B Cell Development and Proliferation in Absence of Phosphoinositide 3-Kinase p85α. *Science*. **283**(5400),pp.393–397.

Fruman, D.A. and Limon, J.J. 2012. Akt and mTOR in B cell activation and differentiation. *B Cell Biology*. **3**,p.228.

Fu, C. et al. 1998. BLNK: a Central Linker Protein in B Cell Activation. *Immunity*. **9**(1),pp.93–103.

Fujieda, S. et al. 1995. IL-4 plus CD40 monoclonal antibody induces human B cells gamma subclass-specific isotype switch: switching to gamma 1, gamma 3, and gamma 4, but not gamma 2. *Journal of Immunology (Baltimore, Md.: 1950)*. **155**(5),pp.2318–2328.

Fujii, C. et al. 2005. Aberrant expression of serine/threonine kinase Pim-3 in hepatocellular carcinoma development and its role in the proliferation of human hepatoma cell lines. *International Journal of Cancer. Journal International Du Cancer*. **114**(2),pp.209–218.

Fujimoto, M. et al. 2000. CD19 Regulates Src Family Protein Tyrosine Kinase Activation in B Lymphocytes through Processive Amplification. *Immunity*. **13**(1),pp.47–57.

Fujinaga, K. et al. 2004. Dynamics of human immunodeficiency virus transcription: P-TEFb phosphorylates RD and dissociates negative effectors from the transactivation response element. *Molecular and Cellular Biology*. **24**(2),pp.787–795.

Fuks, F. et al. 2003. The DNA methyltransferases associate with HP1 and the SUV39H1 histone methyltransferase. *Nucleic Acids Research*. **31**(9),pp.2305–2312.

Fulcher, D.A. et al. 1996. The fate of self-reactive B cells depends primarily on the degree of antigen receptor engagement and availability of T cell help. *The Journal of Experimental Medicine*. **183**(5),pp.2313–2328.

Fulcher, D.A. and Basten, A. 1994. Reduced life span of anergic self-reactive B cells in a double-transgenic model. *The Journal of Experimental Medicine*. **179**(1),pp.125–134.

Furman, R.R. et al. 2000. Modulation of NF-κB Activity and Apoptosis in Chronic Lymphocytic Leukemia B Cells. *The Journal of Immunology*. **164**(4),pp.2200–2206.

Gadewal, N. et al. 2013. Molecular Modeling of Differentially Phosphorylated Serine 10 and Acetylated lysine 9/14 of Histone H3 Regulates their Interactions with 14-3-3ζ, MSK1, and MKP1. *Bioinformatics and Biology Insights*,p.271.

Gagro, A. et al. 2000. CD5-positive and CD5-negative human B cells converge to an indistinguishable population on signalling through B-cell receptors and CD40. *Immunology*. **101**(2),pp.201–209.

Del Gaizo Moore, V. et al. 2007. Chronic lymphocytic leukemia requires BCL2 to sequester prodeath BIM, explaining sensitivity to BCL2 antagonist ABT-737. *The Journal of Clinical Investigation*. **117**(1),pp.112–121.

Galm, O. et al. 2006. The fundamental role of epigenetics in hematopoietic malignancies. *Blood Reviews*. **20**(1),pp.1–13.

Galvani, A. et al. 2008. In vivo study of the nucleosome assembly functions of ASF1 histone chaperones in human cells. *Molecular and Cellular Biology*. **28**(11),pp.3672–3685.

Gan, X. et al. 2011. Evidence for direct activation of mTORC2 kinase activity by phosphatidylinositol 3,4,5-trisphosphate. *The Journal of Biological Chemistry*. **286**(13),pp.10998–11002.

Gao, Y. et al. 2013. A broad activity screen in support of a chemogenomic map for kinase signalling research and drug discovery. *The Biochemical Journal*. **451**(2),pp.313–328.

Gapter, L.A. et al. 2006. Pim-1 kinase expression during murine mammary development. *Biochemical and Biophysical Research Communications*. **345**(3),pp.989–997.

Garapaty-Rao, S. et al. 2013. Identification of EZH2 and EZH1 small molecule inhibitors with selective impact on diffuse large B cell lymphoma cell growth. *Chemistry & Biology*. **20**(11),pp.1329–1339.

Garaud, S. et al. 2011. CD5 Promotes IL-10 Production in Chronic Lymphocytic Leukemia B Cells through STAT3 and NFAT2 Activation. *The Journal of Immunology*. **186**(8),pp.4835–4844.

García-Muñoz, R. et al. 2012. Immunological aspects in chronic lymphocytic leukemia (CLL) development. *Annals of hematology*. **91**(7),pp.981–996.

Garcia, P.D. et al. 2014. Pan-PIM kinase inhibition provides a novel therapy for treating hematologic cancers. *Clinical Cancer Research: An Official Journal of the American Association for Cancer Research*. **20**(7),pp.1834–1845.

Garrone, P. et al. 1995. Fas ligation induces apoptosis of CD40-activated human B lymphocytes. *The Journal of Experimental Medicine*. **182**(5),pp.1265–1273.

Gary-Gouy, H., Harriague, J., Dalloul, A., et al. 2002. CD5-Negative Regulation of B Cell Receptor Signaling Pathways Originates from Tyrosine Residue Y429 Outside an Immunoreceptor Tyrosine-Based Inhibitory Motif. *The Journal of Immunology*. **168**(1),pp.232–239.

Gary-Gouy, H., Harriague, J., Bismuth, G., et al. 2002. Human CD5 promotes B-cell survival through stimulation of autocrine IL-10 production. *Blood*. **100**(13),pp.4537–4543.

Gary-Gouy, H. et al. 2000. The Pseudo-immunoreceptor Tyrosine-based Activation Motif of CD5 Mediates Its Inhibitory Action on B-cell Receptor Signaling. *Journal of Biological Chemistry*. **275**(1),pp.548–556.

Gascan, H. et al. 1991. Anti-CD40 monoclonal antibodies or CD4+ T cell clones and IL-4 induce IgG4 and IgE switching in purified human B cells via different signaling pathways. *The Journal of Immunology*. **147**(1),pp.8–13.

Gasco, M. et al. 2008. Transcriptional silencing of dual specificity phosphatase type 2 (DUSP2) abrogates drug-induced apoptosis and predicts cisplatin resistance in head and neck squamous carcinomas. *ASCO Meeting Abstracts*. **26**(15_suppl),p.11030.

Gauchat, J.F. et al. 1990. Structure and expression of germline epsilon transcripts in human B cells induced by interleukin 4 to switch to IgE production. *The Journal of Experimental Medicine*. **172**(2),pp.463–473.

Gauld, S.B. et al. 2005. Maintenance of B cell anergy requires constant antigen receptor occupancy and signaling. *Nature Immunology*. **6**(11),pp.1160–1167.

Gehani, S.S. et al. 2010. Polycomb group protein displacement and gene activation through MSK-dependent H3K27me3S28 phosphorylation. *Molecular Cell*. **39**(6),pp.886–900.

Gellert, M. 2002. V(d)j Recombination: Rag Proteins, Repair Factors, and Regulation*. *Annual Review of Biochemistry*. **71**(1),pp.101–132.

Gévry, N. et al. 2009. Histone H2A.Z is essential for estrogen receptor signaling. *Genes & Development*. **23**(13),pp.1522–1533.

Gévry, N. et al. 2007. p21 transcription is regulated by differential localization of histone H2A.Z. *Genes & Development*. **21**(15),pp.1869–1881.

Ghosh, A. et al. 2011. Structural Insights to How Mammalian Capping Enzyme Reads the CTD Code. *Molecular Cell*. **43**(2),pp.299–310.

Ghosh, A.K. et al. 1999. MBP-1 Physically Associates with Histone Deacetylase for Transcriptional Repression. *Biochemical and Biophysical Research Communications*. **260**(2),pp.405–409.

Giardine, B. et al. 2005. Galaxy: A platform for interactive large-scale genome analysis. *Genome Research*. **15**(10),pp.1451–1455.

Gille, H. et al. 1992. Phosphorylation of transcription factor p62TCF by MAP kinase stimulates ternary complex formation at c-fos promoter. *Nature*. **358**(6385),pp.414–417.

Goecks, J. et al. 2010. Galaxy: a comprehensive approach for supporting accessible, reproducible, and transparent computational research in the life sciences. *Genome Biology*. **11**(8),p.R86.

Goldberg, A.D. et al. 2010. Distinct factors control histone variant H3.3 localization at specific genomic regions. *Cell*. **140**(5),pp.678–691.

Gómez-Abad, C. et al. 2011. PIM2 Inhibition as a Rational Therapeutic Approach in B-Cell Lymphoma. *Blood*. **118**(20),pp.5517–5527.

Gomez-Curet, I. et al. 2006. c-Myc inhibition negatively impacts lymphoma growth. *Journal of Pediatric Surgery*. **41**(1),pp.207–211; discussion 207–211.

Gomez-Roman, N. et al. 2003. Direct activation of RNA polymerase III transcription by c-Myc. *Nature*. **421**(6920),pp.290–294.

Gong, J. et al. 2009. Serine/threonine kinase Pim-2 promotes liver tumorigenesis induction through mediating survival and preventing apoptosis of liver cell. *The Journal of Surgical Research*. **153**(1),pp.17–22.

Goodfellow, S.J. et al. 2006. Regulation of RNA polymerase III transcription during hypertrophic growth. *The EMBO journal*. **25**(7),pp.1522–1533.

Good, K.L. and Tangye, S.G. 2007. Decreased expression of Kruppel-like factors in memory B cells induces the rapid response typical of secondary antibody responses. *Proceedings of the National Academy of Sciences of the United States of America*. **104**(33),pp.13420–13425.

Goodnow, C.C. et al. 1988. Altered immunoglobulin expression and functional silencing of self-reactive B lymphocytes in transgenic mice. *Nature*. **334**(6184),pp.676–682.

Goodnow, C.C. et al. 1989. Induction of self-tolerance in mature peripheral B lymphocytes. *Nature*. **342**(6248),pp.385–391.
Goto, H. et al. 1999. Identification of a Novel Phosphorylation Site on Histone H3 Coupled with Mitotic Chromosome Condensation. *Journal of Biological Chemistry*. **274**(36),pp.25543–25549.
Grandori, C. et al. 2005. c-Myc binds to human ribosomal DNA and stimulates transcription of rRNA genes by RNA polymerase I. *Nature Cell Biology*. **7**(3),pp.311–318.
Grant, P.A. et al. 1997. Yeast Gcn5 functions in two multisubunit complexes to acetylate nucleosomal histones: characterization of an Ada complex and the SAGA (Spt/Ada) complex. *Genes & Development*. **11**(13),pp.1640–1650.
Graves, P.R. et al. 2005. Regulation of zipper-interacting protein kinase activity in vitro and in vivo by multisite phosphorylation. *The Journal of biological chemistry*. **280**(10),pp.9363–9374.
Greer, E.L. and Brunet, A. 2005. FOXO transcription factors at the interface between longevity and tumor suppression. *Oncogene*. **24**(50),pp.7410–7425.
Gregory, M.A. and Hann, S.R. 2000. c-Myc Proteolysis by the Ubiquitin-Proteasome Pathway: Stabilization of c-Myc in Burkitt's Lymphoma Cells. *Molecular and Cellular Biology*. **20**(7),pp.2423–2435.
Grundler, R. et al. 2009. Dissection of PIM serine/threonine kinases in FLT3-ITD–induced leukemogenesis reveals PIM1 as regulator of CXCL12–CXCR4-mediated homing and migration. *The Journal of Experimental Medicine*. **206**(9),pp.1957–1970.
Gschwendt, M. et al. 1996. Inhibition of protein kinase C mu by various inhibitors. Differentiation from protein kinase c isoenzymes. *FEBS letters*. **392**(2),pp.77–80.
Guarini, A. et al. 2008. BCR ligation induced by IgM stimulation results in gene expression and functional changes only in IgV H unmutated chronic lymphocytic leukemia (CLL) cells. *Blood*. **112**(3),pp.782–792.
Gu, B. et al. 2013. CTD serine-2 plays a critical role in splicing and termination factor recruitment to RNA polymerase II in vivo. *Nucleic Acids Research*. **41**(3),pp.1591–1603.
Guelen, L. et al. 2008. Domain organization of human chromosomes revealed by mapping of nuclear lamina interactions. *Nature*. **453**(7197),pp.948–951.
Guillemette, B. et al. 2005. Variant Histone H2A.Z Is Globally Localized to the Promoters of Inactive Yeast Genes and Regulates Nucleosome Positioning. *PLoS Biol*. **3**(12),p.e384.
Guittard, G. et al. 2009. Cutting edge: Dok-1 and Dok-2 adaptor molecules are regulated by phosphatidylinositol 5-phosphate production in T cells. *Journal of Immunology (Baltimore, Md.: 1950)*. **182**(7),pp.3974–3978.
Gu, J.J. et al. 2009. PIM1 phosphorylates and negatively regulates ASK1-mediated apoptosis. *Oncogene*. **28**(48),pp.4261–4271.
Guo, B. et al. 2004. Protein kinase C family functions in B-cell activation. *Current Opinion in Immunology*. **16**(3),pp.367–373.
Guo, R. et al. 2014. BS69/ZMYND11 Reads and Connects Histone H3.3 Lysine 36 Trimethylation-Decorated Chromatin to Regulated Pre-mRNA Processing. *Molecular Cell*. **56**(2),pp.298–310.
Guo, S. et al. 2010. Overexpression of Pim-1 in bladder cancer. *Journal of Experimental & Clinical Cancer Research*. **29**(1),p.161.
Guo, Z. et al. 2014. PIM inhibitors target CD25-positive AML cells through concomitant suppression of STAT5 activation and degradation of MYC oncogene. *Blood*. **124**(11),pp.1777–1789.
Gurley, L.R. et al. 1978. Histone Phosphorylation and Chromatin Structure during Mitosis in Chinese Hamster Cells. *European Journal of Biochemistry*. **84**(1),pp.1–15.

Habermann, T.M. 2012. New developments in the management of diffuse large B-cell lymphoma. *Hematology (Amsterdam, Netherlands)*. **17 Suppl 1**,pp.S93–97.

Hagerty, L. et al. 2007. ROCK1 phosphorylates and activates zipper-interacting protein kinase. *The Journal of biological chemistry*. **282**(7),pp.4884–4893.

Halsall, J. et al. 2012. Genes Are Often Sheltered from the Global Histone Hyperacetylation Induced by HDAC Inhibitors. *PLoS ONE*. **7**(3),p.e33453.

Hamblin, T.J. et al. 1999. Unmutated Ig VH Genes Are Associated With a More Aggressive Form of Chronic Lymphocytic Leukemia. *Blood*. **94**(6),pp.1848–1854.

Hammerman, P.S. et al. 2004. Lymphocyte transformation by Pim-2 is dependent on nuclear factor-kappaB activation. *Cancer research*. **64**(22),pp.8341–8348.

Hammerman, P.S. et al. 2005. Pim and Akt oncogenes are independent regulators of hematopoietic cell growth and survival. *Blood*. **105**(11),pp.4477–4483.

Hanahan, D. and Weinberg, R.A. 2000. The Hallmarks of Cancer. *Cell*. **100**(1),pp.57–70.

Hann, S.R. et al. 1988. A non-AUG translational initiation in c-myc exon 1 generates an N-terminally distinct protein whose synthesis is disrupted in Burkitt's lymphomas. *Cell*. **52**(2),pp.185–195.

Hann, S.R. and Eisenman, R.N. 1984. Proteins encoded by the human c-myc oncogene: differential expression in neoplastic cells. *Molecular and Cellular Biology*. **4**(11),pp.2486–2497.

Hardy, S. et al. 2009. The Euchromatic and Heterochromatic Landscapes Are Shaped by Antagonizing Effects of Transcription on H2A.Z Deposition. *PLoS Genet*. **5**(10),p.e1000687.

Harris, N.L. et al. 1999. World Health Organization Classification of Neoplastic Diseases of the Hematopoietic and Lymphoid Tissues: Report of the Clinical Advisory Committee Meeting—Airlie House, Virginia, November 1997. *Journal of Clinical Oncology*. **17**(12),pp.3835–3849.

Ha, S. et al. 2013. Phosphorylation of the androgen receptor by PIM1 in hormone refractory prostate cancer. *Oncogene*. **32**(34),pp.3992–4000.

Hatzi, K. and Melnick, A. 2014. Breaking bad in the germinal center: how deregulation of BCL6 contributes to lymphomagenesis. *Trends in Molecular Medicine*. **20**(6),pp.343–352.

Hauser, C. et al. 2002. Activation of the mouse histone deacetylase 1 gene by cooperative histone phosphorylation and acetylation. *Molecular and Cellular Biology*. **22**(22),pp.7820–7830.

Hay, N. and Sonenberg, N. 2004. Upstream and downstream of mTOR. *Genes & Development*. **18**(16),pp.1926–1945.

Haystead, T.A.J. 2005. ZIP kinase, a key regulator of myosin protein phosphatase 1. *Cellular Signalling*. **17**(11),pp.1313–1322.

Hayward, W.S. et al. 1981. Activation of a cellular onc gene by promoter insertion in ALV-induced lymphoid leukosis. *Nature*. **290**(5806),pp.475–480.

Hazan-Halevy, I. et al. 2010. STAT3 is constitutively phosphorylated on serine 727 residues, binds DNA, and activates transcription in CLL cells. *Blood*. **115**(14),pp.2852–2863.

Healy, J.I. et al. 1997. Different nuclear signals are activated by the B cell receptor during positive versus negative signaling. *Immunity*. **6**(4),pp.419–428.

Healy, S. et al. 2012. Histone H3 phosphorylation, immediate-early gene expression, and the nucleosomal response: a historical perspective. *Biochemistry and cell biology = Biochimie et biologie cellulaire*. **90**(1),pp.39–54.

Hediger, F. and Gasser, S.M. 2006. Heterochromatin protein 1: don't judge the book by its cover! *Current opinion in genetics & development*. **16**(2),pp.143–150.

Heidemann, M. et al. 2013. Dynamic phosphorylation patterns of RNA polymerase II CTD during transcription. *Biochimica et Biophysica Acta (BBA) - Gene Regulatory Mechanisms*. **1829**(1),pp.55–62.

Heintzman, N.D. et al. 2007. Distinct and predictive chromatin signatures of transcriptional promoters and enhancers in the human genome. *Nature genetics*. **39**(3),pp.311–318.

Heintzman, N.D. et al. 2009. Histone Modifications at Human Enhancers Reflect Global Cell Type-Specific Gene Expression. *Nature*. **459**(7243),pp.108–112.

Hemann, M.T. et al. 2005. Evasion of the p53 tumour surveillance network by tumour-derived MYC mutants. *Nature*. **436**(7052),pp.807–811.

Herishanu, Y. et al. 2011. The lymph node microenvironment promotes B-cell receptor signaling, NF-κB activation, and tumor proliferation in chronic lymphocytic leukemia. *Blood*. **117**(2),pp.563–574.

Herold, S. et al. 2002. Negative Regulation of the Mammalian UV Response by Myc through Association with Miz-1. *Molecular Cell*. **10**(3),pp.509–521.

Herranz, N. et al. 2008. Polycomb complex 2 is required for E-cadherin repression by the Snail1 transcription factor. *Molecular and Cellular Biology*. **28**(15),pp.4772–4781.

Hervé, M. et al. 2005. Unmutated and mutated chronic lymphocytic leukemias derive from self-reactive B cell precursors despite expressing different antibody reactivity. *The Journal of Clinical Investigation*. **115**(6),pp.1636–1643.

Herz, H.-M. et al. 2012. Enhancer-associated H3K4 monomethylation by Trithorax-related, the Drosophila homolog of mammalian Mll3/Mll4. *Genes & Development*. **26**(23),pp.2604–2620.

Heyman, B. 2003. Feedback regulation by IgG antibodies. *Immunology Letters*. **88**(2),pp.157–161.

He, Z. et al. 2003. Arsenite-induced phosphorylation of histone H3 at serine 10 is mediated by Akt1, extracellular signal-regulated kinase 2, and p90 ribosomal S6 kinase 2 but not mitogen- and stress-activated protein kinase 1. *The Journal of Biological Chemistry*. **278**(12),pp.10588–10593.

Hiasa, M. et al. 2014. Pim-2 kinase is an important target of treatment for tumor progression and bone loss in myeloma. *Leukemia*.

Hiebert, S.W. et al. 1989. E1A-dependent trans-activation of the human MYC promoter is mediated by the E2F factor. *Proceedings of the National Academy of Sciences of the United States of America*. **86**(10),pp.3594–3598.

Hillion, S. et al. 2005. Expression of RAGs in peripheral B cells outside germinal centers is associated with the expression of CD5. *Journal of Immunology (Baltimore, Md.: 1950)*. **174**(9),pp.5553–5561.

Hintermair, C. et al. 2012. Threonine-4 of mammalian RNA polymerase II CTD is targeted by Polo-like kinase 3 and required for transcriptional elongation: CTD Thr4 is required for transcription elongation. *The EMBO Journal*. **31**(12),pp.2784–2797.

Hippen, K.L. et al. 2000. CD5 maintains tolerance in anergic B cells. *The Journal of Experimental Medicine*. **191**(5),pp.883–890.

Hirose, T. et al. 2006. A spliceosomal intron binding protein, IBP160, links position-dependent assembly of intron-encoded box C/D snoRNP to pre-mRNA splicing. *Molecular cell*. **23**(5),pp.673–684.

Hirose, T. et al. 2003. Splicing-Dependent and -Independent Modes of Assembly for Intron-Encoded Box C/D snoRNPs in Mammalian Cells. *Molecular Cell*. **12**(1),pp.113–123.

Hirose, T. and Steitz, J.A. 2001. Position within the host intron is critical for efficient processing of box C/D snoRNAs in mammalian cells. *Proceedings of the National Academy of Sciences of the United States of America*. **98**(23),pp.12914–12919.

Hirota, T. et al. 2005. Histone H3 serine 10 phosphorylation by Aurora B causes HP1 dissociation from heterochromatin. *Nature*. **438**(7071),pp.1176–1180.
Hoellenriegel, J. et al. 2011. The phosphoinositide 3'-kinase delta inhibitor, CAL-101, inhibits B-cell receptor signaling and chemokine networks in chronic lymphocytic leukemia. *Blood*. **118**(13),pp.3603–3612.
Hogan, C. et al. 2008. Elevated Levels of Oncogenic Protein Kinase Pim-1 Induce the p53 Pathway in Cultured Cells and Correlate with Increased Mdm2 in Mantle Cell Lymphoma. *Journal of Biological Chemistry*. **283**(26),pp.18012–18023.
Ho, J.S.L. et al. 2005. p53-Dependent Transcriptional Repression of c-myc Is Required for G1 Cell Cycle Arrest. *Molecular and Cellular Biology*. **25**(17),pp.7423–7431.
Holder, S. et al. 2007. Characterization of a Potent and Selective Small-Molecule Inhibitor of the PIM1 Kinase. *Molecular Cancer Therapeutics*. **6**(1),pp.163–172.
Honigberg, L.A. et al. 2010. The Bruton tyrosine kinase inhibitor PCI-32765 blocks B-cell activation and is efficacious in models of autoimmune disease and B-cell malignancy. *Proceedings of the National Academy of Sciences*. **107**(29),pp.13075–13080.
Hoogeboom, R. et al. 2013. A mutated B cell chronic lymphocytic leukemia subset that recognizes and responds to fungi. *The Journal of Experimental Medicine*. **210**(1),pp.59–70.
Hooker, C.W. and Hurlin, P.J. 2006. Of Myc and Mnt. *Journal of Cell Science*. **119**(2),pp.208–216.
Hoover, D.S. et al. 1997. Pim-1 protein expression is regulated by its 5'-untranslated region and translation initiation factor eIF-4E. *Cell Growth & Differentiation: The Molecular Biology Journal of the American Association for Cancer Research*. **8**(12),pp.1371–1380.
Horton, J.R. et al. 2010. Enzymatic and structural insights for substrate specificity of a family of jumonji histone lysine demethylases. *Nature Structural & Molecular Biology*. **17**(1),pp.38–43.
Hosogane, M. et al. 2013. Ras-Induced Changes in H3K27me3 Occur after Those in Transcriptional Activity. *PLoS Genet*. **9**(8),p.e1003698.
Houzelstein, D. et al. 2002. Growth and early postimplantation defects in mice deficient for the bromodomain-containing protein Brd4. *Molecular and Cellular Biology*. **22**(11),pp.3794–3802.
Hsin, J.-P. et al. 2011. RNAP II CTD Phosphorylated on Threonine-4 Is Required for Histone mRNA 3′ End Processing. *Science*. **334**(6056),pp.683–686.
Hsu, J.-L. et al. 2012. Pim-1 knockdown potentiates paclitaxel-induced apoptosis in human hormone-refractory prostate cancers through inhibition of NHEJ DNA repair. *Cancer Letters*. **319**(2),pp.214–222.
Hsu, P.L. et al. 2014. Rtr1 is a dual specificity phosphatase that dephosphorylates Tyr1 and Ser5 on the RNA polymerase II CTD. *Journal of Molecular Biology*. **426**(16),pp.2970–2981.
Hsu, Y.-L. et al. 2013. Breast tumor-associated osteoblast-derived CXCL5 increases cancer progression by ERK/MSK1/Elk-1/snail signaling pathway. *Oncogene*. **32**(37),pp.4436–4447.
Huang, B. et al. 2009. Brd4 coactivates transcriptional activation of NF-kappaB via specific binding to acetylated RelA. *Molecular and Cellular Biology*. **29**(5),pp.1375–1387.
Huang, J. et al. 2012. SUMO1 modification of PTEN regulates tumorigenesis by controlling its association with the plasma membrane. *Nature Communications*. **3**,p.911.
Huang, Y. et al. 2012. Outcome of R-CHOP or CHOP Regimen for Germinal Center and Nongerminal Center Subtypes of Diffuse Large B-Cell Lymphoma of Chinese Patients. *The Scientific World Journal*. **2012**.

Huang, Y. et al. 2006. Recognition of Histone H3 Lysine-4 Methylation by the Double Tudor Domain of JMJD2A. *Science*. **312**(5774),pp.748–751.
Huang, Z.-Y. et al. 2003. The effect of phosphatases SHP-1 and SHIP-1 on signaling by the ITIM- and ITAM-containing Fcγ receptors FcγRIIB and FcγRIIA. *Journal of Leukocyte Biology*. **73**(6),pp.823–829.
Hu, D. et al. 2013. The MLL3/MLL4 branches of the COMPASS family function as major histone H3K4 monomethylases at enhancers. *Molecular and Cellular Biology*. **33**(23),pp.4745–4754.
Hudson, B.P. et al. 2000. Solution structure and acetyl-lysine binding activity of the GCN5 bromodomain. *Journal of Molecular Biology*. **304**(3),pp.355–370.
Hung, T. et al. 2009. ING4 Mediates Crosstalk between Histone H3 K4 Trimethylation and H3 Acetylation to Attenuate Cellular Transformation. *Molecular Cell*. **33**(2),pp.248–256.
Hurlin, P.J. et al. 1995. Mad3 and Mad4: novel Max-interacting transcriptional repressors that suppress c-myc dependent transformation and are expressed during neural and epidermal differentiation. *The EMBO journal*. **14**(22),pp.5646–5659.
Hurlin, P.J. et al. 1997. Mnt, a novel Max-interacting protein is coexpressed with Myc in proliferating cells and mediates repression at Myc binding sites. *Genes & Development*. **11**(1),pp.44–58.
Hu, S. et al. 2013. MYC/BCL2 protein coexpression contributes to the inferior survival of activated B-cell subtype of diffuse large B-cell lymphoma and demonstrates high-risk gene expression signatures: a report from The International DLBCL Rituximab-CHOP Consortium Program. *Blood*. **121**(20),pp.4021–4031; quiz 4250.
Hüttmann, A. et al. 2006. Gene expression signatures separate B-cell chronic lymphocytic leukaemia prognostic subgroups defined by ZAP-70 and CD38 expression status. *Leukemia*. **20**(10),pp.1774–1782.
Iavarone, C. et al. 2003. The platelet-derived growth factor controls c-myc expression through a JNK- and AP-1-dependent signaling pathway. *The Journal of Biological Chemistry*. **278**(50),pp.50024–50030.
Iizuka, M. et al. 2006. Regulation of replication licensing by acetyltransferase Hbo1. *Molecular and Cellular Biology*. **26**(3),pp.1098–1108.
Ikura, T. et al. 2000. Involvement of the TIP60 Histone Acetylase Complex in DNA Repair and Apoptosis. *Cell*. **102**(4),pp.463–473.
Inabe, K. et al. 2002. Vav3 Modulates B Cell Receptor Responses by Regulating Phosphoinositide 3-Kinase Activation. *The Journal of Experimental Medicine*. **195**(2),pp.189–200.
Inoki, K. et al. 2003. Rheb GTPase is a direct target of TSC2 GAP activity and regulates mTOR signaling. *Genes & Development*. **17**(15),pp.1829–1834.
Inoki, K. et al. 2002. TSC2 is phosphorylated and inhibited by Akt and suppresses mTOR signalling. *Nature Cell Biology*. **4**(9),pp.648–657.
Ionov, Y. et al. 2003. Pim-1 protein kinase is nuclear in Burkitt's lymphoma: nuclear localization is necessary for its biologic effects. *Anticancer Research*. **23**(1A),pp.167–178.
Iqbal, J. et al. 2007. Distinctive patterns of BCL6 molecular alterations and their functional consequences in different subgroups of diffuse large B-cell lymphoma. *Leukemia*. **21**(11),pp.2332–2343.
Ishiai, M. et al. 1999. Cutting edge: association of phospholipase C-gamma 2 Src homology 2 domains with BLNK is critical for B cell antigen receptor signaling. *Journal of Immunology (Baltimore, Md.: 1950)*. **163**(4),pp.1746–1749.
Ishiura, N. et al. 2010. Differential phosphorylation of functional tyrosines in CD19 modulates B-lymphocyte activation. *European Journal of Immunology*. **40**(4),pp.1192–1204.

Ito, D. et al. 2012. CD40 ligand is necessary and sufficient to support primary diffuse large B-cell lymphoma cells in culture: a tool for in vitro preclinical studies with primary B-cell malignancies. *Leukemia & Lymphoma*. **53**(7),pp.1390–1398.

Jackson, V. et al. 1975. Studies on highly metabolically active acetylation and phosphorylation of histones. *The Journal of Biological Chemistry*. **250**(13),pp.4856–4863.

Jacobson, R.H. et al. 2000. Structure and Function of a Human TAFII250 Double Bromodomain Module. *Science*. **288**(5470),pp.1422–1425.

Jacobs, S.A. et al. 2001. Specificity of the HP1 chromo domain for the methylated N-terminus of histone H3. *The EMBO journal*. **20**(18),pp.5232–5241.

Jafarnejad, S.M. et al. 2008. Knocking-down the expression of nucleostemin significantly decreases rate of proliferation of rat bone marrow stromal stem cells in an apparently p53-independent manner. *Cell Proliferation*. **41**(1),pp.28–35.

Jaffe, E.S. 2009. The 2008 WHO classification of lymphomas: implications for clinical practice and translational research. *Hematology / the Education Program of the American Society of Hematology. American Society of Hematology. Education Program*,pp.523–531.

Janeway, C.A. et al. 2001. *Immunobiology* 5th ed. Garland Science.

Jang, J.Y. et al. 2014. Reactive oxygen species play a critical role in collagen-induced platelet activation via SHP-2 oxidation. *Antioxidants & Redox Signaling*. **20**(16),pp.2528–2540.

Jang, M.K. et al. 2005. The Bromodomain Protein Brd4 Is a Positive Regulatory Component of P-TEFb and Stimulates RNA Polymerase II-Dependent Transcription. *Molecular Cell*. **19**(4),pp.523–534.

Janknecht, R. et al. 1995. SAP1a is a nuclear target of signaling cascades involving ERKs. *Oncogene*. **10**(6),pp.1209–1216.

Jelinic, P. et al. 2011. A Novel Mammalian Complex Containing Sin3B Mitigates Histone Acetylation and RNA Polymerase II Progression within Transcribed Loci. *Molecular and Cellular Biology*. **31**(1),pp.54–62.

Jeong, K.W. et al. 2011. Recognition of enhancer element-specific histone methylation by TIP60 in transcriptional activation. *Nature Structural and Molecular Biology*. **18**(12),pp.1358–1365.

Jiang, Y.W. et al. 1998. Mammalian mediator of transcriptional regulation and its possible role as an end-point of signal transduction pathways. *Proceedings of the National Academy of Sciences*. **95**(15),pp.8538–8543.

Ji, H. et al. 2011. Cell-type independent MYC target genes reveal a primordial signature involved in biomass accumulation. *PloS One*. **6**(10),p.e26057.

Jin, B. et al. 2014. PIM-1 modulates cellular senescence and links IL-6 signaling to heterochromatin formation. *Aging Cell*. **13**(5),pp.879–889.

Jin, C. and Felsenfeld, G. 2007. Nucleosome stability mediated by histone variants H3.3 and H2A.Z. *Genes & Development*. **21**(12),pp.1519–1529.

Jin, Y. et al. 2012. Expressions of Osteopontin (OPN), αvβ3 and Pim-1 Associated with Poor Prognosis in Non-small Cell Lung Cancer (NSCLC). *Chinese Journal of Cancer Research = Chung-Kuo Yen Cheng Yen Chiu*. **24**(2),pp.103–108.

John, S. et al. 2008. Interaction of the glucocorticoid receptor with the chromatin landscape. *Molecular Cell*. **29**(5),pp.611–624.

John, S. et al. 2000. The something about silencing protein, Sas3, is the catalytic subunit of NuA3, a yTAF(II)30-containing HAT complex that interacts with the Spt16 subunit of the yeast CP (Cdc68/Pob3)-FACT complex. *Genes & Development*. **14**(10),pp.1196–1208.

Jones, R.M. et al. 1996. An essential E box in the promoter of the gene encoding the mRNA cap-binding protein (eukaryotic initiation factor 4E) is a target for activation by c-myc. *Molecular and Cellular Biology*. **16**(9),pp.4754–4764.

Joshi, A.A. and Struhl, K. 2005. Eaf3 chromodomain interaction with methylated H3-K36 links histone deacetylation to Pol II elongation. *Molecular Cell*. **20**(6),pp.971–978.

Jou, S.-T. et al. 2002. Essential, nonredundant role for the phosphoinositide 3-kinase p110delta in signaling by the B-cell receptor complex. *Molecular and Cellular Biology*. **22**(24),pp.8580–8591.

Julienne, H. et al. 2013. Human genome replication proceeds through four chromatin states. *PLoS computational biology*. **9**(10),p.e1003233.

Jung, D. et al. 2006. Mechanism and Control of V(d)j Recombination at the Immunoglobulin Heavy Chain Locus. *Annual Review of Immunology*. **24**(1),pp.541–570.

Jung, Y. et al. 2014. Plant-Derived Flavones as Inhibitors of Aurora B Kinase and Their Quantitative Structure-Activity Relationships. *Chemical Biology & Drug Design*.

Kabak, S. et al. 2002. The direct recruitment of BLNK to immunoglobulin alpha couples the B-cell antigen receptor to distal signaling pathways. *Molecular and Cellular Biology*. **22**(8),pp.2524–2535.

Kabbout, M. et al. 2014. MicroRNA 17-92 cluster mediates ETS1 and ETS2-dependent RAS-oncogenic transformation. *PloS One*. **9**(6),p.e100693.

Kadamb, R. et al. 2013. Sin3: Insight into its transcription regulatory functions. *European Journal of Cell Biology*. **92**(8–9),pp.237–246.

Kalb, R. et al. 2014. Histone H2A monoubiquitination promotes histone H3 methylation in Polycomb repression. *Nature Structural & Molecular Biology*. **21**(6),pp.569–571.

Kanayama, A. et al. 2004. TAB2 and TAB3 Activate the NF-κB Pathway through Binding to Polyubiquitin Chains. *Molecular Cell*. **15**(4),pp.535–548.

Kanazawa, S. et al. 2003. c-Myc recruits P-TEFb for transcription, cellular proliferation and apoptosis. *Oncogene*. **22**(36),pp.5707–5711.

Kang, S.W. et al. 2001. PKCβ modulates antigen receptor signaling via regulation of Btk membrane localization. *The EMBO Journal*. **20**(20),pp.5692–5702.

Kanhere, A. et al. 2010. Short RNAs are transcribed from repressed polycomb target genes and interact with polycomb repressive complex-2. *Molecular Cell*. **38**(5),pp.675–688.

Katakami, N. et al. 2004. Role of pim-1 in smooth muscle cell proliferation. *The Journal of Biological Chemistry*. **279**(52),pp.54742–54749.

Kato, G.J. et al. 1992. Max: functional domains and interaction with c-Myc. *Genes & Development*. **6**(1),pp.81–92.

Kaustov, L. et al. 2011. Recognition and specificity determinants of the human cbx chromodomains. *The Journal of Biological Chemistry*. **286**(1),pp.521–529.

Kawai, T. et al. 1998. ZIP kinase, a novel serine/threonine kinase which mediates apoptosis. *Molecular and cellular biology*. **18**(3),pp.1642–1651.

Kawai, T. et al. 2003. ZIP kinase triggers apoptosis from nuclear PML oncogenic domains. *Molecular and Cellular Biology*. **23**(17),pp.6174–6186.

Keeton, E.K. et al. 2014. AZD1208, a potent and selective pan-Pim kinase inhibitor, demonstrates efficacy in preclinical models of acute myeloid leukemia. *Blood*. **123**(6),pp.905–913.

Kelly, K.R. et al. 2012. Targeting PIM kinase activity significantly augments the efficacy of cytarabine. *British Journal of Haematology*. **156**(1),pp.129–132.

Kenneth, N.S. et al. 2007. TRRAP and GCN5 are used by c-Myc to activate RNA polymerase III transcription. *Proceedings of the National Academy of Sciences*. **104**(38),pp.14917–14922.

Kent, W.J. et al. 2002. The Human Genome Browser at UCSC. *Genome Research*. **12**(6),pp.996–1006.

Keogh, M.-C. et al. 2005. Cotranscriptional set2 methylation of histone H3 lysine 36 recruits a repressive Rpd3 complex. *Cell*. **123**(4),pp.593–605.

Kessler, D.J. et al. 1992. A novel NF-kappa B element within exon 1 of the murine c-myc gene. *Oncogene*. **7**(12),pp.2447–2453.
Keum, Y.-S. et al. 2012. UVB-induced COX-2 expression requires histone H3 phosphorylation at Ser10 and Ser28. *Oncogene*.
Khan, M. et al. 2014. Idelalisib for the treatment of chronic lymphocytic leukemia. *ISRN oncology*. **2014**,p.931858.
Khodabakhshi, A.H. et al. 2012. Recurrent targets of aberrant somatic hypermutation in lymphoma. *Oncotarget*. **3**(11),pp.1308–1319.
Kim, H.K. et al. 2012. Expression of provirus integration site for Moloney murine leukemia virus 1 is post-transcriptionally regulated by tristetraprolin in cancer cells. *The Journal of biological chemistry*.
Kim, J. et al. 2011. AMPK and mTOR regulate autophagy through direct phosphorylation of Ulk1. *Nature Cell Biology*. **13**(2),pp.132–141.
Kim, J. et al. 2010. Pim1 promotes human prostate cancer cell tumorigenicity and c-MYC transcriptional activity. *BMC cancer*. **10**,p.248.
Kim, J. et al. 2009. RAD6-Mediated Transcription-Coupled H2B Ubiquitylation Directly Stimulates H3K4 Methylation in Human Cells. *Cell*. **137**(3),pp.459–471.
Kim, J. et al. 2006. Tudor, MBT and chromo domains gauge the degree of lysine methylation. *EMBO reports*. **7**(4),pp.397–403.
Kim, J.B. and Sharp, P.A. 2001. Positive transcription elongation factor B phosphorylates hSPT5 and RNA polymerase II carboxyl-terminal domain independently of cyclin-dependent kinase-activating kinase. *The Journal of Biological Chemistry*. **276**(15),pp.12317–12323.
Kim, J.-Y. et al. 2014. A role for WDR5 in integrating threonine 11 phosphorylation to lysine 4 methylation on histone H3 during androgen signaling and in prostate cancer. *Molecular Cell*. **54**(4),pp.613–625.
Kim, K. et al. 2010. Pim-1 Regulates RANKL-Induced Osteoclastogenesis via NF-κB Activation and NFATc1 Induction. *The Journal of Immunology*. **185**(12),pp.7460–7466.
Kim, K.-C. et al. 2003. Inactivation of a histone methyltransferase by mutations in human cancers. *Cancer Research*. **63**(22),pp.7619–7623.
Kim, K.M. and Reth, M. 1995. Signaling difference between class IgM and IgD antigen receptors. *Annals of the New York Academy of Sciences*. **766**,pp.81–88.
Kim, S.-K. et al. 2012. Human Histone H3K79 Methyltransferase DOT1L Methyltransferase Binds Actively Transcribing RNA Polymerase II to Regulate Gene Expression. *Journal of Biological Chemistry*. **287**(47),pp.39698–39709.
Kim, S.Y. et al. 2003. Skp2 Regulates Myc Protein Stability and Activity. *Molecular Cell*. **11**(5),pp.1177–1188.
Kimura, Y. et al. 2007. MM-1 facilitates degradation of c-Myc by recruiting proteasome and a novel ubiquitin E3 ligase. *International Journal of Oncology*. **31**(4),pp.829–836.
Kinney, C.M. et al. 2009. Histone H3 as a novel substrate for MAP kinase phosphatase-1. *American Journal of Physiology. Cell Physiology*. **296**(2),pp.C242–249.
Kishore, S. et al. 2010. The snoRNA MBII-52 (SNORD 115) is processed into smaller RNAs and regulates alternative splicing. *Human Molecular Genetics*. **19**(7),pp.1153–1164.
Kishore, S. and Stamm, S. 2006. The snoRNA HBII-52 regulates alternative splicing of the serotonin receptor 2C. *Science (New York, N.Y.)*. **311**(5758),pp.230–232.
Kiss, T. 2002. Small nucleolar RNAs: an abundant group of noncoding RNAs with diverse cellular functions. *Cell*. **109**(2),pp.145–148.

Kizer, K.O. et al. 2005. A novel domain in Set2 mediates RNA polymerase II interaction and couples histone H3 K36 methylation with transcript elongation. *Molecular and Cellular Biology*. **25**(8),pp.3305–3316.

Klose, R.J. et al. 2006. The transcriptional repressor JHDM3A demethylates trimethyl histone H3 lysine 9 and lysine 36. *Nature*. **442**(7100),pp.312–316.

Knight, Z.A. and Shokat, K.M. 2005. Features of Selective Kinase Inhibitors. *Chemistry & Biology*. **12**(6),pp.621–637.

Kobor, M.S. et al. 2004. A protein complex containing the conserved Swi2/Snf2-related ATPase Swr1p deposits histone variant H2A.Z into euchromatin. *PLoS biology*. **2**(5),p.E131.

Koch, C.M. et al. 2007. The landscape of histone modifications across 1% of the human genome in five human cell lines. *Genome Research*. **17**(6),pp.691–707.

Kocher, B.A. et al. 2014. DAPK3 Suppresses Acini Morphogenesis and is Required for Mouse Development. *Molecular cancer research: MCR*.

Kögel, D. et al. 1998. Cloning and characterization of Dlk, a novel serine/threonine kinase that is tightly associated with chromatin and phosphorylates core histones. *Oncogene*. **17**(20),pp.2645–2654.

Kögel, D. et al. 1999. C-terminal truncation of Dlk/ZIP kinase leads to abrogation of nuclear transport and high apoptotic activity. *Oncogene*. **18**(51),pp.7212–7218.

Kögel, D. et al. 2003. The death associated protein (DAP) kinase homologue Dlk/ZIP kinase induces p19ARF- and p53-independent apoptosis. *European Journal of Cancer (Oxford, England: 1990)*. **39**(2),pp.249–256.

Kohl, N.E. et al. 1983. Transposition and amplification of oncogene-related sequences in human neuroblastomas. *Cell*. **35**(2 Pt 1),pp.359–367.

Koike, N. et al. 2000. Identification of heterochromatin protein 1 (HP1) as a phosphorylation target by Pim-1 kinase and the effect of phosphorylation on the transcriptional repression function of HP1(1). *FEBS Letters*. **467**(1),pp.17–21.

Komarnitsky, P. et al. 2000. Different phosphorylated forms of RNA polymerase II and associated mRNA processing factors during transcription. *Genes & Development*. **14**(19),pp.2452–2460.

Komatsu, S. and Ikebe, M. 2004. ZIP kinase is responsible for the phosphorylation of myosin II and necessary for cell motility in mammalian fibroblasts. *The Journal of Cell Biology*. **165**(2),pp.243–254.

Komatsu, S. and Ikebe, M. 2014. ZIPK is critical for the motility and contractility of VSMCs through the regulation of nonmuscle myosin II isoforms. *American Journal of Physiology. Heart and Circulatory Physiology*. **306**(9),pp.H1275–1286.

Konev, A.Y. et al. 2007. CHD1 motor protein is required for deposition of histone variant H3.3 into chromatin in vivo. *Science (New York, N.Y.)*. **317**(5841),pp.1087–1090.

Konietzko, U. et al. 1999. Pim kinase expression is induced by LTP stimulation and required for the consolidation of enduring LTP. *The EMBO journal*. **18**(12),pp.3359–3369.

Koning, J.J. and Mebius, R.E. 2012. Interdependence of stromal and immune cells for lymph node function. *Trends in Immunology*. **33**(6),pp.264–270.

Kosan, C. et al. 2010. Transcription Factor Miz-1 Is Required to Regulate Interleukin-7 Receptor Signaling at Early Commitment Stages of B Cell Differentiation. *Immunity*. **33**(6),pp.917–928.

Kovacina, K.S. et al. 2003. Identification of a Proline-rich Akt Substrate as a 14-3-3 Binding Partner. *Journal of Biological Chemistry*. **278**(12),pp.10189–10194.

Kracker, S. and Durandy, A. 2011. Insights into the B cell specific process of immunoglobulin class switch recombination. *Immunology Letters*. **138**(2),pp.97–103.

Kretzner, L. et al. 1992. Myc and Max proteins possess distinct transcriptional activities. *Nature*. **359**(6394),pp.426–429.

Krishnan, S. et al. 2011. Structure and Function of Histone H3 Lysine 9 Methyltransferases and Demethylases. *ChemBioChem*. **12**(2),pp.254–263.

Krogan, N.J. et al. 2003. The Paf1 complex is required for histone H3 methylation by COMPASS and Dot1p: linking transcriptional elongation to histone methylation. *Molecular Cell*. **11**(3),pp.721–729.

Krouwels, I.M. et al. 2005. A glue for heterochromatin maintenance: stable SUV39H1 binding to heterochromatin is reinforced by the SET domain. *The Journal of Cell Biology*. **170**(4),pp.537–549.

Krysov, S. et al. 2010. Surface IgM of CLL cells displays unusual glycans indicative of engagement of antigen in vivo. *Blood*. **115**(21),pp.4198–4205.

Kuehn, H.S. et al. 2013. Loss-of-function of the protein kinase C δ (PKCδ) causes a B-cell lymphoproliferative syndrome in humans. *Blood*. **121**(16),pp.3117–3125.

Ku, M. et al. 2008. Genomewide analysis of PRC1 and PRC2 occupancy identifies two classes of bivalent domains. *PLoS genetics*. **4**(10),p.e1000242.

Kumanogoh, A. et al. 2000. Identification of CD72 as a Lymphocyte Receptor for the Class IV Semaphorin CD100: A Novel Mechanism for Regulating B Cell Signaling. *Immunity*. **13**(5),pp.621–631.

Kumar, A. et al. 2005. Crystal Structures of Proto-oncogene Kinase Pim1: A Target of Aberrant Somatic Hypermutations in Diffuse Large Cell Lymphoma. *Journal of Molecular Biology*. **348**(1),pp.183–193.

Kurland, J.F. and Tansey, W.P. 2008. Myc-Mediated Transcriptional Repression by Recruitment of Histone Deacetylase. *Cancer Research*. **68**(10),pp.3624–3629.

Kurosaki, T. et al. 2000. Regulation of the phospholipase C-gamma2 pathway in B cells. *Immunological reviews*. **176**,pp.19–29.

Kwak, H. and Lis, J.T. 2013. Control of Transcriptional Elongation. *Annual Review of Genetics*. **47**(1),pp.483–508.

Kwon, S.H. et al. 2010. Heterochromatin protein 1 (HP1) connects the FACT histone chaperone complex to the phosphorylated CTD of RNA polymerase II. *Genes & development*. **24**(19),pp.2133–2145.

Lachner, M. et al. 2001. Methylation of histone H3 lysine 9 creates a binding site for HP1 proteins. *Nature*. **410**(6824),pp.116–120.

Lagneaux, L. et al. 1998. Chronic lymphocytic leukemic B cells but not normal B cells are rescued from apoptosis by contact with normal bone marrow stromal cells. *Blood*. **91**(7),pp.2387–2396.

Lanasa, M.C. and Weinberg, J.B. 2011. Immunoglobulin class switch recombination in chronic lymphocytic leukemia. *Leukemia & Lymphoma*. **52**(7),pp.1398–1400.

Lane, P. et al. 1992. Activated human T cells express a ligand for the human B cell-associated antigen CD40 which participates in T cell-dependent activation of B lymphocytes. *European Journal of Immunology*. **22**(10),pp.2573–2578.

Lange, M. et al. 2008. Regulation of muscle development by DPF3, a novel histone acetylation and methylation reader of the BAF chromatin remodeling complex. *Genes & Development*. **22**(17),pp.2370–2384.

Langerak, A.W. and Dongen, J.J.M. van 2012. Multiple clonal Ig/TCR products: implications for interpretation of clonality findings. *Journal of Hematopathology*. **5**(1-2),pp.35–43.

Langmead, B. and Salzberg, S.L. 2012. Fast gapped-read alignment with Bowtie 2. *Nature Methods*. **9**(4),pp.357–359.

Lanham, S. et al. 2003. Differential signaling via surface IgM is associated with VH gene mutational status and CD38 expression in chronic lymphocytic leukemia. *Blood*. **101**(3),pp.1087–1093.

Lankester, A.C. et al. 1994. CD5 is associated with the human B cell antigen receptor complex. *European Journal of Immunology*. **24**(4),pp.812–816.
Lanoue, A. et al. 2002. Interaction of CD22 with alpha2,6-linked sialoglycoconjugates: innate recognition of self to dampen B cell autoreactivity? *European Journal of Immunology*. **32**(2),pp.348–355.
Laplante, M. and Sabatini, D.M. 2012. mTOR Signaling in Growth Control and Disease. *Cell*. **149**(2),pp.274–293.
Larochelle, M. and Gaudreau, L. 2003. H2A.Z has a function reminiscent of an activator required for preferential binding to intergenic DNA. *The EMBO journal*. **22**(17),pp.4512–4522.
Lau, P.N.I. and Cheung, P. 2012. Elucidating combinatorial histone modifications and crosstalks by coupling histone-modifying enzyme with biotin ligase activity. *Nucleic acids research*.
Lau, P.N.I. and Cheung, P. 2011. Histone code pathway involving H3 S28 phosphorylation and K27 acetylation activates transcription and antagonizes polycomb silencing. *Proceedings of the National Academy of Sciences*. **108**(7),pp.2801–2806.
Lawson, T.G. et al. 1989. Dissociation of double-stranded polynucleotide helical structures by eukaryotic initiation factors, as revealed by a novel assay. *Biochemistry*. **28**(11),pp.4729–4734.
Lebbink, R.J. et al. 2011. Polymerase II Promoter Strength Determines Efficacy of microRNA Adapted shRNAs. *PLoS ONE*. **6**(10),p.e26213.
Lederman, S. et al. 1992. Identification of a novel surface protein on activated CD4+ T cells that induces contact-dependent B cell differentiation (help). *The Journal of Experimental Medicine*. **175**(4),pp.1091–1101.
Lee, S.-W. et al. 2010. ASXL1 represses retinoic acid receptor-mediated transcription through associating with HP1 and LSD1. *The Journal of Biological Chemistry*. **285**(1),pp.18–29.
Lee, T. et al. 2008. Sensing and integration of Erk and PI3K signals by Myc. *PLoS computational biology*. **4**(2),p.e1000013.
Lee, T.I. and Young, R.A. 2013. Transcriptional Regulation and Its Misregulation in Disease. *Cell*. **152**(6),pp.1237–1251.
Lehman, A.L. and Dahmus, M.E. 2000. The sensitivity of RNA polymerase II in elongation complexes to C-terminal domain phosphatase. *The Journal of Biological Chemistry*. **275**(20),pp.14923–14932.
Von der Lehr, N. et al. 2003. The F-Box Protein Skp2 Participates in c-Myc Proteosomal Degradation and Acts as a Cofactor for c-Myc-Regulated Transcription. *Molecular Cell*. **11**(5),pp.1189–1200.
Leister, P. et al. 2008. ZIP kinase plays a crucial role in androgen receptor-mediated transcription. *Oncogene*. **27**(23),pp.3292–3300.
Leitges, M. et al. 1996. Immunodeficiency in Protein Kinase Cβ-Deficient Mice. *Science*. **273**(5276),pp.788–791.
Lemay, S. et al. 2000. Dok-3, a Novel Adapter Molecule Involved in the Negative Regulation of Immunoreceptor Signaling. *Molecular and Cellular Biology*. **20**(8),pp.2743–2754.
Lenz, G. et al. 2007. Aberrant immunoglobulin class switch recombination and switch translocations in activated B cell–like diffuse large B cell lymphoma. *The Journal of Experimental Medicine*. **204**(3),pp.633–643.
Lenz, G. et al. 2008. Oncogenic CARD11 mutations in human diffuse large B cell lymphoma. *Science (New York, N.Y.)*. **319**(5870),pp.1676–1679.
Lenz, G. et al. 2008. Stromal gene signatures in large-B-cell lymphomas. *The New England journal of medicine*. **359**(22),pp.2313–2323.
Leung, C.O.-N. et al. 2015. PIM1 regulates glycolysis and promotes tumor progression in hepatocellular carcinoma. *Oncotarget*.
Levens, D. 2010. 'You Don't Muck with MYC'*. *Genes & Cancer*. **1**(6),pp.547–554.

Ley, R. et al. 2004. Extracellular Signal-regulated Kinases 1/2 Are Serum-stimulated 'BimEL Kinases' That Bind to the BH3-only Protein BimEL Causing Its Phosphorylation and Turnover. *Journal of Biological Chemistry*. **279**(10),pp.8837–8847.

Liao, B. et al. 2007. Competitive binding of AUF1 and TIAR to MYC mRNA controls its translation. *Nature Structural & Molecular Biology*. **14**(6),pp.511–518.

Li, B., Gogol, M., et al. 2007. Infrequently transcribed long genes depend on the Set2/Rpd3S pathway for accurate transcription. *Genes & Development*. **21**(11),pp.1422–1430.

Li, B., Carey, M., et al. 2007. The Role of Chromatin during Transcription. *Cell*. **128**(4),pp.707–719.

Li, G. et al. 2012. Extensive promoter-centered chromatin interactions provide a topological basis for transcription regulation. *Cell*. **148**(1-2),pp.84–98.

Li, H.L. et al. 1997. Syk is required for BCR-mediated activation of p90Rsk, but not p70S6k, via a mitogen-activated protein kinase-independent pathway in B cells. *The Journal of biological chemistry*. **272**(29),pp.18200–18208.

Li, J. et al. 2001. Transcriptional induction of MKP-1 in response to stress is associated with histone H3 phosphorylation-acetylation. *Molecular and Cellular Biology*. **21**(23),pp.8213–8224.

Lilly, M. et al. 1992. Sustained expression of the pim-1 kinase is specifically induced in myeloid cells by cytokines whose receptors are structurally related. *Oncogene*. **7**(4),pp.727–732.

Limnander, A. et al. 2014. Protein kinase Cδ promotes transitional B cell-negative selection and limits proximal B cell receptor signaling to enforce tolerance. *Molecular and Cellular Biology*. **34**(8),pp.1474–1485.

Limon, J.J. and Fruman, D.A. 2010. B cell receptor signaling: picky about PI3Ks. *Science Signaling*. **3**(134),p.pe25.

Lin, C.Y. et al. 2012. Transcriptional Amplification in Tumor Cells with Elevated c-Myc. *Cell*. **151**(1),pp.56–67.

Lin, J.J. et al. 2011. Mediator coordinates PIC assembly with recruitment of CHD1. *Genes & Development*. **25**(20),pp.2198–2209.

Linn, D.E. et al. 2012. Differential regulation of androgen receptor by PIM-1 kinases via phosphorylation-dependent recruitment of distinct ubiquitin E3 ligases. *The Journal of Biological Chemistry*. **287**(27),pp.22959–22968.

Lin, P.S. et al. 2002. TFIIF-associating carboxyl-terminal domain phosphatase dephosphorylates phosphoserines 2 and 5 of RNA polymerase II. *The Journal of Biological Chemistry*. **277**(48),pp.45949–45956.

Lin, T. et al. 2010. Tumor-initiating function of nucleostemin-enriched mammary tumor cells. *Cancer Research*. **70**(22),pp.9444–9452.

Liokatis, S. et al. 2012. Phosphorylation of histone H3 Ser10 establishes a hierarchy for subsequent intramolecular modification events. *Nature Structural & Molecular Biology*. **19**(8),pp.819–823.

Li, S. et al. 2003. Translation factor eIF4E rescues cells from Myc-dependent apoptosis by inhibiting cytochrome c release. *The Journal of Biological Chemistry*. **278**(5),pp.3015–3022.

Liu, S.-J. et al. 2004. Role of nucleostemin in growth regulation of gastric cancer, liver cancer and other malignancies. *World journal of gastroenterology: WJG*. **10**(9),pp.1246–1249.

Liu, X. et al. 2003. c-Myc Transformation Domain Recruits the Human STAGA Complex and Requires TRRAP and GCN5 Acetylase Activity for Transcription Activation. *Journal of Biological Chemistry*. **278**(22),pp.20405–20412.

Liu, X. et al. 2008. STAGA Recruits Mediator to the MYC Oncoprotein To Stimulate Transcription and Cell Proliferation. *Molecular and Cellular Biology*. **28**(1),pp.108–121.

Liu, Y. et al. 2012. Protein kinase C-δ negatively regulates T cell receptor-induced NF-κB activation by inhibiting the assembly of CARMA1 signalosome. *The Journal of Biological Chemistry*. **287**(24),pp.20081–20087.

Liu, Y.J. et al. 1995. Memory B cells from human tonsils colonize mucosal epithelium and directly present antigen to T cells by rapid up-regulation of B7-1 and B7-2. *Immunity*. **2**(3),pp.239–248.

Li, Y. et al. 2014. MYC through miR-17-92 suppresses specific target genes to maintain survival, autonomous proliferation, and a neoplastic state. *Cancer Cell*. **26**(2),pp.262–272.

Li, Y. et al. 2011. The histone modifications governing TFF1 transcription mediated by estrogen receptor. *The Journal of Biological Chemistry*. **286**(16),pp.13925–13936.

Li, Y. et al. 2009. The target of the NSD family of histone lysine methyltransferases depends on the nature of the substrate. *The Journal of Biological Chemistry*. **284**(49),pp.34283–34295.

Li, Y.-Y. et al. 2009. Essential contribution of Ets-1 to constitutive Pim-3 expression in human pancreatic cancer cells. *Cancer Science*. **100**(3),pp.396–404.

Li, Y.-Y. et al. 2006. Pim-3, a Proto-Oncogene with Serine/Threonine Kinase Activity, Is Aberrantly Expressed in Human Pancreatic Cancer and Phosphorylates Bad to Block Bad-Mediated Apoptosis in Human Pancreatic Cancer Cell Lines. *Cancer Research*. **66**(13),pp.6741–6747.

Li, Z. et al. 2003. A Global Transcriptional Regulatory Role for C-Myc in Burkitt's Lymphoma Cells. *Proceedings of the National Academy of Sciences*. **100**(14),pp.8164–8169.

Lo, D. et al. 2014. Nucleostemin stabilizes ARF by inhibiting the ubiquitin ligase ULF. *Oncogene*.

Loenarz, C. et al. 2010. PHF8, a gene associated with cleft lip/palate and mental retardation, encodes for an Nepsilon-dimethyl lysine demethylase. *Human Molecular Genetics*. **19**(2),pp.217–222.

Van Lohuizen, M. et al. 1991. Identification of cooperating oncogenes in E mu-myc transgenic mice by provirus tagging. *Cell*. **65**(5),pp.737–752.

Van Lohuizen, M. et al. 1989. Predisposition to lymphomagenesis in pim-1 transgenic mice: cooperation with c-myc and N-myc in murine leukemia virus-induced tumors. *Cell*. **56**(4),pp.673–682.

Lomberk, G. et al. 2006. Evidence for the existence of an HP1-mediated subcode within the histone code. *Nature Cell Biology*. **8**(4),pp.407–415.

Lomberk, G. et al. 2012. Sequence-specific Recruitment of Heterochromatin Protein 1 via Interaction with Krüppel-like Factor 11, a Human Transcription Factor Involved in Tumor Suppression and Metabolic Diseases. *Journal of Biological Chemistry*. **287**(16),pp.13026–13039.

Lösing, M. et al. 2013. The Dok-3/Grb2 Protein Signal Module Attenuates Lyn Kinase-dependent Activation of Syk Kinase in B Cell Antigen Receptor Microclusters. *Journal of Biological Chemistry*. **288**(4),pp.2303–2313.

Losman, J.A. et al. 2003. Protein phosphatase 2A regulates the stability of Pim protein kinases. *The Journal of biological chemistry*. **278**(7),pp.4800–4805.

Love, C. et al. 2012. The genetic landscape of mutations in Burkitt lymphoma. *Nature Genetics*. **44**(12),pp.1321–1325.

Lovén, J. et al. 2013. Selective Inhibition of Tumor Oncogenes by Disruption of Super-Enhancers. *Cell*. **153**(2),pp.320–334.

Lo, W.S. et al. 2000. Phosphorylation of serine 10 in histone H3 is functionally linked in vitro and in vivo to Gcn5-mediated acetylation at lysine 14. *Molecular Cell*. **5**(6),pp.917–926.

Lu, B.Y. et al. 2000. Heterochromatin protein 1 is required for the normal expression of two heterochromatin genes in Drosophila. *Genetics*. **155**(2),pp.699–708.

Luciano, F. et al. 2003. Phosphorylation of Bim-EL by Erk1/2 on serine 69 promotes its degradation via the proteasome pathway and regulates its proapoptotic function. *Oncogene*. **22**(43),pp.6785–6793.

Lucio-Eterovic, A.K. et al. 2010. Role for the nuclear receptor-binding SET domain protein 1 (NSD1) methyltransferase in coordinating lysine 36 methylation at histone 3 with RNA polymerase II function. *Proceedings of the National Academy of Sciences of the United States of America*. **107**(39),pp.16952–16957.

Luco, R.F. et al. 2011. Epigenetics in alternative pre-mRNA splicing. *Cell*. **144**(1),pp.16–26.

Luger, K. et al. 1997. Crystal structure of the nucleosome core particle at 2.8 A resolution. *Nature*. **389**(6648),pp.251–260.

Luger, K. et al. 2012. New insights into nucleosome and chromatin structure: an ordered state or a disordered affair? *Nature Reviews Molecular Cell Biology*. **13**(7),pp.436–447.

Van der Lugt, N.M. et al. 1995. Proviral tagging in E mu-myc transgenic mice lacking the Pim-1 proto-oncogene leads to compensatory activation of Pim-2. *The EMBO journal*. **14**(11),pp.2536–2544.

Lutterbach, B. and Hann, S.R. 1994. Hierarchical phosphorylation at N-terminal transformation-sensitive sites in c-Myc protein is regulated by mitogens and in mitosis. *Molecular and Cellular Biology*. **14**(8),pp.5510–5522.

Lynch, M.D. et al. 2012. An interspecies analysis reveals a key role for unmethylated CpG dinucleotides in vertebrate Polycomb complex recruitment. *The EMBO journal*. **31**(2),pp.317–329.

Macdonald, A. et al. 2006. Pim kinases phosphorylate multiple sites on Bad and promote 14-3-3 binding and dissociation from Bcl-XL. *BMC cell biology*. **7**,p.1.

MacDonald, J.A. et al. 2001. Identification of the endogenous smooth muscle myosin phosphatase-associated kinase. *Proceedings of the National Academy of Sciences*. **98**(5),pp.2419–2424.

Macdonald, N. et al. 2005. Molecular basis for the recognition of phosphorylated and phosphoacetylated histone h3 by 14-3-3. *Molecular Cell*. **20**(2),pp.199–211.

Machanick, P. and Bailey, T.L. 2011. MEME-ChIP: motif analysis of large DNA datasets. *Bioinformatics*. **27**(12),pp.1696–1697.

Machida, Y.J. et al. 2005. Right Place, Right Time, and Only Once: Replication Initiation in Metazoans. *Cell*. **123**(1),pp.13–24.

Maclean, K.H. et al. 2003. c-Myc augments gamma irradiation-induced apoptosis by suppressing Bcl-XL. *Molecular and Cellular Biology*. **23**(20),pp.7256–7270.

MacLennan, I.C.M. et al. 2003. Extrafollicular antibody responses. *Immunological Reviews*. **194**(1),pp.8–18.

Maeda, A. et al. 1999. Paired immunoglobulin-like receptor B (PIR-B) inhibits BCR-induced activation of Syk and Btk by SHP-1. *Oncogene*. **18**(14),pp.2291–2297.

Mahadevan, L.C. et al. 1991. Rapid histone H3 phosphorylation in response to growth factors, phorbol esters, okadaic acid, and protein synthesis inhibitors. *Cell*. **65**(5),pp.775–783.

Mahat, D.B. et al. 2012. Coordinated expression of tristetraprolin post-transcriptionally attenuates mitogenic induction of the oncogenic Ser/Thr kinase Pim-1. *PloS one*. **7**(3),p.e33194.

Ma, H. and Pederson, T. 2007. Depletion of the nucleolar protein nucleostemin causes G1 cell cycle arrest via the p53 pathway. *Molecular biology of the cell*. **18**(7),pp.2630–2635.

Maier, C.J. et al. 2012. PIM-1 kinase interacts with the DNA binding domain of the vitamin D receptor: a further kinase implicated in 1,25-(OH)2D3 signaling. *BMC molecular biology*. **13**,p.18.

Maita, H. et al. 2000. PAP-1, a novel target protein of phosphorylation by pim-1 kinase. *European journal of biochemistry / FEBS*. **267**(16),pp.5168–5178.

Maita, H. et al. 2004. PAP-1, the mutated gene underlying the RP9 form of dominant retinitis pigmentosa, is a splicing factor. *Experimental Cell Research*. **300**(2),pp.283–296.

Ma, J. et al. 2007. Negative regulation of Pim-1 protein kinase levels by the B56β subunit of PP2A. *Oncogene*. **26**(35),pp.5145–5153.

Malhotra, S. et al. 2009. B Cell Antigen Receptor Endocytosis and Antigen Presentation to T Cells Require Vav and Dynamin. *Journal of Biological Chemistry*. **284**(36),pp.24088–24097.

Malinen, M. et al. 2013. Proto-oncogene PIM-1 is a novel estrogen receptor target associating with high grade breast tumors. *Molecular and Cellular Endocrinology*. **365**(2),pp.270–276.

Mandal, M. et al. 2009. Ras orchestrates exit from the cell cycle and light-chain recombination during early B cell development. *Nature Immunology*. **10**(10),pp.1110–1117.

Mankaï, A. et al. 2008. Purine-rich box-1-mediated reduced expression of CD20 alters rituximab-induced lysis of chronic lymphocytic leukemia B cells. *Cancer Research*. **68**(18),pp.7512–7519.

Manning, B.D. et al. 2002. Identification of the tuberous sclerosis complex-2 tumor suppressor gene product tuberin as a target of the phosphoinositide 3-kinase/akt pathway. *Molecular Cell*. **10**(1),pp.151–162.

Marais, R. et al. 1993. The SRF accessory protein Elk-1 contains a growth factor-regulated transcriptional activation domain. *Cell*. **73**(2),pp.381–393.

Marani, M. et al. 2004. Role of Bim in the survival pathway induced by Raf in epithelial cells. *Oncogene*. **23**(14),pp.2431–2441.

Marderosian, M. et al. 2006. Tristetraprolin regulates Cyclin D1 and c-Myc mRNA stability in response to rapamycin in an Akt-dependent manner via p38 MAPK signaling. *Oncogene*. **25**(47),pp.6277–6290.

Margueron, R. et al. 2009. Role of the polycomb protein EED in the propagation of repressive histone marks. *Nature*. **461**(7265),pp.762–767.

Marina, O. et al. 2010. Serologic markers of effective tumor immunity against chronic lymphocytic leukemia include nonmutated B-cell antigens. *Cancer research*. **70**(4),pp.1344–1355.

Martinez, E. et al. 2001. Human STAGA complex is a chromatin-acetylating transcription coactivator that interacts with pre-mRNA splicing and DNA damage-binding factors in vivo. *Molecular and Cellular Biology*. **21**(20),pp.6782–6795.

Martin, K.J. and Arthur, J.S.C. 2012. Selective kinase inhibitors as tools for neuroscience research. *Neuropharmacology*. **63**(7),pp.1227–1237.

Martin, P. et al. 2002. Role of ζPKC in B-cell signaling and function. *The EMBO Journal*. **21**(15),pp.4049–4057.

Mateescu, B. et al. 2004. Tethering of HP1 proteins to chromatin is relieved by phosphoacetylation of histone H3. *EMBO reports*. **5**(5),pp.490–496.

Matikainen, S. et al. 1999. Interferon-alpha activates multiple STAT proteins and upregulates proliferation-associated IL-2Ralpha, c-myc, and pim-1 genes in human T cells. *Blood*. **93**(6),pp.1980–1991.

Matsuuchi, L. and Gold, M.R. 2001. New views of BCR structure and organization. *Current Opinion in Immunology*. **13**(3),pp.270–277.

Matthews, S.A. et al. 2003. Regulation of Protein Kinase Cv by the B-cell Antigen Receptor. *Journal of Biological Chemistry*. **278**(11),pp.9086–9091.

McCabe, M.T. et al. 2012. EZH2 inhibition as a therapeutic strategy for lymphoma with EZH2-activating mutations. *Nature*. **492**(7427),pp.108–112.

McEwan, I.J. et al. 1996. Functional Interaction of the c-Myc Transactivation Domain with the TATA Binding Protein: Evidence for an Induced Fit Model of Transactivation Domain Folding†. *Biochemistry*. **35**(29),pp.9584–9593.
McGinty, R.K. et al. 2008. Chemically ubiquitylated histone H2B stimulates hDot1L-mediated intranucleosomal methylation. *Nature*. **453**(7196),pp.812–816.
McGinty, R.K. et al. 2009. Structure-activity analysis of semisynthetic nucleosomes: mechanistic insights into the stimulation of Dot1L by ubiquitylated histone H2B. *ACS chemical biology*. **4**(11),pp.958–968.
McKeown, M.R. and Bradner, J.E. 2014. Therapeutic Strategies to Inhibit MYC. *Cold Spring Harbor Perspectives in Medicine*. **4**(10),p.a014266.
McMahon, S.B. et al. 2000. The Essential Cofactor TRRAP Recruits the Histone Acetyltransferase hGCN5 to C-Myc. *Molecular and Cellular Biology*. **20**(2),pp.556–562.
McMahon, S.B. et al. 1998. The Novel ATM-Related Protein TRRAP Is an Essential Cofactor for the c-Myc and E2F Oncoproteins. *Cell*. **94**(3),pp.363–374.
McManus, E.J. et al. 2004. The in vivo role of PtdIns(3,4,5)P3 binding to PDK1 PH domain defined by knockin mutation. *The EMBO journal*. **23**(10),pp.2071–2082.
Mebius, R.E. and Kraal, G. 2005. Structure and function of the spleen. *Nature Reviews Immunology*. **5**(8),pp.606–616.
Mecklenbräuker, I. et al. 2002. Protein kinase Cδ controls self-antigen-induced B-cell tolerance. *Nature*. **416**(6883),pp.860–865.
Meja, K. et al. 2014. PIM and AKT kinase inhibitors show synergistic cytotoxicity in acute myeloid leukaemia that is associated with convergence on mTOR and MCL1 pathways. *British Journal of Haematology*.
Melamed, D. and Nemazee, D. 1997. Self-antigen does not accelerate immature B cell apoptosis, but stimulates receptor editing as a consequence of developmental arrest. *Proceedings of the National Academy of Sciences of the United States of America*. **94**(17),pp.9267–9272.
Mempel, T.R. et al. 2004. T-cell priming by dendriticcells in lymph nodes occurs in three distinct phases. *Nature*. **427**(6970),pp.154–159.
Mendenhall, E.M. et al. 2010. GC-rich sequence elements recruit PRC2 in mammalian ES cells. *PLoS genetics*. **6**(12),p.e1001244.
Meng, L. et al. 2008. Nucleoplasmic mobilization of nucleostemin stabilizes MDM2 and promotes G2-M progression and cell survival. *Journal of cell science*. **121**(Pt 24),pp.4037–4046.
Merrell, K.T. et al. 2006. Identification of Anergic B Cells within a Wild-Type Repertoire. *Immunity*. **25**(6),pp.953–962.
Mertz, J.A. et al. 2011. Targeting MYC dependence in cancer by inhibiting BET bromodomains. *Proceedings of the National Academy of Sciences of the United States of America*. **108**(40),pp.16669–16674.
Meryet-Figuiere, M. et al. 2014. Temporal separation of replication and transcription during S-phase progression. *Cell Cycle (Georgetown, Tex.)*. **13**(20),pp.3241–3248.
Messmer, B.T. et al. 2005. In vivo measurements document the dynamic cellular kinetics of chronic lymphocytic leukemia B cells. *The Journal of Clinical Investigation*. **115**(3),pp.755–764.
Messmer, B.T. et al. 2004. Multiple Distinct Sets of Stereotyped Antigen Receptors Indicate a Role for Antigen in Promoting Chronic Lymphocytic Leukemia. *The Journal of Experimental Medicine*. **200**(4),pp.519–525.
Metzger, E. et al. 2008. Phosphorylation of histone H3 at threonine 11 establishes a novel chromatin mark for transcriptional regulation. *Nature cell biology*. **10**(1),pp.53–60.
Metzger, E. et al. 2010. Phosphorylation of histone H3T6 by PKCβI controls demethylation at histone H3K4. *Nature*. **464**(7289),pp.792–796.

Meyer, K.D. et al. 2008. Cooperative activity of cdk8 and GCN5L within Mediator directs tandem phosphoacetylation of histone H3. *The EMBO Journal*. **27**(10),pp.1447–1457.

Meyer, N. et al. 2006. The Oscar-worthy role of Myc in apoptosis. *Seminars in Cancer Biology*. **16**(4),pp.275–287.

Middendorp, S. et al. 2003. Function of Bruton's tyrosine kinase during B cell development is partially independent of its catalytic activity. *Journal of Immunology (Baltimore, Md.: 1950)*. **171**(11),pp.5988–5996.

Mikkelsen, T.S. et al. 2007. Genome-wide maps of chromatin state in pluripotent and lineage-committed cells. *Nature*. **448**(7153),pp.553–560.

Mikkers, H. et al. 2002. High-throughput retroviral tagging to identify components of specific signaling pathways in cancer. *Nature Genetics*. **32**(1),pp.153–159.

Mikkers, H. et al. 2004. Mice deficient for all PIM kinases display reduced body size and impaired responses to hematopoietic growth factors. *Molecular and Cellular Biology*. **24**(13),pp.6104–6115.

Milburn, C.C. et al. 2003. Binding of phosphatidylinositol 3,4,5-trisphosphate to the pleckstrin homology domain of protein kinase B induces a conformational change. *The Biochemical Journal*. **375**(Pt 3),pp.531–538.

Mills, J.R. et al. 2008. mTORC1 promotes survival through translational control of Mcl-1. *Proceedings of the National Academy of Sciences of the United States of America*. **105**(31),pp.10853–10858.

Milne, T.A. et al. 2010. Multiple interactions recruit MLL1 and MLL1 fusion proteins to the HOXA9 locus in leukemogenesis. *Molecular Cell*. **38**(6),pp.853–863.

Minc, E. et al. 2000. HP1gamma associates with euchromatin and heterochromatin in mammalian nuclei and chromosomes. *Cytogenetics and Cell Genetics*. **90**(3-4),pp.279–284.

Minc, E. et al. 1999. Localization and phosphorylation of HP1 proteins during the cell cycle in mammalian cells. *Chromosoma*. **108**(4),pp.220–234.

Minden, M.D. et al. 2012. Chronic lymphocytic leukaemia is driven by antigen-independent cell-autonomous signalling. *Nature*. **489**(7415),pp.309–312.

Min, J. et al. 2003. Structural basis for specific binding of Polycomb chromodomain to histone H3 methylated at Lys 27. *Genes & Development*. **17**(15),pp.1823–1828.

Mitchell, K.O. et al. 2000. Bax is a transcriptional target and mediator of c-myc-induced apoptosis. *Cancer Research*. **60**(22),pp.6318–6325.

Miyamoto, A. et al. 2002. Increased proliferation of B cells and auto-immunity in mice lacking protein kinase Cdelta. *Nature*. **416**(6883),pp.865–869.

Mizuki, M. et al. 2003. Suppression of myeloid transcription factors and induction of STAT response genes by AML-specific Flt3 mutations. *Blood*. **101**(8),pp.3164–3173.

Mizuno, K. et al. 2000. Src homology region 2 (SH2) domain-containing phosphatase-1 dephosphorylates B cell linker protein/SH2 domain leukocyte protein of 65 kDa and selectively regulates c-Jun NH2-terminal kinase activation in B cells. *Journal of Immunology (Baltimore, Md.: 1950)*. **165**(3),pp.1344–1351.

Mochizuki, T. et al. 1999. Physical and functional interactions between Pim-1 kinase and Cdc25A phosphatase. Implications for the Pim-1-mediated activation of the c-Myc signaling pathway. *The Journal of biological chemistry*. **274**(26),pp.18659–18666.

Mockridge, C.I. et al. 2007. Reversible anergy of sIgM-mediated signaling in the two subsets of CLL defined by VH-gene mutational status. *Blood*. **109**(10),pp.4424–4431.

Moffat, L.D. et al. 2011. Chemical genetics of zipper-interacting protein kinase reveal myosin light chain as a bona fide substrate in permeabilized arterial smooth muscle. *The Journal of Biological Chemistry*. **286**(42),pp.36978–36991.

Mognol, G.P. et al. 2012. Transcriptional regulation of the c-Myc promoter by NFAT1 involves negative and positive NFAT-responsive elements. *Cell Cycle*. **11**(5),pp.1014–1028.

Möhle, R. et al. 1999. Overexpression of the chemokine receptor CXCR4 in B cell chronic lymphocytic leukemia is associated with increased functional response to stromal cell-derived factor-1 (SDF-1). *Leukemia*. **13**(12),pp.1954–1959.

Mombaerts, P. et al. 1992. RAG-1-deficient mice have no mature B and T lymphocytes. *Cell*. **68**(5),pp.869–877.

Monroe, J.G. 2006. ITAM-mediated tonic signalling through pre-BCR and BCR complexes. *Nature Reviews Immunology*. **6**(4),pp.283–294.

Moon, T.C. et al. 2009. Advances in mast cell biology: new understanding of heterogeneity and function. *Mucosal Immunology*. **3**(2),pp.111–128.

Morcinek, J.C. et al. 2002. Activation of STAT5 triggers proliferation and contributes to anti-apoptotic signalling mediated by the oncogenic Xmrk kinase. *Oncogene*. **21**(11),pp.1668–1678.

Mori, K. et al. 1998. MM-1, a novel c-Myc-associating protein that represses transcriptional activity of c-Myc. *The Journal of Biological Chemistry*. **273**(45),pp.29794–29800.

Morikawa, K. et al. 1993. Induction of CD5 antigen on human CD5− B cells by stimulation with Staphylococcus aureus Cowan strain I. *International Immunology*. **5**(8),pp.809–816.

Morishita, D. et al. 2008. Pim kinases promote cell cycle progression by phosphorylating and down-regulating p27Kip1 at the transcriptional and posttranscriptional levels. *Cancer research*. **68**(13),pp.5076–5085.

Möröy, T. et al. 1991. E mu N- and E mu L-myc cooperate with E mu pim-1 to generate lymphoid tumors at high frequency in double-transgenic mice. *Oncogene*. **6**(11),pp.1941–1948.

Morton, S. et al. 2003. A reinvestigation of the multisite phosphorylation of the transcription factor c-Jun. *The EMBO Journal*. **22**(15),pp.3876–3886.

Movilla, N. and Bustelo, X.R. 1999. Biological and Regulatory Properties of Vav-3, a New Member of the Vav Family of Oncoproteins. *Molecular and Cellular Biology*. **19**(11),pp.7870–7885.

Muntean, A.G. et al. 2010. The PAF complex synergizes with MLL fusion proteins at HOX loci to promote leukemogenesis. *Cancer Cell*. **17**(6),pp.609–621.

Muramatsu, D. et al. 2013. Pericentric heterochromatin generated by HP1 protein interaction-defective histone methyltransferase Suv39h1. *The Journal of Biological Chemistry*. **288**(35),pp.25285–25296.

Muramatsu, M. et al. 2000. Class Switch Recombination and Hypermutation Require Activation-Induced Cytidine Deaminase (AID), a Potential RNA Editing Enzyme. *Cell*. **102**(5),pp.553–563.

Muraski, J.A. et al. 2007. Pim-1 regulates cardiomyocyte survival downstream of Akt. *Nature Medicine*. **13**(12),pp.1467–1475.

Murata-Hori, M. et al. 2001. HeLa ZIP kinase induces diphosphorylation of myosin II regulatory light chain and reorganization of actin filaments in nonmuscle cells. *Oncogene*. **20**(57),pp.8175–8183.

Murata-Hori, M. et al. 1999. ZIP kinase identified as a novel myosin regulatory light chain kinase in HeLa cells. *FEBS letters*. **451**(1),pp.81–84.

Murga, C. et al. 2002. Rac1 and RhoG promote cell survival by the activation of PI3K and Akt, independently of their ability to stimulate JNK and NF-kappaB. *Oncogene*. **21**(2),pp.207–216.

Murphy, L.O. et al. 2004. A Network of Immediate Early Gene Products Propagates Subtle Differences in Mitogen-Activated Protein Kinase Signal Amplitude and Duration. *Molecular and Cellular Biology*. **24**(1),pp.144–153.

Murray, F. et al. 2008. Stereotyped patterns of somatic hypermutation in subsets of patients with chronic lymphocytic leukemia: implications for the role of antigen selection in leukemogenesis. *Blood*. **111**(3),pp.1524–1533.

Müschen, M. et al. 2002. The origin of CD95-gene mutations in B-cell lymphoma. *Trends in Immunology*. **23**(2),pp.75–80.

Muzio, M. et al. 2008. Constitutive activation of distinct BCR-signaling pathways in a subset of CLL patients: a molecular signature of anergy. *Blood*. **112**(1),pp.188–195.

Myhrinder, A.L. et al. 2008. A new perspective: molecular motifs on oxidized LDL, apoptotic cells, and bacteria are targets for chronic lymphocytic leukemia antibodies. *Blood*. **111**(7),pp.3838–3848.

Nagano, T. et al. 2013. Single-cell Hi-C reveals cell-to-cell variability in chromosome structure. *Nature*. **502**(7469),pp.59–64.

Nair, S.K. and Burley, S.K. 2003. X-Ray Structures of Myc-Max and Mad-Max Recognizing DNA: Molecular Bases of Regulation by Proto-Oncogenic Transcription Factors. *Cell*. **112**(2),pp.193–205.

Nasser, M.W. et al. 2008. Down-regulation of Micro-RNA-1 (miR-1) in Lung Cancer SUPPRESSION OF TUMORIGENIC PROPERTY OF LUNG CANCER CELLS AND THEIR SENSITIZATION TO DOXORUBICIN-INDUCED APOPTOSIS BY miR-1. *Journal of Biological Chemistry*. **283**(48),pp.33394–33405.

Nau, M.M. et al. 1985. L-myc, a new myc-related gene amplified and expressed in human small cell lung cancer. *Nature*. **318**(6041),pp.69–73.

Nawijn, M.C. et al. 2011. For better or for worse: the role of Pim oncogenes in tumorigenesis. *Nature reviews. Cancer*. **11**(1),pp.23–34.

Neal, J.W. and Clipstone, N.A. 2001. Glycogen synthase kinase-3 inhibits the DNA binding activity of NFATc. *The Journal of Biological Chemistry*. **276**(5),pp.3666–3673.

Nehru, V. et al. 2013. Interaction of RhoD and ZIP kinase modulates actin filament assembly and focal adhesion dynamics. *Biochemical and Biophysical Research Communications*. **433**(2),pp.163–169.

Nemazee, D.A. and Bürki, K. 1989. Clonal deletion of B lymphocytes in a transgenic mouse bearing anti-MHC class I antibody genes. *Nature*. **337**(6207),pp.562–566.

Ng, H.H. et al. 2003. Targeted recruitment of Set1 histone methylase by elongating Pol II provides a localized mark and memory of recent transcriptional activity. *Molecular Cell*. **11**(3),pp.709–719.

Ngo, V.N. et al. 2011. Oncogenically active MYD88 mutations in human lymphoma. *Nature*. **470**(7332),pp.115–119.

Nielsen, S.J. et al. 2001. Rb targets histone H3 methylation and HP1 to promoters. *Nature*. **412**(6846),pp.561–565.

Niemann, C.U. and Wiestner, A. 2013. B-cell receptor signaling as a driver of lymphoma development and evolution. *Seminars in Cancer Biology*. **23**(6, Part A),pp.410–421.

Nie, Z. et al. 2012. c-Myc is a universal amplifier of expressed genes in lymphocytes and embryonic stem cells. *Cell*. **151**(1),pp.68–79.

Nihira, K. et al. 2010. Pim-1 controls NF-kappaB signalling by stabilizing RelA/p65. *Cell Death and Differentiation*. **17**(4),pp.689–698.

Niiro, N. and Ikebe, M. 2001. Zipper-interacting protein kinase induces Ca(2+)-free smooth muscle contraction via myosin light chain phosphorylation. *The Journal of Biological Chemistry*. **276**(31),pp.29567–29574.

Nikolakaki, E. et al. 1993. Glycogen synthase kinase 3 phosphorylates Jun family members in vitro and negatively regulates their transactivating potential in intact cells. *Oncogene*. **8**(4),pp.833–840.

Nikpour, P. et al. 2009. Differential effects of Nucleostemin suppression on cell cycle arrest and apoptosis in the bladder cancer cell lines 5637 and SW1710. *Cell Proliferation*. **42**(6),pp.762–769.

Nishizumi, H. et al. 1998. A double-edged kinase Lyn: a positive and negative regulator for antigen receptor-mediated signals. *The Journal of Experimental Medicine*. **187**(8),pp.1343–1348.

Nitschke, L. 2005. The role of CD22 and other inhibitory co-receptors in B-cell activation. *Current Opinion in Immunology*. **17**(3),pp.290–297.

Van Noesel, C.J.M. et al. 1993. The CR2/CD19 complex on human B cells contains the src-family kinase Lyn. *International Immunology*. **5**(7),pp.699–705.

Nosaka, T. et al. 1999. STAT5 as a molecular regulator of proliferation, differentiation and apoptosis in hematopoietic cells. *The EMBO journal*. **18**(17),pp.4754–4765.

Nowak, S.J. and Corces, V.G. 2000. Phosphorylation of histone H3 correlates with transcriptionally active loci. *Genes & Development*. **14**(23),pp.3003–3013.

O'Brien, S. et al. 2014. Ibrutinib as initial therapy for elderly patients with chronic lymphocytic leukaemia or small lymphocytic lymphoma: an open-label, multicentre, phase 1b/2 trial. *The Lancet. Oncology*. **15**(1),pp.48–58.

O'Carroll, D. et al. 2000. Isolation and characterization of Suv39h2, a second histone H3 methyltransferase gene that displays testis-specific expression. *Molecular and Cellular Biology*. **20**(24),pp.9423–9433.

Oda, A. et al. 2008. PKC eta directs induction of IRF-4 expression and Ig kappa gene rearrangement in pre-BCR signaling pathway. *International Immunology*. **20**(11),pp.1417–1426.

O'Donnell, K.A. et al. 2005. c-Myc-regulated microRNAs modulate E2F1 expression. *Nature*. **435**(7043),pp.839–843.

Oeckinghaus, A. et al. 2007. Malt1 ubiquitination triggers NF-kappaB signaling upon T-cell activation. *The EMBO journal*. **26**(22),pp.4634–4645.

Ogawa, H. et al. 2002. A complex with chromatin modifiers that occupies E2F- and Myc-responsive genes in G0 cells. *Science (New York, N.Y.)*. **296**(5570),pp.1132–1136.

Ogryzko, V.V. et al. 1996. The transcriptional coactivators p300 and CBP are histone acetyltransferases. *Cell*. **87**(5),pp.953–959.

O'Hayre, M. et al. 2010. Elucidating the CXCL12/CXCR4 signaling network in chronic lymphocytic leukemia through phosphoproteomics analysis. *PloS One*. **5**(7),p.e11716.

Oh-hora, M. et al. 2003. Requirement for Ras Guanine Nucleotide Releasing Protein 3 in Coupling Phospholipase C-γ2 to Ras in B Cell Receptor Signaling. *The Journal of Experimental Medicine*. **198**(12),pp.1841–1851.

Okada, M. 2012. Regulation of the SRC family kinases by Csk. *International Journal of Biological Sciences*. **8**(10),pp.1385–1397.

Okada, T. et al. 2000. BCAP: The Tyrosine Kinase Substrate that Connects B Cell Receptor to Phosphoinositide 3-Kinase Activation. *Immunity*. **13**(6),pp.817–827.

Okamoto, M. et al. 2009. Identification of Death-Associated Protein Kinases Inhibitors Using Structure-Based Virtual Screening. *Journal of Medicinal Chemistry*. **52**(22),pp.7323–7327.

Okazaki, K. and Sagata, N. 1995. The Mos/MAP kinase pathway stabilizes c-Fos by phosphorylation and augments its transforming activity in NIH 3T3 cells. *The EMBO journal*. **14**(20),pp.5048–5059.

Okazaki, T. et al. 2001. PD-1 immunoreceptor inhibits B cell receptor-mediated signaling by recruiting src homology 2-domain-containing tyrosine phosphatase 2 to phosphotyrosine. *Proceedings of the National Academy of Sciences of the United States of America*. **98**(24),pp.13866–13871.

Okkenhaug, K. et al. 2007. Antigen receptor signalling: a distinctive role for the p110? isoform of PI3K. *Trends in Immunology*. **28**(2-2),pp.80–87.

Okkenhaug, K. et al. 2002. Impaired B and T cell antigen receptor signaling in p110delta PI 3-kinase mutant mice. *Science (New York, N.Y.)*. **297**(5583),pp.1031–1034.

Oliver, A.M. et al. 1999. IgMhighCD21high Lymphocytes Enriched in the Splenic Marginal Zone Generate Effector Cells More Rapidly Than the Bulk of Follicular B Cells. *The Journal of Immunology*. **162**(12),pp.7198–7207.

Oliver, P.M. et al. 2006. Loss of the proapoptotic protein, Bim, breaks B cell anergy. *The Journal of Experimental Medicine*. **203**(3),pp.731–741.

Omori, S.A. et al. 2006. Regulation of class-switch recombination and plasma cell differentiation by phosphatidylinositol 3-kinase signaling. *Immunity*. **25**(4),pp.545–557.

O'Neill, S.K. et al. 2011. Monophosphorylation of CD79a and CD79b ITAM motifs initiates a SHIP-1 phosphatase-mediated inhibitory signaling cascade required for B cell anergy. *Immunity*. **35**(5),pp.746–756.

Ono, M. et al. 1996. Role of the inositol phosphatase SHIP in negative regulation of the immune system by the receptor Fc(gamma)RIIB. *Nature*. **383**(6597),pp.263–266.

Ooi, S.K.T. et al. 2007. DNMT3L connects unmethylated lysine 4 of histone H3 to de novo methylation of DNA. *Nature*. **448**(7154),pp.714–717.

O'Rourke, L.M. et al. 1998. CD19 as a membrane-anchored adaptor protein of B lymphocytes: costimulation of lipid and protein kinases by recruitment of Vav. *Immunity*. **8**(5),pp.635–645.

Os, A. et al. 2013. Chronic lymphocytic leukemia cells are activated and proliferate in response to specific T helper cells. *Cell Reports*. **4**(3),pp.566–577.

Page, G. et al. 1999. AATF, a novel transcription factor that interacts with Dlk/ZIP kinase and interferes with apoptosis. *FEBS letters*. **462**(1-2),pp.187–191.

Page, G. et al. 1999. Interaction partners of Dlk/ZIP kinase: co-expression of Dlk/ZIP kinase and Par-4 results in cytoplasmic retention and apoptosis. *Oncogene*. **18**(51),pp.7265–7273.

Pal-Bhadra, M. et al. 2004. Heterochromatic silencing and HP1 localization in Drosophila are dependent on the RNAi machinery. *Science (New York, N.Y.)*. **303**(5658),pp.669–672.

Pan, G. et al. 2007. Whole-genome analysis of histone H3 lysine 4 and lysine 27 methylation in human embryonic stem cells. *Cell stem cell*. **1**(3),pp.299–312.

Panigrahi, A.K. et al. 2012. A cohesin–RAD21 interactome. *Biochemical Journal*. **442**(3),pp.661–670.

Pao, L.I. and Cambier, J.C. 1997. Syk, but not Lyn, recruitment to B cell antigen receptor and activation following stimulation of CD45- B cells. *Journal of Immunology (Baltimore, Md.: 1950)*. **158**(6),pp.2663–2669.

Papamokos, G.V. et al. 2012. Structural role of RKS motifs in chromatin interactions: a molecular dynamics study of HP1 bound to a variably modified histone tail. *Biophysical journal*. **102**(8),pp.1926–1933.

Parelho, V. et al. 2008. Cohesins functionally associate with CTCF on mammalian chromosome arms. *Cell*. **132**(3),pp.422–433.

Park, C.-H. and Kim, K.-T. 2012. Apoptotic Phosphorylation of Histone H3 on Ser-10 by Protein Kinase Cδ. *PLoS ONE*. **7**(9),p.e44307.

Pascual, V. et al. 1994. Analysis of somatic mutation in five B cell subsets of human tonsil. *The Journal of Experimental Medicine*. **180**(1),pp.329–339.

Pasqualucci, L. et al. 2004. Expression of the AID protein in normal and neoplastic B cells. *Blood*. **104**(10),pp.3318–3325.

Pasqualucci, L. et al. 2001. Hypermutation of multiple proto-oncogenes in B-cell diffuse large-cell lymphomas. *Nature*. **412**(6844),pp.341–346.

Pasqualucci, L. and Dalla-Favera, R. 2014. SnapShot: Diffuse Large B Cell Lymphoma. *Cancer Cell*. **25**(1),pp.132–132.e1.

Patel, J.H. et al. 2004. The c-MYC Oncoprotein Is a Substrate of the Acetyltransferases hGCN5/PCAF and TIP60. *Molecular and Cellular Biology*. **24**(24),pp.10826–10834.

Patten, P.E.M. et al. 2008. CD38 expression in chronic lymphocytic leukemia is regulated by the tumor microenvironment. *Blood*. **111**(10),pp.5173–5181.

Paulson, J.R. and Taylor, S.S. 1982. Phosphorylation of histones 1 and 3 and nonhistone high mobility group 14 by an endogenous kinase in HeLa metaphase chromosomes. *The Journal of Biological Chemistry*. **257**(11),pp.6064–6072.

Paumelle, R. et al. 2002. Hepatocyte growth factor/scatter factor activates the ETS1 transcription factor by a RAS-RAF-MEK-ERK signaling pathway. *Oncogene*. **21**(15),pp.2309–2319.

Payne, G.S. et al. 1982. Multiple arrangements of viral DNA and an activated host oncogene in bursal lymphomas. *Nature*. **295**(5846),pp.209–214.

Peltola, K. et al. 2009. Pim-1 kinase expression predicts radiation response in squamocellular carcinoma of head and neck and is under the control of epidermal growth factor receptor. *Neoplasia (New York, N.Y.)*. **11**(7),pp.629–636.

Penn, L.J. et al. 1990. Negative autoregulation of c-myc transcription. *The EMBO journal*. **9**(4),pp.1113–1121.

Pérez-Durán, P. et al. 2007. Oncogenic events triggered by AID, the adverse effect of antibody diversification. *Carcinogenesis*. **28**(12),pp.2427–2433.

Perry, A.M. et al. 2014. MYC and BCL2 protein expression predicts survival in patients with diffuse large B-cell lymphoma treated with rituximab. *British Journal of Haematology*. **165**(3),pp.382–391.

Petesch, S.J. and Lis, J.T. 2012. Overcoming the nucleosome barrier during transcript elongation. *Trends in genetics: TIG*. **28**(6),pp.285–294.

Pfaffl, M.W. 2001. A new mathematical model for relative quantification in real-time RT-PCR. *Nucleic Acids Research*. **29**(9),p.e45.

Phee, H. et al. 2001. Visualization of Negative Signaling in B Cells by Quantitative Confocal Microscopy. *Molecular and Cellular Biology*. **21**(24),pp.8615–8625.

Pieper, K. et al. 2013. B-cell biology and development. *Journal of Allergy and Clinical Immunology*. **131**(4),pp.959–971.

Pierrat, B. et al. 1998. RSK-B, a novel ribosomal S6 kinase family member, is a CREB kinase under dominant control of p38alpha mitogen-activated protein kinase (p38alphaMAPK). *The Journal of Biological Chemistry*. **273**(45),pp.29661–29671.

Pinson, J.-A. et al. 2011. Thiazolidinedione-Based PI3Kα Inhibitors: An Analysis of Biochemical and Virtual Screening Methods. *ChemMedChem*. **6**(3),pp.514–522.

Ponader, S. et al. 2012. The Bruton tyrosine kinase inhibitor PCI-32765 thwarts chronic lymphocytic leukemia cell survival and tissue homing in vitro and in vivo. *Blood*. **119**(5),pp.1182–1189.

Poortinga, G. et al. 2004. MAD1 and c-MYC regulate UBF and rDNA transcription during granulocyte differentiation. *The EMBO journal*. **23**(16),pp.3325–3335.

Postnikov, Y.V. et al. 2006. Chromosomal protein HMGN1 modulates the phosphorylation of serine 1 in histone H2A. *Biochemistry*. **45**(50),pp.15092–15099.

Potter, C.J. et al. 2002. Akt regulates growth by directly phosphorylating Tsc2. *Nature Cell Biology*. **4**(9),pp.658–665.

Van Potter, null 1963. FEEDBACK INHIBITION OF THYMIDINE KINASE BY THYMIDINE TRIPHOSPHATE. *Experimental Cell Research*. **24**,pp.SUPPL9:259–262.

Pracht, C. et al. 2007. Association of protein kinase C-delta with the B cell antigen receptor complex. *Cellular Signalling*. **19**(4),pp.715–722.

Prado, F. and Aguilera, A. 2005. Impairment of replication fork progression mediates RNA polII transcription-associated recombination. *The EMBO journal*. **24**(6),pp.1267–1276.

Preuss, U. et al. 2003. Novel mitosis-specific phosphorylation of histone H3 at Thr11 mediated by Dlk/ZIP kinase. *Nucleic Acids Research*. **31**(3),pp.878–885.

Punnonen, J. et al. 1993. Interleukin 13 induces interleukin 4-independent IgG4 and IgE synthesis and CD23 expression by human B cells. *Proceedings of the National Academy of Sciences*. **90**(8),pp.3730–3734.

Qian, J. et al. 2011. PP1/Repo-man dephosphorylates mitotic histone H3 at T3 and regulates chromosomal aurora B targeting. *Current biology: CB*. **21**(9),pp.766–773.

Qian, K.C. et al. 2005. Structural basis of constitutive activity and a unique nucleotide binding mode of human Pim-1 kinase. *The Journal of biological chemistry*. **280**(7),pp.6130–6137.

Qiao, Q. et al. 2011. The structure of NSD1 reveals an autoregulatory mechanism underlying histone H3K36 methylation. *The Journal of Biological Chemistry*. **286**(10),pp.8361–8368.

Qin, S. and Min, J. 2014. Structure and function of the nucleosome-binding PWWP domain. *Trends in Biochemical Sciences*. **39**(11),pp.536–547.

Qiu, Y. et al. 2012. Combinatorial readout of unmodified H3R2 and acetylated H3K14 by the tandem PHD finger of MOZ reveals a regulatory mechanism for HOXA9 transcription. *Genes & Development*. **26**(12),pp.1376–1391.

Ragvin, A. et al. 2004. Nucleosome binding by the bromodomain and PHD finger of the transcriptional cofactor p300. *Journal of Molecular Biology*. **337**(4),pp.773–788.

Rahl, P.B. et al. 2010. c-Myc regulates transcriptional pause release. *Cell*. **141**(3),pp.432–445.

Rahman, S. et al. 2011. The Brd4 Extraterminal Domain Confers Transcription Activation Independent of pTEFb by Recruiting Multiple Proteins, Including NSD3. *Molecular and Cellular Biology*. **31**(13),pp.2641–2652.

Rahmati, M. et al. 2014. Nucleostemin knocking-down causes cell cycle arrest and apoptosis in human T-cell acute lymphoblastic leukemia MOLT-4 cells via p53 and p21(Waf1/Cip1) up-regulation. *Hematology (Amsterdam, Netherlands)*.

Rainio, E.-M. et al. 2002. Cutting edge: Transcriptional activity of NFATc1 is enhanced by the Pim-1 kinase. *Journal of Immunology (Baltimore, Md.: 1950)*. **168**(4),pp.1524–1527.

Rainio, E.-M. et al. 2005. Pim kinases are upregulated during Epstein-Barr virus infection and enhance EBNA2 activity. *Virology*. **333**(2),pp.201–206.

Raisner, R.M. et al. 2005. Histone variant H2A.Z marks the 5' ends of both active and inactive genes in euchromatin. *Cell*. **123**(2),pp.233–248.

Rakshambikai, R. et al. 2013. Repertoire of protein kinases encoded in the genome of zebrafish shows remarkably large population of pim kinases. *Journal of Bioinformatics and Computational Biology*. **12**(01),p.1350014.

Ramachandran, P. et al. 2013. MaSC: mappability-sensitive cross-correlation for estimating mean fragment length of single-end short-read sequencing data. *Bioinformatics (Oxford, England)*. **29**(4),pp.444–450.

Ramiro, A.R. et al. 2004. AID is required for c-myc/IgH chromosome translocations in vivo. *Cell*. **118**(4),pp.431–438.

Ram, O. et al. 2011. Combinatorial patterning of chromatin regulators uncovered by genome-wide location analysis in human cells. *Cell*. **147**(7),pp.1628–1639.

Rangasamy, D. et al. 2003. Pericentric heterochromatin becomes enriched with H2A.Z during early mammalian development. *The EMBO journal*. **22**(7),pp.1599–1607.

Raval, A. et al. 2007. Downregulation of Death-Associated Protein Kinase 1 (DAPK1) in Chronic Lymphocytic Leukemia. *Cell*. **129**(5),pp.879–890.
Ravetch, J.V. and Bolland, S. 2001. Igg Fc Receptors. *Annual Review of Immunology*. **19**(1),pp.275–290.
Rea, S. et al. 2000. Regulation of chromatin structure by site-specific histone H3 methyltransferases. *Nature*. **406**(6796),pp.593–599.
Reichard, P. et al. 1960. Regulatory mechanisms in the synthesis of deoxyribonucleic acid in vitro. *Biochimica Et Biophysica Acta*. **41**,pp.558–559.
Reif, K. et al. 2002. Balanced responsiveness to chemoattractants from adjacent zones determines B-cell position. *Nature*. **416**(6876),pp.94–99.
Reiser-Erkan, C. et al. 2008. Hypoxia-inducible proto-oncogene Pim-1 is a prognostic marker in pancreatic ductal adenocarcinoma. *Cancer Biology & Therapy*. **7**(9),pp.1352–1359.
Revy, P. et al. 2000. Activation-induced cytidine deaminase (AID) deficiency causes the autosomal recessive form of the Hyper-IgM syndrome (HIGM2). *Cell*. **102**(5),pp.565–575.
Reynolds, L.F. et al. 2002. Vav1 Transduces T Cell Receptor Signals to the Activation of Phospholipase C-γ1 via Phosphoinositide 3-Kinase-dependent and -independent Pathways. *The Journal of Experimental Medicine*. **195**(9),pp.1103–1114.
Richards, J.D. et al. 2001. Inhibition of the MEK/ERK signaling pathway blocks a subset of B cell responses to antigen. *Journal of Immunology (Baltimore, Md.: 1950)*. **166**(6),pp.3855–3864.
Richter-Larrea, J.A. et al. 2010. Reversion of epigenetically mediated BIM silencing overcomes chemoresistance in Burkitt lymphoma. *Blood*. **116**(14),pp.2531–2542.
Rickert, R.C. 2013. New insights into pre-BCR and BCR signalling with relevance to B cell malignancies. *Nature reviews. Immunology*. **13**(8),pp.578–591.
Rigley, K.P. et al. 1989. Analysis of signaling via surface immunoglobulin receptors on b cells from cba/n mice. *European Journal of Immunology*. **19**(11),pp.2081–2086.
Riising, E.M. et al. 2014. Gene Silencing Triggers Polycomb Repressive Complex 2 Recruitment to CpG Islands Genome Wide. *Molecular Cell*. **55**(3),pp.347–360.
Ringshausen, I. et al. 2002. Constitutively activated phosphatidylinositol-3 kinase (PI-3K) is involved in the defect of apoptosis in B-CLL: association with protein kinase Cδ. *Blood*. **100**(10),pp.3741–3748.
Rinn, J.L. et al. 2007. Functional demarcation of active and silent chromatin domains in human HOX loci by noncoding RNAs. *Cell*. **129**(7),pp.1311–1323.
Riss, T.L. et al. 2004. Cell Viability Assays *In*: G. S. SITTAMPALAM et al., eds. *Assay Guidance Manual*. Bethesda (MD): Eli Lilly & Company and the National Center for Advancing Translational Sciences.
Rivera, C.M. and Ren, B. 2013. Mapping Human Epigenomes. *Cell*. **155**(1).
Robak, T. and Robak, P. 2013. BCR signaling in chronic lymphocytic leukemia and related inhibitors currently in clinical studies. *International Reviews of Immunology*. **32**(4),pp.358–376.
Rodriguez, R. et al. 2001. Tyrosine Residues in Phospholipase Cγ2 Essential for the Enzyme Function in B-cell Signaling. *Journal of Biological Chemistry*. **276**(51),pp.47982–47992.
Roifman, C.M. and Ke, S. 1993. CD19 is a substrate of the antigen receptor-associated protein tyrosine kinase in human B cells. *Biochemical and Biophysical Research Communications*. **194**(1),pp.222–225.
Rolli, V. et al. 2002. Amplification of B Cell Antigen Receptor Signaling by a Syk/ITAM Positive Feedback Loop. *Molecular Cell*. **10**(5),pp.1057–1069.

Romanova, L. et al. 2009. Critical role of nucleostemin in pre-rRNA processing. *The Journal of biological chemistry*. **284**(8),pp.4968–4977.

De Rooij, M.F.M. et al. 2012. The clinically active BTK inhibitor PCI-32765 targets B-cell receptor- and chemokine-controlled adhesion and migration in chronic lymphocytic leukemia. *Blood*. **119**(11),pp.2590–2594.

Roose, J.P. et al. 2007. Unusual Interplay of Two Types of Ras Activators, RasGRP and SOS, Establishes Sensitive and Robust Ras Activation in Lymphocytes. *Molecular and Cellular Biology*. **27**(7),pp.2732–2745.

Rosenbloom, K.R. et al. 2013. ENCODE Data in the UCSC Genome Browser: year 5 update. *Nucleic Acids Research*. **41**(D1),pp.D56–D63.

Rosenwald, A. et al. 2002. The Use of Molecular Profiling to Predict Survival after Chemotherapy for Diffuse Large-B-Cell Lymphoma. *New England Journal of Medicine*. **346**(25),pp.1937–1947.

Roskoski Jr., R. 2012. ERK1/2 MAP kinases: Structure, function, and regulation. *Pharmacological Research*. **66**(2),pp.105–143.

Roussel, M.F. et al. 1994. Dual control of myc expression through a single DNA binding site targeted by ets family proteins and E2F-1. *Oncogene*. **9**(2),pp.405–415.

Roux, P.P. et al. 2007. RAS/ERK signaling promotes site-specific ribosomal protein S6 phosphorylation via RSK and stimulates cap-dependent translation. *The Journal of Biological Chemistry*. **282**(19),pp.14056–14064.

Rowland, S.L. et al. 2010. Ras activation of Erk restores impaired tonic BCR signaling and rescues immature B cell differentiation. *The Journal of Experimental Medicine*. **207**(3),pp.607–621.

Rowley, R.B. et al. 1995. Syk protein-tyrosine kinase is regulated by tyrosine-phosphorylated Ig alpha/Ig beta immunoreceptor tyrosine activation motif binding and autophosphorylation. *Journal of Biological Chemistry*. **270**(19),pp.11590–11594.

Roy, C.L. et al. 2012. The degree of BCR and NFAT activation predicts clinical outcomes in chronic lymphocytic leukemia. *Blood*. **120**(2),pp.356–365.

Rozovski, U. et al. 2014. Stimulation of the B-cell receptor activates the JAK2/STAT3 signaling pathway in chronic lymphocytic leukemia cells. *Blood*.

Rudich, S.M. et al. 1988. Anti-IgM-mediated B cell signaling. Molecular analysis of ligand binding requisites for human B cell clonal expansion and tolerance. *The Journal of Experimental Medicine*. **168**(1),pp.247–266.

Rufiange, A. et al. 2007. Genome-wide replication-independent histone H3 exchange occurs predominantly at promoters and implicates H3 K56 acetylation and Asf1. *Molecular Cell*. **27**(3),pp.393–405.

Ruhl, D.D. et al. 2006. Purification of a human SRCAP complex that remodels chromatin by incorporating the histone variant H2A.Z into nucleosomes. *Biochemistry*. **45**(17),pp.5671–5677.

Ruminy, P. et al. 2011. The isotype of the BCR as a surrogate for the GCB and ABC molecular subtypes in diffuse large B-cell lymphoma. *Leukemia*. **25**(4),pp.681–688.

ar-Rushdi, A. et al. 1983. Differential expression of the translocated and the untranslocated c-myc oncogene in Burkitt lymphoma. *Science (New York, N.Y.)*. **222**(4622),pp.390–393.

Russell, D.M. et al. 1991. Peripheral deletion of self-reactive B cells. *Nature*. **354**(6351),pp.308–311.

Ruzinova, M.B. et al. 2010. Altered subcellular localization of c-Myc protein identifies aggressive B-cell lymphomas harboring a c-MYC translocation. *The American journal of surgical pathology*. **34**(6),pp.882–891.

Rybtsova, N. et al. 2007. Transcription-coupled deposition of histone modifications during MHC class II gene activation. *Nucleic Acids Research*. **35**(10),pp.3431–3441.

Sabbattini, P. et al. 2014. An H3K9/S10 methyl-phospho switch modulates Polycomb and Pol II binding at repressed genes during differentiation. *Molecular Biology of the Cell*. **25**(6),pp.904–915.

Sabò, A. et al. 2014. Selective transcriptional regulation by Myc in cellular growth control and lymphomagenesis. *Nature*. **511**(7510),pp.488–492.

Sachdeva, M. et al. 2009. p53 represses c-Myc through induction of the tumor suppressor miR-145. *Proceedings of the National Academy of Sciences*. **106**(9),pp.3207–3212.

Sadikovic, B. et al. 2008. Cause and Consequences of Genetic and Epigenetic Alterations in Human Cancer. *Current Genomics*. **9**(6),pp.394–408.

Saint-André, V. et al. 2011. Histone H3 lysine 9 trimethylation and HP1γ favor inclusion of alternative exons. *Nature Structural & Molecular Biology*. **18**(3),pp.337–344.

Sakabe, K. et al. 2010. β-N-acetylglucosamine (O-GlcNAc) is part of the histone code. *Proceedings of the National Academy of Sciences*. **107**(46),pp.19915–19920.

Sakamuro, D. et al. 1995. c-Myc induces apoptosis in epithelial cells by both p53-dependent and p53-independent mechanisms. *Oncogene*. **11**(11),pp.2411–2418.

Saksouk, N. et al. 2009. HBO1 HAT complexes target chromatin throughout gene coding regions via multiple PHD finger interactions with histone H3 tail. *Molecular cell*. **33**(2),pp.257–265.

Salghetti, S.E. et al. 1999. Destruction of Myc by ubiquitin-mediated proteolysis: cancer-associated and transforming mutations stabilize Myc. *The EMBO Journal*. **18**(3),pp.717–726.

Salzer, E. et al. 2013. B-cell deficiency and severe autoimmunity caused by deficiency of protein kinase C δ. *Blood*. **121**(16),pp.3112–3116.

Sampson, V.B. et al. 2007. MicroRNA let-7a down-regulates MYC and reverts MYC-induced growth in Burkitt lymphoma cells. *Cancer research*. **67**(20),pp.9762–9770.

Sancak, Y. et al. 2007. PRAS40 is an insulin-regulated inhibitor of the mTORC1 protein kinase. *Molecular Cell*. **25**(6),pp.903–915.

Sander, S. et al. 2012. Synergy between PI3K signaling and MYC in Burkitt lymphomagenesis. *Cancer Cell*. **22**(2),pp.167–179.

Santenard, A. et al. 2010. Heterochromatin formation in the mouse embryo requires critical residues of the histone variant H3.3. *Nature Cell Biology*. **12**(9),pp.853–862.

Sapkota, G.P. et al. 2007. BI-D1870 is a specific inhibitor of the p90 RSK (ribosomal S6 kinase) isoforms in vitro and in vivo. *Biochemical Journal*. **401**(Pt 1),pp.29–38.

Sarbassov, D.D. et al. 2005. Phosphorylation and Regulation of Akt/PKB by the Rictor-mTOR Complex. *Science*. **307**(5712),pp.1098–1101.

Saris, C.J. et al. 1991. The pim-1 oncogene encodes two related protein-serine/threonine kinases by alternative initiation at AUG and CUG. *The EMBO journal*. **10**(3),pp.655–664.

Sassone-Corsi, P. et al. 1999. Requirement of Rsk-2 for Epidermal Growth Factor-Activated Phosphorylation of Histone H3. *Science*. **285**(5429),pp.886–891.

Sato, M. et al. 2007. Augmentation of signaling through BCR containing IgE but not that containing IgA due to lack of CD22-mediated signal regulation. *Journal of Immunology (Baltimore, Md.: 1950)*. **178**(5),pp.2901–2907.

Sato, N. et al. 2006. Phosphorylation of threonine-265 in Zipper-interacting protein kinase plays an important role in its activity and is induced by IL-6 family cytokines. *Immunology Letters*. **103**(2),pp.127–134.

Sato, N. et al. 2005. Physical and functional interactions between STAT3 and ZIP kinase. *International Immunology*. **17**(12),pp.1543–1552.

Satou, A. et al. 2001. A Novel Transrepression Pathway of c-Myc RECRUITMENT OF A TRANSCRIPTIONAL COREPRESSOR COMPLEX TO c-Myc BY MM-1, A c-Myc-BINDING PROTEIN. *Journal of Biological Chemistry*. **276**(49),pp.46562–46567.

Sawicka, A. et al. 2014. H3S28 phosphorylation is a hallmark of the transcriptional response to cellular stress. *Genome Research*,p.gr.176255.114.

Sayós, J. et al. 2004. Recruitment of C-terminal Src kinase by the leukocyte inhibitory receptor CD85j. *Biochemical and Biophysical Research Communications*. **324**(2),pp.640–647.

Schatz, J.H. et al. 2011. Targeting cap-dependent translation blocks converging survival signals by AKT and PIM kinases in lymphoma. *The Journal of Experimental Medicine*. **208**(9),pp.1799–1807.

Scheid, M.P. et al. 2002. Multiple phosphoinositide 3-kinase-dependent steps in activation of protein kinase B. *Molecular and Cellular Biology*. **22**(17),pp.6247–6260.

Schlosser, I. et al. 2003. A role for c-Myc in the regulation of ribosomal RNA processing. *Nucleic Acids Research*. **31**(21),pp.6148–6156.

Schmidlin, H. et al. 2009. New insights into the regulation of human B-cell differentiation. *Trends in Immunology*. **30**(6),pp.277–285.

Schmitz, R. et al. 2012. Burkitt lymphoma pathogenesis and therapeutic targets from structural and functional genomics. *Nature*. **490**(7418),pp.116–120.

Schmitz, R. et al. 1996. Catalytic specificity of phosphotyrosine kinases Blk, Lyn, c-Src and Syk as assessed by phage display. *Journal of Molecular Biology*. **260**(5),pp.664–677.

Schmitz, R. et al. 2014. Oncogenic Mechanisms in Burkitt Lymphoma. *Cold Spring Harbor Perspectives in Medicine*. **4**(2),p.a014282.

Schreiber-Agus, N. et al. 1995. An amino-terminal domain of Mxi1 mediates anti-myc oncogenic activity and interacts with a homolog of the Yeast Transcriptional Repressor SIN3. *Cell*. **80**(5),pp.777–786.

Schuebel, K.E. et al. 1998. Phosphorylation-dependent and constitutive activation of Rho proteins by wild-type and oncogenic Vav-2. *The EMBO journal*. **17**(22),pp.6608–6621.

Schultz, D.C. et al. 2002. SETDB1: a novel KAP-1-associated histone H3, lysine 9-specific methyltransferase that contributes to HP1-mediated silencing of euchromatic genes by KRAB zinc-finger proteins. *Genes & Development*. **16**(8),pp.919–932.

Schulz, A. et al. 2011. Inflammatory cytokines and signaling pathways are associated with survival of primary chronic lymphocytic leukemia cells in vitro: a dominant role of CCL2. *Haematologica*. **96**(3),pp.408–416.

Schwab, M. et al. 1983. Amplified DNA with limited homology to myc cellular oncogene is shared by human neuroblastoma cell lines and a neuroblastoma tumour. *Nature*. **305**(5931),pp.245–248.

Schwartz, B.E. and Ahmad, K. 2005. Transcriptional activation triggers deposition and removal of the histone variant H3.3. *Genes & Development*. **19**(7),pp.804–814.

Sears, R. et al. 2000. Multiple Ras-dependent phosphorylation pathways regulate Myc protein stability. *Genes & Development*. **14**(19),pp.2501–2514.

Seidel, J.J. and Graves, B.J. 2002. An ERK2 docking site in the Pointed domain distinguishes a subset of ETS transcription factors. *Genes & Development*. **16**(1),pp.127–137.

Seitz, V. et al. 2011. Deep sequencing of MYC DNA-binding sites in Burkitt lymphoma. *PloS One*. **6**(11),p.e26837.

Seoane, J. et al. 2001. TGFβ influences Myc, Miz-1 and Smad to control the CDK inhibitor p15INK4b. *Nature Cell Biology*. **3**(4),pp.400–408.

Shahbazian, D. et al. 2006. The mTOR/PI3K and MAPK pathways converge on eIF4B to control its phosphorylation and activity. *The EMBO Journal*. **25**(12),pp.2781–2791.

Shani, G. et al. 2004. Death-Associated Protein Kinase Phosphorylates ZIP Kinase, Forming a Unique Kinase Hierarchy To Activate Its Cell Death Functions. *Molecular and Cellular Biology*. **24**(19),pp.8611–8626.

Shankland, K.R. et al. 2012. Non-Hodgkin lymphoma. *The Lancet*. **380**(9844),pp.848–857.

Shay, K.P. et al. 2005. Pim-1 kinase stability is regulated by heat shock proteins and the ubiquitin-proteasome pathway. *Molecular cancer research: MCR*. **3**(3),pp.170–181.

Sheiness, D. and Bishop, J.M. 1979. DNA and RNA from Uninfected Vertebrate Cells Contain Nucleotide Sequences Related to the Putative Transforming Gene of Avian Myelocytomatosis Virus. *Journal of Virology*. **31**(2),pp.514–521.

Shembade, N. et al. 2010. Inhibition of NF-κB Signaling by A20 Through Disruption of Ubiquitin Enzyme Complexes. *Science*. **327**(5969),pp.1135–1139.

Shen, W. et al. 2007. Solution structure of human Brg1 bromodomain and its specific binding to acetylated histone tails. *Biochemistry*. **46**(8),pp.2100–2110.

Shen, X. et al. 2008. EZH1 mediates methylation on histone H3 lysine 27 and complements EZH2 in maintaining stem cell identity and executing pluripotency. *Molecular Cell*. **32**(4),pp.491–502.

Shi, J. and Vakoc, C.R. 2014. The Mechanisms behind the Therapeutic Activity of BET Bromodomain Inhibition. *Molecular Cell*. **54**(5),pp.728–736.

Shilatifard, A. 2012. The COMPASS Family of Histone H3K4 Methylases: Mechanisms of Regulation in Development and Disease Pathogenesis. *Annual Review of Biochemistry*. **81**(1),pp.65–95.

Shimamura, A. et al. 2000. Rsk1 mediates a MEK–MAP kinase cell survival signal. *Current Biology*. **10**(3),pp.127–135.

Shinkai, Y. et al. 1992. RAG-2-deficient mice lack mature lymphocytes owing to inability to initiate V(D)J rearrangement. *Cell*. **68**(5),pp.855–867.

Shinohara, H. et al. 2007. IkappaB kinase beta-induced phosphorylation of CARMA1 contributes to CARMA1 Bcl10 MALT1 complex formation in B cells. *The Journal of Experimental Medicine*. **204**(13),pp.3285–3293.

Shirogane, T. et al. 1999. Synergistic roles for Pim-1 and c-Myc in STAT3-mediated cell cycle progression and antiapoptosis. *Immunity*. **11**(6),pp.709–719.

Shi, X. et al. 2006. ING2 PHD domain links histone H3 lysine 4 methylation to active gene repression. *Nature*. **442**(7098),pp.96–99.

Shi, Y. et al. 2012. PTEN at a glance. *Journal of Cell Science*. **125**(Pt 20),pp.4687–4692.

Shlomchik, M.J. and Weisel, F. 2012. Germinal center selection and the development of memory B and plasma cells. *Immunological Reviews*. **247**(1),pp.52–63.

Shoval, Y. et al. 2011. New Modularity of DAP-Kinases: Alternative Splicing of the DRP-1 Gene Produces a ZIPk-Like Isoform. *PLoS ONE*. **6**(2),p.e17344.

Shoval, Y. et al. 2007. ZIPK: a unique case of murine-specific divergence of a conserved vertebrate gene. *PLoS genetics*. **3**(10),pp.1884–1893.

Shu, F. et al. 2007. Functional characterization of human PFTK1 as a cyclin-dependent kinase. *Proceedings of the National Academy of Sciences of the United States of America*. **104**(22),pp.9248–9253.

Shulman, Z. et al. 2014. Dynamic signaling by T follicular helper cells during germinal center B cell selection. *Science*. **345**(6200),pp.1058–1062.

Siddiqi, S. et al. 2008. Myocardial Induction of Nucleostemin in Response to Postnatal Growth and Pathological Challenge. *Circulation Research*. **103**(1),pp.89–97.

Sidorenko, S.P. et al. 1996. Protein Kinase C μ (PKCμ) Associates with the B Cell Antigen Receptor Complex and Regulates Lymphocyte Signaling. *Immunity*. **5**(4),pp.353–363.

Simboeck, E. et al. 2010. A phosphorylation switch regulates the transcriptional activation of cell cycle regulator p21 by histone deacetylase inhibitors. *The Journal of Biological Chemistry*. **285**(52),pp.41062–41073.

Smolle, M. and Workman, J.L. 2013. Transcription-associated histone modifications and cryptic transcription. *Biochimica et Biophysica Acta (BBA) - Gene Regulatory Mechanisms*. **1829**(1),pp.84–97.

Søgaard, T.M.M. and Svejstrup, J.Q. 2007. Hyperphosphorylation of the C-terminal repeat domain of RNA polymerase II facilitates dissociation of its complex with mediator. *The Journal of Biological Chemistry*. **282**(19),pp.14113–14120.

Sohn, H.W. et al. 2006. Fluorescence resonance energy transfer in living cells reveals dynamic membrane changes in the initiation of B cell signaling. *Proceedings of the National Academy of Sciences of the United States of America*. **103**(21),pp.8143–8148.

Soloaga, A. et al. 2003. MSK2 and MSK1 mediate the mitogen- and stress-induced phosphorylation of histone H3 and HMG-14. *The EMBO Journal*. **22**(11),pp.2788–2797.

Sommer, K. et al. 2005. Phosphorylation of the CARMA1 linker controls NF-kappaB activation. *Immunity*. **23**(6),pp.561–574.

Song, J.H. et al. 2014. Deletion of Pim kinases elevates the cellular levels of reactive oxygen species and sensitizes to K-Ras-induced cell killing. *Oncogene*.

Song, M.S. et al. 2012. The functions and regulation of the PTEN tumour suppressor. *Nature Reviews Molecular Cell Biology*. **13**(5),pp.283–296.

Song, W.-J. et al. 2014. Phosphorylation and Inactivation of GSK3β by Dual-Specificity Tyrosine(Y)-Phosphorylation-Regulated Kinase 1A (Dyrk1A). *The Journal of Biological Chemistry*.

Soper DS 2014. Free p-Value Calculator for Correlation Coefficients. Available from: http://www.danielsoper.com/statcalc3/calc.aspx?id=44 [Accessed September 9, 2014].

Sorrentino, V. et al. 1988. Expression of cellular protooncogenes in the mouse male germ line: a distinctive 2.4-kilobase pim-1 transcript is expressed in haploid postmeiotic cells. *Proceedings of the National Academy of Sciences of the United States of America*. **85**(7),pp.2191–2195.

Soucek, L. et al. 2013. Inhibition of Myc family proteins eradicates KRas-driven lung cancer in mice. *Genes & Development*. **27**(5),pp.504–513.

Souers, A.J. et al. 2013. ABT-199, a potent and selective BCL-2 inhibitor, achieves antitumor activity while sparing platelets. *Nature Medicine*. **19**(2),pp.202–208.

Souza, P.P. et al. 2009. The histone methyltransferase SUV420H2 and Heterochromatin Proteins HP1 interact but show different dynamic behaviours. *BMC cell biology*. **10**,p.41.

Spencer, J. et al. 1998. Human marginal-zone B cells. *Immunology Today*. **19**(9),pp.421–426.

Spender, L.C. and Inman, G.J. 2012. Phosphoinositide 3-kinase/AKT/mTORC1/2 signaling determines sensitivity of Burkitt's lymphoma cells to BH3 mimetics. *Molecular cancer research: MCR*. **10**(3),pp.347–359.

Srivastava, B. et al. 2005. Models for peripheral B cell development and homeostasis. *Seminars in Immunology*. **17**(3),pp.175–182.

Staller, P. et al. 2001. Repression of p15INK4b expression by Myc through association with Miz-1. *Nature Cell Biology*. **3**(4),pp.392–399.

Stavnezer-Nordgren, J. and Sirlin, S. 1986. Specificity of immunoglobulin heavy chain switch correlates with activity of germline heavy chain genes prior to switching. *The EMBO Journal*. **5**(1),pp.95–102.

Stebbins, C.C. et al. 2003. Vav1 Dephosphorylation by the Tyrosine Phosphatase SHP-1 as a Mechanism for Inhibition of Cellular Cytotoxicity. *Molecular and Cellular Biology*. **23**(17),pp.6291–6299.

Steiniger, B. et al. 2005. CD27+ B cells in human lymphatic organs: re-evaluating the splenic marginal zone. *Immunology*. **116**(4),pp.429–442.

Steiniger, B. et al. 1997. The species-specific structure of microanatomical compartments in the human spleen: strongly sialoadhesin-positive macrophages occur in the perifollicular zone, but not in the marginal zone. *Immunology*. **92**(2),pp.307–316.

Stempin, C.C. et al. 2011. The E3 Ubiquitin Ligase Mind Bomb-2 (MIB2) Protein Controls B-cell CLL/Lymphoma 10 (BCL10)-dependent NF-κB Activation. *Journal of Biological Chemistry*. **286**(43),pp.37147–37157.

Stewart, B.E. and Rice, R.H. 1995. Differentiation-associated expression of the proto-oncogene pim-1 in cultured human keratinocytes. *The Journal of Investigative Dermatology*. **105**(5),pp.699–703.

Sthoeger, Z.M. et al. 1989. Production of autoantibodies by CD5-expressing B lymphocytes from patients with chronic lymphocytic leukemia. *The Journal of Experimental Medicine*. **169**(1),pp.255–268.

Stoffel, A. 2005. The NF-κB signalling pathway: a therapeutic target in lymphoid malignancies? *Expert Opinion on Therapeutic Targets*. **9**(5),pp.1045–1061.

Stokoe, D. et al. 1997. Dual Role of Phosphatidylinositol-3,4,5-trisphosphate in the Activation of Protein Kinase B. *Science*. **277**(5325),pp.567–570.

Stoll, S. et al. 2002. Dynamic Imaging of T Cell-Dendritic Cell Interactions in Lymph Nodes. *Science*. **296**(5574),pp.1873–1876.

Stone, K.D. et al. 2010. IgE, mast cells, basophils, and eosinophils. *Journal of Allergy and Clinical Immunology*. **125**(2, Supplement 2),pp.S73–S80.

Stork, B. et al. 2007. Subcellular localization of Grb2 by the adaptor protein Dok-3 restricts the intensity of Ca2+ signaling in B cells. *The EMBO journal*. **26**(4),pp.1140–1149.

Strahl, B.D. and Allis, C.D. 2000. The language of covalent histone modifications. *Nature*. **403**(6765),pp.41–45.

Strelkov, I.S. and Davie, J.R. 2002. Ser-10 phosphorylation of histone H3 and immediate early gene expression in oncogene-transformed mouse fibroblasts. *Cancer Research*. **62**(1),pp.75–78.

Sun, F. et al. 2009. Remodeling of chromatin structure within the promoter is important for bmp-2-induced fgfr3 expression. *Nucleic Acids Research*. **37**(12),pp.3897–3911.

Sun, L. et al. 2004. The TRAF6 Ubiquitin Ligase and TAK1 Kinase Mediate IKK Activation by BCL10 and MALT1 in T Lymphocytes. *Molecular Cell*. **14**(3),pp.289–301.

Sun, M. et al. 2012. Estrogen regulates JNK1 genomic localization to control gene expression and cell growth in breast cancer cells. *Molecular Endocrinology (Baltimore, Md.)*. **26**(5),pp.736–747.

Sutcliffe, E.L. et al. 2009. Dynamic histone variant exchange accompanies gene induction in T cells. *Molecular and Cellular Biology*. **29**(7),pp.1972–1986.

Sutherland, C. et al. 1993. Inactivation of glycogen synthase kinase-3 beta by phosphorylation: new kinase connections in insulin and growth-factor signalling. *The Biochemical Journal*. **296 (Pt 1)**,pp.15–19.

Sutton, L.-A. et al. 2013. Antigen selection in B-cell lymphomas—Tracing the evidence. *Seminars in Cancer Biology*. **23**(6, Part A),pp.399–409.

Suzuki, K. et al. 2010. REAP: A two minute cell fractionation method. *BMC Research Notes*. **3**,p.294.

Swarnalatha, M. et al. 2012. The epigenetic control of E-box and Myc-dependent chromatin modifications regulate the licensing of lamin B2 origin during cell cycle. *Nucleic Acids Research*. **40**(18),pp.9021–9035.

Tachibana, M. et al. 2001. Set domain-containing protein, G9a, is a novel lysine-preferring mammalian histone methyltransferase with hyperactivity and specific selectivity to lysines 9 and 27 of histone H3. *The Journal of Biological Chemistry*. **276**(27),pp.25309–25317.

Tagami, H. et al. 2004. Histone H3.1 and H3.3 Complexes Mediate Nucleosome Assembly Pathways Dependent or Independent of DNA Synthesis. *Cell*. **116**(1),pp.51–61.

Takamoto, N. et al. 2006. Novel ZIP kinase isoform lacks leucine zipper. *Archives of Biochemistry and Biophysics*. **456**(2),pp.194–203.

Talbert, P.B. and Henikoff, S. 2010. Histone variants |[mdash]| ancient wrap artists of the epigenome. *Nature Reviews Molecular Cell Biology*. **11**(4),pp.264–275.

Tamburini, J. et al. 2009. Protein synthesis is resistant to rapamycin and constitutes a promising therapeutic target in acute myeloid leukemia. *Blood*. **114**(8),pp.1618–1627.

Tamir, I. et al. 2000. The RasGAP-binding protein p62dok is a mediator of inhibitory FcgammaRIIB signals in B cells. *Immunity*. **12**(3),pp.347–358.

Tamura, T. et al. 2009. Inducible deposition of the histone variant H3.3 in interferon-stimulated genes. *The Journal of Biological Chemistry*. **284**(18),pp.12217–12225.

Tanaka, M. et al. 2004. Synthesis of anilino-monoindolylmaleimides as potent and selective PKCβ inhibitors. *Bioorganic & Medicinal Chemistry Letters*. **14**(20),pp.5171–5174.

Tanay, A. et al. 2007. Hyperconserved CpG domains underlie Polycomb-binding sites. *Proceedings of the National Academy of Sciences of the United States of America*. **104**(13),pp.5521–5526.

Tang, H.-W. et al. 2011. Atg1-mediated myosin II activation regulates autophagosome formation during starvation-induced autophagy. *The EMBO journal*. **30**(4),pp.636–651.

Tan, M. et al. 2011. Identification of 67 Histone Marks and Histone Lysine Crotonylation as a New Type of Histone Modification. *Cell*. **146**(6),pp.1016–1028.

Tavolaro, S. et al. 2013. IgD cross-linking induces gene expression profiling changes and enhances apoptosis in chronic lymphocytic leukemia cells. *Leukemia research*. **37**(4),pp.455–462.

Taylor, K.H. et al. 2013. Aberrant epigenetic gene regulation in lymphoid malignancies. *Seminars in Hematology*. **50**(1),pp.38–47.

Tee, A.R. et al. 2003. Tuberous sclerosis complex gene products, Tuberin and Hamartin, control mTOR signaling by acting as a GTPase-activating protein complex toward Rheb. *Current biology: CB*. **13**(15),pp.1259–1268.

Tee, W.-W. et al. 2014. Erk1/2 activity promotes chromatin features and RNAPII phosphorylation at developmental promoters in mouse ESCs. *Cell*. **156**(4),pp.678–690.

Teodorovic, L.S. et al. 2014. Activation of Ras overcomes B-cell tolerance to promote differentiation of autoreactive B cells and production of autoantibodies. *Proceedings of the National Academy of Sciences of the United States of America*. **111**(27),pp.E2797–2806.

Teves, S.S. and Henikoff, S. 2011. Heat shock reduces stalled RNA polymerase II and nucleosome turnover genome-wide. *Genes & development*. **25**(22),pp.2387–2397.

Thalmeier, K. et al. 1989. Nuclear factor E2F mediates basic transcription and trans-activation by E1a of the human MYC promoter. *Genes & Development*. **3**(4),pp.527–536.

Thomas, M. et al. 2012. The proto-oncogene Pim-1 is a target of miR-33a. *Oncogene*. **31**(7),pp.918–928.

Thomasova, D. et al. 2012. p53-Independent Roles of MDM2 in NF-?B Signaling: Implications for Cancer Therapy, Wound Healing, and Autoimmune Diseases. *Neoplasia (New York, N.Y.)*. **14**(12),pp.1097–1101.

Thompson, J. et al. 2006. Small carboxyl-terminal domain phosphatase 2 attenuates androgen-dependent transcription. *The EMBO journal*. **25**(12),pp.2757–2767.

Thomson, S. et al. 1999. The nucleosomal response associated with immediate-early gene induction is mediated via alternative MAP kinase cascades: MSK1 as a potential histone H3/HMG-14 kinase. *The EMBO journal*. **18**(17),pp.4779–4793.

Thorne, J.L. et al. 2012. Heterochromatin protein 1 gamma and IκB kinase alpha interdependence during tumour necrosis factor gene transcription elongation in activated macrophages. *Nucleic acids research*.

Tibaldi, E. et al. 2011. Lyn-mediated SHP-1 recruitment to CD5 contributes to resistance to apoptosis of B-cell chronic lymphocytic leukemia cells. *Leukemia*. **25**(11),pp.1768–1781.

Ticchioni, M. et al. 2007. Homeostatic chemokines increase survival of B-chronic lymphocytic leukemia cells through inactivation of transcription factor FOXO3a. *Oncogene*. **26**(50),pp.7081–7091.

Tietjen, J.R. et al. 2010. Chemical-genomic dissection of the CTD code. *Nature Structural & Molecular Biology*. **17**(99),pp.1154–1161.

Till, K.J. et al. 2002. The chemokine receptor CCR7 and α4 integrin are important for migration of chronic lymphocytic leukemia cells into lymph nodes. *Blood*. **99**(8),pp.2977–2984.

Timens, W. et al. 1989. Immaturity of the human splenic marginal zone in infancy. Possible contribution to the deficient infant immune response. *The Journal of Immunology*. **143**(10),pp.3200–3206.

Ting, H.C. et al. 2002. Activation and phosphatidylinositol 3-kinase-dependent phosphorylation of protein kinase C-epsilon by the B cell antigen receptor. *Immunology Letters*. **82**(3),pp.205–215.

Titus, J.A. et al. 1987. Human K/natural killer cells targeted with hetero-cross-linked antibodies specifically lyse tumor cells in vitro and prevent tumor growth in vivo. *Journal of Immunology (Baltimore, Md.: 1950)*. **139**(9),pp.3153–3158.

Tiwari, V.K. et al. 2012. A chromatin-modifying function of JNK during stem cell differentiation. *Nature Genetics*. **44**(1),pp.94–100.

Tobin, G. et al. 2003. Chronic lymphocytic leukemias utilizing the VH3-21 gene display highly restricted Vλ2-14 gene use and homologous CDR3s: implicating recognition of a common antigen epitope. *Blood*. **101**(12),pp.4952–4957.

Tobin, G. et al. 2004. Subsets with restricted immunoglobulin gene rearrangement features indicate a role for antigen selection in the development of chronic lymphocytic leukemia. *Blood*. **104**(9),pp.2879–2885.

Tonegawa, S. 1983. Somatic generation of antibody diversity. *Nature*. **302**(5909),pp.575–581.

Toren, P. and Zoubeidi, A. 2013. Rational cotargeting of Pim-1 and Akt in prostate cancer. *Expert Review of Anticancer Therapy*. **13**(8),pp.937–939.

Toualbi, K. et al. 2006. Physical and functional cooperation between AP-1 and β-catenin for the regulation of TCF-dependent genes. *Oncogene*. **26**(24),pp.3492–3502.

Tourdot, B.E. et al. 2013. Immunoreceptor tyrosine-based inhibitory motif (ITIM)-mediated inhibitory signaling is regulated by sequential phosphorylation mediated by distinct nonreceptor tyrosine kinases: a case study involving PECAM-1. *Biochemistry*. **52**(15),pp.2597–2608.

Tracey, L. et al. 2005. Expression of the NF-κB targets BCL2 and BIRC5/Survivin characterizes small B-cell and aggressive B-cell lymphomas, respectively. *The Journal of Pathology*. **206**(2),pp.123–134.

Traenckner, E.B.-M. et al. 1995. Phosphorylation of human IκB-α on serines 32 and 36 controls IκB-α proteolysis and NF-κB activation in response to diverse stimuli. *EMBO Journal*. **14**(12),pp.2876–2883.

Tridandapani, S. et al. 1997. Recruitment and phosphorylation of SH2-containing inositol phosphatase and Shc to the B-cell Fc gamma immunoreceptor tyrosine-based inhibition motif peptide motif. *Molecular and Cellular Biology*. **17**(8),pp.4305–4311.

Tsubata, T. 2012. Role of Inhibitory BCR Co-Receptors in Immunity. *Infectious Disorders - Drug Targets*. **12**(3),pp.181–190.

Tuveson, D.A. et al. 1993. CD19 of B cells as a surrogate kinase insert region to bind phosphatidylinositol 3-kinase. *Science (New York, N.Y.)*. **260**(5110),pp.986–989.

Usui, T. et al. 2014. Death-associated protein kinase 3 mediates vascular structural remodelling via stimulating smooth muscle cell proliferation and migration. *Clinical Science (London, England: 1979)*. **127**(8),pp.539–548.

Vakoc, C.R. et al. 2005. Histone H3 lysine 9 methylation and HP1gamma are associated with transcription elongation through mammalian chromatin. *Molecular cell*. **19**(3),pp.381–391.

Valentine, M.A. et al. 1995. Anti-immunoglobulin M activates nuclear calcium/calmodulin-dependent protein kinase II in human B lymphocytes. *The Journal of Experimental Medicine*. **182**(6),pp.1943–1949.

Vander Haar, E. et al. 2007. Insulin signalling to mTOR mediated by the Akt/PKB substrate PRAS40. *Nature Cell Biology*. **9**(3),pp.316–323.

Varlakhanova, N. et al. 2011. Myc and Miz-1 have coordinate genomic functions including targeting Hox genes in human embryonic stem cells. *Epigenetics & Chromatin*. **4**(1),p.20.

Vassilev, A. et al. 1998. The 400 kDa Subunit of the PCAF Histone Acetylase Complex Belongs to the ATM Superfamily. *Molecular Cell*. **2**(6),pp.869–875.

Venkataraman, L. et al. 1994. Cyclosporin-a sensitive induction of NF-AT in murine B cells. *Immunity*. **1**(3),pp.189–196.

Venkatesh, S. et al. 2012. Set2 methylation of histone H3 lysine 36 suppresses histone exchange on transcribed genes. *Nature*. **489**(7416),pp.452–455.

Verbeek, S. et al. 1991. Mice bearing the E mu-myc and E mu-pim-1 transgenes develop pre-B-cell leukemia prenatally. *Molecular and cellular biology*. **11**(2),pp.1176–1179.

Verbrugge, A. et al. 2006. Leukocyte-associated Ig-like receptor-1 has SH2 domain-containing phosphatase-independent function and recruits C-terminal Src kinase. *European Journal of Immunology*. **36**(1),pp.190–198.

Vermeulen, L. et al. 2003. Transcriptional activation of the NF-kappaB p65 subunit by mitogen- and stress-activated protein kinase-1 (MSK1). *The EMBO journal*. **22**(6),pp.1313–1324.

Vermeulen, M. et al. 2010. Quantitative Interaction Proteomics and Genome-wide Profiling of Epigenetic Histone Marks and Their Readers. *Cell*. **142**(6),pp.967–980.

Vermeulen, M. et al. 2007. Selective anchoring of TFIID to nucleosomes by trimethylation of histone H3 lysine 4. *Cell*. **131**(1),pp.58–69.

Vervoorts, J. et al. 2003. Stimulation of c-MYC transcriptional activity and acetylation by recruitment of the cofactor CBP. *EMBO reports*. **4**(5),pp.484–490.

Vetterkind, S. et al. 2005. Binding of Par-4 to the actin cytoskeleton is essential for Par-4/Dlk-mediated apoptosis. *Experimental Cell Research*. **305**(2),pp.392–408.

Vezzoli, A. et al. 2010. Molecular basis of histone H3K36me3 recognition by the PWWP domain of Brpf1. *Nature Structural & Molecular Biology*. **17**(5),pp.617–619.

Vicent, G.P. et al. 2006. Induction of progesterone target genes requires activation of Erk and Msk kinases and phosphorylation of histone H3. *Molecular Cell*. **24**(3),pp.367–381.

Vlad, A. et al. 2009. Down-regulation of CXCR4 and CD62L in chronic lymphocytic leukemia cells is triggered by B-cell receptor ligation and associated with progressive disease. *Cancer Research*. **69**(16),pp.6387–6395.

Wagner, E.J. and Carpenter, P.B. 2012. Understanding the language of Lys36 methylation at histone H3. *Nature Reviews. Molecular Cell Biology*. **13**(2),pp.115–126.

Wakabayashi, C. et al. 2002. A Distinct Signaling Pathway Used by the IgG-Containing B Cell Antigen Receptor. *Science*. **298**(5602),pp.2392–2395.

Walter, W. et al. 2008. 14-3-3 interaction with histone H3 involves a dual modification pattern of phosphoacetylation. *Molecular and Cellular Biology*. **28**(8),pp.2840–2849.

Walz, S. et al. 2014. Activation and repression by oncogenic MYC shape tumour-specific gene expression profiles. *Nature*. **511**(7510),pp.483–487.

Wang, G. et al. 2001. Characterization of mediator complexes from HeLa cell nuclear extract. *Molecular and Cellular Biology*. **21**(14),pp.4604–4613.

Wang, H. et al. 2004. Role of histone H2A ubiquitination in Polycomb silencing. *Nature*. **431**(7010),pp.873–878.

Wang, J. et al. 2012. Pim1 kinase is required to maintain tumorigenicity in MYC-expressing prostate cancer cells. *Oncogene*. **31**(14),pp.1794–1803.

Wang, J. et al. 2010. Pim1 kinase synergizes with c-MYC to induce advanced prostate carcinoma. *Oncogene*. **29**(17),pp.2477–2487.

Wang, P. et al. 2009. Global Analysis of H3K4 Methylation Defines MLL Family Member Targets and Points to a Role for MLL1-Mediated H3K4 Methylation in the Regulation of Transcriptional Initiation by RNA Polymerase II. *Molecular and Cellular Biology*. **29**(22),pp.6074–6085.

Wang, Q. et al. 2006. Histone phosphorylation and pericentromeric histone modifications in oocyte meiosis. *Cell Cycle (Georgetown, Tex.)*. **5**(17),pp.1974–1982.

Wang, X. and Proud, C.G. 2011. mTORC1 signaling: what we still don't know. *Journal of Molecular Cell Biology*. **3**(4),pp.206–220.

Wang, Y. et al. 2002. The Physiologic Role of CD19 Cytoplasmic Tyrosines. *Immunity*. **17**(4),pp.501–514.

Wang, Z. et al. 2009. Genome-wide mapping of HATs and HDACs reveals distinct functions in active and inactive genes. *Cell*. **138**(5),pp.1019–1031.

Wang, Z. et al. 2011. MYC protein inhibits transcription of the microRNA cluster MC-let-7a-1~let-7d via noncanonical E-box. *The Journal of Biological Chemistry*. **286**(46),pp.39703–39714.

Wang, Z. et al. 2002. Phosphorylation of the cell cycle inhibitor p21Cip1/WAF1 by Pim-1 kinase. *Biochimica Et Biophysica Acta*. **1593**(1),pp.45–55.

Wang, Z. et al. 2010. Pro Isomerization in MLL1 PHD3-Bromo Cassette Connects H3K4me Readout to CyP33 and HDAC-Mediated Repression. *Cell*. **141**(7),pp.1183–1194.

Wanzel, M. et al. 2008. A ribosomal protein L23-nucleophosmin circuit coordinates Miz1 function with cell growth. *Nature Cell Biology*. **10**(9),pp.1051–1061.

Wardemann, H. et al. 2003. Predominant Autoantibody Production by Early Human B Cell Precursors. *Science*. **301**(5638),pp.1374–1377.

Washington, K. et al. 2002. Protein phosphatase-1 dephosphorylates the C-terminal domain of RNA polymerase-II. *The Journal of Biological Chemistry*. **277**(43),pp.40442–40448.

Watson, C.T. and Breden, F. 2012. The immunoglobulin heavy chain locus: genetic variation, missing data, and implications for human disease. *Genes and Immunity*. **13**(5),pp.363–373.

Watt, R. et al. 1983. The structure and nucleotide sequence of the 5' end of the human c-myc oncogene. *Proceedings of the National Academy of Sciences of the United States of America*. **80**(20),pp.6307–6311.

Weber, C.M. et al. 2014. Nucleosomes are context-specific, H2A.Z-modulated barriers to RNA polymerase. *Molecular cell*. **53**(5),pp.819–830.

Van Weeren, P.C. et al. 1998. Essential role for protein kinase B (PKB) in insulin-induced glycogen synthase kinase 3 inactivation. Characterization of dominant-negative mutant of PKB. *The Journal of Biological Chemistry*. **273**(21),pp.13150–13156.

Weill, J.-C. et al. 2009. Human Marginal Zone B Cells. *Annual Review of Immunology*. **27**(1),pp.267–285.

Weinstein, I.B. and Joe, A.K. 2006. Mechanisms of Disease: oncogene addiction—a rationale for molecular targeting in cancer therapy. *Nature Clinical Practice Oncology*. **3**(8),pp.448–457.

Weitzel, D.H. et al. 2011. Phosphorylation-dependent control of ZIPK nuclear import is species specific. *Cellular signalling*. **23**(1),pp.297–303.

Wei, Y. et al. 1998. Phosphorylation of histone H3 at serine 10 is correlated with chromosome condensation during mitosis and meiosis in Tetrahymena. *Proceedings of the National Academy of Sciences of the United States of America*. **95**(13),pp.7480–7484.

Welcker, M. et al. 2004. The Fbw7 tumor suppressor regulates glycogen synthase kinase 3 phosphorylation-dependent c-Myc protein degradation. *Proceedings of the National Academy of Sciences of the United States of America*. **101**(24),pp.9085–9090.

Wellbrock, C. et al. 2004. The RAF proteins take centre stage. *Nature Reviews Molecular Cell Biology*. **5**(11),pp.875–885.

Weller, S. et al. 2004. Human blood IgM 'memory' B cells are circulating splenic marginal zone B cells harboring a prediversified immunoglobulin repertoire. *Blood*. **104**(12),pp.3647–3654.

Welsh, G.I. and Proud, C.G. 1993. Glycogen synthase kinase-3 is rapidly inactivated in response to insulin and phosphorylates eukaryotic initiation factor eIF-2B. *The Biochemical Journal*. **294 (Pt 3)**,pp.625–629.

Wen, H. et al. 2014. ZMYND11 links histone H3.3K36me3 to transcription elongation and tumour suppression. *Nature*. **508**(7495),pp.263–268.

Whetstine, J.R. et al. 2006. Reversal of histone lysine trimethylation by the JMJD2 family of histone demethylases. *Cell*. **125**(3),pp.467–481.

Whitfield, M.L. et al. 2000. Stem-Loop Binding Protein, the Protein That Binds the 3′ End of Histone mRNA, Is Cell Cycle Regulated by Both Translational and Posttranslational Mechanisms. *Molecular and Cellular Biology*. **20**(12),pp.4188–4198.

Widhopf II, G.F. et al. 2004. Chronic lymphocytic leukemia B cells of more than 1% of patients express virtually identical immunoglobulins. *Blood*. **104**(8),pp.2499–2504.

Wiestner, A. 2012. Emerging role of kinase-targeted strategies in chronic lymphocytic leukemia. *Hematology / the Education Program of the American Society of Hematology. American Society of Hematology. Education Program*. **2012**,pp.88–96.

Wingett, D. et al. 1992. Characterization of the testes-specific pim-1 transcript in rat. *Nucleic acids research*. **20**(12),pp.3183–3189.

Winter, S. et al. 2008. 14-3-3 proteins recognize a histone code at histone H3 and are required for transcriptional activation. *The EMBO journal*. **27**(1),pp.88–99.

Witham, J. et al. 2013. A NF-κB-dependent dual promoter-enhancer initiates the lipopolysaccharide-mediated transcriptional activation of the chicken lysozyme in macrophages. *PloS One*. **8**(3),p.e59389.

Wodarz, D. et al. 2014. Kinetics of CLL cells in tissues and blood during therapy with the BTK inhibitor ibrutinib. *Blood*. **123**(26),pp.4132–4135.

Wood, N.T. et al. 2009. 14-3-3 Binding to Pim-phosphorylated Ser166 and Ser186 of human Mdm2 – Potential interplay with the PKB/Akt pathway and p14ARF. *FEBS Letters*. **583**(4),pp.615–620.

Woyach, J.A. et al. 2014. Resistance Mechanisms for the Bruton's Tyrosine Kinase Inhibitor Ibrutinib. *The New England journal of medicine*.

Wozniak, G.G. and Strahl, B.D. 2014. Hitting the 'mark': Interpreting lysine methylation in the context of active transcription. *Biochimica Et Biophysica Acta*.

Wright, G. et al. 2003. A gene expression-based method to diagnose clinically distinct subgroups of diffuse large B cell lymphoma. *Proceedings of the National Academy of Sciences of the United States of America*. **100**(17),pp.9991–9996.

Wu, C.-J. and Ashwell, J.D. 2008. NEMO recognition of ubiquitinated Bcl10 is required for T cell receptor-mediated NF-kappaB activation. *Proceedings of the National Academy of Sciences of the United States of America*. **105**(8),pp.3023–3028.

Wu, M. et al. 2008. Molecular regulation of H3K4 trimethylation by Wdr82, a component of human Set1/COMPASS. *Molecular and Cellular Biology*. **28**(24),pp.7337–7344.

Wu, Y. et al. 2010. Link of Dlk/ZIP kinase to cell apoptosis and tumor suppression. *Biochemical and Biophysical Research Communications*. **392**(4),pp.510–515.

Xiao, C. et al. 2008. Lymphoproliferative disease and autoimmunity in mice with increased miR-17-92 expression in lymphocytes. *Nature Immunology*. **9**(4),pp.405–414.

Xia, Z. et al. 2009. Synthesis and evaluation of novel inhibitors of Pim-1 and Pim-2 protein kinases. *Journal of Medicinal Chemistry*. **52**(1),pp.74–86.

Xie, Y. et al. 2006. The 44 kDa Pim-1 kinase directly interacts with tyrosine kinase Etk/BMX and protects human prostate cancer cells from apoptosis induced by chemotherapeutic drugs. *Oncogene*. **25**(1),pp.70–78.

Xie, Y. et al. 2008. The 44-kDa Pim-1 Kinase Phosphorylates BCRP/ABCG2 and Thereby Promotes Its Multimerization and Drug-resistant Activity in Human Prostate Cancer Cells. *Journal of Biological Chemistry*. **283**(6),pp.3349–3356.

Xue, Y. et al. 2008. GPS 2.0, a tool to predict kinase-specific phosphorylation sites in hierarchy. *Molecular & cellular proteomics: MCP*. **7**(9),pp.1598–1608.

Yada, M. et al. 2004. Phosphorylation-dependent degradation of c-Myc is mediated by the F-box protein Fbw7. *The EMBO Journal*. **23**(10),pp.2116–2125.

Yaghoobi, M.M. et al. 2005. Nucleostemin, a coordinator of self-renewal, is expressed in rat marrow stromal cells and turns off after induction of neural differentiation. *Neuroscience Letters*. **390**(2),pp.81–86.

Yagi, K. et al. 2002. c-myc is a downstream target of the Smad pathway. *The Journal of Biological Chemistry*. **277**(1),pp.854–861.

Yahi, H. et al. 2008. Differential cooperation between heterochromatin protein HP1 isoforms and MyoD in myoblasts. *The Journal of Biological Chemistry*. **283**(35),pp.23692–23700.

Yahyaoui, W. and Zannis-Hadjopoulos, M. 2009. 14-3-3 proteins function in the initiation and elongation steps of DNA replication in Saccharomyces cerevisiae. *Journal of cell science*. **122**(Pt 24),pp.4419–4426.

Yamamoto, K. and Sonoda, M. 2003. Self-interaction of heterochromatin protein 1 is required for direct binding to histone methyltransferase, SUV39H1.

Biochemical and Biophysical Research Communications. **301**(2),pp.287–292.
Yamamoto, Y. et al. 2003. Histone H3 phosphorylation by IKK-α is critical for cytokine-induced gene expression. *Nature*. **423**(6940),pp.655–659.
Yamanashi, Y. et al. 2000. Role of the rasGAP-associated docking protein p62 dok in negative regulation of B cell receptor-mediated signaling. *Genes & Development*. **14**(1),pp.11–16.
Yamane, K. et al. 2006. JHDM2A, a JmjC-containing H3K9 demethylase, facilitates transcription activation by androgen receptor. *Cell*. **125**(3),pp.483–495.
Yan, B. et al. 2003. The PIM-2 Kinase Phosphorylates BAD on Serine 112 and Reverses BAD-Induced Cell Death. *Journal of Biological Chemistry*. **278**(46),pp.45358–45367.
Yang, B.S. et al. 1996. Ras-mediated phosphorylation of a conserved threonine residue enhances the transactivation activities of c-Ets1 and c-Ets2. *Molecular and Cellular Biology*. **16**(2),pp.538–547.
Yang, Q. et al. 2012. Transcription and translation are primary targets of Pim kinase inhibitor SGI-1776 in mantle cell lymphoma. *Blood*. **120**(17),pp.3491–3500.
Yang, S.-H. et al. 1998. Differential targeting of MAP kinases to the ETS-domain transcription factor Elk-1. *The EMBO Journal*. **17**(6),pp.1740–1749.
Yang, W. et al. 2012. PKM2 phosphorylates histone H3 and promotes gene transcription and tumorigenesis. *Cell*. **150**(4),pp.685–696.
Yang, X.-J. and Seto, E. 2007. HATs and HDACs: from structure, function and regulation to novel strategies for therapy and prevention. *Oncogene*. **26**(37),pp.5310–5318.
Yang, Z. et al. 2005. Recruitment of P-TEFb for Stimulation of Transcriptional Elongation by the Bromodomain Protein Brd4. *Molecular Cell*. **19**(4),pp.535–545.
Yap, K.L. and Zhou, M.-M. 2010. Keeping it in the family: diverse histone recognition by conserved structural folds. *Critical Reviews in Biochemistry and Molecular Biology*. **45**(6),pp.488–505.
Yarkoni, Y. et al. 2010. Molecular underpinning of B-cell anergy. *Immunological Reviews*. **237**(1),pp.249–263.
Yasuda, T. et al. 2008. Erk Kinases Link Pre-B Cell Receptor Signaling to Transcriptional Events Required for Early B Cell Expansion. *Immunity*. **28**(4),pp.499–508.
Ye, J. et al. 2012. Primer-BLAST: a tool to design target-specific primers for polymerase chain reaction. *BMC bioinformatics*. **13**,p.134.
Yeo, M. et al. 2003. A novel RNA polymerase II C-terminal domain phosphatase that preferentially dephosphorylates serine 5. *The Journal of Biological Chemistry*. **278**(28),pp.26078–26085.
Yochum, G.S. et al. 2010. A beta-catenin/TCF-coordinated chromatin loop at MYC integrates 5' and 3' Wnt responsive enhancers. *Proceedings of the National Academy of Sciences of the United States of America*. **107**(1),pp.145–150.
Yuan, W. et al. 2012. Dense Chromatin Activates Polycomb Repressive Complex 2 to Regulate H3 Lysine 27 Methylation. *Science*. **337**(6097),pp.971–975.
Yu, M.K. 2006. Epigenetics and chronic lymphocytic leukemia. *American Journal of Hematology*. **81**(11),pp.864–869.
Yu, X. et al. 2008. Neutralizing antibodies derived from the B cells of 1918 influenza pandemic survivors. *Nature*. **455**(7212),pp.532–536.
Zeller, K.I. et al. 2006. Global mapping of c-Myc binding sites and target gene networks in human B cells. *Proceedings of the National Academy of Sciences of the United States of America*. **103**(47),pp.17834–17839.
Zemskova, M. et al. 2010. p53-dependent induction of prostate cancer cell senescence by the PIM1 protein kinase. *Molecular cancer research: MCR*. **8**(8),pp.1126–1141.

Zemskova, M. et al. 2008. The PIM1 kinase is a critical component of a survival pathway activated by docetaxel and promotes survival of docetaxel-treated prostate cancer cells. *The Journal of Biological Chemistry*. **283**(30),pp.20635–20644.

Zeng, L. et al. 2010. Mechanism and regulation of acetylated histone binding by the tandem PHD finger of DPF3b. *Nature*. **466**(7303),pp.258–262.

Zeng, L. et al. 2008. Structural basis of site-specific histone recognition by the bromodomains of human coactivators PCAF and CBP/p300. *Structure (London, England: 1993)*. **16**(4),pp.643–652.

Zhang, C. et al. 2002. Impaired Proliferation and Survival of Activated B Cells in Transgenic Mice That Express a Dominant-negative cAMP-response Element-binding Protein Transcription Factor in B Cells. *Journal of Biological Chemistry*. **277**(50),pp.48359–48365.

Zhang, F. et al. 2009. PIM1 protein kinase regulates PRAS40 phosphorylation and mTOR activity in FDCP1 cells. *Cancer Biology & Therapy*. **8**(9),pp.846–853.

Zhang, H.-M. et al. 2008. Mitogen-induced recruitment of ERK and MSK to SRE promoter complexes by ternary complex factor Elk-1. *Nucleic Acids Research*. **36**(8),pp.2594–2607.

Zhang, J. et al. 2009. Targeting cancer with small molecule kinase inhibitors. *Nature Reviews Cancer*. **9**(1),pp.28–39.

Zhang, N. et al. 2014. MYC interacts with the human STAGA coactivator complex via multivalent contacts with the GCN5 and TRRAP subunits. *Biochimica Et Biophysica Acta*. **1839**(5),pp.395–405.

Zhang, Q. et al. 2013. Domain-specific c-Myc ubiquitylation controls c-Myc transcriptional and apoptotic activity. *Proceedings of the National Academy of Sciences*. **110**(3),pp.978–983.

Zhang, Q. et al. 2011. Phosphorylation of histone H3 serine 28 modulates RNA polymerase III-dependent transcription. *Oncogene*. **30**(37),pp.3943–3952.

Zhang, S. et al. 2013. B Cell–Specific Deficiencies in mTOR Limit Humoral Immune Responses. *The Journal of Immunology*. **191**(4),pp.1692–1703.

Zhang, S. and Kipps, T.J. 2014. The Pathogenesis of Chronic Lymphocytic Leukemia. *Annual Review of Pathology: Mechanisms of Disease*. **9**(1),pp.103–118.

Zhang, W. et al. 2012. Bromodomain-containing Protein 4 (BRD4) Regulates RNA Polymerase II Serine 2 Phosphorylation in Human CD4+ T Cells. *Journal of Biological Chemistry*. **287**(51),pp.43137–43155.

Zhang, X. et al. 2012. Coordinated silencing of MYC-mediated miR-29 by HDAC3 and EZH2 as a therapeutic target of histone modification in aggressive B-Cell lymphomas. *Cancer Cell*. **22**(4),pp.506–523.

Zhang, X. et al. 2011. Structure of Lipid Kinase p110β/p85β Elucidates an Unusual SH2-Domain-Mediated Inhibitory Mechanism. *Molecular Cell*. **41**(5),pp.567–578.

Zhang, Y. et al. 2010. Chromatin methylation activity of Dnmt3a and Dnmt3a/3L is guided by interaction of the ADD domain with the histone H3 tail. *Nucleic Acids Research*. **38**(13),pp.4246–4253.

Zhang, Y. et al. 2013. Germinal center B cells govern their own fate via antibody feedback. *The Journal of Experimental Medicine*. **210**(3),pp.457–464.

Zhang, Y. et al. 2004. Phosphorylation of Histone H2A Inhibits Transcription on Chromatin Templates. *Journal of Biological Chemistry*. **279**(21),pp.21866–21872.

Zhang, Y. et al. 2010. Pim-1 kinase as activator of the cell cycle pathway in neuronal death induced by DNA damage. *Journal of Neurochemistry*. **112**(2),pp.497–510.

Zhang, Y. et al. 2007. Pim-1 kinase-dependent phosphorylation of p21Cip1/WAF1 regulates its stability and cellular localization in H1299 cells. *Molecular Cancer Research: MCR*. **5**(9),pp.909–922.

Zhang, Y. et al. 2008. Pim kinase-dependent inhibition of c-Myc degradation. *Oncogene*. **27**(35),pp.4809–4819.
Zhao, J. et al. 2008. Polycomb proteins targeted by a short repeat RNA to the mouse X chromosome. *Science (New York, N.Y.)*. **322**(5902),pp.750–756.
Zhao, M. et al. 2001. Phosphoinositide 3-Kinase–Dependent Membrane Recruitment of P62dok Is Essential for Its Negative Effect on Mitogen-Activated Protein (Map) Kinase Activation. *The Journal of Experimental Medicine*. **194**(3),pp.265–274.
Zhao, X.D. et al. 2007. Whole-genome mapping of histone H3 Lys4 and 27 trimethylations reveals distinct genomic compartments in human embryonic stem cells. *Cell Stem Cell*. **1**(3),pp.286–298.
Zheng, H.-C. et al. 2008. Aberrant Pim-3 expression is involved in gastric adenoma-adenocarcinoma sequence and cancer progression. *Journal of Cancer Research and Clinical Oncology*. **134**(4),pp.481–488.
Zheng, Q. et al. 2011. Regulation of C. elegans presynaptic differentiation and neurite branching via a novel signaling pathway initiated by SAM-10. *Development*. **138**(1),pp.87–96.
Zheng, Y. et al. 2005. Phosphorylation of RasGRP3 on threonine 133 provides a mechanistic link between PKC and Ras signaling systems in B cells. *Blood*. **105**(9),pp.3648–3654.
Zhong, S. et al. 2001. Ultraviolet B-induced phosphorylation of histone H3 at serine 28 is mediated by MSK1. *The Journal of Biological Chemistry*. **276**(35),pp.33213–33219.
Zhou, B.P. et al. 2001. HER-2/neu induces p53 ubiquitination via Akt-mediated MDM2 phosphorylation. *Nature Cell Biology*. **3**(11),pp.973–982.
Zhou, H. et al. 2004. Bcl10 activates the NF-κB pathway through ubiquitination of NEMO. *Nature*. **427**(6970),pp.167–171.
Zhuang, J. et al. 2010. Akt is activated in chronic lymphocytic leukemia cells and delivers a pro-survival signal: the therapeutic potential of Akt inhibition. *Haematologica*. **95**(1),pp.110–118.
Zhu, B. et al. 2005. Monoubiquitination of Human Histone H2B: The Factors Involved and Their Roles in HOX Gene Regulation. *Molecular Cell*. **20**(4),pp.601–611.
Zhu, N. et al. 2002. CD40 signaling in B cells regulates the expression of the Pim-1 kinase via the NF-kappa B pathway. *Journal of Immunology (Baltimore, Md.: 1950)*. **168**(2),pp.744–754.
Zieve, G.W. et al. 1980. Production of large numbers of mitotic mammalian cells by use of the reversible microtubule inhibitor Nocodazole: Nocodazole accumulated mitotic cells. *Experimental Cell Research*. **126**(2),pp.397–405.
Zindy, F. et al. 1998. Myc signaling via the ARF tumor suppressor regulates p53-dependent apoptosis and immortalization. *Genes & Development*. **12**(15),pp.2424–2433.
Zippo, A. et al. 2009. Histone crosstalk between H3S10ph and H4K16ac generates a histone code that mediates transcription elongation. *Cell*. **138**(6),pp.1122–1136.
Zippo, A. et al. 2004. Identification of Flk-1 target genes in vasculogenesis: Pim-1 is required for endothelial and mural cell differentiation in vitro. *Blood*. **103**(12),pp.4536–4544.
Zippo, A. et al. 2007. PIM1-dependent phosphorylation of histone H3 at serine 10 is required for MYC-dependent transcriptional activation and oncogenic transformation. *Nature Cell Biology*. **9**(8),pp.932–944.
Zirkin, S. et al. 2013. The PIM-2 kinase is an essential component of the UV damage response that acts upstream to E2F-1 and ATM. *The Journal of biological chemistry*.
Zotos, D. and Tarlinton, D.M. 2012. Determining germinal centre B cell fate. *Trends in Immunology*. **33**(6),pp.281–288.

Zupo, S. et al. 1994. Expression of CD5 and CD38 by human CD5- B cells: requirement for special stimuli. *European Journal of Immunology*. **24**(6),pp.1426–1433.

Zwolinska, A.K. et al. 2011. Suppression of Myc oncogenic activity by nucleostemin haploinsufficiency. *Oncogene*.

10 Appendix

10.1 Quercetagetin kinase screen

This kinase screen was performed by the MRC Protein Phosphorylation and Ubiquiylation Unit (Dundee, UK). The data are available at http://www.kinase-screen.mrc.ac.uk/screening-compounds/348817.

Screening Concentration: 10µM			Screening Concentration: 1µM		
Kinase	% Activity Remaining	Standard Deviation	Kinase	% Activity Remaining	Standard Deviation
PIM3	0	0	PKB beta	21	7
PKB beta	1	0	RSK2	22	0
PRAK	1	0	VEGFR1	27	4
DYRK2	1	0	FGF-R1	27	1
PHK	2	0	NUAK1	33	7
DYRK3	2	0	PIM3	34	1
DYRK1A	3	0	MARK4	34	1
SRPK1	3	0	PIM1	37	6
CHK2	5	1	Src	38	0
TAK1	5	2	MARK1	40	0
MARK3	6	1	YES1	42	1
BRSK1	7	0	DYRK2	45	2
CK2	7	0	CK2	46	3
PIM1	7	0	CHK2	48	12
RIPK2	7	0	CAMK1	49	1
VEGFR1	7	0	PAK4	50	3
Aurora B	8	1	RSK1	51	0
AMPK	9	3	MARK3	51	1
MELK	9	1	MELK	53	3
MST2	9	0	TBK1	54	4
YES1	9	0	SRPK1	55	10
MINK1	10	0	MINK1	56	4
MARK1	11	0	PAK6	58	2
PIM2	11	0	MST2	58	2
HIPK1	11	1	CLK2	58	9
RSK2	12	1	DYRK3	59	3
MNK1	12	4	MNK1	61	2
NUAK1	12	0	BTK	61	2
BRSK2	13	1	PKC zeta	62	0
NEK2a	13	1	MLK3	62	1
JAK2	13	7	HIPK2	62	7
S6K1	14	0	Aurora B	62	4

MAPKAP-K3	14	0	MNK2	63	7
FGF-R1	14	0	PAK5	67	0
RSK1	15	0	MEKK1	67	4
PKD1	15	6	PKD1	69	3
IKK beta	16	5	IKK epsilon	69	4
MLK3	16	0	EPH-B2	69	4
CAMK1	19	3	DYRK1A	71	11
GSK3 beta	19	1	BRSK2	71	10
HIPK2	19	0	CAMKK beta	72	0
PKC zeta	20	0	AMPK	73	6
MARK4	20	0	PIM2	74	1
NEK6	21	1	TTK	75	0
IKK epsilon	21	1	IRR	76	4
IRR	21	1	IRAK4	80	3
SmMLCK	23	0	BRSK1	82	1
PLK1	23	4	RIPK2	83	10
GCK	23	1	MKK1	84	0
MKK1	24	4	EPH-B1	85	8
SGK1	24	2	NEK2a	86	3
MLK1	24	0	MARK2	86	2
Src	25	2	IR	86	0
MNK2	26	5	SmMLCK	87	0
MARK2	26	3	SGK1	87	3
Aurora A	28	2	PRAK	87	1
CK1 delta	29	1	MST4	87	2
TrkA	29	2	MSK1	88	1
CHK1	32	1	HIPK3	88	10
CDK2-Cyclin A	32	0	SYK	89	6
BTK	32	2	ERK8	89	0
TTK	36	6	CDK2-Cyclin A	89	12
MSK1	38	0	EPH-B4	90	13
PAK4	38	6	CK1 delta	90	0
IGF-1R	43	2	JAK2	91	5
HER4	44	2	TrkA	92	9
IRAK4	46	0	MAPKAP-K3	92	3
MAPKAP-K2	53	14	CHK1	92	12
ERK1	54	4	JNK1	93	1
LKB1	55	6	HIPK1	93	5
HIPK3	55	0	GCK	93	1
PAK5	55	6	EPH-B3	93	5
ROCK 2	56	3	TAO1	94	11
EPH-B4	56	11	TAK1	94	10
MST4	58	5	MKK2	94	1

PAK6	60	12
CAMKK beta	61	5
EPH-B3	61	6
IR	62	3
TBK1	64	10
ERK8	65	1
EPH-A2	73	6
MEKK1	74	6
CSK	74	0
EPH-A4	74	6
PKA	79	2
PKC alpha	80	13
PDK1	83	13
p38 gamma MAPK	88	6
JNK3	89	1
p38 beta MAPK	90	0
JNK1	93	3
SYK	93	8
Lck	95	9
p38 delta MAPK	97	8
PAK2	98	2
PKB alpha	99	10
JNK2	100	9
PRK2	102	1
ERK2	105	1
EF2K	109	1
p38 alpha MAPK	119	6

MAPKAP-K2	94	1
GSK3 beta	94	5
EPH-A2	94	14
ROCK 2	95	4
LKB1	95	12
DAPK1	95	11
Aurora A	95	11
PAK2	96	7
p38 delta MAPK	96	7
IGF-1R	96	3
PHK	98	2
PKC alpha	99	7
NEK6	99	8
p38 alpha MAPK	100	4
MLK1	100	5
IKK beta	100	6
p38 beta MAPK	101	7
ERK1	101	2
MKK6	102	7
Lck	102	15
S6K1	104	3
PDK1	104	0
PRK2	106	7
PKB alpha	106	9
JNK2	106	7
PLK1	107	11
p38 gamma MAPK	107	2
JNK3	107	2
ERK2	107	8
PKA	109	7
HER4	109	4
EF2K	110	8
EPH-A4	117	3
ASK1	118	0
CSK	125	12